

IGS

1 9 9 8 A N A L Y S I S

C E N T E R W O R K S H O P

PROCEEDINGS

**DARMSTADT,
FEBRUARY 9-11, 1998**

ESA/ESOC
Darmstadt
Germany

Edited by
J. M. Dow (ESA)
J. Kouba (NRCan)
T. Springer (AIUB)



International GPS Service



Association Internationale de Géodésie

Union Géodésique et Géophysique
Internationale

International Association of Geodesy

International Union of Geodesy and
Geophysics



The Federation of Astronomical and
Geophysical Data Analysis Services

The research described in this publication was sponsored by many agencies who actively participate in the International GPS Service. The Proceedings of the Workshop were prepared and published by the European Space Centre of the European Space Agency.

FOREWORD

The 1998 Analysis Centre Workshop of the International GPS Service for Geodynamics (IGS) held in Darmstadt, Germany from 9 to 11 February 1998 followed a series of workshops dedicated to IGS Analysis Centre issues (1993 in Ottawa, 1994 in Pasadena, 1995 in Potsdam, 1996 in Silver Spring, 1997 in Pasadena; IGS workshops with a more general scope also took place in Bern in 1993 and Paris in 1994).

Discussions between representatives of the Analysis Centres present at IGS Governing Board meetings and Retreat held in San Francisco and Napa Valley in early December 1997 led to the identification of four major topics for the upcoming workshop, which were summarised as follows in the invitation to participate which was sent to some 70 persons from the IGS and user communities:

Topic 1: The IGS Analysis Products and Consistency of the Combination Solutions

The basic IGS analysis products (orbits, earth orientation parameters, clocks) are of very high quality, and should in general be more accurate and reliable than the solutions obtained by the individual analysis centres (ACs). This session will focus on the current combination process, reporting and feedback, along with possible enhancements in precision, consistency, robustness and results presentation. Furthermore, it should address a need (if any) for additional (global) products in order to meet current and future needs of IGS users.

Topic 2: Orbit Prediction and Rapid Products

The IGS is facing ever increasing demands for more precise and more rapid (real-time!) products. The computation of the rapid orbits and especially the orbit predictions, which are available in real-time, therefore are becoming more important and deserve special attention. This session will focus on ways of improving the quality of the rapid and predicted orbits. The current AC methods of generating the rapid products will be reviewed. The main objective will be the improvement of the (orbit) models and the reduction of turn-around time.

Topic 3: IGS Reference Frame Realization and Contributions to ITRF

The stability of the underlying reference frame defined by the global GPS network has been degrading due to the decrease in quality and availability of some stations of the previously selected group of 13 ITRF stations. More ITRF stations and a new approach to solving this problem is urgently required. The future IGS reference frame realisation should be precise, robust and based on the GNAAC station combinations (G-SINEXes). Furthermore, the IGS reference frame realization should ensure a high product consistency in particular for orbits/EOP and the station coordinate (G-SINEX and P-SINEX) combinations. The new ITRF96 should be discussed in this session.

Topic 4: IGS products for Troposphere and Ionosphere

Global tropospheric and ionospheric information can enhance precision and/or efficiency of various GPS and VLBI solutions (including LEO applications). Additionally it is also required for (global) calibration of ground and satellite based atmospheric (i.e. tropospheric/ionospheric) determination by GPS. A combined IGS solution for tropospheric zenith biases already shows

considerable promise. The IGS global ground network is also allowing progress to be made in development of regional and global ionospheric maps. Of particular interest is the assimilation of such maps into global models which may be based on atmospheric physics and/or on alternative sources of measurement data. The main objective will be to define an operational IGS ionospheric product (or products).

Fifty-one active participants representing institutions in more than a dozen different countries (USA, Canada, Australia, France, UK, Switzerland, Italy, Spain, Norway, Denmark, Belgium, The Netherlands and Germany) contributed through presentation of papers, posters and intensive discussion to the workshop. The Proceedings which are documented in the present volume contain, in addition to introductory material (including the IGS Chairman's Report and the Summary Recommendations of the Workshop), a total of 25 full papers, 4 abstracts and 7 poster summary papers, covering in particular **all** workshop contributions relating to the 4 major topics.

I would like to thank all participants for their active involvement in the workshop, and to the speakers and poster presenters who, by the quality of their contributions during the workshop itself and rapid preparation of their manuscripts afterwards, once again demonstrated the amazing motivation of those involved in the IGS. The "Position Papers" relating to the key topics mentioned above were prepared in a short time and distributed to all participants in advance of the workshop. The authors (T. Springer, J. Zumberge, J. **Kouba**; T. **Martin-Mur**, T. Springer, Y. Bar-Sever; J. **Kouba**, J. Ray, M. Watkins; G. Gendt; J. Feltens, S. **Schaer**), working together by e-mail, made a fundamental contribution to the preparation and to the successful outcome of the workshop.

Thanks are due to the members of the Local Organizing Committee (**Siegmar Pallaschke**, Roberta **Mugellesi** Dow and **Hiltrud Grunewald**) for smooth organisation of the workshop logistics, the reception and visit to the satellite control facilities at **ESOC**, and the workshop dinner at **Jagschloss Kranichstein**.

The Scientific Programme Committee for the 1998 IGS Analysis Centre Workshop consisted of myself (as representative of the host institution), Jan **Kouba** (as IGS Analysis Centre Coordinator from 1994 to 1998) and Tim Springer (as future IGS AC Coordinator). Although we three also appear as editors, I would like to dedicate these proceedings to Jan Kouba with thanks for **his** massive contribution to the IGS analysis efforts since the beginning of the IGS, a contribution which will be difficult to match and will certainly not end with his retirement from Natural Resources Canada.

John M. Dow
ESA/ European Space Operations Centre
Darmstadt

April 1998

TABLE OF CONTENTS

Foreword	iii
<i>J.M. Dow</i>	
Programme of Workshop	1
List of Participants	7
Executive Summary	9
<i>G. Beutler</i>	
Summary Recommendations of the Darmstadt Workshop	19
Recommendation and Action Items of the IGS Governing Board Retreat, Napa Valley, December 12-14 1997	25
<i>I.I. Mueller</i>	
 Topic 1: The IGS Analysis Products and Consistency of the Combination Solutions	
The IGS analysis products and the consistency of the combined solutions	37
<i>T. Springer, J. Zumberge, J. Kouba</i>	
Efficient estimation of precise high-rate GPS clocks	55
(Abstract only)	
<i>J. Zumberge, F. Webb, M. Watkins</i>	
Precise high-rate satellite clocks at GFZ	57
<i>W. Söhne</i>	
The IGS/BIPM time transfer project	65
<i>J. Ray</i>	
 Topic 2: Orbit Prediction and Rapid Products	
Orbit predictions and rapid products	73
<i>T. Martin-Mur, T. Springer, Y. Bar-Sever</i>	
A new solar radiation pressure model for the GPS satellites	89
<i>T. Springer, G. Beutler, M. Rothacher</i>	
New solar radiation pressure models for GPS satellites	107
(Abstract only)	
<i>Y. Bar-Sever, D. Jefferson, L. Remans</i>	

A look at the IGS predicted orbit	109
(Abstract only)	
<i>J. Zumberge</i>	
Real time ephemeris and clock corrections for GPS and GLONASS Satellites	111
<i>M. Romay-Merino, J. Nieto-Recio, J. Cosmen-Shortmann, J. Martin-Piedelobo</i>	
Potential use of orbit predictions and rapid products in the GRAS programme	127
<i>P. Silvestrin</i>	

Topic 3: IGS Reference Frame Realisation and Contributions to ITRF

IGS reference frame realisation	139
<i>J. Kouba, J. Ray, M. Watkins</i>	
ITRF96 and follow-on for 1998	173
<i>C. Boucher, Z. Altamimi, P. Sillard</i>	
IGS reference stations classification based on ITRF96 residual analysis	177
<i>Z. Altamimi</i>	
Estimation of nutation terms using GPS	183
<i>M. Rothacher, G. Beutler</i>	
Globally consistent rigid plate motion: Fiducial-free Euler vector estimation	191
<i>G. Blewitt, R. Kowar, and P. Davies</i>	

Topic 4: IGS Products for Troposphere and Ionosphere

IGS Combination of tropospheric estimates - experience from pilot experiment	205
<i>G. Gendt</i>	
Water vapour from observations of the German Geodetic GPS reference network (GREF)	217
(summary)	
<i>M. Becker, G. Weber, C. Köpken</i>	
Estimating horizontal gradients of tropospheric path delay with a single GPS receiver	223
(Abstract only)	
<i>Y. Bar-Sever, P. Kroger, J. Borjesson</i>	
IGS products for the ionosphere	225
<i>J. Feltens, S. Schaer</i>	
IONEX: The Ionosphere Map EXchange, Format Version 1	233

S. Schaer, W. Gurtner, J. Feltens

The study of the TEC and its irregularities using a regional network
of GPS stations249
R. Warnant

Monitoring the ionosphere over Europe and related ionospheric studies.....265
N. Jakowski, S. Schlüter, A. Jungstand

Routine production of ionospheric TEC maps at ESOC - first results.....273
J. Feltens, J. Dow, T. Martin-Mur, C. Garcia-Martinez, P. Bernedo

Chapman profile approach for 3-D global TEC representation285
J. Feltens

The role of GPS data in ionospheric monitoring, mapping and nowcasting299
R. Leitinger

Mapping and predicting the ionosphere307
S. Schaer, G. Beutler, M. Rothacher

Contributed papers on other topics

Experiences of the BKG in processing GLONASS and combined
GLONASS/GPS observations.....321
H. Habrich

Precise autonomous ephemeris determination for future navigation satellites333
M. Romay-Merino, P. van Niftrik

ARP project: Absolute and relative orbits using GPS347
T. Martin-Mur, C. Garcia-Martinez

Poster Summary Papers

IGS related activities at the Geodetic Survey Division
of Natural Resources Canada353
C. Huot, P Tétreault, Y. Mireault, P. Héroux, R. Ferland, D. Hutchison and J. Kouba

ESA/ESOCIGS Analysis Centre poster summary357
C. Garcia-Martinez, J. Dow, T. Martin-Mur, J. Feltens, P. Bernedo

Recent IGS Analysis Center Activities at JPL.....363
D. Jefferson, Y. Bar-Sever, M. Heflin, M. Watkins, F. Webb, J. Zumberge

A review of GPS related activities at the National Geodetic Survey367

M. Schenewerk, S. Mussman, G. Mader and E. Dutton

U.S. Naval Observatory: Center for rapid service and predictions375
J. Ray, J. Rohde, P. Kammeyer and B. Luzum

The IGS Regional Network Associate Analysis Center for South America at DGFI38 1
W. Seemüller, H. Drewes

The Newcastle Global Network Associate Analysis Centre395
R. Kwar, G. Blewitt and P. Davies

IGS Workshop Dinner, Jagdschloß Kranichstein, Darmstadt.....399

Programme of Workshop

IGS ANALYSIS CENTRE WORKSHOP 1998

Sunday 8 February 1998

16:00 IGS Governing Board (GB) Business Meeting (separate invitation by Central Bureau)

Monday 9 February

08:15 Opening of Workshop registration desk

09:00 Welcome and introduction (J.M. Dow, C. Mazza, G. Beutler)

09:20 I. Mueller: Summary of conclusions of the GB Retreat

Topic 1: The IGS Analysis Products and Consistency of the Combination Solutions (Session chair: J. Kouba, M. Rothacher)

09:40 Position paper by T. Springer, J. Zumberge, J. Kouba

10:00 J. Zumberge: Efficient estimation of precise high-rate GPS clocks

10:15 W. Soehne: Precise high-rate satellite clocks at GFZ

10:30 J. Ray: The IGS/BIPM time transfer project

10:45 Coffee break

11:00 Discussion

12:15 Lunch

Topic 2: Orbit Prediction and Rapid Products (Session chair: T. Springer, J. Dow)

13:30 Position paper by T. Martin-Mur, T. Springer, Y. Bar-Sever

13:50 T. Springer, Y. Bar-Sever: Radiation pressure models for GPS

14:10 J. Zumberge: Identification of mismodelled satellites in the GPS predicted orbit

14:25 M. Romay-Merino: Real-time ephemeris corrections for EGNOS based on the computation of accurate orbit predictions

14:40 P. Silvestrin: The GRAS programme and projected requirements for orbit prediction and rapid products

14:55 Discussion

15:30 Coffee break

15:45 Analysis Centre Poster Session

18:00 Reception with buffet at ESOC

IGS ANALYSIS CENTRE WORKSHOP 1998

Tuesday 10 February

**Topic 3: IGS Reference Frame Realization and Contributions to ITRF
(Session chair: M. Watkins, G. Beutler)**

- 09:00 Position paper by J. Kouba, J. Ray, M. Watkins
- 09:20 C. Boucher, Z. Altamimi, P. Sillard: ITRF96 and follow-on for 1998
- 09:35 Z. Altamimi: IGS reference stations classification based on ITRF96 residual analysis
- 09:50 M. Rothacher: Estimation of nutation from GPS
- 10:05 G. Blewitt, R.S. Kwar, and P.B.H. Davies: Fiducial-Free Euler Vector Solutions from the GNAAC Polyhedron Time Series
- 10:20 Coffee break
- 10:40 Discussion
- 12:00 Lunch

**Topic 4: IGS Products for Troposphere and Ionosphere
(Session chair: G. Gendt, M. Schenewerk)**

- 13:30 Position paper (Troposphere) by G. Gendt
- 13:50 M. Becker, G. Weber: Troposphere model estimated from the data of the German permanent GPS net work GREF
- 14:05 Y. Bar-Sever: Tropospheric gradients - a new IGS product?
- 14:20 Discussion
- 15:00 Coffee break
- 15:20 Position paper (Ionosphere) by S. Schaer, J. Feltens
- 15:40 R. Warnant: The study of the TEC and its irregularities using a regional network of GPS stations
- 15:55 N. Jakowski, S. Schlueter, A. Jungstand: Monitoring the ionosphere over Europe and related ionospheric studies
- 16:10 J. Feltens: Routine production of ionospheric maps and Chapman profile approach for 3-D global TEC representation
- 16:25 R. Leitinger: The role of GPS data in ionospheric monitoring, mapping and nowcasting
- 16:40 S. Schaer: Mapping and predicting the ionosphere
- 16:55 Discussion
- 17:45 End of session
- 20:00 Dinner at Jagdschloss Kranichstein

IGS ANALYSIS CENTRE WORKSHOP 199S

Wednesday 11 February

Contributed papers on other topics
(Session chair: Peng Fang)

- 09:00 Y. Bar-Sever: Low elevation tracking by TurboRogue receivers
- 09:10 Y. Bar-Sever, K. Hurst: Site specific antenna phase center calibrations
- 09:20 H. Habrich: Experiences of the Federal Office for Cartography and Geodesy (BKG) in processing GLONASS and combined GLONASS/GPS observations
- 09:35 M. Romay-Merino: Precise autonomous orbit determination for future navigation satellites without degradation during manoeuvres
- 09:50 T. Martin-Mur, C. Garcia-Martinez: ARP project - absolute and relative orbits using GPS
- 10:05 R. Neilan: Status of GPS modernisation effort in the US, including prospects for additional civilian frequencies
- 10:20 Free slot
- 10:30 Coffee break
- 10:50 Discussion on open AC issues (Facilitators by topic groups: J. Dow, J. Kouba, T. Springer)
- 13:00 End of workshop
- 14:30 Wrap-up Business Meeting (GB/CB members, session coordinators)

IGS ANALYSIS CENTRE WORKSHOP 1998

Posters

1. CODE Analysis poster
2. EMR Analysis poster
3. ESA Analysis poster
4. GFZ Analysis poster
5. JPL Analysis poster
6. NGS Analysis poster
7. SIO Analysis poster
8. USNO Analysis Poster
9. Newcastle GNACC processing/ results
10. GFZ CHAMP poster and S/C model
11. SIRGAS (South America) RNAAC poster

IGS ANALYSIS CENTRE WORKSHOP 1998

List of Participants

Zuheir Altamimi, Institut Geographique National, France
Poul Hoeg Andersen, TERMA (CRI), Denmark
Yoaz Bar-Sever, JPL, USA
Matthias Becker, BKG Frankfurt, Germany
Pelayo Bemedo, ESA/GMV
Gerhard Beutler, Univ. of Bern, Switzerland
Geoff Blewitt, Univ. of Newcastle, UK
Claude Boucher, Institut Geographique National, France
Carine Bruyninx, Royal Observatory of Belgium
Stefano Casotto, Univ. of Padova, Italy
Bill Dillinger, NOAA, USA
John Dow, ESA
Bjom Engen, Statens Kartverk, Norway
Peng Fang, Scripps Institution of Oceanography, USA
Joachim Feltens, ESA/eds
Remi Ferland, Natural Resources Canada
Walter Flury, ESA
Daniel Gambis, Observatoire de Paris, France
Carlos Garcia-Martinez, ESA/GMV
Gerd Gendt, GFZ Potsdam, Germany
Ramesh Govind, AUSLIG, Australia
Heinz Habrich, BKG Frankfurt, Germany
Caroline Huot, Natural Resources Canada
Norbert Jakowski, DLR, Germany
Klaus Kaniuth, DGFI, Germany
Ra'ed Kwar, Univ. of Newcastle, UK
Jan Kouba, Natural Resources Canada
Reinhart Leitinger, Univ. of Graz, Austria
Tomas Martin-Mur, ESA
Carlo Mazza, ESA
Ivan Mueller, Ohio State University, USA
Rolf Muench, ESA
Roberta Mugel lesi Dow, ESA
Ruth Neilan, JPL, USA
Guillermo Ortega, ESA
Siegmar Pallaschke, ESA
Hans Peter Plag, Statens Kartverk, Norway
Mostafa Rabah, TU Darmstadt, Germany
Jim Ray, USNO, USA
Jim Rhode, USNO, USA
Miguel Romay, GMV, Spain
Marita Roth, ESA
Markus Rothacher, Univ. of Bern, Switzerland
Stefan Schaer, Univ. of Bern, Switzerland
Mark Schenewerk, NOAA, USA
Wolfgang Secmueller, DGFI, Germany
Pierluigi Silvestrin, ESA
Wolfgang Soehne, GFZ Potsdam, Germany
Tim Springer, Univ. of Bern, Switzerland
Lambert Wanninger, TU Dresden, Germany
Rene Warnant, Royal Observatory of Belgium
Mike Watkins, JPL, USA
Georg Weber, BKG Frankfurt, Germany, Austria
Pascal Willis, Institut Geographique National, France
Jim Zumbege, JPL, USA

EXECUTIVE SUMMARY¹

G. Beutler

The 1998 IGS Analysis Center Workshop took place 9-11 February 1998 in Darmstadt. In addition, a business meeting of the IGS Governing Board was scheduled for Sunday, February 8, a wrap-up meeting of the Governing Board together with the convenors of the AC Workshop and the authors of the position papers concluded the Darmstadt IGS events. As usual I try to summarize the essential events of the Board meetings and of the workshop.

Governing Board Meetings (February 8 and 11)

IGEX-98

Pascal Willis, chair of the CSTG **Subcommission** on "Precise Satellite Microwave Systems", presented the draft call for participation for the "International GLONASS Experiment (**IGEX**)" to the **IGS** Governing Board. In essence it is proposed to organize a three months GLONASS test campaign by the end of 1998. The Experiment is organized by **CSTG**, it is sponsored by the IGS, the ION, and the **IERS**. The call for participation was prepared by the IGEX steering committee consisting of Pascal Willis (**IGN**, chair), Gerhard Beutler (**AIUB**), Werner Gurtner (**AIUB**), Guenther Hein (**UFAF**), Ruth Neilan (**JPL**), and Jim Slater (**NIMA**).

The draft call for participation consists of two parts, a description of the experiment and the actual call for participation. The IGS involvement is indeed essential: Major parts of the IGS infrastructure (network, data links, data centers) will be used. It is furthermore expected that some of the IGS Analysis Centers will answer the **IGS** Call for Participation.

The Steering Committee of the **IGEX-98** is fostering participation in the 1998 International GLONASS Experiment **IGEX-98** in the following areas:

- **IGEX-98** Coordinating Center
- **IGEX-98** Observing Sites
- **IGEX-98** Data Centers
- **IGEX-98** Analysis Centers
- **IGEX-98** Evaluation Center(s)

All GLONASS satellites are equipped with arrays of LASER reflectors allowing the SLR community to range easily (!) to the GLONASS satellites. It was thus decided to closely coordinate the **IGEX-98** with the SLR

SubCommission of CSTG (Werner Gurtner from the **IGEX-98** steering committee is the "liaison officer" to the SLR **Subcommission**). The participation of the SLR community is essential for validating the results and for the development of radiation pressure models for the GLONASS satellites.

The receiver situation is of concern to the IGS Board members. In principle one would like to use uniquely geodetic-type dual **frequency** combined **GPS/GLONASS** equipment (similarly as it was done for the 1992 IGS Test Campaign). In order to have access to a greater number of

¹Reprint of IGS Mail No. 1806, 17 February 1998.

receivers the steering committee decided to be more flexible: In sequence of preference, the following receiver types may be used in **IGEX-98**:

- Combined dual-frequency GPS/GLONASS receivers
- Dual-frequency GLONASS receivers
- Combined single-frequency (L1) GPS/GLONASS receivers
- Single-frequency GLONASS receivers

Receivers must be collocated with or tied to sites that have well-determined ITRF coordinates. IGS sites are preferable. The **ITRF** coordinates should have an accuracy of 1-5 cm.

Not only the receiver situation, but also the satellite situation has to be considered as a crucial issue. Today, there are only 14 operational GLONASS satellites available, Launches of GLONASS satellites have been announced, however. There is not much that the steering committee can do to improve satellite availability (!). Should the number of operational GLONASS satellites fall under a critical level, the **IGEX-98** would of course have to be postponed.

The schedule for **IGEX-98** is as follows:

February 1998	Distribution of IGEX-98 Call for Participation through mail e-mail services of the sponsoring agencies.
May	Proposals due
June	Evaluation of proposal by the Steering Committee Review/approval of the schedule Designation of the Oversight Committee (including Chair) Campaign Planning Meeting
September 20	Campaign begins
December 20	Campaign ends
early 1999	IGEX-98 Evaluation Workshop (possibly combined with the 1999 IGS Analysis Center Workshop)

The **IGS** Governing Board discussed the proposal in detail. It was finally decided that the Call for Participation should be sent out in February 1998 after a few modifications. The modifications underline the experimental (as opposed to operation oriented) character of **IGEX-98**. The chairman thanked Pascal Willis and the **IGEX-98** steering committee for their planning work.

IGS Densification

At the eighth IGS Governing Board meeting in San Francisco (December 1998) it was decided to take the necessary steps to terminate the Pilot Phase of the Densification Project as soon as possible, but not before all discrepancies, errors, etc., in the understanding of station coordinates (and velocities) were removed (**IGS** Mail Message 1763). This condition could not yet be met. The IGS Central Bureau, together with the IGS Infrastructure Committee are still working on that issue. The basis is the list of discrepancies published regularly by the Analysis Coordinator.

It is the policy of the IGS Governing Board to come up with a unique IGS product of coordinates and station velocities. As all three GNAACS are willing to continue with their

activities one has the problem that a unique series of coordinates has to be formed using the resulting SINEX files of the three SINEX files. Norman Beck, Chief of Active Control System, Natural Resources Canada (NRCan), kindly offered in a letter dated January 19, 1998 to produce the SINEX GNAAC combination, based on the three GNAAC solutions by University of Newcastle, JPL and MIT, The IGS Governing Board unanimously accepted this offer and asked the chairman to thank NRCan for providing this service to the IGS community. NRCan will start providing this combination as soon as possible (probably in March 1998).

As a side issue Norman Beck asked the chairman to explore the IGS Governing Boards views concerning an EUREF-like activity for North America. The discussion revealed that the Board and the GNAACS represented at the business meeting would in fact favour such a development. The EUREF solution, coordinated by Carine Bruyninx, is (amongst other) most useful to eliminate all station-related problems. Also, it makes sure that the solution is actually providing the reference frame for the continent, which is accepted and used by the European topography and geodetic services, The chairman was asked to write a letter to the existing and potential RNAACs in North America encouraging this level of cooperation.

"Densification of the ITRF using GPS" will be again on the agenda of the ninth IGS Governing Board Meeting, to be held end of May 1998 in Boston. I hope (and assume) that the Board will be in a position to decide about the operational phase of the densification issue.

1997 IGS Annual Report

Ruth Neilan and Jim Zumberge came up with a new format for the 1997 IGS Annual Report. They propose to produce the report in two parts (corresponding to 2 volumes). Part 1 would contain, so to speak, the top level information (CB report, IGS Analysis Center Coordinator report, report about current projects, etc.), Part 2 would contain the Analysis Center reports, the station reports, etc. Part 1 would be edited by the Central Bureau in a similar way as it was done with the 1996 Annual Report. Part 2 would be published based on "camera ready manuscripts". In order to reduce the size of the Annual Report, page limits will be given to the authors. Both reports will be made available also in electronic form.

The proposal aims at reducing the costs of the Annual Reports and at having the Annual Report available much earlier.

After extensive discussions and after positive feedback from the Analysis Centers the Board accepted the proposal. The authors of the 1997 Annual Report will be notified concerning the expected contributions in the near future. The Annual report -- if possible both parts, but certainly Part 1 should be available in July 1998.

GPS Modernization Process and IGS Involvement

Ruth Neilan informed the Board that she was asked to chair a working group of the "US GPS Interagency Advisory Council (GIAC)" jointly setup by the U.S. Department of Defence (DoD) and the Department of Transportation (DoT). Ruth Neilan views this assignment as an important interface between the international scientific community represented in the IGS and operators of the GPS.

The IGS Governing Board in turn viewed this as a very positive development and encouraged

the Central Bureau to play a very active role in this working group. The hope was expressed that views of the IGS community on issues like the “second civil frequency” or on the attempt to assign the frequency range 1559-1567 MHz to Mobile Satellite Services (**MSS**) (latest attempt made at the the **WRC-97** in Geneva) could more easily be made known. The **CB** was in particular asked to coordinate efforts in such matters with other organizations like, e.g., the ION.

IGS Retreat, December 1998

At the seventh IGS Governing Board Meeting in Rio de Janeiro it was decided to organize an “IGS Retreat” in December 1997 with the IGS Governing Board Members and a very limited group of IGS Associates with the goal to come up with a plan for the future development of the IGS which then should be discussed by the entire **IGS** community and the Board (IGS Mail Message No 16S3).

About half of the time of the Sunday business meeting of the IGS Governing Board was devoted to the discussion of the “recommendations and action items” of the IGS Governing Board retreat in Napa Valley, December 12-14, 1997. The report was prepared by Ivan I. Mueller, who was also the program chair of the retreat. It was clear that the report could only be discussed at the business meeting; decisions on this matter will be taken at the next official **IGS** Governing Board Meeting (28 May 1998 in Boston). The complete report containing all recommendations and action items may be retrieved by ftp (see attachment). Let me point out that comments on the action items and recommendations are **welcome!**: no decisions have been taken so far, the process may still be influenced till the end of May.

The report contains fourteen recommendations and thirteen action items emerging from them. Let me comment a few of these recommendations and action items.

Recommendation 1 proposes to change the name “International GPS Service for **Geodynamics**” to “International GPS Service”. The acronym “**IGS**” remains the same. The Board is in **favour** of this recommendation.

Recommendation 2 asks the “IGS to produce combined, internally consistent, **global** products”. Product will include in future orbit parameters, station coordinates and velocities, earth rotation parameters, GPS clock corrections, IGS time scale, tropospheric zenith delays, and ionosphere models. Consistency of all products is the central issue, which was also discussed at the workshop (see below). The **IGS/BIPM** Project addresses the time-related issues.

Recommendation 5 asks that “the global IGS Network should be enhanced in the overall sense”. An important (actually **THE** important) action item related to this recommendation is to appoint a Network Manager or Coordinator, within or outside the **CB**.

Recommendation 7 asks for a review of the definition of the terms “IGS Analysis Center”, “Associate Analysis Center” at the Analysis Center Workshop in Darrnstadt.

Recommendation 8 recommends that Working Groups be appointed for “troposphere products”, “ionosphere products”, for “**ITRF densification**”, and possibly for others. The working groups should have clear charters and structures.

Recommendations 9 to 12 are related to the **IGS** Central Bureau. It is in particular recommended that the tasks of the **CB** (as described in the Terms of Reference) are regularly reviewed, that

future tasks **are** clearly defined. Moreover, requirements concerning the minimum number of persons working for the CB were stated.

Recommendation 14 asks the Governing Board to consider forming a committee, with external participation, with the task to prepare the IGS Long Range and Strategic Plan.

The above selection of recommendations and action items emerging from the IGS Retreat 1997 is of course a personal one. Everybody is encouraged to retrieve the complete report.

The Governing Board considers the “recommendations and action items” of the IGS Governing Board retreat in Napa Valley, December 12-14, 1997 as prepared by Ivan I. Mueller as an extremely useful document defining the development of the IGS at least till the end of the millenium (!). The Board thanked Ivan I. Mueller for his excellent work.

1998 IGS Analysis Center Workshop (9-11 February, 1998)

4 topics (see below) were dealt with in detail at the 1998 IGS Analysis Center Workshop. The first presentation within each topic was a position paper, topic 4 even was dealt with in two position papers. AU of the position papers were available over the internet prior to the workshop (**ftp-address**: see attachment). The final versions of the position papers will be available no later than March 15, 1998 under the same ftp-address. These remarks underline how well the workshop was prepared by the programme committee, consisting of **John Dow**, **Jan Kouba**, and **Tim Springer**.

The workshop was formally opened on Monday, February 9 at 9 a.m. with a welcome address by **Carlo Mazza**, Head of Ground Systems Engineering Department of ESA, with an introduction by **John Dow**, and an overview of previous IGS workshops by **Gerhard Beutler**.

Topic 1: The IGS Analysis Products and Consistency of the Combination Solutions (Session Chair: **Jan Kouba, **Markus Rothacher**)**

The position paper entitled “the IGS Analysis Products and the Consistency of the Combined Solutions” written by **T.A. Springer**, **J.F. Zumberge**, and **J. Kouba** reviewed the quality, consistency, and reliability of current IGS analysis products (orbits, Earth orientation parameters, station coordinates, and clocks). The paper focused on current procedures to derive these products, on reporting and feedback. Seven recommendations were given at the end of the paper. All of them were accepted, some will ask for significant work by the IGS Analysis Centers in the near future, As the proceedings of the workshop (containing all position papers and resolutions) should be available rather soon, and as people interested in the resolutions may retrieve preliminary versions of the position papers under the ftp address mentioned, we may confine ourselves to highlight only a few of these resolutions.

First of all it is recommended that the IGS ACS include ephemerides for ALL operational satellites in the daily **SP3-files**, and that these ephemerides are characterized by **MEANINGFUL** accuracy codes. No format changes are necessary for this step, most of the analysis centers already provide such accuracy information. It was also discussed, however, that the user community of IGS products must be made aware of these accuracy codes, and that this community should be strongly encouraged to make use of these codes. This aspect might be more important in future, when more orbit information of “modest quality” will available (due

to this resolution).

Precise single point positioning developed by **Zumberge** et al. is used extensively today. Consistency of orbit and clock information is crucial for this technique, The required consistency level (of millimeters) is much easier to achieve if the same software package is used to produce the global products (orbits and clocks) AND the coordinates using the single point positioning technique. It was/is most encouraging to see that already today, thanks to an essential upgrading of the combination technique, the consistency level for the combined IGS products is not far away from the best possible consistency level that may be reached (using one and the same software). It seems feasible that sub-centimeter point-positioning using IGS products should be possible in the very near future.

Other recommendations dealt with the “densification project”. It was recommended that deadlines in compliance with other deadlines in the IGS are used, that EOP information is included by all analysis centers in the GNAAC solutions, and that all discrepancies/errors in the **RINEX** files are removed.

Also, the minimal requirements (**performance-wise**) to become an IGS Analysis Center were reviewed (and probably clearly defined for the first time). As this recommendation was extensively discussed and modified at the workshop, it is advisable to wait for the final version of this position paper.

There were other interesting contributions in the first session. Jim **Zumberge** presented a technique at JPL to produce in an efficient way high-rate GPS clocks, Wolfgang **Soehne** from GFZ presented the GFZ procedures developed for the same purpose. Jim Ray gave a short status report of the **IGS/BIPM** project: the call for participation was issued in January, the next phase will consist of evaluating the proposals received in spring 1998.

Topic 2: Orbit Prediction and Rapid Products (Session Chair: Tim Springer, John Dow)

Tomas Martin Mur (**ESA**), Tim Springer (**CODE**) and **Yoaz** Bar Sever (**JPL**) reviewed the procedures for “Orbit Prediction and Rapid Products” in the position paper for topic 2. With the increasing demand for close to real-time products this issue becomes more and more important. It came out very clearly that data availability is **THE** critical issue. Global coverage is far more important than the number of stations (provided a minimum number of about **30** stations is available).

The paper also reviewed the prediction techniques used by individual IGS Analysis Centers and in the combination. Usually, IGS predictions are much better than broadcast orbits (the former, when compared to the IGS final orbits are of about 30-50 accuracy (extrapolation over 2 days), the latter are of 2-3 meter accuracy). There are exceptions, however, which are not always predictable. Two measures may improve the reliability of IGS predicted orbits: (a) reduction of the delay of data availability (see primary recommendation below), (b) reduction of the number of “unknown” parameters for prediction process.

New orbit models developed by **Yoaz** Bar-Sever at JPL and by Tim Springer at CODE are promising in area (b). Only improved data transmission may help in area (a): Therefore, the first and probably the primary recommendation of the position paper asks the operational and global data centers to give highest priority to the delivery of stations outside Europe and North America (!). This does not mean, of course, that data from Europe and North America are not important;

but due to the usually excellent infrastructure ftp retrieval guarantees quick availability of a sufficiently high number of stations (data outside these areas often have to be retrieved by the operational centers by telephone or other links).

All in all seven recommendations were given in the position paper for Topic 2. The first three addressed data availability (including more frequent than daily data download), the third recommends extensive tests of the two new radiation pressure models (which are made available by CODE and JPL) by all IGS ACS. The other three resolutions dealt with EOP series to be used with the predictions, studies to improve the accuracy codes for prediction, and the use of the NANU messages to reduce the number of blunders. An important issue, the change of the deadline for the IGS Analysis Centers to deliver the rapid orbits/cops to 4 p.m. U.T. by January 1, 1999 (from 9 p.m. U.T.), was extensively discussed at the workshop. A recommendation related to that topic will be contained in the final version of position paper 2.

The position paper was followed by technical papers related to topic 2: Tim Springer presented his "latest and greatest" radiation pressure model and compared it to the model developed by Bar-Sever. Jim Zumberge addressed the problem of identifying mismodeled satellites in GPS predicted orbits. A presentation by M. Romay-Merino dealt with considerations concerning real-time orbit computation for navigation using orbit predictions of the GPS, GLONASS, etc., in the context of GNSS. A contribution by P. Silvestrin described the GRAS (GPS/GLONASS) receiver being developed by ESA for support of atmospheric sounding and other applications.

Topic 3: IGS Reference Frame Realization and Contribution to ITRF (Session Chair: Mike Watkins, Gerhard Beutler)

The position paper by J. Kouba, J. Ray and M.M. Watkins addressed "IGS Reference Frame Realization" within/by the IGS. It was stated in particular that the current set of 13 ITRF94 stations and the current IGS approach to realize the ITRF are no longer appropriate. A new set of about fifty reference frame stations (based essentially on an IGS history of station coordinates AND the new ITRF96 as made available through the IERS) are about to replace the "old" set of 13 stations. It is expected that this measure will "dramatically" improve the IGS rapid EOPs. This in turn will improve the Bulletin A values of the IERS.

The paper also compares in detail the ITRF96 station positions and velocities with the purely IGS derived quantities for the selected fifty stations (and subsets of it). The agreement is excellent, indeed. It is therefore natural that recommendation 1 demands the IGS to adopt ITRF96 as early as March 1, 1998.

Other recommendations deal with technical aspects of producing the SINEX solutions, like, e.g., the inclusion of EOPs. Last but not least, it is recommended that a "super" combination of G-SINEXes for station coordinates, velocities and EOPS is researched and initiated on behalf of the IGS. The participants of the workshop were very much pleased to learn that NRCAN would take on this new combination task (compare report about GB Meeting, topic "densification").

Very interesting and informative presentations concerning the establishment of ITRF96 followed the position paper. It became quite clear that the IGS is an important contributor to the ITRF. The histograms dealing with coordinate accuracies are interesting, as well. It might be worthwhile to look into the technique specific aspects: it seems in particular that the distribution of SLR-derived height errors supports the conclusion that, due to the unproblematic modeling of the troposphere in SLR, the SLR determined heights may significantly contribute to the height

datum of the ITRF96.

Markus Rothacher et al. summarized their attempts to extract short-period nutation terms from CODE/IGS eop series. Apparently, for periods up to about 20 days, the results obtained by GPS are of equal or better quality than those obtained by VLBI. The work was motivated by the simple idea that “there is no reason NOT to solve for nutation drifts, if one is solving for led-values” ! It is expected that the results can be significantly improved, if a more appropriate orbit model (radiation pressure model) is adopted.

Geoff Blewitt et al. proposed to extract “fiducial-free Euler vectors” from the GNAAC Polyhedron time series. The method presented allows it very well to separate “normal” plate motion (represented through the Euler vectors, resp. their first derivatives) from “abnormal” (e.g., subsidence) or “apparent” (e.g., induced through antenna changes . . .) motion. It might be worthwhile to explore the interest within the IGS and the IERS community for such vectors as a regular IGS product.

Topic 4: IGS Products for Troposphere and Ionosphere (Session Chair: Gerd Gendt, Mark Schenewerk)

Troposphere

The position paper “IGS Combination of Tropospheric Estimates - Experiences from Pilot Project” was presented by Gerd Gendt from the GFZ Analysis Center, GFZ was gaining experience since more than one year of comparing and combining troposphere estimates for about 100 sites of the IGS Global Network stemming from individual IGS Analysis Centers.

Despite the fact that rather different processing options were used by the Analysis Centers (different levels of **differencing**, different binning, different cut-off angles) the consistency level reached is in general quite good. There was general agreement that the combined series of **total** zenith path delays for the entire IGS network are of interest for **climatological** studies. Gerd Gendt recommends furthermore that the troposphere combination product should become an **official IGS** product, that the weekly summary reports are made publicly available (in the IGS report series), and that the product distribution is performed using the ftp server of GFZ.

The IGS troposphere product would be of much greater value, if a significant number of permanent, accurate, reliable surface meteorology measurements series would be available. This is a station specific issue to be addressed by the Central Bureau, the Infrastructure Committee and the future Network Coordinator.

Gerd Gendt’s recommendations were unanimously accepted, We are thus looking forward to see the announcement through **IGS-mail** that official IGS troposphere products are available.

Matthias Becker and Georg Weber from BKG Frankfurt (former **IfAG**) presented a study to use the German permanent GPS network (**GREF**) to extract regional troposphere information on a routine basis. The results are promising and should be seen as an attempt to make optimum use of a permanent network.

Yoaz Bar-Sever discussed troposphere gradient estimates performed at the JPL Analysis Center. He concludes that gradient estimates are significant and tend to improve station coordinate repeatability. The drawback has to be seen in the considerably increased number of parameters. Comparisons of monthly mean values for the JPL gradient parameters with those of the CODE Analysis Center show a good agreement. More work has to be done in this area.

Ionosphere

The position paper "IGS Products for the Ionosphere" was given by **Joachim Feltens** (ESA) and **Stefan Schaer** (CODE). They reviewed the ionosphere related activities within the IGS in previous years and they came up with a list of ten potential participating institutions in a future "IGS ionosphere service". Based on an e-mail inquiry they furthermore gave an overview of analysis methods and models used by the institutions mentioned. An important part of the presentation dealt with the definition of a future IGS ionosphere product. They recommend that all IGS ionosphere products

- must be based on the **IONEX** format,
- should refer to a two-dimensional grid in a (single layer) shell,
- should refer to the same shell height,
- should use identical reference epochs for subsequent ionosphere models,
- that one, maybe two, time resolutions have to be agreed on, and
- that naming conventions for ionosphere model files have to be defined.

The authors and the interested institutions are convinced that the development of an IGS ionosphere product makes sense and that a continuous series of IGS products should be produced at least over one full 11 years cycle of solar activity. It is of particular importance that the IGS models are covering the next period of maximum of solar activity (years 2001-2003). The key recommendation was to establish a pilot phase for such an IGS ionosphere service as soon as possible.

It was most encouraging that the experts in the field of ionosphere physics, in particular Drs. N. Jakowski (DLR **Neustrelitz**), R. Leitinger (TU **Graz**), and R. Warnant (Royal Observatory of Belgium, Brussels), and L. Wanninger (TU Dresden) were attending the workshop to give their input for the development of an IGS product. Their presentations showed that many activities in the ionosphere community are regional in nature -- and that there are good reasons for this. It became clear that the IGS (at least in a first phase) should stay out of regional ionosphere modeling, but should rather focus on global aspects. One had to conclude from the discussions that there is a great interest of the ionosphere community in a continuous series of global IGS ionosphere models.

That the modeling capabilities were **significantly** improved over the last few years emerged from two technical presentations given by Stefan Schaer and by **Joachim Feltens**. The former presentation showed (among other) that the parameters of the CODE models maybe successfully predicted, the latter presentation was also addressing mathematical aspects using a so-called "Chapman profile approach".

In the discussion portion of the session and in the wrap-up meeting at the end of the workshop the following procedure was proposed:

- **Joachim Feltens** and Stefan Schaer, in close cooperation with the existing "IGS ionosphere club", should come up with
- a proposal for global IGS ionosphere products (including the specification of parameters, formats, etc.)
- a clear proposal how to proceed (test phase, pilot phase, etc.)
- a proposal for the structure of the working group (what positions have to be created (e.g., IGS (Associate) Ionosphere Analysis Centers, Ionosphere Combination Center, Validation Center),
- a list of members for the future IGS Ionosphere Working Group.

- These specifications should be included in the final version of their position paper.
- John Dow and **Gerhard Beutler** should
 - draft a general “charter” for setting up Working Groups within the IGS and circulate this draft within the Governing Board,
 - develop in close cooperation with the “ionosphere club” the charter for the ionosphere working group and circulate this draft within the “ionosphere group” (which probably is the nucleus for the working group).
- Assuming that the structure of the ionosphere working group is acceptable to all parties interested in **IGS** ionosphere monitoring, the ionosphere working group should be established by the IGS Governing Board by the end of May 1998 in Boston.

This procedure was unanimously accepted by the IGS Governing Board and the session convenors at the wrap-up meeting on Wednesday, February 11. It should thus be possible to start an IGS pilot ionosphere service in the near future.

The workshop was concluded with a session addressing topics other than those treated in the previous four sessions. Let us mention in particular presentations by T. **Martin-Mur** and C. Garcia-Martinez (absolute and relative orbit determination using spaceborne GPS receiver), Y. Bar-Sever (low elevation tracking of TurboRogue receivers, site specific antenna phase center calibrations), H. Habrich (processing of GLONASS and combined GLONASS/GPS observations), and by Ruth Neilan (GPS modernization effort in the US).

Hospitality experienced in Darmstadt

As one may conclude from the above report, the Darmstadt **IGS** event really was a **WORKshop**. That the IGS Analysis Centers forma very dynamic group of enthusiasts became also clear at the reception on Monday evening and at the dinner at **Jagdschloss Kranichstein**. Despite its name there was no hunting before the dinner, one even had the option of a vegetarian menue (and this in a **Jagdschloss** -- “o tempera, o mores”!).

The Analysis Centers took the opportunity to thank Jan **Kouba** for his personal engagement and his great performance as IGS Analysis Coordinator. A Swiss railway clock presented to him will undoubtedly help him to understand the subtleties of the **IGS/BIPM** project. The clock is also complicated enough (it has at least two buttons and may be used in at least two different ways, e.g., as a pocket clock or as a clock on his desk) to represent a challenge for his technical skills. Jan will continue to serve as IGS Analysis Center Coordinator till the end of 1998. As the next IGS AC Workshop will take place only in 1999, the Darmstadt workshop was presumably the last workshop with Jan **Kouba** “in command” as AC coordinator.

The chairman also took the opportunity at the dinner to express the gratitude of all workshop participants to the **local** organizers from **ESA**, in particular John Dow, his wife Roberta, Siegmarr **Pallaschke**, Rolf Muench, and **Hiltrud** Grunewald for their perfect organization of the 1998 IGS events in Darmstadt,

Gerhard Beutler
Chair, IGS Governing Board

SUMMARY RECOMMENDATIONS OF THE DARMSTADT WORKSHOP

Position Paper 1: The IGS Analysis Products and Consistency of the Combination Solutions

1. Inclusion of all satellites, which were used in the data analysis, with meaningful accuracy codes in the orbit products from all individual ACS. Use of these accuracy codes, or accuracy measures from the long-arc analysis, to identify and consequently downweight “bad” satellites in the orbit combination. In addition the IGS should increase the user awareness of the availability and importance of the accuracy codes in the SP3 files (see also Recommendation 4).
2. Enhancement of clock products. All ACS which submit clocks must also submit clock estimates from a, yet to be determined, subset of “core time stations”! All ACS are urged to submit clock estimates. Furthermore the ACS are encouraged to increase the sampling rate of the satellite clock products to 30 seconds. A format for station and satellite clocks, also suited for 30 seconds satellite clocks, will have to be defined.
3. Improved and automatic feedback to Data Centers (DC) and station managers in case there are discrepancies between **RINEX files** and station logs, data problems and unexpected problems (jumps) in the station coordinate solutions.
4. Create a central place (**WWW**) for feedback and information about the IGS products and their use.
5. **Definition** of minimal requirements for becoming an IGS AC. Any AC must produce all core products, i.e. orbits, **EOPs**, and **SINEX**, both on time and with sufficient (high) quality. The IGS terms of reference will be changed accordingly,
6. Additional accuracy digit for the **IERS/IGS EOP file** format. New format to be defined before June 28, 1998 by Jan **Kouba** in cooperation with Dennis McCarthy.

Position Paper 2: Orbit Prediction and Rapid Products

- 1, Ask the Operational, Regional and Global Data Centers to give the highest priority to the prompt retrieval and distribution of data from sites outside Europe and North America.
2. Ask the Operational, Regional and Global Data Centers to investigate and implement ways of reducing data retrieval and distribution delays.
3. Ask the Operational, Regional and Global Data Centers to study and implement more frequent down-loading of the data.
4. Ask those Analysis Centers that are evaluating more precise radiation pressure models to make them publicly available, and encourage all Analysis Centers to implement and use them when they have been validated.

5. Ask the IERS Rapid Service and the Analysis Centers to investigate and propose ways to obtain predicted cops (pole and UT1) for use in the calculation of IGS predicted orbits.
6. Ask the Analysis Centers and the AC Coordinator to study, monitor, and, if possible, improve the fitness of the accuracy codes for the predicted orbits.
7. Ask the **Analysis** Centers to investigate the ways and the consequences of reducing the turn-around time for rapid and predicted products.
8. Review data and rapid product delivery times at July 1 and October 1 in order to evaluate the change of the deadline for rapid products to no later than 16:00 UTC by January 31999.

Position Paper 3: IGS Reference Frame realisation and Contributions to ITRF

In order to increase the IGS product consistency and to prepare ground for adaptation of the new approach of ITRF realizations, the following recommendations were accepted by the workshop participants:

1. That IGS adopts **ITRF96** as early as March 1, 1998 to replace the currently ailing and problematic IGS realization of **ITRF94**, which currently is based only on less than 13 ITRF stations.
2. As an interim measure and to facilitate an immediate ITRF realization improvement it is recommended that the selection of the new **ITRF96** station positions and velocities for a large subset of the RF station is finalized at this workshop. This newly selected **ITRF96** set of the 47 globally distributed IGS stations is to be used for **ITRF96** realization in all IGS products beginning as early as March 1, 1998. IGS realization of **ITRF** is then accomplished by the above **ITRF96** station coordinates/velocities together with the current official **igs.snx**, which contains antenna offset and height information in the **SINEX** format.
3. That all weekly submitted AC **SINEX** solutions (**A-SINEXes**) contain the EOP of the current week and that the submitted AC orbits/clocks (**sp3**) and EOP (**erp**) files are consistent with the above **A-SINEX** solutions. This is essential not only for the increased **IGS** product consistency but also for the future (improved) ITRF realization and IGS products. It is recommended that this is implemented and ensured by all ACS by June 28, 1998.
4. That the **GNAAC** combinations retain (and adjust) the submitted AC EOP information of the current week in their G- **SINEX** combined products, along with the usual station position solutions. It is recommended to be implemented by June 28, 1998.
5. The **SINEX** extensions as outlined in the Appendix IV, allowing the minimum datum and transformation parameter constraints to be coded in the **SINEX** format, are accepted and used by **IGS** on or before March 1, 1998. Furthermore, that IGS submits the **SINEX** extension for acceptance to Prof. Tom Herring of CSTG, who is currently responsible for the **SINEX** format. This will provide a means and encouragement to ACS and other IGS users to use (minimum) datum constraints, as well as it allow an efficient and safe monitoring of geocenter and scale changes (e.g. Ray, 1997). It is further recommended that only the AC Final products, which are based on minimum or no datum constraints, be accepted for the IGS Final orbit/clock/EOP/station combinations after June 28, 1998.

6. That a (super) combination of G-SINEXes for station coordinates and EOP is researched and initiated on behalf of IGS. This EOP (**G-SINEX** combination) cumulative solution would replace the current IGS EOP combination and it would lead to an official **SINEX** station solution product (both for global as well as the polyhedron stations). The polyhedron **SINEX** solutions could be produced by back substitution when P-SINEXes are made available to produce the IGS **P-SINEX** products (station positions/velocities only). The implementation goal should also be by June 28, with the official IGS **SINEX** (G and P) products on or before January 3, 1999 !

Position Paper 4a: IGS Products for the Troposphere

1. The pilot phase for the IGS Combined Tropospheric Estimates **will** be finished and the combined zenith path delay (**ZPD**) estimates will become an official product. The conversion into **precipitable** water vapor will be postponed until a sufficient number of surface met packages is available. At the moment it is to the customer to convert the ZPD by relying both on the existing **RINEX** met files as well as on interpolation within global or regional meteorological fields. The product will be archived at the global Data Centers.

2. All network operators will be encouraged to enforce the installation of met packages.

3. The Analysis Centers should strive to constrain the RF stations during the computation of the tropospheric estimates to reduce the biases in the ZPD estimates as much as possible.

4. *All* Analysis Centers provide **TRO-SINEX** files which are compatible to the weekly **SINEX file**, i.e. the daily station coordinates of the TRO-SINEX files should refer to the site description blocks given in the weekly **SINEX** file.

5. IGS will strive to get water vapor estimates from collocated water vapor radiometer and **VLBI**. During a calibration campaign all Analysis Centers will be asked to include those sites in their analysis for investigation of the biases in the ZPD estimates.

6. For each **SINEX file** the shortened version ***.ssc** without all matrices **should** be **archieved** too. The **ssc-files** should be formed at the Data Centers unless the ACS already submit both ***.snx** and ***.ssc**. This way also ***.ssc** versions for all the old **SINEX** files can be formed.

Paper 4b: IGS Products for the Ionosphere

1. Initially, the IGS should focus on two kinds of products:

- (a) TEC maps in grid form and
- (b) differential code biases (**DCBs**).

2. IGS TEC maps are global maps. Only global maps will be compared and perhaps combined, This policy may be reviewed after one year of pilot operations.

3. **All TEC** maps must be delivered to the IGS in the **IONEX** format [Schaer et al., 1998]. TEC maps delivered to the IGS thus are “snapshots” of the electron density referring to a particular epoch and to an earth-fixed reference frame.

4. Global **TEC** maps from each contributing Analysis Center are given the name **cccGddd0.yyI**,

where ccc is a 3-figure acronym for the AC (in uppercase), “G” says that this file contains global maps, ddd is the day of the year, “O” indicates a daily file, yy specifies the 2-digit year, and the last letter “T” stands for “ionosphere maps”. Example: CODGO41O.98I (or CODGO41O.98I.Z). These files are {compressed} and sent to the IGS Global Data Centers and are available to the interested user. Access Fortran routines are also made available.

5. The daily **IONEX** file, as produced by an IGS Analysis Center, should have a 2-hour resolution referring to the epochs 01, 03, 23 hours UT. RMS files corresponding to the 2-hourly TEC maps maybe included in the **IONEX** files. **TEC/RMS** maps refer to a two-dimensional grid in a single layer, The height of the single layer should be 450 km adopting a base radius of 6371 km. The latitude ranges from 87.5 to -87.5 degrees in steps of 2.5 degrees; the longitude ranges from -180 to 180 degrees in steps of 5 degrees. **TEC/RMS** values have to be given in units of 0.1 **TECU**.

6. Daily sets of differential code biases (**DCBs**) for the GPS satellites are recommended to be included in **IONEX files**. The exchange of satellite-specific DCBS is IONBX-supported, too. Note that the DCB reference maybe chosen arbitrarily and can be taken into account in the combination procedure.

Annex

IGS Fiducials for ITRF Reference Frame Control, ITRF96 47 stations, Darmstadt AC workshop, Topic 3, Rec. #2

id	City	Location	lon (E)	lat (N)	ht (m)	Agency
algo	Algonquin Park, Ontario	Canada	-78.0714	45.9558	201.9000	NRCan/GSD
areq	Arequipa	Peru	-71.4928	-16.4655	2489.9506	NASA/JPL
braz	Brasilia	Brazil	-47.8779	-15.9475	1107.0570	IBGE-JPL
brmu	Bermuda	Bermuda Islands	-64.6963	32.3704	-10.6158	NOAA
davl	Davis	Antarctica	77.9726	-68.5773	45.4584	AUSLIG
drao	Penticton	Canada	-119.6250	49.3226	542.8755	NRCan/GSC
fair	Fairbanks, AK	USA	-147.4990	64.9780	320.0126	JPL-GSFC
fort	Fortaleza	Brazil	-38.4256	-3.8774	20.4850	NOAA
gode	Greenbelt, MD	USA	-76.8268	39.0217	15.5186	NASA/GSFC
gol2	Goldstone, CA	USA	-116.8890	35.4252	987.6665	NASA/JPL
graz	Graz	Austria	15.4935	47.0671	539.3059	I SR
guam	Dededo	Guam	144.8684	13.5893	202.9268	NASA/JPL
hark	Pretoria	South Africa	27.7077	-25.8871	1555.0000	CNES
hob2	Hobart, Tasmania	Australia	147.4387	-42.8047	42.0872	AUSLIG
irkt	Irkutsk	Russia	104.3162	52.2190	503.3754	DUT
kerg	Port aux Francais	Kerguelen Islands	70.2555	-49.3515	74.0583	CNES
kit3	Kitab	Uzbekistan	66.8854	39.1348	623.5264	GFZ
kokb	Kokee Park, HI	USA	-159.6650	22.1263	1168.3669	NASA/JPL
kosg	Kootwijk	The Netherlands	5.8096	52.1784	97.8582	DUT
kour	Kourou	French Guiana	-52.8060	5.2522	-24.7597	E SA
kwj1	Kwajalein Atoll	Kwajalein Atoll	167.7302	8.7222	39.2028	NASA/JPL
lhas	Lhasa	China	91.1040	29.6573	3625.6824	I fAG
mac1	MacQuarie Island	Australia	158.9358	-54.4995	-5.7467	AUSLIG
mad2	Robledo	Spain	-4.2497	40.4292	830.4708	NASA/JPL
mali	Malindi	Kenya	40.1944	-2.9959	-22.3241	ESA
mas1	Maspalomas	Spain	-15.6333	27.7637	198.1606	E SA
mate	Matera	Italy	16.7045	40.6491	536.6528	ASI
mdo1	Fort Davis, TX	USA	-104.0150	30.6805	2005.4936	NASA/JPL
nlib	North Liberty, IA	USA	-91.5749	41.7716	208.0427	NASA/JPL
nyal	Ny Alesund	Norway	11.8651	78.9296	79.4598	NMA
ohig	O'Higgins	Antarctica	-57.9003	-63.3207	31.6952	I fAG
onsa	Onsala	Sweden	11.9255	57.3953	46.5782	OsO
pert	Perth	Australia	115.8852	-31.8020	13.7867	ESA
piel	Pie Town, NM	USA	-108.1190	34.3015	2348.7138	NASA/JPL
pot s	Potsdam	Germany	13.0661	52.3793	145.4281	GFZ
sant	Santiago	Chile	-70.6686	-33.1503	724.0539	NASA/JPL
shao	Sheshan	China	121.2004	31.0996	23.0701	SAO-JPL
thul	Thule	Greenland	-68.7880	76.5373	56.0093	KMS-JPL
tid2	Tidbinbilla	Australia	148.9800	-35.3992	666.3630	NASA/JPL
t rom	Tromsø	Norway	18.9383	69.6627	133.4530	NMA
tskb	Tsukuba	Japan	140.0875	36.1057	68.2591	GSI
vill	Villafranca	Spain	-3.9520	40.4436	648.3720	ESA
wes2	Westford, MA	USA	-71.4933	42.6133	86.0138	NOAA
wtzr	Koetzing	Germany	12.8789	49.1442	667.0379	I fAG
yar1	Yaragadee	Australia	115.3470	-29.0466	242.3113	NASA/JPL
yell	Yellowknife, NW Terr.	Canada	-114.4810	62.4809	181.8642	NRCan/GSD
zwen	Zwenigorod	Russia	36.7586	55.6993	206.0122	GFZ

RECOMMENDATIONS AND ACTION ITEMS
IGS Governing Board Retreat
Napa Valley, December 12-14,1997

Ivan L Mueller

One of the conclusions of the Retreat has been that the IGS Terms of Reference (January 1996 version), with some "fine tuning", still reflects the current needs. For this reason and also to provide a framework for the Retreat's Recommendations (**Rs**) and Action Items (**As**) relevant portions of the terms are reproduced below, between dotted lines, with the **Rs** and **As** inserted at the appropriate locations.

In order to keep the Retreat as conducive for open discussion as possible formal Minutes were not kept. A short **handS/informal** record suitable to jog the memories of the participants is available from the Central Bureau.

The Recommendations/Action Items and the explanatory text as presented below are based on the final summary discussion of the Retreat Coordinators on December 14, 1998, on correspondence and conversations after the Retreat.

INTERNATIONAL GPS SERVICE FOR GEODYNAMICS
TERMS OF REFERENCE

The term "Geodynamics" in the name of IGS, at its inception, was meant to indicate that the primary users of the service are scientists involved in geodynamics, specifically using GPS for determining and/or monitoring positions on the surface of the Earth with the highest accuracy. Since other types of users (especially from the atmospheric and oceanic science communities) are appearing on the horizon the suggestion was made to eliminate the term "Geodynamics" from the title of IGS.

- **R 1:** The name of the Service be the "International GPS Service".
 - **AI:** Governing Board (**GB**) needs to consider **R1** and vote.
-

The primary objective of the IGS is to provide a service to support, through GPS data products, geodetic and geophysical research activities. Cognizant of the immense growth in GPS applications the secondary objective of the IGS is to support a broad spectrum of operational activities performed by governmental or selected commercial organizations. The Service also develops the necessary standards/specifications and encourages international adherence to its conventions.

IGS collects, archives and distributes GPS observation data sets of sufficient accuracy to satisfy the objectives of a wide range of applications and experimentation. These data sets are used by the IGS to generate the following data products:

- **high accuracy GPS satellite ephemerides**
- **earth rotation parameters**

- **coordinates and velocities of the IGS tracking stations**
- **GPS satellite and tracking station clock information**
- **ionospheric information**
- **tropospheric information.**

The accuracies of these products are sufficient to support current scientific objectives including:

- **realization of global accessibility to and the improvement of the International Terrestrial Reference Frame (ITRF)**
- **monitoring deformations of the solid earth**
- **monitoring earth rotation**
- **monitoring variations in the liquid earth (sea level, ice-sheets, etc.)**
- **scientific satellite orbit determinations**
- **ionosphere monitoring**
- **climatological research, eventually weather prediction.**

In the past the IGS combined products used primarily have been those related to the **IGS Reference Frames**, both terrestrial and inertial, recommended for GPS users. These are the station coordinates with their variations in time (defining the terrestrial frame) and the orbits of GPS satellites (defining the inertial frame), and the transformation parameters relating the two (the earth-rotation parameters). There have been some questions as to the internal consistencies of the above products.

Due to user requirements for using the GPS signals in various efficient modes and/or leading to more accurate results, it appears necessary for **IGS** to produce combined, timely and consistent additional products, specifically GPS clock corrections, possibly an **IGS** time scale, tropospheric zenith biases and global and possibly regional ionosphere models. **These**, together with the reference **frames** (all based on the IERS Conventions, 1996), constitute the **IGS Reference System** assuring consistency for all GPS users of positioning in all modes.

Although non-positioning GPS user requirements are not clear at this time, it appears that there is (or will be in the near future) an increasing demand for rapid (real-time) and more accurate GPS orbits as well as the satellites in the IGS framework (primarily the GLONASS and LEO satellites).

- **R2: IGS** is to produce combined, internally consistent, global products based on GPS observations as follows (several of these to a fair extent are already accomplished):
 - a) station coordinates and velocities (incl. **IGS SINEX** products)
 - b) orbital parameters
 - c) earth rotation parameters
 - d) GPS clock corrections
 - e) **IGS** time scale
 - f) tropospheric zenith delays
 - g) ionosphere models
- **A2.1: The Analysis Center Workshop in Darmstadt** should address the issues a) - d) and f) and g) and make recommendations.
- **A2.2** The recently established **IGS-BIPM Pilot Project** should address issue e) as already decided by the GB.

- R3: IGS should continue producing accurate orbits based on rapid and/or high rate data, investigate new requirements (e.g., for real time meteorology forecasting a twenty-station network providing 30s data down loaded every 6-12 hours is suggested. For LEO see A4.2 below) and suggest and implement improvements in availability (IGR) and precision (IGP).
- A3: The Analysis Center Workshop in Darmstadt should address this issue and make recommendations.
- R4: IGS should support the tracking of GLONASS and LEO satellites.
- **A4.1:** The GB should support tracking of GLONASS satellites by actively promoting within IGS the International GLONASS Experiment (IGEX), currently scheduled Sep. -Dec., 1998, pending on the discussion on GLONASS at the GB business meeting in Darmstadt.
- A4.2: The LEO Working Group should continue its work (in collaboration with various groups involved in the use of LEOS for atmospheric science). Specific recommendations are to be made on the appropriate number of tracking stations and sampling rate (1 -5s?) and on the feasibility of IGS processing of occultation and/or other flight data.

The IGS accomplishes its mission through the following components:

- **networks of tracking stations**
- **data centers**
- **Analysis and Associate Analysis Centers**
- **Analysis Coordinator**
- **Central Bureau**
- **Governing Board.**

NETWORKS OF TRACKING STATIONS

IGS Stations provide continuous tracking using high accuracy receivers and have data transmission facilities allowing for a rapid (at least daily) data transmission to the data centers (see below). The stations have to meet requirements which are specified in a separate document. The tracking data of IGS stations are regularly and continuously analyzed by at least one IGS Analysis Center or IGS Associate Analysis Center

IGS Stations which are analyzed by at least three IGS Analysis Centers for the purpose of orbit generation, where at least one of the Analysis Centers lies on a different continent than the station considered, are in addition called IGS Global Stations.

All IGS stations are qualified as reference stations for regional GPS analyses. The ensemble of the IGS stations forms the IGS network (polyhedron).

The IGS global network needs an overall enhancement. The IGS Infrastructure Committee is involved considering issues related to the existing network e.g., instrumentation, monumentation, reporting, performance, data communication and flow, quality control,

archiving, site and **RINEX** standards. Plans for a coordinated systematic effort to **expand/densify** the network to the proposed (about 200 stations) Polyhedron is still lacking, On the other hand, the regional densification efforts are progressing, and limits are to be set up as to the inclusion of the regional stations into the IGS Polyhedron (being pro-active at the same time). Use of the network for climatology would also require the installation of high stability accurate barometers.

- R5: The global IGS Network should be enhanced in the overall sense.
- **A5.1:** The IGS Infrastructure Committee is to continue its work and report to the GB at its next regular meeting in Boston.
- **A5.2:** The GB should consider appointing a Network Manager/ Coordinator, within or outside the CB, to coordinate a systematic effort to complete the IGS Polyhedron. The responsibility would include the formulation of network standards and checking performance.
- **A5.3:** The **CB/GB** should make a systematic and concerted effort to request stations to install high stability/accuracy barometers (the alternative of using routinely produced atmospheric pressure grids should be explored, although their availability in near real time might be a challenge).
- **A5.4:** The GB should consider organizing an **IGS Network Workshop** to have an open discussion on network/station issues and to develop a direct interaction between the GB and the stations, upon which rest all IGS activities.

DATA CENTERS

The data centers required fall into three categories: Operational, Regional, and Global Data Centers

The Global Data Centers are the main interfaces to the Analysis Centers and the outside user community. Their primary tasks include the following:

- **receive/retrieve, archive and provide on line access to tracking data received from the Operational/Regional Data Centers**
- **provide on-line access to ancillary information, such as site information, occupation histories, etc.,**
- **receive/retrieve, archive and provide on-line access to IGS products received from the Analysis Centers**
- **backup and secure IGS data and products.**

It was noted that, with the exception of **CDDIS** (which is doing an admirable job), not all Global Data Centers are producing regularly their Access Reports, In view of the importance of keeping track of the users of IGS products it is recommended that such reports be published on a regular basis.

- R6: It is recommended that all Global Data Centers publish Access Reports on a monthly basis.
- **A6:** The **CB** is to contact the relevant Global Data Centers and encourage them to comply with R6.

ANALYSIS CENTERS

The analysis centers fall into two categories: Analysis Centers and Associate Analysis Centers.

The Analysis Centers receive and process tracking data from one or more data centers for the purpose of producing IGS products. The Analysis Centers are committed to produce daily products, without interruption, and at a specified time lag to meet IGS requirements. The products are delivered to the Global Data Centers and to the IERS (as per bilateral agreements), and to other bodies, using designated standards.

The Analysis Centers provide as a minimum, ephemeris information and earth rotation parameters on a weekly basis, as well as other products, such as coordinates, on a quarterly basis. The Analysis Centers forward their products to the Global Data Centers.

Associate Analysis Centers are organizations that produce unique products, e.g., ionospheric information or Fiducial Station coordinates and velocities within a certain geographic region. Organizations with the desire of becoming Analysis Centers may also be designated as Associate Analysis Centers by the Governing Board until they are ready for full scale operation.

- **R7:** Depending on the outcome of the Analysis Center Workshop in Darmstadt the above descriptions of the Analysis and Associate Analysis Centers should be reviewed. The GB decisions in San Francisco/Napa Valley re. the GNAACs/RNAACs, may also have an effect.
- **A7:** The AC Coordinator together with the Chair of the Densification Project recommend the necessary changes to the Terms of Reference as per R7, if necessary.

ANALYSIS COORDINATOR

The Analysis Centers are assisted by the Analysis Coordinator.

The responsibility of the Analysis Coordinator is to monitor the Analysis Centers activities to ensure that the IGS objectives are carried out. Specific expectations include quality control, performance evaluation, and continued development of appropriate analysis standards. The Analysis Coordinator is also responsible for the appropriate combination of the Analysis Centers products into a single set of products. As a minimum a single IGS ephemeris for each GPS satellite is to be produced. In addition, IERS will produce ITRF station coordinates/velocities and earth rotation parameters to be used with the IGS orbits.

The Analysis Coordinator is to fully interact with the Central Bureau and the IERS. Generally the responsibilities for the Analysis Coordinator shall rotate between the Analysis Centers with appointments and terms specified by the Governing Board.

In view of R2 above, the present Analysis Coordinator's role will be significantly expanded and

it is unlikely that a single person (or organization) will be able to handle the responsibilities related to all the different combined global products now contemplated. There is also a question of coordinating the regional **densification** projects (connected to the Polyhedron) in some central way. One of the responsibilities here would also be the education of users on how to use IGS products.

- R8: It is recommended that Working Groups be appointed for **Tropospheric Products**, for **Ionospheric Products**, for **ITRF Densification** and possibly others (pending on the recommendations of the Analysis Center Workshop in Darmstadt). The Analysis Center Coordinator should be an **ex-officio** member of all Working Groups. The alternative of appointing individual “Coordinators” for each application (instead of the Working Groups) may also be considered.
- **A8.1:** Based on the recommendations of the Darmstadt Analysis Workshop, the GB should appoint new Working Groups or Coordinators as per R8 and clarify their relationship/interaction (reporting requirements, etc.) with the CB and the GB.
- **A8.2:** The concept of Working Groups or additional Coordinators, together with their responsibilities and reporting/interaction requirements should be incorporated in the Terms of Reference.

CENTRAL BUREAU

The Central Bureau (CB) is responsible for the general management of the IGS consistent with the directives and policies set by the Governing Board. The primary functions of the CB are to facilitate communications, coordinate IGS activities, establish and promote compliance to IGS network standards, monitor network operations and quality assurance of data, maintain documentation, and organize reports, meetings and workshops, and insure the compatibility of IGS and IERS by continuous interfacing with the IERS. To accomplish these tasks the CB fully interacts with the independent Analysis Coordinator described above.

Although the Chairperson of the Governing Board is the official representative of the IGS at external organizations, the CB, consonant with the directives established by the Governing Board, is responsible for the day-to-day liaison with such organizations

The CB coordinates and publishes all documents required for the satisfactory planning and operation of the Service, including standards/specifications regarding the performance, functionality and configuration requirements of all elements of the Service including user interface functions.

The CB operates the communication center for the IGS. It maintains a hierarchy of documents and reports, both hard copy and electronic, including network information, standards, newsletters, electronic bulletin board, directories, summaries of IGS performance and products, and an Annual Report,

In summary, the Central Bureau performs primarily a long term coordination and communication role to ensure that IGS participants contribute to the Service in a consistent and continuous manner and adhere to IGS standards.

The Central Bureau has performed well, especially in the areas of coordinating the network and communication. However, partly due to the rapid expansion of IGS over the past several years, other **CB** tasks described in the Terms of Reference either had to be farmed out to persons(usually volunteers) outside the CB, contracted to other organizations (e.g., UNAVCO) or neglected.

In addition to the rapid expansion of IGS, the other major difficulty the **CB** is facing when trying to fulfill its responsibilities is primarily structural/ organizational in nature. Although it is difficult to assess the situation from the outside, it seems evident that partly due to the fact that probably no single person has full time responsibility within the CB, every one is “spread too thin” and fragmented. The Director of the **CB** has at least three jobs and it appears that only one person reports to her (the liaison to UNAVCO). The UNAVCO contract to help with the network involves one staff position spread out over six persons. Others working for the CB, instead of reporting to the Director, in fact report to one of JPLUS Group Supervisors, who **inturn** reports to certain Section/Division heads, not directly in charge of the Director of the CB. It appears that such a structure (although maybe efficient for other purposes), combined with the fragmentation of individual responsibilities, lead to difficulties in meeting JPLUS original commitment to IGS and in some cases even to conflicts of interests within JPL.

- **R9:** It is recommended that the tasks of the CB as described in the Terms of Reference be reviewed and the future tasks of the CB clearly defined, with the **Rleft-overS** responsibilities appropriately assigned to organizations or individuals outside the CB, which will closely interact with the CB.
- **R10:** It is recommended that the host organization of the CB review and streamline the CB organization, with fragmentation reduced to a minimum and lines of reporting and responsibilities clearly defined.
- **R 11:** It is also recommended that at least two persons should be given full time responsibility within the CB. One of these should be the Director, the other may be the Network Coordinator (see **A5.2** above).
- **R 12:** It is recommended that, provided that the recommendation for the additional Coordinators are adopted (see R8 above), their interaction with the CB be clearly defined.
- **A9:** The Director of the CB should discuss **R9- 11** with the appropriate officials of the host organization and present a plan to eliminate the above difficulties to the GB and the progress at its next regular meeting in Boston.
- **A 10:** The GB should appoint a small sub-committee to work with the Director of the **CB** to accomplish R9 and R12.
- **A1 1:** The Central Bureau section of the Terms of Reference will have to be modified after the fact.

GOVERNING BOARD

The Governing Board (GB) consists of fifteen members. They are distributed as follows:

Elected by IGS Associates (see below):

Analysis Centers' representatives	3
Data centers' representative	1
Networks' representatives	2

Elected by the Governing Board upon recommendations from the Central Bureau, for the next term:

Representatives of Analysis, Data Centers or Networks	2
Members at large	2

Appointed members:

Director of the Central Bureau	1
Representative of the IERS	1
IGS representative to the IERS	1
IAG/FAGS representative	1
President of IAG Sect. II or Com.VIII (CSTG)	1

Total 15

The appointed members are considered *ex officio* and are not subject to institutional restrictions. The other ten persons must be members of different organizations and are nominated for each position by the IGS components they represent as listed above (six persons) , or by the Central Bureau (four persons) for a staggered four year term renewable once. The GB membership should be properly balanced with regard to supporting organizations as well as to geography.

The election for each position is by the number of nominations received from the relevant IGS component, i.e., from the networks (for this purpose organizations operating two or more Global Stations are considered a network), from the Analysis Centers and from the Data Centers. In case of a tie, the election is by the members of the Governing Board and the IGS Associate Members (see below) by a simple majority of votes received. The election will be conducted by a nominating committee of three members, the chair of which will be appointed by the Chair of the IGS Governing Board...

The IAG / FAGS representative is appointed by the IAG Bureau (or by FAGS) for a maximum of two four-year terms...

The secretariat of the GB is provided by the Central Bureau...

The experience of the past several years indicate that the nomination procedure for both groups of elected GB members, i.e., those nominated by the IGS Associates and those by the CB may be improved to assure wider participation in the nomination process. In addition, it has been suggested to include all (or most) Coordinators in the deliberations of the GB. The appointed representation of IAG and FAGS on the GB needs clarification as well.

- **A1 2:** The GB should appoint a sub-committee to review the current nomination/appointment procedures for GB membership and to recommend improvements by the end of 199S.
-

Additional Recommendations/Action Items:

- **A13:** Periodic performance review requirement for each IGS component be incorporated in the Terms of Reference. The GB is to set up procedures for such regular reviews (how often and how?) and for the follow up of the recommendations (whether positive or negative).
- **R13:** The GB should consider forming an Advisory Committee for Commercialization of IGS products. The Committee should include representatives of organizations experienced in such ventures, e.g., WMO, UCAR/NCAR, IRIS, ESA (its business arm).
- **R14:** The GB should consider forming a committee, with external participation, with the task to prepare the IGS Long Range and Strategic Plan. Reporting should be at the IAG General Assembly in 1999.

(January 31, 1998)

**Topic 1: The IGS Analysis Products and Consistency of
the Combination Solutions**

The IGS Analysis Products and the Consistency of the Combined Solutions

T.A. Springer, J.F. Zumberge, J. Kouba

Abstract

The basic IGS analysis products (orbits, Earth orientation parameters, station coordinates, and clocks) are of very high quality, and should in general be more reliable and at least as accurate (if not more so) than the solutions obtained by the individual analysis centers (**ACs**). This position paper focuses on the current combination procedures, reporting and feedback. Possible enhancements in precision, consistency, robustness, presentation and feedback of the results are discussed. Furthermore, it addresses a need for additional products in order to meet the needs of IGS users.

Introduction

Many different combination activities are going on within the IGS. Ideally every AC would provide just one single file each day containing all estimated parameters, including orbit, Earth orientation parameters (**EOPs**), clocks, coordinates, and troposphere estimates together with their **full covariance** matrix. These solutions could then be rigorously combined in one single combination scheme! Of course this is not feasible for many reasons at this time; one obvious reason being the different models which are used. Another is that results **from** different ACS are not likely to be independent, since they are based on datasets which are largely common.

Therefore different combination activities were initiated by the **IGS** over the last years. The orbit combination, the first and most **well** known **IGS** combination, has played a major **part in the** improvement of the **IGS** products and has been the key to the overall success of the **IGS**. Based on its success other combinations have been initiated including the EOP, clock, and station coordinate combinations by the GNAACS (in the framework of the **densification** project), and the troposphere combinations by Gerd **Gendt** at **GFZ**. Currently others are planned like combination of station clock estimates, (in the framework of the time-transfer project), and ionosphere estimates.

Due to the diversity of the combination activities and consequently the different methods

used, the consistency between **all** these IGS combined products is not (automatically) guaranteed. The complete decoupling of the orbit- and coordinate-combinations can lead to some problems. The resulting **IGS-coordinates**, which essentially represent the IGS reference frame, are not necessarily compatible with the **IGS-orbits** and **EOPs**. Furthermore the feedback to the AC's and other users of **IGS** products, coming from the different combinations, has very different levels of quality and usefulness. Some reports are very good and extensive whereas others give practically no information. The different combinations and resulting products also make it very difficult for "outsiders" to get and keep a good overview of the IGS activities and developments. It is even hard for those within the **IGS** to keep track of all activities and to find the necessary information!

In this position paper we critically review all different combination activities which are currently performed within the IGS. We review the:

- combination procedures which are currently used,
- consistency of the products within a combination (e.g. orbits, **EOPs**, and clocks),
- consistency of the products between different combinations (e.g. orbits, EOPS, clocks, and **Sinex**),
- feedback **from** the different combinations, and
- ways of improving any of the above.

One other aspect of the IGS which is discussed here will be the quality control of the data from all the IGS stations! Although the observational data in the **Rinex** format is one of the most important **IGS** products, if not **the** most important, the IGS has not been very successful in setting up and maintaining a standard for IGS stations.

IGS Combination Activities

Currently the following combination activities are performed within the IGS:

- Combinations by the IGS Analysis Center Coordinator for the Final, Rapid and Predicted results:
 - Orbit combination
 - EOP combination (polar motion, polar motion rates, UT, LOD)
 - Satellite Clock combination
- Station Coordinate combination

- JPL, Michael Heflin,
- MIT, Tom Herring,
- NCL, Phil Davies, and

- Troposphere Combination at **GFZ**, Gerd Gendt.

As mentioned before ideally every AC would provide just one single product file each day containing all currently available products. Because this is not possible for obvious reasons we have the different IGS combinations listed above. This means that the resulting combined **IGS** products are not necessarily consistent at the required level of accuracy.

Another issue which we have to address is the extent to which the products of the individual ACS are internally consistent. For instance some ACS provide satellite clock estimates although they use double difference observations for their orbit estimates. We have to know and understand to what extent the orbits, EOPS and clocks of these ACS are consistent. Other possible inconsistencies exist, for instance high rotations sometimes observed in the orbit combinations indicate that for some ACS the orbit and pole estimates are inconsistent.

So besides the consistency of the IGS combined products we should also look for possible inconsistencies within the individual AC products. **All** inconsistencies, if any, should be detected and corrected, or reduced to an acceptable level, as soon as possible.

Review of ACC Combination

The **IGS** orbit combination was originally developed in 1993, [*Beutler et al.*, 1995]. Since then many improvements and additions have been made by the Analysis Center Coordinator (**ACC**) and his colleagues at **NRCan**, [*Kouba*, 1995; *Kouba and Mireault*, 1996]. However, the basic method of the combination, the L1 -norm, was not changed.

It is our impression that the **IGS** final orbits, EOPS and clocks are of very high quality and are in general more accurate and reliable than the solutions obtained by the individual ACS. Nevertheless, there are possibly a few improvements which can be made. First of all the consistency between the combined orbits and the combined clocks can, and should, be improved, especially with respect to those users who want to perform precise point positioning [*Zumberge et al.*, 1997a]. A second improvement maybe found, as envisioned during the initial development in 1993, in the use of a priori weights for the individual satellites.

Consistency between the IGS orbits and clocks

The quality of the satellite clock estimates provided by the ACS has improved dramatically over the 1996--1997 timeframe. Thanks to the increased accuracy of the AC satellite clocks and the growing number of people interested in using precise point positioning (using precise orbits *and* satellite clocks) it became clear that the IGS orbits and clocks were inconsistent at the 200 mm level. To improve the consistency between the combined IGS orbits and the combined IGS **clocks** two changes were made recently to the clock combination algorithm.

The two new features are:

- an improved clock weighting scheme, using the clock estimates from one AC as reference instead of the satellites without Selective Availability (SA, only 1 remaining), and
- correcting the AC clocks, before the combination, based on the difference in the radial component between the AC orbit and the **IGS** combined orbit.

Different ACS use different reference clocks. Therefore the AC clocks have to be aligned before the combination to correct for the differences between the different reference clocks. For this purpose the satellites without SA were used, because their clocks can be accurately modeled fitting only an offset and a drift. At the same time the **RMS** of this fit was used for the clock weighting. Because only one satellite remains without SA the alignment has **become** unreliable. Therefore the alignment was changed by using one of the ACS as reference. The selected reference AC is aligned to GPS time, based on the broadcast clocks, using all satellites. All other centers are then to this reference AC.

Providing the orbits and the clocks of the individual ACS ax-e consistent then orbit differences between the ACS should show up in the clocks as well. **In** a first order approximation only the radial differences are important. Therefore **an** attempt to improve the consistency between the orbit and clocks, by correcting the AC clocks based on the radial AC orbit differences, was made **and** coded almost 3 years ago! It was only implemented recently due to other more urgent combination improvements/enhancements and because 3 years ago no improvement was found!

One way to evaluate the IGS clock/orbit product is to use it in precise point positioning [*Zumberge et al.*, 1997a] to analyze data from a single **receiver**. We have selected nine sites (Figure 1) and the 6-week period beginning November 16, 1997 to perform such an evaluation. The sites were selected to give reasonable global coverage. To ensure that the results using the JPL product wouldn't look artificially good, it was decided to exclude sites that were used by JPL for its IGS contribution during the test period.

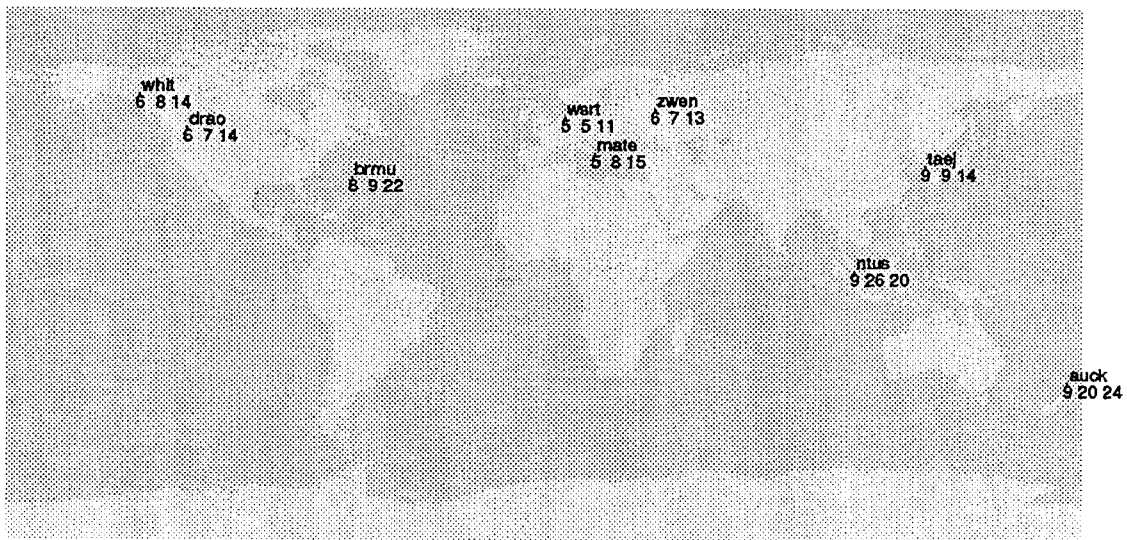


Figure 1. Sites used. The numbers indicate the observed daily repeatability for site coordinates in the North, East, and Vertical dimensions, using the latest clock combination technique, for the period December 7-- December 27, 1997.

The SP3 product contains both orbits and clock information for each satellite, once every 15 minutes. SA results in large and rapid fluctuations in the GPS clock correction. Thus only data that are on the even quarter hour in a daily Rinex file can be modeled to the sub-centimeter level for phase and half-meter for pseudorange, given a precise orbit/clock product. For each day and site, the data are used to estimate site coordinates, with satellite parameters -- orbits and clocks -- held fixed at their values in the SP3 file. For eclipsing satellites, the yaw angle was fixed at its value as estimated in JPL's contribution to the IGS. One could alternatively use the nominal yaw rates and obtain similar results. Gipsy/Oasis-II was used for all processing. On a given day, only satellites that are in both SP3 product files were kept. The JPL product contains only satellites which JPL considered usable, so this criterion attempts to exclude poorly modeled satellites.

Shown in Table 1 is the median of the daily repeatabilities of site coordinates as a function of orbit product and time window (the numbers indicate only fluctuations, and do not include any average offset). The product labelled 'IGSO' used the original clock combinations, For the product labelled 'IGS 1' the improved weighting scheme was used and for the 'NEW' product the radial corrections were applied in addition to the improved weighting scheme. For reference the results using the JPL orbits and clocks using the same timespan and sites are also given. Note that the solutions 'IGSO' and 'IGS 1' are based on the official IGS products for those timeframes whereas the the "NEW" product represents the now operational (current state of the art) IGS clock combination (active since GPS-week 0938, day 0 for IGS and GPS-week 0940, day 1 for IGR).

With the latest implementations regarding the IGS satellite clock combination we find

Table 1. Median daily repeatabilities as a function of time and orbit/clock product. The table contains the median value of the nine sites. A change in the clock weighting scheme was implemented on Dec 7, and a proposed improvement using radial variations in contributed orbits was also evaluated (*NEW*). The JPL results, using the same timeframes and sites, are shown for **comparison**.

<i>Product</i>	<i>period</i>	<i>North (mm)</i>	<i>East (mm)</i>	<i>Vertical (mm)</i>
IGS0	Nov 16-- Dec 06	11	17	24
IGS1	Dec 07-- Dec 27	8	10	16
NEW	Dec 07-- Dec 27	6	8	14
JPL	Nov 16-- Dec 06	4	4	7
JPL	Dec 07-- Dec 27	4	6	8

typical daily **repeatabilities** of 10 mm horizontal and 14 mm vertical for stationary site coordinates. These are approximately a factor of two better than before these improvements were implemented and are approaching the individual AC consistency. This is quite an achievement in view of the very inhomogeneous input for the clock combination: not all ACS submit clocks, the quality of the clocks are very different and one AC provides clocks only every 30 minutes. However, the results using JPL's SP3 product indicate that there is still some additional room for improvement for the **IGS** product.

One feature of the results that is not well understood are significant variation among sites in the repeatabilities, which are indicated in Figure 1. An extreme case is Auckland, New **Zealand**, where the **repeatabilities** are approximately a factor of two larger than the median (this is not observed when the JPL product is used). Further enhancements maybe necessary to reduce these significant site-to-site variations.

One possibility to further improve the consistency of the combined **IGS** clocks may be found in the alignment of the AC clocks. Currently the alignment of the AC clocks is achieved by estimating one offset and drift per AC with respect to a chosen reference AC. In order to do proper clock alignment amongst ACS, i.e. to remove the effects of a single reference station, we need AC station clock solutions (e.g. also at 15 min sampling), or at least a subset of consistent AC station clock solutions. The station clock solutions are also essential to the time transfer pilot project [Ray, 1998]. Furthermore an important quality control could be realized by analyses of the stable hydrogen maser clock subnet of stations.

Note that there are some significant hurdles in the clock combination. The quality of the individual AC clock solutions are very different. Only three ACS (EMR, GFZ, and JPL) provide satellite clocks based on processing undifferenced phase (and code) data. Of these, GFZ has a sampling rate of only 30-minutes with respect to the nominal 15-minutes sampling. This may cause problems in the combination, something which will have to be studied. Note that for the rapid products the USNO AC also provides satellite clock estimates based on processing undifferenced phase (and code) data.

The clock estimates of two other ACS (CODE and ESA) are based on (phase-) smoothed code observations and may be noisier than the true “phase-clocks”. This may have some negative influence on the combined IGS clocks as well. It should also be investigated to what extent the clocks of these ACS are consistent with their other products, because for both ACS the primary products (orbit, EOP and coordinates) are based on double difference processing!

Clearly it would be very advantageous if all ACS would provide satellite and station clock estimates at least as frequently as every 15-minutes. Preferably the clocks should be of similar quality, comparable to the quality of the orbits.

Use of a priori satellite weights

One limiting factor in the orbit combination scheme is the fact that there is no (a priori) information about the quality of the individual satellites! Although the orbit exchange format (**SP3**) allows for the inclusion of (meaningful) accuracy codes for each individual satellite this option is not used by many ACS. In the combination scheme this information is only used, when available, a posteriori to compute the weighted RMS.

During the original development of the orbit combination software, using the L2-norm (least squares instead of the **L1-norm**) it was envisioned that at some stage a priori weights would be used for each satellite and possibly also for the ACS [*Springer and Beutler, 1993*]. Because satellite specific weights were not readily available in 1993 it was decided to switch to the **L1-norm**, a much more robust estimator than the L2-norm, to be less sensitive to bad satellites and therefore make the use of satellite specific weights obsolete.

However, looking at recent orbit combination reports several ACS exclude supposedly “bad” satellites from their orbit solutions. In many cases the bad satellites, however, were used in the actual data analysis and only removed from the final (**SP3**) product. The reason behind this is to ensure that users do not by mistake use these bad satellites. If all ACS would remove all, and the same, bad satellites there would be no problem except that we would lose (based on recent combinations) about 2 satellites each day! Because not all IGS users are interested in the highest precision this would be disadvantageous for several users. It is our conclusion that also “bad” satellites are to be considered **IGS** products, and therefore should be included in all AC submissions.

Another reason for this is that the omission of bad satellites in some, but not all, of the AC solutions could distort the combination. To avoid any distortions from missing satellites the combination, and its statistics, should be based on the common satellites only! The satellites submitted by only a few ACS can be combined a posteriori using the estimated transformation parameters and weights.

Of course the inclusion of bad satellites in the combination could, despite the robustness of the L1 -norm, distort the combination. It would therefore be sensible to start using a priori satellite weights. The weights would, ideally, be based on the accuracy codes found in the SP3-header. However they could also be based on the 7-day arc fit which is performed in the orbit combination, In this way the bad satellites can easily be detected and downweighted in the combination. In any case the **IGS** should put more emphasis on the availability and the usefulness of the accuracy codes in the orbit files and request the ACS to submit solutions for **all** satellites, with the possible exception of satellite **manoeuvres** and exceptionally large modeling problems.

Review of GNAAC Combination

The combination methods of the three different **GNAACs** are described in detail in the **IGS** Annual Reports. The coordinate combination, based on the weekly **SINEX** files, has one very **large** advantage over the orbit combination. It has access to the full **covariance** matrix of the coordinate estimates. Therefore the combination method is both easier and more accurate than the orbit combination where we have no statistical information whatsoever.

It has been shown in several publications, [*Davies and Blewitt, 1997*] that the **GNAAC** combinations are better than most if not **all** AC solutions. We therefore conclude that the **GNAAC** combinations are in very good shape and can not significantly be improved. However, there are some persisting problems with site names, site ties, antenna types etc. etc. which have to be sorted out once and for **all soon**. Because these inconsistencies are a more generic **IGS** problem they are discussed in a later section.

The only “problem” with the **GNAAC** activities is that there is not yet an official **IGS** product! There is no official **IGS** combined solution and therefore no **IGS** reference frame. This is confusing for many of the **IGS** users and also quite illogical. Essentially we need **only** one **GNAAC** but redundancy may be useful. Therefore the easiest, and politically correct, decision would be that a combined **IGS** solution is based on a combination of the three **GNAAC** combinations, the “super” combination.

One **planned** addition to the **Sinex** submissions is the inclusion of the EOP parameters. This will facilitate and improve the **IGS** EOP combination. This improved combined **IGS** EOP can then be used in the orbit combination. In this way the **IGS** combined orbit will be consistent with the **IGS** reference frame, [*Kouba et al., 1998*]. However, this requires that the **GNAAC** combinations are done prior to the (**final**) orbit combination, e.g. before or on the second Wednesday (1 O days) after the end of the **GPS-week**.

Review of Troposphere Combination

For several months the tropospheric zenith delay estimates of most ACS, as provided in the (pseudo-)Sinex format, have been combined [Gendt, 1998]. For this combination it is essential that the differences in the zenith delays, caused by differences in the station coordinates, are corrected prior to the combination. This is very similar to the correction of the satellite clocks based on the radial orbit differences. Clearly a consistent IGS coordinate (and velocity) set, the IGS reference frame, is helpful, if not essential, for the troposphere combination. The individual AC troposphere solutions can then be made consistent with this official IGS reference frame prior to their combination. In this way the troposphere estimates would be related to the “true” and constant reference frame.

One aspect that should be mentioned here is that in small networks there is a large advantage if a global station is included together with its estimated tropospheric delay. In a small network (few 100 km) it is difficult to estimate the absolute tropospheric delay. The inclusion of one “global” station with its previously determined tropospheric delay held fixed while adjusting the troposphere delays of all other stations solves this problem. This may be very important for future meteorological investigations. Here similar consistency problems, as encountered in the case of precise point positioning between the orbit and the clocks, may be encountered between the IGS combined tropospheric zenith delays and the IGS combined station coordinates.

One additional problem in the troposphere combination is the use of different mapping functions by the different ACS. The effect different mapping functions have on the zenith delay estimates should be studied. It should also be investigated how an IGS user can use the combined zenith delay, e.g. which mapping function he should use. Analogous to how the clocks are adjusted based on different reference clocks the zenith delay estimates should be corrected, calibrated, to account for the usage of different mapping functions. Other complicating factors are the estimation of tropospheric gradients and the antenna phase center variations.

Finally it is very likely that future troposphere estimates will include tropospheric gradients; at this time gradients are already routinely estimated at CODE and JPL. The current tropospheric Sinex format does not allow for the inclusion of tropospheric gradients.

Consistency between the Combinations

It is essential that all submitted AC products be either consistent, or sufficient info is included (e.g. EOP) that they can be made consistent before IGS combinations. This applies to all products, i.e. orbit, EOP, clock, Sinex, and troposphere.

Therefore the inclusion of the EOP parameters in the AC Sinex submissions and GNAAC combinations is absolutely essential in order to make the IGS orbits, EOPS and clocks

consistent with the IGS reference frame [*Kouba et al., 1998*]. All ACS therefore **must** include EOPS in their **Sinex** solutions **as soon as possible**. A nice benefit from this will be the (much) improved quality of the combined **IGS** EOP because it will be done using the full **covariance** matrix.

Review of feedback

In general **all** the results and combinations produced in the framework of the IGS are unique in the (scientific) world. However, there is always room for improvement! Therefore here it is tried to identify in what way **all** the information **from** the different IGS activities can be improved, enhanced, streamlined, and so on.

Because the troposphere combination is in its pilot phase it is not considered here. However, we would like to state that it already looks to be in good shape and the reports should soon become official and distributed using the **IGSREPORT** e-mail system.

In our opinion there is one central problem with respect to the feedback. The information is coming **from** very different sources and in very different formats. Therefore it is suggested that **all** interesting results are gathered and made available at a central place. The information should be made available both numerically and graphically, and automatically updated. The most likely way of providing this kind of service is by using the World-Wide-Web (**WWW**). Essentially **all** kind of routinely produced information should be made available. Besides feedback and results from all different combinations the site should also provide documents describing the IGS, its products and how to access and use the different IGS products.

Some items which this **WWW** (feedback) site could contain are:

- . time series of the transformation parameters coming from the orbit combination,
- . time series of station positions,
- time series of **network/station** performance,
- . access to the EOP plots and statistics as provided by USNO,
- documents describing different facets of the IGS,
- documents describing access to the **IGS** products,
- documents describing usage of **IGS** products,
- and many many more.

Some of these features are already available at the IGS Central Bureau (**CB**), and others have been proposed by CODE when it assumes the role of Analysis Center Coordinator (**ACC**). We expect cooperation and coordination between the CB and ACC to provide improved feedback.

ACC Final and Rapid Combination Feedback

The feedback as provided by the (final) IGS orbit combination is one of the most valuable within the IGS. It is clear that it provides excellent information. One point which can be improved is the navigation solution. Currently smoothed code observations are used which are not really capable of showing the quality of the orbits and clocks. Therefore it should be enhanced by using the carrier phase measurements. In this way it will automatically provide feedback about the consistency between the orbits and the clocks.

The feedback from the rapid orbit combination is also quite good, although the long arc test is not included here because, the rapid combination is done on a daily rather than a weekly basis. Therefore the feedback about the rapid orbits, of the individual ACS, maybe improved by performing a weekly comparison in the same way as is being done for the final orbits, In this weekly comparison the long arc test would then be included. One other positive effect of this is that it will give the rapid orbits more visibility and thus create some more awareness about the availability of these products.

The predicted orbit combination provides good feedback for all participants. However, if the combined IGS predicted orbit would be included in the proposed weekly rapid comparison, in the same way as the rapid orbit is included in the **final** combination, then the visibility and awareness of the prediction products and efforts is also guaranteed.

One upcoming problem for the rapid and predicted orbit is the change of time-zone which will take place when the ACC activities change from EMR to CODE (sometime in 1998). The deadline for the rapid products will have to be adjusted to allow the combination to be performed during "normal" office hours. Assuming that the rapid combination should be performed before **19:00** MET (e.g. **17:00** or 18:00 UTC depending on daylight saving time), this would mean a effective deadline around **16:00** hours UTC! In view of the increasing demands for real-time products (especially troposphere) this would be a (small) step in the right direction. It should be investigated if an earlier deadline is feasible (12:00 hours **UTC?**).

GNAAC Combination Feedback

The feedback of the individual GNAACS is very different. Thanks to the fact of having three different GNAACS the **total** feedback is sufficient. The recent addition, by the MIT

GNAAC, of providing station coordinates residual file is valued highly. Nevertheless there are some problems with the GNAAC combinations.

Most important y, and most disturbing, are the problems with station names, receiver and antenna types, and antenna heights and phase center variations. These are well known IGS problems which are not caused by the GNAACS. These station inconsistencies encountered in the **GNAAC** activities underline the bad situation of the **IGS** global network. Furthermore, the persistence of these problems, despite the **GNAAC** combinations, shows that the GNAACS are not very well embedded in the IGS structure. This situation should be *much* improved before any form of IGS reference frame realization can be based on the GNAAC results. Hopefully the “super combination” will help to close the gap between the GNAACS, the ACS, the stations, and the data centers.

One other confusing part of the GNAAC feedback is the time at which the different GNAAC combinations are performed. The delay is usually much larger than that of the orbit combination and on several occasions a GNAAC center has provided several weeks at one time. For successful and timely realization of the **IGS** reference frame the GNAAC combinations will have to be performed both more regularly and more timely. The **proposed** implementation of the EOPS in **Sinex** and the use of the combined EOP in the **orbit combination** implies that the deadline for all GNAAC combinations will be 10 days after the end of the GPS-week. This will solve this problem.

Feedback to Data Centers and Station Managers

The IGS has not been very successful in controlling the quality of the stations, their data, their **Rinex** files and the resulting coordinate estimates despite several different checks which are being performed routinely, including:

- JPL network reports,
- **CDDIS** Rinex checking,
- **IGSCB** station log and **Rinex** checking.
- CODE Rinex checking,
- several GNAAC checks, and
- coordinate residuals from the MIT GNAAC.

Little action is taken based on all the available information. All different information pieces should be gathered at a central place (**IGSCB**, DCS, or ACC) and erroneous stations should be informed of their errors and their data files flagged by the IGS *automatically*.

The (still unexplained !!) problems with the station of Madrid, throughout 1997, showed that the way station problems are currently handled within the IGS is completely insufficient. Many **IGS** customers used the station as fiducial for their local network which resulted in severe problems (due to the several cm apparent shift of the station). Also the list of discrepancies in antenna heights, antenna types between station logs and **Rinex** files, and consequently between ACS and GNAACS, is (still) almost endless.

Despite **all** the checks being performed the situation has not really improved over the last two years. Therefore it is time to specify some (strict) guidelines on what the *minimal* requirements are to become and to remain an IGS station. In our opinion the absolute minimal requirement is the availability of a complete station log file at the **IGSCB** and **Rinex files** which contain information corresponding to the station log. The IGS should aim to provide *only* data from official IGS stations. This should take effect as soon as possible but no later than July 1998. Data from **non-IGS** sites may be made available but it should be clearly flagged by either putting the data in a separate directory at the **DCs** or by **(re)naming** the file.

The Rinex "file sequence number" maybe abused for flagging files in the following way:

- **XXXXOO1 0.9802** -- normal name for an **IGS** station
- **XXXX001Z.980.Z** -- for an **non-IGS** station

Flagging **non-IGS** files in addition to improved and automatic feedback to the Data Centers (DC) and station managers is the only way to improve the current (bad) situation of the global network, It is the key to ensure and maintain a high quality global network! The details on how exactly to define a non-conforming station need to be worked out,

Future Products

It is very difficult to predict the **future** and especially the future of the **IGS** which is still developing rapidly. Nevertheless, we can reasonably anticipate some future demands and, consequently, products.

Combined troposphere and ionosphere estimates will possibly become official **IGS** products. A combined troposphere solution is already being generated routinely and may soon become official. For the ionosphere the situation is less clear but already an exchange format has been defined (**IONEX**) and at least one AC (CODE) already routinely produces ionosphere "maps". So the generation of combined ionosphere solutions could be started very soon if enough participants are found. One "problem" with the ionosphere is that it is not a **(by-)product** of the normal processing algorithms, which use the ionosphere-free linear combination of the two carrier phase observations.

One large future "customer" of IGS products will be the Low Earth orbiter (LEO) missions. At the moment it seems that at a large amount, if not all, of the LEO data will be processed using precise point positioning. For most of the LEO missions it will be mandatory to have satellite clock estimates with a higher rate than the current 15 minutes. For the meteorological LEO missions (e.g. tomography) it will be mandatory to have access to satellite clock estimates with a 30 second sampling rate (assuming precise point positioning is used). If higher sampling rates are required than also a subset of the ground network stations will have to sample the observations at a higher rate. This poses no real problems because there is already a large number of sites with higher sampling rates. Only the data are not made available as official IGS data.

Finally, as discussed during the 1996 IGS AC workshop, there should be a "short" **SINEX** file format; a **SINEX** file without the **covariance** matrix. This would enable users to study time series of station coordinate solutions more easily. It might be wise to generate only a short **SINEX** file from the official IGS reference frame solution rather than generating short **SINEX** files for **all** available **SINEX** files, which could very easily confuse the IGS users!

Summarizing we foresee the following future **IGS** products:

- Troposphere and Ionosphere
- 30 sec satellite clocks
- 15 min station clocks
- Short **Sinex** file, only for the official IGS "super combination"

One other product might be estimates of the Earth's Center of Mass, which could be included in the **Sinex** files. These estimates may also be useful for the orbit combination.

Furthermore the upcoming GLONASS test campaign (end of 1998) should be mentioned. Although not organized by the **IGS**, it may lead to some new products like, GLONASS orbits, the time difference between GLONASS and UTC and others.

Other, more distant, products may include:

- Earth's center of mass estimates (included in **Si nex**)
- EOPS with a higher time resolution (hourly?) to verify and possibly improve sub-daily polar motion models.

- Estimation of **nutaton** drifts. This has similar problems as the estimation of LOD (UTC drifts).
- Station coordinate solutions with a higher time resolution (hourly?) to verify and possibly improve Earth tide models.
- GLONASS products.
- ""
- and probably many many more!

Generation of accurate high rate Satellite clocks

One drawback to the clock portion of the IGS combined **orbit/clock** product is that precise clock solutions are available only once every 15 minutes. Unlike the orbits, which vary smoothly with time, one cannot interpolate precise GPS clocks that are computed only four times an hour (due to SA). Thus only low rate data --4 measurements per hour -- can be analyzed with the precise point positioning technique. To apply this technique to upcoming missions with low-Earth-orbiting (LEO) satellites carrying GPS receivers, one will need nearly continuous knowledge of the GPS clocks. They must be determined frequently enough, therefore, that interpolation is feasible.

Zumberge et al. [1997b] describe a **computationally** efficient method for determining precise GPS clocks at the full rate of the ground **network**; the JPL AC computes such solutions operationally. The method exploits the globally distributed subset of the IGS network which has precise frequency references. The JPL high-rate solutions, and potential similar ones from other ACS, could be used to augment the existing IGS combined clock solution in a simple way.

Recommendations

Recommendation 1: Inclusion of **all** satellites, which were used in the data analysis, with meaningful accuracy codes in the orbit products from all individual ACS, Use of these accuracy codes, or accuracy measures from the long-arc analysis, to identify and consequent y downweight' 'bad" satellites in the orbit combination. In addition the IGS should increase the **user awareness** of the availability and importance of the accuracy codes in the SP3 files (see also Recommendation 4).

Recommendation 2: Enhancement of clock products. All ACS which submit clocks **must also** submit clock estimates from a, yet to be determined, subset of" 'core time stations" ! All ACS are **urged** to submit clock estimates. Furthermore the ACS are **encouraged** to increase the sampling rate of the satellite clock products to 30

seconds. A format for station and satellite clocks, also suited for 30 seconds satellite clocks, will have to be defined.

Recommendation 3: Improved and automatic feedback to Data Centers (DC) and station managers in case there are discrepancies between **Rinex** files and station logs, data problems and unexpected problems (jumps) in the station coordinate solutions.

Recommendation 4: Create a central place (**WWW**) for feedback and information about the IGS products and their use.

Recommendation 5: Definition of minimal requirements for becoming an IGS AC. Any AC must produce **all** core products, i.e. orbits, EOPS, and **Sinex**, both on time and with sufficient (high) quality. The **IGS** terms of reference will be changed accordingly.

Recommendation 6: Additional accuracy digit for the **IERS/IGS** EOP file format. New format to be defined before June 28, 1998 by Jan **Kouba** in cooperation with Dennis McCarthy.

add 1: To achieve the highest consistency of the orbit and clock combination it is mandatory that all ACS provide estimates for all satellites which were used in the analysis. Only **manoeuvring** satellites and very bad satellites (**modelling** problems larger than 1 meter) which ‘ ‘darnage” the solution may be removed. Bad satellites should be flagged by inclusion of meaningful accuracy codes in the orbit files. This will allow a priori weighting of the satellites in the orbit combination which should improve the combination and its consistency. At the same time the users of the **IGS** products can, and should, use these accuracy codes to weight or remove bad satellites. The **IGS** should put some effort into increasing the user awareness of the availability and importance of the accuracy codes in the SP3 files. It should also be investigated if the commercial GPS softwares (can) use the SP3 accuracy codes. To avoid any distortions from missing satellites, in some of the AC solutions, the combination, and its statistics, should be based on the common satellites only!

add 2: “**Core** clock stations” are necessary to improve the AC clock alignment. Jan **Kouba**, Jim Ray will work out a list of clock stations by June 28, 1998. A higher clock sampling rate is necessary, or at least very advantageous, for several future missions but also for the precise point positioning users. Hopefully some of the ACS can provide 30 sec satellite clock and 15 min station clock estimates by June 28, 1998. Consequently a format for the clock products (TIMEX?) should be available by June 28 as well. The **IGSGB** will write a letter to **all** ACS requesting them to submit clock estimates.

add 3: Stations which are performing poorly or have incorrect/inconsistent documentation should be identified in a timely fashion. A file containing a list of such stations as a function of time, should be maintained and accessible by anonymous ftp from the Central Bureau, In addition the DCS should flag the **Rinex** data files. It is hoped

the first step in the data “flagging” can be started by June 28, 1998. In the first step data from stations giving inconsistent information in the station logs and **Rinex** headers should be flagged. Ideally the flagged stations will not be used by the IGS ACS but at least they should not show up in the official IGS products. Further refinement and feedback will have to be controlled by the **IGSCB** and/or a future Network Coordinator. A necessary requirement here is a clear definition of an ‘IGS-station’.

add 4: To enable a better overview of all IGS activities, products, combinations, and feedback a central **WWW-site** should be developed. This (feedback) site should contain descriptions of **all** the IGS activities. It should also contain documentation on how to use the **IGS** products, The information can either be at this site or provided using “links”. (This recommendation was part of the CODE **ACC** proposal)

add 5: At present there are no (clear) guidelines about what an **IGS AC** is required to do nor how to become one. Therefore a list with the **minimal requirements to be and to become an IGS AC** should be generated. The minimal requirements are the generation of Orbits, EOPS, Coordinates with sufficient accuracy. Estimation of satellite (and station) clocks and tropospheric estimates are highly recommended. Furthermore a long-term commitment is necessary.

References

- Beutler, G., J. Kouba, and T. A. Springer (1995), Combining the Orbits of the IGS Processing Centers, *Bulletin Geodesique*, 69(4), 200--222.
- Davies, P. B.H., and G. Blewitt (1997), Newcastle-Upon-Tyne Global Network Associate Analysis Centre Annual Report, in *IGS 1996 Annual Report*, edited by J.F. Zumberge et al., pp. 237--252, IGS Central Bureau, Jet Propulsion Laboratory, Pasadena, California U. S. A., November 1997.
- Gendt, G. (1998), IGS Combination of Troposphere Estimates -- Experience from Pilot Experiment, in *Proceedings of the IGS Analysis Center Workshop*, ESA, Darmstadt, Germany, February 1998, This Volume.
- Kouba, J. (1995), Analysis Coordinator Report, in *IGS 1994 Annual Report*, edited by J.F. Zumberge et al., pp. 59--94, IGS Central Bureau, Jet Propulsion Laboratory, Pasadena, California U. S. A., September 1995.
- Kouba, J., and Y. Mireault (1996), IGS Analysis Coordinator Report, in *IGS 1995 Annual Report*, edited by J.F. Zumberge et al., pp. 45--77, IGS Central Bureau, Jet Propulsion Laboratory, Pasadena, California U.S.A., September 1996.
- Kouba, J., J. Ray, and M.M. Watkins (1998), IGS Reference Frame Realization, in *Proceedings of the IGS Analysis Center Workshop*, ESA, Darmstadt, Germany, February 1998, This Volume.
- Ray, J. (1998), The IGS/BIPM Time Transfer Project, in *Proceedings of the IGS Analysis Center Workshop*, ESA, Darmstadt, Germany, February 1998, This Volume.
- Springer, T. A., and G. Beutler (1993), Towards an Official IGS Orbit by Combining the Results of all IGS Processing Centers, in *Proceedings of the 1993 IGS workshop*, edited by G. Beutler and E. Brockmann, pp. 242--249, Beme, Switzerland, March 25--26 1993.

- Zumberge, J. F., M. B. Heflin, D. C. Jefferson, M. M. Watkins, and F. H. Webb (1997a), Precise point positioning for the efficient and robust analysis of GPS data from large networks, *Journal of Geophysical Research*, **102(B3)**, 5005--5017.
- Zumberge, J. F., M. M. Watkins, and F. H. Webb (1997b), Characteristics and applications of precise GPS clock solutions every 30 seconds, *Navigation*, submitted.

EFFICIENT ESTIMATION OF PRECISE HIGH-RATE GPS CLOCKS

J. F. Zumberge, F. H. Webb, M. M. Watkins
Jet Propulsion Laboratory, California Institute of Technology
Pasadena, CA 91109 USA

SUMMARY

Using carrier phase and pseudorange data from a small network of globally distributed GPS receivers with precise time references, we are able to estimate GPS clock parameters every 30 sec, with sub-decimeter accuracy, in a computationally efficient manner. Over time and the Earth's surface, there are usually five or more satellites above 15 deg elevation angle with well determined clock solutions, although occasionally some isolated locations view fewer than four. The accuracy obtained is a factor of 100 to 1000 times better than that of clocks in the broadcast navigation message, and allows post-processing of high-rate single-receiver kinematic GPS data with few-cm-level precision when used in conjunction with precise GPS orbits. The clock estimates can be interpolated to arbitrary times, with an additional error due to Selective Availability (SA) clock dithering, of approximately 7 cm rms. The interpolation error could be reduced to about 2 cm if 15-sec data were analyzed instead of 30-sec data. The amplitude of the daily clock variability y is typically 24 m for satellites affected by SA. Temporal variations are well modeled by an auto correlation function $p(d) = \exp(-d^2/2\tau^2)$ with $\tau \approx 106$ sec.

Acknowledgments The full paper "Characteristics and applications of precise GPS clock solutions every 30 seconds" has been accepted for publication in Navigation. The research described here was carried out by the Jet Propulsion Laboratory, California Institute of Technology, under a contract with the National Aeronautics and Space Administration.

PRECISE HIGH-RATE SATELLITE CLOCKS AT GFZ

Wolfgang Söhne

GeoForschungsZentrum Potsdam,
Telegrafenberg A 17, D-14473 Potsdam, Germany

INTRODUCTION

Within the routine IGS rapid and final analysis the raw GPS data is in general sampled to a lower data rate to reduce noticeably the amount of data and the computation time. At **GFZ** a sampling rate of 6 minutes was used up to now, since early 1998 it is changed to 5 minutes.

However for some applications like Precise Point Positioning or estimating the orbits of the so-called Low Earth Orbiters (**Kang** et al., 1995, Foeckersperger et al., 1997) it may be useful or necessary to determine the orbits and the clocks of the GPS satellites with the higher rate of the original data given in the **RINEX** files, i.e. 30 seconds. Whereas it is relatively easy to determine the satellites orbit position by means of interpolation within the orbit position file which is obtained by integration this method is not applicable to the satellite clock due to its non-smooth behaviour as a result of Selective Availability.

A straightforward way of estimation is the full treatment of the 30 second data within the IGS processing scheme instead of the computation with the sampled data. This procedure is not suitable due to the huge amount of computation time which would be necessary for processing 30 second data. So a more practical way was found by using the results of the **IGS** final computation as an input into the estimation process with the higher data rate.

FIXED AMBIGUITIES APPROACH

After the IGS final processing the GPS satellite orbits are available with a high accuracy of few cm (**Gendt** et al., 1997). Therefore they can be introduced as known parameters. The satellite positions are taken from the SP3 file and can be fixed during further adjustments. On the other hand all ambiguities within the sampled 6 minute data are found and estimated within the IGS adjustment as well as all bad data and **outliers** are identified and written into the so-called LOG files. With this information the raw **high-rate RINEX** data files are reduced to those parts for which the ambiguities are valid, New data before or after is neglected. As a result of such **pre-processing** new ambiguities may not be found within the high rate data. Beyond this the GPS data between the 6 minute

epochs is separately inspected for bad records. Figure 1 shows the principle of this modified **IGS-like** analysis. For **further** reduction of the computation time the number of stations should be reduced to the minimum necessary to estimate the highest number of satellite clocks. On the other hand a good coverage must be maintained, especially on the southern hemisphere. In some cases it is better to include stations with worse clocks into consideration to avoid problems with gaps over problematic regions. These clocks are provided with very low weights during the analysis.

Because the number of stations used in the high-rate clock analysis in general will be smaller than the number of stations used in the IGS final analysis the starting time of the ambiguities is not identical to the starting time of the original scene. Therefore the ambiguities have to be shifted to the correct new epochs to avoid the problem that new ambiguities were automatically found by the program. With a number of about 20 stations which in general is sufficient for a good coverage the time of the estimation process including the time for the pre-processing part can sufficiently be reduced compared to the routine IGS analysis.

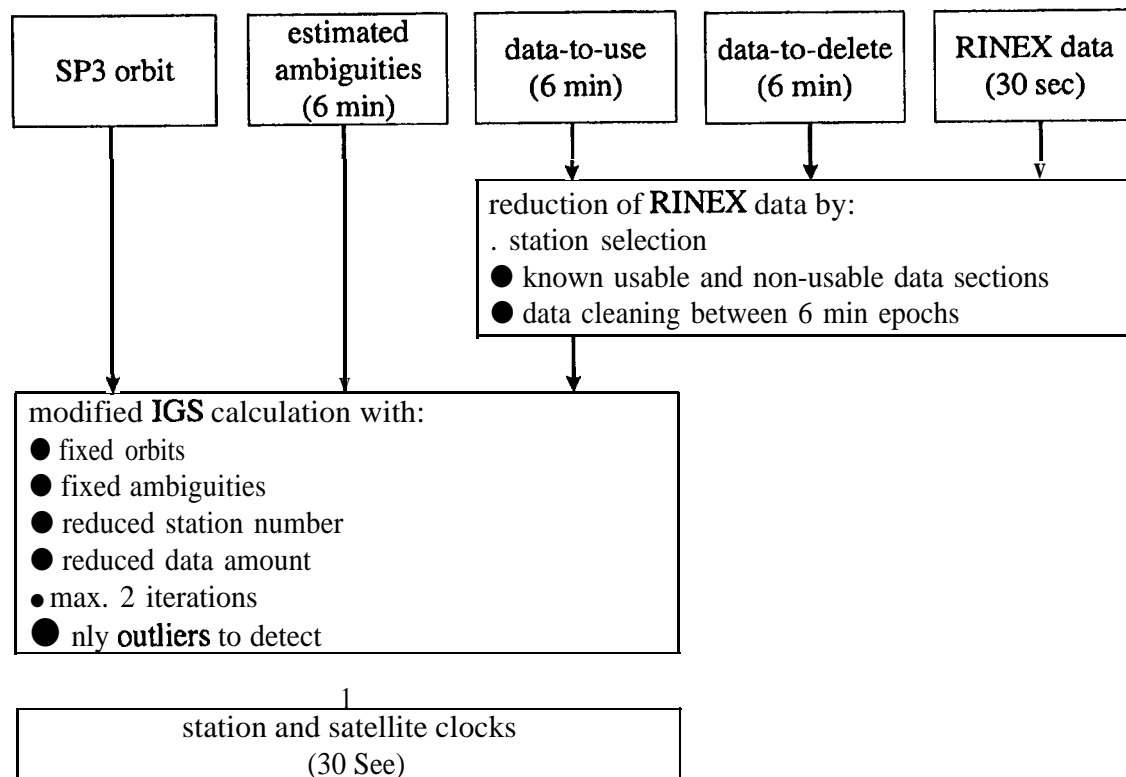


Fig. 1: Scheme of 30 second clock estimation with fixed ambiguities

FIXED STATION CLOCKS APPROACH

A second approach is based on the introduction of fixed station clocks besides the fixed orbits (Jefferson et al., 1997, Zumberge, 1998). Only stations with smooth and stable clocks are taken into account, This is tested by forming the differences to the mean of the nearest neighbors which have to be very small (few tenth of a nanosecond). After this selection the station clocks are interpolated to the necessary data rate of 30 seconds. This approach can be performed with a very small number of stations.

The advantage of the approach is the greatly reduced computation time due to the small number of stations and, of course, if only few iterations are necessary. The problem is that only few IGS stations with very stable clocks are available (~ 12-14) which, in addition, are not well distributed.

RESULTS

Results of differences between the various approaches are shown in Table 1. The first column of Table 1 shows the internal consistency of the two GFZ products, i.e. the IGS final clock solution against the 30 second solution with fixed ambiguities and fixed orbit. It can be seen that with the beginning of 1998 the fit became very small. This can be explained by a change within the IGS final computation which removed an inconsistency at the end of the final analysis.

The rms values concerning the solutions with fixed station clocks are slightly higher but mainly below 0.5 ns. One reason for the differences in the last column between the two 30 second clock solutions with fixed station clocks may be the different number of stations used: whereas JPL took 8 stations (Jefferson et al., 1997) the GFZ solution included all selected stations (11 - 12).

Tab. 1: rms values of differences between different satellite clock solutions, in nanoseconds

Day of year	GFZ-SP3 <-> GFZ with fixed ambiguities	GFZ-SP3 <-> GFZ with fixed station clocks	GFZ-SP3 <-> JPL with fixed station clocks	JPL with fixed station clocks <-> GFZ with fixed station clocks
97355	0.28	0.58	0.45	0.44
97356	0.26	0.83	0.46	0.65
97357	0.23	2.00	0.36	2.27
97358	0.27	0.49	0.45	0.35
98001	0.04	0.40	0.42	0.46
98002	0.02	0.45	0.46	0.39
98003	0.02	0.35	0.58	0.36

Besides the accuracy the number of the estimated 30 second satellite clocks is of particular interest, It clearly depends on the number of stations and on their distribution. For a routine IGS final estimation with about 50 stations usually 1-2 % of satellite clocks can not be estimated. If a number of about 20 equally distributed stations is used within the ambiguity fixed approach between 5 and 7 % of the clocks are not determinable. Within the fixed station clocks solution only 12-14 stations are usually available. In this case the number of lost satellite clocks is much higher: between 10 and 25 %. However these missing clocks are not equally distributed: usually great gaps are located over the South America and the pacific region whereas there are nearly no gaps over North America and Europe.

The Figures 2a and 2b show in detail the differences between the JPL and the GFZ satellite clocks for a single day. Figure 2a shows the full differences whereas Figure 2b is corrected for a linear trend. This trend can be explained as follows: Within the estimation process the satellite clocks are reduced to a specified reference clock. This clock is usually one of the very stable station clocks. But this connection leads to an offset and to a drift compared to GPS time because of the **behaviour** of the reference clock. Therefore beginning with GPS week 921 the clock solution at **GFZ** is corrected for these offset and trend. The offset correction is performed by calculating an average over all satellites. The drift correction is evaluated by an average over **all** stable station clocks; within this step possible resets or jumps of the reference clock are also detected and corrected, missing epochs of the reference clock are now bridged over by using other stable clocks.

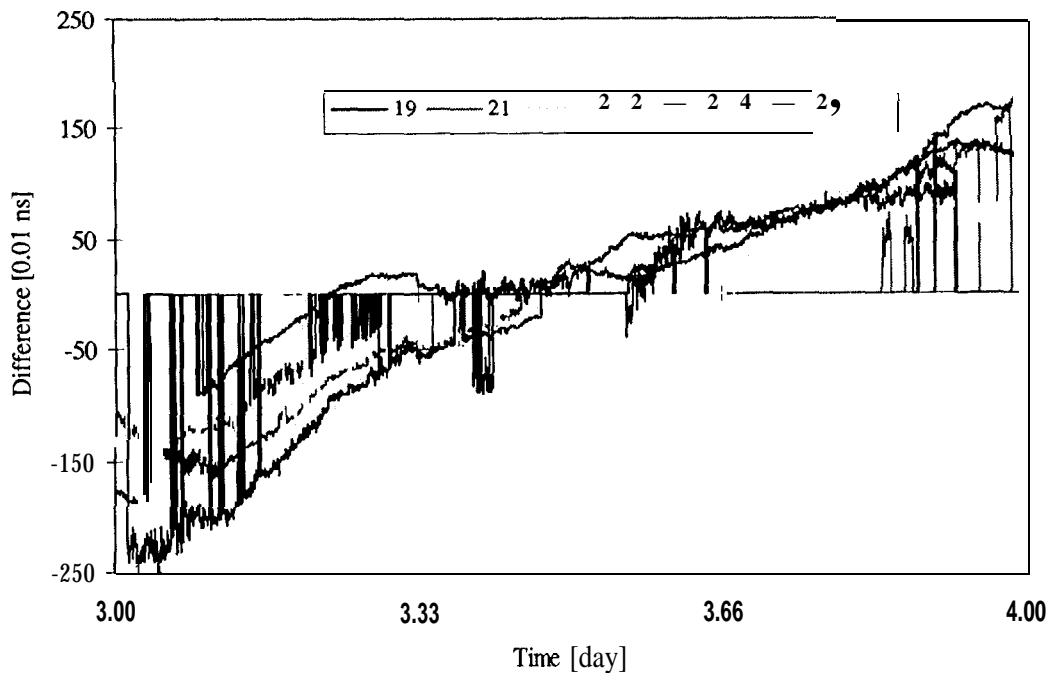


Fig. 2a: Differences between JPL and GFZ 30 second satellite clocks

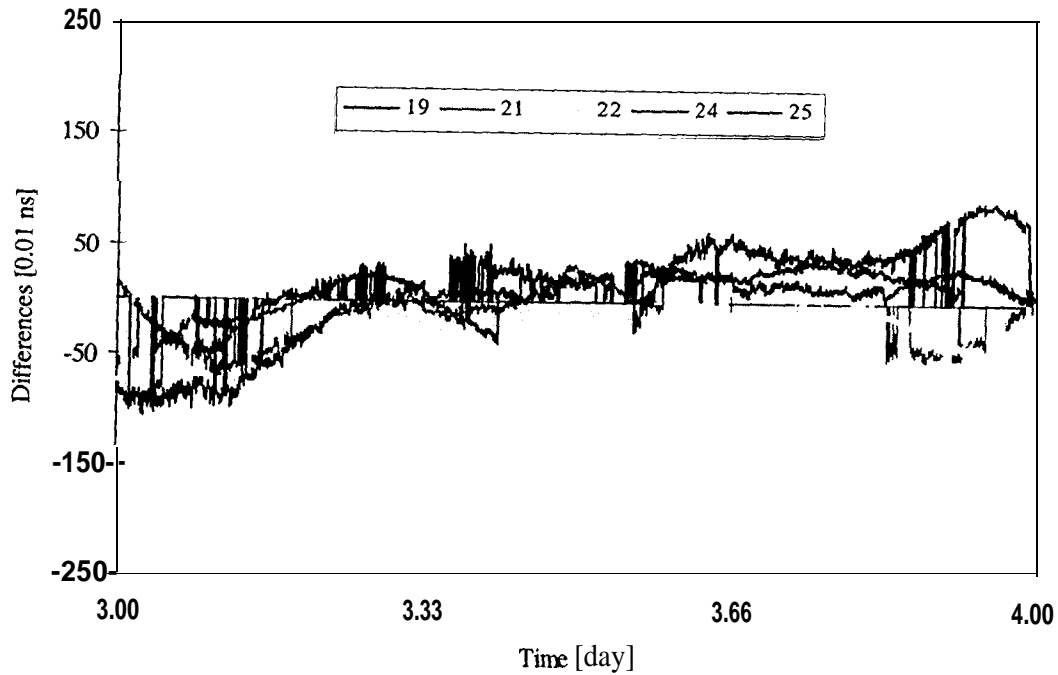


Fig. 2b: Differences between JPL and **GFZ** 30 second satellite clocks after trend correction

The Figures 3a and 3b show the improvement of the **IGS** final clocks of **GFZ** as a result of the changes starting with GPS week 921 for both offset and trend. Before week 921 the trend is nearly constant in the range of 90 nanoseconds per day whereas after the changes it is in the order of the accuracy of other Analysis Centers, e.g. CODE. In Figure 3a the gradual drift and the reset of the reference station clock before week 921 can clearly be seen in the **GFZ** offset.

The remaining differences in Figure 2b can be explained by the differences within the fixed orbits of the two variants. These differences mainly appear at the day boundaries where the **GFZ** orbit estimation still allows small jumps within the three day orbit combination process. A second explanation is the different handling of the ambiguities which are real values at **GFZ** whereas they were fixed to integer at JPL.

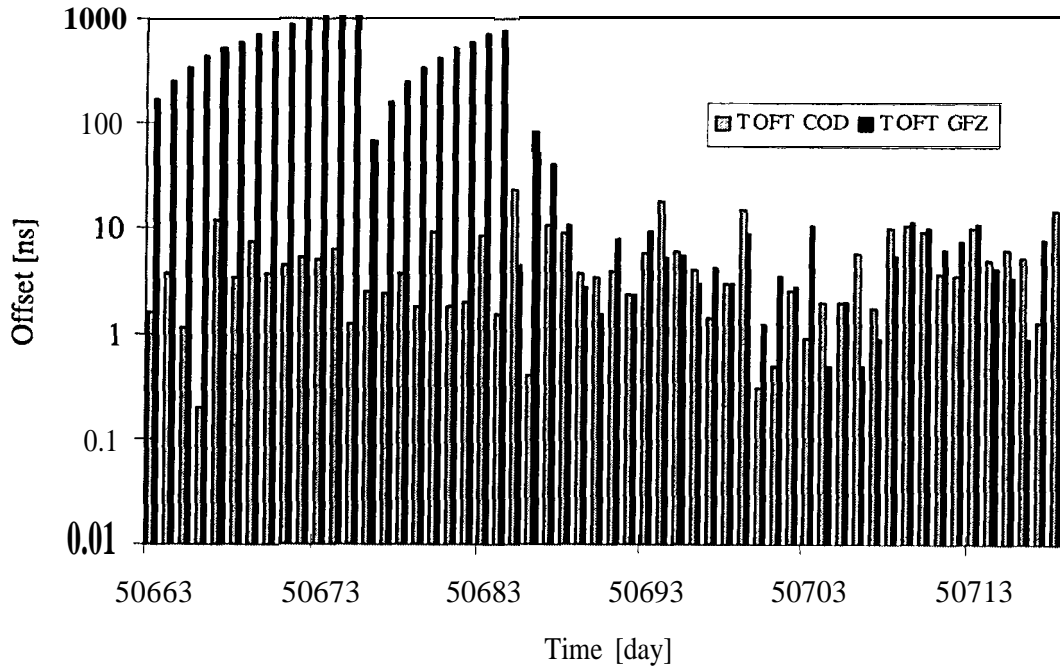


Fig. 3a: Offset of **GFZ** and **COD** IGS final clocks compared to GPS time, taken from IGS summary (logarithmic presentation)

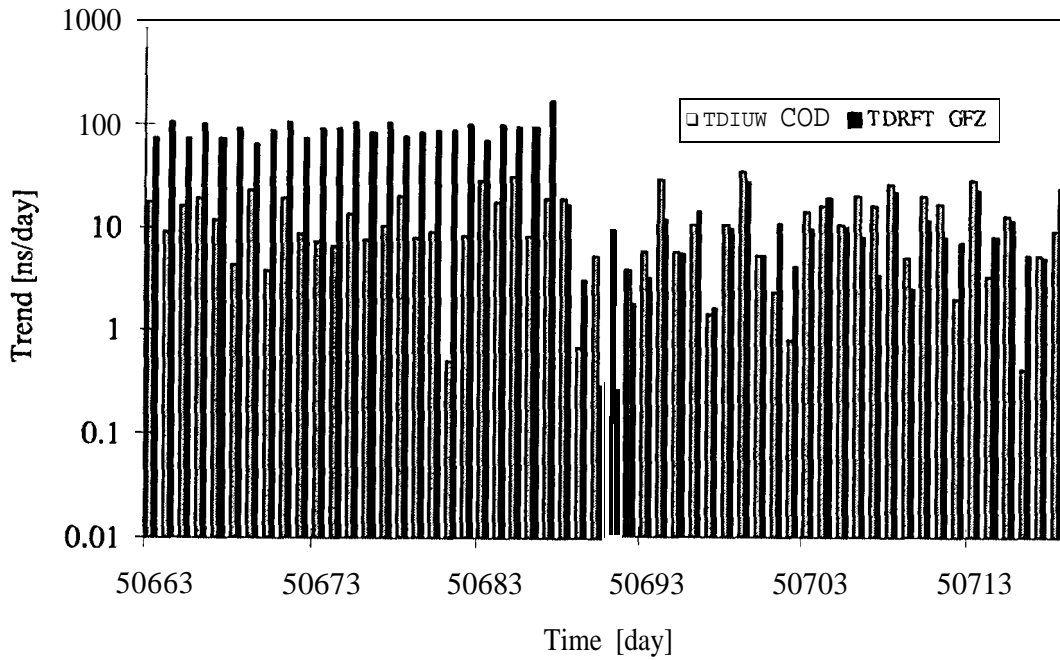


Fig. 3b: Drift of **GFZ** and **COD** IGS final clocks compared to GPS time, taken from IGS summary (logarithmic presentation)

HIGH-RATE STATION CLOCKS

One advantage of the fixed ambiguities approach is the simultaneous estimation of high-rate station clocks. Figure 4 shows the differences between the estimated 30 second station clocks and the interpolated clocks which are used as input in the fixed station clocks approach. The differences are exemplary shown for two stations, one of them (Onsala) with a very stable station clock.

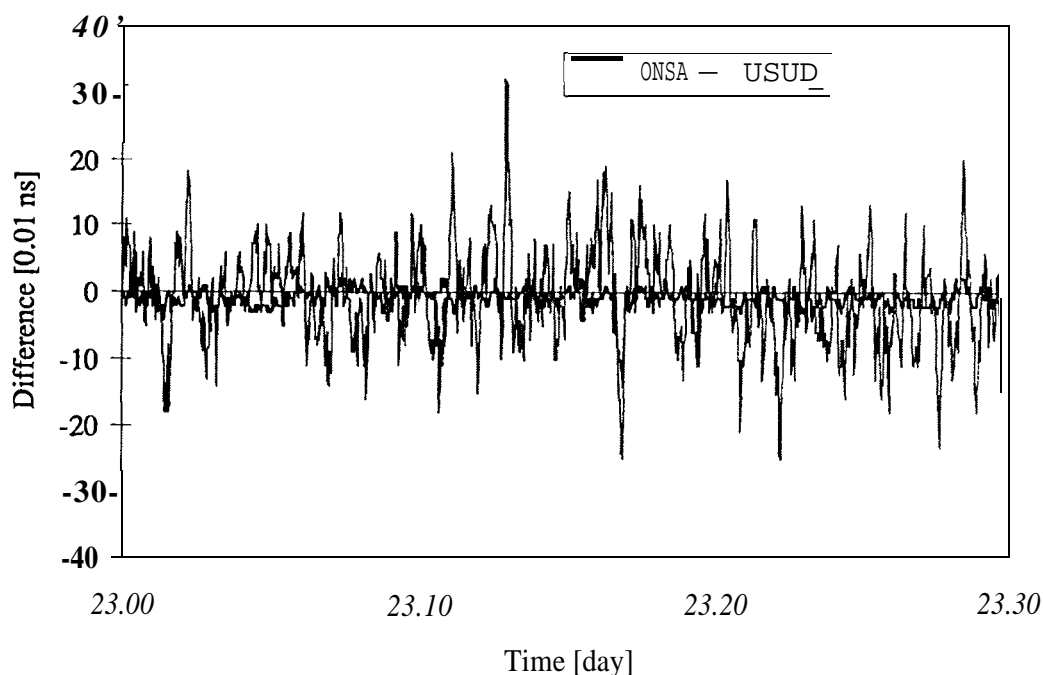


Fig. 4: Differences between adjusted and linear interpolated high-rate station clocks

It can be seen that for Onsala a linear interpolation is sufficient to keep well within a 0.1 nanosecond limit whereas for Usuda (which is only an example for some other stations with quite stable station clocks) a polynomial interpolation is necessary to use them as input in the fixed station clocks approach. On the other hand with the fixed ambiguities approach it is possible to estimate the high-rate station clocks with the same accuracy (clearly below 0.5 nanoseconds) as the satellite clocks.

REFERENCES

Foekersperger et al., 1997: Foekersperger, S., R. Hollmann, G. Dick, and Ch. Reigber - On Board MIR: Orienting Remote Images with MOMSNAV, *GPS World* 10/97

Gendt et al., 1997: Gendt, G., G. Dick and W. Söhne - GFZ Analysis Center of IGS - Annual Report 1996, in *IGS 1996 Annual Report*, JPL publications 97-20, pp. 169-181

Jefferson et al., 1997: Jefferson, D. C., M. B. Heflin, M. M. Watkins, F. H. Webb, J. F. Zumberge, and Y. E. Bar-Sever - Jet Propulsion Laboratory IGS Analysis Center Report, 1996, in *IGS 1996 Annual Report*, pp. 183-191

Kang et al., 1995: Kang, Z., P. Schwintzer, Ch. Reigber, and S.Y. Zhu - Precise Orbit Determination for TOPEX/Poseidon Using GPS-SST Data, *Adv. Space Res.* Vol. 16, No. 12, pp. (12)59-(12)62

Zumberge, 1998: Zumberge, J. F. - Efficient estimation of precise high-rate GPS clocks, in *Proceedings of the 1998 IGS Workshop (this volume)*

THE IGS/BIPM TIME TRANSFER PROJECT

J.R. Ray
Earth Orientation Dept., U.S. Naval Observatory
Washington, DC 20392 USA

INTRODUCTION

The "IGS/BIPM Pilot Project to Study Accurate Time and Frequency Comparisons using GPS Phase and Code Measurements" was authorized in December 1997 jointly by the International GPS Service for **Geodynamics (IGS)** and the Bureau International des Poids et **Mesures (BIPM)**. A general Call for Participation was issued shortly afterwards with responses requested by 15 March 1998. The respondents will form a working group co-chaired by C. Thomas, **BIPM**, and J. Ray, U.S. Naval Observatory (USNO).

A number of groups have been working for several years to develop the capability of using geodetic GPS techniques for accurate time transfer. A variety of convincing demonstrations has already been performed showing the potential for determining clock differences at the level of a few hundred picosecond. The current state of maturity of both the global tracking network and data analysis techniques now allows practical applications to be considered. The central goal of this Pilot Project is to investigate and develop operational strategies to exploit GPS measurements for improved availability of accurate time and frequency comparisons worldwide. This will become especially significant for maintaining the international UTC **timescale** as a new generation of frequency standards emerges with accuracies of 10^{-15} or better.

AREAS OF PARTICIPATION

It is expected that the Pilot Project will benefit from activities **in** a range of areas, including those listed below. Investigators have been invited to participate in one or more of these areas, or to indicate others.

Deployment of GPS receivers

In addition to the GPS receivers already installed as part of the IGS global tracking network, other receivers at laboratories having accurate time standards are sought. These should be high-quality geodetic receivers capable of recording and rapidly transmitting dual-frequency pseudorange and carrier phase observations. The station configuration and data distribution should conform to IGS standards and appropriate documentation must be filed with the IGS Central Bureau. General instructions for adding a new station to the IGS network are available at

<http://igscb.jpl.nasa.gov/igscb/resource/newstation.txt>.

A log file should be completed and sent to the IGS Central Bureau for each IGS station. For this Project, due consideration should be given to electronic stability, environmental control, and other factors which might affect the timing results. Upgrading of existing tracking stations for better timing performance is also encouraged. Deployment of **dual-frequency** GLONASS receivers, especially collocated at IGS sites, would provide an

additional data source of interest.

GPS data analysis

Strategies for analyzing GPS phase and pseudorange observations must be developed, consistent with other IGS products, to allow the routine, accurate characterization of time standards at a large number of independent GPS receiver sites and onboard the GPS satellites. This work will be done in close cooperation with the IGS Analysis Center Coordinator. It is expected that regular reports will be issued by participating analysis centers, analogous to those distributed by the IGS for other activities, and filed in the IGS Electronic Reports series.

The precise relationship between the analysis activities that are needed for this Pilot Project and those required for the official products of the IGS is not entirely clear at this point. Certainly, the Project should build and rely upon the existing IGS structure. There may, however, exist a need for clock analysis and related products beyond the charter of the IGS. Also, some changes in the current analysis procedures of the IGS may be advantageous for enhanced timing performance. For these reasons it is essential that the Analysis Coordinator be actively involved.

Analysis of instrumental delays

In order to relate clock estimates derived from GPS data analysis to external timing standards it is necessary to understand the instrumental electronic delays introduced by the associated hardware. Studies are sought to characterize the short-term and long-term sensitivities to environmental changes and to develop suitable calibration methods. Differences for the L1 and L2 frequencies must be considered. Studies of both GPS ground sites as well as the GPS satellites are sought.

Time transfer comparisons

Simultaneous, independent time and frequency comparison data are needed to compare with the GPS-derived estimates. Collaborations are sought with groups performing time transfer experiments using a variety of techniques. Close cooperation is expected with the Consultative Committee for Time and Frequency (CCTF) of the Comité International des Poids et Mesures (CIPM).

OBJECTIVES

To accomplish the overall goal of improved global accessibility to accurate time and frequency using GPS, several specific objectives can be set.

Accurate and consistent satellite clocks

Satellite clock estimates are among the "core" products of the IGS (Kouba *et al.*, 1998). The IGS combined solutions for satellite clocks are distributed together with the IGS combined orbits in the sp3 product files. It is essential that the clock information be as accurate as possible and also that it be fully consistent with the other IGS products. Kouba *et al.* (1998) describe the importance of global consistency to ensure that the point positioning technique (Zumberge *et al.*, 1997) can be applied without degradation.

A type of point positioning likely to become increasingly important is for tracking low Earth-orbiting satellites equipped with onboard GPS receivers. For this application the 15-minute tabulation interval of the sp3 orbit files is not adequate because the SA corruption of the broadcast clocks does not allow accurate interpolation over intervals longer than about 30 s (Zumberge *et al.*, 1998a). For this and other applications, the IGS ACS have been asked to provide satellite clock products with 30-s sampling rates and the IGS will probably begin producing a corresponding combined product (Springer *et al.*, 1998). Methods for efficiently computing high-rate satellite clocks have been presented by Zumberge *et al.* (1998b) and Soehne *et al.* (1998). A new exchange format will be needed to permit easy distribution of the new high-rate results.

Accurate and consistent station clocks

Presently, the IGS does not produce clock information for the GPS ground stations although doing so is mentioned in the IGS Terms of Reference. There is a clear interest in the user community for this information. Apart from time transfer uses, it could be used to characterize and monitor the performance of station frequency standards. Clock solutions from stations equipped with very stable frequency standards (especially H-masers) are needed to apply the method of Zumberge *et al.* (1998a) to estimate high-rate satellite clocks. For this purpose, station clock determinations at intervals of about 5 minutes can be accurately interpolated to the 30-s intervals needed to solve for the satellite clocks provided that the ground stations are referenced to stable clocks.

For time transfer applications, such as envisioned for this Pilot Project, accurate analysis results for the station clocks are mandatory. As with high-rate satellite clocks, a suitable exchange format must be developed. Regular summary reports to describe the analysis results characterizing satellite and station clocks will be encouraged. These should be publicly distributed in the IGS Electronic Reports series. Some IGS ACS, particularly JPL and EMR, already include valuable clock information in the weekly analysis summary reports that accompany their Final product submissions.

From geodetic analyses of the GPS data, the effective "clock" of each station is determined for the ionosphere-corrected L3 phase center of the antenna displaced by the electronic delay to the point in the receiver where the time tags are assigned to the phase measurements. These clock determinations are relative measurements in the sense that usually a single station is chosen as a time reference and not adjusted. From the viewpoint of geodetic applications, the precise reference point of the analysis clocks is irrelevant. As a result, manufacturers of geodetic receivers have generally not taken care to provide easy or accurate access to the time reference points. However, for timing applications, such as time transfer comparisons with other techniques, the precise location of the clock reference and accurate access to it are essential. Consequently, the investigation of instrumental path delays and access points is critical to the success of the Pilot Project.

Even if one imagines a shift in the timing paradigm so that the GPS receivers are eventually regarded as a part of the outer "electronics package" of stable frequency standards, it is nonetheless vital to establish accurate access to the clock reference points. The effects of environmental influences will be even more important in that case and must be minimized. Doing so will require new approaches for isolating GPS receiver equipment, such as efforts by Ovmey *et al.* (1997).

Accurate and stable reference timescale

Ultimately, it is necessary that all clock information, for satellites and stations, be referenced to a common, consistent **timescale**. Individual sets of results from different ACS generally refer to different reference clocks. Thus, in the IGS combination process, the AC submissions must be realigned. This is currently done by choosing one submission as a reference solution, realigning its satellite clock estimates to GPS time based on the broadcast clocks for all the satellites (using only daily offset and rate terms), and then realigning all the other AC submissions to the reference solution (Springer *et al.*, 1998). Corrections are applied to each solution set to account for radial orbit differences compared to the IGS combined orbits. The IGS combined satellite clock estimates are then formed from the weighted average of the realigned, corrected submissions.

It has been suggested that the clock realignment and combination process would be improved if a common set of "fiducial" station clocks were used in all analyses and included in the IGS submissions (Springer *et al.*, 1998). Naturally, only stations equipped with very stable frequency standards (preferably geometrically well distributed) should be considered as candidate **fiducials**. Recommendations for this station set will likely be made during 1998.

Likewise, it is questionable whether GPS time is an appropriate choice for the underlying **IGS timescale**. The ideal choice should be accurate, accessible, and stable over all relevant time intervals (namely, 30s and longer). GPS time is readily accessible but not with an accuracy comparable to other IGS products due to SA effects. Nor is GPS time particularly stable. The clocks of the GPS constellation are monitored from US NO and this information is provided to GPS operations with the goal of maintaining GPS time within 28 ns (**RMS**) of **UTC(USNO)**, allowing for accumulated leap second differences. In practice, the two **timescales** have been kept within about 6.5 ns (**modulo** 1 s) over the last two years (for 24-hour averages). However, the GPS time steering algorithm has a "bang-bang" character resulting in a saw-tooth variation with **typical** cycle of about 25 days. This is equivalent to a frequency error greater than 10^{-11} over days to weeks, which changes periodically in an abrupt, nearly step-like fashion.

Almost certainly, an internal ensemble of the **frequency** standards used in the IGS network can be formed which would possess better stability than GPS time (Young *et al.*, 1996). There are currently about 27 **IGS** stations using H-masers, and about 40 with **Cesium** or Rubidium standards. Addition of new IGS sites located at primary timing laboratories would only improve this situation. A purely internal **IGS timescale** would probably not be stable against long-term drifts so some linkage to external laboratory **timescales** is required. Indeed, traceability to **UTC(BIPM)** is most desirable. In principle, this could be accomplished using the instrumental calibration data mentioned above, especially for the fiducial clock sites. It will be technically difficult, however, to achieve comparable accuracies for the calibration measurements to the few hundred picosecond level possible for the data analysis clocks. This will be one of the greatest challenges for this Pilot Project.

An alternative approach to provide external linkage that can be readily implemented uses monitor data for the GPS constellation that are collected and compared at the timing labs. USNO collects such data using pseudorange timing observations and makes the results publicly available. Using the observed offsets of GPS time relative to **UTC(USNO)**, the corresponding IGS clock estimates can be related to **UTC(USNO)**. Because of the effects of SA such comparisons would only be useful to remove long-term

differences. This is probably sufficient, at least for an initial realization. Other timing laboratories would be encouraged to provide similar monitor data for a more robust tie to UTC(BIPM). A potential problem with this approach is possible biases between the effective clocks transmitted by the satellites as measured from the pseudorange and carrier phase observable.

Challenges for an IGS timescale

Apart from the issues discussed above concerning calibration and external referencing for an IGS timescale, there are other practical questions that must be resolved. In particular, it may be difficult to form and maintain a timescale within the IGS product delivery schedule. This is likely to be especially true for the Rapid products even though that is probably also where the greatest user interest lies. Fundamentally, this does not seem overwhelming although it will require entirely new and highly automated IGS processes.

Other practical concerns are minimizing discontinuities at day boundaries, dealing with clock discontinuities and drop-outs in the ensembling process, and finding an appropriate robust ensembling algorithm. These subjects, together with those mentioned above, should be studied during this Pilot Project.

SCHEDULE

It is anticipated that the schedule of activities will be flexible, as dictated by technical progress. However, for planning purposes the following milestones are envisioned:

01 Jan. 1998	--	Call for Participation distributed
15 Mar. 1998	--	responses to Call for Participation due
01 Apr. 1998	--	establishment of Pilot Project Working Group
01 Jun. 1998	--	target for publication of first analysis report
Dec. 1998	--	interim report to the IGS Governing Board
Spring 1999	--	report to Consultative Committee for Time and Frequency
Dec. 1999	--	final report to the IGS Governing Board and BIPM

By the year 2000, those aspects of this Pilot Project which are suitable for integration into the operational activities and official products of the IGS or BIPM should be underway. To the extent that some functions may not be suitable for the existing structure of the IGS, a new coordinator for this might be appropriate.

INFORMATION EXCHANGE

An e-mail exploder list has been assembled to allow a free exchange of ideas among Pilot Project participants. In addition, a Web site has been created at the URL

<http://maia.usno.navy.mil/gpst.html>

with information about IGS stations and frequency standards, a bibliography of background publications, a list of the participants, and an archive of e-mail.

REFERENCES

- Kouba, J., J. Ray, and M.M. Watkins, IGS reference frame realization, in **1998 IGS Analysis Center Workshop Proceedings**, European Space Operations Centre, Darmstadt, Germany, (this volume), in press 1998.
- Overney, F., Th. **Schildknecht**, and G. Beutler, GPS time transfer using geodetic receivers: Middle-term stability and temperature dependence of the signal delays, *Proc. 11th European Frequency and Time Forum*, 504-508, 1997.
- Soehne**, W., *et al.*, Precise high-rate satellite clocks at **GFZ**, in **1998 IGS Analysis Center Workshop Proceedings**, European Space Operations Centre, Darmstadt, Germany, (this volume), in press 1998.
- Springer, T. A., J.F. Zumberge, and J. Kouba, The IGS analysis products and the consistency of the combined solutions, in **1998 IGS Analysis Center Workshop Proceedings**, European Space Operations Centre, Darmstadt, Germany, (this volume), in press 1998.
- Young, L.E., D.C. Jefferson, S.M. Lichten, R.L. Tjoelker, and L. Maleki, Formation of a GPS-linked global ensemble of Hydrogen masers, and comparison to JPL's linear ion trap, *Proc. 50th Annual Institute of Electronics Engineers (IEEE,) International Frequency Control Symposium*, 1159-1162, 05-07 June 1996.
- Zumberge, J.F., M.B. Heflin, D.C. Jefferson, M.M. Watkins, and F.H. Webb, Precise point positioning for the efficient and robust analysis of GPS data from large networks, *J. Geophys. Res.*, **102(B3)**, 5005-5017, 1997.
- Zumberge, J.F., M.M. Watkins, and F.H. Webb, Characteristics and applications of precise GPS clock solutions every 30 seconds, *Navigation*, in press 1998a.
- Zumberge, J.F.**, *et al.*, Efficient estimation of precise high-rate GPS clocks, in **1998 IGS Analysis Center Workshop Proceedings**, European Space Operations Centre, Darmstadt, Germany, (this volume), in press 1998b.

Topic 2: Orbit Prediction and Rapid Products

ORBIT PREDICTIONS AND RAPID PRODUCTS

Tomás J. Martín Mur

European Space Operations Centre, European Space Agency
D-64293 Darmstadt, Germany

Tim Springer

Astronomical Institute, University of Bern
CH-3012 Bern, Switzerland

Y. Bar-Sever

Jet Propulsion Laboratory, California Institute of Technology
Pasadena, CA 91109 USA

ABSTRACT

The IGS is facing ever increasing demands for more precise and more rapid (**real-time!**) products. The computation of the rapid **orbits** and especially the orbit predictions, which are available in real-time, therefore are becoming more important and deserve special attention, This position paper reviews the methods of generating the rapid and predicted products and proposes ways to improve the prediction accuracy and to reduce the turn-around time.

INTRODUCTION

The use of GPS techniques for near real time data processing requires fast availability of relatively precise GPS products. New fields of application require availability of GPS orbits with high precision and at short delay after the observations are taken. An example of this is the developing field of operational meteorology using GPS. The GPS derived **precipitable water vapor (PWV)** measurements have to be processed within hours after the observation so they can be used for weather forecast. In order to get the best observability of PWR precise predicted orbits have to be available.

The IGS have been producing orbits and cops with a 24 hour delay and predictions for the next day since 1996. These products are obtained as a combination of the results of a number of Analysis Centers and are currently available before **22:00 UTC** (rapid products) and before **23:00 UTC** (orbit prediction for the following day).

The factors that limit the accuracy of the rapid and predicted products are the availability of a sufficient set of tracking data and the accuracy of the orbit prediction models.

The IGS community has been working to speed the delivery of the measurement data, but we have not yet achieved a satisfactory status, because many stations are still late and this is normally the case for stations outside Europe and North America. Faster or more frequent delivery of the data could also allow for more frequent (sub-daily) delivery of precise and rapid products.

Progress has been made in the accuracy of orbit prediction models, with investigations on new radiation pressure models being presented in this session, but we still have problems for some satellites and some improvement is possible. It is also very important for users of predicted orbits to have a good estimate of their accuracy so they can de-weight or exclude those satellites that can not be well predicted.

DATA AVAILABILITY AND REDUCTION OF THE TURN-AROUND TIME

There are two aspects in the reduction of the turn-around time, measurement data and data processing. Data from a sufficient number of well distributed stations should be available before the rapid orbits can be computed. The current deadline for data to be used in rapid orbits is 05:00 UTC, but most ACS start computing their orbits later due to the lack data from stations in the southern hemisphere. In order to obtain a good rapid orbit the criticality is not only the number of stations but their distribution. We have studied the availability of data at **CDDIS**, as listed in the reports of **CDDIS** GPS tracking data holdings, and for the purpose of this study we have grouped the stations in six regions. The selection is of course arbitrary, the stations in the border between two regions could belong to one or the other region, but it is useful in order to analyze the arrival of the data. The regions that we have selected are:

- **AS**: Central and Eastern Asia
- **EU**: Europe, Asia Minor and the Canary Islands
- **IN**: Indian Ocean rim and islands
- **NA**: North America and Greenland
- **PA**: South Pacific, Micronesia and Polynesia
- **SA**: Caribbean and South America

These regions are shown in Figure 1.

We have checked the number of stations available at the following times:

- Within two hours of tracking. This is time enough for data retrieval at the operational data center, reformatting, and transmission to the global data center.
- Within five hours of tracking. This is the theoretical Rapid Orbit deadline.
- Within twelve hours of tracking. This represents a typical AC Rapid Orbit deadline.
- Within forty-eight hours of tracking. This is the theoretical Final Orbit deadline.

GPS TRACKING NETWORK
International GPS Service for Geodynamics

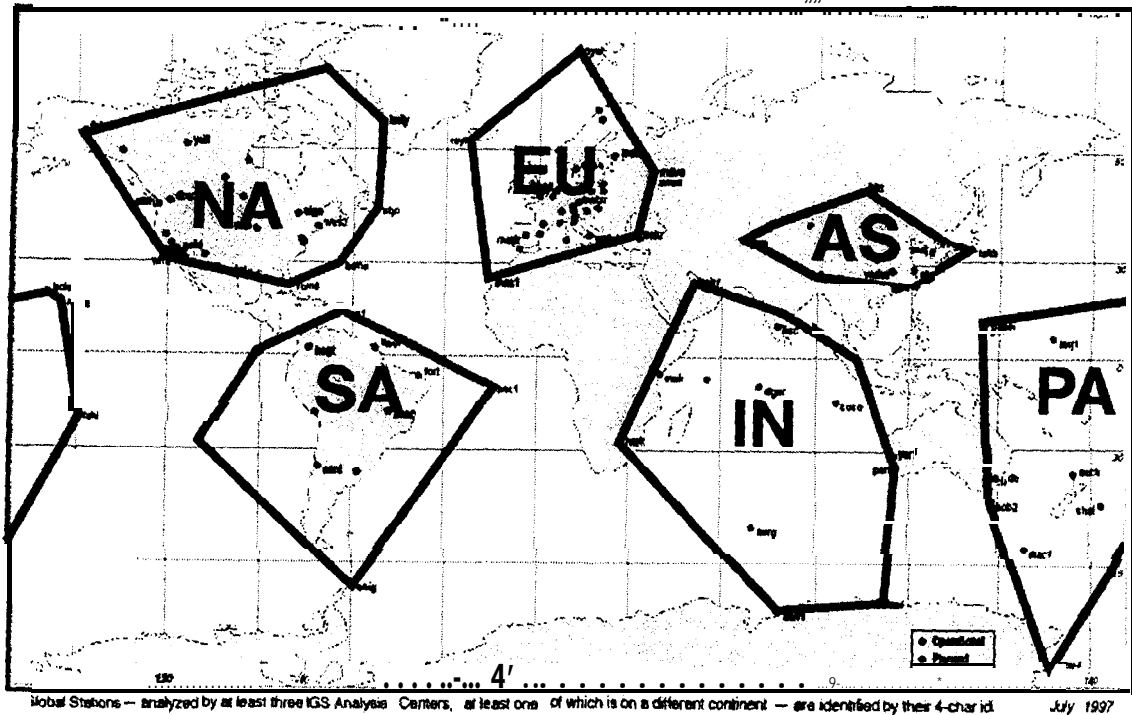


Fig. 1. Grouping of stations in order to study availability

The number of stations that were available at CDDIS for the period from Nov. 29th 1997 to Jan. 27th 1998 are shown in Table 1. The two values that are shown are the minimum and maximum number of stations that were available at that time. Detailed plots for the studied period are in Figures 2 to 5.

There are days for which no station is available at 12:00 UTC for some of the less covered regions (PA, SA). This means that the rapid orbits are calculated without taking in account any observations from a substantial part of the satellite orbits. This also affects the predicted orbits that will be obtained based on the rapid orbits. The ideal would be to have a minimum of 4 stations available from each of the regions at the time of the calculation of the rapid orbits. The maximum number of stations available at the different times also tells the capability of the system when everything goes well and for +5 hours a minimum of 6 stations are available from each of the regions when the data retrieval and transfer is at its best.

One of the ways to reduce the delay in the availability of data and to increase the probability of data being available would be to perform incremental downloads during the day. The data could be retrieved by the Operational Data Centers every 6 or 8 hours, processed and sent to the Global Data Centers where it would be available to the ACS. The current RINEX file naming convention can accommodate multiple files per day. It could be agreed that the *statdoy0.yyo* file name would correspond to a whole day and that *statdoyi.yyo* with $i > 1$

Table 1. Number of stations available at CDDIS for the last two months

Region	Delay after 00:00 UTC			
	< 2 h	< 5 h	<12h	<48h
NA	2 - 18	11-41	20-50	25-54
EU	3 - 12	5 - 16	8-22	16-26
IN	0 - 3	2 - 9	4-11	5 - 12
AS	0 - 5	0 - 6	2 - 7	4 - 13
SA	0 - 3	0 - 8	1-11	3-13
PA	0 - 2	0 - 8	1-12	1-13
All	12-34	29-79	45-103	57-126

corresponds to a fraction of the day. Fractional files could be stored in a different directory accessible to the ACS and then combined in a whole day file for final archiving. Incremental delivery would insure that some data would be available for rapid orbits even if there were communication problems right after 00:00 UTC. It would also allow for more frequent computation of rapid and predicted orbits. Reduction of the turn-around time leads to improved predictions because the predicted orbit is less "old" and therefore better. At the moment we have a 24 hour delay of the predictions, but this could easily be reduced to 12 hours .

ORBIT MODELS

The most characteristic features of the orbit models that are used by the ACS for rapid and predicted orbits are listed in Table 2. Special emphasis is given to the description of radiation pressure models, stochastic accelerations and the handling of eclipsing satellites. One of the points that are handled differently by every center is the prediction of cops. To make the orbits more consistent the IGS could produce a set of predicted Earth orientation parameters, based on the rapid cops and that could be used for generating and using orbit predictions.

As can be seen in the Figure 6 the IGS rapid orbits are very close to the final orbits and it is believed that the best way to improve them would be through the increase in the amount of data that is available to the Analysis Centers, more data from remote regions and more recent data. Data from the same day could be used to improved the rapid orbits, if an incremental delivery system for the data from the IGS stations is implemented.

The situation for the predicted orbits is not so good, see Figure 7, even when the comparison wrms with the rapid orbits sometimes goes down to under 50 cm, other times it is much worse. In Figures 8 to 11 it can also be seen the rms for individual satellites, both for the

Table 2. Rapid and predicted processing at the Analysis Centers

	CODE	EMR	ESA	GFZ	JPL	NGS	S10	USNO
RAPID ORBITS								
Started at (hours)	+8 to +12	+13	+14	+11	+8 to +11	+6.5	+15.5	+5
Duration (hours)	3.5	3.0	4.0	2.5	10.0	4.0	3.0	10.0
ROCK 4(2)T	yes	yes	yes	yes	yes	yes		yes
CODE orbit model	ye-s	-					yes	
stochastic DVs	along track - per rev		3 comp.	at 3 comp. eclipse exit at 12:00				
stochastic accel.					yes	-		X+Z
cycle per rev. ace.	-		radial (c+s) -					
est. orb. par. per arc	6+5	6+3	6+2+2	6+2	6+2	6+2	6+9	6+2
est. orb. par. per rev.	1		(3)	3/2				
est. orb. par. per step					3			2
yaw rate estimated				yes	yes	-		yes
PREDICTIONS						N/A		N/A
IGR days fitted	-	4	4or1	3or1	4			
ACR days fitted	3		(1)	1	(1)		2	
cops	CODE	IGR/Bull.A	IGR	GFZ	JPL		S10	
ROCK 4 T			yes	yes	yes			
CODE orbit model	all	all	-	all	ax, ayc		all	
cycle per rev. ace.	-		all	(c+s) -	-			
est. orb. par.	6+9	6+9	6+2+6	6+9	6+2+4		6+9	
standard aat	rms of fit	rms of fit	ae = 9	?	rms of fit		overlap	
bad fit sat.	rms of fit	rms of fit	ae= 13	100 cm	rms of fit		overlap	
eclipsing sat.	rms of fit	rms of fit	ae = 16	200 cm	rms of fit		overlap	
maneuvering sat.	-		excluded	-				

predicted orbits and for the broadcast orbits and for non-eclipsing and eclipsing satellites. It can be seen that there are problematic satellites (**PRN#23**) and that the rms for eclipsing satellites is higher than that for others. In general the predicted orbits are much better than the broadcast orbits but this is not always true.

Table 3. Effect of different perturbations on the GPS satellites over 24 hours

Perturbation	Magnitude (m)			Total
	Radial	Along	Cross	
Earth oblateness	1335	12902	6101	14334
Moon (gravitation)	191	1317	361	1379
Sun (gravitation)	83	649	145	670
C(2,2), S(2,2)	32	175	9	178
Solar Radiation Pressure	29	87	3	92
C(n,m), S(n,m) (n,m=3..8)	6	46	4	46

Orbit models could be improved to improve the prediction accuracy for those satellites that are not problematic and especially to improve the prediction of eclipsing satellites.

The largest non gravitational effect on the GPS satellite orbits is the Solar radiation pressure (RPR). Table 3 shows the effect that different perturbations have on the GPS satellites. The values in Table 3 were computed by integrating a given set of osculating Keplerian elements over a time period of one day (24 hours) with the respective parameters turned on or off. Given is the RMS of the orbit differences over the full 24 hour arc-length over all satellites (using the full satellite constellation of 1-1- 1998). As can be seen the size of the perturbation caused by the Solar radiation pressure is only exceeded by the effects of the Earth oblateness, the gravitational effects from Sun and Moon and the lower harmonics (C(2,2) and S(2,2)) of the Earth gravity field. Clearly an accurate Solar radiation pressure model is as important as an accurate gravity model of the Earth.

The basis of the RPR-models currently used was furnished by Rockwell International, the spacecraft contractor for Blocks I and II [Fliegel et al., 1992]. The computer programs that embody this model became known for Block I as ROCK4, [Fliegel et al., 1985] and for Block II as ROCK42, [Fliegel and Gallini, 1989] although they are also known as the Porter models. The ROCK models are expressed in the satellite fixed coordinate system. This system has its origin in the center of mass of the satellite. Its Z-axis points in the direction to the center of mass of the Earth, and therefore along the satellite antennas. The X-axis is positive toward the half plane that contains the Sun and the Y-axis completes a right-handed system and points along one of the solar panel beams. For high precision geodetic work it is advised to estimate a scale term and a force in the Y-direction, the Y-bias, in addition to the ROCK model. The ROCK model therefore only serves as a-priori information. Both the scale term and the Y-bias are parameters which are supposed to vary slowly in time. Although the cause of the Y-bias is unknown its effect on the orbit is very significant. The claimed accuracy of the ROCK models is about 3%. Taking the nominal value of $1 \cdot 10^{-7} m/s$ for the solar radiation pressure and the claimed accuracy of 3% of the T20 model the expected error is approximately

$3 \cdot 10^{-7} m/s$. Furthermore the size of the Y-bias, which is not included in the ROCK models, is about $1 \cdot 10^{-9} m/s$. The effect of both error sources is about 3 meters (RMS over 24-hours). Of course we have to keep in mind here that the ROCK models were developed for orbit estimation using pseudo-range data! With pseudo ranges the orbit estimates have an accuracy of about 1 meter. For this type of accuracy the ROCK model is adequate to serve as a-priori model provided the scale term and the Y-bias are estimated,

Clearly for IGS type of accuracies, e.g. centimeter type orbit accuracies, the ROCK-models are inadequate, even when the scale and Y-bias are estimated. This is also obvious from the additional orbit parameters which most of the IGS ACS are estimating, be it deterministic and/or stochastic parameters. However, additional orbit parameters may weaken the GPS solutions significantly, especially the LOD estimates. Therefore it should be studied if an improved **RPR-model** can be found. Possibly it can be derived from the available IGS products and experiences. When developing a new **RPR-model** there are two questions which should be asked:

- How accurate/reliable can a new **RPR-model** be derived?
 - which parameters should be estimated/modeled
 - how accurate can these parameters be estimated
 - . . . from real GPS data
 - . . . from precise orbits
 - how accurate can we model these parameters (to what extend are the selected parameters correlated).
- What may be expected from a new (improved) **RPR-model**:

Improved (orbit) estimates. With a good **RPR-model** less orbit parameters will have to be estimated, or the estimated parameters may be (more) constrained, e.g. stochastic pulses. This may be especially useful for the rapid orbits.

More reliable orbit predictions. If less parameters are used for the orbit predictions they will become more reliable. This, however, depends on the type of parameters. Constant accelerations are much more “dangerous” than periodic (e.g. once per revolution) accelerations. Nevertheless good a-priori knowledge of the value of the **RPR**-parameters will help in identifying “bad” predictions.

Better orbit predictions This will be difficult because, a better **RPR-model** will not directly lead to better predictions. For the predictions usually the precise orbits are used as pseudo observations. This means that the “observations” are 3-dimensional positions which are a very strong observation type; much stronger than the double difference phase observations normally used. This implies that a relatively large number of parameters can be estimated without too much problem. However, if the **RPR-model** improves the rapid orbits then also the predictions will become better. The quality of the orbit predictions depends quite strongly on the quality of the rapid orbits.

Table 4. Orbit fit (7-day) and orbit extrapolation (2-day) using different RPR models. Only scale (or Do) and Y-bias estimated

RPR MODEL	Fit	Prediction	
	RMS (cm)	Median (cm)	RMS (cm)
No Model	75	133	159
T20	76	134	161
T20 Scaled	72	119	151
JPL Scaled	10	45	58
CODE	6	17	31
CODE-9	5	17	22

The CODE and JPL IGS analysis centers have successfully developed new and improved **RPR-models** over the last years, [Bar-Sever 1997, Springer et al. 1997]. Table 4 list the results of a test using the different available RPR-models. It shows the RMS of fit using seven days of precise orbits. The orbit resulting from the 7-day fit was extrapolated for 48-hours. The last 24-hours of this extrapolation were compared with the “true” orbit. The CODE IGS Final products (orbit and **EOPs**) were used. In all cases only the scale term (or a constant acceleration in the direction sun-satellite) and the Y-bias were estimated. Only for the solution **labelled** CODE-9 more RPR-parameters (9) were estimated. This solution is given as reference to show the best obtainable predicted orbit for the selected test.

Table 4 shows that including the ROCK-model as a-priori **RPR-model** does hardly give any improvement, both in fit and in prediction. Although it was clear for a long time that the ROCK-models are not very accurate, this is a still surprise! Very clearly both the CODE and JPL RPR-models perform much better than the ROCK-model. The results also show that indeed it is very difficult to get better orbit predictions. However, the reduction of the number of parameters (from 9 to 2) without significant loss of accuracy should make the prediction more reliable. More important will be to study the effect on the orbit estimates. If the **RPR-models** help to improve the (rapid) orbit estimates then also the predictions will be improved.

QUALITY ASSURANCE

The inter-comparison of rapid orbits provides for **an** accurate assessment of the quality of the **IGS** rapid orbits. That is not the case for predicted orbits, where the different ACS are using basically the same information to generate the predictions. There are ways to decide which satellites are less predictable, like checking the fit rrns for the four days and considering whether they are in the eclipse season or a maneuver is going to be performed. This is a very

important matter because users of the predicted orbits should use them in combination with the accuracy exponents that define the prediction error in order to get the best estimate of their derived products.

Lets assume that we have a parameter that we want to estimate based on the values of other variables and the estimation error for the parameter linearly depends on the error or the values of the variables. The estimates of the variables have an accuracy estimate attached and also a true accuracy. The accuracy estimate is used to weight the variables (that are used as observations) in the estimation of the parameter. For simplicity lets assume that the all variables provide the same observability for the parameter, and lets suppose that this is unity. The least-squares error for the parameter will be:

$$\epsilon_x = \frac{\sum_i \frac{\hat{\sigma}_i^2}{\sigma_i^2}}{\sum_i \frac{1}{\sigma_i^2}} \quad (1)$$

It can be observed that the error itself would be the same if all the accuracy estimates would be multiplied by a constant. That is not the case for the estimate of the accuracy of the **parameter**. Assuming that the values of the variables are not correlated:

$$\sigma_x^2 = \frac{1}{\sum_i \frac{1}{\hat{\sigma}_i^2}} \quad (2)$$

We can also compute the actual accuracy of the parameter:

$$\sigma_x^2 = \frac{\sum_i \frac{\sigma_i^2}{\hat{\sigma}_i^4}}{\left(\sum_i \frac{1}{\hat{\sigma}_i^2} \right)^2} \quad (3)$$

The optimal set of weights (accuracy estimates of the variables) will be the one that would minimize the actual accuracy of the parameter. The values of the accuracy estimate that result are:

$$\hat{\sigma}_i = K \cdot \sigma_i \quad (4)$$

As an example the IGS predicted orbits for day 0942/0 produced the following values:

$$\begin{aligned} rms &= 137.8cm \\ wrms &= 49.0cm \\ wrms_{optimal} &= 20.1cm \end{aligned}$$

A more than twofold improvement in accuracy for the users of the orbits could have been achieved by setting the accuracy exponents to the (at the time of the combination unknown) optimal values!

It can be shown that the critical factor for the degradation of the accuracy is to set a low value for the accuracy exponent of a satellite that has not been predicted accurately. To mistakenly tag a good satellite as bad has a much smaller impact.

RECOMMENDATIONS

1. Ask the Operational, Regional and Global Data Centers to give the highest priority to the prompt retrieval and distribution of data from sites outside Europe and North America.
2. Ask the Operational, Regional and Global Data Centers to investigate and implement ways of reducing the data retrieval and distribution delays.
- 3. Ask the Operational, Regional and Global Data Centers to study and implement more frequent down-loading of the data.**
4. Ask those Analysis Centers that are evaluating more precise radiation pressure models to make them publicly available, and encourage all Analysis Centers to implement and use them when they have been validated.
5. Ask the IERS Rapid Service and the Analysis Centers to investigate and propose ways to obtain predicted cops (pole and UT1) for use in the calculation of IGS predicted orbits.
6. Ask the Analysis Centers **and** the AC Coordinator to study, monitor, and, if possible, improve the fitness of the accuracy codes for the predicted orbits.
7. Ask the Analysis Centers to investigate the ways and the consequences of reducing the turn-around time for rapid and predicted products.
8. Review data and rapid product delivery times at July 1 and October 1 in order to evaluate the change of the deadline for rapid products to no later than 16:00 UTC by January 31998.

REFERENCES

- Bar-Sever, **Yoaz** E. (1997), New and Improved Solar Radiation Models for GPS Satellites Based on Flight Data, Final Report for the Air Force Materiel Command Space and Missile Systems **Center/CZSF**, April 121997.
- Fliegel**, H. F., and T. E. **Gallini** (1989), Radiation Pressure Models for Block II GPS Satellites, in Proceedings of the Fifth International Symposium on Precise Positioning with the Global Positioning System, pp. 789--798, National Geodetic Survey, NOAA, **Rockville, Md.**, April 1989.

- Fliegel, H. F., W. A. Feess, W. C. Layton, and N. W. Rhodus (1985),** The GPS Radiation Force Model, in Proceedings of the First International Symposium on Precise Positioning with the Global Positioning System, edited by Clyde Goad, pp. 113--119, National Geodetic Survey, NOAA, **Rockville, Md.**, March 1985.
- Fliegel, H. F., T. E. Gallini, and E. R. Swift (1992),** Global Positioning System Radiation Force Model for Geodetic Applications, *Geophysical Research Letters*, 97(B 1), 559--568.
- Springer, T. A., G. Beutler, and M. Rothacher (1997),** Improving the GPS Orbit Model, presented at the 1997 AGU Fall Meeting, *EOS Transactions*, 00(00), 00--00, December 9 1997.

Data Available Before 02:00 UTC

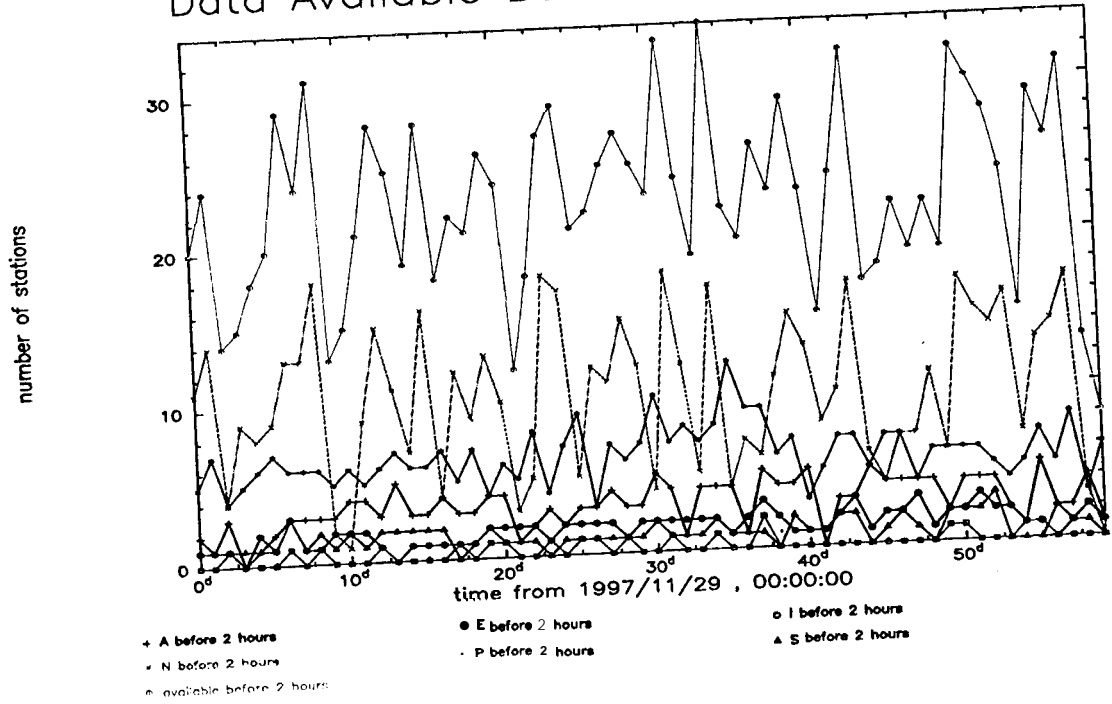


Fig. 2. Data available at CDDIS before 02:00 UTC

Data Available Before 05:00 UTC

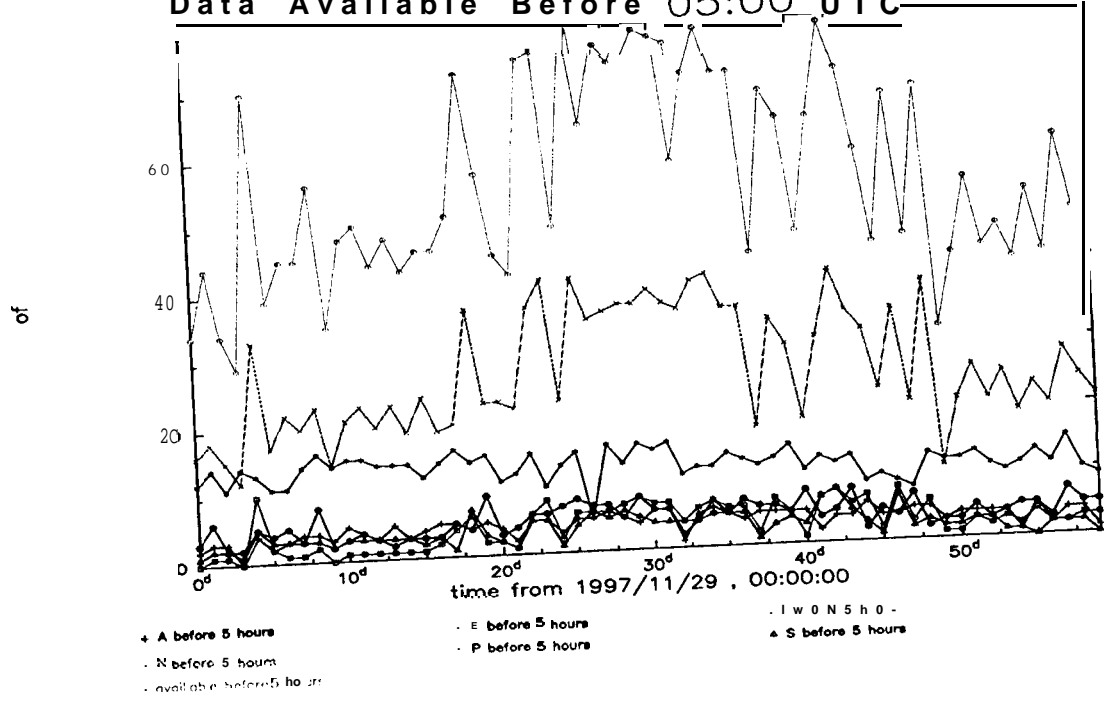


Fig. 3. Data available at CDDIS before 05:00 UTC

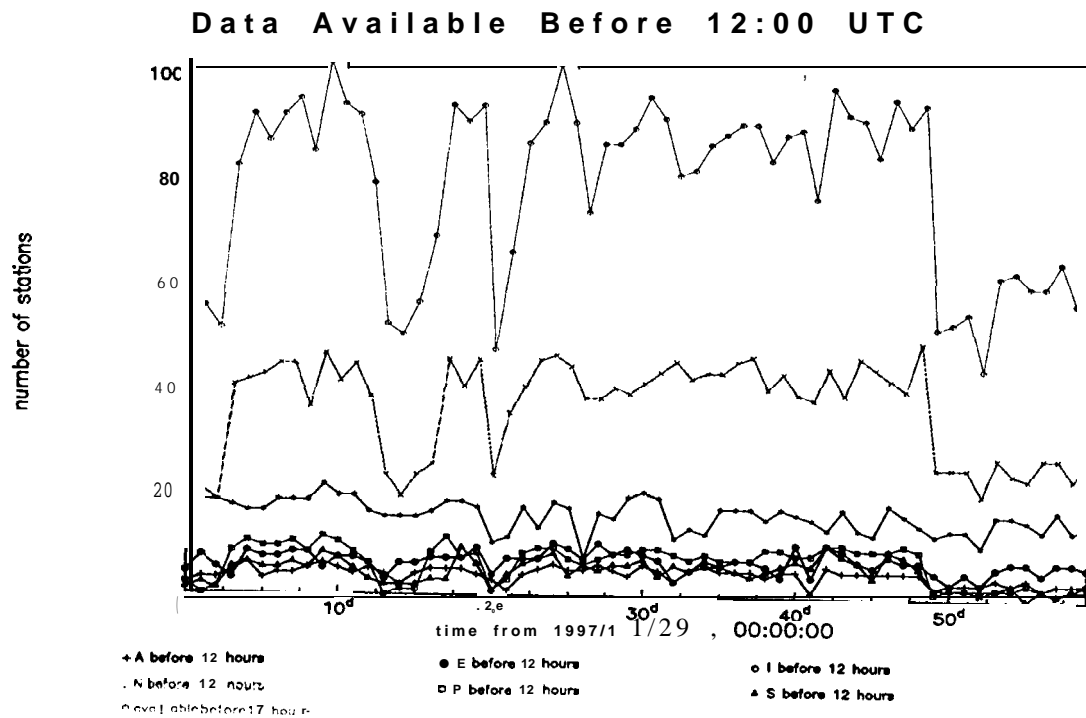


Fig. 4. Data available at CDDIS before 12:00 UTC

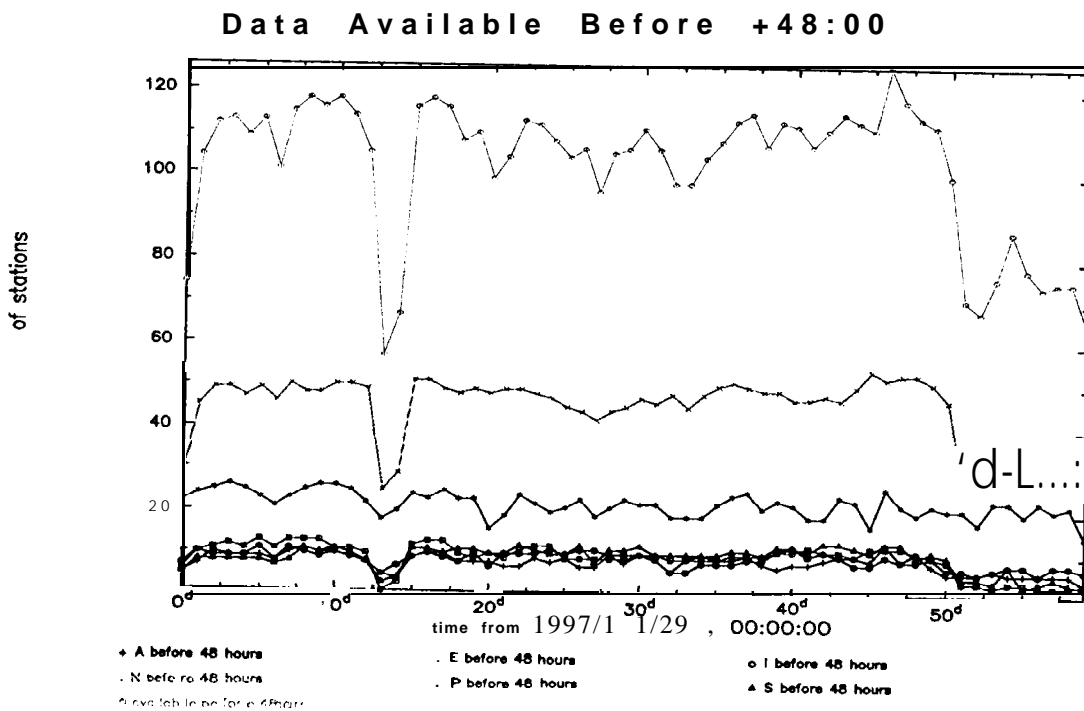


Fig. 5. Data available at CDDIS before 48 hours after collection

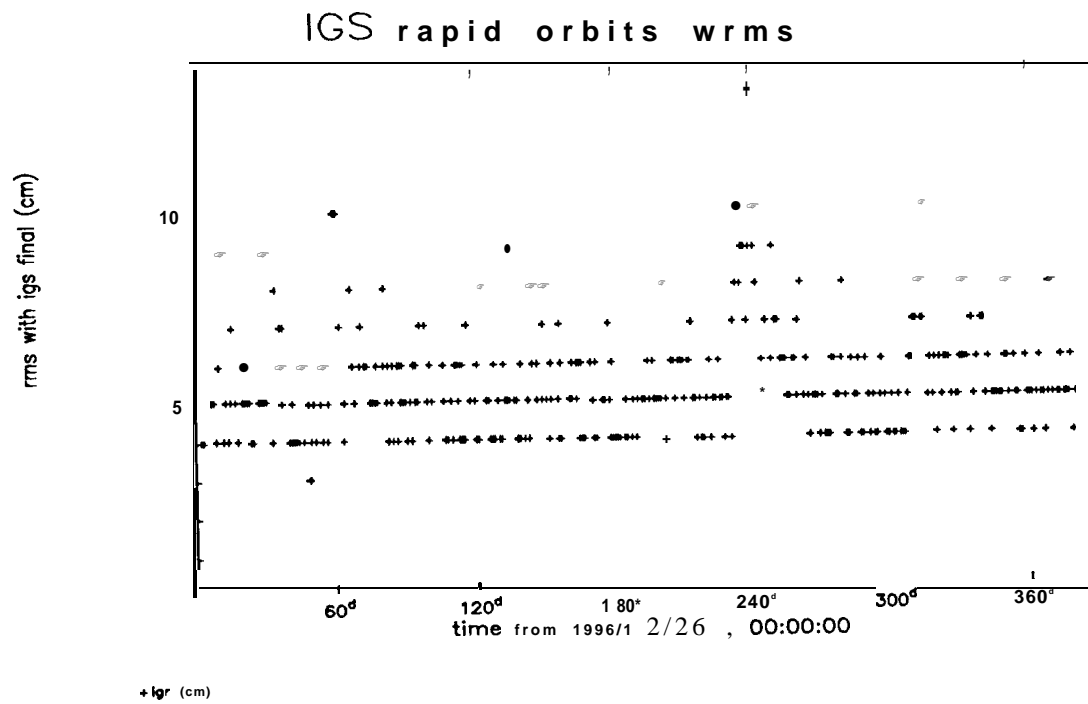


Fig. 6. Comparison weighted rms of rapid orbits with respect to final orbits

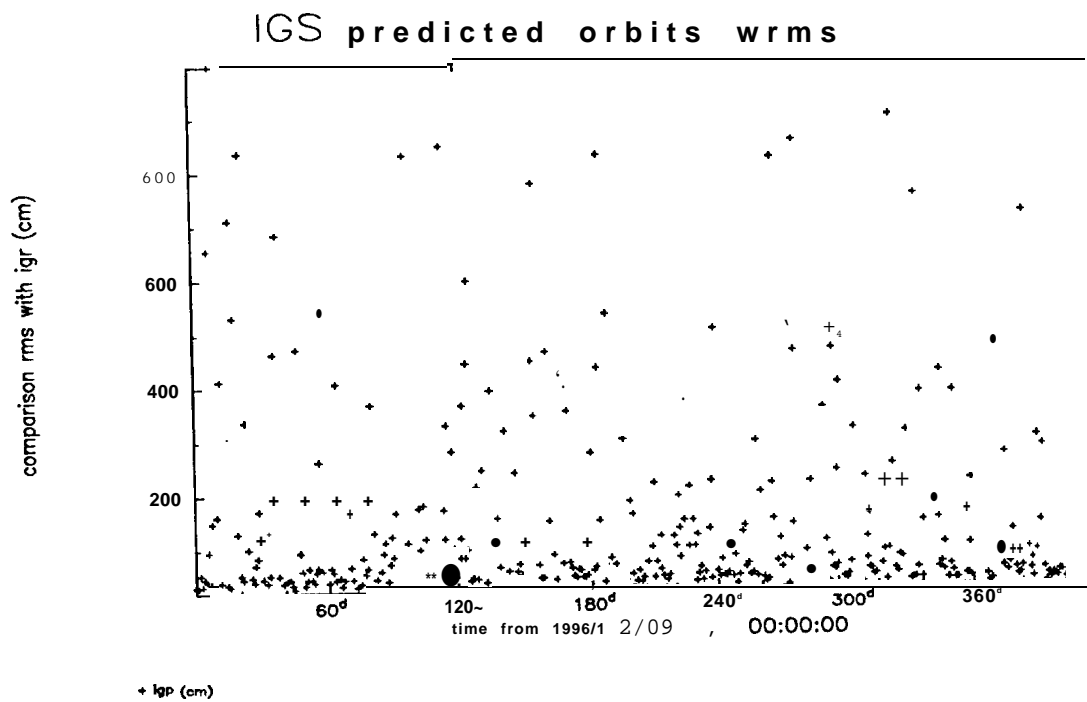


Fig. 7. Comparison weighted rms of predicted orbits with respect to rapid orbits

IGS predicted orbits for non-eclipsing satellites

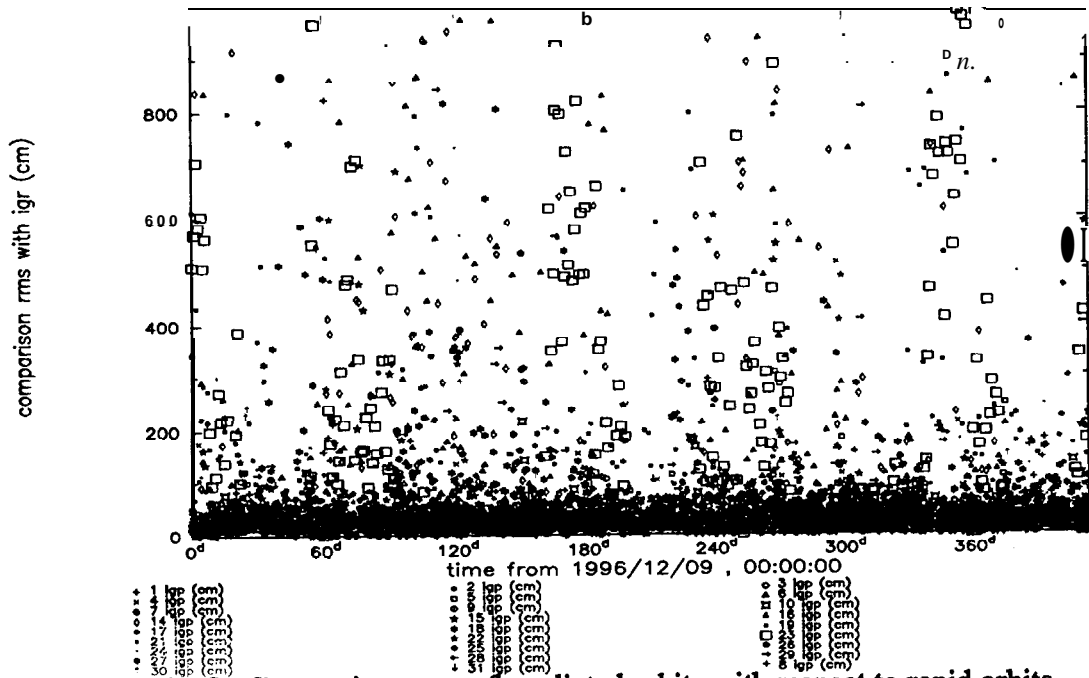


Fig. 8. Comparison rms of predicted orbits with respect to rapid orbits for non-eclipsing satellites

IGS predicted orbits for eclipsing satellites

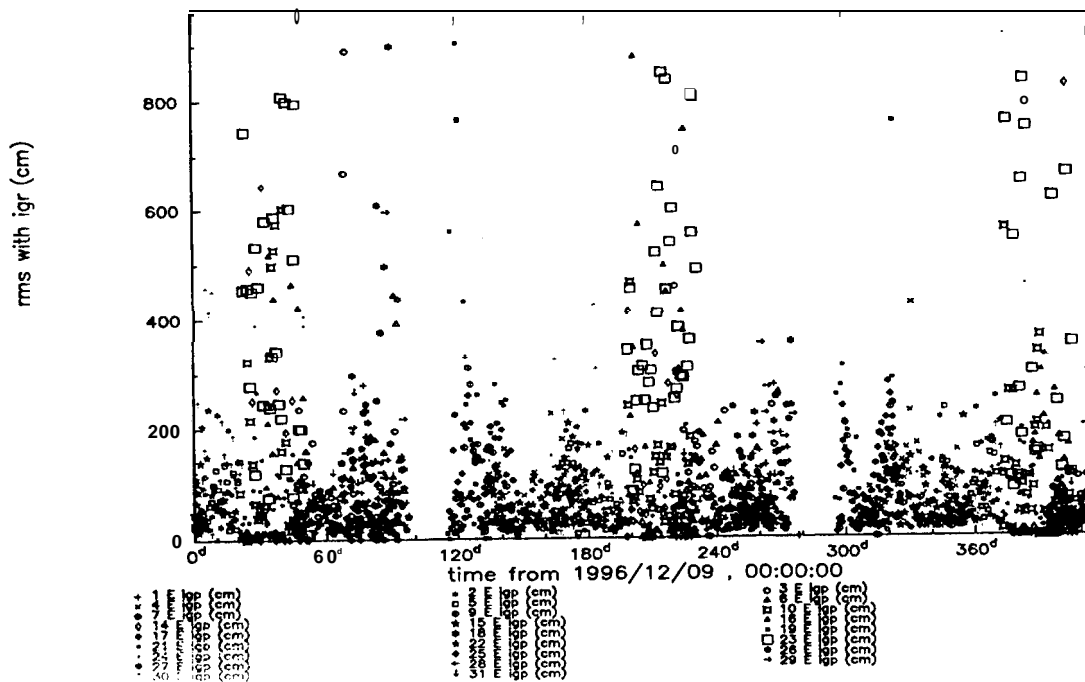


Fig. 9. Comparison rms of predicted orbits with respect to rapid orbits for eclipsing satellites

Broadcast orbits for non-eclipsing satellites

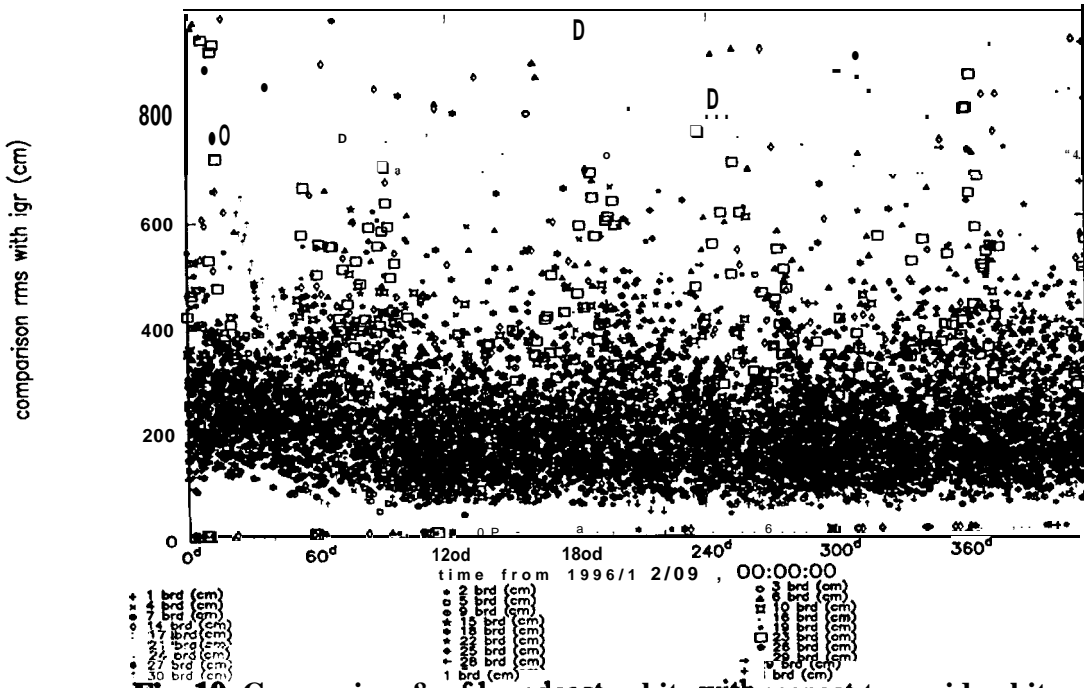


Fig. 10. Comparison of broadcast orbits with respect to rapid orbits for non-eclipsing satellites

Broadcast orbits for eclipsing satellites

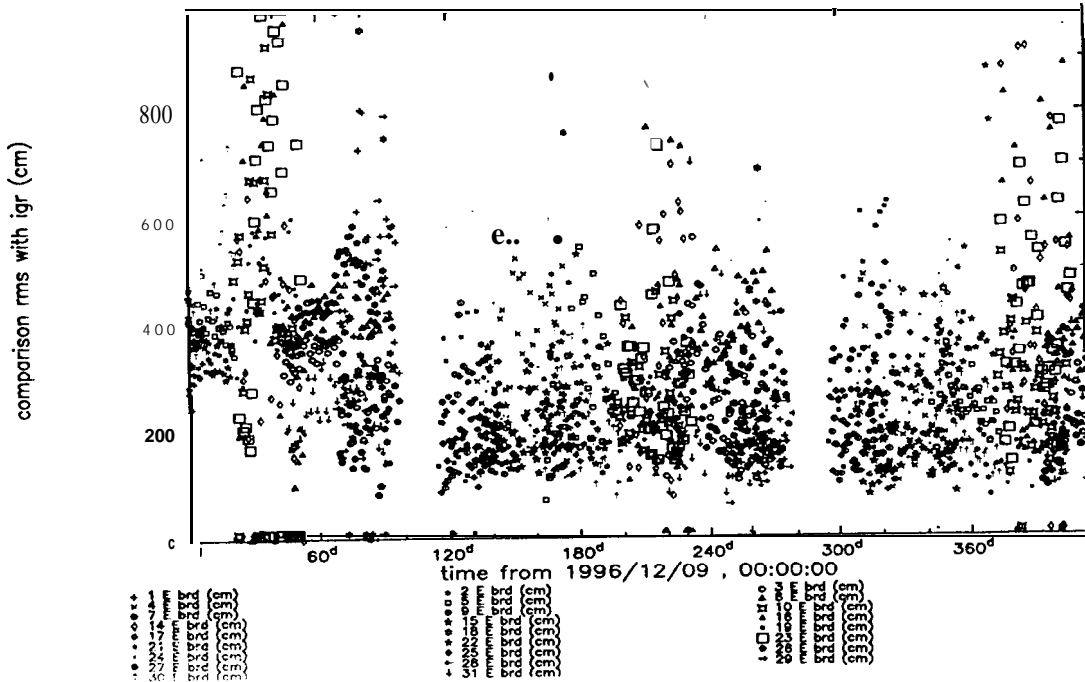


Fig. 11. Comparison rms of broadcast orbits with respect to rapid orbits for eclipsing satellites

A new Solar Radiation Pressure Model for the GPS Satellites

T.A. Springer, G. Beutler, M. Rothacher
Astronomical Institute, University of Bern
Sidlerstrasse 5, CH-3012 Bern, Switzerland

Abstract

The largest error source in GPS orbit modeling is due to the effect of the solar radiation pressure. Over the last few years many improvements were made in modeling the orbits of GPS satellites within the IGS. However, most improvements were achieved by increasing the number of estimated orbit and/or solar radiation pressure parameters. This increase **in** the number of estimated satellite parameters weakens the solutions of **all** estimated parameters. Due to correlations the additional parameters may cause biases in other estimated quantities like, e.g., the length of day.

In this paper a recently developed solar radiation pressure model for the GPS satellites is presented. This model is based on experiences and results acquired at the Center of Orbit Determination in Europe (CODE) Analysis Center during its IGS activities since June 1992. The new model outperforms the existing ROCK models by almost an order of magnitude. It also allows a reduction of the number of orbit parameters that have to be estimated!

Introduction

The largest non-gravitational effect on the GPS satellite orbits is the solar radiation pressure (RPR). To underline this, Table 1 shows the effect of different perturbations on the GPS orbits. The results in Table 1 are based on integrating a given set of osculating **Keplerian** elements over a time period of one day (24 hours) with the respective perturbations turned on or off. Table 1 gives the RMS of the differences between the resulting two orbits, one with the perturbation turned on and one with the perturbation turned off. The RMS was computed using the full 24-hour arc length and all satellites (using the **full** satellite constellation of January 1, 1998). It can be seen that the size of the perturbation caused by the solar radiation pressure is only exceeded by the effects of the Earth **oblateness**, the gravitational attraction by Sun and Moon, and the lower harmonics (**C(2,2)** and **S(2,2)**) of the Earth's

Table 1. Effect of different Perturbations on the GPS satellites over 24 hours

Perturbation	Magnitude (m)					
	Radial	Along	Cross	Total		
Earth oblateness	1335	12902	6101	14334		
Moon (gravitation)	191	1317	361	1379		
Sun (gravitation)	83	649	145	670		
C(2,2), S(2,2)	32	175	9	178		
Solar Radiation Pressure	29	87	3	92		
C(n,m), S(n,m) (n,m=3..8)	6	4	6	4	4	6

gravity field. The results clearly show that an accurate solar radiation pressure model for the GPS satellites is as important as an accurate gravity model of the Earth.

The basis of the RPR models currently used was furnished by Rockwell International, the spacecraft contractor for the Block I, **II** and **IIa** satellites [Fliegel *et al.*, 1992]. The computer programs that embody this model became known as **ROCK4** for Block **I** [Fliegel *et al.*, 1985], and **ROCK42** for Block **II** and **IIa** satellites [Fliegel and Gallini, 1989]. They are *also known* as “the Porter models”. The ROCK models are expressed in the satellite-fixed coordinate system. This system has its origin in the center of mass of the satellite. Its Z-axis points in the direction of the center of mass of the Earth, and therefore along the satellite antennas. The X-axis is positive toward the half plane that contains the Sun and the Y-axis completes a right-handed system and points along one of the solar panel beams.

For high precision geodetic work it is necessary to estimate a scale term and a force in the Y-direction, the Y-bias, in addition to using the ROCK model. The ROCK model, therefore, only serves as a priori information. Both, the scale term and the Y-bias, are parameters which are supposed to vary slowly in time. Although the cause for the Y-bias is unknown, its effect on the orbit is significant. The claimed accuracy of the ROCK models is about 3%. Taking the nominal value of $1 \cdot 10^{-7} m/s^2$ for the solar radiation pressure acceleration of a GPS satellite and the claimed accuracy of 3% for the T20 model, the expected error in acceleration is approximately $3 \cdot 10^{-9} m/s^2$. Furthermore the size of the Y-bias, which is not included in the ROCK models, is about $1 \cdot 10^{-9} m/s^2$. The effect of both error sources is about 3 meters (RMS) over 24-hours! Of course, we have to keep in mind that the ROCK models were developed for orbit estimation using pseudo-range data. With pseudo-ranges, position estimates with an accuracy of about 1 meter may be obtained, For this type of accuracy the ROCK models are adequate to serve as (a priori) model, provided, the scale term and the Y-bias are estimated.

The ROCK models are inadequate for **IGS-type** accuracies, e.g., centimeter-type orbit accuracies, even if the scale and Y-bias are estimated. This is also obvious from the additional orbit and solar radiation pressure parameters which most of the IGS ACS are estimating, be they deterministic and/or stochastic in nature. However, additional orbit parameters may weaken the GPS solutions significantly, especially the the LOD (length

of day) estimates, Therefore it would be advantageous if an improved RPR model could be developed. The experiences gained from our IGS analysis efforts in recent years have indicated that it will indeed be possible to derive an improved RPR model [Springer *et al.*, 1998].

Below we first present a summary of the most recent orbit results. Because these results are based on the extended CODE orbit model (ECOM) [Beutler *et al.*, 1994], a short description of the ECOM is given as well. Secondly, results from orbit estimation using the GPS (IGS) precise orbits as pseudo-observations (orbit fit) are presented. Based on these results an “optimal” orbit parameterization is proposed. Using this parameterization and all CODE final orbits and EOPS, as submitted to the IGS, a long time series for the selected (optimal) set of RPR parameters is generated. The last two years (1996 and 1997) of this time series are then used to generate our new solar radiation pressure model. The article concludes with an evaluation of the quality of our RPR model and a short summary.

The Extended CODE Orbit Model

In Beutler *et al.* [1994] our orbit model, ECOM, is presented and discussed in detail. We only summarize its basic characteristics. The considerations behind the ECOM are similar to those underlying the Colombo model [Colombo, 1989]. The principal difference resides in the fact that the ECOM considers the Sun as the major ‘error source’ for the orbits, whereas the gravity field of the Earth plays this role in the Colombo model. The Colombo model uses the radial, along-, and cross-track directions as the three orthogonal directions whereas, the D-, Y-, and B-directions are used by the ECOM. Notice that in earlier publication the B-axis was referred to as X-axis. To avoid confusion with the X-axis of the ROCK models, the B-axis is introduced hereto designate the third axis of the ECOM. Beutler *et al.* [1994] demonstrated that the performance of the ECOM is superior to that of the Colombo model, which is a clear indication that solar radiation pressure is indeed the major error source in the GPS satellite orbit model. In the ECOM the acceleration \vec{a}_{rpr} due to the solar radiation pressure is written as:

$$\vec{a}_{rpr} = \vec{a}_{ROCK} + \vec{a}_D + \vec{a}_Y + \vec{a}_B \quad (1)$$

where \vec{a}_{ROCK} is the acceleration due to the ROCK model, and

$$\begin{aligned} \vec{a}_D &= [a_{D0} + a_{DC} \cdot \cos u + a_{DS} \cdot \sin u] \cdot \vec{e}_D = D(u) \cdot \vec{e}_D \\ \vec{a}_Y &= [a_{Y0} + a_{YC} \cdot \cos u + a_{YS} \cdot \sin u] \cdot \vec{e}_Y = Y(u) \cdot \vec{e}_Y \quad \& \\ \vec{a}_B &= [a_{B0} + a_{BC} \cdot \cos u + a_{BS} \cdot \sin u] \cdot \vec{e}_B = B(u) \cdot \vec{e}_B \end{aligned} \quad (2)$$

where a_{D0} , a_{DC} , a_{DS} , a_{Y0} , a_{YC} , a_{YS} , a_{B0} , a_{BC} , and a_{BS} are the nine parameters of the ECOM, and

\vec{e}_D is the unit vector Sun-satellite,

\vec{e}_Y is the unit vector along the spacecraft's solar-panel axis,

$\vec{e}_B = \vec{e}_Y \times \vec{e}_D$, and

u is the argument of latitude

The ECOM is a generalization of the standard orbit model which uses only two parameters to account for the solar radiation pressure, namely a_{D0} and a_{ye} . Note that the Y-direction of the ECOM corresponds to the Y-direction of the body-fixed coordinate system. Although not really a solar radiation pressure model in the sense of the ROCK models, the ECOM does consider solar radiation pressure to be the major perturbing force acting on the GPS satellites. Therefore the ECOM provides an excellent tool to study the effects of the solar radiation pressure on the GPS satellites. It allows to detect in which direction the most significant **unmodeled RPR** forces act on the GPS satellites.

There are two methods to study the effects different parameters of the ECOM have on the orbit estimates. **The first, and most reliable method is to use the ECOM in real orbit estimation procedures using GPS observations, very much like the routine orbit estimation performed** at CODE as part of its IGS activities. **The second method** is to use the orbits as provided by CODE as "pseudo-observations" estimating an arc extending over several days which gives the best fit, in a least squares sense, to the observations. This second method is less correct but **computationally** much more efficient than the first. The generation of a 3-day arc using the "orbit fit" method typically takes 1 minute whereas the "orbit estimation" method will take several hours. Results **from** both methods, orbit estimation and orbit fit, will be discussed in the following sections.

Orbit estimation using GPS observations

In 1996 the ECOM was **fully** implemented into the **Bernese** GPS Software. It was expected that not all nine parameters of the ECOM can (and should) be estimated when estimating 3-day arcs from real GPS data. Initial tests [*Springer et al., 1996*] indicated that it is best not to solve for "B-terms", but to estimate the constant and periodic terms in the **D**- and **Y**-directions plus small velocity changes (pseudo-stochastic pulses) in the radial and along-track directions. A careful analysis of this parameterization showed that it leads to a significant degradation of the quality of the LOD estimates. It was therefore decided to systematically test the different parameters of the ECOM in order to find the "optimal" parameterization. In [*Springer et al. [1998]*] a detailed description of the results from two extensive tests using the ECOM is given. The difference between the two extensive test series is, that in the first test series pseudo-stochastic pulses [*Beutler et al., 1996*] were always estimated (stochastic test series) whereas in the second test series they were never estimated (deterministic test series),

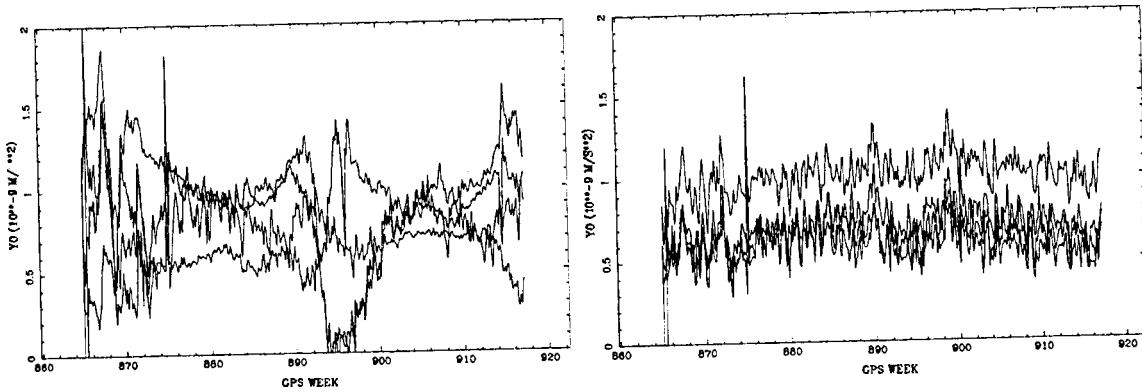
The stochastic test series showed that the estimation of the constant and periodic terms in the B-direction, in addition to the estimation of the constant terms in the D- and Y-direction, and the pseudo-stochastic pulses in the radial and along-track directions, significantly improves the quality of the orbit estimates. An improvement was seen in all estimated parameters: orbits, station coordinates, and EOPS. Only for the LOD estimates a small, but significant, degradation in quality was observed. The improvement of the orbit quality was estimated to be a factor of two to three, compared to the results without estimating the three terms in the B-direction! As a direct consequence of these tests the estimation of the B-terms was implemented for the generation of the CODE contributions to the IGS on September 29, 1996.

The second, deterministic, test series confirmed that the periodic terms in the B-direction most significantly reduce the orbit model deficiencies. Evidence was presented that the periodic signals in the Y-direction reduce the orbit model deficiencies as well. The periodic signals in the B-direction, however, were shown to be more important than those in the Y-direction. The deterministic test series further showed that a purely deterministic orbit parameterization, consisting of the constant terms in the D- and Y-directions plus periodic terms in the D- and B-directions, gives excellent orbit results. Because of a degradation of the LOD estimates this deterministic orbit model is currently not considered for the IGS activities at CODE.

The results based on one full year of routine orbit estimates using **the** standard (R3) and new (X3) orbit parameterizations (3 B-terms) showed that the **behaviour** of the estimated stochastic and deterministic orbit parameters significantly improves with the new orbit parameterization. This is true in particular for the Y-bias (see Figure 1), and the radial pseudo-stochastic pulses (see Figure 2). Tests without estimating the radial pseudo-stochastic pulses showed that with the new orbit parameterization these pulses no longer have to be estimated. Considering the fact that pseudo-stochastic pulses are meant to absorb orbit model deficiencies it is clear that the modeling deficits are significantly reduced in the new orbit parameterization. Because the **behaviour** of all estimated RPR parameters in the X3 solutions is "predictable" it is expected that an improved RPR model may be developed.

Orbit estimation using satellite positions as pseudo-observations

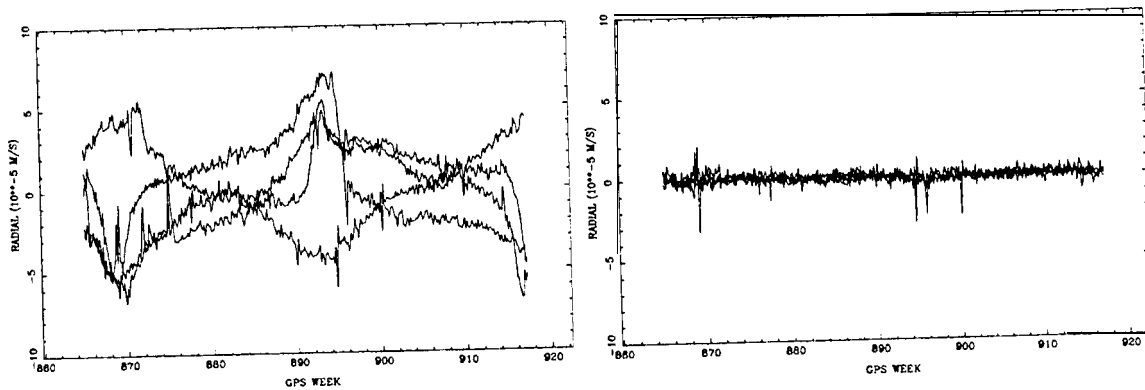
The essential difference between orbit estimation, using real (GPS) data, and orbit fit, using previously determined satellite positions as pseudo-observations, lays in the type of observations used. For the orbit estimation double-difference GPS carrier phase observations are used whereas for the orbit fit the observations are the position vectors of the satellites. The position vectors are very strong observations for orbit estimation whereas the double-difference carrier phases do not contain very much information about the satellite position. Only thanks to the dense global network it is possible to get accurate GPS orbit estimates based on carrier phase data. Due to this significant difference the



(a) Standard Orbit Parametrization

(b) New Orbit Parametrization

Figure 1. Estimated Y-bias (Y_0) using the two different CODE orbit parameterizations. Only PRNs 3,6,7, and 31 in orbital plane C are shown.



(a) Standard Orbit Parametrization

(b) New Orbit Parametrization

Figure 2. Estimated radial pseudo-stochastic pulses using the two different CODE orbit parameterizations. Only PRNs 3,6,7, and 31 in orbital plane C are shown.

results from orbit fit tests always have to be verified using real GPS data analysis.

The goal of the orbit fit tests was to find the optimal orbit parameterization. For this purpose a “standard test” was developed in order to be able to compare the results. The selected standard test consists out of a 7-day orbit fit using the CODE final products, e.g., precise orbits plus their respective Earth Orientation Parameters (**EOP**). The resulting 7-day arc is extrapolated, using orbit integration, for 48 hours. The last 24 hours of this orbit prediction are compared to the CODE final orbit for the same day. The period from March 13 to March 21 in 1997 was selected as test interval. The following quantities are considered as quality indicators for the orbit parameterization:

- the RMS of the residuals of the 7-day fit,
- the RMS of the residuals of the orbit prediction comparison, and
- the median of the residuals of the orbit prediction comparison.

First, we studied whether our standard orbit fittest gives similar results as the deterministic orbit estimation test discussed earlier. It was verified that the results were indeed very similar. Only one **small** anomaly was detected in the estimation of the periodic terms in the Y- and B-direction. In the orbit fit the effect of the periodic terms in these two directions are almost identical whereas in the orbit estimation test a significant difference was observed favoring the periodic terms in the B-direction,

As mentioned above the orbit fit method is based on a strong observation type making it possible to estimate a large number of orbit parameters. Therefore, our software was enhanced to estimated periodic terms up to six times per orbital revolution. Furthermore, modifications were made to allow for periodic terms in two other coordinate systems: the satellite-fixed reference frame (**Z, Y, X**) and the ‘classical’ orbit system radial, along-, and cross-track (R, S, W). In addition, the argument for the periodic terms was slightly changed to account for the position of the Sun with respect to the ascending node. This change is a consequence of the assumption that the solar radiation pressure is the major ‘error source’ in the GPS orbit modeling. It is therefore logical to relate the time argument of the periodic signals to the position of the Sun in the orbital plane. Thus, the argument of latitude is corrected for the latitude of the Sun in the orbital plane (u_0), [*Rothacher et al., 1995*]. After extensive tests, using many different combinations of the available parameters, a small set of optimal orbit parameterizations was found, Table 2 lists these “best” parameterizations.

All candidate parameterizations were subsequently used in real orbit estimation using one full week of GPS data, This test confirmed that all 5 parameterizations perform very **well** apart from some correlation with the LOD. Because of the slightly better performance and its resemblance with the ROCK model, “model 5” (Table 2) was selected as the ‘optimal’ orbit parameterization. It consists of three constant terms in the D-, Y-, and B-directions

Table 2. Selected “optimal” orbit parameterizations.

Model	Constant Terms	Periodic Terms
1	D, Y, and B	B sin($u - u_0$) and D sin($u - u_0$)
2	D, Y, and B	B sin($u - u_0$) and B sin($2u - u_0$)
3	D, Y, and B	Z sin($u - u_0$) and X sin($u - u_0$)
4	D, Y, and B	Z sin($u - u_0$) and X sin($3u - u_0$)
I 5	D, Y, and B	Z sin($u - u_0$), X sin($u - u_0$), and X sin($3u - u_0$)

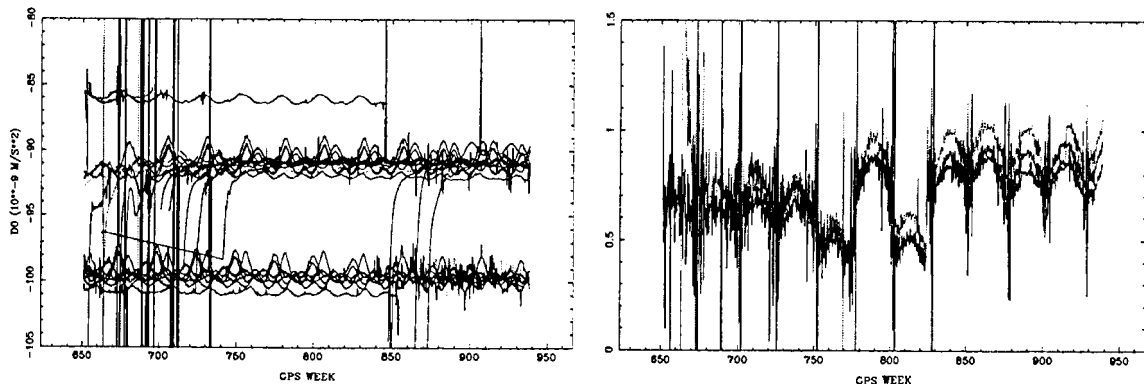
and three periodic sine terms: once-per-revolution terms in the Z-, and X-direction and one three-times per revolution term in the X-direction.

The New Solar Radiation Pressure Model

Using the “optimal” orbit parameterization (model 5 in Table 2) all final CODE orbits with their respective **EOPs**, as submitted to the IGS since June 1992, were used in an orbit fit. An arc length of 5 days was chosen and **no** a priori solar radiation pressure model was used. This resulted in a long time series, covering 5.5 years, of estimates for the selected (optimal) set of **RPR** parameters. It was hoped that, after careful analysis, this time series may be used to derive a new solar radiation pressure model. Figure 3 shows the estimated values for the direct solar radiation pressure (D_0) and for the Y-bias (Y_0) accelerations as function of time over the full 5.5 years. Jumps are visible in the Y-bias time series. These jumps are related to the “bias” changes in the attitude system of the GPS satellites. These biases have been kept constant since approximately November 1995. Furthermore, the eclipse phases can clearly be seen in the Y-bias estimates: the estimates are somewhat anomalous during these phases.

A careful analysis of the estimated parameters as a **function** of time showed that the **behaviour** of satellites within one orbital plane is very similar. Clear annual and semiannual signals are present. Assuming that the Sun causes the observed signals it is logical to study the **behaviour** of the **RPR** parameters as function of the angle of the Sun above the orbital plane (angle β_0). **Note** that, if the absolute value of this angle is $\leq 14^\circ$, the satellite is in eclipse. In Figure 4 the same two time series for the direct solar radiation pressure and Y-bias accelerations are shown but now as function of the angle of the Sun above the orbital plane. For the Y-bias a shorter time interval was selected to exclude the observed jumps, but more satellites are shown.

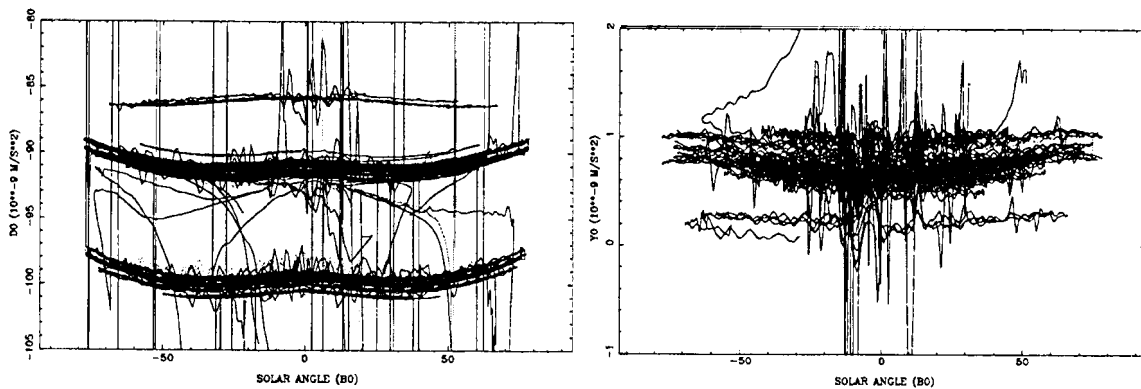
Clearly, the **behaviour** of the estimates of the direct solar radiation pressure acceleration and the Y-bias acceleration is very similar for all (Block II and **IIa**) satellites which indicates that a model can be easily derived for these parameters. The same is true for the constant term in the B-direction and for the once per revolution periodic term in the Z-direction. Both periodic signals in the X-direction do not show a very clear signal, nevertheless a model was estimated for these parameters as well. The Block I satellites, the uppermost



(a) Direct solar radiation pressure acceleration for the Block I, 11, and IIa satellites

(b) Y-bias acceleration for the satellites in orbital plane A (PRNs 9,25, 27)

Figure 3. Estimated direct solar radiation pressure acceleration (D_0) and Y-bias (Y_0) acceleration as function of time over the interval from June 1992 to 1997



(a) Direct solar radiation pressure acceleration for the Block I, 11, and IIa satellites

(b) Y-bias acceleration for the Block II and IIa satellites

Figure 4. Estimated direct solar radiation pressure acceleration (D_0) and Y-bias (Y_0) acceleration as function of the angle of the Sun above to the orbital plane. (for D_0 the complete interval from June 1992 to 1997 is shown whereas for Y_0 only the last two years (1996, 1997) are included)

lines in both plots showing the D_0 estimates, behave in a slightly different way. Although their **behaviour** is also predictable, no attempts were made to create a model for the Block I satellites. Due to the “jumps” in the estimates of the Y-bias, the model for this parameter had to be based on the estimates since 1996 only. It turned out that the performance of the complete model was better if all model parameters were uniquely based on the most recent results (since 1996). Apparently the (significant) modeling improvements made over the last few years are important when deriving a solar radiation pressure model.

Based on the careful analysis of the orbit fit results the following terms were included in the radiation pressure model:

$$\begin{aligned}
 a_D &= D_0 + D_{C2} \cos(2\beta_0) + D_{C4} \cos(4\beta_0) \\
 a_Y &= Y_0 + Y_C \cos(2\beta_0) \\
 a_B &= B_0 + B_C \cos(2\beta_0) \\
 a_{z_p} &= \{Z_0 + Z_{C2} \cos(2\beta_0) + Z_{S2} \sin(2\beta_0) \\
 &\quad + Z_{C4} \cos(4\beta_0) + Z_{S4} \sin(4\beta_0)\} \sin(u - u_0) \\
 a_{X_p} &= \{X1, + X1_C \cos(2\beta_0) + X1_S \sin(2\beta_0)\} \sin(u - u_0) \\
 &\quad + \{X3_0 + X3_C \cos(2\beta_0) + X3_S \sin(2\beta_0)\} \sin(3u - u_0)
 \end{aligned} \tag{3}$$

Note that all three constants (D_0 , Y_0 , B_0) were chosen to be satellite-specific and that the Z_0 -term was chosen to be Block type dependent. The values for **all** of the above parameters are given in the Appendix. Please note that the model is only valid for Block II and **IIa** satellites. Furthermore, the values given for PRN8 should be used with care because this satellite was launched late in 1997 and by the end of the year was **still** in its ‘outgassing’ phase. Of course, satellite PRN23 should be used with care as well due to the problems with the orientation of its solar panels, The results indicate, however, that it should be possible to derive a tailored RPR model for PRN23.

Evaluation of the New Solar Radiation Pressure Model

Four different investigations were performed to evaluate the new solar radiation pressure model.

- The effect of the parameters of our **RPR** model on the satellite positions was determined to get an idea of the significance of the individual terms of the model.
- An error budget of the model was derived, based on the residuals of the **RPR** series, to get an idea of the remaining model errors.
- The model was compared, using our standard test, to other **RPR** models to check its performance.
- Finally, the model was tested in a real parameter estimation, using one full week of GPS observations.

The effects of the different parameters of the new **RPR** model on the orbit were estimated by integrating a given set of osculating **Keplerian** elements over a time period of one day (24 hours), once with the parameter turned on and once with the parameter turned off. The RMS of the difference between the two resulting orbits, over the full 24 hour period, was then computed to get an idea of the size of the effect. The results are given in Table 3.

Table 3. Effect of the individual parameters of the new **RPR** model on the GPS satellite orbits over 24 hours.

Parameter	Effect			
	Radial	Along	Cross	Total
<i>DO</i> (m)	29	87	3	92
<i>Y</i> ₀ (cm)	49	350	8	354
<i>B</i> ₀ (cm)	2	29	3	29
Z sin(<i>u</i> - <i>u</i> ₀) (cm)	15	32	0	36
X sin(<i>u</i> - <i>u</i> ₀) and X sin(3 <i>u</i> - <i>u</i> ₀) (cm)	2	11	0	11

As expected the *Do* (direct solar radiation term) and *Y*. (*Y*-bias) give the largest contributions. However, the contributions of the *Be*-term and the periodic term in the **Z**-direction (radial **direction!**) are not negligible! Note that the periodic **Z**-term has a signature very similar to the periodic terms in the **B**-direction, which CODE uses when computing its IGS orbit products. The periodic terms in the **X**-direction have an effect of only **11** cm. The typical RMS of the 5-day fits, used for the model development, is at the level of 5 cm. This means that the 11 cm effect is close to the noise level of the solutions. However, the IGS orbit combinations show an orbit consistency of about 4 cm between the orbits of different **ACs**. Thus, an 11 cm effect maybe significant.

The RPR model is based on the time series of parameter estimates computed by fitting 5-day arcs through the final products from CODE. The RMS of the residuals of the parameter estimates, after subtracting the estimated RPR model, is used to estimate the remaining errors in the model. For this purpose the RMS value was introduced as a “bias” in the corresponding RPR parameter and a 24-hour orbit integration was performed with this bias included. The difference between the biased orbit and the original orbit are a measure of the remaining orbit model errors. The results are given in Table 4. The total error budget was estimated by introducing the RMS value for all parameters as bias.

Table 4. Estimated model errors based on the parameter residuals

Error Source	Model Fit ($10^{-9}m/s^2$)	Magnitude (cm)			
		Radial	Along	Cross	Total
D_0	0.0724	2	7	0	7
Y_0	0.0416	2	15	1	15
B_0	0.2318	1	15	2	15
$Z \sin(u - u_0)$	0.1187	2	4	0	4
$X \sin(u - u_0)$	0.1454	5	36	1	36
$X \sin(3u - u_0)$	1.5252	8	61	2	62
Total Error budget		11	79	4	79
RMS of 7-day fit (no par. est.)					52

Surprisingly enough the largest error source stems from the two periodic terms in the X-direction. This is remarkable in view of the very small effect these parameters have on the orbit. The estimated errors from the other parameters are all below the 20 cm level. The total error budget is estimated to be about 80 cm. To verify this, our standard test was used without estimating any parameters (except the 6 osculating Keplerian elements). The RMS of this 7-day fit may then be comparable to the estimated model error. The results are comparable but the error budget seems to be somewhat pessimistic. This may be caused by the relatively large error of the X-periodic terms. Also, the arc length of our standard test (7 days) is longer than the arc length used for the RPR parameter estimates (5 days). Therefore the remaining orbit model error is estimated to be of the order of 50 cm only!

Apart from CODE also the JPL analysis center has successfully developed a new RPR model [Jar-Sever, 1997]. To test the performance of different RPR models our standard test was used once more. Table 5 gives the results of the standard test using the different RPR models available: ROCK, JPL, and CODE. It shows the RMS of fit using 7 days of precise orbits and the RMS and median of the residuals of the prediction comparison. Again the CODE final products (orbit and EOPs) were used. In all cases only the scale term (or a constant acceleration in the direction sun-satellite (D_0)) and the Y-bias (Y_0) were estimated. Only for the solution labelled ‘BEST’ more RPR parameters (all 9 parameters of the ECOM) were estimated. This solution is given as a reference, Furthermore, the ROCK model was used in two different ways. First, it was used as a priori model and the accelerations D_0 and Y_0 were estimated on top of the model (solution: T20), which represents the way the ROCK

model is normally used in the **Bernese** GPS Software. Secondly, it was used by estimating a scale factor for the complete ROCK model and the acceleration in the Y-direction (solution: T20 scaled), which represents the recommended usage of the ROCK model.

Table 5. Orbit Fit (7 days) and orbit extrapolation (2 days) using different RPR models. Only scale (or D_0) and Y-bias estimated.

RPR-MODEL	RMS of FIT (cm)	Prediction	
		Median (cm)	RMS (cm)
No Model	75	133	159
T20	76	134	161
T20 Scaled	72	119	151
JPL Scaled	10	45	58
CODE	6	17	31
“BEST” (9 RPR par.)	5	17	22

Table 5 shows that including the ROCK model as a priori RPR model does hardly give any improvement, both in the fit and in the prediction, compared to not including an a priori model. Although it was clear for a long time that the ROCK models are not very accurate, this is a surprise! Both the CODE and JPL RPR models perform much better than the ROCK model. The results of the CODE model are close to the “best possible” results. This means that the reduction of the number of estimated RPR parameters (from 9 to 2!), does not significantly degrade the accuracy of the results. This reduction of parameters should make the GPS orbit predictions more reliable! This is very important because it has become clear that the integrity of the predicted orbits is the most crucial factor for real time GPS data analysis [*Martin Mur et al., 1998*].

Finally, the new RPR model was tested in a real GPS data processing experiment using one full week of data (7 days of 3-day solutions). Four different solutions were generated. For the first two solutions our standard (D_0, Y_0) and new ($D_0, Y_0, 130, B_p$) orbit solutions were generated using the ROCK model as a priori model. For the second two solutions the same two orbit solutions were generated but now using the new CODE RPR model as a priori model. The results are given in Table 6.

Table 6. Results from real GPS data analysis using both the ROCK and CODE RPR models

	ROCK + CODE+		ROCK + CODE +	
	$D_0 Y_0$	$D_0 Y_0$	$D_0 Y_0 B_0 B_p$	$D_0 Y_0 B_0 B_p$
Orbit Overlap (mm)	106	34	31	32
Orbit Comparison (mm)	66	54	50	51

A significant improvement can be seen for the standard solution (D_0, Y_0). In fact, the standard solution using the CODE model has become almost as good as the two X3-type (D_0, Y_0, B_0, B_p) solutions. This is an important result because it means that three orbit parameters (the three B-terms) become obsolete! The slight difference in quality is most

likely caused by the eclipsing satellites, which are not treated in any special way in the CODE model. The similarity in quality of both X3 (DO, Y_0, B_0, B_p) solutions shows once more that the periodic B-terms behave very similar as the periodic Z-terms.

Summary and Outlook

It has been shown that the new solar radiation pressure model as developed by CODE is superior to the ROCK model by almost one order of magnitude. The remaining model error was estimated to be about 50 cm, whereas for the ROCK model the error is about 300 cm. Although a significant improvement could be achieved with the new RPR model, it should be considered as a “first attempt” only. In the near future more time and effort will (have to) be spent on RPR models. Different models are required for the Block I and IIr satellites and also for PRN23. Furthermore, the **behaviour** of some of the parameters of the RPR model is significantly different, but not erratic, during the eclipse phases. Therefore, it is very likely that a special eclipse model maybe derived, One minor problem was discovered in the model. The so-called X3 orbit solutions, the official CODE solutions since September 1996, show a small scale difference with respect to the standard (R3) solutions and also with respect to the IGS combined orbit, Because the model was based mainly on our X3 orbits (only for the first few months of 1996 the R3 solutions were used) this scale effect has propagated into the RPR model. This means that all orbit estimates generated with this new RPR model will have a small scale difference of approximately 0.2 ppb (5 mm). Keep in mind that the “true scale” is not known,

The implementation of the CODE RPR model may improve the quality of the orbit estimates. In addition, the number of required (orbit) parameters maybe reduced. This will strengthen the GPS solutions significantly. Especially the generation of the so-called ‘rapid’ products may profit from this development. The predicted orbits may also improve; maybe not in accuracy, but certainly in integrity, thanks to the reduction of the required number of orbit parameters. Last but not least we hope that the model will enable us to generate GPS orbits based on SLR observations only. So far, the limited number of SLR observations and the large number of required orbit parameters made it almost impossible to generate accurate GPS orbits based on SLR data only. With our new RPR model we are in a much better position because, it allows a 7-day fit at the 6 cm **level** solving for only two parameters.

References

- Bar-Sever, Yoaz E. (1997), New and Improved Solar Radiation Models for GPS Satellites Based on Flight Data, Final Report fo Air Force Materiel Command Space and Missile Systems Center/CZSF, April 121997.
- Beutler, G., E. Brockmann, W. Gurtner, U. Hugentobler, L. Mervart, and M. Rothacher (1994), Extended Orbit Modeling Techniques at the CODE Processing Center of the International

- GPS Service for Geodynamics (IGS): Theory and Initial Results, *Manuscripta Geodaetica*, 19, 367--386, April 1994.
- Beutler, G., E. Brockmann, U. Hugentobler, L. Mervart, M. Rothacher, and R. Weber (1996), Combining Consecutive Short Arcs into Long Arcs for Precise and Efficient GPS Orbit Determination, *Journal of Geodesy*, 70, 287--299.
- Colombo, O. L. (1989), The Dynamics of Global Positioning Orbits and the Determination of Precise Ephemerides, *Journal of Geophysical Research*, 94(B7), 9167--9182.
- Fliegel, H. F., and T. E. Gallini (1989), Radiation Pressure Models for Block II GPS Satellites, in *Proceedings of the Fifth International Symposium on Precise Positioning with the Global Positioning System*, pp. 789--798, National Geodetic Survey, NOAA, Rockville, Md., April 1989.
- Fliegel, H. F., W. A. Feess, W. C. Layton, and N. W. Rhodus (1985), The GPS Radiation Force Model, in *Proceedings of the First International Symposium on Precise Positioning with the Global Positioning System*, edited by Clyde Goad, pp. 113--119, National Geodetic Survey, NOAA, Rockville, Md., March 1985.
- Fliegel, H. F., T. E. Gallini, and E. R. Swift (1992), Global Positioning System Radiation Force Model for Geodetic Applications, *Geophysical Research Letters*, 97(B1), 559--568.
- Martin Mur, T.J., T.A. Springer, and Y. Bar-Sever (1998), Orbit Predictions and Rapid Products, in *Proceedings of the IGS Analysis Center Workshop*, ESA, Darmstadt, Germany, February 1998, This Volume.
- Rothacher, M., G. Beutler, and L. Mervart (1995), The Perturbation of the Orbital Elements of GPS Satellites Through Direct Radiation Pressure, in *ZGS Workshop Proceedings on Special Topics and New Directions*, edited by G. Gendt and G. Dick, pp. 152--166, GeoForschungsZentrum, Potsdam, Germany, May 15--18 1995.
- Springer, T. A., M. Rothacher, and G. Beutler (1996), Using the Extended CODE Orbit Model: First Experiences, in *IGS 1996 Analysis Center Workshop*, edited by R.E. Neilan *et al.*, pp. 13--25, Central Bureau, JPL, Pasadena, Ca, March 19--21 1996.
- Springer, T. A., G. Beutler, and M. Rothacher (1998), Improving the Orbit Estimates of the GPS Satellites, *Journal of Geodesy*, January 1998, Submitted.

Appendix

This Appendix gives some statistics of the RPR model estimation and the values of the CODE solar radiation pressure model.

Table 7. Results from the CODE solar radiation pressure model estimation

Parameters	#Est.	RM _s ($10^{-9}m/s^2$)
D_0	15961	0.0724
Y_0	15815	0.0416
B_0	15406	0.2318
$Z \sin(u - u_0)$	15348	0.1187
$X \sin(u - u_0)$	15187	0,1454
$X \sin(3u - u_0)$	15760	1.5252

Table 8. The values of the CODE solar radiation pressure model

Parameters	Estimate (10^{-97} ?2/s2)	Formal Error ($10^{-11}m/s^2$)
D_{C2}	-0.813	0.176
D_{C4}	0.517	0.124
Y_C	-0.067	0.104
B_C	0.385	0.572
2_0 Block II	1.024	0.299
2_0 Block IIa	0.979	0.184
Z_{C2}	0.519	0.248
Z_{S2}	0.125	0.149
Z_{C4}	0.047	0.261
Z_{S4}	-0.045	0.164
$X1_0$	-0.015	0,157
$X1_C$	-0.018	0.297
$X1_S$	-0.033	0.168
$X3_0$	0.004	1.655
$X3_C$	-0.046	3.118
$X3_S$	-0.398	1.773

Table 9. The values for the CODE solar radiation pressure model. The values for PRN8 and PRN13 should be used with care. PRN8 was launched by the end of 1997 and was still in its ‘outgassing’ phase. PRN13 was also launched by the end of 1997 and is a completely new type of satellite (Block **IIr**). This new Block type most likely will have a different solar radiation pressure model.

PRN	Block	D_0 ($10^{-9}m/s^2$)	Y_0 ($10^{-9}m/s^2$)	B_0 ($10^{-9}m/s^2$)
2	II	-99.373	0.6362	0.0480
14	II	-99.290	0.9064	-0.2510
15	II	-98.985	0.7048	-0.4749
16	II	-99.108	0.6496	-0.1170
17	II	-99.010	0.6604	-0.0770
18	II	-99.359	0.8683	-0.4783
19	II	-99.850	0.7057	-0.1449
20	II	-100.396	0.6642	-0.4997
21	II	-99.477	0.2592	0.0996
1	IIa	-91.088	0.7458	-0.4868
3	IIa	-90.395	0.5637	-0.3960
4	IIa	-90.502	0.7856	-0.2487
5	IIa	-90.414	0.7612	-0.2309
6	IIa	-90.354	0.7589	-0.3092
7	IIa	-90.238	1.0376	-0.2241
8	IIa	-93.342	1.8394	-0.7143
9	IIa	-90.317	0.7955	-0.3569
10	IIa	-89.546	0.7819	-0.1772
22	IIa	-90.944	0.7319	-0.0179
23	IIa	-78.592	0.7440	-1.0843
24	IIa	-91.436	1.0537	-0.2214
25	IIa	-90.785	0.8556	-0.3851
26	IIa	-90.377	0.9750	-0.4144
27	IIa	-90.291	0.9482	-0.4224
28	IIa	-90.951	0.8210	-0.1303
29	IIa	-91.015	0.9078	-0.5188
30	IIa	-90.455	0.8285	-0.5409
31	IIa	-90.370	0.6269	-0.6173
13	IIr	-99.599	-0.2801	-1.6732

NEW SOLAR RADIATION PRESSURE MODELS FOR GPS SATELLITES

Y. Bar-Sever, D. Jefferson, and L. Remans

Jet Propulsion Laboratory/California Institute of Technology

The mismodeling of solar radiation forces is currently the largest error source in the precise orbit determination of GPS satellites. Consequently, it is a dominant error source in many precise applications of the GPS, such as, geodesy, determination of Earth orientation, and low Earth orbiter tracking. We have developed a new approach to the problem of modeling the solar radiation forces on GPS satellites that significantly improves the quality of the model. The approach is aiming to replace the conventional re-launch design phase of solar pressure and heat reradiation models by a more accurate post-launch phase. The approach is also suitable for many other Earth-orbiting satellites.

The current GPS constellation of Block II and Block 11A satellites was used as a prototype for developing and validating our approach. We used the daily JPL GPS precise ephemerides over a period of 9 months to adjust a parametrized model of the solar pressure so as to obtain best fit. The resulting model proved to be significantly more accurate than the standard solar pressure model for GPS satellites (Bar-Sever, 1997). For example, 4-day orbit prediction accuracy has increased by 63% for non-eclipsing GPS satellites, and by 28% for eclipsing satellites. The new models will be made available to all IGS Analysis Centers.

References

Bar-Sever, Y. E., New and Improved Solar Pressure Models for GPS Satellites Based on Flight Data, Final Report, Prepared for Air Force Materiel Command SMC/CZSF, April 12, 1997.

A LOOK AT THE IGS PREDICTED ORBIT

J. F. Zumberge

Jet Propulsion Laboratory, California Institute of Technology
Pasadena, CA 91109 USA

SUMMARY

The quality of the IGS predicted orbit has been assessed by comparing it to the IGS final orbit. For each satellite and day during the 6-week period beginning November 16, 1997, the 3-D rms difference over the day between the predicted and final orbit was computed. The distribution of this quantity is shown in Figure 1. Each count corresponds to one satellite and one day.

The median 3-D rms is 57 cm, which is approximately a factor of seven smaller than the corresponding number for the broadcast ephemeris. However, the high-end tail in Figure 1 – 8.5% are above 3 m – limits the use of the IGS predicted orbit. It would be beneficial to identify problematic satellites when the prediction is published.

It was found that poorly performing satellites are not well correlated with either (i) the smoothness of the broadcast ephemeris or (ii) time. There is, however, some correlation with pm, as indicated in Figure 2. For example, predictions of prn14 and prn23 are consistently poor. Although not indicated in Figure 2, the eclipse status is also a consideration, at least for some satellites. For example, the predictions for prn1 0 are typically worse when that satellite is in shadow.

With additional work, one might be able to develop a not-too-complicated algorithm using prn and shadow/sun status to flag many of the problematic satellite-days in the IGS predicted orbit. To realize the full potential of the IGS predicted orbit, however, one probably needs to use near-real-time data to flag the outlier satellites and days.

Acknowledgment The research described here was carried out by the Jet Propulsion Laboratory, California Institute of Technology, under a contract with the National Aeronautics and Space Administration.

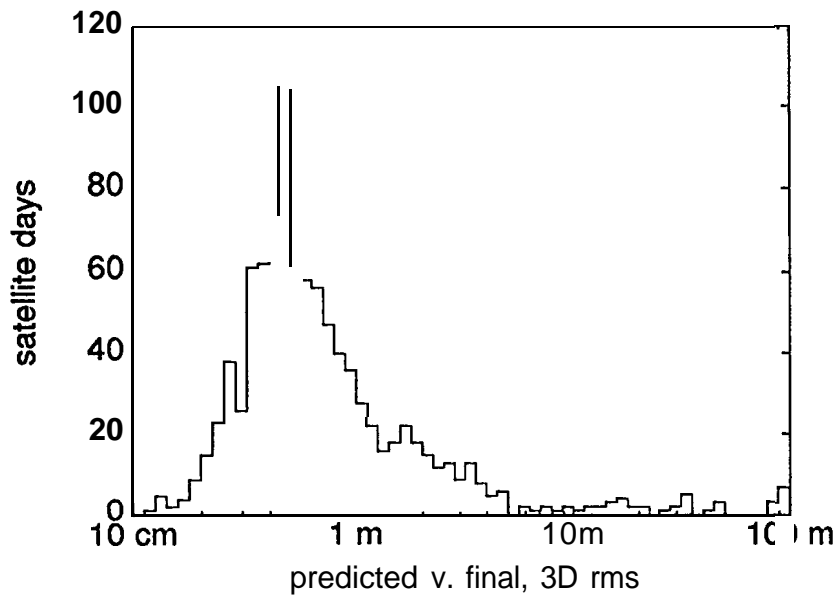


Figure 1: Distribution of the daily 3D-rms difference between the IGS predicted and final orbits.

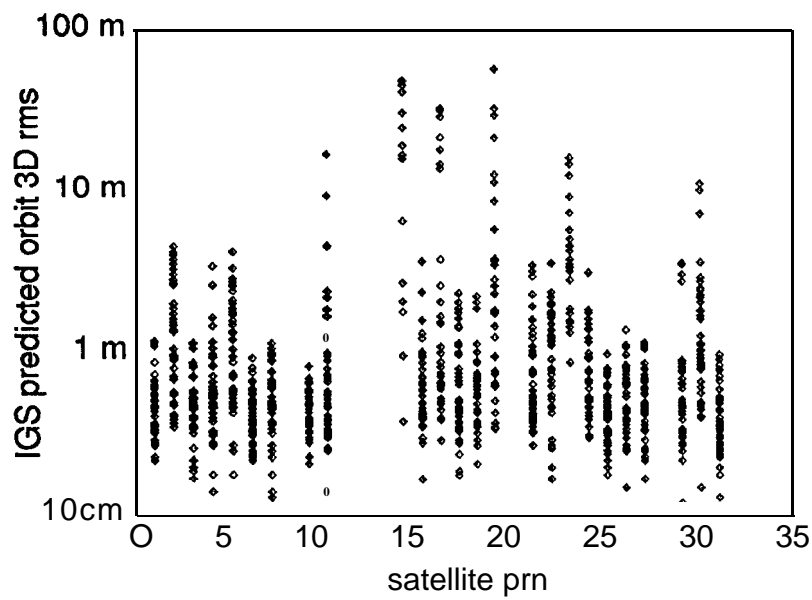


Figure 2: Correlation of predicted performance with pm.

REAL TIME EPHEMERIS AND CLOCK CORRECTIONS FOR GPS AND GLONASS SATELLITES

M.M. Romay-Merino, J. Nieto-Recio, J. Cosmen-Shortmann, J.R. Martin-Piedelobo
GMV, Isaac Newton 11, P.T.M. Tres Cantos, E-28760 Madrid, Spain

ABSTRACT

Algorithms computing clock and ephemeris corrections for GPS and GLONASS satellites as the basis for GIC (Ground Integrity Channel) and WAD (Wide Area Differential) services constitute one of the most important part of the EGNOS (European Geostationary Navigation Overlay Service) system. Using the GPS/GLONASS broadcast data it is not possible to compute the user position with the desired accuracy and integrity for high demanding users, such as aeroplanes. To achieve the desired user positioning requirements some corrections should be applied to the broadcast data. These corrections must be computed in real time, and they will be transmitted to the user via a geostationary satellite. Corrections can be divided in ephemeris or orbit corrections, satellite clock corrections, and ionospheric corrections. These corrections shall be valid in the regional area to be analysed, Europe in this case.

This paper summarises the results obtained using the most promising algorithms, based on the use of a state of the art orbit determination algorithm (BAHN developed at ESOC/OAD). These results have been obtained using real data from a dedicated campaign. Eight GPS and GLONASS receivers have been deployed in Europe to evaluate the performances of the algorithms to compute ephemeris and clock corrections. The use of orbit and clock corrections allows to determine the user position in real time with an accuracy about one meter, which fully satisfy the EGNOS performances requirements.

INTRODUCTION

Europe's primary contribution to GNSS -1 will involve signal relay transponders carried on geostationary satellites, and a network of ground stations. They are intended to provide a regional augmentation service for GPS and GLONASS signals over Europe. Thus improving considerably the positioning accuracy of a user located in the coverage area. This augmentation is called an "overlay", and the European programme is known as EGNOS (European Geostationary Navigation Overlay Service).

Using the current GNSS systems, user positioning accuracy of about 100 meters (for GPS satellites) can be achieved when no augmentation system is used. The following figure illustrates the typical user positioning errors when GPS data is used:

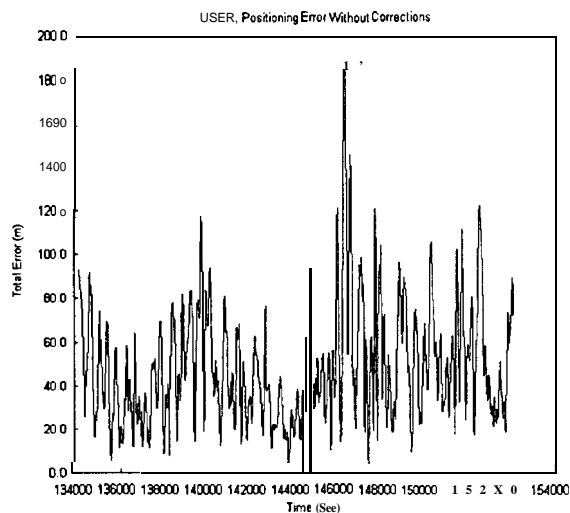


Figure 1 GPS Typical user positioning errors

EGNOS is expected to improve considerably the user positioning accuracy. EGNOS will reach its Advanced Operational Capability in 1999, when it can be used as primary source of navigation and positioning for applications such as aircraft landing approaches

EGNOS provide the backbone for three essential navigation services: ranging, integrity monitoring and wide-area differential corrections.

Ranging service. The ranging service will enable the EGNOS transponders to broadcast GPS-like navigation signals. As a result, these satellites become two more sources of space-based navigation data for users. This is important because neither GPS nor GLONASS systems can guarantee that the minimum number of six satellites required for safety-critical applications is in view at all time and all locations world-wide.

Integrity service. Range errors estimates for each GPS, GLONASS, or EGNOS navigation signal are broadcasted. The EGNOS integrity service will enable users to known within 10 seconds whether a navigation satellite signal is out of tolerance, allowing action to be taken before any critical situation arises.

Wide area differential correction service. Correction signals to improve the precision of satellite navigation are broadcasted to the users. With the wide area differential service, the satellite navigation precision will dramatically increase to 5 to 10 meters well above the approximate] y 100 meters for the currently available non-encrypted signals from GPS.

This paper describes the algorithms to be used to provide the Wide Area Differential (WAD) ephemeris and clock correction service. The most promising technique is analysed to some extent, and the results obtained when using this algorithm are presented.

ALGORITHMS SELECTION AND DESCRIPTION

Three different types of algorithms can be considered to perform an accurate orbit determination:

- . Dynamic methods
- Geometric methods
- . Reduce dynamic methods

The algorithm used to compute clock corrections is the same for all above mentioned algorithms, Once the ephemeris corrections have been computed the clock corrections will be computed from the measurement's residuals.

Dynamic methods. These methods are based in the integration of the equations of motion:

$$m \frac{d^2 x}{dt^2} = \sum_{i=1}^n F_i$$

Where F_i account for all perturbation acting on the satellite, like: gravitational perturbations, surface force perturbations, tidal perturbations, manoeuvres, etc.

Combining dynamic with observations:

$$y = Hx + \varepsilon$$

it is possible to improve the knowledge of the state variables, and therefore the satellite orbit determination. The major problem of the dynamic methods is the required computational time. A significant amount of computational time is required to compute the ephemeris corrections, thus they are in principle not suitable for real time operations. In the other hand they are able to compute accurate predictions. The state equations can be used to propagate the satellite ephemeris into the future, and the propagated ephemeris can be used in real time to compute the ephemeris corrections.

Once the satellite ephemeris corrections have been computed, satellite clock corrections can be easily computed. To estimate satellite clock corrections, the satellite must be at least visible for two reference stations simultaneously.

It can be concluded that it is possible to use dynamic methods for real time applications if it is possible to compute accurate predictions. Preliminary analyses, using globally distributed data show that predictions over 24 hours have an accuracy (rms) of about one

meter, this will be sufficient to provide accurate ephemeris and clock corrections to the EGNOS users.

Precise orbits for the GPS satellites can be computed operationally at regular time intervals. The objective of this operational orbit determination process will be to determine the GPS orbits in the past and to produce accurate orbit predictions for the future.

The objective of the tests to be performed here will be to evaluate the possibility of computing accurate GPS/GLONASS orbits using only tracking data from the dedicated ground stations. The possibility of using external data from IGS stations will be considered.

Geometric methods. These methods do not make any use of information coming from the dynamics. They are also identified as inverse GPS methods. The position of the reference stations is accurately known, therefore if four or more than four stations are simultaneously tracking the satellite, the satellite position and clock error can be estimated. To apply these methods station clocks must be synchronised. This is normally done by using common view techniques. Station clocks synchronisation failures will severely influence the accuracy of the satellite ephemeris and clock corrections. These methods do not aim to provide real ephemeris corrections. They provide corrections that are valid for the region of interest, therefore the extrapolation of the correction to other areas may not be possible.

Reduce dynamic methods. These methods are a combination of the two previously described methods. They combine dynamical information with geometric information coming from the measurements. These methods can provide more accurate corrections than the dynamic or geometric methods, but as they are using relatively simple dynamic models, they can not provide accurate orbit predictions. Reduce dynamic methods are using dynamic models, therefore a significant amount of computational time is still required to evaluate the perturbations coming from those models, and they will not be able to operate in real time. These methods will not be considered in this analysis. Some examples have been performed by considering Keplerian propagation, no significant improvement was obtained with respect to the kinematic propagation.

DATA CAMPAIGN DESCRIPTION

A dedicated GPS/GLONASS campaign has provided the required data in order to evaluate the performances provided by the different algorithms to compute ephemeris and clock corrections.

The objective of the GPS/GLONASS Measurement Campaign was to provide a consistent dataset from widely distributed sites in Europe, with suitable equipment including dual-frequency GPS, single frequency GLONASS receivers, Atomic Frequency

Standards and meteorological logging devices. The location of the deployed receivers is represented in the figure below:

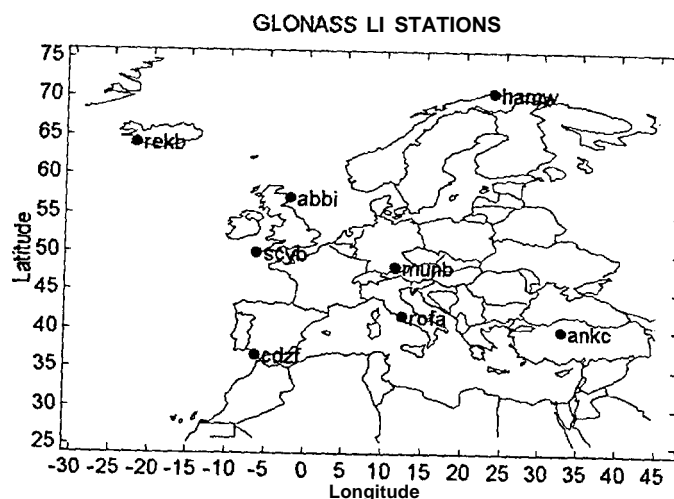


Figure 2 Ground stations used during the analysis

ALGORITHMS EVALUATION APPROACH

In order to evaluate the performances of the algorithms, to compute ephemeris and clock corrections, some already developed software packages have been integrated with some new developed software packages in a single tool.

Five different algorithms to compute ephemeris and clock corrections have been considered:

1. Dynamic algorithm, using the at ESOC developed GPSOBS and BAHN software packages.
2. Snapshot algorithm based in single differences
3. Snapshot algorithm based in double differences.
4. Snapshot and Kalman filter algorithm based in single and double differences
5. Clock correction algorithm common to all ephemeris computation algorithms

The implemented tool covers the following functionalities:

- Data generation
- Data pre-processing
- Computation of ephemeris and clock corrections
- User positioning determination

Standards and meteorological logging devices. The location of the deployed receivers is represented in the figure below:

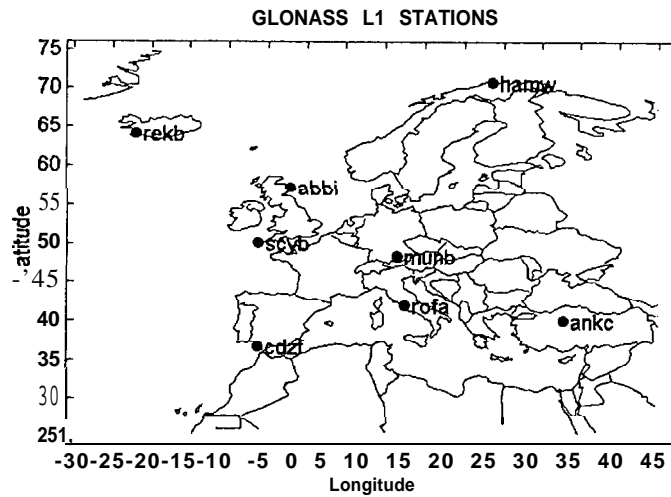


Figure 2 Ground stations used during the analysis

ALGORITHMS EVALUATION APPROACH

In order to evaluate the performances of the algorithms, to compute ephemeris and clock corrections, some already developed software packages have been integrated with some new developed software packages in a single tool.

Five different algorithms to compute ephemeris and clock corrections have been considered:

1. Dynamic algorithm, using the at ESOC developed GPSOBS and BAHN software packages.
2. Snapshot algorithm based in single differences
3. Snapshot algorithm based in double differences.
4. Snapshot and Kalman filter algorithm based in single and double differences
5. Clock correction algorithm common to all ephemeris computation algorithms

The implemented tool covers the following functionalities:

- . Data generation
- . Data pre-processing
- . Computation of ephemeris and clock corrections
- User positioning determination

with the data from the dedicated campaign to try to determine accurate GLONASS orbits and to establish the best orbit determination strategy for those satellites, as no accurate orbits are available for those satellites. Unfortunately a very limited amount of SLR data was available, so very precise orbits could not be computed. The availability of SLR data during the month of June 1996 is summarised in the table below:

<i>Satellite</i>	<i>Number of SLR observations</i>
GL-63	421
GL-66	137
GL-67	1031

Table 1 GLONASS SLR data available

Meteorological data are required in order to remove tropospheric delays from the measurements. Some facilities to generate RINEX files from the campaign data have also been implemented.

GPSOBS. GPSOBS is a state of the art GPS data pre-processing software package developed at ESOC. This program is used at ESOC to pre-process RINEX files, the output of this module is directly usable by the orbit determination package BAHN.

As it has been mentioned before, BAHN has been used to compute accurate GPS and GLONASS orbits. Unfortunately GPSOBS is not able to handle GLONASS data, therefore GLONASS data have not been processed to the same extent as GPS data.

GPSOBS has been used to generate double differences of carrier phase and pseudorange measurements from the ESA GNSS - 1 campaign, from the at GMV installed receiver, and from some IGS stations.

Data from all satellites have been generated. Antenna corrections and ionospheric corrections have been applied to those data. Cycle slips have been removed, and eclipses perturbations have been modelled. The interval between observations has been selected as 6 minutes, and a minimum elevation of 20 degrees has been selected. Initial values for clock parameters are computed.

Pre-processing for real-time algorithms. This module is not really part of the algorithms to compute ephemeris and clock corrections, but it is required in order to perform those corrections, and in order to compute the user position.

The pre-processing is valid for real (GPS and GLONASS) and simulated measurements, but the methods used depend on which case is considered. This algorithm is intended to provide a iono-free, tropo-free, carrier phase smoothed pseudorange to the algorithms working in real time.

Ephemeris computation algorithms. Different algorithms have been used to compute accurate ephemeris corrections to the GPS and GLONASS satellites.

The core of the dynamic algorithms is the general utility orbit determination program BAHN. BAHN is a state of the art package developed at ESA/ESOC over the last

decades, This package has been extensively used to compute precise orbits for many different types of satellites and using different types of tracking data systems. In particular ESOC is actively participating as an Analysis Centre and Operational Data Centre in IGS. In the scope of this analysis BAHN has been extensively used to compute accurate orbits for GPS and GLONASS satellites.

Geometric algorithms have been implemented, those algorithms use pre-processed data, the position of the satellite can be computed if four or more stations are simultaneously tracking the satellites. Some of the implemented methods use a Kalman filter to smooth the computed corrections.

User Positioning Algorithm. This algorithm is intended to provide the user position using GPS or GLONASS measurements. Pre-processed measurements for the selected user, and ephemeris and clock corrections generated by any of the algorithms are used to obtain the position of the user.

The analysis of the user positioning errors is required in order to assess the performances of the algorithms. The accuracy of the ephemeris corrections for GPS satellites can be evaluated just by comparing with accurate IGS orbits. For clock corrections no accurate solutions are available. To have an estimation of the errors associated with the clock estimation the user position errors are estimated, and from those values an upper limit of the contribution of the clock corrections to the total UERE (User Equivalent Range Error) can be estimated.

ALGORITHMS EVALUATION TESTS RESULTS.

The performances of the different algorithms to compute accurate ephemeris and clock corrections have been evaluated using real data from the dedicated tracking data campaign. One of the stations of the campaign will be used to simulate the user performances in terms of positioning errors. This section summarises the results obtained in terms of accuracy of the ephemeris and clock corrections, and also in terms of the accuracy of the user positioning.

Geometric algorithms.

The following table represents for all satellites and algorithms the rms in meters of the ephemeris corrections errors. All stations (eight) have been used to compute the solutions. Due to the large correlations between ephemeris and clock corrections similar errors may be expected for clock corrections, as it was concluded from the tests based on simulated data

	Single Differences Snapshot	Single Differences Kalman Filter	Double Differences Snapshot	Double Differences Kalman Filter
TOTAL	489	524	101	112

Table 2 RMS of the ephemeris corrections in meters

From the above results the following conclusions can be addressed:

- For single differences algorithms different behaviour has been observed for different satellites. Corrections for low elevation satellites are worse than corrections for high elevation satellites,
- Almost the same results are obtained for **all** satellites when using double differences algorithms (ephemeris errors around 100 meters).
- Algorithms based in **Kalman** filters are providing worse performances than snapshot algorithms.
- Ephemeris corrections errors computed using double differences algorithms are significantly smaller than when using single differences algorithms. Although they are bigger than the typical ephemeris broadcast errors.

The use of geometric algorithms to solve for the satellites ephemeris and clocks represents the inverse GPS problem. The position of some reference ground stations is accurately known, and the unknown is the satellite position and clock. The concept of DOP (Dilution of Precision) needs to be redefined as in this case the user is the satellite, and the “satellites” are the reference ground stations. Therefore the “inverse DOP” is computed. The precision of the ephemeris and clocks computed using geometric methods will depend on the “inverse DOP” value and the measurements errors. The satellite position errors can be represented as the product of the “inverse DOP” by the measurements errors. This is basically the same concept applied to the user in the typical GPS case, but now applied to a satellite.

The figure below represents the “inverse DOP” values for two satellites and for the reference geometrical configuration (eight stations):

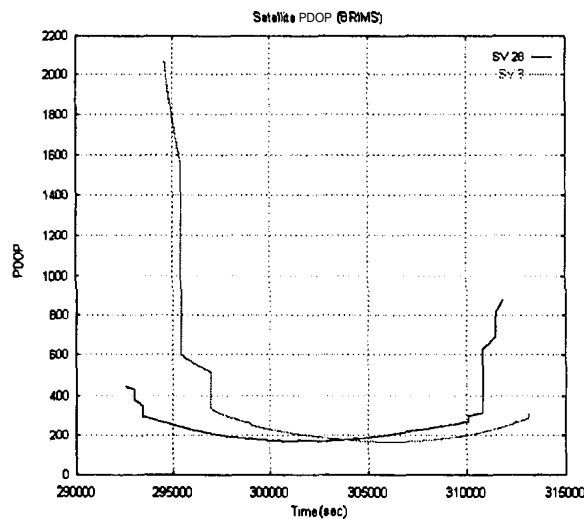


Figure 4 Inverse GPS DOP values

This explains the large ephemeris errors obtained. Maximum PDOP values can be up to 2000, and in optimal geometrical conditions they are about 200. This is certainly worse than for a typical GPS user where those values are typically between 2 and 5. This is

mainly due to the bad geometrical conditions, distances between stations are smaller than distances between satellites.

Measurements errors of about 50 cm will address to ephemeris errors among 100 and 1000 meters. These measurements errors can be considered as realistic for a low elevation satellite. These errors are slightly smaller for a higher elevation satellite.

It can be concluded that using geometric algorithms it is only possible to compute accurate ephemeris if the measurements were almost perfect.

Performances have also been evaluated from the user point of view. For all the cases the user positioning errors will be represented as the total error divided by the PDOP, this represents an indication of the total UERE.

The accuracy to be achieved for a user located at Rome without transmitting any correction is:

	User Error (m)
UERE	23.0

If ephemeris and clock corrections based in geometric algorithms are applied the user position accuracy change to:

	Single Differences Snapshot	Single Differences Kalman Filter	Double Differences Snapshot	Double Differences Kalman Filter
UERE (m)	0.80	2.86	0.52	0.73

This relatively good results, despite of the large ephemeris errors, have been obtained because clock corrections are compensating ephemeris corrections. This compensation may not be valid for all user locations. A theoretical analysis shows that this compensation is higher for a user located close to centre or the area covered by the stations. For a user located far from this location the user position errors will increase with the ephemeris corrections errors. For a user close to the borders of the investigated area (ECAC) this degradation has been estimated as a 10-15 % of the ephemeris errors.

To analyse the influence of the user location. The same tests have been repeated for a user out of the area covered by the stations. Reykjavik has been selected as user. Only one algorithm has been selected to perform this test: snapshot single differences.

The table below represents the user position errors:

	User Error (m)
UERE	5.04

- It can be concluded that the performances of the geometric algorithms are severely depending on the user location. Ephemeris errors are compensated with clock errors for a user close to the centre of the area covered by the stations, but this is not valid when the user is relatively far from this location.

- The situation will not improve by increasing the number of stations, or by modifying the location of the stations. This will only modify the location where clock corrections compensate ephemeris corrections.
- The only way to improve the performance is reducing the correlation between ephemeris and clock corrections by reducing the errors in the computed ephemeris corrections.

Dynamic algorithms.

Dynamic algorithms have been used to compute the orbits of the GPS satellites. The orbit determination package BAHN (developed at ESOC/OAD) has been used in combination with data from the eight stations involved in the dedicated tracking data campaign. The computed orbits were compared against the very accurate IGS orbits in order to have an estimation about the accuracy of the determined orbits. It shall be indicated that only data from a European network of stations has been used, while to compute the IGS orbits data from a world-wide network have been used.

GPS orbits with an accuracy of about 1.11 meters have been computed.

Some effort has been devoted to compute ephemeris corrections in a well-defined reference frame, in particular in the ITRF-93 reference frame. The success is demonstrated by the small values obtained for the seven parameters defining the transformation between the computed orbits and the IGS orbits. The translations are at the 1 cm level, rotations at the 1 mas level, and the scale factor is about 0.1 parts per billion. The accuracy of the orbit predictions, which is defining the accuracy of the ephemeris corrections to be transmitted to the user, is presented below as a function of the prediction length:

prediction interval	Total rms
3 h	3.14
6 h	3.42
12 h	3.43
24 h	4.71

Table 3 Orbit predictions accuracy in meters

The influence of the number of stations and their location in the orbit prediction accuracy have been evaluated. It can be concluded that better results are obtained when the eight stations are used, but still acceptable results can be obtained if only four stations are used. Orbits are computed using as observable double difference carrier phase measurements. So the addition of an isolate station out of Europe will not improve the results. Some improvements have been observed when two stations located in USA have been added (to perform this tests real data from IGS stations have been used).

Correlations between ephemeris and clock corrections can mask the results, because the performances of the algorithms are usually validated from the user point of view. It was already mentioned when evaluating geometric algorithms that wrong ephemeris

corrections can be compensated by clock corrections. This compensation is expected to be high for a location close to the centre of the configuration defined by the stations. Different conclusions may be obtained by considering different user locations. The following figure represents the percentage of the non compensated ephemeris errors as a function of the user location. The horizontal plane represents the ECAC area, and the vertical axis the percentage of non absorbed ephemeris errors:

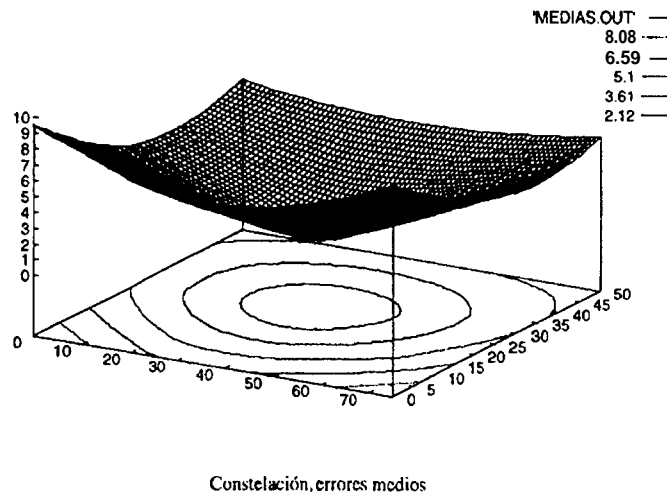


Figure 5 Percentage of the non compensated ephemeris errors as function of the location

From the above figure it can be observed that for a user located close to the corners of the ECAC zone the non absorbed ephemeris errors can amount up to a 10 % of the total ephemeris errors. Other tests performed using different orbit errors suggest that those values are never bigger than 15% for the mean values. The worst location user is at the corners of the area covered by the stations. In these tests the selected user location is close to the centre, to extrapolate the conclusions to the worst user, a 15% of the total ephemeris error will be added to the UERE value. Figures below represent the computed ephemeris and clock corrections

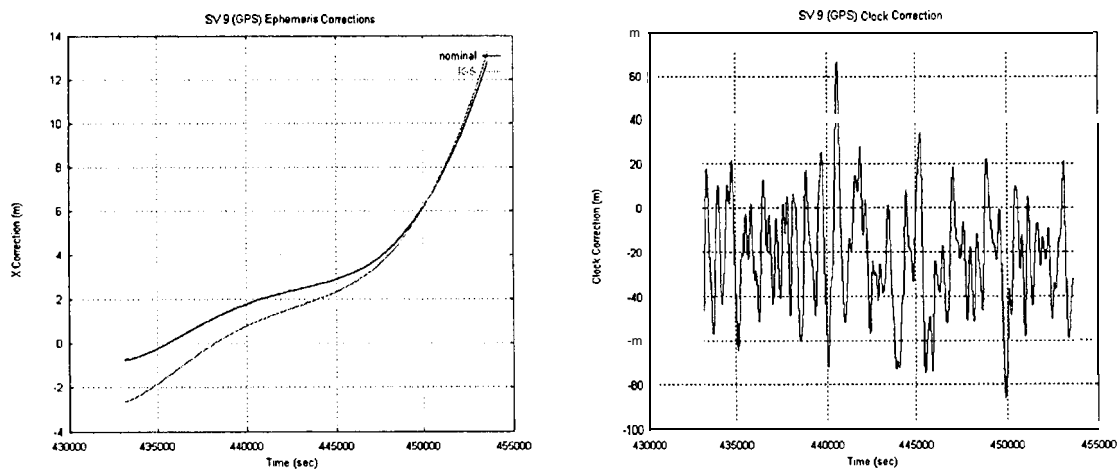


Figure 6 Estimated ephemeris and clock corrections

The performances of the dynamic algorithms have also been evaluated from the user point of view, the obtained results are represented in the table and figure below:

UERE (m)	0.51
----------	------

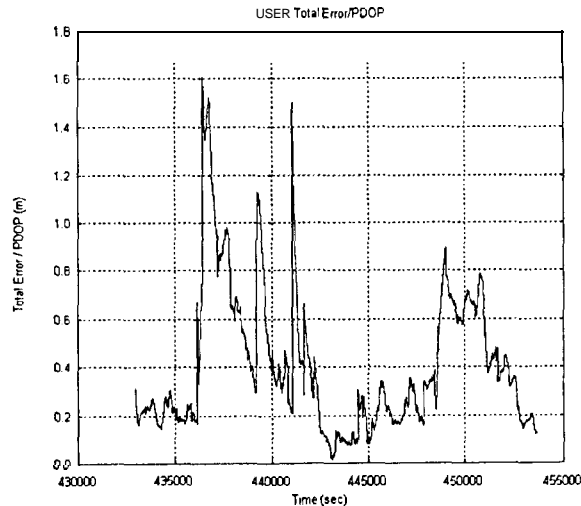


Figure 7 UERE after applying of corrections based in dynamic algorithms

The following conclusions can be addressed:

- Dynamic algorithms are able to provide accurate user positioning. Also ephemeris and clock corrections are quite accurate.
- The estimated UERE value for a user at a central location is about 0.5 meters.
- Similar behaviour are observed for the horizontal and vertical components of the user positioning errors

Another central location (Munich instead of Rome) has been selected as user to confirm the results from the previous test. The time interval selected to perform the test is different, as data from a previous day have been used. The orbits used to perform this test have relatively high orbit errors, about five meters.

The results obtained are presented in the table below:

UERE (m)	0.46
----------	------

To analyse the sensitivity of the algorithm to different user locations several tests modifying the user location have been performed. It should be considered that the station selected as user has not been used to compute ephemeris and clock corrections. Ephemeris and clock corrections have been computed for each of the cases. The results will be affected by the different geometrical conditions associated to each of the cases.

These results can be compared with the results obtained when the user was located at Rome.

The table below summarises the obtained results for the different cases:

	Ankara	Reykjavik	Hammerfest
UERE (m)	0.56	0.58	0.41

It can be concluded that the performances of the dynamic algorithms from the user point of view are less sensitive to the user location than the geometric algorithms.

Some tests have been performed for **GLONASS satellites**. **No accurate ephemeris are available for these satellites, so it has not been possible to get an estimation about the orbit determination accuracy achieved in this case. In addition to that no accurate pre-processor for GLONASS data was available, so the orbit determination was based in pseudorange measurements, The computed orbits are believed to have an accuracy of a few meters. In addition to that** clock corrections have also been computed for GLONASS satellites.

The performances of the algorithms to compute ephemeris and clock corrections have been evaluated from the user point of view, and the obtained results are summarised in the table below:

Error	Without corrections	Clock & Ephemeris corrections
UERE (m)	7.20	2.98

The table above represent the user position errors for a user located at Rome with and without corrections. The following conclusions can be addressed:

- The positioning user errors obtained without corrections are in agreement with the expected performances of the GLONASS system.
- The user positioning errors are substantially reduced when applying corrections. The non availability of accurate GLONASS orbits makes difficult to conclude anything about the quality of the computed ephemeris corrections, although from the results of these tests it seems that the computed ephemeris corrections are not very accurate.
- The user positioning errors obtained are mainly due to the large noise of the measurements, and not only due to errors in the clock estimation.

CONCLUSIONS

A complex infrastructure has been specifically developed, this has made possible the evaluation and assessment of different algorithms. The following items related to the developed infrastructure and the way the experiment has been conducted are highlighted:

- . Geometric and Dynamic algorithms to compute ephemeris and clock corrections have been evaluated.
- . Algorithms have been evaluated using different sources of data, namely: simulated, ESA GNSS-1 campaign, GMV GPS receiver, IGS, and SLR.
- Dynamic algorithms have been evaluated for GPS and GLONASS satellites. Geometric algorithms have been only evaluated with GPS data.
- . The results obtained are affected by the applied pre-processing and the quality of the data used.

It can be concluded that **dynamic algorithms are providing better performances than the geometric algorithms. Geometric algorithms can not be considered as a valid alternative for the EGNOS system.**

From the results of this experiment, the UERE (1 σ value) associated to the ephemeris and clocks correction is estimated in about 0.65 metres. However the reduced amount of data used in the experiment as well as the fact that additional ionospheric errors could appear for high solar activity. A **risk margin of 15%** could be considered to account for those effects.

REFERENCES

B. Hoffman-Wellenhof, H. Lichtenegger and J. Collins. Global Positioning System, Theory and Practice.

Global Positioning System. Standard Positioning Service. Signal Specification. GPS NAVSTAR.

Yeou-jyh Tsai et al. Evaluation of Orbit and Clock Models for Real Time WAAS. Standford University. ION-95.

Changdon Kee, Bradford W. Parkison, Penina Axelrad. Wide Area Differential GPS. Navigation Journal of The Institute of Navigation, Vol. 38, No. 2, 1991.

J.M. Dow, T.J. Martin Mur, M.M. Romay ESA's Precise Orbit Determination Facility, Merino. ESA bulletin, number 78, may 1994.

GLONASS Interface Control Document, 1995.

P.N. Misra, R.I. Abbot, E.M. Gaposchkin. Integrated use of GPS and GLONASS: Transformation between WGS 84 and PZ-90. ION GPS-96

Minimum Operational Performance Standards for Sensors Using Global Positioning System/Wide Area Augmentation System, RTCA Paper No. 240-95/SC 159-664, April 20.1995.

M.M. Romay Merino et al. Experiment 2.2a Test Report. Evaluation of Real Time Integrity and Differential Correction Algorithms for WAD Systems, ref.: GMVSA 2170/96

POTENTIAL USE OF ORBIT PREDICTIONS AND RAPID PRODUCTS IN THE GRAS PROGRAMME

Pierluigi Silvestrin

Earth Observation Preparatory Programme
Directorate of Applications Programmed
European Space Agency
ESTEC, NL-2200AG Noordwijk, The Netherlands

BACKGROUND

The European Space Agency (ESA) is currently developing instrumentation and data analysis tools for atmospheric sounding by radio occultation (**RO**). The GNSS Receiver for Atmospheric Sounding (GRAS) is a space instrument based on the use of RO technique with global navigation satellite systems such as GPS and GLONASS (collectively indicated as **GNSS**) as sources of opportunity. The final program objective is to provide data products of a specified quality for operational meteorology, climate monitoring and prediction, and studies of atmospheric processes and space weather physics.

The RO method is widely considered a mature technique for atmospheric remote sensing. It benefits from a long scientific and technical heritage from planetary exploration experiments, starting with the Mariner IV mission in 1964. Concepts for RO measurements of GPS signals to probe the Earth's atmosphere have been published since 1987 [**Gurvich** and **Krasilnikova**, 1987]. Since then, the quality of derived data products has been proved to be, in several respects, superior to that of current observation techniques, such as spaceborne radiometry or in situ monitoring by e.g. **radio-sondes** [see e.g. Melbourne et al., 1994, **Kursinski** et al., 1997; **Rocken** et al., 1998].

Within the ESA programmed, theoretical and simulation-oriented studies included a validation of error analyses using data from the GPS-MET experiment and the development of improved calibration and retrieval algorithms [**DMI** et al., 1995; **CRI** et al., 1998]. Combined with the GRAS instrument development, these activities enabled European meteorologists and climatologists to propose a dedicated space program, the 'Atmospheric Profiling Mission' within the Earth Explorers framework [ESA, 1996]. The mission proposal, consisting of a constellation of 12 small satellites each carrying a GRAS instrument and the required ground segment, was partly successful since it resulted in the decision to embark GRAS as a co-passenger instrument in all suitable Earth Explorers. It is planned to launch these satellites at two years intervals starting in 2004.

Meanwhile, the European Organisation for the Exploitation of Meteorological Satellites (**Eumetsat**) has added GRAS to the payload of the MetOp satellites for meteorology and climatology. These satellites are being developed by ESA for **Eumetsat**, which will take over the operations and the data exploitation. Each satellite carries a set of instruments including a wind **scatterometer**, an imaging radiometer, three temperature and humidity sounders, an ozone monitoring instrument and **telecom** equipment for data dissemination. The orbit will be a sun-synchronous frozen orbit at 820 km altitude, with a 5 days repeat period and local solar time at the descending node of **9:30** a.m. The on-going MetOp- 1 development is on schedule for a launch in 2003, to be followed by the **MetOp-2** launch in 2007 and **MetOp-3** in 2011.

THE GRAS INSTRUMENT

GRAS provides measurements of the code and carrier phases of signals from both GPS and GLONASS at the **L1** and **L2** bands. Both descending (set) and ascending (rise) occultation signals are observed through two antenna arrays placed on the anti-velocity and velocity sides of the spacecraft, respectively. Each array features 15 antenna elements and provides **~12 dB** gain in a field of view which includes the atmosphere in an azimuth range of $\pm 53^\circ$. This allows some 1000 occultation profiles per day to be observed, assuming full operation of both GPS and GLONASS. A conventional zenith-looking antenna receives signals for real-time navigation and precise orbit determination (POD).

GRAS uses 16 dual-band channels, of which 6 are reserved for **GPS-based** POD. Its Ultra-Stable Oscillator (**USO**) has an overall stability better than 10^{-12} over 0.1 s - 100s observation intervals, enabling the use of a **single-differencing** approach in the ground processing of occultation measurements. This minimises the number of required ground stations and improves performance by reducing thermal noise, **multipath** and tropospheric scintillation errors.

The main observable for occultation processing will be carrier phase and amplitude measurements at 50 Hz sampling rate. Amplitude measurements with a precision of 0.2 dB will be used mainly for diffraction correction processing. The preliminary requirements for the signals undergoing an occultation have been established on the basis of analyses and simulations of the retrieval process. The main carrier phase requirements are outlined in Table 1. Measurements of the L2 band signals are not required when crossing the lowest height region ($h < 12$ km). In this case, the instrument operation will take advantage of the possibility to make ionospheric corrections based on extrapolated ionospheric **doppler** (or refraction angle) and of the strong signature by refraction in the troposphere on the **L1** signal phase.

Height region	Measurement error (rms)	Observation bandwidth
$h > 30$ km	< 1 m m	> 10 Hz
30 km $> h > 12$ km	$< 3 + (12-h)/9$ mm	10 to 25 Hz
1 km $< h < 12$ km	$< 30 + 27(1-h)/11$ mm	> 25 Hz

Table 1: GRAS Carrier Phase Measurement Requirements

The space qualification and reliability/availability requirements mandate the use of **radiation-tolerant** components, which are being tested in GRAS prototypes. Earlier receiver breadboards

were used to validate the basic design [Riley et al., 1995]. Flight equipment production will start in 1999. A similar instrument, the GPSOS (GPS Occultation Sensor) is being designed for the U.S. National Polar-orbiting Operational Environmental Satellite System (NPOESS) programme by the same European industrial consortium developing the GRAS. It is also planned that the instrument functionality be extended to measure signals reflected by the sea surface so as to derive scatterometric information [Martin-Neira, 1993].

OBSERVATION REQUIREMENTS AND DATA PRODUCTS

The observation requirements for a GRAS-based system have been compiled by a Science Advisory Group including numerical weather prediction (NWP) experts. They are formulated separately for the three application domains, namely operational meteorology, climate monitoring and prediction, and space weather, as detailed in Tables 2-4 for a **MetOp-type** mission. In the tables, the horizontal resolution indicates the mean distance of individual soundings over the specified time window (defined as the time required to achieve global coverage). The timeliness requirements are referred to the time of observation. For operational meteorology, these stringent requirements have top priority and drive the design of the ground processing subsystem. On the other hand, the main performance requirements (accuracy, vertical domain) are slightly relaxed compared to the performance achievable with the most sophisticated retrieval algorithms.

	Temperature	Humidity	Refraction angle
Geographic coverage	global	global	global
Horizontal resolution	<1000 km	< 1000 km	< 1000 km
Vertical resolution	0.5-1.0 km	0.5 km	< 0.5 km
Vertical range	500 hPa to 10 hPa (5-30 km)	surface to 300 hPa (0-10 km)	surface to 80 km
Time window	< 12 hours	c 12 hours	c 12 hours
Absolute accuracy	< 1.0 K	< max{10 %, 0.2g/kg}	< max{1 prd, 0.4 %}
Timeliness	3 hours	3 hours	2.25 hours

Table 2: Observation Requirements for Operational Meteorology

	Temperature	Humidity
Horizontal domain	global	global
Horizontal resolution	< 1000 km	< 1000 km
Vertical domain	surface to 1 hPa (< 50 km)	surface to 300 hPa (< 10 km)
Vertical resolution	0.5 km/1.0 km (Troposphere/Stratosphere)	0.5 km
Time domain	> 10 years	> 10 years
Absolute accuracy	< 0.2 K (monthly average)	< 3 % (monthly average)
Long term stability	< 0.1 K/decade	< 2 %/decade
Timeliness	1-2 months	1-2 months

Table 3: Observation Requirements for Climate Monitoring and Prediction

	Ionospheric monitoring, modelling and prediction		E layer analysis	Plasmaspheric analysis and modelling
	large-scale	meso-scale		
Horizontal domain	global	global	global	global
Horizontal resolution	< 1000 km	< 1000 km	< 1000 km	< 5000 km
Vertical domain	100- 800 km	100- 800km	90- 130km	103-2 10 ⁴ km
Vertical resolution	10 km	5km	0.5 km	500-5000 km
Time domain	> 1 year	> 1 year	> 1 year	> 1 year
Time window	< 12 hours	< 12 hours	< 12 hours	c 12 hours
Accuracy: TEC	0.5-5%	0.1-5%	0.5-5%	2-20%
electron density	1-20%	1-10%	1-10%	10-30%
Timeliness	3 hours	1 - 2 months	1-2 month	1 - 2 months

Table 4: Space Weather Observation Requirements

The currently assumed architecture for the MetOp space and ground systems is outlined in Fig. 1 (where PCDA = Polar Command and Data Acquisition; PDIF = Polar Data Ingestion Facility; PSCC = Polar Satellite Control Centre). Two high-latitude ground stations will be used, e.g. in Kiruna and Fairbanks, so ensuring a data **downlink** at each orbit.

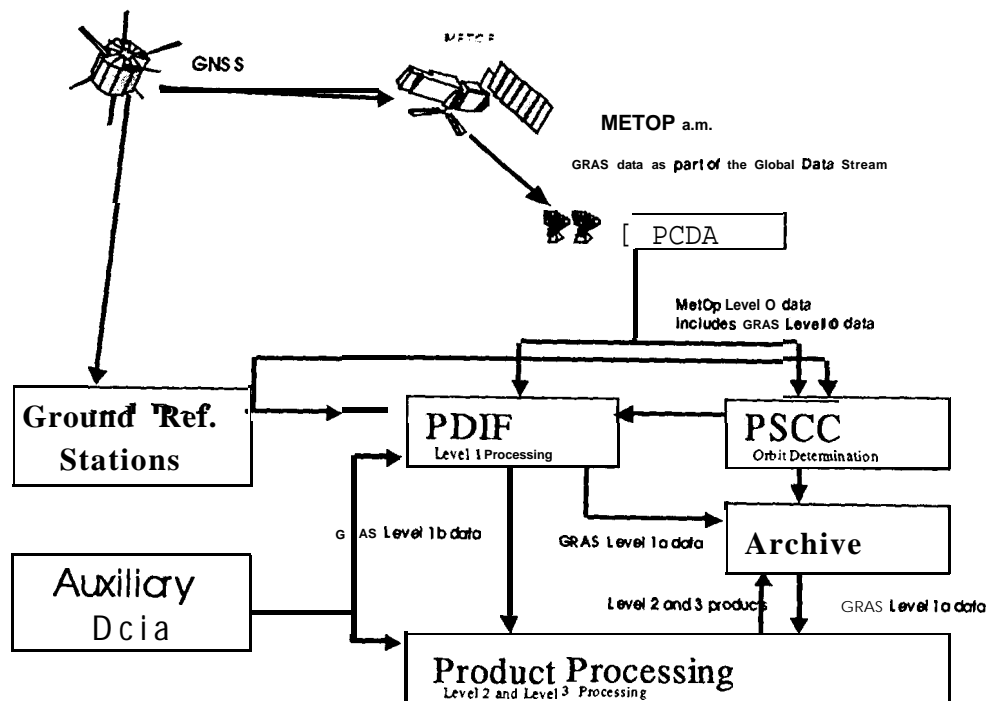


Figure 1: Space/Ground Segments Architecture

Following the CEOS (Committee for Earth Observation Systems) guidelines, the GRAS data products have been defined for various processing levels:

- Level 1a: tracking and occultation data (code and carrier phases, amplitudes), ground station tracking data (for occultation processing), ancillary spacecraft and ground station data;
- Level 1b: GRAS POD data, GNSS POD data, L1 and L2 excess phase and amplitude data, L1 and L2 refraction angles (functions of the ray impact parameter);
- Level 2: refractivity profiles, temperature, pressure and humidity profiles, total electron content and electron density profiles;
- Level 3: profiles (1D), images (2D) and fields (3 or 4D) of atmosphere parameters.

A simplified outline of the data processing (from level 1a to levels 1b and 2) is given in Fig. 2. Level 1b data should be available to users within 2.25 h and level 2 data within 3 h. Apart from the POD step, the other processing steps to derive level 1b and level 2 data (referred to as the occultation processing) are not computationally demanding and can be performed well within the timeliness requirement. This applies also when advanced retrieval methods based e.g. on the Fresnel transform for diffraction correction are applied [CRI et al., 1998].

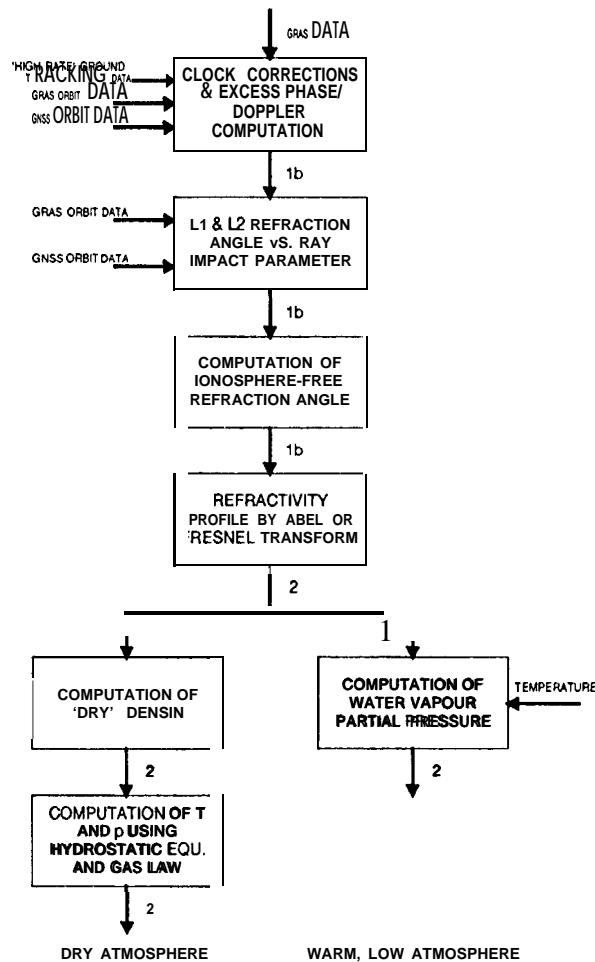


Fig. 2: Data processing from 1a to 1b and 2

PROCESSING REQUIREMENTS

GRAS and GNSS POD data is required in the first processing step (computation of the excess phase delay and **doppler** shift caused by the atmospheric refraction) and in the second step (computation of refraction angles). Ground tracking data is also required in the first step to derive single differences (SD) of carrier phases, which remove GNSS oscillator instability errors. It is expected that ionosphere-free refraction angles will be the preferred input to NWP systems for data assimilation [Eyre, 1994].

The ground tracking data will be taken from a set of -10 reference stations properly distributed over the globe. These stations must be equipped with high-availability **geodetic**-class GNSS receivers and clocked by high-performance USO. The data retrieval must occur at least as often as the orbital period, About 12 to 15 stations would be needed if the processing were based on the use of double-differences, with some increase in the operation costs.

The POD requirements for both the GRAS-carrying satellite and the GNSS satellites have been assessed using a software simulator. The EGOPS (End-to-end GNSS Occultation Performance Simulator) tool is used to perform sensitivity analyses with respect to several

parameters of both the 'model world', which include detailed models of the signal propagation and of the observing system, and the retrieval system (i.e., the ground processing chain) [CRI et al., 1998]. The **EGOPS** retrieval system can accept an input of simulated data or real data. This feature was used to validate the tool, GPS-MET phase measurements being reproduced within the 'model world' to mm-level precision. Atmospheric parameters were also retrieved from **GPS-MET** data and successfully compared with in situ measurements and with the results of analyses using NWP systems.

The POD position accuracy for both GNSS and GRAS affects only the determination of the measurement geometry. The accuracy needed for the ray impact parameter and the ray perigee is related in general to the maximum refractivity gradients found during a tropospheric occultation. If it is insufficient, the error on the height level attributed to a given temperature or humidity measurement can exceed the vertical resolution of the RO technique. However, for operational meteorology a vertical resolution of 0.5 km is acceptable, hence the position determination accuracy can be fairly relaxed. A formal requirement for POD of GRAS and GNSS of 1 m rms has been set, which is expected to be feasible without special developments.

The velocity estimation accuracy is the 'driving' requirement, since a velocity error maps directly in the excess **doppler** shift in the first processing step. The **doppler** error is proportional to the projection of the velocity estimation error on the ray path, therefore, because of the occultation geometry, the main error components are the along-track one for GRAS and the radial one for GNSS. The challenging requirement is on the velocity estimation accuracy of the low-orbiting GRAS. Analyses and EGOPS simulations agree that a GRAS along-track error of 0.05 mm/s, corresponding to -0.2 K error in the temperature retrieval under average conditions, should be the goal. For operational meteorology, a 1 K error at 30 km implies a maximum along-track velocity error of 0.2 -0.3 mm/s, assuming the system is designed in such a way as to make the other error contributors negligible in comparison. The velocity estimates are also used in the computation of the refraction angles from excess **doppler** shifts, but the impact on the final accuracy is negligible if the velocity error is at the sub-mm/s level.

USE OF PREDICTED GNSS ORBITS AND RAPID PRODUCTS

GPS rapid orbits and orbit predictions are now established IGS products of high quality. Efforts are underway to improve them further, in particular to continuously ensure predicted orbits at the decimeter level. This will exceed what is needed for the GPS POD data in the data processing to level 1b. As regards the prediction of velocities, thermal errors obtained by comparing predicted GPS orbits with GPS precise orbits have been computed and found to remain below 0.05 mm/s over a 24 hours prediction period. The accuracy of GPS predicted orbits, both in terms of position and velocities, is therefore not considered critical. No results are yet available about the performance of GLONASS POD or orbit predictions.

For the MetOp satellites, the current baseline assumes that the dedicated ground network needed for occultation processing is used also for POD. Previous experience suggests however that the required POD (velocity) accuracy will be reached only after augmenting the network to at least -20 reference stations properly distributed in the northern and southern hemispheres. Considering that, in this initial approach, the POD must be performed in near-

real time (within -20 minutes from downlink of GRAS data), this scenario is particularly demanding for both data transmission and computation time.

A possible alternative consists in taking advantage of the IGS rapid orbit products to perform POD and precise orbit predictions for the MetOp satellite or other low Earth orbiter (LEO). Recent results obtained at the Delft Institute for Earth-Oriented Space Research (DEOS) indicate that the accuracy to which the orbit of an ERS-class LEO can be predicted may suffice for occultation processing [Visser et al., 1996]. The DEOS work included a comparison between ERS-2 predicted orbits and precise orbits for April 1996. The GEODYN software was used for both POD and orbit prediction, the POD being based on laser ranging data. The predicted radial position rms accuracy was found to deteriorate from about 14 cm for the first day to about 54 cm for the fifth day. For the predicted along-track velocity, the rms accuracy was about 0.06 mm/s over the first day and 0.09 mm/s over the second day. The caveat is of course that these results have been obtained in a low solar activity period, i.e. a favorable situation for air density prediction. For future LEOS, continuous tracking with GPS which will improve the POD accuracy, while prediction accuracy will benefit from better dynamic models.

A timeline for this processing scenario is sketched in Fig. 3. Assuming that rapid combined orbit/clock products are available at sub-daily intervals, e.g. every 6-12 hours, with clock data at relatively high rate (30 s period or less), the LEO POD can be performed after each rapid product delivery using the rapid products and all the GRAS tracking data available at the end of the period of validity of the rapid products (period no. 1 in Fig. 3; here all the GRAS tracking data up to retrieval m together with the rapid products delivered at the end of period 2 can be used for POD). The POD is followed by a precise orbit prediction over a period of e.g. 48 hours. The process is repeated when new rapid products are delivered. The occultation processing following a generic retrieval n of the GRAS data and of the ground tracking data will therefore use predicted orbits for both GPS and LEO. Only the occultation processing will be performed after each GRAS data retrieval, hence at the LEO orbital rate. Two benefits are obtained, namely the time needed for the LEO POD becomes much less critical and the need to augment the dedicated ground network to cater also for LEO POD is removed.

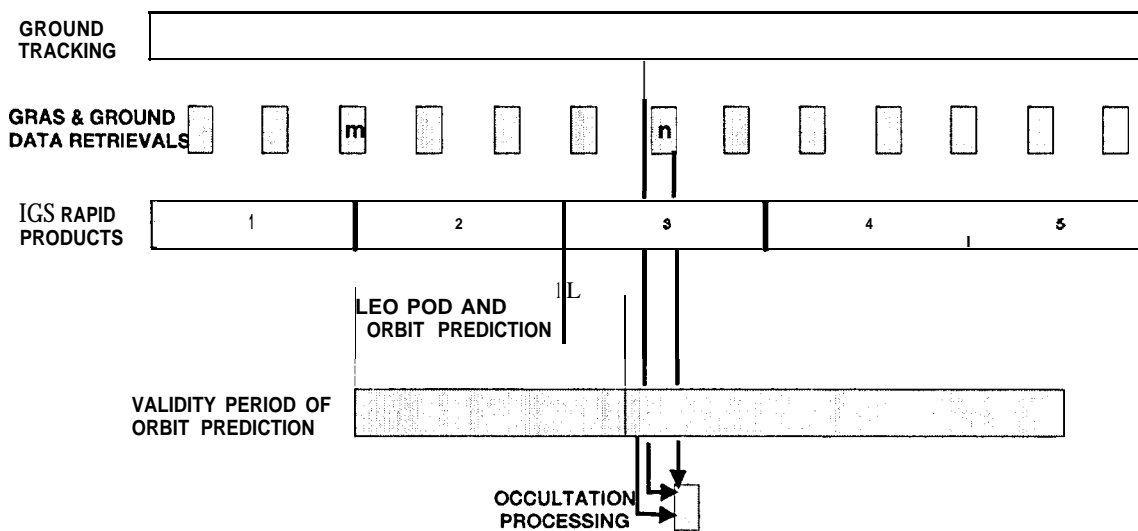


Figure 3: Timeline for Ground Processing using Rapid Orbit and Clock Products

A critical aspect is given by the delivery rate of the rapid products, which equals the rate at which the LEO orbit predictions are updated. It remains to be investigated whether delivery of rapid products every 12 hours (with 12 hours latency, as assumed here) is sufficient for accurate orbit predictions also with high solar activity. On the other hand, since the GPS tracking data from the dedicated ground network will be available anyway, it should also be investigated whether these can be used to correct the predicted LEO orbits with limited computational effort.

CONCLUSIONS

The GRAS programme aims at providing atmospheric soundings for operational meteorology and other applications. The operational use of the data products puts severe constraints on delivery time and consequently drives the complexity and cost of the ground data processing. A possible approach relying on the availability of precise GPS orbit predictions and of combined orbit/clock rapid products has been outlined. To be useful for this application, the rapid products should be provided at a sub-daily rate and include 'high rate' clock solutions based on tracking data from ground stations with reference clocks.

Acknowledgements: discussions with P. Visser of Delft University of Technology and G. Kirchengast of Graz University are gratefully acknowledged.

REFERENCES

- CRI et al., 1998, Using Global Navigation Satellite Systems (GNSS) for Operational Meteorology and Climatology, Final report of ESA Contract 11930, ESA Publication Division, ESTEC, Noordwijk, The Netherlands
- DMI et al., 1995, Derivation of Atmospheric Properties using a Radio Occultation Technique, Final report for ESA Contract 11024, ESA Publication Division, ESTEC, Noordwijk, The Netherlands
- ESA, Atmospheric Profiling Mission, 1996, SP-1 196(7), ESA Publication Division, ESTEC, Noordwijk, The Netherlands
- Eyre, J.R., 1994, Assimilation of Radio Occultation Measurements into a Numerical Weather Prediction Model, ECMWF Technical Memorandum 199, ECMWF, Reading, UK
- Gurvich, A. S., T.G. Krasilnikova, 1987, Navigation Satellites for Radio Sounding of the Earth Atmosphere, in *Issled. Zemli Kosmosa*, 6, pp. 89-93, March 1987
- Kursinski, E.R, et al., 1997, Observing Earth's Atmosphere with Radio Occultation Measurements using Global Positioning System, in *Journal of Geophysical Research*, 102, no. D19
- Martin-Neira, M., 1993, A Passive Reflectometry and Interferometry System (PARIS): Application to Ocean Altimetry, in *ESA Journal*, Vol. 17, pp 331-355

Melbourne, W.G., et al., 1994, The Application of Spaceborne GPS to Atmospheric Limb Sounding and Global Change Monitoring, JPL Publication 94-18, JPL, Pasadena, USA

Riley, S., et al., 1995, A Combined GPS/GLONASS High Precision Receiver for Space Applications, in *Proc. of ION-GPS International Technical Meeting*, Palm Springs, USA

Rocken, C. et al., 1998, Analysis and Validation of GPS/MET Data in the Neutral Atmosphere, to appear in *Journal of Geophysical Research*

Visser, P. N.A.M., et al., Operational Orbit Computation of ERS- 1 and -2 at DEOS, presented at AGU Fall Meeting, San Francisco, December 1996

Topic 3: IGS Reference Frame Realisation and Contributions to ITRF

IGS REFERENCE FRAME REALIZATION

J. Kouba

Geodetic Survey Division, **Geomatics Canada, NRCan**
615 Booth Str., Ottawa, Canada KIA OE9
e-mail: kouba@geod.emr.ca

J. Ray

Earth Orientation Dep., U.S. Naval Observatory
3450 Massachusetts Ave, NW, Washington, DC 20392-5420 USA
e-mail: jimr@maia.usno.navy.mil

M.M. Watkins

Jet Propulsion Laboratory (**JPL**)
M/S 238-600,4800 Oak Grove Drive, Pasadena, Cal. 91109 USA
e-mail: mmw@cobra.jpl.nasa.gov

ABSTRACT

The current set of 13 ITRF94 stations and the **IGS** approach to **ITRF** realization are no longer adequate for high precision frame reference definition. A new set of 52 Reference Frame (RF) Stations has been identified and is proposed to be used for a new IGS realization of **ITRF**. The new approach of **ITRF** realization is based on a nearly rigorous accumulated combination of weekly GNAAC SINEX solutions for station positions and EOPS of the current week. The **orbit/clock** solutions can then be obtained by an approximation of back substitution. This way the consistency of all IGS products, including the future IGS **SINEX** products, is enforced. It is proposed that this new, **nearly** optimal IGS realization of **ITRF** should be implemented preferably by June 28, 1998, but not later than January 3, 1999. The ITRF96 station coordinates and velocities for the set of 52 RF stations were evaluated and compared to an accumulated combination of GNAAC **SINEX** solutions, resulting in an rms agreement of a few mm horizontally and less than 10 mm vertically. For an interim and immediate improvement of the **IGS** realization of **ITRF**, it is suggested that a large subset of 47 **ITRF96** station positions and velocities be selected and used, starting as early as March 1, 1998. This new set of **ITRF96** stations is to replace the current 13 **ITRF94** station set.

INTRODUCTION

The prime objective of **IGS** is to provide a global **IGS** reference system, including realization, maintenance, and easy accessibility for all **IGS** users and GPS applications.

“A global IGS reference system” here is used in a broad sense. It encompasses not only a traditional reference system (with its **imbedded** reference frames, e.g. **ITRF**, **ICRF**, etc.), but also the standards and calibrations for ionosphere, troposphere and other, yet unforeseen, **GPS-related** information. Such a reference system, in addition to traditional theory, constants, conventions, documentation and monitoring, can be realized and represented in discrete and/or model forms. As with any global reference system, the IGS reference system must strive for global coverage and the utmost accuracy and consistency, both internally and with respect to the internationally adopted standards (e.g. **IERS**, **BIPM**, etc.). This is precisely what the IGS Terms of Reference imply. Even the components which contribute to the IGS reference system are listed, giving the specific IGS products for its realization, namely, orbits, EOP, station coordinates, clocks, along with (global) tropospheric and ionospheric information. The first four components (**orbits/EOP/station coordinates/clocks**) are fundamental in nature, although only the first three are generally considered to be absolutely essential, thus requiring the utmost precision to support IGS users. However, the recent precise point positioning approach (**Zumberge et al., 1997**) and the precise time transfer initiative (Ray, 1998) make the IGS clock product component equally important and fundamental in nature. Thus, the IGS quadruplet **orbits/EOP/station coordinates/clocks** must all be consistent and highly accurate. They should include GPS (and possibly **GLONASS**) satellites only and about 200 (polyhedron) stations. Not all possible (e.g. LEO) satellites and not all possible stations computed by ACS /AACs or observed by IGS users should or need to be included in the above IGS (reference system) product components. The **tropospheric/ionospheric** delay products should also be global (i.e. with global resolution), highly accurate and consistent within the IGS reference system. For more discussions on **clock/orbit** consistency and possible product additions and/or enhancements, see the other position papers and presentations at this workshop (e.g. Springer et al., 1998; Ray, 1998; Gendt, 1998; **Schaer and Feltens, 1998**).

The stability of the underlying reference frame (ITRF), realized by the global GPS network, **is crucial and an** integral part of, perhaps the basis of the whole IGS reference system as described above. However, the current IGS realization of ITRF has been gradually degrading due to the decrease in quality and availability of some of the 13 **ITRF** stations that are used for the current **IGS** realization of **ITRF94**. More specifically, the **ITRF94** realization is obtained by constraining the 13 **ITRF** station coordinates and velocities (**Kouba and Mireault, 1997, p. 56**). More and better ITRF station **position/velocities** and new approaches are required to solve this urgent problem. The future IGS reference frame realization should not only be precise, robust, consistent, and stable but it should also take advantage of the **GNAAC** station combinations (**G-SINEXes**). Furthermore, the **IGS** reference **frame** realization should ensure a high product consistency, in particular for the core products, viz., the IGS orbit, EOP, station coordinate (**G-SINEX** and **P-SINEX**) and clock combinations. The new ITRF96, which was recently released, can contribute significantly to the IGS reference frame realization, thus it is also discussed here.

CONSISTENCY OF IGS REFERENCE SYSTEM AND IGS PRODUCTS

Some constants and models defining a reference frame may not be accurately known, however the reference system should always be consistent, i.e. all the derived constants and reference system components must be consistent with these, albeit not accurately known, constants. Then transformation and relations to a new and improved reference system can be realized with greater precision and ease. The same is true for the underlying reference frames (i.e. positioned, oriented and scaled coordinate systems). A good example of the importance of reference system/frame consistency is the case of the core **IGS** products. The **IGS** orbit and IGS station solutions imply two realizations of **IGS** reference **frame**; i.e. they imply two sets of reference frame positions, orientations and scales that are not necessarily identical. Furthermore, the **IGS** EOPS imply an orientation for the reference **frame**. Clearly the implied reference frames should all be the same so that **IGS** users, when using any combination of the core products, will not detect any conflicts and (statistically speaking) will obtain the same results. For example, users of the new precise point positioning approach (**Zumberge** et al., 1997) realize the **ITRF** implied by the IGS orbits and clocks rather than a mixture of the two reference frames implied by stations and orbits, which is the case for more traditional GPS positioning approaches. This example also demonstrates the importance not only of the IGS orbits, EOPS, and stations but also clock solutions must be consistent with the other **IGS** products. It should be mentioned that the consistency of orbits and EOPS has been attempted from the very beginning, as evident from the fact that the initial **IGS** orbit combination enforced **orbit/EOP** consistency by rotating submitted orbits to adopted IERS (Bull. A and B) EOPS prior to the IGS combinations (**Beutler** et al., 1995). This was later abandoned in favor of separate orbit and EOP combinations as the AC orbits and EOPS were (and still are) considered to be sufficiently consistent (**Kouba** and **Mireault**, 1997). The need for **EOP/station** consistency, i.e. the need to include EOP in the **SINEX** station solutions, has also been recognized at an early stage (**Blewitt** et al., 1994). However, so far, less than half of ACS include EOPS in their **SINEX** submissions and the **SINEX** submissions for most ACS are not consistent with the **orbits/EOPs** submitted to IGS and the AC EOPS submitted to **IERS!** This is clearly unacceptable and a serious deficiency, which should be corrected as soon as possible!

The need for **clock/orbits/EOP/station** solution consistency is nowadays quite accepted, as it became evident thanks to the modern precise point positioning mentioned above. This will be **even** more accentuated with the time transfer project. However, that the tropospheric and ionospheric **IGS** products must also be consistent with the **IGS** core products is not as widely appreciated, but the same condition applies to these two atmospheric products. Specifically, tropospheric delays require the corresponding station solutions and (radial station error) corrections prior to the IGS tropospheric delay combinations (**Gend**, 1996). Clearly, **IGS** tropospheric delays should be harmonized (refer to) the **IGS** station coordinates (combined), or the adopted station solutions. Similarly for the ionospheric delay combination, the crucial component here is the (L1 -L2) calibration delay for both satellite and station hardware. This is important not only for single frequency (**L1**) users who use the ionospheric delay information for improved position

determinations (largely free of the ionospheric effects) (Huot et al., 1998), but it also has significant implications for precise time transfers. All the IGS clock products (be it the current satellite clock or the **future** station clock products) have the **L1/L2** delays imprinted in them; consequently the **L1/L2** calibrations are required and need to be applied when compared to external (time transfer) measurements at the ns and sub-ns level. Clearly, the **L1/L2 station/satellite** biases and **L1/L2** satellite and station clock corrections, be they implied or externally corrected for independent clock **comparisons/time** transfer such as in the proposed pilot project (Ray, 1998), must be precise and consistent (preferably the same, in this case). So we also have a strong “connection” of ionospheric and clock products and in turn a strong connection between clocks and the **orbit/station** position products (the station positions are required for receiver clocks, too).

REVIEW OF CURRENT STATUS OF IGS REFERENCE FRAME REALIZATION

Since the official start of IGS, the IGS reference frame realization has been accomplished by simply fixing, constraining or aligning **IGS/AC** solutions to the adopted ITRF coordinates of the same 13 stations: ALGO, FAIR, GOLD, HART, KOKB, KOSG, MADR, SAINT, **TIDB, TROM**, WETI', YAR1, YELL (see Figure 1). All the 13 stations have, or have had multi-technique (in most cases **VLBI**) collocations. Since January 1994, three official versions of **ITRF** have been used (**ITRF92, ITRF93** and **ITRF94**). Changes of ITRF versions introduced apparent station coordinate discontinuities that can reach up to 3 cm, in particular the changes to and from **ITRF93**, which was differently aligned by up to 1 mas with respect to the other **ITRFs** (Boucher et al., 1994). For more details and the specific estimates of transformation parameters between different **ITRF** versions used by IGS, please consult the Analysis Coordinator Report in the 1996 IGS Annual Report (Kouba & Mireault, 1997). Consult also the **IGSMail#1391** (<http://igs.cb.jpl.nasa.gov/igs.cb/mail/mess.1391>) which gives the information about a simple program facilitating the transformation of the current **IGS** sp3 orbit files to and from one of the above **ITRF** versions. In order to aid its users and prevent possible misuse and confusions connected with the past and future **ITRF** changes, IGS should consider transforming all past products based on previous **ITRF** realizations into the currently adopted **ITRF**. Even better, IGS should consider implementing, at the DC level, a simple user interface, e.g. based on the transformation program mentioned above, which would allow users to get all the **IGS** core products in an **ITRFyy** of their choice. However, it should be noted here that all such **ITRF** transformations of **IGS** products are only approximate due to limitations of the past and current ITRF realizations as discussed below.

Due to systematic errors in **ITRF** and GPS solutions, as well as the limited number, distribution and precision of the 13 (**ITRF94**) stations, the **station** position errors are mapped into the constrained **IGS/AC** solutions (and the implied reference frame). The distortions and reference frame variations vary amongst ACS and also in time, with possible small, periodical systematic and random effects. Even when a more optimal

approach, such as applying minimum datum constraints to unconstrained (“fiducial free”) AC solutions (see e.g. Heflin et al. 1997; Jefferson et al., 1997), the **ITRF** and GPS systematic errors as well as changes in station geometry and of processing approaches cause systematic reference frame variations (errors). For example, the current deficiency of the (13) **ITRF** station distribution is responsible for an increased noise and a decrease of the stability of **IGS** and AC solutions for PM y especially (Springer, 1998 personal comm.). More recently, the problems have been magnified since at least two or three **ITRF** stations have become unusable (e.g. **TROM**, **MADR**), leaving at times only 9 or even 8 **ITRF** stations available and usable as **fiducials**. Such a low number of stations can compromise all the **IGS/AC** products as reference frame errors can easily exceed the formal errors. The situation is particularly acute for the **IGS** Rapid products where timely availability of data is critical.

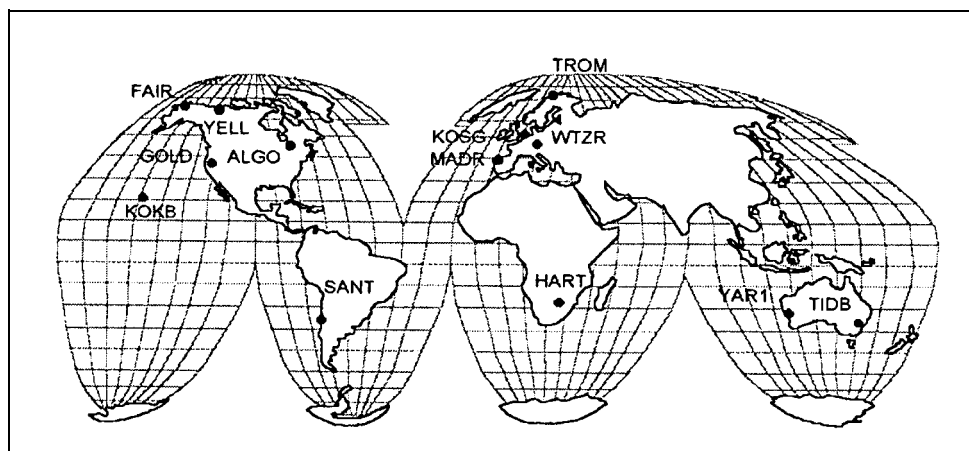


Fig. 1. The set of the 13 **ITRF** stations used by **IGS** for the current **ITRF94** realization

Clearly, a much larger number of **ITRF** stations and more consistent set of **ITRF** station coordinates than the currently adopted **ITRF94** coordinate/velocity set are urgently needed. That is why a search for a new much larger set of **ITRF** station was initiated during the AC Workshop held in March 1997 at JPL. An initial set of about 50, well distributed global stations, was identified as potential candidates at the workshop and the discussions continued by e-mail until August 1997 when a more definitive set of 52 stations was identified and agreed upon by all ACS (Figure 2). All the 52 stations survived a rigorous test and criteria of GPS data and solution quality, consistency and timeliness. Unlike for the 13 **ITRF** station selection, good multi-technique and **ITRF** coordinates, though important, are not as essential as long as there is a sufficient number of multi-technique stations remaining in the station set. This is so because there is already a sufficient number of **GPS-only** stations with a very high level of internal consistency which can effectively and reliably interpolate/realize **ITRF** even when some of the few crucial **ITRF** stations are missing, thus mitigating the current reference frame problems discussed above. Accordingly, this new set is termed reference **frame** (RF) station set, rather than an **ITRF** station set - the term used for the current 13 (**ITRF/multi-technique**) station set. For more details on the RF station list, the selection criteria as well as the individual station “performance”, please refer to Appendix I.

A relatively fast and efficient resolution of the current IGS reference frame “crisis” is to replace the 13 ITRF stations with **ITRF96** station coordinate/velocity set for most if not all the selected 52 RF stations. This is only an interim step as it does not address nor incorporate the **ITRF Densification** project and its potential impact and improvements in IGS ITRF realization. Before using the RF station ITRF96 coordinates and velocities they must first be evaluated and tested for precision and consistency. That indeed the new **ITRF96** version is highly consistent with ITRF94 is evident from Table 1, where the **ITRF96/ITRF94** alignment and coordinates/velocities for the 13 **ITRF** stations are compared. As one can see in Table 1, both **ITRF94** and **ITRF96** are almost identical in translation and orientation with the exception of small misorientations (of about -0.2 mas) in **R_x** and **R_z**, which are barely statistically **significant** (the formal sigmas are about 3 mm, 0.1 mas, 0.4 ppb). Even more encouraging is that the rates are practically zeros (equal or less than the formal sigmas of about 1 mm y⁻¹, 0.03 mas y⁻¹, 0.2 ppb y⁻¹). In the second part of Table 1, the alignment of each ITRF94 & 96 is checked with respect to NNR NUVELIA (McCarthy, 1996), using only the respective ITRF station velocities. Also shown are position/velocity rrms after the transformations, Both **ITRF** solutions are well aligned in velocity, with nearly zero rates. The differences between ITRF96 and ITRF94 rates in the last line of Table 1 compare quite well to the relative transformation rates in the second line. The formal sigmas for these NNR alignments are about the same as above, i.e. 1 mm y⁻¹, 0.03 mas y⁻¹ and 0.2 ppb y⁻¹. This should be no surprise as **ITRF94** and **ITRF96** time evolution should, by definition, be consistent with the NNR NUVELIA (Boucher, 1990).

Table 1: Transformation ITRF94 to ITRF96 (using the 13 ITRF station positions/velocities)

Epoch	T _x	T _y	T _z	R _x	R _y	R _z	S _{cl}	rms (mm)		
	mm	mm	mm	mas	mas	mas	ppb	dN	dE	dH
Param 1997	0.1	0.5	0.8	-0.190	-0.005	-0.230	-0.5	8.2	8.4	10.5
Rate ./y	-0.5	-0.2	-0.6	0.018	0.033	-0.002	-0.01	2.4	1.3	2.9
Rates with respect to NNR Nuvelia, computed from the velocities of 11 of the 13 ITRF stations; SANT & GOLD excluded due to plate margin effects .										
	mm/y	mm/y	mm/y	mas/y	mas/y	mas/y	ppb/y	rms (mm/y)		
ITRF96	-0.6	-1.8	-0.3	-0.03	0.02	0.02	0.00	1.6	2.2	2.7
ITRF94	0.2	-1.2	-0.6	-0.03	0.00	0.01	0.12	1.7	1.5	2.5
ITRF96-94	-0.8	-0.6	0.3	0.00	0.02	0.01	-0.12			

The **ITRF96** station coordinates of the newly selected 52 RF station set are evaluated in Table 2 and Fig. 3 where the **ITRF96** solution is compared to a combination of more than 100 GNAAC **SINEX** weekly combinations (GPS Weeks 830-933). The weekly GNAAC (**G-SINEX**) files are routinely produced by the three **GNAACs** (i.e. MIT, NCL and JPL) as a part of the **ITRF Densification** Project (Herring, 1997; Davies and **Blewitt**, 1997; **Heflin** et al., 1997). Remi **Ferland** of **NRCAN AC** (formerly EMR) kindly produced this “**IGS SINEX**” combined solutions (labeled here as **IGS97P05**), using his **SINEX** combination

software. As seen from Table 2 and Fig. 3, both **ITRF96** and IGS station positions are highly consistent and precise, at least for the 52 RF station set and for the epoch of 1997.0. The station position rms agreement (after a 14-parameter transformation) is at the 2-mm and 7-mm level for horizontal and vertical directions, respectively. Even for a more representative and useful epoch of 1998.0 the rms agreement is still at about 4-mm horizontal and about 10-mm vertical precision levels, which is significantly better than the **ITRF94/ITRF96** position agreement (see Table 1). For completeness, position rms values for epoch 1999.0 are also shown in Table 2 and Fig. 3. Individual station position residuals are listed in the Appendix II. It is expected that, except for one or two questionable **ITRF96** station velocities, the rms increases for the 1998 and 1999 epochs are largely due to weaker station velocities for the **IGS97P05** solution, since they are based on less than two years of GPS data. This can be seen in Fig. 3 but also in Table 3 where the **ITRF96** and **IGS97P05** station velocity solutions are compared to the NNR **NUVEL1 A** plate motion model.

Table 2: ITRF96 and combined (**IGS97P05**) station coordinates residuals for 52 RF stations at 1997.0 (**IGS97P05-ITRF96**) after 14-parameter transformation.

	Dx	Dy	Dz	dN	dE	dH	Epoch	Excluded from means & sig.
	mm	mm	mm	mm	mm	mm		
Mean	0.4	-0.7	0.1	-0.2	-0.3	0.0	1997	none
Sig	4.9	5.2	5.5	1.6	2.3	7.2		
Mean	1.8	0.4	1.9	0.2	0.0	0.0	1998	AUCK , CHAT dE & MCM4 dH
Sig	7.0	7.8	11.3	3.7	4.2	10.8		
Mean	3.1	1.5	3.6	0.5	0.0	-0.1	1999	AUCK, CHAT dE & MCM4 dH
Sig	10.3	12.6	19.1	6.0	7.2	17.4		

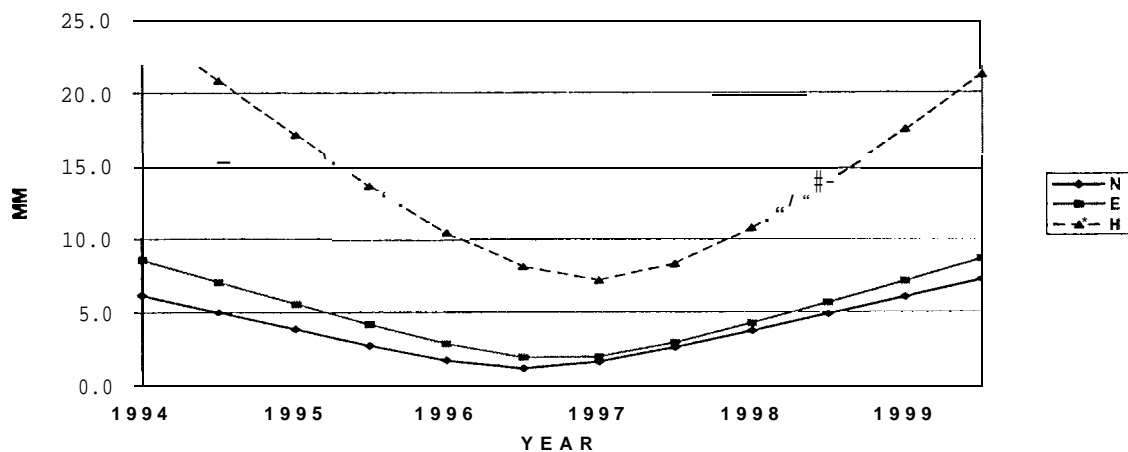


Fig.3: ITRF96 and combined (**IGS97P05**) station coordinates rms for 52 RF stations after a 14-parameter transformation.

While the IGS97P05 horizontal velocities compare equally well to NNR NUVEL1A, the vertical velocities show considerably worse agreement than ITRF96 (i.e. assuming the zero vertical motion which is implied by NNR NUVEL1 A). However, two ITRF96 station velocities (for AUCK and CHAT) appear to be anomalous (see the Appendix III, where individual station velocity residuals are listed), thus likely cannot be included in the new ITRF station coordinate/velocity set. Also, two Antarctic stations (MCM4 and CAS 1) appear to have erroneous vertical ITRF96 velocities. Thus the stations AUCK, CHAT, MCM4 and CAS 1, together with BHR, which has rather large ITRF96 residuals, were not recommended for inclusion into the new ITRF96 station set. Altogether 47 RF stations has been recommended for the new ITRF96 station set (Altamimi, 1998). IGS97P05, in addition to the same two Antarctic stations above, has additional problems with the vertical velocities at stations GRAZ, TROM, NYAL and LHAS (see Appendix III).

Table 3: ITRF96 and IGS97P05 differences from NNR NUVELIA (EURA, NOAM, AUST, ANTA, SOAM Plates) for RF stations (see the Appendix III for specific station exclusions to mitigate plate margin effects on the means and sigmas below).

STATION	PLATE	IGS97P05 - NNR NUVEL1A			ITRF96 - NNR NUVELIA		
		N (mm/y)	E (mm/y)	H (mm/y)	N (mm/y)	E (mm/y)	H (mm/y)
Mean	EURA	1.75	-2.18	3.81	1.37	0.36	0.52
Sigma	EURA	3.50	2.74	9.53	1.89	2.05	1.98
Mean	NOAM	-1.09	0.04	-0.63	-1.07	0.82	-0.52
Sigma	NOAM	1.45	1.80	4.85	1.07	1.52	2.34
Mean	AUST	2.53	-3.93	-3.74	-0.75	4.70	-1.40
Sigma	AUST	2.43	1.91	3.72	3.10	0.74	1.60
Mean	ANTA	-0.98	-3.17	0.75	-4.36	0.05	10.27
Sigma	ANTA	1.97	4.49	17.40	3.77	6.21	10.84
Mean	SOAM	1.12	1.73	3.18	-0.70	2.53	-2.50
Sigma	SOAM	0.57	2.38	4.97	1.42	3.08	6.64

It would be very useful if all ACS compare their best station **position/velocity** solutions to the ITRF96 coordinates/velocities of the 52 RF stations above, in particular for the problematic station solutions in both ITRF96 and/or IGS97P05 solutions. It is hoped that exclusions of stations (e.g. AUCK, CHAT, MCM4, CAS 1, BHR) from the new ITRF96 station set could be finalized at the workshop so that the new RF set of 47 stations could be adopted by IGS and used instead of the ailing 13 ITRF94 stations. It is proposed that this finalized RF station set, with the ITRF96 coordinates/velocities, together with the official **igs.snx** (SINEX Header template of antenna heights), is then used, starting as early as March 1, 1998, as an interim IGS realization of ITRF96. Since some small discontinuities

of about 0.2 mas are expected, it is essential that, as in the past, all ACS and the IGS products make this **ITRF96** change at the same time. Also note that it would be preferable that all ACS use minimum datum constraints (e.g. **Blaha**, 1971), based on this new **ITRF96** set, as recommended in the following sections. It is, however, recognized that, given the rather short time frame and the urgency, the usual (sigma) constraining should be acceptable. Besides, since the new set is highly consistent it is no longer so important (to apply the minimum datum constraints). In fact it may even be advantageous to apply sigma constraints, as the new **ITRF** set may be less prone to systematic effects (biases) than individual, minimally constrained AC and IGS solutions. This is applicable and important to IGS and AC Rapid solutions. Note that **all** stations of the new RF set, including some stations with possibly questionable **ITRF96** collocations, can be used for the new and nearly optimal IGS **ITRF** realization proposed in the next section because the new RF set is so internally consistent. Thus the IGS **ITRF96** realization will be defined by the adopted **ITRF96** positions/velocities of a large subset (47) of the RF stations, together with the current **igs.snx** template containing the antenna heights and offsets, The **igs.snx** file is maintained and available at the following **IGSCB** WWW site:

ftp:/ /igsb.jpl.nasa. gov/igsb/station/general/igs.snx

The adoption of the new **ITRF96** station set should result in significant improvements of stability and precision of all IGS core products and EOPS, in particular.

PROPOSED IGS REFERENCE FRAME REALIZATION AND MAINTENANCE

As already discussed above, it is essential that all **IGS** reference system components, i.e. all IGS combined products, be consistent and precise. In an ideal case this can be accomplished when all the submitted AC solutions are combined in a single rigorous (**SINEX**) adjustment of **all** the **IGS** products as unknown parameters. However this is not possible both for theoretical as well as practical reasons. Namely, strictly speaking, GPS global analyses cannot be (rigorously) subdivided into overlapping portions of networks (stations). In addition, it is very difficult to parametrize global adjustments and yet allow different and innovative approaches, For example, satellite state vectors are generally incompatible amongst ACS unless identical models and (stochastic) error models are employed, and yet satellite **ITRF** positions are largely independent of the modeling effects and thus are better suited for exchange, comparisons and combinations. Only approximations to an ideal and rigorous method are possible. There are several possible approaches, each with varying degrees of **complexity** and approximation.

It is important to free the **IGS** products from changes and errors in the fiducial stations set. These changes can occur either **from** upgrades in **ITRF** or the RF station set, which involved improvement of the relative site positions, or from errors either due to blunders at the AC's or due to unplanned configuration changes at fiducial sites. All of these have occurred in the last few years with the 13 **ITRF** stations, Therefore it is suggested to ACS and to GNAACS that always only minimum constraints (not "sigma constraints") are used

in the final solutions. The ITRF frame is then realized from a Helmert transformation of unconstrained solutions with proper outlier detection in the computation of the transformation parameters. This means a site by site review of station residuals after the transformation, and editing out any outlying site, and re-computing the transformation. This makes it possible to reduce or remove the “warping” like effect of an anomalous site. As seen from the above discussion, it is essential for precise, robust solutions in a consistent reference frame to have a large set of highly consistent RF station set.

Another relatively simple but well proven approach is an extension to the IGS combination of the “fiducial free” method which has been developed and used at JPL for a number years (see e.g. Jefferson et al., 1997). Here “fiducial **free**” orbit solutions are requested and then combined, resulting in a “fiducial free” **IGS** orbits **and** clocks. Then using a sufficiently large and well-distributed subset of **IGS** stations with the combined “fiducial **free**” orbits held fixed in a regular global analysis for “fiducial free” station positions and **other** pertinent parameters. In order to economize, the **new** precise point positioning approach can be used here, provided that the IGS clock information is precise, consistent and frequent enough. Finally, a reference frame is attached, **i.e. the** “fiducial free” combined orbits are transformed according to the transformation between the “fiducial free” station positions and the adopted set of **ITRF** stations. The advantage of **this** approach is the relative insensitivity to problems or changes of **ITRF** (i.e. “fiducial”) stations of the individual AC orbit solutions; i.e. the corresponding AC “fiducial free” station solutions need not to be used. However, the disadvantages are that the method does not use the valuable information contained **in AC station/EOP SINEX** solutions. The current orbit (and future station) reference frame consistency feedback to ACS, contained in the current **IGS** summary Tables 1, 2 and 4, would not be possible. Furthermore, the method relies on single software to provide the **station/orbit** datum connection, which could potentially result in a decrease of reliability and precision; and there is additional processing workload at the raw data level (even when the efficient point position method is used).

The approach highlighted here is based on a nearly rigorous (**SINEX**) combination of station **positions/velocities/EOP** (Blewitt et al., 1997). **It** is a method endorsed by the recent **IERS/ITRF** workshop held in October 1996 in Paris, Fr. (Reigber and Feissel, 1997). It was developed during the **ITRF densification** pilot project, thus it is fully compatible with the project. It also closely approximates a simultaneous adjustment of all the core IGS products, i.e. **orbits/EOP/clocks** and stations, while it maintains the core product consistency, as long as the submitted AC products themselves are consistent. The scheme is outlined below:

a. First, assume that **all** the submitted AC core solutions -- i.e. **orbits/clocks/EOP** (in SP3 and ERP files) and **A-SINEX** files also containing EOP -- are consistent, either unconstrained, or minimum datum constrained. For a detail description of the method of the minimum datum constraints see (e.g. Blaha, 1971; Vaníček and Krakiwsky, 1982, p.275). Note that this condition is not currently satisfied.

b. All the **A-SINEX** files (with **station/EOP**) are combined weekly by GNAACS and the resulting combinations (**G-SINEXes**) are then timely submitted (with **EOP!**) for a weekly **IGS** cumulative, unconstrained solution for station **position/velocities** and **EOP** (for the current week **EOP** only). This combination is called “accumulated kinematic solution” in **Blewitt et al. (1997)**. Note that the **A-SINEXes** could alternatively be used here, but this may not be optimal, as it would not take advantage of the **GNAAC** combinations, thus potentially it could be less robust and precise. This combination of **G-SINEXes** is, in fact, equivalent to a simultaneous **station/velocity** adjustment of all **A-SINEXes**, or all the GPS data accumulated **from** the start to the current week.

c. An ITRF reference frame is then attached to the unconstrained IGS combined SINEX solution of **station/velocity** and **EOP** (of the current week only). The reference **frame** attachment can be e.g. accomplished by minimum datum constraints, based on the soon to be finalized list of 47 RF stations with good ITRF96 positions/velocities. (See the previous section for detail discussions on the **ITRF96** station set). Altogether 14 minimum datum constraints are required (7 **Helmert** parameters and the corresponding rates). The values and sigmas used (derived at least from the **ITRF96** sigmas (or matrix) and the IGS matrix) should be entered in the **SINEX apriori** block, so that the original unconstrained SINEX file can be recovered. The above constrained file can be designated e.g. as **IGS(SSC/SSV/EOP)yyPww** (**yy-year; ww-the** week of the year), and considered the official (Final) IGS station/position and **EOP** product, and it would, in fact, represent the current and official **IGS** realization of **ITRF** as well. Note that **Blewitt et al. (1997)** also propose independent weekly combinations which, once ITRF is attached in a way which is consistent to the accumulated solution above, represent another type of IGS realization of **ITRF**. This discrete (weekly) realization should have a distinct **IERS** designation, e.g. **IGSyyPwww**, here **www** could stand for the GPS week.

d. Using the weekly **A-SINEXes** (the short (**SSC**) AC **SINEX** files would be preferred here) a 7-parameter transformation between the **IGSyyPww** above and each of the AC solutions is computed. The AC transformation parameters are then used to transform the submitted AC orbits and **EOP** (one transformation per each week and AC) to be consistent with the **IGSyyPww**. Furthermore, the AC orbits for each day are rotated according the AC PM differences between AC and **IGS EOP** (of step c, i.e. the **IGS(EOP)yyPww**), very much as it used to be done during the initial years for the IGS Rapid using **IERS Bull A** and the **IGS** Final using **IERS Bull B** orbit combinations (**Beutler et al., 1995**), Note that here, in place of or in addition to the daily PM rotations, full 7-parameter transformations can also be applied to AC orbit, while maintaining the history of transformation parameters in Tables 1 and 2 of the IGS (Final) combinations. This forms an important AC feedback on solution datum connections and consistency amongst orbit, **EOP** and station coordinate solutions. The check of consistency here is that the weekly mean PM **x, y** differences and the corresponding **Ry, Rx** rotations are statistically the same.

e. Finally, the transformed AC orbits (i.e. weekly by the 7-parameter transformations and daily by the AC PM **y,x** differences) are then combined into the consistent **IGS** orbits. Subsequently the AC clocks are corrected for the **AC-IGS** orbit radial differences as it is

already being done for the current IGS **orbit/clocks** combinations.

In this way, a new and unique official **IGSyyPww SINEX** product would be introduced which would also contribute to much higher consistency of the other IGS core products as **well** as more precise and stable **IGS ITRF** realization (through the **IGS** core products) than it is the case today. ACS would be well advised to use the **IGSyyPww station position/velocities** of RF stations for their ITRF needs, in particular for the AC and IGS Rapid solutions. In fact the above concept of ITRF realization is, due to its complexity and inherent delays, only practical for the IGS Final products. Timely (i.e. the weekly) **IGSyyPww station/EOP** solutions would greatly benefit all IGS users and the AC Rapid analyses and the **IGS** Rapid products generation in particular, including the **IGS** timely contributions to **ITRF**. When attaching a reference frame to the IGS Final **SINEX** “cumulative kinematic” solution it is important that the accumulation include weekly solution for geocenter and scale and this information is also entered into the in **IGSyyPww SINEX** file. This way a precise geocenter and monitoring is maintained as well as unique and exact (i.e. stable with no drift) reference frame attachment is enforced.

It should be noted here that the above “accumulated kinematic solution” (IGSyyPww) is optimal in terms of station positions/velocities only, as it uses all past and present GPS data in a rigorous way (Helmert blocking). While, the above proposed orbit solutions with minimum or no constraints (i.e. “fiducial free”) are, strictly speaking, sub-optimal as only GPS data from the current day or week is utilized in AC orbit solutions. The IGS (Final) orbit solution would be optimal only if the IGSyyPww position/velocity matrix (of the previous week) is used for constraining in the AC solutions (of the current week) in this way all data, including the past data are used in a rigorous way.

Although the AC solutions, constrained according to sigmas as it is currently done by most ACS, or according to the **IGSyyPww** matrix, can in principle, be used here, it is recommended that AC apply minimum or no datum constraints in all AC Final solutions. Currently, the sigma/matrix constraining can potentially introduce small reference frame inconsistency even when a highly consistent and precise station coordinate set such as the future **IGSyyPww** set is used. This situation, as discussed above, should change fairly quickly with proper and efficient feedback on AC **orbit/EOP** and station solution consistency and frame relative biases, That is why the proposed scheme of orbit combination (“back-substitution”) and the question of sigma/matrix versus minimum or no constraints in AC Final solutions, should be reviewed after several years of operation of the proposed scheme, or when AC Rapid solutions that use **sigma/matrix** become more precise and stable than the corresponding AC Final ones.

For the **AC/IGS** Rapid solutions, the **sigma/matrix** constraining of RF stations with **IGSyyPww** positions/velocities, could be quite acceptable or even desirable due to lack of data availability. Besides it is only meaningful to maintain and realize IGS realization of ITRF from more definite and also more precise **IGS/AC** Final solutions. By using the recent **IGSyyPww** station positions/velocity maximum consistency between **IGS** Rapid and Final products is ensured. Note that regardless of which method of constraining ACS

choose (unconstrained, minimum) to apply for their Final solutions, their **orbit/EOP/clocks** (i.e. SP3 and **ERP** files) must be transformed to be consistent with the corresponding weekly AC **SINEX/EOP** files.. This should not be a major effort, and in fact should have been enforced from the beginning, and besides, it has already been the case for some ACS for several years now! (See the Appendix VI for more detail information and practical suggestions on AC product consistency).

It is important that a unique (and official) IGS station polyhedron product is established, In that regard it would be preferable if the **GNAAC** polyhedron combinations (i.e. **P-SINEXes**) are used instead of **G-SINEXes** in the step *b* above, however the use of **P-SINEXes** would introduce delays of up to several weeks which may not be acceptable. Besides it is advantageous that RNAACS, as it is currently required, use the IGS Final **orbit/clock/EOP** products in their (**R-SINEX**) analyses. In this regard, it is far more efficient and convenient to obtain an official IGS station polyhedron product (**P-SINEX**) by a back substitution, using the above IGSyyPww global solution. The **IGSP-SINEX** products would then have the same IERS designation, i.e. **IGSyyPww**.

SUMMARY AND RECOMMENDATIONS

It is essential that all the **IGS** products are made highly consistent and in particular the **IGS** core products (i.e. **orbits/EOP/clocks** and station positions) must be consistent as they are used in various combinations for different applications or realizations of the **IGS** reference frame. This necessitates that all the AC core products submitted to IGS and IERS must be self-consistent, The urgent need for a larger and more precise **ITRF** station set than is the case for the currently used 13 **ITRF94** stations can quickly and sufficiently be met by adopting **ITRF96** positions/velocities of a new **ITRF** set of about 47 stations. This interim step should be adopted as early as March 1, 1998.

A new and nearly optimal **ITRF** realization should utilize the **GNAAC** combinations. It is nearly optimal in terms of station positions/velocities and EOPS; in fact it is the same approach recently recommended by IERS for simultaneous solutions of EOP and positions. In order to increase the IGS product consistency and to prepare ground for adaptation of the new approach of **ITRF** realizations, the following recommendations are offered for consideration to the workshop:

1. That IGS adopts **ITRF96** as early as March 1, 1998 to replace the currently ailing and problematic IGS realization of **ITRF94**, which currently is based only on less than 13 **ITRF** stations.
2. As an interim measure and to facilitate an immediate **ITRF** realization improvement it is recommended that the selection of the new **ITRF96** station positions and velocities for a large subset of the RF station is finalized at this workshop. This newly selected **ITRF96** set of the 47 globally distributed IGS stations is to be used for **ITRF96** realization in all IGS products beginning as early

as March 1, 1998. IGS realization of ITRF is then accomplished by the above ITRF96 station coordinates/velocities together with the current official **igs.snx**, which contains antenna offset and height information in the **SINEX** format.

3. That all weekly submitted AC **SINEX** solutions (A-SINEXes) contain the EOP of the current week and that the submitted AC orbits/clocks (**sp3**) and EOP (**erp**) files are consistent with the above A-SINEX solutions. This is essential not only for the increased **IGS** product consistency but also for the future (improved) ITRF realization and IGS products. It is recommended that this is implemented and ensured by all ACS by June 28, 1998.
4. That the **GNAAC** combinations retain (and adjust) the submitted AC EOP information of the current week in their **G-SINEX** combined products, along with the usual station position solutions. It is recommended to be implemented by June 28, 1998.
5. The **SINEX** extensions as outlined in the Appendix IV, allowing the minimum datum and transformation parameter constraints to be coded in the **SINEX format**, are accepted and used by IGS on or before March 1, 1998. Furthermore, that IGS submits the **SINEX** extension for acceptance to Prof. Tom Herring of **CSTG**, who is currently responsible for the **SINEX format**. This will provide a means and encouragement to ACS and other IGS users to use (minimum) datum constraints, as well as it allow an **efficient** and safe monitoring of geocenter and scale changes (e.g. Ray, 1997). It is further recommended that only the AC Final products, which are based on minimum or no datum constraints, be accepted for the **IGS Final orbit/clock/EOP/station** combinations after June 28, 1998. (See the Appendix V for more details and suggestions on coding the minimum datum constraints in the AC (A-SINEX) submissions).
6. That a (super) combination of **G-SINEXes** for station coordinates and EOP is researched and initiated on behalf of IGS. This EOP (**G-SINEX** combination) cumulative solution would replace the current IGS EOP combination and it would lead to an official **SINEX** station solution product (both for global as well as the polyhedron stations). The polyhedron **SINEX** solutions could be produced by back substitution when P-SINEXes are made available to produce the **IGS P-SINEX** products (station **positions/velocities** only). The implementation goal should also be by June 28, with the **official IGS SINEX (G and P)** products on or before January 3, 1999!

Remarks: The current **IGS orbit/clock** combination would require only minor modifications, i.e. the prior transformations based on one set of (up to 7) transformation parameters for each week and AC, and for each AC a pair of **daily PM x,y** difference rotations (and/or up to 7 transformation parameters), all with respect to the current **IGSyyPww SINEX** solution. This step **can** be viewed as an approximation of a back substitution adjustment process for the (IGS Final) satellite orbit solutions. Due to annual

and semiannual effects for some stations in most current AC solutions (see the AC poster presentations at this workshop), it is mandatory that, until these effects are removed or mitigated, that the new **ITRF** realization use only the **IGSyyPww** solutions that are only derived from an exact multiple of years.

REFERENCES

- Altamimi, Z. , 1998, IGS Reference Station Classification Based on **ITRF96** Residual Analysis, *1998 IGS AC Workshop* held at ESOC Darmstadt, February 9-11.
- Beutler, G., J. Kouba and T. Springer, 1995, Combining the orbits of the IGS Analysis Centers, *Bull. Geod.* **69**, pp. 200-222; also in the *Proceedings of the IGS Analysis Center Workshop*, held in Ottawa, Canada, October 12-14, 1993, pp. 20-56,
- Blaha, G., 1971, Inner adjustment constraints with emphasis on range observations, *Depart. Of Geodetic Science Report 148*, The Ohio State University, Columbus, Oh., U.S.A.
- Blewitt, G., Y. Bock and J. Kouba, 1994, Constructing the IGS Polyhedron by Distributed Processing, *Proceedings of the IGS workshop on the ITRF densification*, held at JPL, Pasadena, Cal., Nov. 30-Dec 2, pp.21-36.
- Blewitt, G., C. Boucher and J. Kouba, 1997, Procedure for **ITRF** continuous realization, the report to the IGS GB, a draft dated Sep. 15, 1997, distributed to all ACS on November 14, and presented to The IGS Governing Board Meeting held in San Francisco, Cal on Dec. 11.
- Boucher, C, 1990, definition and realization of terrestrial reference systems for monitoring Earth rotation, in *variation in Earth rotation*, D.D. McCarthy and W.E. Carter(eds.), pp. 197-201.
- Boucher,C, Z. Altamimi and L. Duhem, 1994, Results and Analysis of the **ITRF93**, *IERS Technical Note 18*, Observatoire de Paris, October,
- Boucher, C, Z. Altamimi, M. Feissel and P. Sillard, 1996, Results and Analysis of the **ITRF94**, *IERS Technical Note 20*, Observatoire de Paris, March,
- Davies, P. and G. Blewitt, 1997, Newcastle-upon-Tyne IGS GNAAC Annual Report 1996, *International GPS Service for Geodynamics (IGS) 1996 Annual Report*, pp. 237-252.
- Gendt, G., 1996, Comparison of IGS Tropospheric Estimations, *IGS AC Workshop Proceedings*, Silver Spring, Md, March 19-21, pp.151-164.
- Gendt, G., 1998, IGS Combination of Tropospheric Estimates – Experience From Pilot Experiment, *1998 IGS AC Workshop* held at ESOC Darmstadt, February 9-11.

- Heflin, M.B., D.C. Jefferson, M.M. Watkins, F.H. Webb and J.F. Zumberge**, 1997, Comparison of Coordinates, Geocenter, and Scale from All IGS Analysis Centers: GNAAC Activities at the Jet Propulsion Laboratory, *International GPS Service for Geodynamics (IGS) 1996 Annual Report*, pp. 253-254.
- Herring, T.A.**, 1997, MIT T2 Associate Analysis Center Report, *International GPS Service for Geodynamics (IGS) 1996 Annual Report*, pp. 255-270.
- Huot, C., P. Tetreault, Y. Mireault, P. Heroux, R. Ferland, D. Hutchison and J. Kouba**, 1998, IGS Related Activities at the Geodetic Survey Division, Natural Resources Canada, "EMR" Analysis Center poster presentation, *1998 IGS AC Workshop* held at ESOC Darmstadt, February 9-11.
- Jefferson, D. C., M.B. Heflin, M.M. Watkins and F.H. Webb, J.F. Zumberge, Y.E. Bar-Saver**, 1997, Jet Propulsion Laboratory IGS Analysis Center Report, *International GPS Service for Geodynamics (IGS) 1996 Annual Report*, pp. 183-192.
- Kouba, J.**, 1997, Status of The IGS Pilot Project to Densify the ITRF, *International GPS Service for Geodynamics (IGS) 1996 Annual Report*, pp. 101-116.
- Kouba, J. and Y. Mireault**, 1997, Analysis Coordinator Report, *International GPS Service for Geodynamics (IGS) 1996 Annual Report*, pp. 55-100.
- McCarthy, D.D.** (cd.), 1996. IERS Conventions (1996), *IERS Technical Note 21*, Observatoire de Paris, July.
- Ray, J.**, 1997, IERS Geocenter Campaign /IERS Working Group on the ITRF Datum, see <http://maia.usno.navy.mil/geoc.html>.
- Ray, J.**, 1998, The IGS/BIPM time transfer project, *1998 IGS AC Workshop* held at ESOC Darmstadt, February 9-11.
- Reigber, C. and M. Feissel.** (cd.), 1997, IERS missions, present and future, Report on the 1996 IERS Workshop, *IERS Technical Note 22*, Observatoire de Paris, January.
- Schaer, S. and J. Feltens**, 1998, Position paper on IGS ionospheric delay products, 1998 *IGS AC Workshop* held at ESOC Darmstadt, February 9-11.
- Springer, T., J.F. Zumberge and J. Kouba**, 1998, The IGS Analysis Products and Consistency of Combination Solutions, 1998 *IGS AC Workshop* held at ESOC Darmstadt, February 9-11,
- Vaniček P. and Krakiwsky, E.J.**, 1982, *Geodesy - The Concept, The North* Holland Publishing Co., Amsterdam, New York, Oxford.

Zumberge, J. F., M.B. Heflin, D.C. Jefferson, M.M. Watkins and F.H. Webb, 1997, Precise point positioning for the efficient and robust analysis of GPS data from large networks, *Journal of Geophysical Research (JGR)*, Vol. 102, No. B3, pp. 5005-5017.

APPENDIX I

(August 15, 1997)

ITRF station selection criteria. (For fuller explanations, see the Remarks at the bottom of the table.)

- 1) Stable and permanent monumentation, possibly with local stability nets (not used, but see Remarks below)
- 2) ACS *not* including site in SINEX submissions
- 3) High quality and reliable station hardware
- 4) Performance including timely data communications; based on igsnet and G-SNX GCOMP Reports: >0 - above, <0 below average; (#)- # of inclusions in GCOMP (=22 max; 0- local or not operating station (wk 0878-900))
- 5) Favorable station data quality (RFI, multipath, etc.) based on igsnet includes phase/Code quality: >0- above; <0 below average.
- 6) Supportive and responsive station staff
- 7) Good quality ITRF94 position and velocity
- 8) Multi-techniques collocations (R=VLBI, L=SLR, D=DORIS G= absolute G)
- 9) Established GPS observing history (> 2 years) (not used)
- 10) Comments from CODE Analysis Center

CODE	1)	2)	3)	4)	5)	6)	7)	8)	9)	10)
	Used	Hrdw.	Perf.	Qual.	Staff	ITRF	Tech.			AC
----- ----- ----- ----- .---. ----- ----- ----- ----- -----										
[For explanation of notations, see Remarks below]										

Europe:

*KOSG			R12	1.0(22)	0.6		A	1		Move !
* MADR			R8	-.5(4)	-1.7	X	A	R		x
MATE	r,e,j,s		TR	-1.3(11)	-1.7		A	RL		
NYAL	r		R8	-5.6(7)	-3.1		B	R D		x
ONSA	r,j		TR	0.7(22)	0.5		A	R		
* TROM			R8	-3.0(13)	-3.0		B	E-V r		Rec.
VILL	c,r,g,j,n,s		TR	2.5(0)	0.7		NONE			x
*WTZR			TR	0.1(22)	0.0		A	RL		
GRAZ			TR	-1.7(2)	-1.7		A	L		
POTS			TR	1.9(16)	1.9		A	L		
ZWEN			TR	-4.7(16)	-0.8		NONE			

Asia:

KIT3			TR	-0.3(13)	0.2		CT	D		
SHAO	r,g		TR	0.3(15)	0.2		CT	RL		
TSKB			TR	2.3(19)	0.6		B	r		
IRKT			TR	-2.0(9)	0.5		NONE			
LHAS			TR	-1.3(16)	-0.5		NONE			

Africa/Arabia :

BAHR	r,e,n,s	Z12	0.9(5)	-0.2		NONE		New
* HART		TR	-0.7(18)	0.0		B	RLD	
MALI		RC	-4.3(8)	-3.7		NONE		Rec.
MAS1	r,n,j,s	TR	N/A (to be completed ASAP)			ASAP)		

N. America

*ALGO		TR	2.7(22)	0.6		B	R	
BRMU	r,j	TR	2.7(22)	0.6		CT	r	
DRAO	e,j	TR	2.6(15)	0.7		z	r	
*FAIR		R8	2.6(20)	0.6		B	R D	x
* GOLD		R8	-1.6(19)	-1.6	x	CT	RLD	x
MDO1	r,j,s	TR	2.3(20)	0.6		A	RL	
NLIB	r,e,j,s	TR	2.1(6)	0.7		B	R	
PIE1	r,e,g,n,s	TR	2.6(0)	0.7		B	R	
THU1	r,e,n	R12	-0.6(0)	0.7		NONE		
*YELL		TR	2.0(22)	0.1		B	R D	
GODE		TR	2.4(0)	0.6		A	rL	
WES2		TR	1.3(20)	0.3		dU=4cm	Rl	

S. America

AREQ		TR	-1.0(17)	0.4		B	L D	
FORT		TR	-0.5(18)	-0.5		B	R	
* SANT		TR	1.1(17)	-0.3		B	R D	
BRAZ		TR	-1.3(12)	-0.3		NONE		
KOUR		RC	0.1(14)	-1.9		B	D	Rec.

Astralia:

HOB2	r,e	TR	-2.0(18)	-0.2		CT	R	
*TID2		TR	2.2(21)	0.7	x	?	RLD	x
*YAR1		R8	-2.1(21)	-1.9		B	LD	Rec.
MAC1	r	TR	-1.4(12)	0.1		NONE		
PERT		TR	2.4(22)	0.6		NONE		
CHAT		TR	0.4(2)	-0.2		NONE		
AUCK		TR	1.3(0)	0.2		NONE		

Antarctica:

CAS1	r,e	TR	-1.1(20)	0.0		c		
DAV1		TR	-1.4(17)	-0.4		c		
KERG		RC	-2.5(19)	-2.3		B	D	Rec.
MCM4		TR	1.7(19)	0.4		c		
OHIG	r	TR	-2.3(18)	-1.0		z	R	

Pacific

* KOKB		TR	2.2(21)	0.5	B	R D	
KWJ1	r	TR	2.4(2)	0.6	NONE	r	New
GUAM		TR	1.0(12)	0.5	NONE	D	

* current fiducial stations

=====
Columns Remarks:

- 1) Some stations have large antenna heights (> 2m) eg, NYAL, TROM, BAHR HART and MATE is mounted on a roof.
- 2) This column lists the analysis centers not using the station. The Information was obtained from the AC's weekly analysis report. (Letter code represents first letter of AC's name except for EMR which is "r")
- 3) Hardware codes are:
 - r8 for big rogue,
 - RC for mini rogue,
 - TR for 8 channel turborogue
 - R12 for 12 channel turborogue
 - Z12 for 12 channel ashtech
 - TE for 8 channel Trimble SSE
- 4) and 5) The code used are the average of the "igsnet" latency and **quality** code respectively. The average was computed using 4 randomly selected weeks of 1997.
- 6) X = poor response, likely should not be recommended
- 7) A = Class A: collocated sites with quality <2 cm at 1988 and 1993
 B = Class B: collocated sites with quality <3 cm at 1993
 c = Class C: not Class A or B, with no large residuals
 Z = Class Z: sites with large residual (blunder or poor determination); DRAO & OHIG have large height discrepancies
 T = local tie to GPS not available
 ? = TID2 not in ITRF94 (although TIDB is) and no site log available
 NONE = not included in ITRF94
 E-V = East velocity inconsistency with VLBI
 dU=4cm = GPS vs. VLBI height discrepancy of -4 cm at WES2
- 8) R=VLBI, L=SLR, D=DORIS G=absolute G; lower case letters indicate mobile site, poor data quality, or discontinued operations
- 10) X-means : Do NOT use as fiducial station.
 - New Relatively new station
 - Rec. Receiver change necessary (big or mini rogue)
 - Move Site will be moved!
 KOSG will be moved to Westerbork (tens of kilometers away).

However there will be something like a year "overlap" using both receivers; the old one in KOSG and new one at new site Westerbork.

=====

NOTE BY JF Zumberege's performance & quality coefficient determination

Col. 4:

Based on 169 daily IGSnet reports spanning the period October 12, 1996 through April 11, 1997, we show in Table 1 a summary of statistics. Scores from each of the following three categories have been normalized to zero mean and unit sigma: (1) number of times the site occurred with non-trivial entry in the daily IGSnet reports; (2) the quality field from the daily report; and (3) the latency field from the daily report (only nonzero latencies are considered). The sum of the three normalized numbers is then averaged for each site. Roughly, positive scores are above average.

Col. 4 (xx) # of weeks station survived GCOMP's (max 22); see GCOMP for rejection criteria

Col.5 the same as Col 4. except that only IGSnet quality considered

APPENDIX 11

ITRF96 and combined (IGS97P05) station coordinates residuals for 52 RF stations at 1997.0 (IGS97P05-ITRF96) after 14-parameter transformation.

1997.0 IGS97P05-ITRF96	(nun)					
	D _x	D _y	D _z	dN	dE	dH
ALGO	-1.0	0.0	-2.2	-1.4	-1.0	-1.8
AREQ	-0.4	-6.7	1.1	2.8	-2.5	5.7
AUCK	13.7	4.6	8.6	-0.9	-5.8	-15.7
BAHR	-7.0	-7.1	-5.4	-0.5	0.9	-11.3
BRAZ	0.8	-1.7	1.9	2.3	-0.5	1.2
BRMU	-0.6	-0.3	-0.9	-0.8	-0.7	-0.5
CAS1	-3.1	4.8	-10.6	0.8	1.2	11.9
CHAT	3.9	8.9	3.1	-0.8	-8.7	-5.4
DAV1	-2.6	3.8	-1.6	2.4	3.3	2.6
DRAO	1.2	-0.8	-2.5	-1.7	1.4	-1.8
FAIR	3.7	1.3	-7.7	0.2	0.9	-8.6
FORT	-1.4	-0.5	1.5	1.4	-1.3	-0.9
GODE	5.5	-15.3	10.7	-1.8	1.8	19.2
GOL2	2.4	-5.1	1.9	-0.4	4.5	4.0
GRAZ	-13.3	-4.3	-14.3	0.4	-0.6	-20.0
GUAM	-1.1	-1.8	-1.2	-1.2	2.2	-0.4
HART	-0.1	-0.5	-3.5	-3.3	-0.4	1.3
HOB2	0.1	1.0	-3.5	-2.3	-0.9	2.7
IRKT	-1.6	0.8	1.2	-0.1	1.3	1.6
KERG	-4.7	0.4	3.0	1.1	4.6	-3.0
KIT3	1.2	-2.0	-1.1	0.0	-1.8	-1.7
KOKB	5.0	0.3	-3.9	-1.8	1.4	-5.9
KOSG	-1.1	-1.1	-1.3	0.2	-1.0	-1.8
KOUR	1.4	-9.8	1.9	1.1	-4.8	8.8
KWJ1	2.2	-2.8	-2.8	-2.4	2.3	-3.1
LHAS	0.4	19.6	9.6	-1.3	-0.7	21.8
MAC 1	0.1	3.5	-1.2	0.2	-3.3	1.7
MADR	-2.7	3.1	-9.9	-5.7	2.9	-8.7
MALI	-2.5	-0.1	-0.2	-0.3	1.6	-2.0
MAS1	-3.6	0.7	-2.6	-0.6	-0.3	-4.4
MATE	-0.4	-1.4	-1.1	-0.3	-1.2	-1.3
MCM4	1.2	0.9	5.9	0.3	-1.1	-4.9
MDO1	0.5	-2.3	1.7	0.4	1.0	2.7
NLIB	0.7	-1.7	0.4	-0.8	0.7	1.5
NYAL	1.8	-0.8	6.7	-0.3	-1.1	6.9
OHIG	0.3	-4.6	0.0	3.6	-2.2	1.8
ONSA	1.5	0.0	4.0	1.0	-0.3	4.2
PERT	2.8	1.1	-0.5	-0.6	-3.0	0.1
PIE1	-0.7	-6.7	5.5	0.9	1.5	8.5
POTS	-1.6	-1.0	-1.8	0.3	-0.6	-2.5
SANT	0.2	-0.8	4.2	4.0	-0.1	-1.6
SHAO	-0.5	-0.6	-0.6	-0.3	0.7	-0.6
THU1	0.9	-2.7	4.5	-1.8	-0.1	5.1
TID2	5.3	-3.4	3.4	-0.9	0.2	-7.1

TROM	1.4	0.8	6.4	0.8	0.3	6.5
TSKB	0.1	-0.7	-0.5	-0.1	0.5	-0.7
VILL	-3.7	0.4	-2.1	0.8	0.1	-4.2
WES2	-2.3	-3.0	2.6	0.5	-3.1	3.3
WTZR	-2.3	-1.2	-2.1	0.6	-0.6	-3.2
YAR1	-0.3	8.7	-4.3	0.1	-3.5	9.1
YELL	2.2	2.2	-7.0	-0.7	1.1	-7.6
ZWEN	-3.5	0.1	-3.3	0.4	2.2	-4.3

Mean	0.4	-0.7	0.1	-0.2	-0.3	0.0	Epoch Excluded 1997 none
Sig	4.9	5.2	5.5	1.6	2.3	7.2	
Mean	1.8	0.4	1.9	0.2	0.0	0.0	1998 AUCK, CHAT
Sig	7.0	7.8	11.3	3.7	4.2	10.8	dE, MCM4 dH
Mean	3.1	1.5	3.6	0.5	0.0	-0.1	1999 AUCK, CHAT
Sig	10.3	12.6	19.1	6.0	7.2	17.4	dE, MCM4 dH

APPENDIX III

ITRF96 and IGS97P05 differences from NNR NUVEL1 A for RF stations. (* stations excluded from the averages and sigmas below)

STATION PLATE		IGS97P05- NNR NUVEL1A			ITRF96 -NNR NUVEL1A		
		N (mm/y)	E (mm/y)	H (mm/y)	N (mm/y)	E (mm/y)	H (mm/y)
GRAZ	EURA	0.7	-1.7	22.9	1.1	1.5	0.8
KOSG	EURA	2.2	-4.1	-0.3	0.6	-0.4	0.8
MADR	EURA	-7.0	1.9	-1.6	-0.5	1.4	3.9
VILL	EURA	-1.8	-4.7	-9.1	-0.9	0.1	1.5
WTZR	EURA	1.5	-3.3	-2.3	-0.3	0.7	-2.4
POTS	EURA	1.8	-3.2	-1.1	0.5	0.7	4.2
ONSA	EURA	1.7	-3.7	3.6	-0.6	-0.7	0.1
MATE	EURA	7.1	-2.8	2.6	5.6	2.3	-0.7
TROM	EURA	4.8	-6.0	19.5	3.0	-3.8	-0.8
NYAL	EURA	1.5	-4.0	14.8	1.1	-1.4	-2.0
ZWEN	EURA	5.5	-0.7	3.7	2.4	-1.8	-0.5
IRKT	EURA	1.0	3.1	1.8	2.6	2.3	-0.1
KIT3	EURA	3.8	0.9	-5.0	3.3	4.0	1.8
SHAO *	EURA	0.9	6.9	1.4	-0.6	10.2	-1.0
TSKB*	EURA	5.8	-26.7	-4.1	4.6	-21.0	-5.3
Mean	EURA	1.75	-2.18	3.81	1.37	0.36	0.52
Sigma	EURA	3.50	2.74	9.53	1.89	2.05	1.98
ALGO	NOAM	-1.9	0.4	-1.1	-2.2	1.2	-0.5
DRAO	NOAM	0.0	0.3	0.5	1.5	2.7	1.2
FAIR	NOAM	-3.4	1.4	-8.1	-2.4	2.3	-0.1
GODE	NOAM	-2.5	0.8	-3.3	-0.4	-2.1	-3.8
MDO1	NOAM	-0.9	0.7	-5.2	-1.5	1.4	2.0
NLIB	NOAM	-0.6	-0.3	-3.7	-1.2	0.9	-3.7
THU1	NOAM	-2.6	-0.4	9.0	-0.7	-1.9	-3.8
PIE1	NOAM	0.4	0.0	0.1	-1.5	1.0	1.2
WES2	NOAM	1.4	-5.0	6.0	-1.9	1.2	-1.4
BRMU	NOAM	-1.6	0.9	0.3	-0.5	0.8	2.4
YELL	NOAM	-0.3	1.5	-1.4	-0.9	1.7	0.7
GOL2*	NOAM	5.8	-6.0	-9.7	6.8	-2.5	0.1
Mean	NOAM	-1.09	0.04	-0.63	-1.07	0.82	-0.52
Sigma	NOAM	1.45	1.80	4.85	1.07	1.52	2.34
HOB2	AUST	2.6	-5.1	-5.9	1.5	5.2	-1.1
PERT	AUST	2.0	-4.2	-3.8	-3.4	4.9	-0.1
TID2	AUST	5.7	-1.1	-6.8	2.3	5.1	-3.7
YAR1	AUST	-0.2	-5.3	1.5	-3.5	3.6	-0.6
AUCK*	AUST	2.9	-4.8	-8.8	2.3	17.1	-0.6
MAC1*	AUST	-16.0	-6.7	-6.6	-17.9	3.8	0.8
Mean	AUST	2.53	-3.93	-3.74	-0.75	4.70	-1.40

Sigma	AUST	2.43	1.91	3.72	3.10	0.74	1.60
CAS1	ANTA	-3.0	-0.1	29.7	-7.3	2.2	13.9
DAV1	ANTA	-1.9	-5.1	-3.9	-8.0	-4.0	1.3
MCM4	ANTA	1.7	3.1	-16.5	0.3	9.5	27.4
OHIG	ANTA	0.5	-6.3	-6.7	-1.1	-0.8	1.8
KERG	ANTA	-2.2	-7.5	1.1	-5.7	-6.5	6.9
Mean	ANTA	-0.98	-3.17	0.75	-4.36	0.05	10.27
Sigma	ANTA	1.97	4.49	17.40	3.77	6.21	10.84
BRAZ	SOAM	1.5	0.6	-2.2	-2.3	-0.9	-10.1
FORT	SOAM	0.5	0.1	7.6	-0.1	3.3	2.3
KOUR	SOAM	1.4	4.5	4.2	0.3	5.1	0.3
AREQ*	SOAM	7.7	10.4	1.3	3.1	14.6	-1.1
SANT*	SOAM	7.4	18.9	-1.1	4.2	19.1	8.1
Mean	SOAM	1.12	1.73	3.18	-0.70	2.53	-2.50
Sigma	SOAM	0.57	2.38	4.97	1.42	3.08	6.64
BAHR	AFRC	12.1	2.5	1.0	15.6	1.9	2.0
HART	AFRC	-5.2	-15.8	0.3	-1.2	-4.1	1.5
MAS1	AFRC	-1.6	-4.2	-1.3	-1.8	-0.1	3.1
KOKB	PCFC	3.6	-6.5	-8.9	0.9	-2.5	-1.6
KWJ1	PCFC	1.6	-11.3	-6.0	3.2	-7.7	-4.2
CHAT	PCFC	3.5	-3.7	-7.6	2.5	25.3	-0.4
MALI	INDI	-4.2	-9.8	2.4	-5.6	-4.2	2.7
LHAS	INDI	-28.1	8.4	-20.6	-25.2	6.5	1.8
GUAM	PHIL	7.2	28.5	3.0	4.7	32.1	-0.5

APPENDIX IV

PROPOSED SINEX 1.00 EXTENSION EXTENSIONS FOR DATUM CONSTRAINTS AND TRANSFORMATION PARAMETER SOLUTION

By

Remi Ferland, NRCan

(Nov 20, 1997)

Transformation parameters and inner constraints are routinely estimated/applied during coordinates computations. Currently, there is no explicit definition to incorporate those in SINEX. This is an attempt to correct this minor problem by proposing standard names and usage.

The transformation parameters may be estimated and/or applied or their sigmas used to constrain the solution

When the transformations parameters are estimated, they can appear in the ESTIMATE block and optionally in the APRIORI block as is currently done for the station parameters. The sign convention should follow IERS convention.

When the transformation parameter sigmas are used to provide the reference frame constraint with the inner constraints technique, those constraints are unfortunately not explicitly provided.

The general SINEX practice has been to have a one to one explicit correspondence between APRIORI and ESTIMATED parameters. For the inner constraints case, the transformation parameters would only appear in the SOLUTION/APRIORI and optionally in the SOLUTION/MATRIX_APRIORI blocks. This would provide the 7 (or less) constraints to apply and code explicitly in the SINEX format.

Names should be reserved for the transformation parameters and their rates (units) such as:

RX RY RZ TX TY TZ SC (mas mas mas m m m ppb)
RXR RYR RZR TXR TYR TZR SCR (ma/y ma/y ma/y m/y m/y m/y pb/y)

When used as inner constraints, the variables Code, Point and Solution could be respectively '-----' '---' '-----'
The apriori values would not be needed.

Example #1:

Minimum datum (rotational) constraints only:

```

*-----
+SOLUTION/APRIORI
*Index  _Type_  Code Pt Soln  _Ref_Epoch_  Unit S  _Apriori Value_____  _Std_Dev____
  1  RX  -----  -  00:000:00000  mas  O  .000000000000000E+00  .1000000E+0
  2  RY  -----  -  00:000:00000  mas  O  .000000000000000E+00  .1000000E+0
  3  RZ  -----  -  00:000:00000  mas  O  .000000000000000E+00  .1000000E+0
-SOLUTION/APRIORI
*-----

```

Example #2:

Transformation from ITRF94 to ITRF93:

```

*-----
+SOLUTION/APRIORI
*Index  _Type_  Code Pt Soln  _Ref_Epoch_  Unit S  _Apriori Value_____  _Std_Dev____
  1  RX  -----  -  88:000:00000  mas  O  -.390000000000000E+00  .1000000E-1
  2  RY  -----  -  88:000:00000  mas  O  .800000000000000E+00  .1000000E-1
  3  RZ  -----  -  88:000:00000  mas  O  -.960000000000000E+00  .1000000E-1
  4  TX  -----  -  88:000:00000  m  o  .006000000000000E+00  .1000000E-1
  5  TY  -----  -  88:000:00000  m  O  -.005000000000000E+00  .1000000E-1
  6  TZ  -----  -  88:000:00000  m  O  -.015000000000000E+00  .1000000E-1
  7  se  -----  -  88:000:00000  ppb  O  .400000000000000E+00  .1000000E-1
  8  RXR  -----  -  88:000:00000  ma/y  O  -.110000000000000E+00  .1000000E-1
  9  RYR  -----  -  88:000:00000  ma/y  O  -.190000000000000E+00  .1000000E-1
 10  RZR  -----  -  88:000:00000  ma/y  O  .050000000000000E+00  .1000000E-1
 11  TXR  -----  -  88:000:00000  m/y  O  -.002900000000000E+00  .1000000E-1
 12  TYR  -----  -  88:000:00000  m/y  O  .000400000000000E+00  .1000000E-1
 13  TZR  -----  -  88:000:00000  m/y  O  .000800000000000E+00  .1000000E-1
 14  SCR  -----  -  88:000:00000  pb/y  O  .000000000000000E+00  .1000000E-1
-SOLUTION/APRIORI
*-----

```

(The **Apriori** Values are real but the **Std_Dev** were made-up for this example)

APPENDIX V

SUGGESTIONS FOR AC SUBMISSIONS OF MINIMUM DATUM CONSTRAINT A- SINEX SOLUTIONS

As proposed in the paper it is recommended that the ACS final orbit/EOP/station/clock solutions be only minimally constrained and that they be consistent. More details on possible approaches and suggestions on how to make all the AC solutions consistent can be found in the Appendix VI. Here it is only suggested how a minimum constrained AC Final (A-SINEX) station/EOP solution can be coded in the SINEX format.

Although in principle unconstrained (consistent) solutions could be used, it is convenient or even necessary to constrain (i.e. attach a datum to) the AC solutions for several reasons. As already discussed in the paper, at least for the time being it is essential that the datum constraints be minimal in order to preserve the relative station/orbit precision and/or datum connections. In this way it is hoped that an efficient feedback on orbit/EOP/station consistency can result in significant consistency improvements .

Since only the three orientation parameters (Rx, Ry, Rz) are nearly singular (with sigmas of a few 10's of mas), by definition, the minimum datum constraints can only include the three rotational parameters. In fact the example #1 of the Appendix IV already demonstrates how such a minimum (datum) constraint A-SINEX submission could be coded. In this way, the important geocenter and scale information implied from the Global AC analysis is preserved. Note that in principle (due to near singularity) any values Rx, Ry, and Rz can be used, so they are of little significance and need not even be coded (i.e. zero values could be used instead) . However the apriori sigmas, or the apriori matrix used, must be coded properly in the apriori SINEX blocks, so that the original (unconstrained) matrix can be recovered. The apriori minimum (rotation) constraints are thus somewhat arbitrary and could be based on e.g. a transformation between the original unconstrained station solution and the IGSyyPww solutions of the 52 RF station set. Alternatively, until IGSyyPww becomes available, the new ITRF96 station set of 47 stations can be used instead.

Analogously for the GNAAC weekly combined SINEXes only the minimum (i.e. rotation) datum constraints could also used, or alternatively, a complete 7-parameter solution (and the corresponding apriori information) could be coded (see e.g. the example #2 of the Appendix IV). When the IGSyyPww RF set becomes available it could be used for the transformation solutions/apriori or alternatively it can be used directly as apriori information. The important consideration here is that all apriori (datum) constraints be fully removable and the original geocenter and scale information be retained.

APPENDIX VI

SUGGESTIONS AND DISCUSSIONS ON AC SOLUTION/PRODUCT CONSISTENCY

It is essential that the consistency of all AC solutions be maintained. This is true for the proposed new ITRF realization in particular. The consistency of the Final orbit, EOP, station, clock and tropospheric delay solutions are to be maintained regardless of whether minimum datum or no constraints are used. (Note that after June 28, 1998 it is proposed that only minimum or no constraints be used for all Final AC solutions; see the Appendix V for more details and the proposed coding in the SINEX format). Since ionospheric delays are not sensitive to reference frame changes and are only needed to connect the IGS clock solutions to external standards, they are not discussed here.

The fact that AC station solutions are currently accumulated and submitted to the IGS on a weekly basis somewhat complicates the product consistency. (Note that weekly-accumulated station solutions were adopted by IGS as a compromise between daily and yearly station submissions.) Depending on the degree of sophistication and the additional CPU time expense, there are at least three possible approaches available to ACS:

1. A rigorous adjustment for all products based on the whole weeklong period. Though preferable, for practical considerations and given the current submission and CPU limitations, this is difficult to realize.

2. A rigorous adjustment for a part of the AC products, e.g. station positions and EOP, accumulated over a one-week period. Then the remaining parameters are obtained by a rigorous back-substitution. This approach may already be feasible for some ACS; in fact, some ACS are already doing this. Note that the solutions for the remaining parameters, while fixing all the relevant parameters obtained from the above-accumulated rigorous (partial parameter) solution, are equivalent to rigorous back-substitution in terms of the parameter values only, but not in terms of the corresponding covariance matrix. So, if the matrix is not required (as is currently the case for the AC orbit/clock/tropo solutions), this back-substitution by parameter fixing could also be a practically viable alternative.

3. A rigorous adjustment for a part of the AC products, e.g. Station positions and EOP, accumulated over a one-week period. All the remaining parameters are then obtained by approximations of back-substitution. More specifically, approximate solutions consistent with the weekly-accumulated SINEX station/EOP solutions can be obtained by applying appropriate parameter transformations computed between the daily (minimum datum or no constraint) station solutions and the accumulated AC A-SINEX solution for the current week. Since this is relatively easy to implement and likely will be a choice for most ACS, below are more details for all the relevant AC product solutions.

EOP (erp-format): The EOP and sigmas from the A-SINEX solution are coded in the erp weekly file, which accompanies the sp3 daily orbit files.

Orbits (sp3 format): 7 parameter transformations between each daily (minimum or no constraint) station solutions and the weekly A-SINEX solution are applied to the corresponding (minimum or no datum constraint) daily orbits. In this way the daily transformed orbits approximate back-substitutions and are consistent with the A-SINEX.

Satellite clocks: The (minimum or no datum constraint) daily clocks are increased by the height corrections computed from the daily station dx , dy , dz shift and scale (Sc) transformations. I.e. the following consistency corrections are added to the daily satellite clock solutions:

$$Dt = ((dx.Xs + dy.Ys + dz.Zs)/Rs + Sc.Rs)/c;$$

where Xs , Ys , Zs , are the ITRF SV coordinates, Rs is the SV radius vector and c is the speed of light. Note this correction accounts for the origin changes of the daily station solutions. The second correction, based on the orbit height errors (with respect to the daily station origin) also needs to be applied but with the opposite sign (see the test below for more details), however this is already being done during the current IGS orbit/clock combinations.

Station clocks: the daily station clocks (to be submitted for some stations in the near future, in a yet to be specified format) need to be corrected only for relative height errors, i.e. the daily station height residuals after 7 parameter transformation between the daily and the A-SINEX station solution. The daily station height residuals with respect to the A-SINEX, expressed in time units, are subtracted from the corresponding daily (minimum or no datum constraint) station clock solutions. Note that the daily transformation parameters (shift and scale) should not be included in this correction.

Tropospheric delays: The tropospheric (tropo) delay corrections are completely analogous to the station daily clocks, i.e. the only difference is that the daily station height residuals are scaled by an empirical scaling factor of about .15 to .30. This factor is likely COntant for an AC, but could vary from AC to AC. It may be a function of the elevation cut-off and/or elevation dependent weighting used.

EXAMPLE : Consistency transformation between EMR sigma constrained and unconstrained solution for Feb 02, 1998 (wk 0943, day 01)

In addition to the regular EMR09431 Final solution, which uses the ITR94 position and sigmas of the 13 ITRF stations as apriori constraints, the second, unconstrained solution was generated with large (at least 10 m) apriori position sigmas for all stations. The Table 1 summarizes the parameter transformations between the corresponding orbit as well as between station solutions.

Table 1: 7 parameter orbit and station transformations for unconstrained -constrained solutions

Product	dx	dy	dz	Sc	R x	Ry	Rz	2D	H
	mm	mm	mm	ppb	mas	mas	mas	RMs(mm)	
Orbits	3	66	43	0.0	.48	-.36	.26	73	40
Stations	-4	140	84	-0.1	.76	-.42	.24	9	13
Difference	1	-74	-41	0.1	-.28	.06	.02		

As one can see, except for the shift parameters dy, dz and the rotation Rx, both the orbit and station transformations are quite consistent. The large and disturbing dy bias, typically also seen for the EMR unconstrained (weekly SINEX) solutions (see the weekly GNAAC summary reports by JPL, MIT and NCL) is also seen for this daily solution. The smaller dy, dz orbit shifts are likely due to orbit dynamics and gravity field which should mitigate (or resist to) any geocentre offset, more than for the station solution. For most ACS the geocentre offsets of unconstrained solutions are much better behaved and usually they are small, within 10-20 mm. This EMR example, in fact, could represent a worst scenario case. The differences in Table 1 also indicate the need for daily 7 parameter transformations in the IGS orbit combinations to account for larger variations in the shift and orientation biases for some AC (minimum or no constraint) solutions.

As outlined above, the approximate transformations/corrections were applied to the unconstrained clock and tropo delay solutions and then they were compared to the constrained solution. The results of comparisons are summarized in Table 2. **Note that** for the satellite clocks, the orbit height error (which includes the daily orbit offsets and scales) were subtracted in addition to adding the above height corrections based on the daily stations offsets and scale transformations. The first (orbit height error) correction, in fact **simulates** the orbit height corrections available and applied in the current IGS clock combinations. In other words the orbit height corrections applied here effectively only include the differential dx, dy, dz and scale offsets listed in the last row of Table 1.

As one can see the consistency transformations/corrections of step 3) seem to be quite acceptable with respect to the formal sigmas. Although the formal sigmas are likely rather pessimistic due to significant correlation amongst the above solution parameters.

Table 2. Comparisons of the unconstrained and constrained clock, tropo EMR Final solutions for Feb 02, 1998.

Solution	RMS (unconstrained - constrained)		Average formal sigma
	Original	transformed	
Sat. clocks	.195 ns	.061 ns	.123 ns
Sta. clocks	.056 ns	.040 ns	.087 ns
Tropo delays	2.7 mm	1.7 mm	4.6mm

A final note on the 7-parameter transformation between unconstrained **daily** solution and the minimally constrained **A-SINEX** solution: Due to the near rotational singularity of the daily unconstrained solutions one can only use the identity matrix weighting. Alternatively, if matrix weighting is desired, one should first "condition" the unconstrained matrix by applying minimum rotation datum constraints, with the daily rotation solution values unchanged (see the example #1 of Appendix IV) .

ITRF96 AND FOLLOW ON FOR 1998

Claude Boucher, Zuheir Altamimi, Patrick Sillard
Institut Géographique National
ENSG/LAREG

6-8 Avenue Blaise Pascal
Cite Descartes, Champs-sur-Marne
77455 Marne-la-Vallee, FRANCE

E-mail: boucher@ensg.ign.fr, altamimi@ensg.ign.fr, sillard@ensg.ign.fr

INTRODUCTION

The **ITRF96** solution represents a new generation of realization of the International Terrestrial Reference System (**ITRS**). It is achieved by combining simultaneously positions and velocities using full variance - **covariance** information provided, in **SINEX** format, by the IERS analysis centers. Moreover, a rigorous weighting scheme is used, based on the analysis and estimation of the variance components using **Helmert** method.

The reference frame definition (origin, scale, orientation and time evolution) is achieved in such away that **ITRF96** is in the same system as the **ITRF94**. In addition, station velocities are constrained to be the same for all points within each site.

INPUT DATA

Solutions from the IERS analysis centers

The solutions provided by the IERS analysis centers and selected for the **ITRF96** analysis are 4 VLBI, 2 SLR, 8 GPS and 3 DORIS solutions. These data are listed in Table 1.

Local ties

As an improvement of the use of the local ties, all the eccentricities of **colocated** sites were converted into a complete set of positions for each site, provided in **SINEX** format. Each **SINEX** file reflects correlations between the **cartesian** components of the points within each site.

ITRF96 DATA ANALYSIS

The current strategy adopted for Terrestrial Reference Frame comparison/combination analysis is twofold: simultaneous combination of positions and velocities using full variance/**covariance** matrices; rigorous weighting scheme based on the analysis and estimation of the variance components using **Helmert** method.

The data analysis performed in view of the **ITRF96** establishment are mainly: comparison of the individual solutions with **ITRF94**, combination of the solutions within each technique and a global combination of all the solutions together with the local ties of **co-located** stations.

Among those selected for the ITRF96 combination, each individual solution was compared to the ITRF94 in order in one hand to estimate the transformation parameters of the system attached to the solution with respect to ITRF94 and, on the other hand, the level of agreement with the ITRF94 values.

In order to assess the relative quality of the individual solutions, independently from the influence of local ties, a combination within each technique was also performed. Matrix Scaling Factors have been rigorously estimated during the combined adjustment of the solutions.

The ITRF96 global combination is achieved with the following properties:

- It includes the 17 selected space geodetic solutions provided by the IERS analysis centers and 70 SINEX files containing positions and covariances, computed from local ties.
- The reference frame definition (origin, scale, orientation and time evolution) of the combination is achieved in such a way that ITRF96 is in the same system as the ITRF94.
- Velocities are constrained to be the same for all points within each site.
- Matrix Scaling Factors have been rigorously estimated during this combined adjustment which was then iterated.

Figure 1 shows the coverage of the 290 sites of the ITRF96. The position formal errors at epoch 1993.0 plotted in Figure 2 demonstrate an improvement of the ITRF96 with respect to ITRF94. Table 1 gives the quality analysis of the ITRF96 results, based more specifically on global residuals per solution.

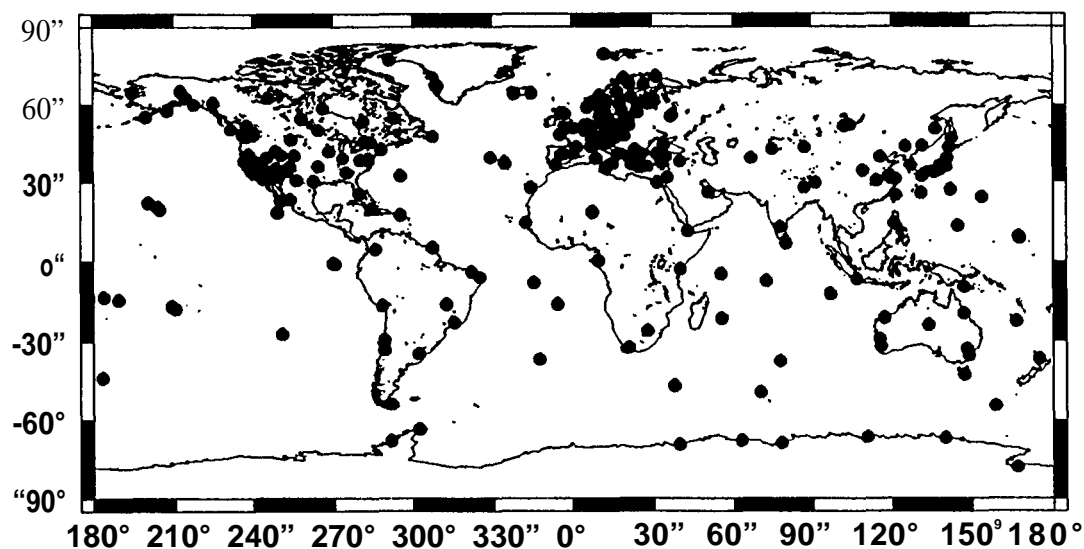


Fig. 1: ITRF96 Sites

Table 1. Global ITRF96 residuals per solution.

Solution	Number of points	Data Span YY-YY	Position RMS mm	Epoch yy:doy	Velocity RMS mm/y
<u>VLBI</u>					
SSC(GSFC) 97 R 01	120	79-97	5.80	93:001	1.90
SSC(GIUB) 97 R 01	43	84-96	13.60	93:001	.50
SSC(NOAA) 95 R 01	111	79-94	14.70	93:001	1.90
SSC(JPL) 97 R 01	8	91-96	20.70	93:001	
<u>SLR</u>					
SSC(CSR) 96 L 01	89	76-96	11.10	93:001	3.80
SSC(GSFC) 97 L 01	38	80-96	10.90	86:182	1.70
<u>GPS</u>					
SSC(EMR) 97 P 01	36	95-97	10.00	96:001	3.50
SSC(GFZ) 97 P 02	66	93-96	16.80	94:365	3.30
SSC(CODE) 97 P 02	100	93-97	7.10	95:076	1.90
SSC(EUR) 97 P 04	39	95-96	2.40	96:090	.30
SSC(EUR) 97 P 03	58	96-97	2.90	96:339	.30
SSC(MIT) 97 P 01	132	94-97	8.50	97:151	9.20
SSC(NCL) 97 P 01	114	95-97	5.40	96:001	6.30
SSC(JPL) 97 P 02	113	91-96	9.40	96:001	3.80
<u>DORIS</u>					
SSC(GRGS) 97 D 01	48	93-96	26.90	93:001	8.00
SSC(CSR) 96 D 01	54	93-96	26.10	93:001	10.60
SSC(IGN) 97 D 04	62	90-97	28.30	95:100	12.80

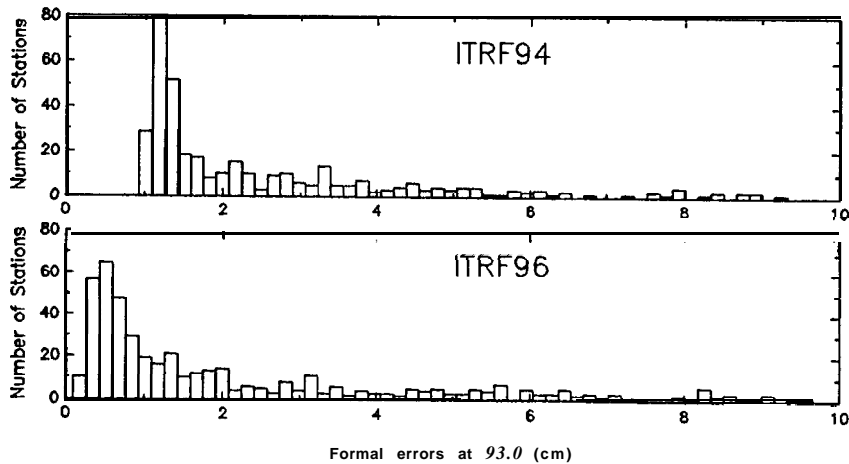


Fig. 2: Position formal errors

ITRF96 RESULTS

All the ITRF96 related files are available via Internet:

http: //lareg.ensg.ign.fr/ITRF/ITRF96.html

The SINEX files are available by anonymousftp:

ftp lareg.ensg.ign.fr (195.220.92. 14)

u sername: anonymous

password: e-mail address

move to the itr96 directory (cd pub/itr96)

compressed ITRF96 SINEX file (ITRF96.SNX.gz, about 52 Mbytes)

compressed ITRF96_VLBI SINEX file (ITRF96_VLBI.SNX. gz, about 3.7 Mb ytes)

compressed ITRF96_SLR SINEX file (ITRF96_SLR.SNX. gz, about 3.3 Mbytes)

compressed ITRF96_GPS SINEX file (ITRF96_GPS.SNX. gz, about 7.6 Mb ytes)

compressed ITRF96_DORIS SINEX file (ITRF96_DORIS.SNX.gz, about 0.8 Mbytes)

compressed ITRF96_EUR_GPS_PERM SINEX file (ITRF96_EUR_GPS_PERM. SNX.gz, about 0.6 Mbytes)

compressed ITRF96_EUROPE SINEX file (ITRF96_EUROPE. SNX.gz, about 4.1 Mbytes)

compressed ITRF96_IGS_RS47 SINEX file (ITRF96_IGS_RS47 .SNX.gz, about 0.5 Mbytes)

CONCLUSIONS

The IERS activities related to the Terrestrial Reference Systems will continue and be expanded in 1998. The main goals are:

to produce a new annual global solution (**ITRF97**) For that, detailed technical specifications will be issued in March 98.

to develop a pilot campaign to collect weekly solutions from the various techniques, in addition to GPS already organized in this way by IGS. A weekly combination in **ITRS** will then be determined. This will be a pilot experiment. The need and interests for such new IERS products should be investigated thanks to this campaign.

IGS REFERENCE STATIONS CLASSIFICATION BASED ON ITRF96 RESIDUAL ANALYSIS

Zuheir Altamimi
Institut Géographique National / ENSG/LAREG
6-8 Avenue Blaise Pascal
Cite Descartes, Champs-sur-Marne
77455 Marne-la-Vallee, FRANCE
E-mail: altamimi@ensg.ign.fr

INTRODUCTION

Using **ITRF96** results, we attempt in this report to classify and qualify the Provisional set of the IGS Reference Stations proposed by the IGS AC's which will replace the current 13 ITRF stations. **This provisional set contains 52 GPS stations, 32 of them are colocated with at least one of the 3 other IERS techniques (VLBI, SLR, DORIS).**

Position residuals of **all** the individual solutions included in the **ITRF96** are computed at **epoch 1997.0, taking into account velocity residuals. Based on 1997.0 position and velocity residuals, the provisional IGS Reference Stations were classified according to the 3 following criteria:**

- Agreement of GPS solutions for positions at epoch 1997.0
- Agreement of solutions for positions at epoch 1997.0 in the collocation sites
- Agreement of solutions for velocities

POSITION AGREEMENT OF THE GPS SOLUTIONS

If we consider **GPS_only** position estimates, disregarding if the GPS point is **colocated** with another technique or not, the 52 GPS proposed stations could be classified in the following classes:

Class A: Position residuals at epoch 97.0 below 1 cm over the 3 components for at least **THREE** individual solutions

Class B: Position residuals at epoch 97.0 below 2 cm over the 3 components for at least **THREE** individual solutions

Class C: Position residuals at epoch 1997.0 larger than 2 cm

POSITION AGREEMENT IN THE COLLOCATION SITES

Focusing on collocation sites, the following 4 classes could be distinguished:

Class A:

- **Site must contain a GPS class A station**
- The agreement between GPS and at least one **colocated** technique should be better than 2 cm over the 3 components.
- The local tie residuals should be below 2 cm

Class B:

- Site must contain at least a GPS class B station
- The agreement between GPS and at least one **colocated** technique should be better than 3 cm over the 3 components.
- The local tie residuals should be below 3 cm

Class C: Discrepancy between GPS and the **colocated** technique larger than 3 cm and less than 5 cm,

Class D: Poor collocation: discrepancy larger than 5 cm.

VELOCITY AGREEMENT

We Remind that in ITRF96, velocities were constrained to be the same for all points within each site. The analysis of the **ITRF96** velocity residuals for the 52 GPS stations leads to classify them into 4 classes:

Class A:

- For **GPS_only** sites, velocity residuals below 5 mm/y over the 3 components for at least **THREE** individual solutions
- For collocation sites, velocity residuals below 5 mm/y over the 3 components for at least **THREE** different solutions coming from at least 2 different techniques

Class B: Criteria as in Class A, but velocity residuals below 10 mm/y over the 3 components

Class C: Criteria as in Class A, but velocity residuals below 15 mm/y over the 3 components

Class D: Velocity residuals larger than 15 mm/y.

Table 1 summarizes the classification of the 52 GPS stations. For comparison, the ITRF94 classes are also listed in this table. A summary of the number of stations per class is given in Table 2, and illustrated on Figure 1. Figure 2 shows the coverage of the 52 sites.

Table 1, Classification of the IGS Reference Stations.

CODE	DOMES	nb.	Positions GPS	at 1997.0 Collocation	Velocities	ITRF94 class
ALGO	401	O4MOO2	A	A	A	B
AREQ	42202	MO05	A	A	B	B
AUCK	50209	MO01	c		c	
BAHR	24901	MO02	c		D	
B R A Z	41606	M001	B		B	
BRMU	42501	S004	A	m ¹	A	c
CAS1	66011	M001	B		c	c
CHAT	50207	MO01	B		D	
DAV1	6601	OMOO1	B		B	c
DRAO	401	O5MOO2	A	D	D	z
FAIR	40408	MO01	A	A	A	B
FORT	41602	M001	A	A	A	B
GODE	40451	M123	A	B	A	A
GOLD	40405	S031	A	m	A	c
GRAZ	11001	MOO2	A	A	A	A
GUAM	50501	M002	A	A	B	
HART	30302	MO02	B	B	A	B
HOB2	50116	M004	A	m	A	c
IRKT	123	13M001	B		B	
KERG	91201	M002	B	D	c	B
KIT3	12334	M001	A	B	A	c
KOKB	40424	MO04	A	A	A	B
KOSG	13504	MO03	A	c	D	A
KOUR	97301	M210	B	B	B	B
KWJ1	50506	M001	A		B	
LHAS	21613	M001	A		B	
MAC1	50135	M001	A		B	
MADR	13407	S012	A	A	A	A
MALI	33201	M001	B		B	
MAS 1	31303	MO02	A		A	c
MATE	12734	MO08	A	A	A	A
MCM 4	66001	M003	B		D	c
MDO1	40442	M012	A	A	A	A

m: missing local tie

Table 1. Classification of the IGS Reference Stations (continued).

CODE	DOMES nb.	Positions at 1997.0			Velocities	ITRF94 class
		GPS	Collocation			
NLIB	40465MO01	A	A	A	B	
NYAL	10317MO01	A	B	A	B	
OHIG	66008MO01	B	B	B	z	
ONSA	10402MO04	A	A	A	A	
PERT	50133M001	A		B		
PIE1	40456MO01	B	B	A	B	
POTS	14106MO03	A	c	B	A	
SANT	41705MO03	A	A	A	B	
SHAO	21605MO02	A	A	A	c	
THU1	43001MO01	A		B		
TIDB	501 03M108	A	A	B	B	
TROM	10302MO03	A	D	c	B	
TSKB	21730S005	A	A	B	B	
VILL	13406MO01	A		B	c	
WES2	40440S020	A	B	A	z	
WTZR	14201MO10	A	A	A	A	
YAR1	50107MO04	A	B	A	B	
YELL	40127MO03	A	A	A	B	
ZWEN	12330M001	A		B		

Table 2. Number of stations per class.

	Class A	Class B	Class C	Class D/Z
GPS_only	38	12	2	
Collocation	18	9	2	3
Velocity	25	18	4	5
ITRF94	9	17	10	3

CONCLUSION

-Based on this selection, it is suggested to exclude from the IGS Reference Stations list, stations having position or/and velocity class C or/and D. These stations are listed in Table 3 and are of two types:

- 5 pure GPS stations (not collocated with any other geodetic technique): (AUCK 50209MO01), (BAHR 24901 MO02), (CAS 16601 1M001), (CHAT 50207MO01),

(MCM466001M003). These stations should be rejected from IGS Reference Stations list.

5 colocated sites appear to have velocity or/and local tie problems: (DRAO 401 O5M002), (KERG 91201 M002), (KOSG13504M003), (POTS 14106M003), (TROM 10302M003). But if based on GPS-only estimates, they could be maintained in the IGS Reference Stations list.

Table 3. Class C or/and D stations.

CODE	DOMES nb.	Positions		at 1997.0 Velocities		ITRF94 class
		GPS	Collocation			
A U C K	50209M001	C			C	
B A H R	24901M002	C			D	
C A S 1	66011M001	B			c	c
C H A T	50207M001	B			D	
D R A O 401	O5M002	A	D		D	z
K E R G	91201M002	B	D		C	B
K O S G	13504M003	A	c		D	A
M C M 4	66001M003	B			D	c
P O T S	14106M003	A	C		B	A
T R O M	10302M003	A	D		c	B

(W13S240440S020) could be selected, but under a close watch, since the “best” position (at 1997.0) agreement between some GPS and VLBI solutions, **plus local tie, is estimated to be about 21 mm.** Meanwhile the “worst” agreement is about 51 mm.

ITRF96 demonstrates real improvement **for 14 GPS colocated sites with respect to ITRF94.**

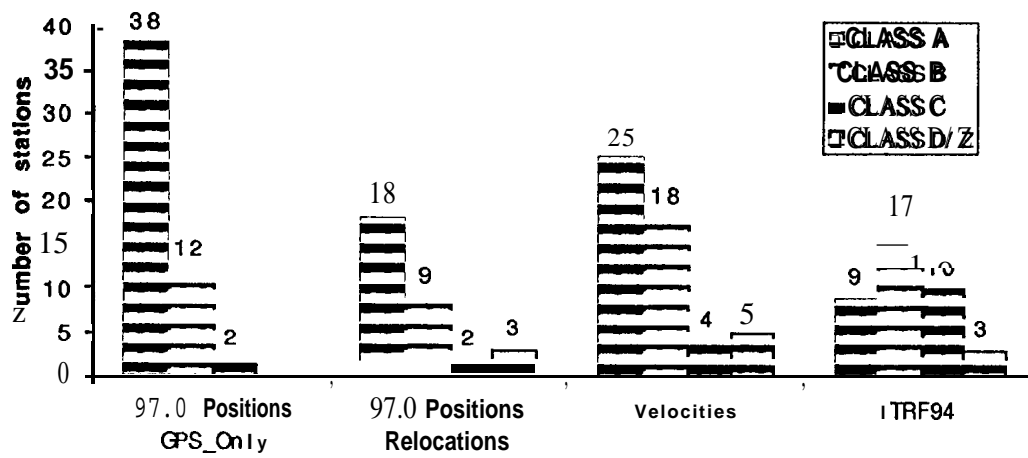


Fig. 1. Classification of the IGS reference stations.

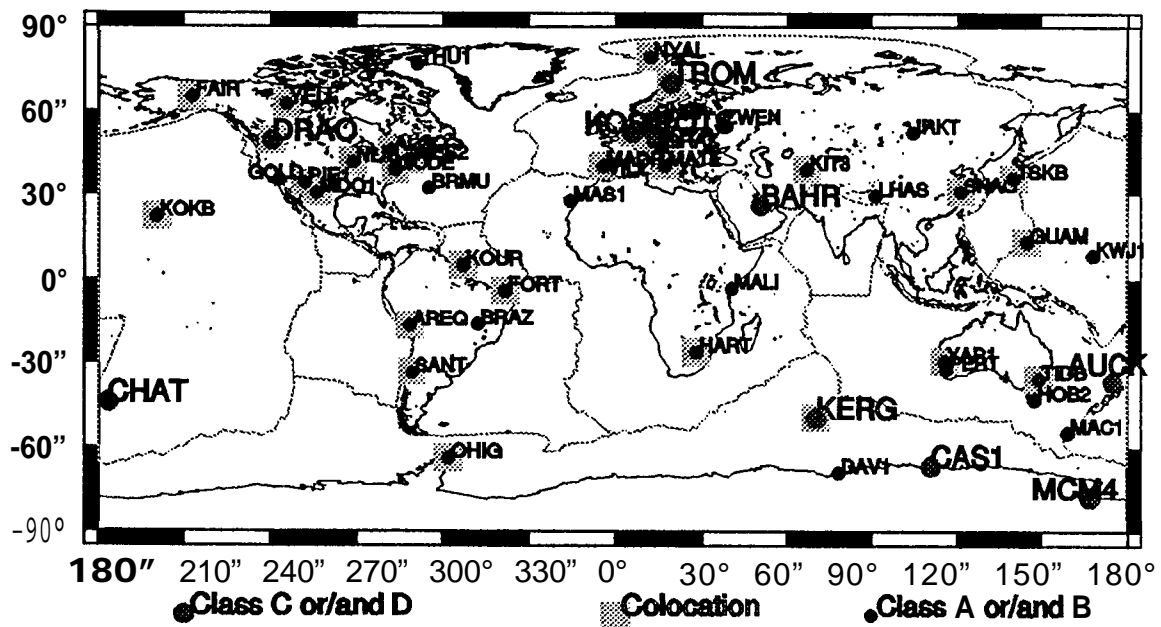


Fig. 2. Distribution of the IGS reference stations

References

Boucher C., Z. Altamimi, P. Sillard, 1998, Results and Analysis of the ITRF96, IERS Technical Note 24, Observatoire de Paris.

ESTIMATION OF **NUTATION** TERMS USING GPS

Markus Rothacher, Gerhard Beutler
Astronomical institute, University of Berne
CH-3012 Berne, Switzerland

ABSTRACT

Satellite space-geodetic measurements have been used since a long time to determine UT1-UTC rates (or length of day values). The estimation of nutation rates (in longitude and obliquity), however, was thought to be reserved to VLBI and LLR. It can be shown, that there is no fundamental difference between the estimation of UT1-UTC rates and nutation rates. Significant contributions to nutation by GPS may be expected in the high frequency domain, i.e., for periods below about 20 days.

CODE, the Center for Orbit Determination in Europe, started to estimate nutation rates in March 1994 using the data of the global IGS network. By now, the series of nutation rates from 3-day solutions has a length of about 3.5 years. From this series corrections to the coefficients of 34 nutation periods between 4 and 16 days have been determined. The resulting coefficients show an agreement of 10 μ as with the IERS 1996 nutation model. The GPS results are very consistent with the most recent model by Souchay and Kinoshita, too. GPS thus allows an independent verification of theoretical nutation models and results from VLBI and LLR. A thorough description and discussion of the estimation of nutation amplitudes using GPS may be found in [Rothacher et al., 1998].

INTRODUCTION

CODE, a cooperation of the Astronomical institute, University of Berne (Switzerland), the Swiss Federal Office of Topography, Wabern (Switzerland), the Bundesamt für Kartographie und Geodäsie, Frankfurt (Germany), and the Institut Géographique National, Paris (France), started to derive celestial pole offset parameters (nutation rates) in March 1994 in order to study whether GPS could be used to contribute to nutation theory.

From a mathematical point of view it can be shown [Rothacher et al., 1998] that the estimation of nutation rates in obliquity $\Delta\epsilon$ and longitude $\Delta\psi$ is very similar to the estimation of UT1-UTC rates: the offsets in all three components (Δt , $\Delta\psi$, and UT1-UTC) are fully

correlated with the orbital parameters describing the orientation of the orbital planes of the satellites (ascending node, inclination, and argument of latitude) and unmodeled orbit perturbations lead to systematic errors in the rate estimates. Major biases may be expected at a period of one revolution of the satellites or at annual and semi-annual periods (orientation of the orbital plane with respect to the sun) due to solar radiation pressure.

With a simple variance-covariance analysis it is possible to deduce in what frequency range corrections to nutation amplitudes may be computed with sufficient accuracy using GPS nutation rate estimates. Assuming a continuous nutation rate series of 1280 days and an RMS scatter of 0.27 mas/d for the nutation rate estimates – values taken from the actual GPS series produced at CODE – we find that the formal error $\sigma(A_T)$ of the nutation amplitude A_T at a nutation period T (in days) grows linearly with the period according to:

$$\sigma(A_T) \approx 0.0017 \cdot T \text{ mas} \quad (1)$$

When estimating nutation amplitude corrections from nutation *offsets*, as in the case of VLBI and LLR, the formal errors of the amplitudes are constant over a wide range of periods (i.e., for periods much longer than the typical spacing of the series and much shorter than the time interval covered by the series considered). From the literature ([Herring *et al.*, 1991], [Charlot *et al.*, 1995], [Souchay *et al.*, 1995], [Herring, 1997]) we obtain the formal errors of nutation amplitudes when using VLBI and LLR data. These formal errors are shown in Figure 1 together with those expected from GPS.

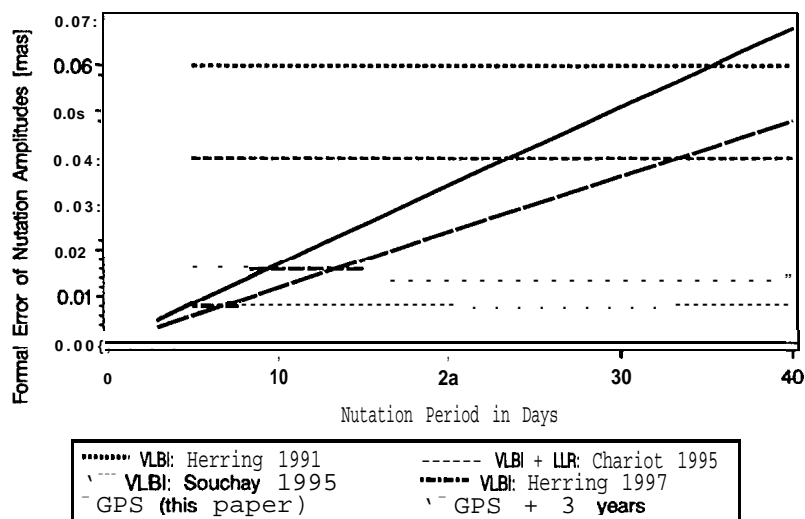


Figure 1. Precision of amplitude estimation from nutation offsets (VLBI and LLR) and from nutation rates (GPS) derived using a simple variance-covariance analysis.

Figure 1 clearly shows, that no major contributions to nutation theory may be expected from GPS for periods above about 20 days with the current orbit modeling. But GPS is in a good position to contribute at high frequencies (periods below 20 days). Let us mention

that the VLBI formal errors will only slowly improve from now on. Another 13 years of VLBI data will be needed to reduce the formal errors by $\sqrt{2}$, whereas for GPS, a factor of $\sqrt{2}$ can be gained with another 3 years of data even without modeling improvements.

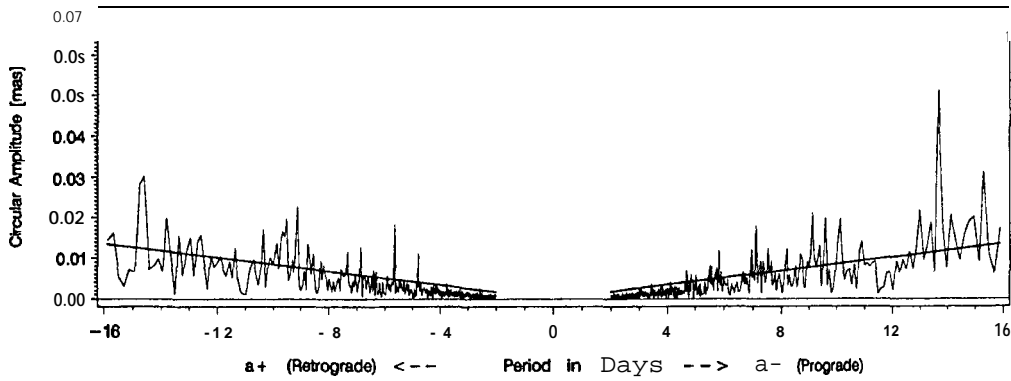
NUTATION RATE SERIES FROM GPS

The GPS nutation rate estimates were obtained from overlapping global 3-day solutions with 3-day satellite arcs using the data of up to 90 IGS sites. Over the three days one set of nutation rates was estimated in the two directions (obliquity and longitude) relative to the a priori nutation model, i.e. relative to the IAU 1980 Theory of Nutation (see [McCarthy, 1996]). It should be pointed out that rate estimates from 3-day solutions are more accurate than those from 1-day solution by about a factor of five. The reference frame was realized by heavily constraining 12 sites to their ITRF94 coordinates and velocities (see [Boucher et al., 1996]). All other site coordinates were freely estimated. Troposphere zenith delays were determined for each site with 6-hour intervals. During the 3.5 years covered by the nutation rate series (from March 1994 to November 1997) two important modeling changes took place. First, starting in January 1995, the ambiguities for baselines with a length below 2000 km were fixed to integers (80-90%) and secondly, end of September 1996, the satellite orbit parameterization was changed from the "classical" radiation pressure model with two parameters (direct radiation pressure coefficient and y-bias) to the extended CODE orbit model [Springer et al., 1998], where five parameters are routinely estimated in the 3-day solutions (constant radiation pressure coefficients in all three directions and periodic terms in X-direction). Both changes had an important effect on the nutation rate estimates. Whereas the ambiguity fixing improved the formal uncertainties of the rate estimates by almost a factor of three, the orbit model change deteriorated them by about the same factor. The worse formal uncertainties in the case of the new orbit parameterization is a consequence of the correlations between the nutation rates and the new radiation pressure parameters.

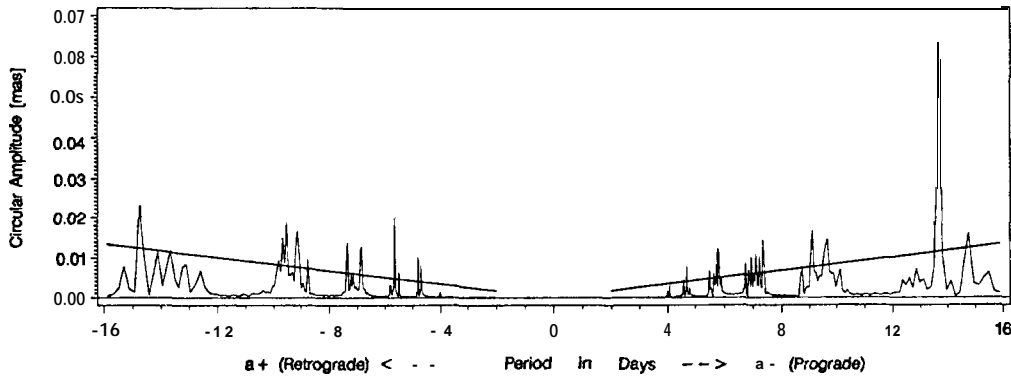
To give an impression of the type of signal contained in the GPS rate series, Figure 2a shows the high frequency spectrum derived from the nutation rate corrections relative to the IAU 1980 model. The *rate amplitudes* were thereby converted to actual amplitudes and transformed from $\Delta\epsilon$ and $\Delta\psi \cdot \sin \epsilon_0$ to amplitudes a^+ and a^- of *circular nutation* according to Eqn. (4) (see next section). For comparison the spectrum of the differences between the IAU 1980 and the IERS 1996 nutation model is depicted in Figure 2b. Many of the deficiencies of the IAU 1980 theory visible in Figure 2b, discovered by VLBI about a decade ago, are clearly seen by GPS, as well. The dashed lines in Figures 2 give the $1-\sigma$ uncertainties of the amplitudes estimates according to the Equation (1) (divided by a factor of 2 to account for the conversion to circular components of nutation).

ESTIMATION OF NUTATION AMPLITUDES

Starting with the GPS nutation rate corrections with respect to the IAU 1980 nutation model, a series of *total* nutation rates was generated by adding the rates given by the IAU 1980 model in order to obtain a series that is independent of the a priori model used.



(a) Spectrum of nutation corrections from GPS relative to the IAU80 model



(b) Spectrum of differences between the IERS96 and the IAU80 model

Figure 2. Spectrum of circular nutation amplitudes (see Eqn. (4) below) at low periods generated from (a) the GPS series of nutation rates converted to actual nutation amplitudes and (b) the differences between the IERS96 and the IAU80 model. The dashed lines indicate the $1\text{-}\sigma$ uncertainties of the amplitudes as expected according to Eqn. (1) (and (4)).

The nutation rate series was then used to estimate corrections to the nutation coefficients of a number of $n=34$ selected nutation periods relative to the more accurate IERS 1996 nutation model (IERS96) [McCarthy, 1996]. The corrections $\delta\Delta\epsilon$ and $\delta\Delta\psi$ in the nutation angles were thereby represented by

$$\delta\Delta\epsilon(t) = \sum_{j=1}^n (\delta\epsilon_{rj} \cos \theta_j(t) + \delta\epsilon_{ij} \sin \theta_j(t)) \quad (2a)$$

$$\delta\Delta\psi(t) = \sum_{j=1}^n (\delta\psi_{rj} \sin \theta_j(t) + \delta\psi_{ij} \cos \theta_j(t)) \quad (2b)$$

the GPS results and the IERS96 model over all 136 coefficients amounts to about 10 μs . No major deviations from the IERS96 model can be detected by GPS. The actual values of the nutation coefficients from GPS for the 34 periods may be found in [Rothacher et al., 1998].

A more detailed comparison of various VLBI and LLR results given in the literature and the GPS results with the most recent model by Souchay and Kinoshita (SKV972) [Herring, 1997] may be seen in Figure 4.

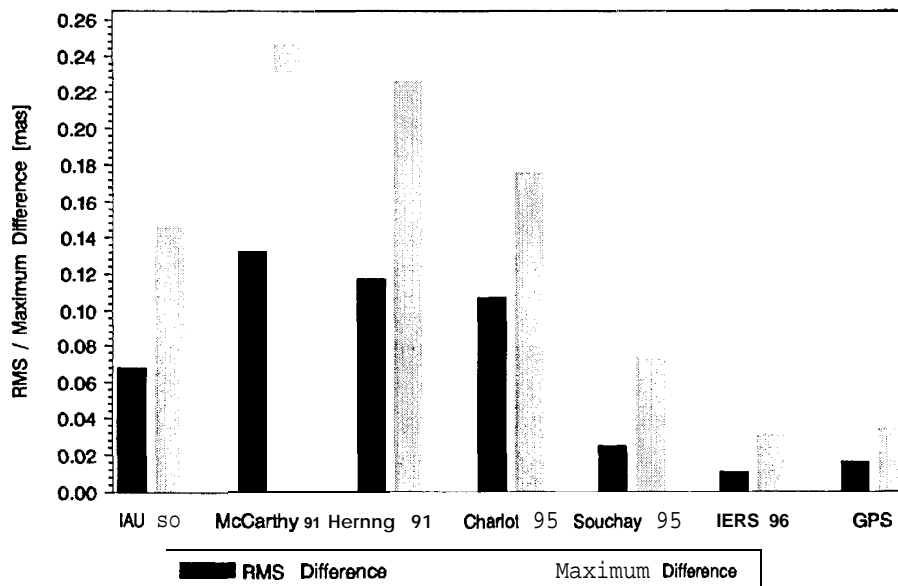


Figure 4. Rms difference and maximum difference over all terms of 4 major nutation periods, namely 13.66, 9.13, 14.77, 9.56 days, relative to the most recent model by Souchay/Kinoshita 1997.2.

Apart from the IAU 1980 (IAU 80), the IERS96 model and the GPS results, the comparison involves the results from [McCarthy and Luzum, 1991] (combined analysis of 10 years of VLBI and about 20 years of LLR data), [Herring et al., 1991] (9 years of VLBI data), [Charlot et al., 1995] (16 years of VLBI and 24 years of LLR data), and [Souchay et al., 1995] (14 years of VLBI data). Figure 4 depicts the rms differences as well as the maximum differences between these various results and SKV972 over all coefficients of the four major nutation periods at 13.66, 9.13, 14.77, 9.56 days (a total of 16 coefficients). We clearly see that the GPS results are in better agreement with the SKV972 model than most of the VLBI/LLR results.

A similar picture emerges when looking in detail at the coefficients of the 13.66 day period (see Figure 5), which is of special interest to geophysicists because of its large amplitudes. Again, the GPS results are very consistent with the results of the most recent model by Souchay and Kinoshita.

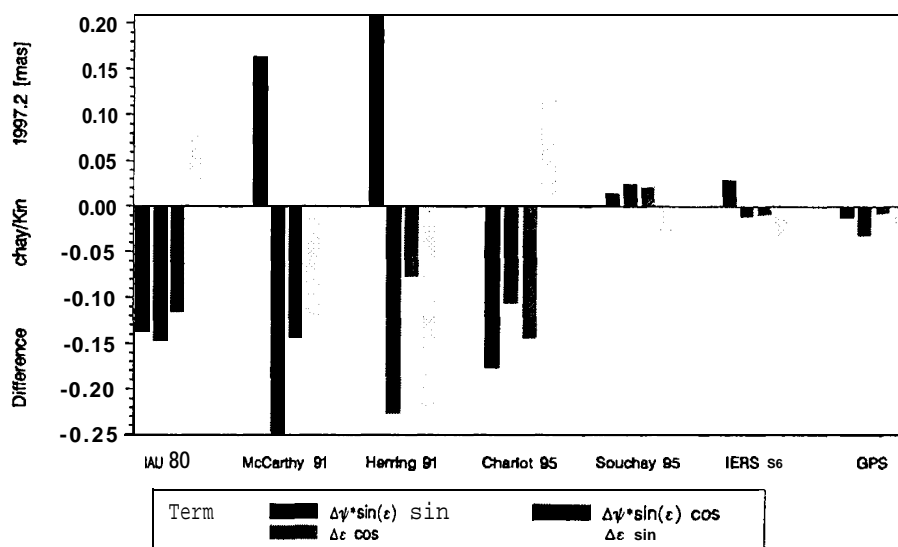


Figure 5. Comparison of the 13.66-day nutation coefficients from different sources with the most recent model by Souchay/Kinoshita 1997.2 .

CONCLUSIONS

Prom the above results we conclude that GPS may give a significant contribution to nutation in the high frequency range of the spectrum (periods below 20 days). The long term behavior is, however, reserved to VLBI and LLR. The nutation coefficients estimated from the GPS rate series show an overall agreement (median) of about $10 \mu\text{as}$ with the most recent nutation models by Souchay and Kinoshita. Using more refined orbit modeling techniques, carefully taking into consideration the correlations between the nutation rates and the orbital parameters, there is certainly much room for improvements. But already now GPS allows an independent check of present-day theoretical nutation models and VLBI/LLR results at the high frequency end of the spectrum. In future a combined analysis of VLBI, LLR, and GPS nutation series promises to give the most accurate nutation results.

REFERENCES

- Boucher, C., Z. Altamimi, M. Feissel, and P. Sillard (1996), Results and Analysis of the ITRF94, Central Bureau of IERS - Observatoire de Paris, Paris.
- Charlot, P., O. J. Severs, J. G. Williams, and X. X. Newhall (1995), Precession and Nutation From Joint Analysis of Radio Interferometric and Lunar Laser Ranging Observations, *The Astronomical Journal*, 109(1), 418-427.
- Herring, T. A. (1997), Most recent nutation model by Souchay and Kinoshita, Version 97.2 (private communication).
- Herring, T. A., B. A. Buffett, P. M. Mathews, and I. 1. Shapiro (1991), Forced Nutations of the Earth: Influence of Inner Core Dynamics, 3. Very Long Interferometry Data Analysis, *Journal of Geophysical Research*, 96(B5), 8259-8273.

- McCarthy, D. D., and B. J. Luzum (1991), Observations of Luni-Solar and Free Core Nutation, *The Astronomical Journal*, 102(5), 1889-1895.
- McCarthy, D.D. (1996), IERS conventions (1996), *IERS Technical Note 21*, Observatoire de Paris, Paris, July 1996.
- Rothacher, M., G. Beutler, T.A. Herring, and R. Weber (1998), Estimation of Nutation Using the Global Positioning System, *JGR*, submitted in March 1998.
- Souchay, J., M. Feissel, C. Bizouard, N. Capitaine, and M. Bougeard (1995), Precession and Nutation for a Non-Rigid Earth: Comparison Between Theory and VLBI Observations, *Astronomy and Astrophysics*, 299, 277-287.
- Springer, T. A., G. Beutler, and M. Rothacher (1998), Improving the Orbit Estimates of the GPS Satellites, *Journal of Geodesy*, January 1998, Submitted.

GLOBALY CONSISTENT RIGID PLATE MOTION: FIDUCIAL-FREE EULER VECTOR ESTIMATION

Geoffrey Blewitt, Ra'ed S. Kawar, and ¹Philip B.H. Davies

Department of Geomatics, University of Newcastle,
Newcastle upon Tyne, NE 7RU, UK

Abstract

IGS will begin in 1998 to routinely produce estimates of station velocities which will contribute to the definition of the terrestrial reference frame. The next logical step, is to use these velocities to estimate Euler vectors according to rigid plate tectonics theory. This will serve geophysicists who require kinematic boundary conditions to their regional analyses. Not only is IGS in the best position to do this (using GPS data), but also this type of analysis is important to IGS in terms of quality assessment of velocity products and station performance, and to enhance reference frame definition. We present some theoretical aspects of Euler vector determination, especially in the context of fiducial-free networks. We define and consider the "Chasles Effect," which must be considered due to imperfect realization of the Earth centre of mass. Preliminary results indicate that the weekly IGS polyhedron solutions provide an excellent dataset for the determination of plate motion. This provides one motivation for the IGS Analysis Centres to reprocesses data back to 1992.5 using today's models and standards.

1. Introduction

IGS Global Network Associate Analysis Centers (GNAACs) are now routinely producing weekly station coordinate solutions (with full covariance matrices) for over 100 stations worldwide [Blewitt *et al.*, 1995]. These weekly solutions can then be used to estimate station velocities and other types of motion (e.g., co-seismic displacement) [Blewitt *et al.*, 1998]. Unlike dense regional networks designed for the study of crustal deformation, the kinematics of the IGS polyhedron can be almost entirely explained in terms of angular velocities known as Euler vectors. The IGS is therefore in a position to estimate these Euler vectors in a globally self-consistent model, using full covariance information.

This paper explores how Euler vectors can be estimated using GNAAC solutions, and why IGS should be interested in this. Applying the philosophy underlying the IGS densification pilot project, the theory of rigid plate kinematics is first considered geometrically, so that the role of the reference frame can clearly be seen in contrast to the physical kinematics, which are necessarily frame-independent. This leads logically to a fiducial-free approach to the estimation of Euler vectors, similar to the situation with station coordinates and velocities. The

¹ Now at Royal Ordnance Survey, Southampton, UK

Newcastle **GNAAC** has undertaken a preliminary investigation to assess the feasibility of an operational estimation of Euler vectors and station velocity residuals, applying ideas presented here. Geodetic tools have been implemented to allow a more rigorous analysis, including generalized **outlier** detection, and variance component estimation.

This leads to our conclusion that IGS should routinely produce Euler vectors and station velocity residuals as a service to geophysicists and to IGS itself. Reprocessing of all past IGS data using current data processing models and strategies would strongly enhance the value of such products; therefore **IGS** should consider organizing such an activity, performed by IGS Analysis Centers.

2. Rigid Plate Kinematics

Introduction to Euler vectors

Rigid plate kinematics starts with the assumptions that (i) the plate does not deform, and (ii) the motion is constrained to the surface of a sphere. This is obviously equivalent to assuming rigid body motion with one point fixed at the **centre** of a sphere. Now Euler's theorem states that

“the general displacement of a rigid body with one point fixed is a rotation about some axis”
[e.g., Goldstein, p. 158, 1980]

Therefore, rigid plate motion at any instant in time is completely specified by an angular velocity vector, known as the “Euler vector” $\underline{\Omega}_i$ for each plate i (Fig. 1).

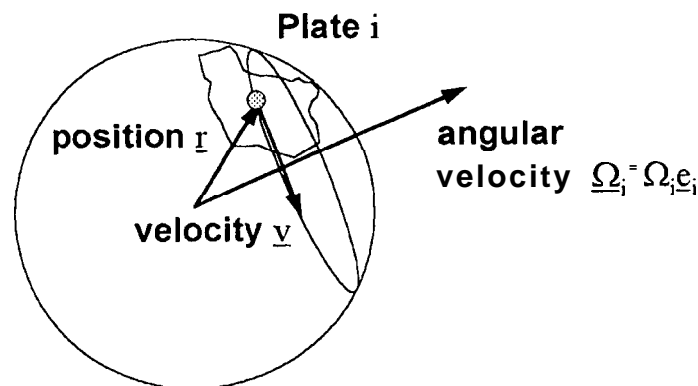


Fig. 1: Kinematics of a rigid plate as described by an angular velocity vector

The magnitude of this vector Ω_i represents the rate of rotation of the plate, often expressed in units of degrees per million years. The direction of this vector \underline{e}_i is known as the “Euler pole,” often expressed in terms of longitude λ_i and latitude ϕ_i computed on the sphere. The cartesian components of the Euler vector can be computed as follows:

$$\begin{aligned}\Omega_{ix} &= \underline{\Omega}_i \cdot \underline{e}_x = \Omega_i (\underline{e}_i \cdot \underline{e}_x) = \Omega_i \cos \phi_i \cos \lambda_i \\ \Omega_{iy} &= \underline{\Omega}_i \cdot \underline{e}_y = \Omega_i (\underline{e}_i \cdot \underline{e}_y) = \Omega_i \cos \phi_i \sin \lambda_i \\ \Omega_{iz} &= \underline{\Omega}_i \cdot \underline{e}_z = \Omega_i (\underline{e}_i \cdot \underline{e}_z) = \Omega_i \sin \phi_i\end{aligned}$$

The velocity of a point that is attached to plate i at position vector \underline{r} is given by the following vector cross product:

$$\underline{v} = \underline{\Omega}_i \times \underline{r}$$

Model Error due to Spherical Approximation

Note that the position vector should be expressed such that the origin is at the center of the sphere. The fact that the Earth is not exact] y spherical introduces the following problems: (i) rotation about an axis constrains a plate to the surface of a sphere, not the surface of an ellipsoid; and (ii) motion of an object constrained to an ellipsoidal surface generally introduces deformations, because the radius of curvature is a function of latitude. It can be shown that the velocity errors introduced by both these problems are of the order

$$\delta v \approx f v$$

where f is the ellipsoidal flattening factor, approximately $1/298$. Since plate velocities are limited to the order 100 mm/yr, the spherical approximation introduces errors at the level of a fraction of a millimetre per year (which is small, but not entirely insignificant as geodetic precision can approach this level).

Presumably due to the ambiguous nature of how to map ellipsoidal surface onto the sphere, the IERS [p. 15-16, 1996] publishes a standard FORTRAN subroutine (originally by Bernard **Minster**) which computes station velocities given the station coordinates, using Euler vectors from the geophysical model **NNR-NUVEL1 A** [DeMets et al. 1994]. It can be seen from the source code, that the cross product formula is applied using geocentric position vectors. As the **geocenter** does not generally coincide with the center of curvature for the surface of the ellipsoid, it can therefore be expected that very small but non-zero height velocities will be introduced. However, the IERS approximation does preserve plate rigidity. Alternatively, the user could ignore the height velocity and thus forego plate rigidity, Either way, the effects are fractions of a millimetre per year.

Reference Frame Dependence

Another problem with the model is that it is frame dependent. The geodetic results give velocity components which general] y include (i) relative rotational motion between the frame axes and the polyhedron, and (ii) relative translational motion between the origin of coordinate frame and the polyhedron. The adoption of frames which have a different evolution of origin or orientation will lead to different velocity results, and therefore different Euler vector results.

Reference Frame Dependence: Rotational Ambiguity

The first problem of frame dependence arises **because** we desire an Earth-fixed frame, yet **all points on the Earth’s surface are in relative motion**, therefore “**Earth-fixed**” is **somewhat arbitrary**. Earth polar motion requires estimation, introducing an ambiguity as to whether the polyhedron is rotating, or the pole is moving. The data can only resolve the **relative rotation between the celestial ephemeris pole (CEP) and the polyhedron**. Moreover, a **global rotation of all plates around the CEP can be interpreted as either Earth rotation, or plate tectonic motion about the CEP - the data cannot separate the two effects, as the observations do not refer to the mantle (if indeed the mantle may be viewed as somehow absolute)**. The **velocity field from a fiducial-free solution therefore has a 3-rank deficiency**, which will propagate into the Euler vector estimates.

Euler vectors are therefore, strictly speaking, non-estimable, and require some form of datum constraints (which may be minimal). Velocity vectors determined by constraining a subset of station velocities to a specific frame will produce Euler vectors consistent with that frame. Therefore, Euler vectors determined in different frames will generally have a common angular velocity bias, which can itself be thought of as an Euler vector (Fig. 2).

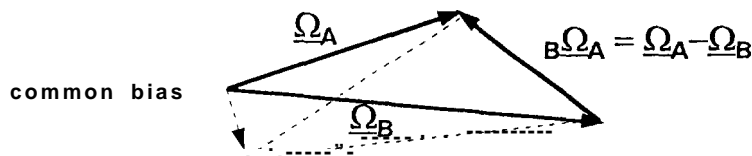


Fig. 2: Relative Euler vector, shown herein angular velocity space, is insensitive to a global reference frame rotation

In Fig. 2, it obvious that a common rotational bias does not affect the difference between two Euler vectors. This difference is known as the “relative Euler vector.” The relative Euler vector has more physical significance than the absolute Euler vector, as it is independent of frame rotation, and is therefore estimable. The absolute version is, however, convenient, because it is far simpler (and better to ensure consistency) to specify a list of absolute Euler vectors rather than a ‘much longer list of pairs.

Reference Frame Dependence: The Chasles Effect

M. Chasles (1 793-1 881) proved a stronger form of Euler’s Theorem,

“the most general displacement of a rigid body is a translation plus a rotation”
 [e.g., Goldstein, p 63, 1980]

We define the “Chasles Effect” as the source of error introduced into Euler vectors due to net translational motion of the polyhedron with respect to the coordinate origin. Why is the Chasles Effect relevant, if we assume that rigid plates move effectively with one point fixed? The problem is that geodetic network solutions cannot perfectly realize the Earth centre of

mass (which we assume to be Euler's fixed point). GPS fiducial-free network solutions will have a small **drift** relative to the Earth **centre** of mass due to imperfect dynamic orbit models. This drift will cause a systematic error in the determination of plate rotations, which doesn't entirely cancel for relative Euler vectors. (The situation for VLBI is even more extreme, as there is no inherent dynamic origin.)

The essence of the problem is that we don't know the exact location of Euler's "fixed point" relative to the GPS stations. Under such circumstances we should instead assume Chasles' theorem is applicable rather than Euler's theorem. Therefore station motions relative to the coordinate origin can be modelled as a plate rotation about the coordinate origin, plus a global translational rate bias.

Frame Independent Analysis

Geodetic observable and estimable should only be a function of relative Euler vectors, not absolute Euler vectors. In fact, if an equation for a kinematic variable cannot be expressed in terms of relative Euler vectors, and if absolute Euler vectors are absolutely necessary in the formulation, then we can conclude that this kinematic variable is reference frame dependent. For example, it can be shown that baseline length rate between two points on arbitrary plates A and B can be written in terms of the relative Euler vector:

$$v_{L(A,B)} = {}_A\Omega_B \frac{(\underline{r}_A \times \underline{r}_B)}{\underline{r}_A - \underline{r}_B}$$

On the other hand, relative velocity cannot be written **only** in terms of relative Euler vectors, and is therefore frame dependent.

$$\begin{aligned} {}_B v_A &= v_A - v_B \\ &= (\Omega_A \times r_A) - (\Omega_B \times r_B) \\ &= (\Omega_A - \Omega_B) \times r_A + \Omega_B \times (r_A - r_B) \\ &= ({}_B\Omega_A \times r_A) + (\Omega_B \times {}_B r_A) \end{aligned}$$

It can be seen, however, that if the baseline is sufficient] y short, then the second term becomes negligible, and relative velocity is then only a function of relative Euler vector, and therefore frame independent. This is a logical result, considering the geophysics. Physical quantities, such as strain and stress buildup at plate boundaries must be a function of local kinematic quantities, such as relative velocity between two nearby points, either side of the plate boundary. The results of physical predictions can not be frame dependent, and therefore it is satisfying to see that the kinematic theory is consistent with this notion.

It therefore makes sense to talk unambiguously about relative velocity at a plate boundary, on the understanding that the limit of zero baseline length is taken. The predicted relative velocity at a plate boundary will determine the boundary's character: whether it be strike slip, spreading, or converging (and if so, at what angle relative to the boundary). Therefore, if we know where plate boundaries lie, the relative Euler vectors can be used to predict the nature of the plate boundary, and the integrated rate of strain accumulation as

we **move** across the boundary. This is the geophysical significance of relative Euler vectors. Conversely, one can therefore understand how it is that geophysicists can invert observations of plate boundary features to estimate relative Euler vectors.

Now that we have established the importance of relative Euler poles, and the rank-3 deficiency of absolute Euler poles, we are in a position to deduce a logical approach from geodesy. We propose that absolute Euler vectors be estimated from fiducial-free (loosely constrained) estimate of station velocities, taking adequate care to minimize the **Chasles** Effect. In the **preliminary** results presented in this paper, we have simply estimated and applied a 14-parameter transformation (i. e., the usual 7 **Helmert** parameters plus their 7 time derivatives) of our loose solution into **ITRF**. This effectively removes the global rotational bias as well as the global translational rate bias (and scale rate, although this may prove to be unnecessary). This is then followed by estimation of the Euler vectors. This is not the only scheme possible, but it is simple and appropriate to implement for an initial test, and it does ensure a good degree of consistency with the SLR realization of the **geocentre**. For **future** work, we intend to investigate the **Chasles** Effect, including the class of methods which do not rely on an externally supplied frame, but may rely on internal constraints and Earth models. We note that the estimation of all absolute Euler vectors is of course not strictly possible due to the 3-rank deficiency, however the application of loose constraints will ensure stability in relative Euler vector estimates, without distorting their values.

3. Why should IGS be interested in Euler vectors?

The horizontal motions of most stations of the IGS polyhedron can be almost completely explained in terms of the Euler vector model. The exceptions would be stations in zones of active **crustal** deformation, such as plate boundaries, and stations which, for whatever reason, are not representative of the plate (e.g., the monument is not anchored to bedrock).

The rigid plate motion model together with a map of plate boundaries provides us with a model of horizontal motion anywhere on the sphere. Any such model which covers the entire sphere allows us to overcome problems in reference frame definition arising from the fact that we do not monitor every possible point on the Earth's surface. If we were to define a frame independent of plate motion models, we would be forced to depend on internal constraints, such as no net rotation of stations; however, these types of constraints are strongly dependent on the selected network, and would have very different effects if applied to a future network with additional stations. The problem of sampling bias would be essentially insurmountable. Therefore, Euler vectors have an important role to play in the definition of a reference system, which is why they appear in the IERS Terrestrial Reference System.

Despite this, the link between the ITRF and plate motion models has in recent years become weaker in **favour** of internally consistent constraints. While internal consistency is **laudible**, there is no reason why a reference frame cannot be both internally consistent with itself, and externally consistent with a plate motion model. The external consistency would be on the evolution of the frame axes with respect to the polyhedron, whereas the internal consistency would be on the deformation of the polyhedron. The fact that ITRS is supposed to have no net plate rotation is explicitly realized when we consider that solutions are

rotated into ITRF using a 14-parameter transformation. It is therefore easy to see why the role of Euler vectors is often overlooked due to these procedures.

In principle, IGS could define its own frame, just as the geophysicists have done for geological models. IGS should investigate the polyhedron kinematics as far as possible prior to contributing to ITRF. From the point of view of potential users, IGS is in a position to produce Euler vector estimates, station velocity residuals, and to classify stations according to their kinematics.

4. Developments at NCL GNAAC

As part of the IGS ITRF Densification Pilot Project, global network solutions with **full covariance** matrices (in SINEX format) are produced every week by several IGS Analysis Centers (ACs). These are combined into a global polyhedron solution (GSINEX) by the IGS Global Network Associate Analysis Center (GNAAC) at Newcastle (NCL) every week, beginning September 1995 [Davies and Blewitt, 1997]. This global combination analysis features variance component estimation to optimize relative weighting, and **outlier** detection (which requires each station to be analyzed by a minimum of 3 ACs). Since July 1996, regional network solutions have been produced every week by several IGS Regional Network Associate Analysis Centers (RNAACs). NCL has attached these RNAAC solutions onto the global combination (so as not to perturb it), thus producing a **densified IGS polyhedron solution (PSINEX)**.

NCL has also been conducting a second stream of analysis for research and development purposes, including reanalysis of past SINEX files using the latest combination software (TANYA), and producing "kinematic solutions" where station positions are parameterized as a **function** of epoch position and a velocity vector. Such a kinematic solution was submitted to IERS and has since been incorporated into ITRF96. The feedback from IERS has been that the NCL solution had one of the lowest **WRMS** statistics with respect to the final ITRF96 [Z. Altamimi, presented at this IGS workshop]. This may be expected, as a GNAAC solution already represents a combination of solutions which are being separately submitted to IERS.

Going beyond simple velocity solutions, NCL is moving towards interpretation and **modelling** of these velocities. The approach taken is to develop a geographical information system (GIS) that is **sufficiently** sophisticated to **identify** and **classify** tectonic zones according to the observed kinematics of geodetic stations. Specifically, we are developing a bootstrapping procedure identifies clusters of stations that, according to the data, appear to be co-rotating as if attached to the rigid plate interior. The idea is that clusters of stations are iteratively augmented while solving for Euler rotation vectors, and testing the plate rigidity hypothesis. Stations are classified as *regular* or *irregular*, depending on whether they are a cluster member (contributing to Euler vector estimation) The estimated rigid-plate velocity field with computed errors are then mapped onto the entire globe, and compared with regional geodetic data (e.g., data from the irregular stations) to investigate crustal deformation

The GIS under development would use object-oriented approach to defining a kinematic Earth model, which is based on a set of plates, with attributes including closed boundaries. These boundaries can be redefined by the user to test new hypotheses. The GIS would facilitate hypothesis testing using built in functions, and using any selection of geodetic data supplied to

it. Estimated relative Euler vectors could be mapped into relative plate velocities at respective plate boundaries, allowing us to objectively categorize boundary segments, and determine boundary parameters (e.g., rate and angle of convergence/spreading; rate of slip). This GIS could then allow for comparison of this geodetic classification with other geophysical data and geophysical interpretations.

While this GIS is under development, NCL has been testing the feasibility of some of these ideas, and has conducted preliminary research into appropriate tools to be incorporated as GIS **functions**. Such **functions** include variance component estimation when combining different geodetic data sets, **outlier** detection, and more importantly, generalized **outlier detection** (as applied to clusters of data suspected of not fitting the model) to allow more rigorous testing of hypotheses.

5. Preliminary Analysis and Results

Analysis

The input to this preliminary analysis are weekly **GSINEX** solutions, spanning 18 months, which include the coordinates and **full covariance** matrix of **IGS** stations that have been analyzed by a minimum of **3 ACS**. The union of all the input files contains 150 stations **satisfying** this criteria. The time series of coordinates were then scanned to ensure that obvious **step functions** (mainly due to equipment replacement) were detected and, if possible corrected.

This screening process has proved to be the most time consuming part of the analysis, which is why only 18 months of data have been processed here. We expect this problem to be mitigated in future due to the recent adoption of a central database at the IGS Central Bureau (the “**loghist**” file) with information on station configuration changes. In fact, this file is now the starting point of our routine **GNAAC** analysis, but the problem still remains until all ACS adopt this procedure.

These weekly coordinate solutions were then input to our processing software, **TANYA**, to **solve** for station velocities and epoch station positions, with a **full covariance** matrix. The solution at this point is fiducial-free, meaning that the reference frame is only loosely defined through loose station coordinate constraints (tight enough to prevent numerical instability, but loose enough not to influence internal **geometry**). A datum definition was then applied to this solution through a 14 parameter **Helmert** transformation to ITRF94 (which, as discussed, also mitigates the **Chasles** Effect).

This kinematic solution was then processed by **TANYA** to solve for Euler vectors and **full covariance** matrix. A manual iterative process (later to be automated) was applied to remove stations not fitting the Euler vector model. This is necessary, because some stations lie in zones of **crustal** deformation.

In addition to producing Euler vector estimates (in the ITRF96 frame) with **full covariance** matrix, station velocity residuals to the resulting estimated model were produced for subsequent analysis. Station velocity residuals can be interpreted in terms of random error, systematic error, or blunders. For example, residuals exceeding their computed 99% confidence ellipses may be interpreted **as** either systematic errors or blunders. Systematic error

can arise because the station actually is in a zone of **crustal** deformation, or because the station is **not** representative of the underlying rigid plate (e.g., due to monument instability). Errors due to change of instrumentation or monumentation can be classified as blunders.

Results

In contrast with station velocities, which in many cases are more than 5 cm/yr, the residual station velocities (after estimating Euler poles) are relatively small, typically several millimetres per year [Fig. 3.].

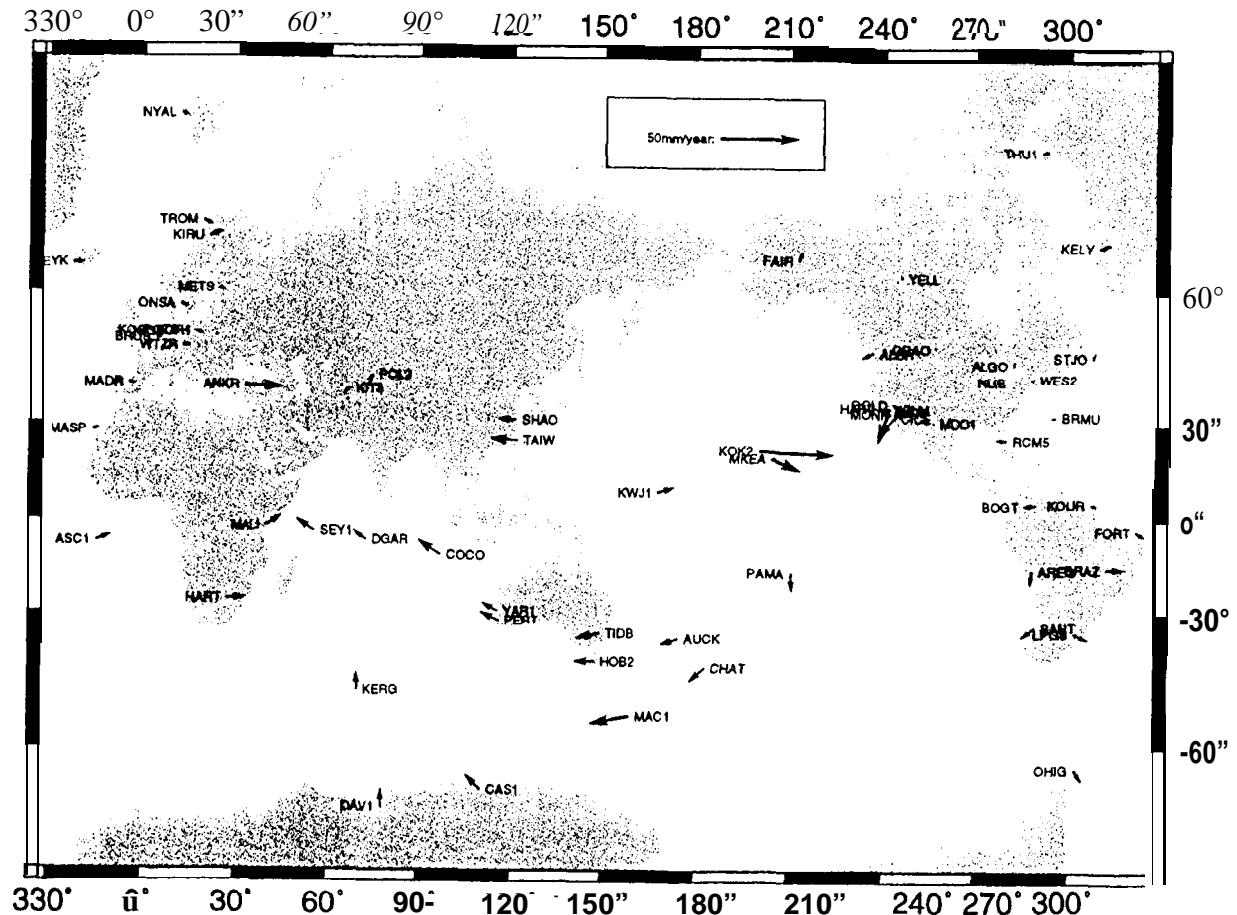


Fig. 3: Estimated station velocity residual vectors. (Note that the direction of the arrows should be reversed if these are to be interpreted as velocity relative to respective plates).

Clearly, the Euler vector model explains a significant proportion of the station velocities. Discrepancies from the Euler vector model can be seen at plate boundaries, and occasionally (e.g., Hawaii) within plate interiors. North America appears to be extremely stable, whereas Eurasia appears to be extended East-West, possibly as a result of the **extrusional** tectonics in Central Asia caused by the collision with the Indian subcontinent. The velocity residual of station **ANKR** in Turkey can be interpreted as that station moving due West relative to the Eurasian plate, which confirms that ANKR is actually on a different plate (namely, the

Anatolian block). The larger residuals in south west United States are due to regional deformation near the Pacific-North American plate boundary.

We emphasise that this analysis is preliminary and no checks have been made to reconcile discrepancies, for example, with misinformation on antenna configuration. Therefore, we should be **careful** in drawing conclusions about specific sites. Rather, we simply point out the potential of this approach at discriminating between sites which appear to behave as expected, and sites which require **further** investigation. (For example, we have not yet attempted to explain the discrepant behaviour of the two GPS stations on the Hawaiian Islands.)

Fig 4. shows that the estimated Euler poles largely agree within the expected errors with the NNR NUVEL- 1 A mode. (The one exception is the South American plate - a problem we are currently investigating). These preliminary results suggest that both the GNAAC solutions and estimated errors are reasonable.

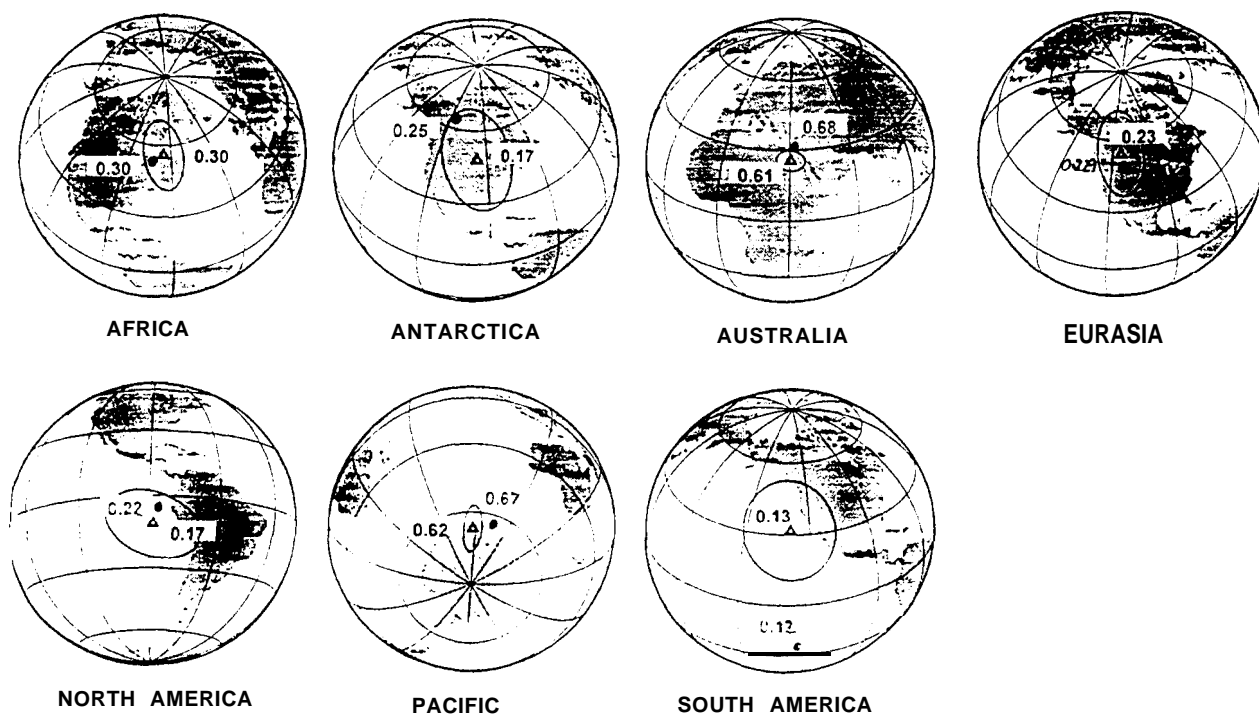


Fig. 5: Estimated Euler vectors and 1-standard deviation error ellipses

Africa-Eurasia kinematic boundary conditions

Certainly, more work is needed to provide results for serious geophysical interpretation, but the potential for this type of analysis is promising. The relative Euler vector solutions are particularly elucidating. For example, the estimated relative Euler vector between Eurasia and Africa can be used to compute relative plate motions at various points in the region of the plate boundary.

- . In northern Algeria, convergence of 5 mm/yr is computed with an azimuth of -310 (which happens to be normal to the general trend of the Atlas mountain range)
- . In northern **Italy**, convergence of 8 mm/yr is computed with direction -350 (which happens to be normal to the general trend of the Alps mountain range)
- . In the eastern **Mediterranean** around Cyprus, convergence of 11 mm/yr is computed precisely due North.

These computation are in close agreement with the **NUVEL- 1A** model, suggesting that current day collision of Africa and Europe has not changed significantly over recent geological time. Only regional measurements distributed around the plate boundary can locate where the convergence is being accommodated, but these types of computations do provide a “kinematic boundary condition” on the total path integral of relative motion across the boundary.

6. Conclusions

(1) We propose that **IGS** provide a service to geophysicists who are investigating **crustal** dynamics, by providing estimates of Euler vectors, station velocity residuals, and a classification of stations according to there observed kinematics. We argue that **IGS** is in the best position to do this (for GPS data), as **IGS** has and will continue to implement a very successful level of quality control, and adherence to standards. The alternative is for geophysicists to continue to derive their own Euler vectors, which due to limited resources, would tend to be limited to analyzing a subset of all data available to **IGS**. From the few examples given, station motions can in most cases be interpreted in simple geophysical terms. Much more **confidence** can be placed in geophysical interpretation if the Euler velocity residuals form a spatially recognizable pattern, rather than discrepant results which would be expected from station configuration problems.

(2) We also suggest that it is in **IGS'S** best interest to perform these type of activities. It is the logical progressive step after station velocity analysis, and allows for a new type of quality assessment of the station velocity products. Moreover, Euler vector analysis can be incorporated into processing schemes, and solutions can be easily updated on a weekly basis. The developments proposed here will allow **IGS** to gain better insight into reference frame realization, which is important for its own “reference system,” for example, in the selection of core stations used in orbit production. As an example of where insight can be gained, we note that the “Chasles Effect” should be carefully considered when estimating plate motions.

(3) Finally, it is clear that a more robust and accurate analysis can be performed using data extending back to the beginning of the **IGS** pilot project, in mid 1992, This would require **ACS** to reprocess data using today's software and analysis strategies to produce a more homogeneous time series. It should also help eliminate some of the problems associated with station configuration information, which now exists at the Central Bureau,

Acknowledgments

The authors gratefully acknowledge financial support from the Natural Environment Research Council, including grant GR3/10041 and studentship GT4/94/386/G.

References

- Blewitt, G., C. Boucher, P.B.H. Davies, M.B. Heflin, T.A. Herring, and J. Kouba, "ITRF densification and continuous realization by the IGS," in *Proc. of the IAG General Assembly*, held in Rio de Janeiro, 1997 (in press 1998).
- Blewitt, G., Y. Bock, and J. Kouba, "Constructing the IGS polyhedron by distributed processing," in *Proc. of the IGS Workshop*, ed. by J. Zumberge, IGS Central Bureau, Pasadena, Calif., USA, p. 21-36 (1995)
- Davies, P.B.H. and G. Blewitt, "Newcastle upon Tyne Global Network Associate Analysis Centre Annual Report 1996," *IGS Annual Report 1996*, p. 237-252, IGS Central Bureau, Jet Propulsion Lab., Pasadena, California (1997)
- DeMets, C., R. Gordon, D. Argus, and S. Stein, "Effect of recent revisions to the geomagnetic reversal time scale on estimates of current plate motions," *Geophys. Res. Lett.*, 21, pp. 2191-2194 (1994)
- Goldstein, H., *Classical Mechanics (2nd Ed.)*, Addison-Wesley Pub. Co., Reading, Massachusetts (1980)
- IERS, *Technical Note 21: IERS Conventions (1996)*, Ed. Dennis D. McCarthy, Paris Observatory (1996).

Topic 4: IGS Products for Troposphere and Ionosphere

IGS COMBINATION OF TROPOSPHERIC ESTIMATES - EXPERIENCE FROM PILOT EXPERIMENT

Gerd Gendt
GeoForschungsZentrum Potsdam
D-14473 Potsdam, Telegrafenberg A17, Div. 1

INTRODUCTION

The existing global and regional networks of permanent GPS receivers installed for geodetic and navigational applications can be used with marginal additional cost for determination of atmospheric water vapor with high temporal and spatial resolution. In different countries projects are under way in which the impact of GPS derived water vapor on the improvement of weather forecast are studied. Within the IGS a network of 100 globally distributed sites are analyzed on a daily basis. The zenith path delay (ZPD) values obtained should be converted into **precipitable** water vapor (**PWV**) and should be made available to the scientific community.

This IGS product could meet the demands for **climatological** studies. Here a time resolution of 2 hours (this is what IGS will provide) is sufficient, because long-term characteristics are of interest only, and a time delay of a few weeks for product delivery is acceptable.

In the past some experiments had demonstrated the capability of IGS (Gendt, 1996, 1997) and on 26 January 1997 (GPS week 890) the Pilot Experiment for the determination of IGS Combined Tropospheric Estimates has started.

GENERATION OF THE COMBINED IGS TROP PRODUCT

Since the beginning of the Pilot Experiment six of the global IGS Analysis Centers (**ACs**) have regularly contributed. Different **mapping** functions and elevation cutoff angles of 10, 15 or 20 degrees are implemented (see Table 1.). Three of the ACS, CODE, GFZ and JPL, have made changes in these parameters during 1997. The number of sites per AC varies from 30 to 85, and we have **~100** sites in total (Fig. 1.). More than 60 sites are used by at least three ACS, so that sufficient statistical information about the quality of the tropospheric estimates can be gained. For the other sites poor or no quality checks are possible, only some conclusions from neighboring sites may be drawn.

Input to the weekly combination are seven daily files from each AC with the estimates of ZPD and station coordinates from all sites (in the format **TRO-SINEX**), as well as the weekly AC **SINEX** file from which the site description blocks are taken. The combination (details see Gendt 1997) starts with the derivations of 2h mean values for each AC. The mean is formed **epochwise** taking into account AC dependent biases not to get jumps by missing data. Additionally, the mean daily station coordinates are computed. Here a homogenization of all used antenna heights and types is performed, so

that all coordinates refer to the same physical point. **Vital to this step is that the daily coordinates from the AC TRO-SINEX files are based on the site descriptions given in the weekly SINEX file. Unfortunately, as checked by Helmert transformation residuals, this is not always the case. The product from the combination is a weekly file for each site containing the ZPD estimates and precipitable water vapor if conversion is possible. Additionally, a combination report will summarize some statistics on the differences to the IGS Mean (bias, standard deviation), for the global mean of each AC and separately for all sites.**

Table 1. Contributing Analysis Centers with some relevant parameters

	ZPD [minutes]	cutoff [deg]	Mapping Function	No. Sites	No. Sites 1 AC only
CODE (week 926)	120	20 10	Saastmoinen Dry Niell	85	14
EMR	60	15	Lanyi	30	2-4
ESA	120	20	Saastmoinen	50	
GFZ (week 929)	60	20	Saastmoinen Dry Niell	55	3-6
JPL (week 920)	5	15	Lanyi Niell	37	1-5
NGS	120	15	Niell	55	1-3

COMPARISONS, RESULTS

The results from 48 weeks in 1997 are used to estimate the achieved consistency. No information about the absolute accuracy could be obtained, with the exception of POTS - the only site for which water vapor radiometer (WVR) data were available.

In Figs. 3, 4 some statistics on the differences between individual AC estimates and the IGS Mean are shown. The information is given separately for about 60 sites, more or less classified into sites with smaller (left) and larger (right) standard deviation (**stddev**). For most sites and ACS the stddev is ± 6 mm ZPD (which corresponds to ± 1 mm PWV) and it approaches in many cases the ± 3 mm level. The magnitude of the stddev is of course highly correlated with the magnitude in the repeatability of the estimated station coordinates. In Fig. 2 the geographical distribution of the magnitude for the stddev is shown. The largest stddevs can be found in the equatorial region. The bias for most sites is below ± 3 mm. Even for sites with a larger bias its repeatability is very high.

In Fig. 5 global mean values (mean over all sites) of the difference to the IGS Mean are given. The mean stddev of the best ACS is at the 4 mm level. Only a small global

bias at the 1 mm ZPD level can be stated. However, significant effects of $\pm 1-2$ mm from AC to AC exist. The three ACS having changed their parameters (crop. Table 1) are extracted in the separate graph at the bottom. Only a slight indication for a bias shift of JPL is indicated at week 920. An more interesting effect can be noticed in the biases of CODE and GFZ. CODE has a large jump at week 926 where changes both from **Saastamionen** to **Niell** mapping function and from 20 to 10 degree cutoff angle were introduced (with elevation dependent weighting). Three weeks later GFZ also switches to **Niell** mapping function, leaving the elevation cutoff angle at 20 degrees. The resulting jump in the GFZ series brings the biases of CODE and GFZ to the same level again, but now 2 mm higher than before week 926. From this one may conclude that the influence of the mapping function on the bias seems to be higher than the influence of the elevation cutoff angle.

In Fig.6 the biases for all weeks and each AC for selected sites are shown. In the top typical examples for fiducial (or other well determined) sites are displayed. The biases are very small, and the repeatability is at the 2 mm ZPD level. Larger systematic effects can be found for some sites as given in the bottom. Here systematic effects of about ± 6 mm exist with single peak to peak differences in the weekly biases of 20 mm. The bias differences could be reduced by taking into account the well-known correlation between the station height and the ZPD estimates. This works rather good for some sites (see Fig. 7), but not for all. However, such a procedure will be not recommended because any corrections to the estimates are dangerous. It is better to reduce the scattering in the determined station heights. One step in this direction will be the enlarged set of 30 to 50 fiducials, which will be constrained to a certain extent by all the ACS. The introduction of a smaller elevation cutoff angle may also help to reduce the bias.

CONVERSION INTO PRECIPITABLE WATER VAPOR

The ZPD estimate must be converted into PWV. The directly estimated ZPD values are of interest for some special applications only, such as atmospheric corrections for collocated VLBI or two-color SLR instruments.

For the conversion meteorological surface measurements are needed. At the moment 19 sites report regularly their met data to the global data centers. Ten further sites have announced the installation of met packages, but the data are not yet available. The met data must be of high precision (1 mbar corresponds to 0.35 mm in PWV) and reliability (continuous time series). In Fig. 8 all sites with met sensors available in 1997 are given. For some sites too many missing days or larger gaps must be stated. In those cases no meaningful series of PWV could be produced. Unfortunately, only 10 to 15 reliable sites with met sensors exist at the moment (a small percentage of all analyzed sites).

The GPS derived PWV estimates can be compared with WVR measurements to get a measure for the absolute accuracy. Only at POTS measurements of a collocated WVR were available. A WVR-1100 of Radiometries Corporation is operated by Meteorological Observatory Potsdam of the German Weather Service, and is located 400m apart from the GPS receiver. In Fig. 10 the time series from WVR, CODE and

GFZ are extracted for 90 days at the end of 1997. Due to a lot of rainy days the WVR series has many gaps. The agreement of the GPS results (both CODE and GFZ) with the WVR is at the 1 mm level (**Fig. 9**). The stddev of the difference approaches ± 0.5 mm, the bias has a level of ± 1 mm and shows some long-periodic behavior for both GPS results. The difference between the two GPS solutions is smaller than their differences to the WVR measurements, The changes in the parameters of CODE (day 926.0 is 97/278) and GFZ (97/299) have obviously not caused any significant changes, neither in the difference between both solutions nor in their differences to WVR, although with 10 and 20 degrees rather different elevation cutoff angles are used.

SUMMARY

During the one year experiment all components involved in the combination have performed well and timely. Some small inconsistencies concerning the description of the station coordinate solutions must be avoided in future. It would be also more effective if the planned short **SINEX** version, containing no matrices, could be introduced soon.

The ZPD estimates have a high quality for all the weeks. The consistency is at the 4 to 5 mm level both for the bias and for the **stddev**. For sites in the equatorial region the quality is not as good - by a factor of 1.5 to 2 worse. The bias is highly correlated with the station height. A lower elevation cutoff angle and the enlarged set of **fiducials** can help to reduce the bias by smaller scattering in the daily station height solutions.

The importance of the IGS contribution to climate research will not only depend on the quality of the ZPD estimates but also on the number of sites which could be equipped with met packages. The number of instruments available now is not sufficient.

To get a better insight into the behavior of the bias more collocated WVR should be made available, either at existing IGS sites or at **non-IGS** sites which then should be analyzed by all **IGS ACS** for some test periods.

REFERENCES

- Gendt, G., 1996a, IGS Tropospheric Estimations - Summary, in *Proceedings Analysis Center Workshop Silver Spring 1996*, Eds. R E Neilan, P A Van Scoy, J F Zumberge, Pasadena, CA U. S. A., pp. 147-149
- Gendt, G., 1996b, Comparison of IGS Tropospheric Estimations, in *Proceedings Analysis Center Workshop Silver Spring 1996*, Eds. R E Neilan, P A Van Scoy, J F Zumberge, Pasadena, CA U.S. A., pp. 151-163
- Gendt, G., 1997, IGS Combination of Tropospheric Estimates (Status Report), in *Proceedings Analysis Center Workshop Pasadena 1997*, in press

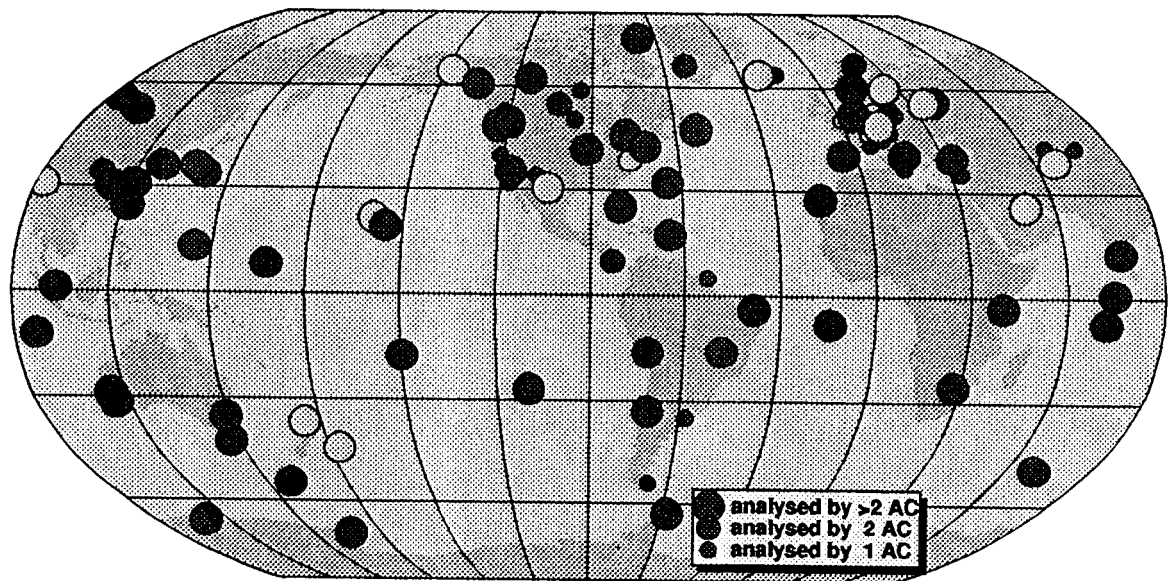


Fig. 1. IGS network with tropospheric estimates (Sites in gray have meteorological packages)

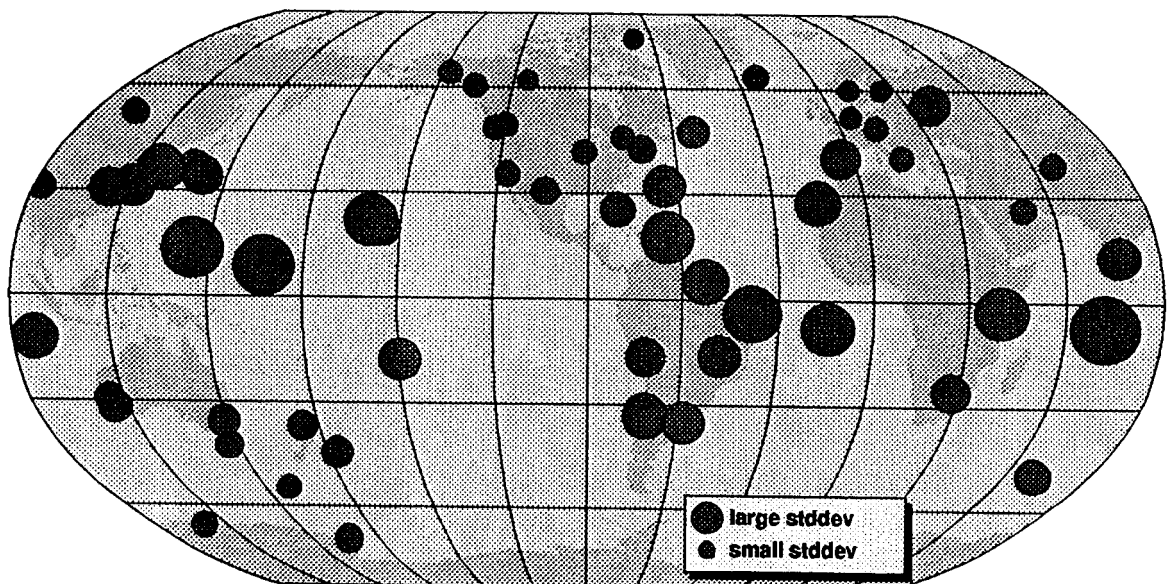


Fig.2. Geographical distribution for mean standard deviation of ZPD estimates

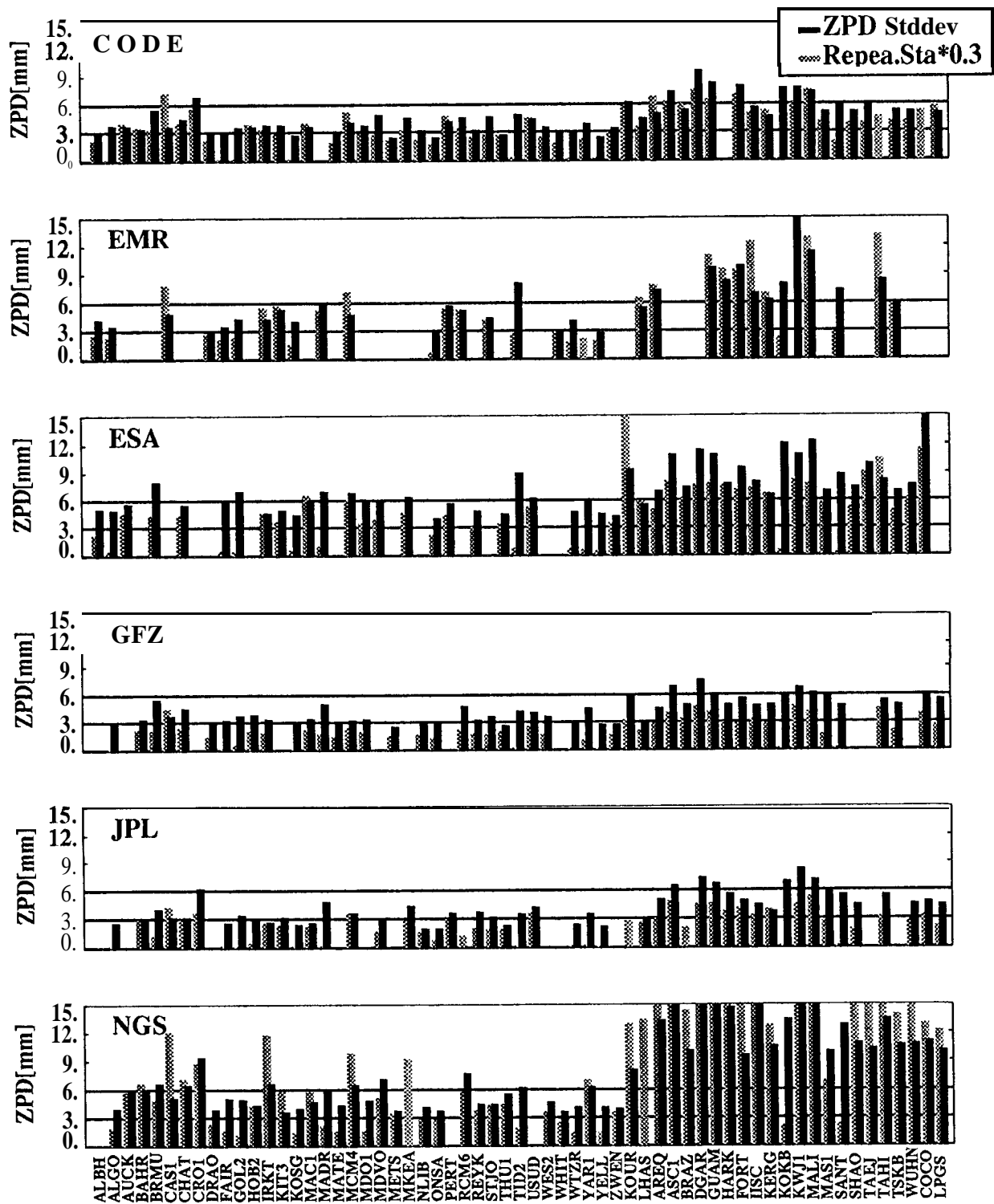


Fig.3. Difference between AC ZPD and IGSC Combined ZPD. Mean of weekly standard deviation for individual sites. Repeatability of station solutions (scaled by correlation factor 0.3) are given for comparison.

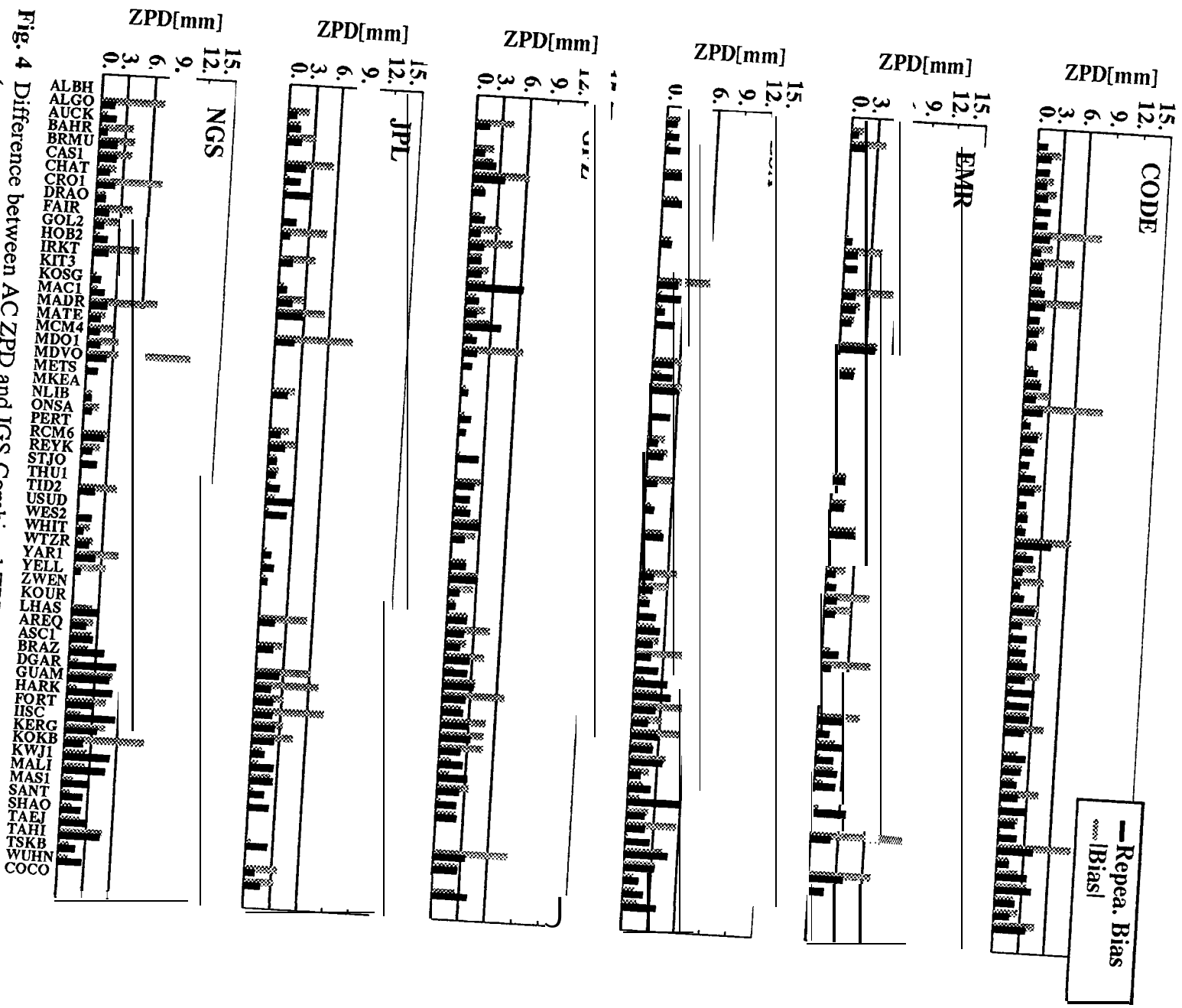


Fig. 4 Difference between AC ZPD and IGS Combined ZPD. Mean of weekly bias (magnitude of bias) and bias repeatability from week to week

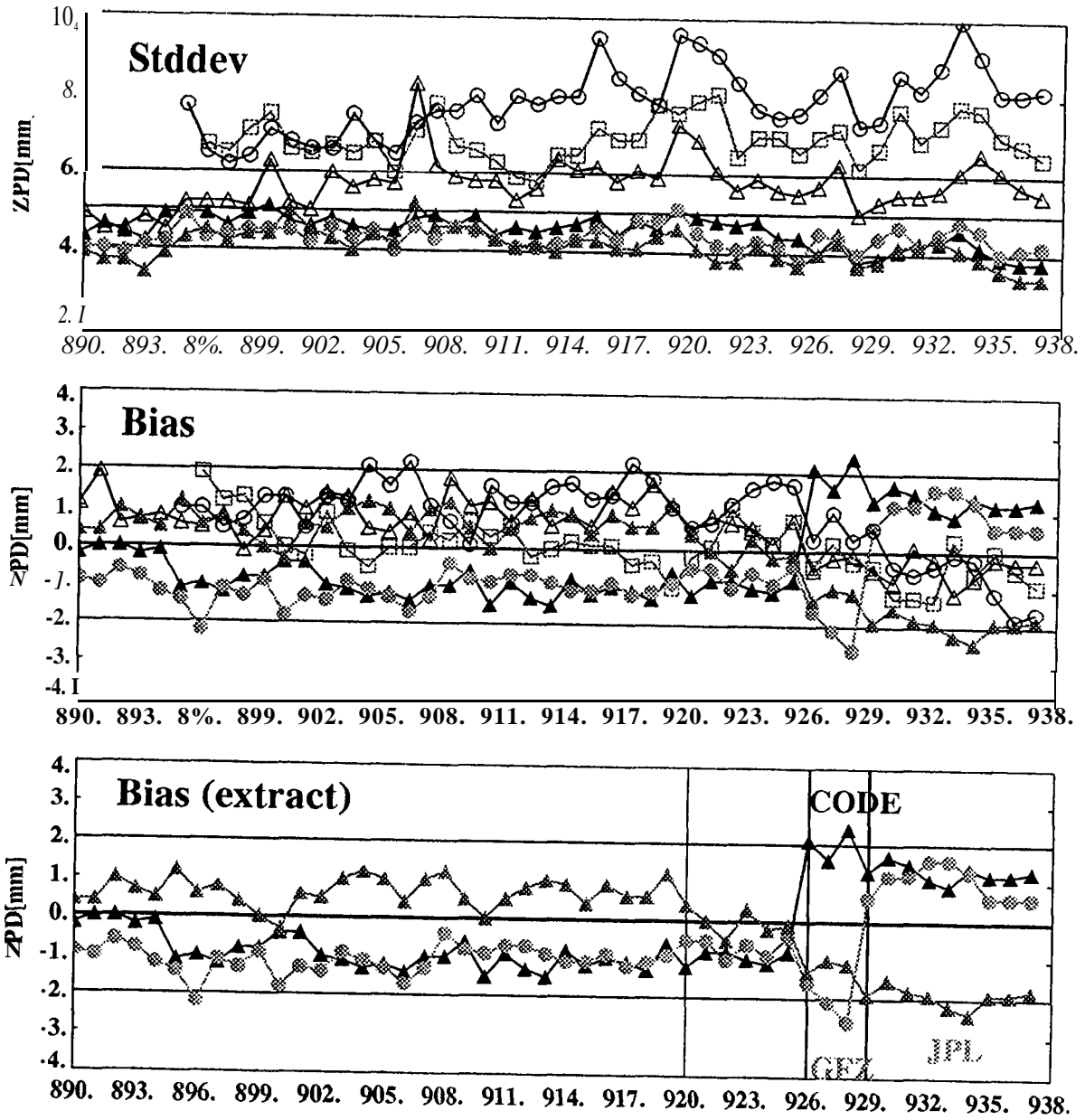


Fig. 5. Difference between AC ZPD and IGS Combined ZPD.
 Mean values (mean over all sites) per week and Analysis Center

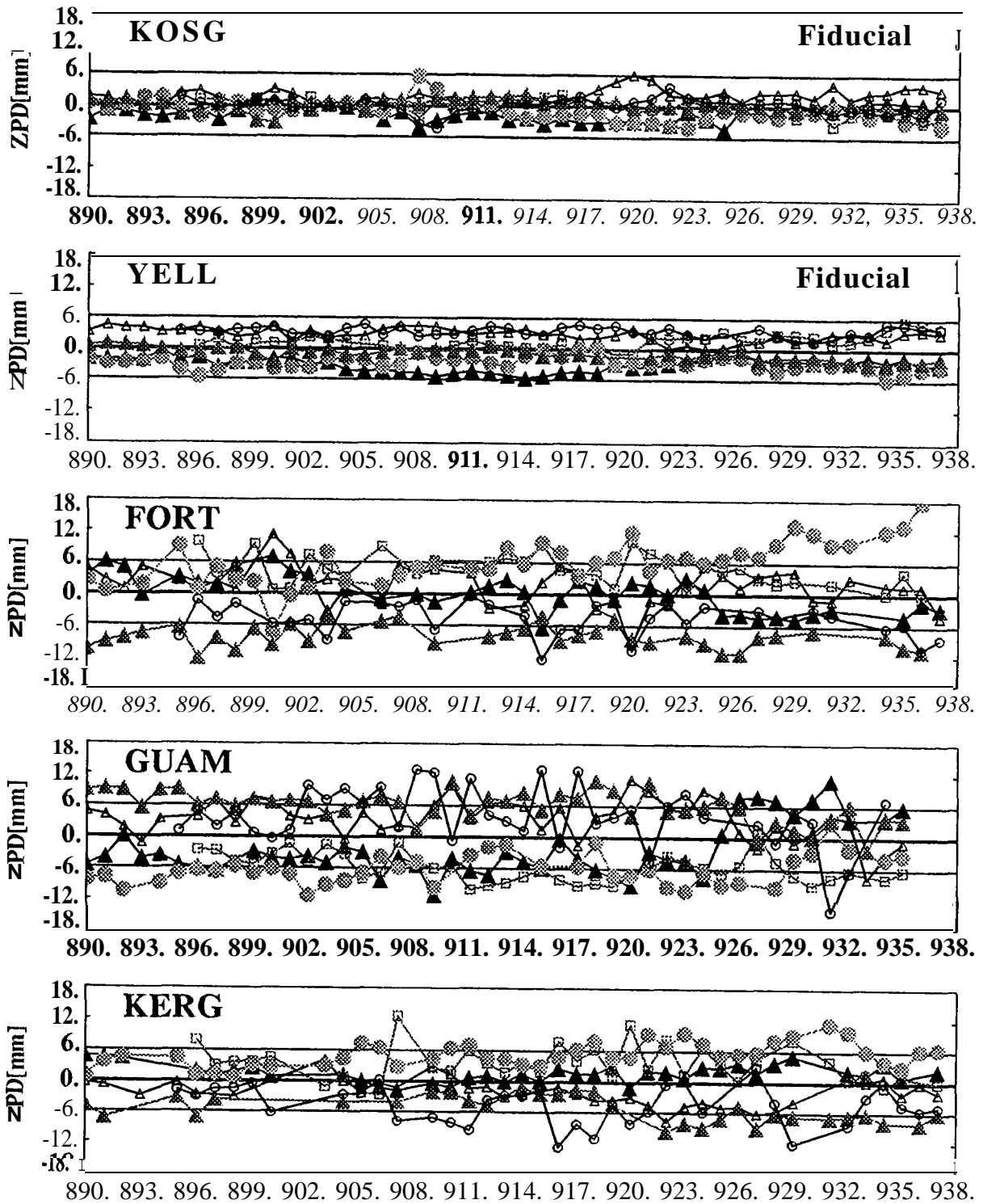


Fig. 6. Difference between AC ZPD and IGS Combined ZPD.
Mean bias per week and Analysis Center

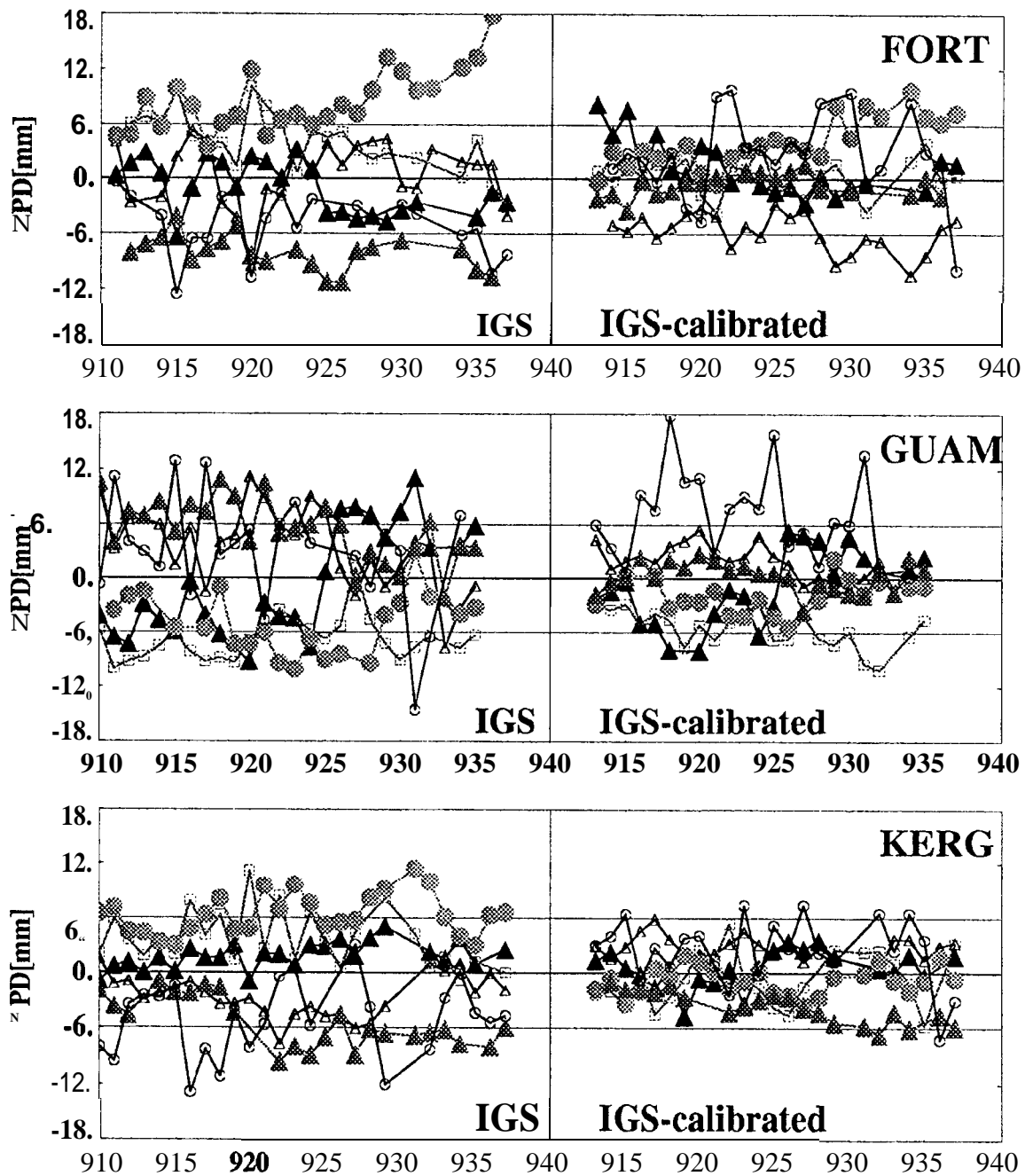


Fig. 7. Difference between AC ZPD and IGS Combined ZPD. Mean bias per week and Analysis Center. Left: Values from Fig. 6. Right: Results with bias corrections by correlation between station height and ZPD.

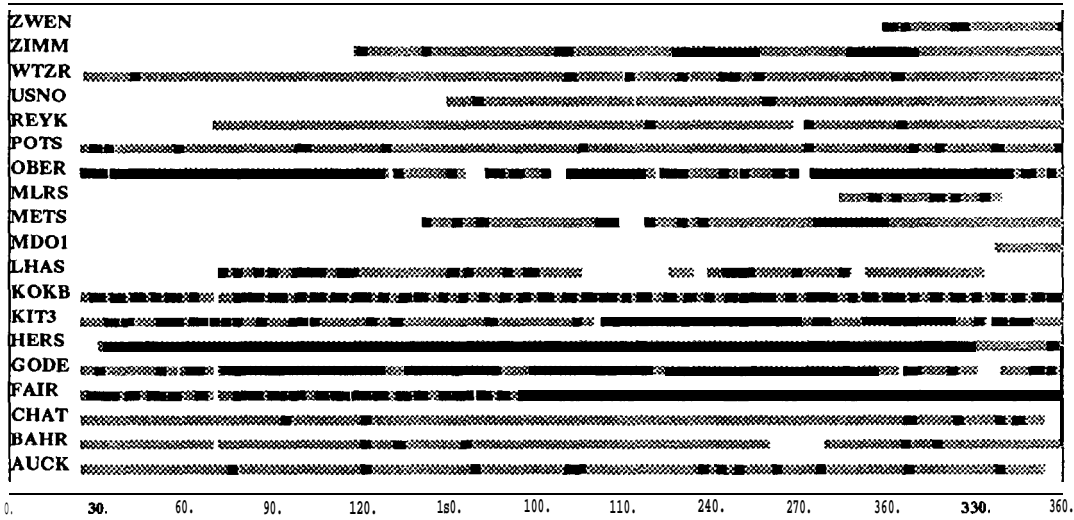


Fig.8. Statistics for existing RINEX Met Files at CDDIS.
 Days with gaps >2 hours are marked with ■ .

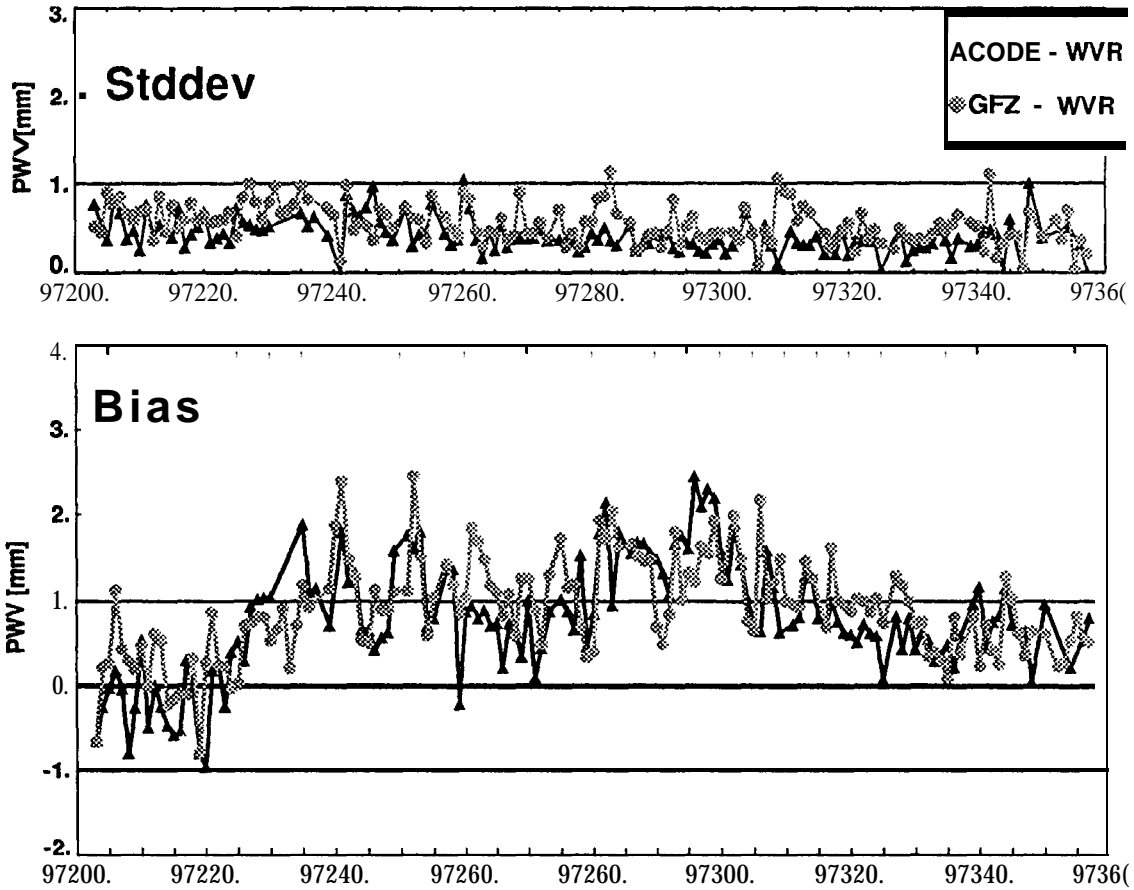


Fig. 9. Comparison of PWV estimates from GPS and WVR at POTS.
 GPS results are from IGS site POTS (CODE and GFZ solutions) and WVR data are from the Meteorological Observatory Potsdam, 400m apart from GPS receiver

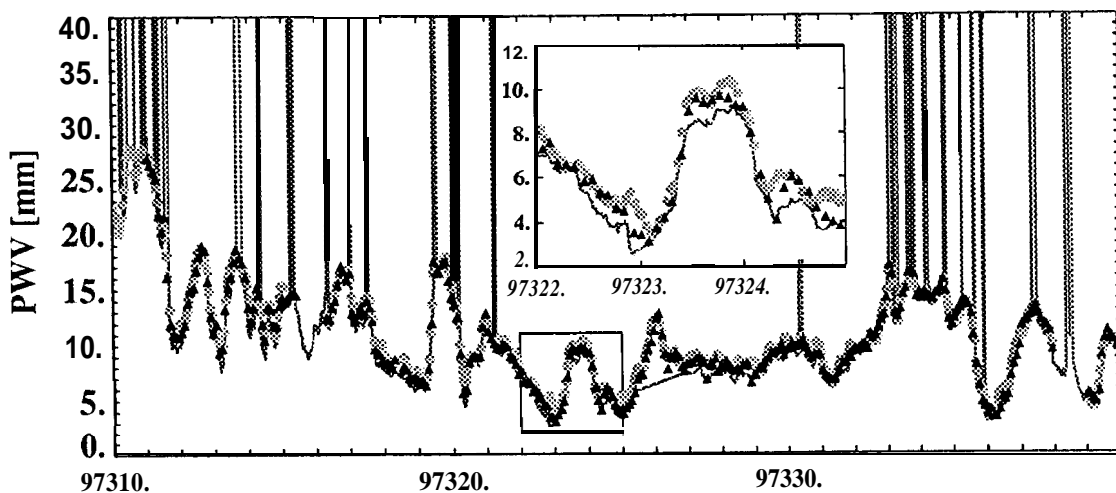
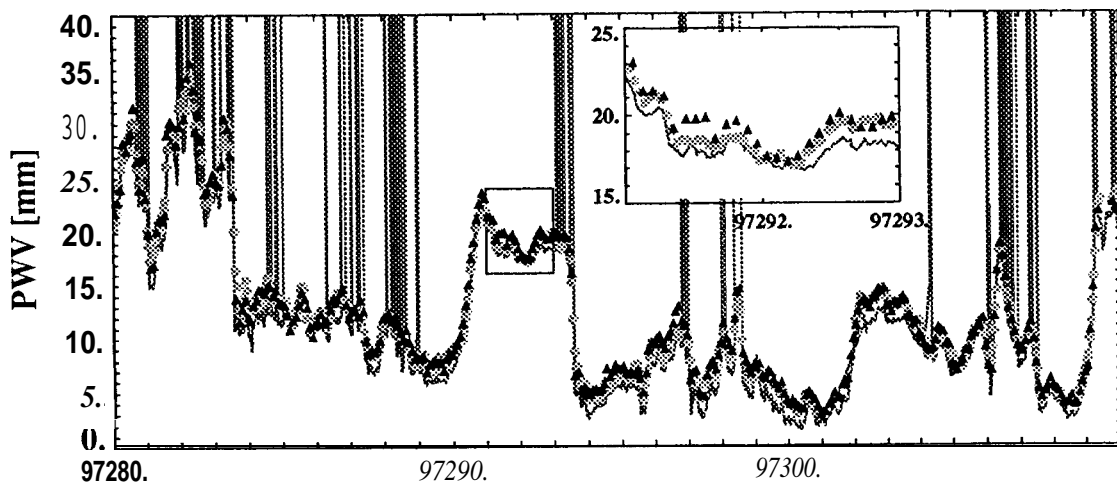
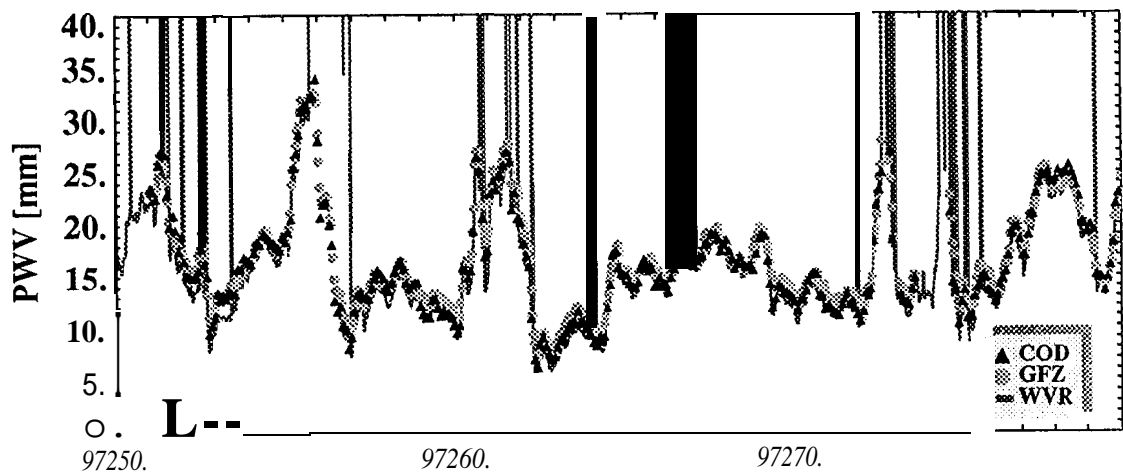


Fig.10. Comparison of PWV estimates from GPS and WVR at POTS.
 GPS results are from IGS site POTS (CODE and GFZ solutions) and WVR data are from the Meteorological Observatory Potsdam, 400m apart from GPS receiver

Water Vapour from Observations of the German Geodetic GPS Reference Network (GREF)

M. Becker, G. Weber

Bundesamt für Kartographie und Geodäsie, Frankfurt a. M., Germany

C. Köpken

German Weather Service (DWD), Offenbach

SUMMARY

Since middle of 1996 the BKG computes daily solutions for a set of German and European permanent GPS stations using the Bernese software. The EUREF permanent network is to be **densified** by a set of up to twenty stations in Germany currently under installation. Presently about twelve stations are operating. Results for a subset of the EUREF network from the BKG processing center are submitted to the EUREF Analysis Center in Bern to be included to the European weekly EUREF solution. The BKG processing is used further to produce sets of tropospheric zenith delay parameters in two hour intervals. These are combined and compared to the **Wettzell** Water Vapour Radiometer of BKG operating since October 1997. In a joint research project with the German Weather Service the potential use of the vertically integrated water vapour (**IWV**) content as derived from the tropospheric zenith delay for the improvement of numerical weather forecasts is studied. As a first step, the derived **GPS-IWV** is compared to **IWV** derived from weather forecast models and the influence of ancillary numerical model data used in the derivation of **GPS IWV** is studied. This is a summary of the main objectives based on the slides of the IGS Analysis Center Workshop 1998, Darmstadt, 9-11 Feb. 1998

1. Verification of DWD Weather Forecasts

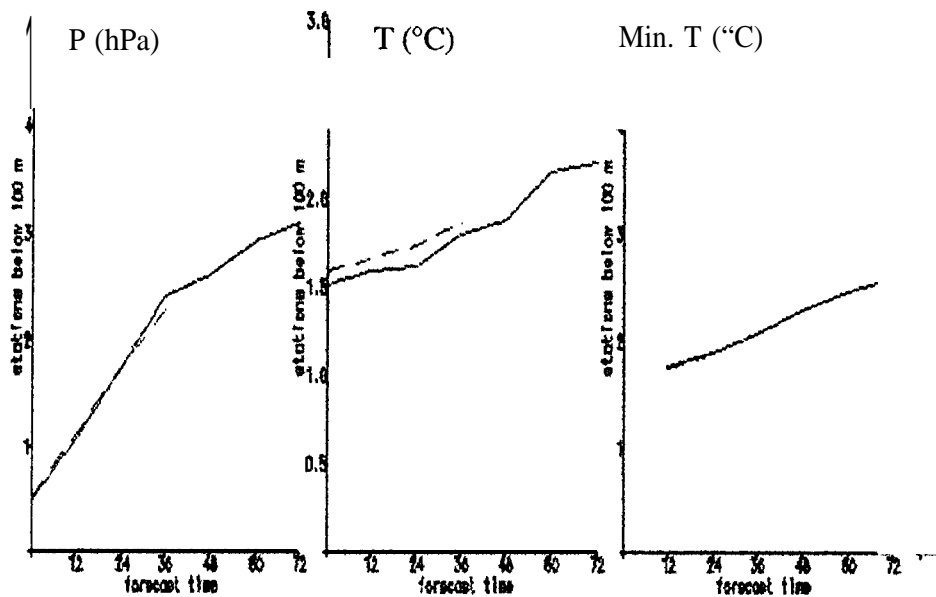


Fig. 1. RMS differences of predicted values to ground truth.

2. CALCULATION OF VERTICALLY INTEGRATED WATER VAPOUR

Integrated vertical water vapour from numerical weather prediction model (NWP):

$$IWV = \int_0^{z_{top}} \rho_{VAP} \cdot dz \quad [\text{kg/nZ}']; \quad dp = -\rho_{WET} \cdot g \cdot dz$$

$$IWV = -\frac{1}{g} \int_{p_s}^{p_{top}} q \cdot dp ;$$

ρ_{vap} = density of water vapor;

z_{top} = height of upper model edge

$\rho_{wet} = \rho_{DRY} + \rho_{VAP}$, density of wet air

p_{top} = pressure at upper edge of model;

p_s = bottom pressure

$q = \frac{\rho_{VAP}}{\rho_{WET}}$ specific humidity of water vapor

given in the model

Integrated precipitable water:

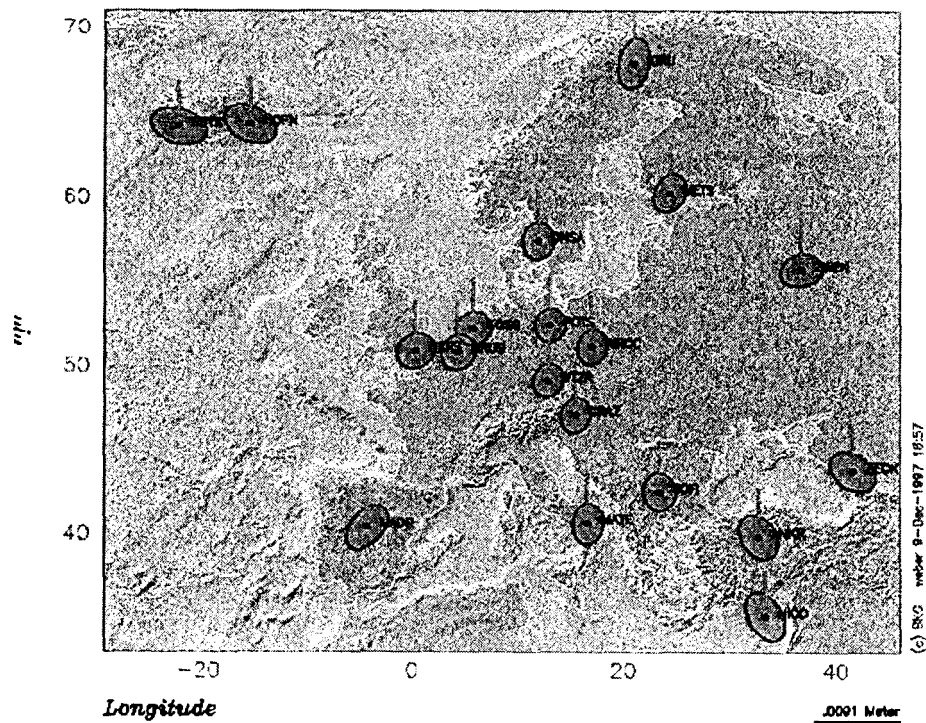
$$IPW = \frac{1}{\rho_w} \cdot IWV \quad [m]; \quad \rho_w = \text{density of water}$$

3. GREF-PERMANENT

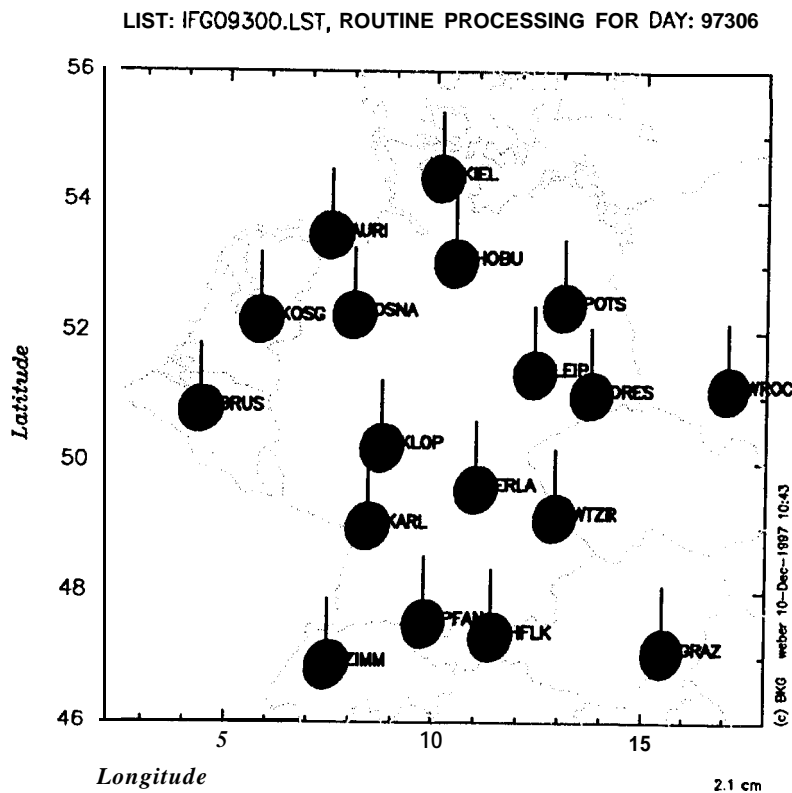
- . Establishing of GPS permanent stations in Germany for daily analysis since 1996
- . Currently 15 stations in Germany
- . Intention
 - Integration in European Reference System
 - Densification for Germany
 - Support of DGPS activities
 - Near real time station control

4. WEEKLY BKG SOLUTION, EUREF PART, GPS-WEEK 0930

Weekly Solution, Federal Agency for Cartography and Geodesy, GPS-Week 0930



5. DAILY BKG SOLUTION, GREF PART, DAY 97306



6. GREF PROCESSING FOR IPWV

- Presently 32 stations with 2 h interval Tropospheric Zenith Delay Estimation
Problem: On] y few met-sensors
- Surface pressure and surface temperature from NWP
- GPS Zenith Path Delay:

$$\text{ZWD (GPS)} = \text{ZTD} - \text{ZHD} = \text{Total Delay} - \text{Hydrostatic Delay}$$

$$\text{ZHD} = f(p_s), p_s = \text{Measured/Model}$$
- Integrated Precipitable Water IPW

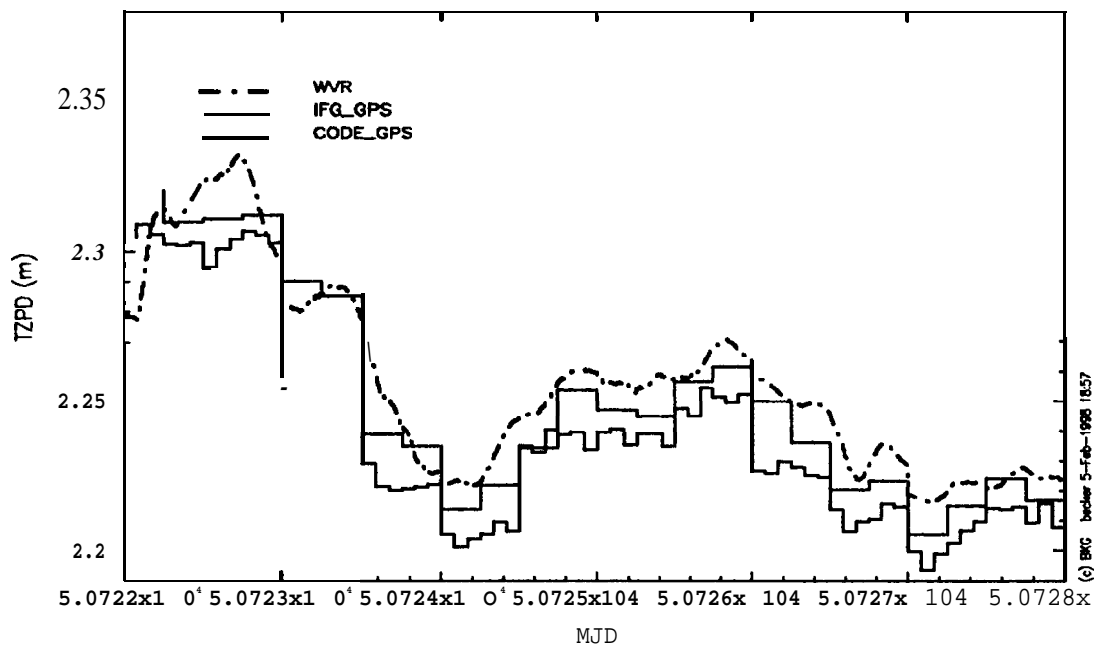
$$\text{IPW} = \Pi * \text{ZWD}; \quad \Pi = f(T_m), T_m \text{ by Regression of } T_s$$
- B KG routine processing problems before optimization of troposphere estimation:
 - bias
 - addition of global stations
 - use of WVR data

7. BKG WATER VAPOUR RADIOMETER

3 WVR'S supplied to BKG by ETH Zurich

- . WVR recording **permanently** at **WETTZELL**
- data provided to **IGS** after software revision
- . WVR for experiments **t.b.d.**
- WVR for **TIGO** missions

8. ZPD FROM GPS AND WVR



9. STATUS OF THE EXPERIMENT AND OUTLOOK

- Data extraction and formatting from NCM
- GPS test computations in the GREF Network
- Reprocessing of WVR Data with improved software
- Numerical results to be presented at **EGS-98** conference

- Met-Packages for **GREF** stations
- Integration of WVR data and ZPD estimation procedures in routine analysis
- Study of numerical weather prediction with near real time requirements for ZPD availability

ESTIMATING HORIZONTAL GRADIENTS OF TROPOSPHERIC PATH DELAY WITH A SINGLE GPS RECEIVER

Yoaz E Bar-Sever¹, Peter M. Kroger¹ and Jorgen A. Borjesson²

¹Jet Propulsion Laboratory, California Institute of Technology

²Onsala Space Observatory, Chalmers University of Technology, Sweden

(in press, *Journal of Geophysical Research*, 1998)

ABSTRACT

We present evidence that modeling troposphere delay gradients in precise GPS geodesy improves the accuracy and precision of the estimated quantities, and that the estimated gradients resemble real atmospheric moisture gradients observed with a water vapor radiometer (WVR). Using a low elevation angle cutoff, combined with a model of the atmospheric delay gradient as a random walk process leads to 19.5% and 15% average improvement in radial and horizontal site position repeatabilities, respectively, relative to a current state-of-the-art estimation strategy that does not model horizontal gradients and imposes high elevation angle cutoff. The agreement between estimated values of zenith wet delay from collocated GPS receivers and WVRs was improved by at least 25%. Merely lowering the elevation angle cutoff improves the repeatability of the radial component of the site's position vector but tends to degrade the repeatability of the horizontal components of the position vector if troposphere gradients are not properly modeled. The estimates of wet delay gradients from a collocated GPS receiver and a WVR at Onsala, Sweden, seem to be correlated over timescales as short as 15 min (Figure 1). The agreement in azimuth between the GPS-based and the WVR-based gradients was at the 10° level, for significant gradients. The GPS was found to under-estimate the magnitude of the gradients by about 60% relative to the WVR-based gradients. The ability to sense atmospheric moisture gradients from a single GPS receiver increases the useful information content from networks of GPS receivers by providing additional spatial information for weather forecasting applications.

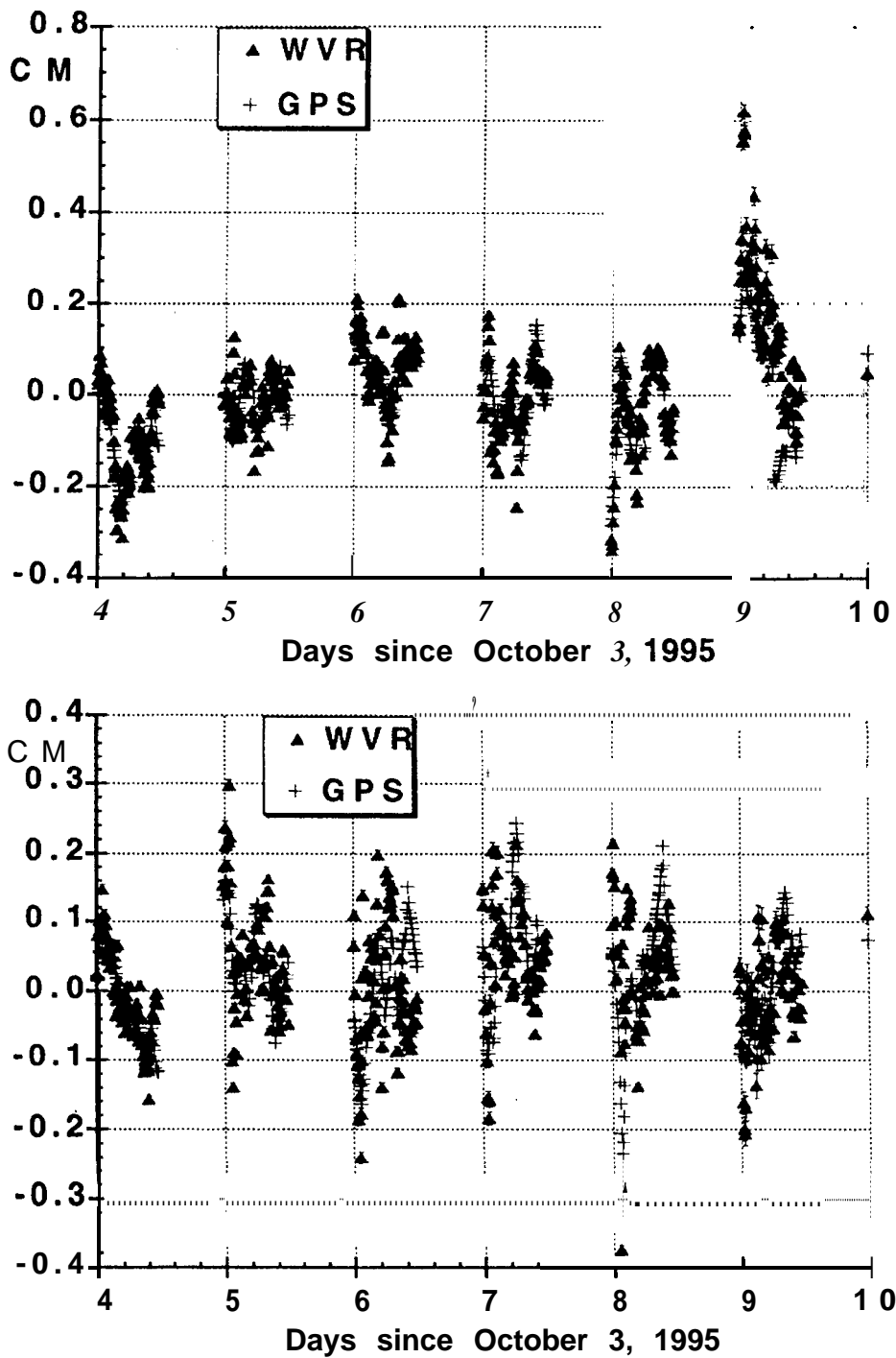


Figure 1. GPS- and WVR-based estimates of north component of the gradient vector, G_N (top), and the east component, G_E (bottom), for 6 12-hour segments during October 1995. Note, the bias between the GPS and the WVR estimates for each segment was removed. Only 6 segments are shown for clarity. Other segments are similar.

IGS PRODUCTS FOR THE IONOSPHERE

J. Feltens

EDS **Industrien (Deutschland)** GmbH, based at
Flight Dynamics Division,
ESA, European Space Operations Centre,
Robert-B **osch-Str.** 5, D-64293 Darrnstadt, Germany

S. Schaer

Astronomical Institute, University of **Berne**,
Sidlerstr. 5, **CH-3012 Berne**, Switzerland

ABSTRACT

In June 1992 the International GPS Service for **Geodynamics (IGS)** started with the routine provision of precise GPS orbits and earth orientation parameters. In the meantime other products were included into the product palette: rapid orbits, predicted orbits, GPS satellite clock information, station coordinates and velocities (**SINEX**), and station-specific tropospheric zenith delays.

For a long time the IGS community has been well aware of the fact that the world-wide **IGS network** offers a unique opportunity to extract ionospheric information on a global scale. At the IGS workshops held **in Potsdam** in May 1995 and in Silver Spring in March 1996, sub-sessions were dedicated to the ionosphere. Main subject of the ionosphere **sub-session** in Silver Spring **in** March 1996 was an **intercomparison** of ionosphere products provided by several Analysis Centers in order to get an idea of the accuracies that can be achieved. In addition it was identified for the first time, which Analysis Centers are interested to contribute to an **IGS** ionosphere product.

Since 1996 considerable progress in ionosphere modeling has been achieved at the different Analysis Centers. **Today** most centers are able (or close to that state) to provide ionosphere information on a routine basis. An official format for the exchange of ionosphere maps, called **IONEX**, has been developed and approved. It was the main task of the 1998 **IGS** Workshop to prepare the start of a coordinated routine processing and a combination of future IGS ionosphere products,

INTRODUCTION AND MOTIVATION

Since mid 1996 we are approaching the next solar maximum. Therefore good and fast knowledge about the ionosphere's actual state becomes increasingly important: Users of satellite navigation systems need accurate corrections to remove signal degradation caused by the ionosphere, information on the ionosphere's behavior is of great importance for radio

signal propagation applications, scientists will benefit from up-to-date and **long-term** ionosphere information, as well. **ESOC** is, for instance, interested to use IGS ionosphere maps to support other ESA missions, like ERS and **ENVISAT**.

As part of the IGS activities **GPS dual-frequency data are collected from a global net of ground stations for years. Due to the fact that the ionosphere is a dispersive medium for microwave signals, dual-frequency GPS data provides thus a direct measure of the ionosphere's activity and can be used to extract global ionospheric information.**

Since 1992 the IGS Analysis Centers demonstrate that they are capable to routinely determine orbits, earth orientation and rotation parameters, and other parameters of geophysical interest. In principle, it is a small step for them to derive ionospheric parameters on a regular basis - provided special software for ionosphere modeling is available.

The main motivation for the **IGS** to get involved in regular ionosphere modeling and mapping is a continuous monitoring of the ionosphere for (at least) the next period of high solar activity and to study in particular the impact of the ionosphere on the "traditional" IGS products (IGS core products).

REVIEW OF IONOSPHERE IGS ACTIVITIES SINCE MARCH 1996

Several of the Analysis Centers participating in the **IGS** have experience with the evaluation of ionospheric parameters from dual-frequency GPS data and develop corresponding software. Institutions, which do currently not contribute to the IGS with products (like orbits, etc.) but indicated their willingness to contribute routinely to IGS ionosphere products, will be denoted as "Analysis Centers", as well, below. Table 1 gives an overview over all Analysis Centers involved and provides detailed information about their ionosphere modeling.

Looking back over the preceding two years, it can be noticed positively that some of the Analysis Centers have achieved considerable progress and improvement in their ionosphere processing. And, as reaction on an e-mail inquiry initiated in preparation to this 1998 workshop, new Analysis Centers have manifested their interest to enter into future IGS ionosphere activities. It must be noticed, however, that most ionosphere-related efforts of the Analysis Centers dealt with internal improvements. Apart from the **intercomparison** of ionosphere maps and differential code biases, performed as a part of the 1996 **IGS** workshop session, and the definition and approval of the so-called Ionosphere Map EXchange Format (**IONEX**) (**Schaer** et al., 1997), no significant contributions to a common IGS activity could be registered.

Many Analysis Centers are ready to participate in a routine **IGS** ionosphere service or are being very close to do so. Therefore, in principle it should only be a small step to start with a routine provision of ionosphere products within the **IGS**.

POTENTIAL PARTICIPANTS IN A ROUTINE IGS SERVICE FOR IONOSPHERE PRODUCTS

In order to get an overview over the possible participants and their individual ionosphere products, an inquiry via e-mail was initiated prior to the 1998 workshop. The reactions on this inquiry are condensed in the following table:

Analysis Center	CODE	DLR	ESOC	JPL	NOAA	NRCan	ROB	UNB	UPC	WUT
IGS Analysis Center ?	yes	no	yes	yes	yes	yes	no	no	no	no
Extent of Ionosphere maps	global & regional (Europe)	regional (Europe)	global	global	regional (US) + global (planned)	regional (Canada) + global (planned)	regional (Belgium)	regional + global (planned)	global	regional
Temporal resolution	24 ^d / 2 ^h in preparation	1 ^h	24 ^d	15 ^m	24 ^d	24 ^h	15 ^m		1 ^h	
Observable(s) used	doubly differenced phase or carrier phase leveled to code	carrier phase leveled to code	carrier phase leveled to code	carrier phase leveled to code	GPS phase information	carrier phase leveled to code	carrier phase leveled to code	carrier phase leveled to code	carrier phases and differences	doubly differenced phase
Shell height	400 km	400 km	450 km for 2-d models	450 km		350 km		400 km and calculated from IRI		400 km
Elevation Swell angle	10°	10°	20°	10°		15°				15°
event dependent observation weighting			yes	yes		yes				
TEC representation	spherical harmonics, n=12, m=8	NTCM model	2-d GE-functions & 3-d Chapman profile models	composition of local basis functions	specific models		Station-specific profile	spatial linear approximation	3-d tomography models	spherical harmonics, n,m=3
Grid width	2.5°	2.5° / 5°	2.5°			3°				2.5°
Differential scd biases	yes	yes	yes	yes	no	yes	yes	isa	no	no
Reference frame internally used	sun-fixed / geographic		sun-fixed / geomagnetic	sun-fixed / geomagnetic		sun-fixed / geographic		sun-fixed / geomagnetic	sun-fixed	sun-fixed
Mapping function	1/cosZ	1/cosZ	1/cosZ, integrated in Chapman profile models	elevation scaling function based on extended-slab model		1/cosZ		1/cosZ		1/cosZ
Single layer shape	spherical		spherical for 2-d models			spherical		spherical		spherical
IONEX format implemented ?	yes	in preparation	yes	in preparation		planned		planned		yes
Ready for routine processing ?	yes	yes	yes	yes	planned	regional: yes global: planned				yes

Analysis Center	CODE	DLR	ESOC	JPL	NOAA	NRCan	ROB	UNB	UPC	WUT
RMS maps provided ?	yes		planned							no
Delay of availability	rapid: 12 ^h , final: 4 ^d	2 ^d	final: 11 ^d rapid: planned	3 ^d						

Table 1: Potential participants and their ionosphere products.

The Analysis Center identifiers are in alphabetical order:
CODE (AIUB): Center for Orbit Determination in Europe, Berne, Switzerland,
DLR: DLR/DFD Fernerkundungsstation Neustrelitz, Germany,
ESOC: ESA/European Space Operations Centre, Darmstadt, Germany,
JPL: Jet Propulsion Laboratory, Pasadena, CA, U.S.A.,
NOAA: National Oceanic and Atmospheric Administration, Silver Spring, U.S.A.,
NRCan (EMR): Natural Resources Canada, Ottawa, Ontario, Canada,
ROB: Royal Observatory of Belgium, Brussels, Belgium,
UNB: University of New Brunswick Fredericton, N.B., Canada,
UPC: Politechnical University of Catalonia, Barcelona, Spain,
WUT: Warsaw University of Technology, Warsaw, Poland.

A blank field indicate-s that no information is available for the Analysis Center.

The University of New Brunswick (uN'B), Fredericton, N. B., Canada, intends (at least in the near future) to contribute with intercomparisons of technique-s and scientific findings rather than with routine ionosphere products.

Table 1 shows that the number of methods of ionospheric modeling corresponds to the number of Analysis Centers!

POTENTIAL USERS OF IGS IONOSPHERE PRODUCTS

When developing IGS ionosphere products, potential users of such ionosphere products should be specified. Ionospheric electron density models are of greatest interest to GPS/GLONASS users with single-frequency receivers. The same information may of course be used for other than GPS/GLONASS satellite tracking data, too. Regular information on ionospheric conditions may also be helpful in other fields of radio signal propagation and for scientific interpretation of phenomena in the high atmosphere, the magnetosphere, and solar activity.

Depending on the interests of different users, different kinds of ionosphere products are required. Users may be grouped into two categories:

- 1) Users interested in fast access to up-to-date ionosphere information, but do not require highest accuracy. We think, e.g., of geodetic survey, navigation applications, road and shipping transport companies. Ionosphere models are only of interest to obtain reasonable corrections for tracking data.

TOWARDS A COMBINED IGS IONOSPHERE PRODUCT

From Table 1 we can see that ten Analysis Centers are prepared to contribute with ionosphere products to the IGS. The analysis procedures are well established at each center, and they differ considerably. We conclude that it does not make sense for the IGS to come up with very stringent requirements concerning the generation of such products. The IGS should, however, define minimum standards, formats, and deadlines for product delivery. These are the basic considerations underlying the following recommendations which emerged from the **Darmstadt** workshop:

Recommendations

- (1) Initially, the IGS should focus on two kinds of products:
 - (a) **TEC** maps in grid form and
 - (b) differential code biases (**DCBs**).
- (2) **IGS TEC** maps are global maps. Only global maps will be compared and perhaps combined. This policy may be reviewed after one year of pilot operations.
- (3) All **TEC** maps must be delivered to the **IGS** in the **IONEX** format [Schaer et al., 1998]. **TEC** maps delivered to the **IGS** thus are “snapshots” of the electron density referring to a particular epoch and to an earth-fixed reference frame.
- (4) Global **TEC** maps from each contributing Analysis Center are given the name *cccGddd0.yy1*, where *ccc* is a 3-figure acronym for the AC (in uppercase), “G” says that this file contains global maps, *ddd* is the day of the year, “O” indicates a daily file, *yy* specifies the 2-digit year, and the last letter “1” stands for “ionosphere maps”. Example: *CODG0410.981* (or *CODG0410.981.Z*). These files are {compressed} and sent to the IGS Global Data Centers and are available to the interested user. Access **Fortran** routines are also made available.
- (5) The daily **IONEX** file, as produced by an IGS Analysis Center, should have a 2-hour resolution referring to the epochs *01, 03, . . . 23 hours UT*. RMS files corresponding to the 2-hourly **TEC** maps may be included in the **IONEX** files. **TEC/RMS** maps refer to a two-dimensional grid in a single layer. The height of the single layer should be 450 *km* adopting a base radius of **6371 km**. The latitude ranges from 87.5 to -87.5 degrees in steps of -2.5 degrees; the longitude ranges from -180 to **180 degrees in** steps of **5 degrees**. **TEC/RMS** values have to be given in units of 0.1 **TECU**.
- (6) Daily sets of differential code biases (**DCBs**) for the GPS satellites are recommended to be included in **IONEX** files. The exchange of satellite-specific DCBS is **IONEX**-supported, too. Note that the DCB reference may be chosen arbitrarily and can be taken into account in the combination procedure.

- 2) Scientists interested in highly accurate ionosphere models. To get precise ionosphere information, this group will accept time delays in having ionosphere products available. Scientists have already signaled their interest in an IGS ionosphere product.

We assume that the majority of potential users will belong to the first category.

PROGRESS MADE AT THE 1998 WORKSHOP

The ionosphere sub-session started with the presentation of the position paper prepared by S. Schaer and J. Feltens. Thereafter contributions covering different aspects relevant for the development of an IGS ionosphere product followed:

- R. Warnant from ROB presented results of a study dealing with the short-term resolution of TEC and its irregularities from GPS data in a regional network.
- N. Jakowski from DLR Neustrelitz reported about their monitoring of the ionosphere over Europe using a model developed at Neustrelitz and discussed its applicability to related ionosphere studies.
- J. Feltens from ESOC presented the basics of a mathematical model to describe the TEC with a 3-d "Chapman profile approach", together with first results obtained - a first attempt in the direction of a 3-d TEC map establishment.
- R. Leitinger from TU Graz pointed out the importance of GPS in ionospheric monitoring, mapping, and **nowcasting** for atmospheric research. He also pointed out that regional differences are considerable. Nevertheless there is a clear interest in global ionospheric models.
- S. Schaer from AIUB showed long-time series of global TEC parameters and demonstrated that it is possible to predict the parameters of CODE ionosphere maps.

The above presentations and the subsequent discussion revealed that there is a great interest of the ionosphere community in a continuous series of global IGS ionosphere models. However, some of the above presentations indicated that many activities in the ionosphere community are regional in nature. Nevertheless, it was decided that the IGS (at least in a first phase) should stay out of regional ionosphere modeling, but should rather focus on global aspects.

In summary it can be said that the authors and the interested institutions are convinced that the development of an IGS ionosphere product is an important task. A continuous series of IGS TEC maps should be produced at least over one full 11-year cycle of solar activity. It is of particular importance that the IGS TEC maps are covering the next period of maximum solar activity (years 2000-2003).

GOALS AND NEXT STEPS

For the near future (about two years) we see the following goals:

- (1) **Global ionosphere maps (TEC maps) including satellite-specific differential code biases (DCBs) from contributing Analysis Centers are made available in IONEX format through the IGS Global Data Centers. The start of the pilot ionosphere service is scheduled for June 28, 1998 (GPS week 964).**
- (2) **Minimum analysis and performance standards are prescribed:**
 - **Minimum analysis standards are listed in recommendation (5), above.**
 - **Ionosphere products are made available not later than the IGS Final Orbits and EOPS, i.e., 11 days after the observations.**
- (3) **TEC maps and DCB values as produced by individual Analysis Centers are compared by the "IGS Ionosphere Coordinating Center". A weekly report has to be produced.**
- (4) **Individual TEC maps and DCB sets are combined into a preliminary "IGS Combined Ionosphere Product". The weekly report now contains also "rms values" relative to the combined product.**
- (5) **Deadlines for ionosphere product delivery after at least six months of pilot service are reviewed. Define an "IGS Rapid Ionosphere Product".**
- (6) **An "IGS Ionosphere Model" based on the available combined (or individual) time series of IGS ionosphere maps (IGS TEC maps) is developed.**

In order to accomplish these goals we propose to establish an "IGS Ionosphere Working Group" proceeding as follows:

- Terms of Reference for the "IGS Ionosphere Working Group":

A draft for these Terms of Reference will be developed jointly by the authors of this position paper, and, as agreed upon at the Darmstadt Governing Board Meeting, by Gerhard **Beutler** and John Dow.

- Membership:

This group should contain representatives of those Analysis Centers which will (with utmost certainty) contribute to the "IGS Ionosphere Service". The list of names will be provided by those IGS parties which intend to participate in the "ionosphere club".

From the ionosphere research community representatives will be

Norbert **Jakowski** (DLR Neustrelitz),

Reinhard **Leitinger** (TU Graz),

and, as IGS Analysis Center Coordinator,

Jan **Kouba**.

Further participation will be called for through an **IGS-mail** message (see below).

- Chairperson:

The **IGS** Governing Board will appoint the first chairperson for the IGS Ionosphere Working Group.

- Announcement, call for participation:

The establishment of the IGS Ionosphere Working Group containing the Terms of Reference, the goals, the next steps, and the list of WG members is published through IGS mail. Further participation is sought in this message. The working group should not have more than 20 members.

- Time frame:

The IGS Ionosphere Working Group should be formally established at the IGS GB Meeting of May 28, 1998 in Boston. This implies that

- draft Terms of Reference for the IGS Ionosphere Working Group and

- draft IGS message containing information and a **call** for further participation

must be available not later than May 7, 1998 for distribution to the IGS Governing Board.

REFERENCES

Feltens, J., 1996a, Ionosphere Models - A New Product of IGS ? **IGS** Position Paper, IGS Analysis Center Workshop, Silver Spring, MD, U. S.A., March 19-21, 1996.

Feltens, J., **1996b**, Ionosphere Maps - A New Product of IGS ? IGS Summary, in *Proceedings of the 1996 IGS Analysis Center Workshop*, Silver Spring, MD, U.S.A., March 19-21, 1996, pp 177-180.

Schaer, S., W. Gurtner, and J. Feltens, 1997, **IONEX**: The Ionosphere Map EXchange Format Version 1, February 25, 1998, in *Proceedings of the 1998 IGS Analysis Centers Workshop*, **ESOC, Darmstadt**, Germany, February 9-11, 1998.

IONEX: The ionosphere Map EXchange Format Version 1

Stefan Schaer, Werner Gurtner

Astronomical Institute, University of Berne, Switzerland
stef an. `schaer@aiub.unibe.ch`

Joachim Feltens

ESA/ESOC, Darmstadt, Germany

February 25, 1998

Introduction

The International GPS Service for Geodynamics (IGS) provides precise GPS orbits, earth orientation parameters (EOPs), station coordinates, satellite clock information, and - on a test basis - tropospheric zenith delays. The IGS community is well aware of the fact that the IGS network can also be used to extract information about the total electron content (TEC) of the ionosphere on a global scale. One may expect that the IGS will include TEC maps into its product palette in the near future.

As part of the 1996 IGS Workshop in Silver Spring, a first effort has been made to compare GPS-derived TEC maps produced by IGS Analysis Centers (CODE and ESA/ESOC) as well as external processing centers (DLR Neustrelitz and University of New Brunswick) [Feltens, 1996a]. For this purpose, a very simple data exchange format proposed by Wilson (JPL) has been used.

One essential conclusion of the ionosphere-related discussion was that a common data format to exchange, compare, or combine TEC maps has to be defined. Based on a first format proposal by [Schaer, 1996], which strongly follows the Receiver INdependent EXchange format (RINEX) [Gurtner and Mader, 1990], [Schaer and Gurtner, 1996], and [Feltens, 1996b], we present a revised version of the so-called Ionosphere map EXchange format (1 ONEX) that supports the exchange of 2- and 3-dimensional TEC maps given in a geographic grid.

The most important modifications with respect to [Schaer and Gurtner, 1996] are:

- Ionosphere maps given in an earth-fixed reference frame are supported only.
- Ionosphere maps are epoch-specific, i. e., they have to be interpreted as "snapshots" at certain epochs. Guidelines how to use IONEX TEC maps are formulated in the next section.
- in addition to TEC and RMS error maps, single-layer height maps are allowed, too.
- The option of 3-dimensional TEC maps has been included into IONEX, i. e., multi-layer models may be handled very easily by performing an additional loop over an equidistant height grid.
- TEC values are written using format m15 instead of m (X1, 14). The definition of an exponent (see "EXPONENT") should help to cover the necessary dynamic range of electron density.
- Further satellite systems and techniques have been added to the list (see "IONEX VERSION / TYPE").
- A general escape sequence has been defined to include technique-related auxiliary data blocks in the header part of IONEX files.

Application of IONEX TEC Maps

We may use three different procedures to compute the TEC E as a function of *geocentric* latitude β , longitude λ , and universal time t , when we have the TEC maps $E_i = E(T_i)$, $i = 1, 2, \dots$, at our disposal:

- Simply take the nearest TEC map $E_i = E(T_i)$ at epoch T_i :

$$E(\beta, \lambda, t) = E_i(\beta, \lambda), \quad (1)$$

where $|t - T_i| = \min$.

- Interpolate between consecutive TEC maps $E_i = E(T_i)$ and $E_{i+1} = E(T_{i+1})$:

$$E(\beta, \lambda, t) = \frac{T_{i+1} - t}{T_{i+1} - T_i} E_i(\beta, \lambda) + \frac{t - T_i}{T_{i+1} - T_i} E_{i+1}(\beta, \lambda), \quad (2)$$

where $T_i \leq t < T_{i+1}$.

- Interpolate between consecutive *rotated* TEC maps:

$$E(\beta, \lambda, t) = \frac{T_{i+1} - t}{T_{i+1} - T_i} E_i(\beta, \lambda'_i) + \frac{t - T_i}{T_{i+1} - T_i} E_{i+1}(\beta, \lambda'_{i+1}), \quad (3)$$

where $T_i \leq t < T_{i+1}$ and $\lambda'_i = \lambda + (t - T_i) \omega$. The TEC maps are rotated by $t - T_i$ around the Z-axis in order to compensate to a great extent the strong correlation between the ionosphere and the Sun's position. Note that method (1) can be refined accordingly by taking the nearest *rotated* map: $E(\beta, \lambda, t) = E_i(\beta, \lambda')$.

From method (1) to method (3), one may expect an improvement of the interpolation results, therefore we recommend to use the last approach (3).

Grid interpolation algorithms to be used are not discussed in detail here. However, a simple 4-point formula should be adequate, if the IONEX grid is dense enough:

$$E(\lambda_0 + p \Delta\lambda, \beta_0 + q \Delta\beta) = (1 - p)(1 - q) E_{0,0} + p(1 - q) E_{1,0} + q(1 - p) E_{0,1} + pq E_{1,1},$$

where $0 \leq p < 1$ and $0 \leq q < 1$. $\Delta\lambda$ and $\Delta\beta$ denote the grid widths in longitude and latitude.

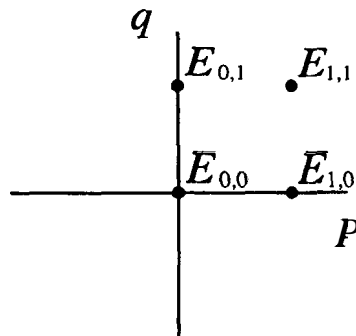


Figure 1: Bivariate interpolation using the nearest 4 TEC values $E_{i,j}$

General Format Description

Each IONEX file consists of a header section and a data section. The header section contains global information for the entire file and is placed at the beginning of the file. The header section contains header labels in columns 61-80 for each line contained in the header section. These labels are mandatory and must appear exactly as given in the IONEX descriptions. Note that the maximum record length is 80 bytes per record.

As record descriptors in columns 61-80 are mandatory, the programs reading an IONEX file should be able to decode the header records with formats according to the record descriptor, provided the records have been first read into an internal buffer.

We propose to allow free ordering of the header records, with the following exception:

- The "IONEX VERSION / TYPE" record must be the first record in a file.

There are further rules to be considered:

- Each value remains valid until changed by an additional header record!
- Fields of lines with formatted numbers must contain at least a "0" to facilitate reading with C language routines, i. e., empty fields are not permitted here.

- In principle there should be no blank lines. We recommend however to anticipate blank line skipping by the reading routines.

Writing and reading IONEX files one has to perform loops over up to a maximum of five arguments, namely: time (EPOCH), latitude (LAT), longitude (LON), height (HGT), and map type. Possible loops are:

- (a) map type, EPOCH, HGT, LAT, LON,
- (b) EPOCH, map type, HGT, LAT, LON.

Both enclosed examples have been created according to loop (a).

The proposed format descriptions as well as examples are given in the tables at the end of this paper.

Exchange of **IONEX** Files

We recommend to use the following naming convention for IONEX files:

cccedddh.yyI,

where

- ccc:** 3-figure Analysis Center (AC) designator
- e:** extension or region code ("G" for Global ionosphere maps)
- ddd:** day of the year of first record
- h:** file sequence number (1, 2,...) or hour (A, B,...) within day;
- O:** file contains all existing data of the current day
- yy:** 2-digit year
- I:** file type ("I" for Ionosphere maps).

Example: CODG2880. 951. It is recommended to specify IONEX file names in uppercase.

When data transmission time or storage volume are critical we recommend to compress the files prior to storage or transmission using the UNIX compress und decompress programs. Compatible routines are available for VAX/VMS and PC/DOS systems.

Proposed naming conventions for compressed files:

System	Ionosphere files
UNIX	cccedddh.yyI.Z
VMS	cccedddh.yyI_Z
DOS	cccedddh.yyJ

Reading and Writing **IONEX** Modules

Fortran-77 routines to read and write IONEX files are available, for instance, via AIUB's anonymous ftp server `ubcclu.unibe.ch` (or 130.92.6.18) — type “`cd aiub$ftp`” after login — in the directory [IONEX.SOURCE]. The main modules are `RDIXFL` (read IONEX file) and `WTIXFL` (write IONEX file). They use the subroutines `RDIXHD/WTIXHD` (read/write IONEX header) and `RDIXDT/WTIXDT` (read/write IONEX data). Auxiliary subroutines are: `DJUL` (date-to-MJD conversion), `JMT` (MJD-to-date conversion), and `RADGMS` (converts a day-fraction into hours-minutes-seconds). Note that the `OPNFIL-OPNERR` sequence must be replaced by an own file opening sequence.

References

- Feltens, J. (1996a): *Ionosphere Maps — A New Product of IGS?* Summary of the Ionosphere Session, IGS Workshop, Silver Spring, MD, USA, March 19–21, 1996.
- Feltens, J. (1996b): *IONEX Format*, GPS-IONO mail, October 30, 1996.
- Gurtner, W., G. Mader (1990): *Receiver Independent Exchange Format Version 2*. CSTG GPS Bulletin, Vol. 3, No. 3, September/October 1990, National Geodetic Survey, Rockville.
- Schaer, S. (1996): *Proposal Concerning VTEC Data Format*. GPS-IONO mail, February 6, 1996.
- Schaer, S., W. Gurtner (1996): *IONEX: The Ionosphere Map EXchange Format Version 0 (Proposal, August 1996)*. GPS-IONO mail, September 3, 1996.

Appendix A: IONEX Version 1 Format Definitions and Examples

Table 1: Ionosphere map file — header section description

HEADER LABEL I (columns 61-80) I	DESCRIPTION	FORMAT
IONEX VERSION / TYPEI	o Format version (1.0)	F8.1,12X,
	o File type ('1' for Ionosphere maps)	A1,19X,
	o Satellite system or theoretical model:	A3,17X
	- 'BEN': BENT	
	- 'ENV': ENVisat	
	- 'ERS': ERS	
	+ 'GEO': GEOstationary satellite(s)	
	- 'GLO': GLOnass	
	- 'GNS': GNSS (gps/glonass)	
	- 'GPS': GPS	
	- 'IRI': IRI	
	+ 'MIX': MIXed/combined	
	- 'NNS': NNSS (transit)	
	- 'TOP': TOPex/poseidon	
	This record has to be the first one in an IONEX file!	
	For techniques marked by a '+', description lines should be added identifying the satellite(s) or roughly specifying the technique used.	
PGM/ RUN BY / DATE	o Name of program creating current file	A20,
	o Name of agency creating current file	A20,
	o Date and time of file creation	A20
* I DESCRIPTION	It is highly recommended to give a brief description of the technique, model, . . . I Please distinguish between description and pure comment.	A60
* I COMMENT	Comment line(s). Note that comment lines are not allowed right at the beginning I of a file or within TEC/RMS/HGT data I blocks (see 'LAT/LON1/LON2/DLON/H'). I	A60
IEPOCH OF FIRST MAP	Epoch of first TECmap (UT): year (4 digits), month, day, hour, rein, sec (integer)	616,24X I
EPOCH OF LAST MAP	Epoch of last TEC map (UT): year (4 digits), month, day, hour, rein, sec (integer)	616,24X
INTERVAL	Time interval between the TEC maps, in seconds (integer). If '0' is specified, 'INTERVAL' may be variable.	16,54X I
# OF MAPS IN FILE	Total number of TEC/RMS/HGT maps	16,54X I

```

|                                     | contained in current file. |                                     |
+-----+-----+-----+-----+-----+-----+-----+-----+
|MAPPING FUNCTION | Mapping function adopted for TEC deter- | 2X,A4,54X | | | | | | |
| I mination: | | | | | | | |
| | 'NONE' : no MF used (e.g. altimetry), | | | | | | | |
| | 'COSZ' : 1/cos(z), | | | | | | | |
| | 'QFAC': Q-factor. | | | | | | | |
| | Others might be introduced. | | | | | | | |
+-----+-----+-----+-----+-----+-----+
|ELEVATION CUTOFF | Minimum elevation angle in degrees. | F8.1,52X |
| | '0.0', if unknown; '90.0' for altimetry. | | | | | | | |
+-----+-----+-----+-----+-----+-----+
|OBSERVABLES USED | One-line specification of the observ- | A60 | | | | | | |
| | able(s) used in the TEC computation (or | | | | | | | |
| | blank line for theoretical models). | | | | | | | |
+-----+-----+-----+-----+-----+-----+
*|# OF STATIONS | I Number of contributing stations. | 16,54X | I*
+-----+-----+-----+-----+-----+-----+
*|# OF SATELLITES | | Number of contributing satellites. | 16,54X | I*
+-----+-----+-----+-----+-----+-----+
|BASE RADIUS | Mean earth radius or bottom of height | F8.1,52X |
| | grid (in km), e.g.: 6371 km or 6771 km. | | | | | | | |
+-----+-----+-----+-----+-----+-----+
|MAP DIMENSION | Dimension of TEC/RMS maps: 2 or 3. | 16,54X |
| | I See also 'TEC VALUES'. | | | | | | | |
+-----+-----+-----+-----+-----+-----+
|HGT1 / HGT2 / DHGT | Definition of an equidistant grid in | 2X,3F6.1, | | | | | | | |
| | height: | I 40X |
| | | 'HGT1' to 'HGT2' with increment 'DHGT' | | | | | | | |
| | | (in km), e.g.: ' 200.0 800.0 50.0'. | | | | | | | |
| | | For 2-dimensional maps, HGT1=HGT2 and | | | | | | | |
| | | DHGT=0, e.g.: ' 400.0 400.0 0.0' or | | | | | | | |
| | | ' 0.0 0.0 0.0' | | | | | | | |
| | | (see also 'BASE RADIUS'). | | | | | | | |
+-----+-----+-----+-----+-----+-----+
|LAT1 / LAT2 / DLAT | Definition of the grid in latitude: | 2X,3F6.1, | | | | | | | |
| | | 'LAT1' to 'LAT2' with increment 'DLAT' | I 40x |
| | | (in degrees). | | | | | | | |
| | | 'LAT1' and 'LAT2' always have to be | | | | | | | |
| | | multiples of 'DLAT'. | | | | | | | |
| | | Example: ' 87.5 -87.5 -2.5'. | | | | | | | |
+-----+-----+-----+-----+-----+-----+
|LON1 / LON2 / DLON | Definition of the grid in longitude: | 2X,3F6.1, | | | | | | | |
| | | 'LON1' to 'LON2' with increment 'DLON' | I 40x |
| | | (in degrees), where LON equals east | | | | | | | |
| | | longitude. | | | | | | | |
| | | 'LON1' and 'LON2' always have to be | | | | | | | |
| | | multiples of 'DLON'. | | | | | | | |
| | | Example: ' 0.0 357.5 2.5' or | | | | | | | |
| | | ' -180.0 177.5 2.5'. | | | | | | | |
+-----+-----+-----+-----+-----+-----+
*| EXPONENT | Exponent defining the unit of the values | 16,54X | I*
| | | listed in the following data block(s). | I | | | | | | |
| | | I Default exponent is -1. | | | | | | | |
| | | I See also 'TEC VALUES', 'RMS VALUES', and | | | | | | | |
| | | 'HGT VALUES', | | | | | | | |
+-----+-----+-----+-----+-----+-----+
*| ISTART OF AUX DATA | Record opening general escape sequence | I A60 | I*

```

	that contains technique-related		
	auxiliary data (e.g. differential code		
	biases for GPS).		
	Note that such data blocks may be		
	skipped if you are interested in		
	ionospheric information only.		
	Format definitions end examples are		
	given in Appendix B.		
+-----+-----+-----+			
* END OF AUX DATA	Record closing auxiliary data block.	A60	*
+-----+-----+-----+			
END OF HEADER	Last record of the header section.	60X	
+-----+-----+-----+			
I START OF TEC MAP	Record indicating the start of the i-th	16,54X	
	TEC map, where i=1,2, . . . ,n denotes the		
	internal number of the current map. All		
	maps have to be ordered chronologically.		
+-----+-----+-----+			
EPOCH OF CURRENT MAP I	Epoch of current map (UT):	616,24X	
	I year (4 digits), month, day, hour,		
	I rein, sec (integer).		
	'EPOCH OF CURRENT MAP' must be specified		
	at the first occurrence of the		
	associated map!		
+-----+-----+-----+			
LAT/LON1/LON2/DLON/H	Record initializing a new TEC/RMS/HGT	2X,5F6.1,	
	data block for latitude 'LAT' (end	28X	
	height 'H(GT)'), from 'LON1' to 'LON2		
	(with increment 'DLON').		
	In case of 2-dimensional maps, it is		
	recommended to define H=HGT1.		
	Neither other types of records nor		
	comment lines are allowed after this		
	record and within the subsequent data		
	block!		
+-----+-----+-----+			
END OF TEC MAP	Record indicating the end of the i-th	16,54X	
	TEC map (see also 'START OF TEC MAP').		
+-----+-----+-----+			
* START OF RMS MAP	Record indicating the start of an RMS	16,54X	*
	map related to the i-th TEC map (see		
	also 'START OF TEC MAP').		
+-----+-----+-----+			
* END OF RMS MAP	I Record indicating the end of an RMS map.	I 16,54X	I*
+-----+-----+-----+			
* START OF HEIGHT MAP I	Record indicating the stint of a HEIGHT	16,54X	*
	map related to the i-th TEC map (see		
	I also 'START OF TEC MAP').		
+-----+-----+-----+			
* END OF HEIGHT MAP	Record indicating the end of a HGT map.	16,54X	*
+-----+-----+-----+			
END OF FILE	Last record closing the IONEX file.	60X	
+-----+-----+-----+			

(Records marked with "*" are optional)

Table 2: Ionosphere map file — data record description

OBS. RECORD	DESCRIPTION	FORMAT
TEC VALUES	TEC values in 0.1 TECU. After 16 values (per latitude band) continue values in next data record. Non-available TEC values are written as '9999'. If an exponent k is specified, the TEC values are given in units of 10**k TECU. The default exponent is -1. See also 'EXPONENT'. If 3-dimensional maps are provided, TEC values should correspond to the surface electron densities at the grid points times 'DHGT' (again in 10**k TECU), that means, you can derive the surface electron densities by simply dividing the TEC values by 'DHGT'. However, if you estimate electron densities integrated over voxels (volume elements), you should ensure that the height grid specified in 'HGT1 / HGT2 / DHGT' refers to the heights of the voxel centers.	m15
* RMS VALUES	RMS values are formatted exactly in the same way as TEC values (see above).	m15
* HGT VALUES	HGT values are formatted exactly in the same way as TEC values (see above). If an exponent k is specified, the HGT values are given in units of 10**k km. The default exponent is -1, too, i.e. in this case the unit corresponds to 0.1 km. The actual heights (with respect to the 'BASE RADIUS') are computed as the sum of 'HGT1' and 'HGT VALUES'.	m15

(Records marked with "*" are optional)

Table 3: Ionosphere map file-example 1: 2-d TEC maps

```

----1---110---1---210---1 ---310---4---4 10---|---5|0--- |---6|0---|---7 |0---|---8|

      1.0          IONOSPHERE MAPS      GPS          IONEX VERSION / TYPE
ionpgm v1.0      aiub                   29-jan-96 17:29  PGM / RUN BY / DATE
example of an ionex file containing 2-dimensional tec maps COMMENT
global ionosphere maps for day 288, 1995 DESCRIPTION
modeled by spherical harmonics . . . DESCRIPTION
      1995  10  15      0      0      0      EPOCH OF FIRST MAP
      1995  10  16      0      0      0      EPOCH OF LAST MAP
21600          INTERVAL
      5          # OF MAPS IN FILE
  
```

COSZ
 20.0
 double-difference carrier phase
 80
 24
 6371.0
 2
 400.0400.0 0.0
 85.0 -85.0 -5.0
 0.0355.0 5.0
 -1
 tec values in 0.1 tec units; 9999, if no value available
 height values in 0.1 km

MAPPING FUNCTION
 ELEVATION CUTOFF
 OBSERVABLE USED
 # OF STATIONS
 # OF SATELLITES
 BASE RADIUS
 MAP DIMENSION
 HGT1 / HGT2 / DHGT
 LAT1 / LAT2 / DLAT
 LON1 / LON2 / DLON

EXPONENT
COMMENT
 COMMENT
 END OF HEADER
 START OF TEC NAP
 EPOCH OF CURRENT NAP
LAT/LON1/LON2/DLON/H

1
 1995 10 15 0 0 0
 85.0 0.0 355.0 5.0 400.0
 1000 1000 1000 1000 1000 1000 1000 1000 1000 1000 1000 1000 1000 1000 1000 1000
 1000 1000 1000 1000 1000 1000 1000 1000 1000 1000 1000 1000 1000 1000 1000 1000
 1000 1000 1000 1000 1000 1000 1000 1000 1000 1000 1000 1000 1000 1000 1000 1000
 1000 1000 1000 1000 1000 1000 1000 1000 1000 1000 1000 1000 1000 1000 1000 1000
 1000 1000 1000 1000 1000 1000 1000 1000 1000 1000 1000 1000 1000 1000 1000 1000
 80.0 0.0 355.0 5.0 400.0
LAT/LON1/LON2/DLON/H

...
 -85.0 0.0 355.0 5.0 400.0
LAT/LON1/LON2/DLON/H
 1000 1000 1000 1000 1000 1000 1000 1000 1000 1000 1000 1000 1000 1000 1000 1000
 1000 1000 1000 1000 1000 1000 1000 1000 1000 1000 1000 1000 1000 1000 1000 1000
 1000 1000 1000 1000 1000 1000 1000 1000 1000 1000 1000 1000 1000 1000 1000 1000
 1000 1000 1000 1000 1000 1000 1000 1000 1000 1000 1000 1000 1000 1000 1000 1000
 1000 1000 1000 1000 1000 1000 1000 1000 1000 1000 1000 1000 1000 1000 1000 1000

1
 2
 1995 10 15 6 0 0
 85.0 0.0 355.0 5.0 400.0
LAT/LoN1/LoN2/DLoN/H
 1000 1000 1000 1000 1000 1000 1000 1000 1000 1000 1000 1000 1000 1000 1000 1000
 1000 1000 1000 1000 1000 1000 1000 1000 1000 1000 1000 1000 1000 1000 1000 1000
 1000 1000 1000 1000 1000 1000 1000 1000 1000 1000 1000 1000 1000 1000 1000 1000
 1000 1000 1000 1000 1000 1000 1000 1000 1000 1000 1000 1000 1000 1000 1000 1000
 1000 1000 1000 1000 1000 1000 1000 1000 1000 1000 1000 1000 1000 1000 1000 1000

...
 5
1
 85.0 0.0 355.0 5.0 400.0
LAT/LON1/LON2/DLON/H
 1000 1000 1000 1000 1000 1000 1000 1000 1000 1000 1000 1000 1000 1000 1000 1000
 1000 1000 1000 1000 1000 1000 1000 1000 1000 1000 1000 1000 1000 1000 1000 1000
 1000 1000 1000 1000 1000 1000 1000 1000 1000 1000 1000 1000 1000 1000 1000 1000
 1000 1000 1000 1000 1000 1000 1000 1000 1000 1000 1000 1000 1000 1000 1000 1000
 1000 1000 1000 1000 1000 1000 1000 1000 1000 1000 1000 1000 1000 1000 1000 1000
 80.0 0.0 355.0 5.0 400.0
LAT/LON1/LON2/DLON/H
 1000 1000 1000 1000 1000 1000 1000 1000 1000 1000 1000 1000 1000 1000 1000 1000
 1000 1000 1000 1000 1000 1000 1000 1000 1000 1000 1000 1000 1000 1000 1000 1000
 1000 1000 1000 1000 1000 1000 1000 1000 1000 1000 1000 1000 1000 1000 1000 1000
 1000 1000 1000 1000 1000 1000 1000 1000 1000 1000 1000 1000 1000 1000 1000 1000

```

1000 1000 1000 1000 1000 1000 1000 1000
...
-85.0 0.0 355.0 5.0 400.0 LAT/LON1/LON2/DLON/H
1000 1000 1000 1000 1000 1000 1000 1000 1000 1000 1000 1000 1000 1000 1000
1000 1000 1000 1000 1000 1000 1000 1000 1000 1000 1000 1000 1000 1000 1000
1000 1000 1000 1000 1000 1000 1000 1000 1000 1000 1000 1000 1000 1000 1000
1000 1000 1000 1000 1000 1000 1000 1000 1000 1000 1000 1000 1000 1000 1000
1000 1000 1000 1000 1000 1000 1000 1000 1000 1000 1000 1000 1000 1000 1000
1
END OF RMS NAP
2
START OF RMS NAP
85.0 0.0 355.0 5.0 400.0 LAT/LON1/LON2/DLON/H
1000 1000 1000 1000 1000 1000 1000 1000 1000 1000 1000 1000 1000 1000 1000
1000 1000 1000 1000 1000 1000 1000 1000 1000 1000 1000 1000 1000 1000 1000
1000 1000 1000 1000 1000 1000 1000 1000 1000 1000 1000 1000 1000 1000 1000
1000 1000 1000 1000 1000 1000 1000 1000 1000 1000 1000 1000 1000 1000 1000
1000 1000 1000 1000 1000 1000 1000 1000 1000 1000 1000 1000 1000 1000 1000
...
5
END OF RMS MAP
1
START OF HEIGHT MAP
85.0 0.0 355.0 5.0 400.0 LAT/LON1/LON2/DLON/H
0 0 0 0 0 0 0 0 0 0 0 0 0 0 0
0 0 0 0 0 0 0 0 0 0 0 0 0 0 0
0 0 0 0 0 0 0 0 0 0 0 0 0 0 0
0 0 0 0 0 0 0 0 0 0 0 0 0 0 0
0 0 0 0 0 0 0 0 0 0 0 0 0 0 0
80.0 0.0 355.0 5.0 400.0 LAT/LON1/LON2/DLON/H
0 0 0 0 0 0 0 0 0 0 0 0 0 0 0
0 0 0 0 0 0 0 0 0 0 0 0 0 0 0
0 0 0 0 0 0 0 0 0 0 0 0 0 0 0
0 0 0 0 0 0 0 0 0 0 0 0 0 0 0
0 0 0 0 0 0 0 0 0 0 0 0 0 0 0
...
-85.0 0.0 355.0 5.0 400.0 LAT/LON1/LON2/DLON/H
0 0 0 0 0 0 0 0 0 0 0 0 0 0 0
0 0 0 0 0 0 0 0 0 0 0 0 0 0 0
0 0 0 0 0 0 0 0 0 0 0 0 0 0 0
0 0 0 0 0 0 0 0 0 0 0 0 0 0 0
0 0 0 0 0 0 0 0 0 0 0 0 0 0 0
1
END OF HEIGHT MAP
2
START OF HEIGHT NAP
85.0 0.0 355.0 5.0 400.0 LAT/LON1/LON2/DLON/H
0 0 0 0 0 0 0 0 0 0 0 0 0 0 0
0 0 0 0 0 0 0 0 0 0 0 0 0 0 0
0 0 0 0 0 0 0 0 0 0 0 0 0 0 0
0 0 0 0 0 0 0 0 0 0 0 0 0 0 0
0 0 0 0 0 0 0 0 0 0 0 0 0 0 0
..
5
END OF HEIGHT NAP
END OF FILE

```

```

----1--1]0--1---2 IO---I---310---! ---4|0---|---5|0--- 1---610---1---710---1---81

```

Table 4: Ionosphere map file — example 2: 3-d TEC maps

```

'---1---110---1---2 |0---|---3|0---|---4 |10---1---510---1---610--- |---7|0---|---8|

1.0 IONOSPHERE MAPS GPS IONEX VERSION / TYPE
ionpgm v1.0 aiub 29-jan-96 17:29 PGM / RUN BY / DATE
example of an ionex file containing 3-dimensional tec maps COMMENT
global ionosphere maps for day 288, 1995 DESCRIPTION
modeled by spherical harmonics . . . DESCRIPTION
1995 10 15 0 0 0 EPOCH OF FIRST MAP
1995 10 16 0 0 0 EPOCH OF LAST MAP
21600 INTERVAL
5 # OF MAPS IN FILE
COSZ MAPPING FUNCTION
20.0 ELEVATION CUTOFF
double-difference carrier phase OBSERVABLE CUTOFF
80 # OF STATIONS
24 # OF SATELLITES
6371.0 BASE RADIUS
3 MAP DIMENSION
200.0 800.0 50.0 HGT1 / HGT2 / DHGT
85.0 -85.0 -5.0 LAT1 / LAT2 / DLAT
0.0355.0 5.0 LON1 / LON2 / DLON
END OF HEADER
1 START OF TEC MAP
1995 10 15 0 0 0 EPOCH OF CURRENT MAP
-3 EXPONENT
85.0 0.0 355.0 5.0 200.0 LAT/LON1/LON2/DLON/H
1000 1000 1000 1000 1000 1000 1000 1000 1000 1000 1000 1000 1000 1000 1000 1000
1000 1000 1000 1000 1000 1000 1000 1000 1000 1000 1000 1000 1000 1000 1000 1000
1000 1000 1000 1000 1000 1000 1000 1000 1000 1000 1000 1000 1000 1000 1000 1000
1000 1000 1000 1000 1000 1000 1000 1000 1000 1000 1000 1000 1000 1000 1000 1000
1000 1000 1000 1000 1000 1000 1000 1000 1000 1000 1000 1000 1000 1000 1000 1000
80.0 0.0 355.0 5.0 200.0 LAT/LON1/LON2/DLON/H
1000 1000 1000 1000 1000 1000 1000 1000 1000 1000 1000 1000 1000 1000 1000 1000
1000 1000 1000 1000 1000 1000 1000 1000 1000 1000 1000 1000 1000 1000 1000 1000
1000 1000 1000 1000 1000 1000 1000 1000 1000 1000 1000 1000 1000 1000 1000 1000
1000 1000 1000 1000 1000 1000 1000 1000 1000 1000 1000 1000 1000 1000 1000 1000
1000 1000 1000 1000 1000 1000 1000 1000 1000 1000 1000 1000 1000 1000 1000 1000
-85.0 0.0 355.0 5.0 200.0 LAT/LON1/LON2/DLON/H
1000 1000 1000 1000 1000 1000 1000 1000 1000 1000 1000 1000 1000 1000 1000 1000
1000 1000 1000 1000 1000 1000 1000 1000 1000 1000 1000 1000 1000 1000 1000 1000
1000 1000 1000 1000 1000 1000 1000 1000 1000 1000 1000 1000 1000 1000 1000 1000
1000 1000 1000 1000 1000 1000 1000 1000 1000 1000 1000 1000 1000 1000 1000 1000
1000 1000 1000 1000 1000 1000 1000 1000 1000 1000 1000 1000 1000 1000 1000 1000
-2 EXPONENT
85.0 0.0 355.0 5.0 250.0 LAT/LON1/LON2/DLON/H
1000 1000 1000 1000 1000 1000 1000 1000 1000 1000 1000 1000 1000 1000 1000 1000
1000 1000 1000 1000 1000 1000 1000 1000 1000 1000 1000 1000 1000 1000 1000 1000
1000 1000 1000 1000 1000 1000 1000 1000 1000 1000 1000 1000 1000 1000 1000 1000
1000 1000 1000 1000 1000 1000 1000 1000 1000 1000 1000 1000 1000 1000 1000 1000
1000 1000 1000 1000 1000 1000 1000 1000 1000 1000 1000 1000 1000 1000 1000 1000
80.0 0.0 355.0 5.0 250.0 LAT/LON1/LON2/DLON/H
1000 1000 1000 1000 1000 1000 1000 1000 1000 1000 1000 1000 1000 1000 1000 1000
1000 1000 1000 1000 1000 1000 1000 1000 1000 1000 1000 1000 1000 1000 1000 1000
1000 1000 1000 1000 1000 1000 1000 1000 1000 1000 1000 1000 1000 1000 1000 1000
1000 1000 1000 1000 1000 1000 1000 1000 1000 1000 1000 1000 1000 1000 1000 1000

```


Appendix B: Auxiliary Data Blocks

GPS/GLONASS-Related Data Block

If single-frequency GPS users apply precise ephemerides and precise satellite clock information — which always refers to the ionosphere-free linear combination (LC) — as well as IONEX TEC maps to eliminate or greatly reduce ionosphere-induced errors, they may also be interested in having a set of differential code biases (DCBs) of the satellites to correct their C/A- or P-code measurements accordingly (to make them consistent to the LC satellite clocks — or vice versa). The DCBs b are estimated simultaneously with the TEC parameters using the relationship

$$c b = (P_1 - P_2)_{\text{observed}} - (P_1 - P_2)_{\text{corrected}},$$

where P_1 and P_2 denote the C/A- or P-code observable in meters on L1 (under AS or non-AS conditions) and L2, respectively. The DCB correction for the P_1 measurements or for the LC satellite clock values T_{LC} (from SP3 orbit file) are given by

$$P_{1\text{corrected}} = P_{1\text{observed}} - \kappa_2 C b$$

and

$$T_{\text{corrected}} = T_{LC} + \kappa_2 b,$$

where $\kappa_2 = -\nu_2^2 / (\nu_1^2 - \nu_2^2) = -1.55$ is the second LC factor, ν_i is the frequency of the i -th carrier, c is the vacuum speed of light, and $b = b_1 - b_2$ is the (geometry-free) DCB of the SV considered (usually in nanoseconds).

Since the DCB information is a by-product of the TEC determination when analyzing dual-band code measurements, DCB estimates may be included in IONEX files. The GPS/GLONASS-related data block has to be labelled with “DIFFERENTIAL CODE BIASES” (see example in Table 2).

Table 1: Differential code biases — format definitions

HEADER LABEL	DESCRIPTION	FORMAT
I (columns 61-80) I		
PRN / BIAS / RMS	Pseudo Random Number (PRN), differential (L1-L2) code bias, and its RMS error in nanoseconds. Note that the PRN consists of a character indicating the satellite system ('G' or blank for GPS and 'R' for GLONASS) and the actual PRN (2 digits).	3X, A1, 12.2, 2F10.3, 34X
* COMMENT	Comment lines are allowed.	A60 *

(Records marked with “*” are optional)

Table 2: Differential code biases — example

```

'---1---110---1---2 10-1---310---1---4{0--- 1---510---1---610--- |---7|0---|---8|

DIFFERENTIAL CODE BIASES                                START OF AUX DATA
   01      0.000      0.000                             PRN / BIAS / RMS
   02      0.000      0.000                             PRN / BIAS / RMS
...
   31      0.000      0.000                             PRN / BIAS / RMS
11-12 biases and rms in ns                             COMMENT
sum of biases constrained to zero                       COMMENT
DIFFERENTIAL CODE BIASES                                END OF AUX DATA

----1---110---1---2 10---1---310---1---410--- 1---510---1---610---1---710---1---81

```

THE STUDY OF THE TEC AND ITS IRREGULARITIES USING A REGIONAL NETWORK OF GPS STATIONS.

Rene Warnant

Royal Observatory of Belgium
Avenue Circulaire, 3
B-1 180 Brussels
Belgium

ABSTRACT

In this paper, we outline the procedure used at the Royal Observatory of Belgium in order to compute the TEC using GPS measurements with a precision of 2-3 TECU. This procedure requires the determination of the so-called receiver and satellite differential group delays. The combined biases (receiver + satellite) are determined using the geometry-free combination of code observations where the TEC is modelled using a simple polynomial in latitude and local time; the long-term behaviour of the biases is studied. In addition, the reliability of the computed TEC is discussed.

The paper also presents a very simple method allowing to detect medium-scale Traveling Ionospheric Disturbances and scintillation effects by observing the high frequency changes in the geometry-free combination of GPS phase measurements. The method has been applied to the GPS measurements gathered at Brussels (mid-latitude European station) during more than 8 years: only a few scintillations were detected during this period but TIDs were very regularly observed. Statistics concerning the occurrence of Traveling Ionospheric Disturbances at Brussels are presented.

COMPUTING THE TEC USING GPS MEASUREMENTS

The Global Positioning System has already proved to be a very useful tool to study the ionosphere. Indeed, GPS code and carrier phase measurements can be processed in order to determine the Total Electron Content (Lanyi and Roth (1988), Warnant (1996)).

In practice, the TEC can be obtained from:

1) the so-called geometry-free combination of dual frequency code measurements, $P'_{p,GF}$;

$$P'_{p,GF} = P_{p,L1}^i - P_{p,L2}^i \quad (1)$$

This equation can be rewritten in **function** of the Total Electron Content, TEC_p^i :

$$P_{p,GF}^i = -1.0510 \cdot 10^{-17} TEC_p^i + (DG_p - DG^i) \quad (2)$$

with TEC_p^i slant TEC measured along the path going from satellite i to receiver p ;
 DG^i, DG_p the satellite i and receiver p differential group delays;
 $P_{p,L1}^i, P_{p,L2}^i$ the $L1, L2$ P-code measurements made by receiver p on satellite i .

When the Anti-spoofing is active (as it is the case since January 31 1994), the code observations have a precision ranging from a few decimeters to more than one metre. These measurements are not ambiguous but contain biases called receiver and satellite **differential group delays**. The existence of these biases is due to the fact that the two GPS frequencies undergo different propagation delays inside the receiver and satellite hardware.

2) the geometry-free combination of dual frequency phase measurements $\Phi_{p,GF}^i$;

$$\Phi_{p,GF}^i = \Phi_{p,L1}^i - \frac{f_{L1}}{f_{L2}} \Phi_{p,L2}^i \quad (3)$$

or rewritten in **function** of the TEC:

$$\Phi_{p,GF}^i = -5.5210 \cdot 10^{-17} TEC_p^i + N_{p,GF}^i \quad (4)$$

with f_{L1}, f_{L2} the frequency of the $L1, L2$ carriers;
 $\Phi_{p,L1}^i, \Phi_{p,L2}^i$ the $L1, L2$ carrier phase measurements made by receiver p on satellite i ;
 $N_{p,GF}^i$ a real ambiguity.

Phase measurements usually have a precision better than one millimetre but contain an initial ambiguity which is real in the case of the geometry-free combination. In the absence of cycle slips, $N_{p,GF}^i$ has to be solved for every satellite pass.

3) a combination of geometry-free code and phase measurements.

$$P_{p,GF}^i - \lambda_{L1} \Phi_{p,GF}^i = (DG_p - DG^i) - \lambda_{L1} N_{p,GF}^i \quad (5)$$

with λ_{L1} the $L1$ carrier wavelength.

This combination is used to solve the ambiguity $N_{p,GF}^i$ which is injected in equation (4) in order

to determine the TEC. This third method which is applied at the Royal Observatory of Belgium allows to combine the advantages of both measurement types: the TEC is obtained from the precise phase measurements but the **information** contained in the code observations is used to solve the ambiguity. Nevertheless, the procedure requires the determination of the receiver and satellite differential group delays. In most of the cases, these biases have to be computed:

- *the satellite biases*: they are measured by the manufacturer before the satellites are launched but in most of the cases, these values are not valid anymore when the satellites are on their orbit (see, for example, Wilson and **Mannucci** (1993), Wanninger et al. (1994), Wamant (1996)).

- *the receiver biases*: in the past, the old Rogue receivers (the so-called Big-Rogue and Mini-Rogue) had an auto-calibration **function** allowing to measure the receiver bias. **Unfortunately**, this **function** does not exist any more on the Turbo Rogue receiver. To our knowledge, no other receiver has this capability.

THE HARDWARE BIASES

The Royal Observatory of Belgium has a network of 7 permanent GPS stations (figure 1). The station of Brussels is in continuous operation since April 1993. Dentergem, Dourbes and Waremmme were installed in January 1994; Bree, **Meeuwen** and Membach were installed in 1997. **All** the stations are equipped with Turbo Rogue receivers. In this **section**, we outline the method we have developed to study the hardware biases. The method has been applied to our Turbo Rogue network. In fact, the error made in the determination of the differential group delays is the largest error source when computing the **TEC** using **GPS** measurements. It is clear that these biases cannot be neglected: for example the bias of one of our receivers (serial number 238) is +5.33 ns. The fact to neglect it would give an error of 16 TECU on the computed TEC.

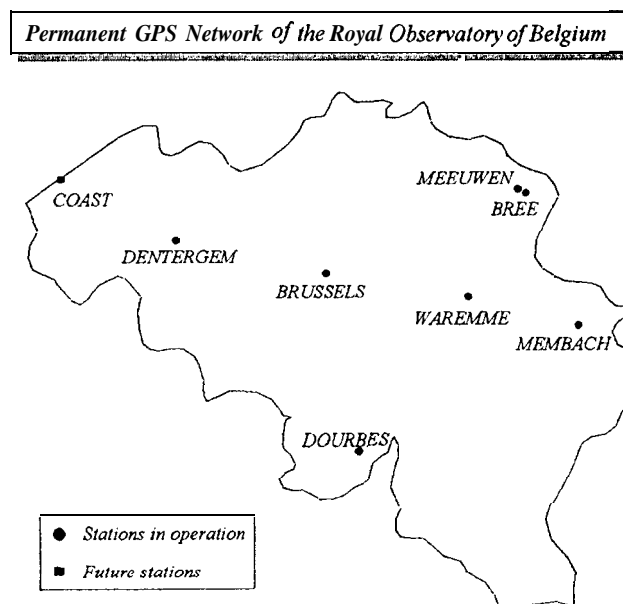


Figure 1. The permanent network of the Royal Observatory of Belgium.

In practice, the combined biases (receiver+ satellite) are determined using equation (2) where the ionosphere is **modelled** by means of a simple polynomial in latitude and local time. Every model (i.e. polynomial) is computed using periods of about 6 hours of data. During this procedure, the “usual” assumptions are made:

- the ionosphere is concentrated in a spherical shell of infinitesimal thickness located at a height of 350 km; the intersection between this layer and the satellite line of sight is called the *ionospheric point*;
- “static” **behaviour** of the ionosphere on short periods (6 hours): the TEC only depends on latitude and local time;
- the receiver and satellite biases are constant on short periods. In the case of the Turbo Rogue biases, we have verified this assumption: during a period of a few hours, the biases remain constant within 0.2 ns(Wamant(1996)).

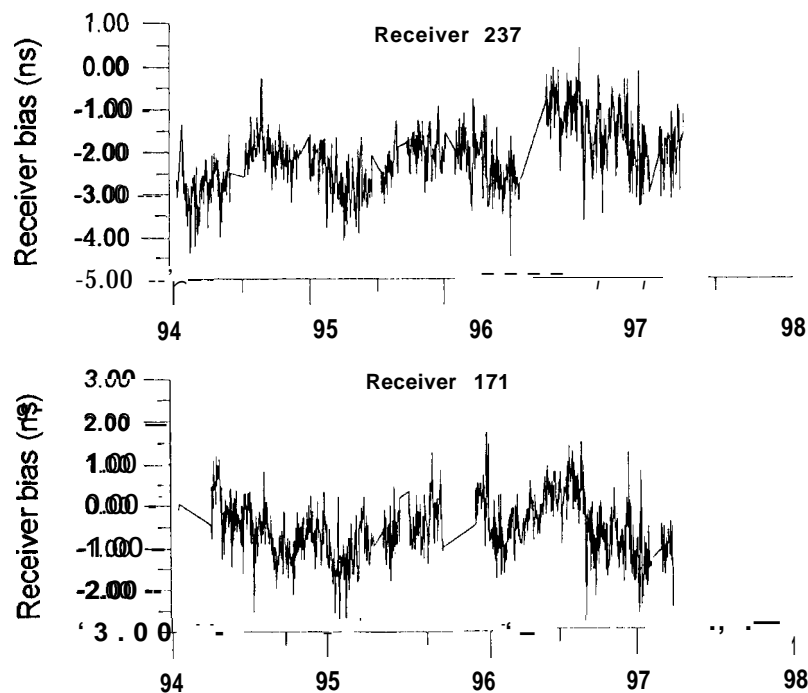


Figure 2. Computed biases for Turbo Rogue receivers 237 and 171.

The combined biases are determined on a daily basis (i.e. one solution a day). We only process night-time observations with an elevation mask of 20°: in most of the cases, the ionosphere is “quieter” during the night. This procedure which has been applied to our 7 Turbo Rogue GPS receivers has allowed us to study the long-term behaviour of the computed biases. The main results obtained with this network can be summarized as follows:

- The Turbo Rogue bias changes according as the Anti-Spoofing is activated or not: we have observed that, in most of the cases, the difference between the two values (i.e. with Anti-Spoofing on or off) is about ± 0.5 ns. Since January 31 1994, the Anti-spoofing is activated but sometimes, it is turned off on a few or all the satellites.

- the biases of two “identical” receivers even with two consecutive serial numbers can be very different from each other: for example, the biases of receivers 237 and 238 are respectively -2.37 ns and +5.33 ns;

- the bias depends on the temperature; the effect is visible during hot summer days;

- Figure 2 shows the computed differential group delays for 2 receivers (serial numbers 237 and 171) on a period of about 3 years. By looking at this figure, it can be seen that the bias changes (sometimes much) as soon as a little change is made to the hardware (after a repair, for example): in June 1996, we have replaced the microprocessor of receiver237: you can see very clearly a jump in the computed biases **after** this change; a similar upgrade has been applied to receiver 171 at the end of December 1995 and a repair has been performed in September 1996.

In addition, the computed biases have a (short-term) day-to-day repeatability of about 1 ns and have a periodic (seasonal) **behaviour**. Which is the origin of these variations in the **computed biases** ? **There are 2 possible explanations: the variations are due to a real change of the receiver bias or they are due to the fact that the use of our simple polynomial to model the ionosphere gives rise to residual errors which vary from day to day, from season to season, . . .** as it is the case for the ionosphere. If this last explanation is true, then we would expect that the residual errors would be similar for the different receivers: from figure 2, it is **clear** that the seasonal behaviors of receivers 171 and 237 are very similar; it is also the case of the other Belgian receivers. If these seasonal variations were real changes of the biases, the effect would be different for the different receivers. It could be argued that this seasonal trend could be due to the environmental parameters in which the receivers are placed: the external temperature also depends on the season. Nevertheless, in our case, this explanation cannot be true: the receiver installed at Brussels which is placed in a room where the temperature remains constant within 2 or 3 ‘K undergoes the same seasonal variations as the other receivers.

For these reasons, the value of the bias adopted to determine the TEC is obtained by computing the mean of **all** the daily solutions on a period of which the duration depends on data availability: it ranges from one month to more than one year. This technique has the advantage to reduce the influence of the ionospheric residual errors: most of the effects are **cancelled** in the mean,

- in addition to these “artificial” variations, the receiver biases also undergo real (sometimes unexplained) changes; such variations can be detected by forming the difference between the bias computed for 2 different receivers: the difference has the advantage to remove the common seasonal effects; figure 3 shows the difference between the delays computed for receivers 238 and 321. Receiver 321 was installed at Brussels in a room where the temperature remains stable. In March 96, the difference suddenly increases of about 2 ns, remains stable during a few days and then goes back to the original value, In fact, the bias of receiver 238 has changed: we have seen it by forming differences with other receivers. We have no idea about the origin of this problem.

We have explained in the previous paragraph that we adopt the long-term mean of **all** the daily computed biases to determine the TEC in order to reduce the residual ionospheric errors. **In** the case of receiver238, the bias variation was real; as a consequence, we have seen a corresponding jump in the **TEC** coming **from** receiver 238 as compared with the other Belgian receivers (figure 3). For this reason, it is clear that the receiver bias has to be very regularly controlled.

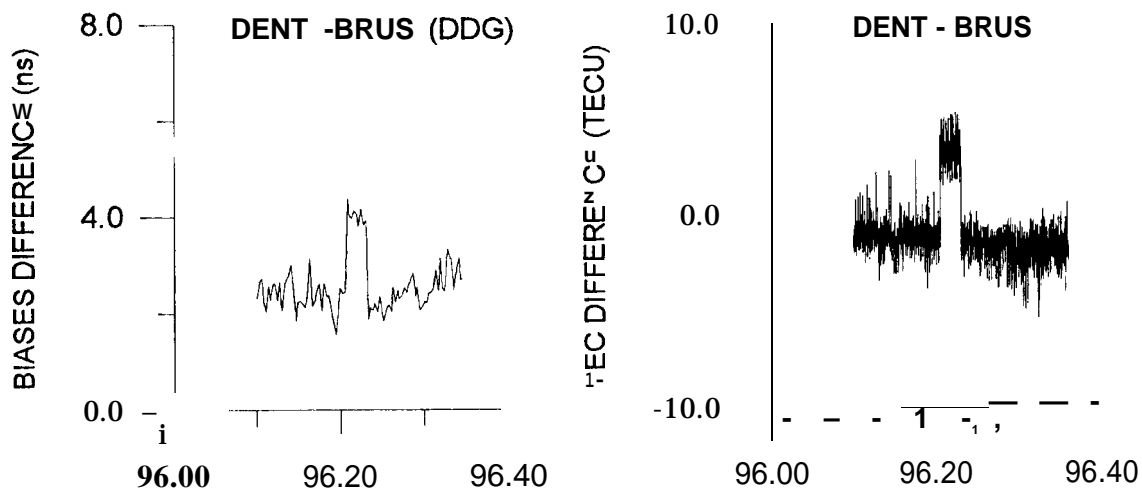


Figure 3. Difference between the biases (left) and the TEC (right) computed for the receivers installed at *Dentergem* (sn 238) and *Brussels* (sn 321).

TEC ABOVE THE OBSERVING STATION

When the biases have been determined, the TEC is computed in function of latitude and local time (or longitude) of the ionospheric point. For example, the data collected at Brussels (latitude= 50.8 °N, longitude = 4.40 E) allow to compute the TEC from about 35 °N to 60° N in latitude and from -20 °W to 25° E in longitude.

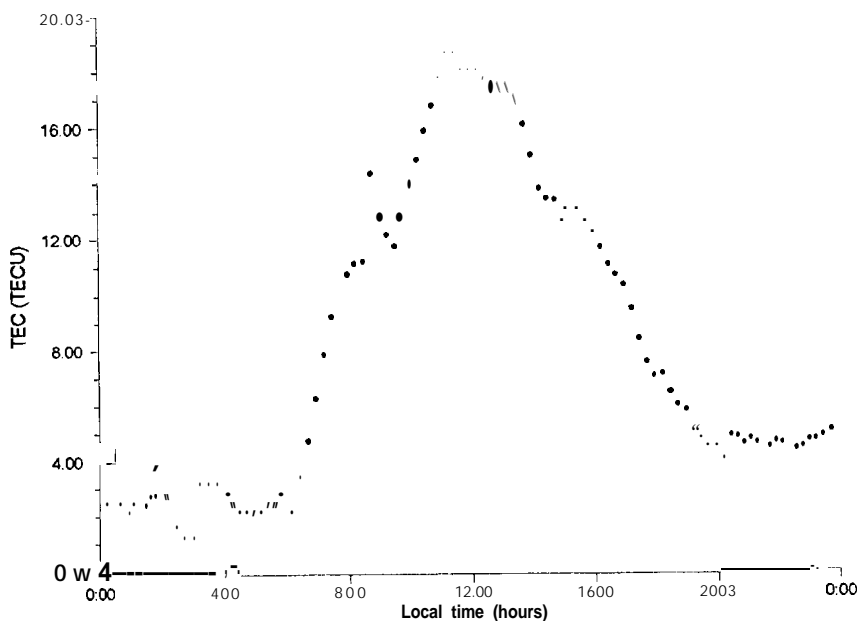


Figure 4. TEC at Brussels on October 30 1994.

To obtain TEC profiles representative of the ionosphere above the observing station, we apply the following procedure:

- we select all the TEC values corresponding to an ionospheric latitude, L_{iono} , given by :

$$L_{sta} - 1.50 < L_{iono} \leq L_{sta} + 1.5^\circ$$

where L_{sta} is the latitude of the observing station;

- we compute the mean of these TEC values on 15 minute periods.

Figure 4 shows the TEC profile above Brussels on October 30 1994 obtained by this method. The procedure outlined here above has been applied to a data set covering a period of more than 8 years.

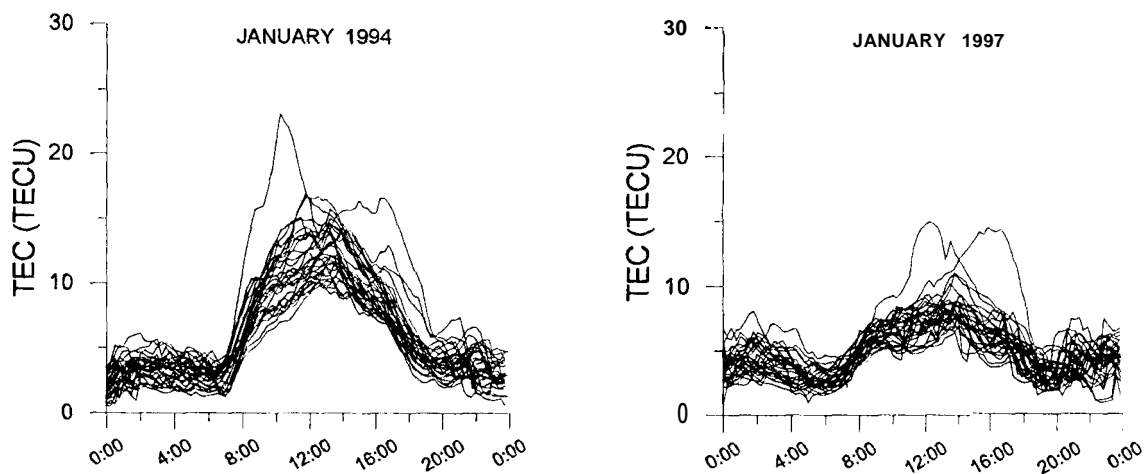


Figure 5. TEC at Brussels during 2 month (January 94 and January 97).

Figure 5 shows, as example, the results obtained at Brussels for two months (January 94 and January 97): in this figure, **all** the TEC profiles corresponding to the same month are represented on the same graph.

To **verify** the reliability (precision and accuracy) of the TEC determined by the method developed at ROB, two experiments have been **performed**:

1. **Precision:** we have compared the TEC obtained at Brussels with the TEC computed at Dentergem, Dourbes and Waremmé (the typical station inter-distance is about 70 km) during a period of more than 3 years: in most of the cases, the difference between the TEC at Brussels and the TEC in the other Belgian stations remains within 2-3 TECU (figure 6).

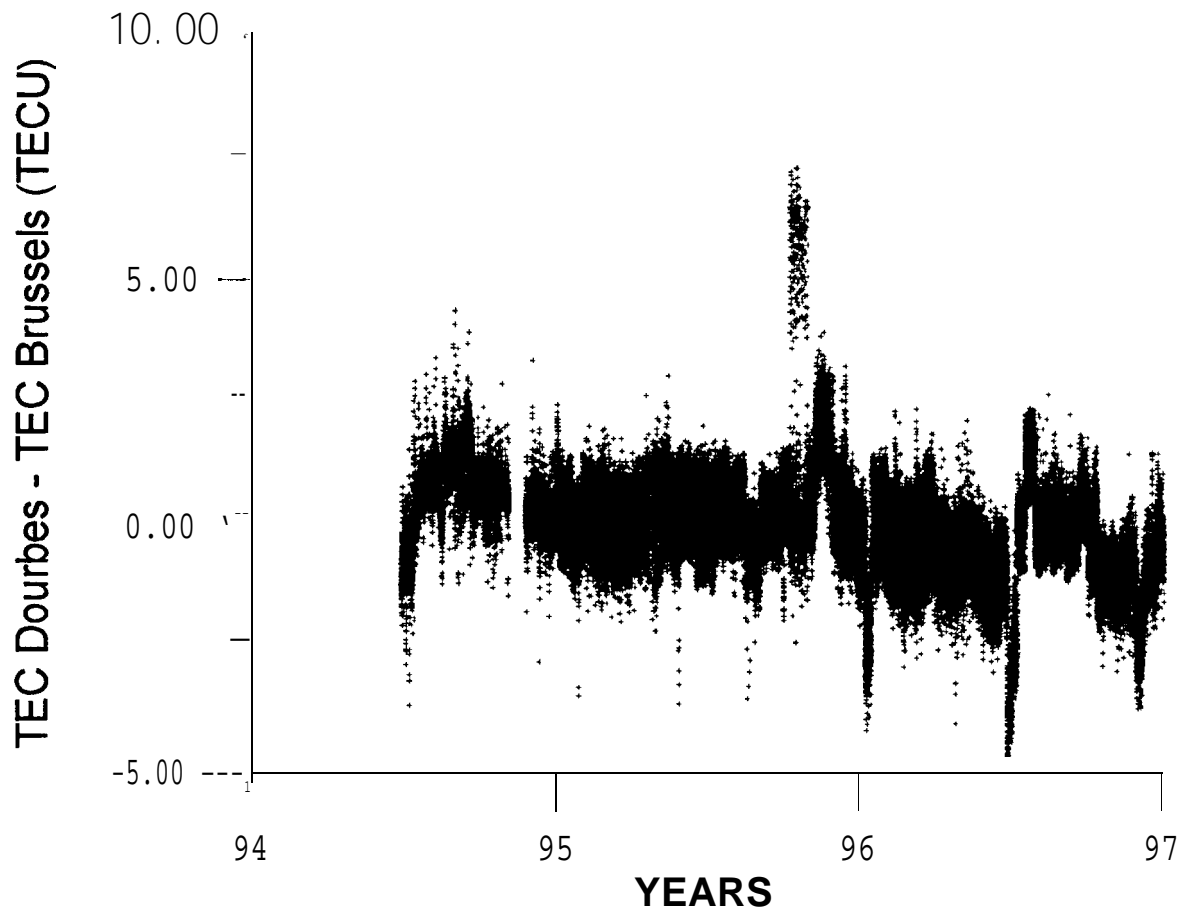


Figure 6. Difference between the *value* of the TEC computed at *Dourbes* and *Brussels*.

2. Accuracy: at Dourbes, an ionosonde which is the property of the Royal Meteorological Institute of Belgium is collocated with our GPS station. This ionosonde produces an electron concentration profile up to the maximum of the F2-layer. The ionosonde measurements are used to compute the Total Electron Content above **Dourbes**:

- in a first step, numerical integration of the measured bottomside electron concentration profile gives the bottomside part;
- in a second step, analytical integration of a Chapman function modelling the topside electron concentration profile gives the topside part; the parameters of the Chapman function are evaluated using the information contained in measured bottomside profile; we assume that the electron concentration is constant in the protonosphere.

This TEC has been compared with the TEC obtained by GPS on a period of 2 years (1995 and 1996). The results of both methods are in very good agreement: in most of the cases, the difference between “GPS” TEC and “ionosonde” TEC remains within 2-3 TECU; the mean and the standard deviation of the difference computed on this period are respectively 0.46 TECU and 1.72 TECU. More details can be found in Warnant and Jodogne (1997).

DETECTION OF IRREGULARITIES IN THE TOTAL ELECTRON CONTENT

From equation (4), it can be seen that the geometry-free combination also allows to monitor the evolution of the TEC in function of time, A $TEC_p^i(t_k)$:

$$A TEC_p^i(t_k) = 9.5241016 \frac{(\Phi_{p,GF}^i(t_k) - \Phi_{p,GF}^i(t_{k-1}))}{(t_k - t_{k-1})} \quad (6)$$

where A $TEC_p^i(t_k)$ is defined as:

$$A TEC_p^i(t_k) = \frac{TEC_p^i(t_k) - TEC_p^i(t_{k-1})}{(t_k - t_{k-1})} \quad (7)$$

It is important to stress that the computation of A $TEC_p^i(t_k)$ does not require the estimation of the **real** ambiguity, $N_{p,GF}^i$, as long as no **cycleslip** occurs.

The TEC variations in function of the time can be divided in 2 classes:

- the *regular gradients*: the usual gradients observed in the TEC; for example, the TEC has a minimum value during the night and reaches its maximum around 14h00 (local time). Consequently, there is a gradient depending on local time;
- the *irregular gradients*: gradients due to irregular ionospheric phenomena such as Traveling Ionospheric Disturbances and scintillation effects.

Traveling Ionospheric Disturbances (or **TIDs**) appear as waves in the electron density (and consequently in the TEC) due to interactions between the neutral atmosphere and the ionosphere. They have a wavelength ranging from a few tens of **kilometres** to more than thousand **kilometres**. Their occurrence **often** cause important gradients in the TEC even on short distances. **Scintillation** effects are variations in phase and amplitude of a radio signal passing through small scale irregularities in the ionosphere. Scintillation effects are very **often** observed in the polar and equatorial regions and are sometimes detected in the mid-latitude regions.

In this paper, we present a method allowing to detect medium-scale Traveling Ionospheric Disturbances (**MSTIDs**) and scintillation effects using GPS measurements. MSTIDs have horizontal wavelengths of several hundreds of **kilometres**, periods ranging from about 12 minutes to about 1 **hour** and **horizontal phase speeds ranging from 100 to 300 m/s** (Van Velthoven, 1990).

Traveling Ionospheric Disturbances and scintillation effects cause high frequency changes in the TEC. Consequently, these phenomena can be studied by detecting such changes in A TEC_p^i . In order to do that, we filter out the low frequency changes in the TEC by modelling A TEC_p^i using a low order polynomial. The residuals R_j of this adjustment (i.e. A TEC_p^i - polynomial) contain the high frequency terms.

In a similar way as Wanninger (1994), we define the *ionospheric variability*, V_I , using the standard deviation of the residuals R_I (table 1):

$$V_I = 0 \text{ when } 0.00 \leq \sigma_{R_I} < 0.08 \text{ TECU/min}$$

$$V_I = 1 \text{ when } 0.08 \leq \sigma_{R_I} < 0.10 \text{ TECU/min}$$

...

V_I	σ_{R_I} (TECU/min)
0	$0.00 \leq \sigma_{R_I} < 0.08$
1	$0.08 < \sigma_{R_I} < 0.10$
2	$0.10 \leq \sigma_{R_I} < 0.15$
...	...
8	$0.40 < \sigma_{R_I} < 0.45$
9	$\sigma_{R_I} \geq 0.45$

Table 1. Definition of the ionospheric variability

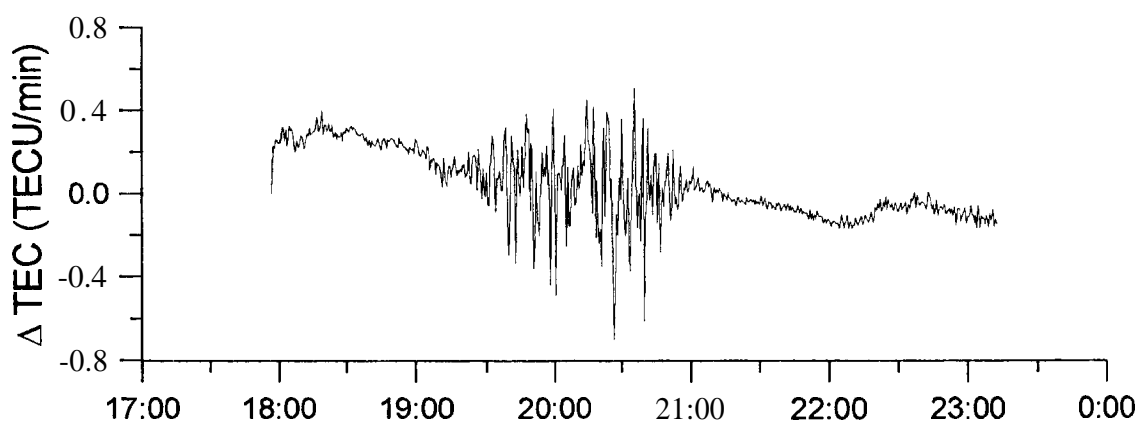


Figure 7. Scintillations observed at Brussels on May 28 1993.

In practice, the ionospheric variability is computed for every observed satellite, using periods of 15 minutes of measurements. When V_I is different from zero, we decide that an “event” is detected. Such an “event” is presented in figure 7. This figure displays the TEC gradients, ΔTEC , observed at Brussels on May 28 1993. These gradients are caused by scintillations effects. Figure 8 shows the gradients observed in 3 GPS stations operated by the Royal Observatory of Belgium. These effects are due to a (Medium-Scale) Traveling Ionospheric Disturbance. In fact, most of the “events” detected in Belgium are due to TIDs.

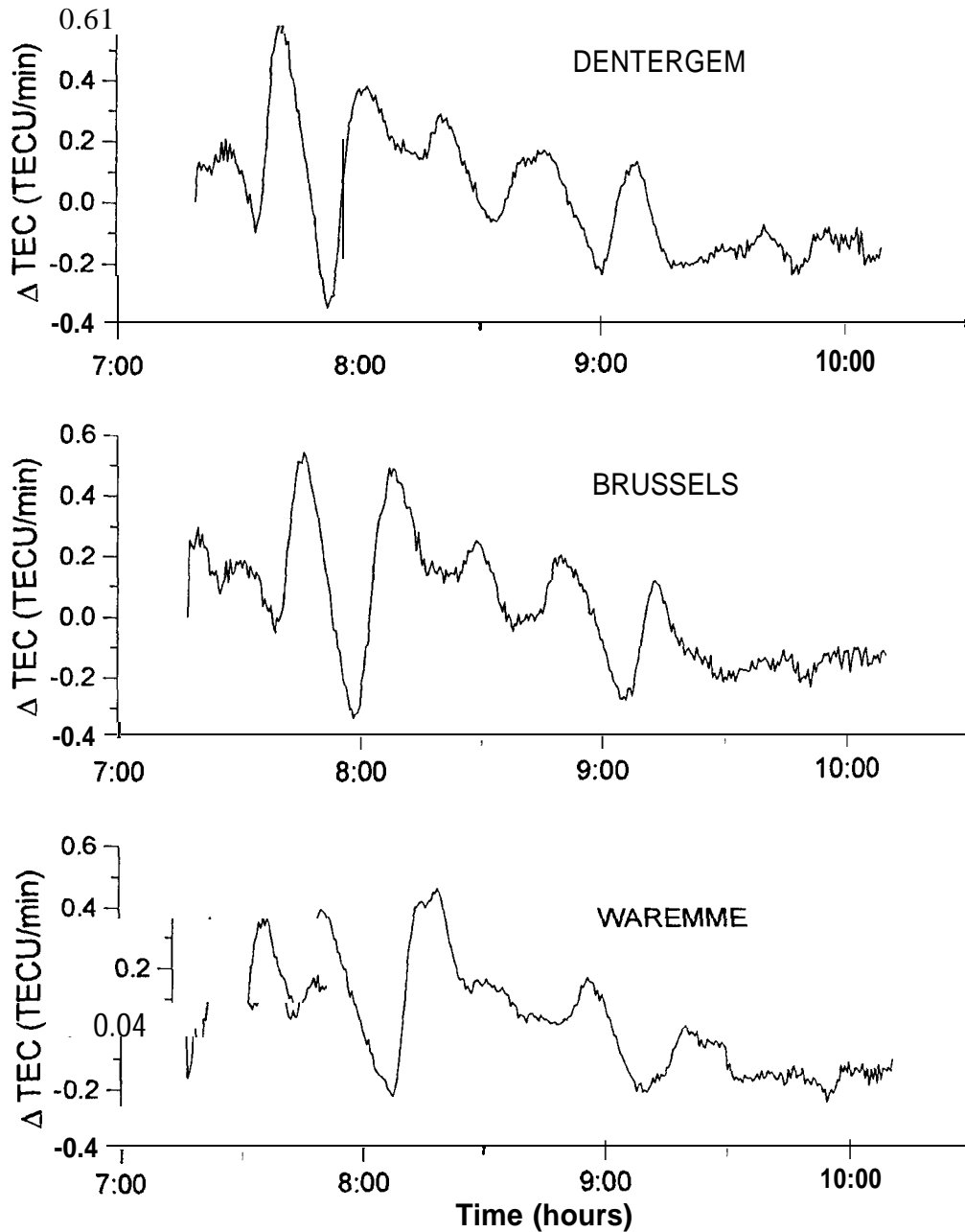


Figure 8. TEC gradients due to a TID observed on October 30 1994 in 3 Belgian stations.

With a sampling interval of 30 seconds, 24 hours of GPS measurements in the RINEX format are stored in a file of which the size is ranging from 1.5 Mb to more than 2 Mb. To perform any long term study based on GPS measurements, it is thus indispensable to develop automatic data processing procedures. In particular, it is not realistic to imagine that an operator could screen the residuals to decide “manually” if a TID is present or not. For this reason, we must choose threshold values which will be used by the computer to take an automatic decision. The choice of 0.08 TECU/min as threshold value to decide if an event is taken into account comes from the fact that the multipath also gives rise to high frequency changes in the geomet-free combination. This site-dependent effect can reach several centimetres on phase measurements and has periods

ranging from a few minutes to several hours depending on the distance separating the reflecting surface from the observing antenna (if this distance is shorter, the period is longer). The multipath effect being more frequent at low elevation, we have chosen an elevation mask of 20° . In the case of the Belgian permanent GPS network, a threshold value of 0.08 TECU/min is large enough to avoid to interpret multipath effects as ionospheric phenomena. This value should be valid for most of the GPS sites but should be applied with care in locations where the multipath is particularly important. An additional verification is then performed: the comparison of the ionospheric variability observed in neighboring GPS stations allows also to distinguish between multipath and ionospheric phenomena: indeed, large residuals observed at the same time in different stations cannot be due to multipath.

Two other error sources can affect our method: cycles slips and phase surges. *Cycle slips are* jumps of an integer number of cycles which occur when the receiver loses lock on the satellite signal. In an automated data processing procedure, an uncorrected cycle slip could result in a σ_{R_i} above the threshold value even if no ionospheric perturbation is present.

Phase surges give rise to several successive jumps in the GPS phase measurements. These jumps are not integer numbers of cycles. For this reason, this error is much more difficult to detect. In addition, this effect is related to the receiver-to-satellite geometry: it means that a similar effect can be observed in several neighboring GPS stations at the same time (Sleewaegen, 1997). Nevertheless, these jumps can be identified because their period is always shorter (a few minutes) than the periods of ionospheric disturbances.

The choice of 15 minute periods to compute the ionospheric variability is due to the fact that most of the MSTIDs have periods ranging from 5 to 30 minutes. If we choose a too short period, the TID will not have the time to cause TEC changes large enough to be detected. On the other hand, if the period is too long, the large residuals in $\Delta TEC_p'$ due to the TID will be lost among the other residuals and the resulting σ_{R_i} will remain under the threshold of 0.08 TECU/min.

STATISTICS CONCERNING THE OCCURRENCE OF TIDs

The procedure outlined here above has been applied to the Belgian GPS network. This experiment has allowed us to compute statistics concerning the occurrence of TIDs above Belgium (i.e in a mid-latitude European station) and to answer the following questions: are TIDs unusual phenomena, do they appear during specific periods in the day, in the year, in the solar cycle, ..?

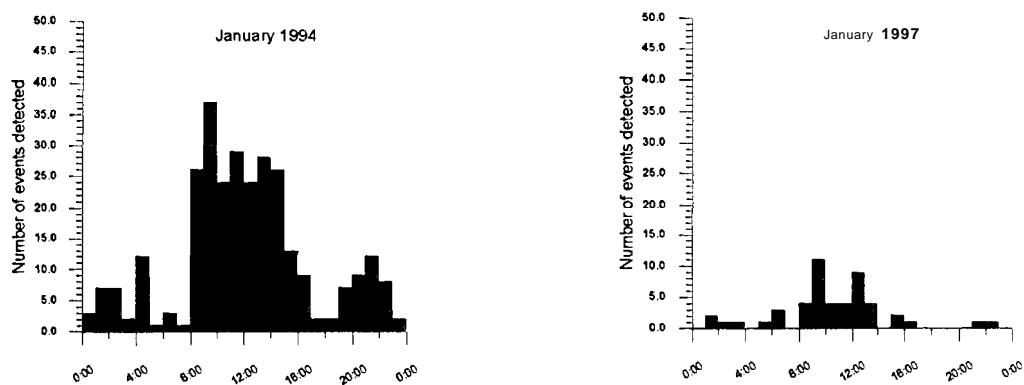
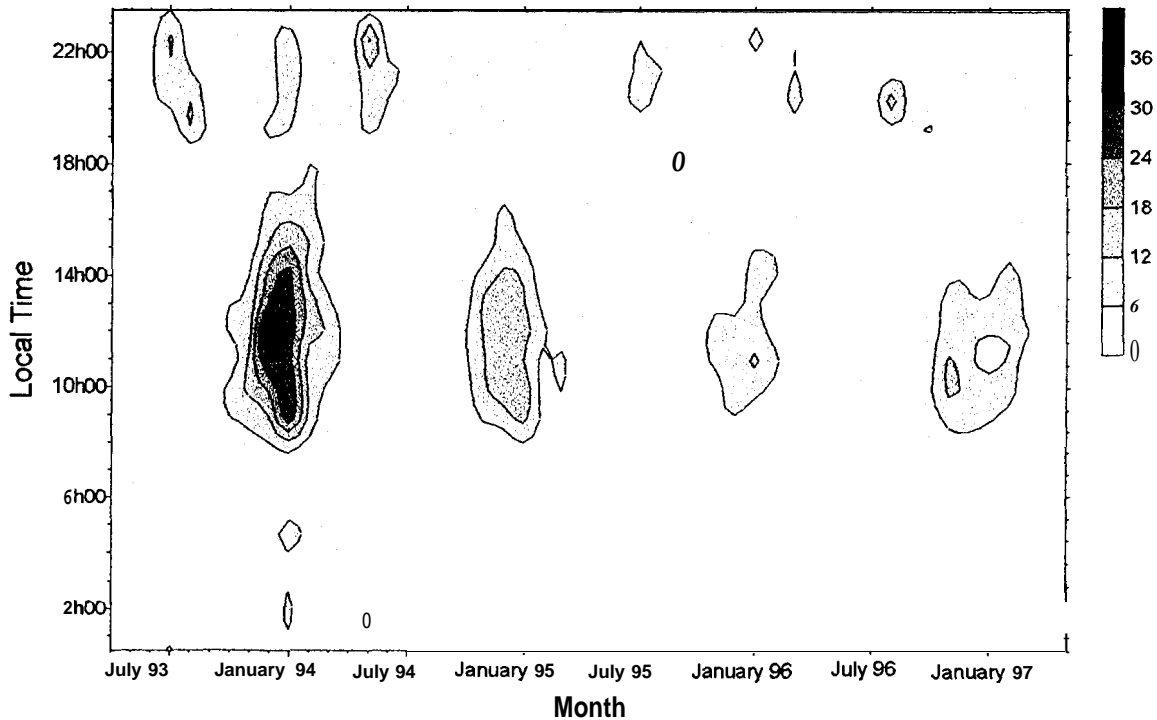


Figure 9. Number of events detected in function local time in January 94 and January97,

Figure 9 shows the statistics of the observed **TIDs** for two month: January 1994 and January 1997. This figure displays the number of **TIDs** encountered during these month in **function** of the time in the day. It means that a sum of all events **occurring** at a specific time (for example between 10h00 and 11h00) during a whole month is made.



*Figure 10. Number of **TIDs** detected from April 93 to May 97 in function of local time.*

Figure 10 shows the number of events (**TIDs**) detected from April 93 to May 97 in **function** of the local time. The different levels of grey represent the number of events detected. By looking at this figure, several conclusions can be drawn concerning the number of detected **TIDs** :

- there is a main maximum between 10h00 and 16h00 (local time) during the winter;
- there is a secondary maximum during the night;
- it decreases with decreasing solar activity.

The case of scintillation effects is different: only a few “events” are observed in one year. These results confirm the conclusions of previous studies performed by means of other independent techniques (see for example, Van Velthoven (1 990)).

CONCLUSIONS

The paper has outlined the method developed at the Royal Observatory of Belgium in order to compute the Total Electron Content. This method requires the determination of the receiver and satellite differential group delays. The combined biases (receiver + satellite) are obtained on a daily basis from the geometry-free combination of code observations. The computed biases undergo day-to-day and seasonal variations; in most of the cases these variations are "artificial": they are due to ionospheric residual errors. For this reason, we adopt the mean value of all the computed biases on a long period to reduce the influence of these errors. Nevertheless, the biases also undergo "real" changes: they are sometimes due to the temperature (during hot summer days) but we have not been able to explain all these variations. For this reason, the receiver bias has to be regularly controlled.

The precision (internal consistency) and the accuracy of our method has also been verified:

- the TEC computed at Brussels has been compared to the TEC obtained at Dentergem, **Dourbes** and **Wareme**: they agree within 2-3 TECU;

- the GPS TEC has been compared with the TEC computed from ionosonde measurements: the mean and the standard deviation of the differences "GPS" TEC - "ionosonde" TEC computed on two years (1995 and 1996) are respectively 0.46 TECU and 1.72 TECU.

In addition, the paper has presented a very simple method allowing to detect medium-scale **Travelling** Ionospheric Disturbances and scintillation effects using the geometry-free combination of GPS carrier phase measurements. This method has been applied to the GPS measurements gathered in the Belgian GPS network since 1989. This experiment has allowed to compute statistics concerning the occurrence of TIDs and scintillations above Belgium. The results which are in good agreement with previous independent studies show that TIDs are very common phenomena at Brussels but only a few scintillation effects have been detected.

REFERENCES

Lanyi G. E., T. Roth (1988), "*A comparison of mapped and measured total ionospheric electron content using global positioning system and beacon satellite observations*", Radio Science, 23, 483-492.

Sleewaegen J-M.. (1997), Personal communication Royal Observatory of Belgium,

Van Velthoven P. J. (1990), "*Medium-scale irregularities in the ionospheric electron content*", Ph. D. Thesis, Technische Universiteit Eindhoven.

Wanninger L. (1994), "*Der Einfluß der Ionosphäre auf die Positionierung mit GPS*", Ph. D. Thesis, Wissenschaftliche Arbeiten der Fachrichtung Vermessungswesen der Universität Hannover, Nr. 201, 137p.

Wanninger L., E. Sardon, R. Warnant (1994), "*Determination of the Total Ionospheric Electron Content with GPS - Difficulties and their Solution*", Proceedings of Beacon Satellite Symposium '94, ed. By Dept. of Physics of University of Aberystwyth, 13-16.

Warnant R. (1996), *“Etude du comportement du Contenu Electronique Total et de ses irregularities dans une station de latitude moyenne. Application aux calculs depositions relatives par le GPS”*, Ph. D. Thesis (in French), Série Géophysique (N° Hors-Série) de l’ Observatoire Royal de Belgique, Bruxelles.

Warnant R. , J.-C.Jodogne(1997), *“A Comparison between the TEC Computed using GPS and Ionosonde Measurements”*, paper presented at the Beacon Satellite Symposium '97, to be published in Acts Geodaetica et Geophysics Hungarica.

Wilson B. D. , A. J. Mannucci (1993), *“Instrumental Biases in Ionospheric Measurements derived from GPS data”*, Proceedings of ION GPS'93, Salt Lake City.

MONITORING THE IONOSPHERE OVER EUROPE AND RELATED IONOSPHERIC STUDIES

N. Jakowski, S. Schlüter and A. Jungstand

Deutsches Zentrum für Luft- und Raumfahrt e. V.
Femerkundungsstation Neustrelitz
Kalkhorstweg 53, D-17235 Neustrelitz

ABSTRACT

The rather dense network of GPS ground receivers of the IGS geodetic community is used to monitor the total electron content (**TEC**) of the ionosphere on a routine base. TEC maps are generated by combining GPS-derived **TEC** data with a well-qualified regional **TEC** model. Taking into account the achieved RMS accuracy of **TEC** in the order of $2 \times 10^6 \text{ m}^{-2}$ the **TEC** maps provide a lot of information for more detailed ionospheric studies. So the **TEC** monitoring data will help to develop and improve ionospheric models, to study complex solar-terrestrial relationships and to explore large scale ionospheric perturbations. The mapping technique is also recommended for real time applications in navigation and geodesy.

INTRODUCTION

Space based radio navigation systems such as the US Global Positioning System (GPS) and the Russian Global Navigation Satellite System (**GLONASS**) offer the unique opportunity to monitor the ionosphere on global scale.

Due to the dispersive nature of the ionosphere the total electron content (**TEC**) can be derived from code and carrier phase measurements on **L1/L2 frequencies** by difference methods. The same technique is applied to compensate ionospheric propagation errors in space based navigation satellite systems.

Since first-order ionosphere induced range errors are proportional to **TEC**, ionospheric **TEC** maps are helpful in different geodetic and navigation applications especially for single frequency GPS and **GLONASS** users to enhance the accuracy and reliability of measurements.

Ionospheric **TEC** maps are generated in **DLR/DFD** Femerkundungsstation **Neustrelitz** since February 1995 on a regular base. Corresponding hourly maps are available in the Internet via <http://www.nz.dlr.de/gps/gps-ion.html> with a time delay of about two days,

TEC MONITORING OVER EUROPE

The algorithm for TEC estimation from GPS measurements is described by Sardon et al. (1994). Assuming a second-order polynomial approximation for TEC variations over the observing GPS ground station, both TEC as well as the instrumental satellite-receiver biases are estimated by a Kalman filter run over 24 hours. The 30s data of GPS stations of the European IGS network thus allow the determination of slant TEC values along more than 100 satellite-receiver links over the European area with high time resolution. The slant TEC data are then mapped to the vertical by applying a mapping function which is based on a single layer approximation at $h_{sp}=400\text{km}$ (Jakowski et al., 1996a). Ionospheric maps are generated by combining the observed TEC data with the regional TEC model (Neustrelitz TEC Model-NTCM) in such a way that the map represents measured values near measuring points and model values at regions without measured data. This procedure has the advantage that also in case of a low number of measurements physically reasonable TEC data are provided to users. So this method is strongly recommended for application in real time ionosphere monitoring systems. The NTCM model is described elsewhere (e.g. Jakowski et al., 1996, a, b). It has to be mentioned that the TEC maps cover the area of $32.5^{\circ}\leq\phi\leq70^{\circ}\text{N}$ and $-20^{\circ}\leq\lambda\leq60^{\circ}\text{E}$ in latitude and longitude, respectively. The grid resolution is 2.5° in latitude and 5° in longitude resulting in 272 grid values for one map. Due to the low data density in the eastern part of the area, the eastward border of the maps is temporarily fixed at 40°E .

COMPARISON WITH IONOSPHERIC MODELS (IRI95)

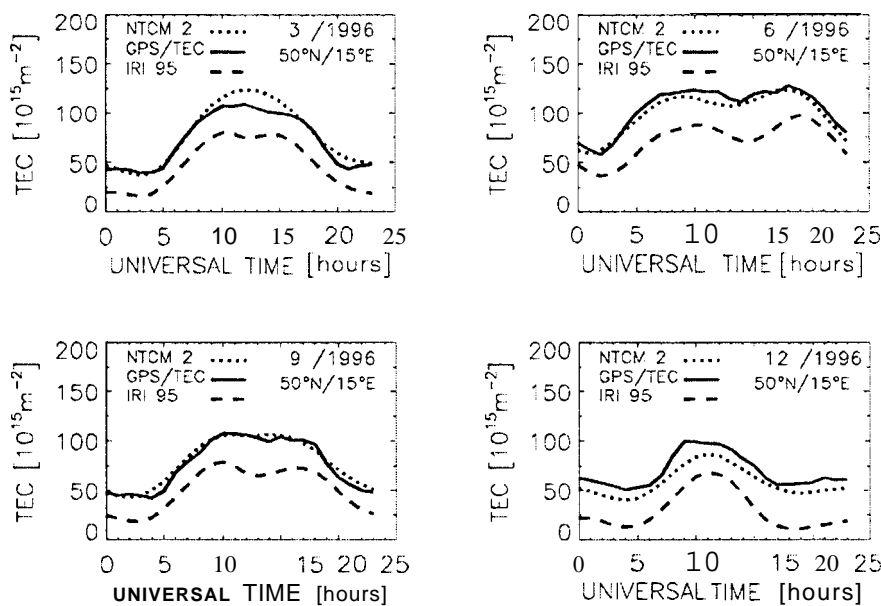


Fig. 1: Diurnal variation of TEC derived from NTCM2, IRI95 and GPS measurements for different seasons at $50^{\circ}\text{N}/15^{\circ}\text{E}$.

Long-term observations of TEC over large areas are well suited for the development and check of ionospheric models. Thus, GPS-derived TEC monitoring data over Europe have been used to derive the regional TEC model NTCM2. On the other hand, the TEC monitoring data can be used to

check and/or improve well-known ionospheric models such as **IRI95** or Bent. A comparison between monthly averaged TEC monitoring data, NTCM2 and corresponding **IRI95-derived TEC** data is made in Fig. 1 at a fixed grid point at **50°N/ 15°E** for different seasons. It has to be mentioned that the **IRI95-TEC** data were derived by integrating **IRI95** electron density profiles up to 1000km height, i.e. these values doesn't include the **plasmaspheric** electron content. **Indeed**, the permanent difference between **TEC** monitoring/NTCM2 data and **IRI95-TEC** in the order of $1-4 \times 10^{16} \text{m}^{-2}$ could be explained by the **plasmaspheric** content not considered in **IRI95-TEC**. This fits quite well with **plasmaspheric** content estimations made by **Kersley and Klobuchar** (1978) using **ATS 6** radio beacon observations.

Taking into account the growing solar activity during the next years, it is evident that regional and global TEC monitoring activities by several groups will contribute to essential improvements of already well-prepared ionospheric models. **On** the other hand the development of special TEC models should be possible on a high standard.

SOLAR CONTROL OF TEC

It is a well-known fact that the solar extreme ultraviolet radiation (EUV) is the major source of ionospheric ionization. Several studies have indicated that there exist a nearly linear relationship between the solar flux $F_{10.7}$ (rough measure of the EUV intensity) and TEC (e.g. **Jakowski and Paasch**, 1984; **Davies et al.**, 1992). The sensitive response of TEC to solar activity variations becomes evident in its solar rotation dependence (**Jakowski et al.**, 1991). To check these relationships, the cross correlation function was computed between the $F_{10.7}$ index and corresponding TEC data obtained at fixed grid points during 1996. The results illustrated in Fig. 2 indicate again a certain delay

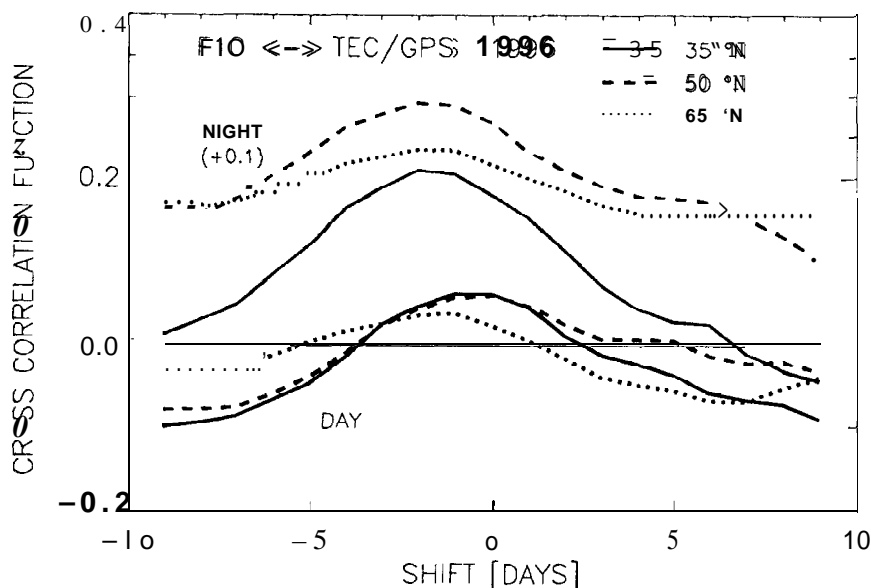


Fig. 2: Cross correlation between GPS based 3-hourly averaged TEC data at 15°E longitude and the solar radio flux index $F_{10.7}$ (Day-time: 11-13 UT; night-time: 1-3 UT).

between the solar radio flux index $F_{10.7}$ and the ionospheric response up to 2 days with some interesting features related to the geographic latitude. The increasing level of solar activity and improved knowledge of the EUV- $F_{10.7}$ relationships are good conditions to explore this phenomenon in the near future.

LARGE SCALE PERTURBATIONS IN THE IONOSPHERE

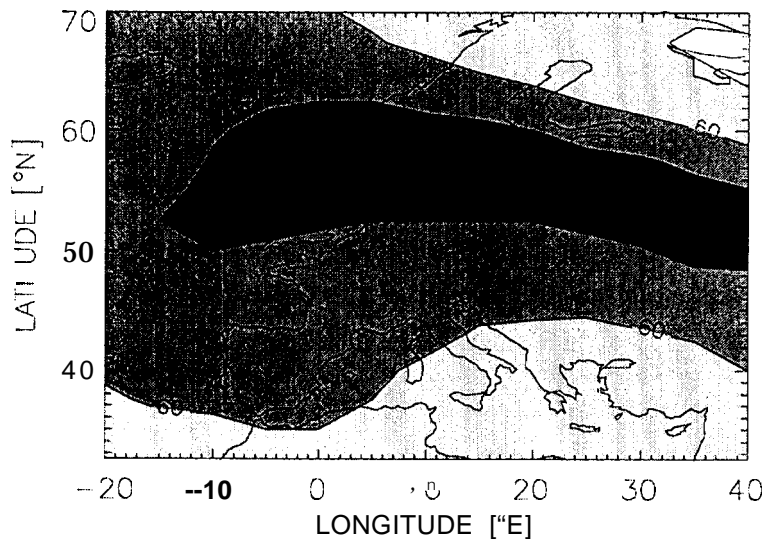


Fig. 3: Electron density trough over Europe in the course of the ionospheric perturbations on 11 April 1997, 00:00 UT (Difference between contour lines is $15 \times 10^{15} \text{ m}^{-2}$).

activity. The competing character of these magnetosphere-ionosphere-thermosphere interactions leads to a rather stochastic **behaviour** of the ionosphere during ionospheric storms. Nevertheless, ionospheric storms indicate some common features as **f.i.** the so-called „**positive**“ and „**negative**“ phases of ionization when referring to the mean **behaviour**. The variation with time of TEC deviations from corresponding mean or „**normal**“ values is called storm pattern.

Since common signatures of the storm **behaviour** should be pronounced in storm statistics, we have superposed such storm periods whose geomagnetic activity or its time gradient exceeds certain critical levels. The synchronization of storm pattern is reached by simple local time dependence (LTV) or by defining a selected geomagnetic activity phase (maximum of three-hourly A_p values or A_p -increase during the onset phase) as the reference storm time (**ST=0**). So local time controlled effects might be separated from storm time driven effects. In agreement with former studies (Jakowski et al., 1990) the preliminary analysis of 23 storm periods over Europe indicate a clear seasonal dependence of storm pattern. Superposed storm time pattern for summer (May-August) and winter months (November-February) illustrate this phenomenon in Figs. 4-6. Summer storms over Europe are characterized by a rather short positive phase (about 10 hours) which is followed by a well-pronounced negative phase starting at high latitudes. In contrast to this **behaviour**, winter storms over Europe are characterized by a **well**-developed positive phase lasting more than 24 hours. As Fig. 6 indicates, the positive phase is more pronounced at high latitudes in winter and at lower latitudes in summer. These seasonal differences can be explained by the global **thermospheric** circulation directed from the summer to the winter hemisphere in an average sense (Jakowski et al.,

GPS based ionospheric monitoring provides an outstanding tool to study large scale processes in the ionosphere (e.g. Jakowski, 1995). So the horizontal extension of large scale structures can easily be detected as it is shown in Fig. 3 for the mid-latitude trough. This trough has been developed in the course of a geomagnetic/ionospheric storm on April 11, 1997, 00:00 UT. As a consequence of various coupling processes, ionospheric perturbations are closely related to geomagnetic

1990). Collecting more and more TEC data during the next years, the statistical analysis of storm pattern can essentially be improved.

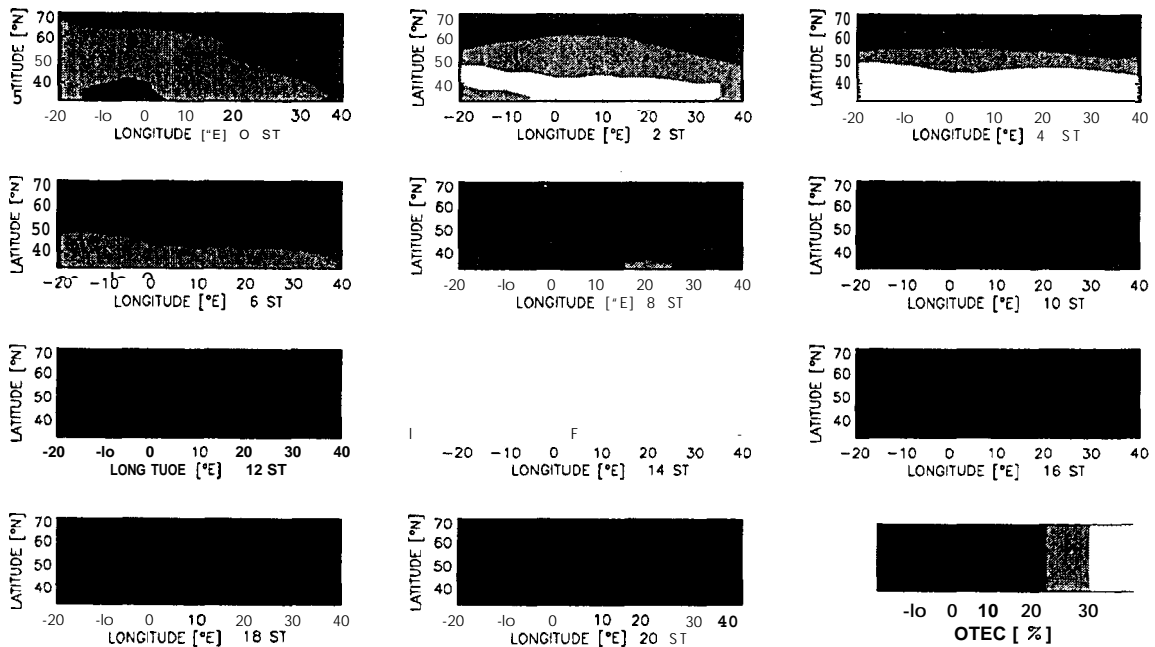


Fig. 4: Two-hourly maps of percentage TEC perturbation pattern for summer storms (May-August during 1995-1997).

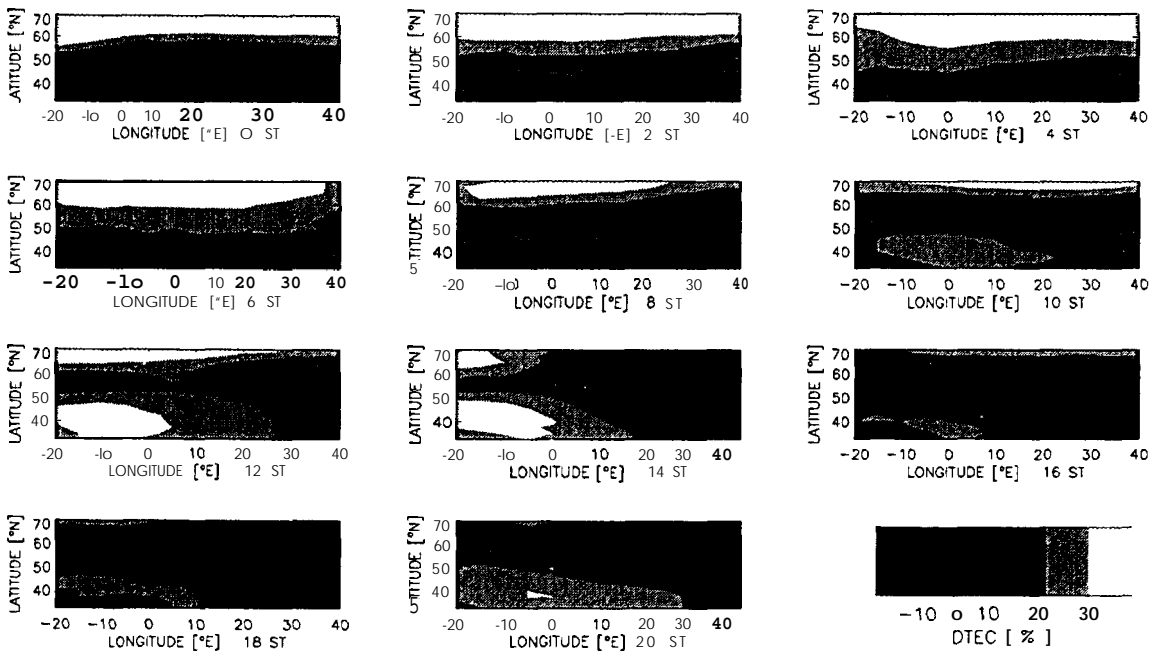


Fig. 5: Two-hourly maps of percentage TEC perturbation pattern for winter storms (November-February during 1995-1997).

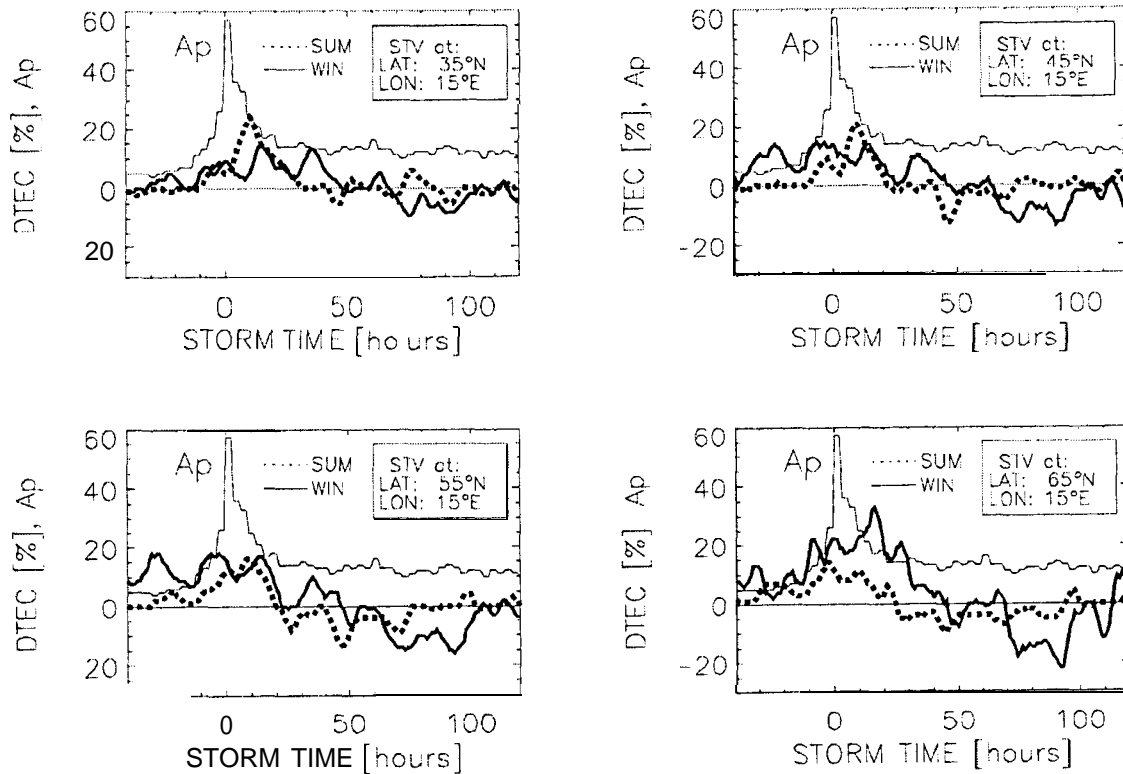


Fig. 6: Superposition of percentage TEC perturbation pattern for summer and winter storms selected from the time interval 2/95-8/97. Storm time $ST=00$ is defined by Ap_{max} , selection criteria for storm periods are: $Ap_{max} > 30$, $Ap < 20$ for prestorm conditions (3 days).

CONCLUSIONS

It has been shown that the rather dense network of well-qualified GPS ground stations of the IGS network provides a unique opportunity for reliable ionospheric monitoring. Considering a RMS error of TEC in the order of 2×10^{-2} tGm⁻² the described mapping technique is suited to reconstruct large scale horizontal structures in the ionosphere. Real time ionospheric monitoring and the delivery of TEC maps to GPS and/or GLONASS users should enhance accuracy and integrity of navigation satellite systems.

The ionospheric monitoring technique based on global and regional GPS measurements contributes directly to „Space Weather” reports and predictions.

Furthermore it becomes evident that GPS based ionospheric monitoring is a powerful tool for developing and/or checking ionospheric models, for studying solar-terrestrial relationships and for exploring large-scale ionospheric perturbations.

Acknowledgement

The authors are grateful to the international IGS community for making available the high-accurate GPS data sets.

References

- Davies K., W. Degenhardt, G.K. Hartmann, N. Jakowski, R. Leitinger, Relationship between Ionospheric Electron Content and Solar Fluxes, Proc. of the Int. Beacon Sat. Symp. (Ed.: Min-Chang Lee), Cambridge, July 6.-10, 188-191, 1992.
- Jakowski N. and E. Paasch, Report on the observations of the total electron content of the ionosphere in Neustrelitz/GDR from 1976 to 1980, Ann. Geophys. 2, 501-504, 1984.
- Jakowski N., E. Putz, and P. Spalla, Ionospheric storm characteristics deduced from satellite radio beacon observations at three European stations, Ann. Geophys. 8, 343-352, 1990.
- Jakowski N., B. Fichtelmann, and A. Jungstand, Solar activity control of ionospheric and thermospheric processes, J. Atmos. Terr. Phys., 53, 1125-1130, 1991.
- Jakowski N., Ionospheric Research and Future Contributions of the IGS Network, Proc. IGS Workshop, Potsdam, 15.-17.05.1995, 17-29, 1995.
- Jakowski N., E. Sardon, E. Engler, A. Jungstand, and D. Klähn, About the use of GPS Measurements for Ionospheric Studies, GPS Trends in precise Terrestrial Airborne, and Spaceborne Applications", IAG Symposium 115, (Eds.: Beutler, Hein, Melbourne, Seeber), Springer-Verlag, 248-252, 1996a.
- Jakowski N., E. Sardon, E. Engler, A. Jungstand, D. Klähn, Relationships between GPS-signal propagation errors and EISCAT observations, Ann. Geophys. 14, 1429-1436, 1996b.
- Kersley L. and J.A. Klobuchar, Comparison of protonospheric electron content measurements from the American and European sectors, Geophys. Res. Lett. 5, 123-125, 1978.
- Sardon E., A. Rius, N. Zarraoa, Estimation of the transmitter and receiver differential biases and the ionospheric total electron content from Global Positioning System observations, Radio Science, VO1.29, N. 3, 577-586, 1994.

ROUTINE PRODUCTION OF IONOSPHERE TEC MAPS AT ESOC - FIRST RESULTS

J. Feltens¹, J.M. Dow², T.J. Martín-Mur²,
C. García Martínez³ and P. Bernedo³

1. EDS at Flight Dynamics Division,
ESA, European Space Operations Centre,
Robert-Bosch-Str. 5, D-64293 Darmstadt, Germany
2. ESOC
3. GMV at ESOC

ABSTRACT

The first version of ESOC'S Ionosphere Monitoring Facility (**IONMON**) software has become operational. The routine production of TEC maps and receiver/satellite differential code bias values has started in January 1998. ESOC intends to contribute with these products to an **IGS** ionosphere service as well as to use the ionosphere maps for the support of other **ESA-missions**, e.g. ERS and ENVISAT.

This paper condenses the results obtained from the first month of routine IGS ionosphere processing at ESOC with different kinds of TEC modeling. A comparison between **TEC** maps obtained **from** these distinct mathematical TEC models is made in order to assess the internal accuracy that can be achieved. A verification with TEC maps provided by other Analysis Centers will be possible when the **IONEX** format (**Schaer** et al., 1997) has been commonly implemented. The ESOC **TEC** maps are available in **IONEX** format. Verification of satellite differential code biases was done by comparison with values obtained from some other centers.

Based on the experiences made with the first month of operational ionosphere maps production, a fine-tuning of the models and last improvements could be made in order to optimize routine ionosphere processing.

INTRODUCTION

It is the task of this paper to give an overview on how routine **IGS** ionosphere processing is done at ESOC and to present an analysis of the first results obtained.

The paper will start with an overview over ESOC'S ionosphere processing under the aspects of observation data used, geographical extent, mathematical models invoked, number of TEC maps produced daily, time resolution and delay of availability.

The main part of the paper will thereafter concentrate on the results achieved during the first month of routine ionosphere processing at ESOC. Until now, validation had to be restricted to internal comparisons only. The implementation of the Ionosphere Map EXchange Format (IONEX) (Schaer et al., 1997) at the other Analysis Centers will enable an easy exchange of ionosphere products and thus allow for intercomparisons. The assessment of internal accuracy was done by the comparison of TEC maps obtained from different mathematical models. For the verification of estimated satellite differential code biases, corresponding values from some other Analysis Centers were available and could be used.

Finally this paper will conclude with an outlook on intended future activities and software extensions planned at ESOC in the area of the ionosphere.

ROUTINE IONOSPHERE PROCESSING AT ESOC

The operational evaluation of ionosphere products at ESOC is currently coupled to the final orbit processing. If a certain routine and experience has been achieved, the provision of ionosphere products in rapid mode can be taken into consideration. The software's structure and environment allows principally for a rapid processing.

Carrier phase leveled to code measurements - so called "TEC observable" - enter into the Ionosphere Monitoring Facility (IONMON) software. The sampling rate is 6 minutes.

Currently 4 IONMON runs are made per day, using TEC observable collected from a global net of about 50 stations, 24 hours of observation data enter into each fit. The 4 daily runs are:

- 1) Determination of a set of receiver/satellite differential code bias values. In order to cleanly extract the influence of the differential code biases from the TEC observable, only nighttime tracking data is enter into that fit. The ionosphere's part (which is expected to be quite small over nighttime) is absorbed by a low degree and order spherical harmonic of $n = 4, m = 2$, with the degree and order l coefficients kept fixed to zero. The differential code bias values thus obtained serve then as reference values for the other 3 fits of that day, and are introduced with a constraint of 0.5 ns there.
- 2) Global TEC model by fitting a GE-function (Feltens et al., 1996) of degree and order $n = 10, m = 8$ to the TEC observation data. In the GE-function fit the ionosphere's electron density is assumed to be condensed within an infinitesimal thin layer enclosing the Earth as hollow sphere in a height of 450 km . The mapping function is $1 / \cos Z$. In the analyses of next chapter this fit will be denoted as "GE".
- 3) Global 3-d Chapman Profile model (Feltens, 1998). The maximum electron density N_0 is represented by a degree and order $n = 10, m = 8$ GE-function, and the height of maximum electron density h_0 is modeled with an extended sin-function. The allowed height range is $400 \text{ km} \leq h_0 \leq 450 \text{ km}$. The output of this Chapman Pro-

file model are 6 maps: A **TEC** map obtained by integration over the Chapman Profile, a N_0 map, a h_0 map and maps of electron density at heights of 250, 500 and 750 km. In the analyses of next chapter this fit will be denoted as "CP".

- 4) Global 3-d Chapman Profile model. The maximum electron density N_0 is represented by a degree and order $n = 10, m = 8$ GE-function, and h_0 is estimated as global constant. The output are also a **TEC** map, a N_0 map and maps of electron density at $h = 250, 500, 750$ km. A h_0 map does not make sense in this case, since h_0 is constant. In the analyses of next chapter this fit will be denoted as "CP1".

All fits use a 20° elevation cutoff, and elevation-dependent weights are applied to the **observables**. The internal evaluation of all these models is done in the solar-magnetic reference frame.

Polynomial models to represent the **TEC** within the local area around a single ground station can be evaluated upon special request and over limited time for **ESOC-internal** use only. It is not intended to deliver these local polynomial models to the IGS. 6 hours of observation data enter into such a polynomial fit.

Once a certain routine has been achieved, the ionosphere products processing can be enhanced, e.g. every 6 hours a global model with 24 hours of TEC data.

FIRST RESULTS

TEC Maps

As already pointed out above, no access to TEC maps from outside ESOC was available for the analysis of the first results of operational processing. So only an **ESOC-internal** verification between the **TEC** maps originating from the different mathematical models could be done so far. An application of **GE-function** TEC models to ERS altimeter and S-band data during a period covering February '97 provided corrections for ionospheric signal delays with accuracies comparable to that obtained from the **IRI-95** model (Feltens et al., 1997). The GE-functions shall thus serve here as reference with respect to which the 3-d Chapman Profile models shall be compared. The results presented here were obtained over the period from 28 December 1997 (97362) to 23 January 1998 (98023).

One indicator of accuracy is the daily repeatability of statistical parameters, such as %-age of measurements used and *rms*, in the one and in the other **TEC** model fit. Figures 1a and 1b show these two parameters for the three fits GE, CP and CP1:

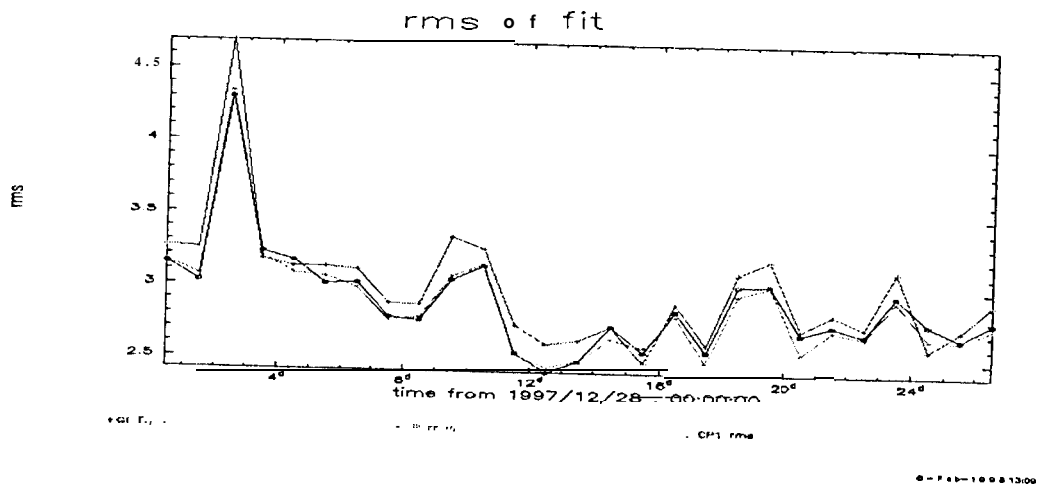


Figure 1a: Daily *rms* obtained for the GE, CP and CP1 fits.

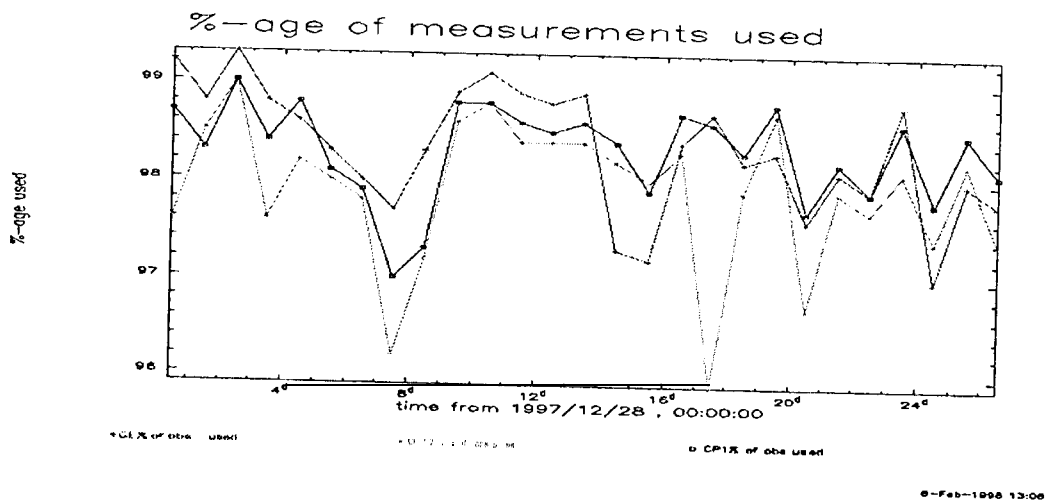


Figure 1b: Daily %-age of measurements used in the GE, CP and CP1 fits.

The curves of Figures 1a and 1b seem to indicate that GE-function fits and Chapman Profile fits are of comparable accuracy, with the Chapman Profile models showing a tendency to be slightly better. The **CP** fits show the lowest *rms*, but also the lowest 96-age of measurements used. The *rms* of the **CP1** fits are slightly higher, but more observations were taken. When comparing GE-functions with Chapman Profile models it must be kept in mind, that the Chapman Profile models show more flexibility because of more unknowns that are estimated.

The next Figure 2 presents the daily variation of estimated height h_0 of maximum electron density from the CP1 fits.

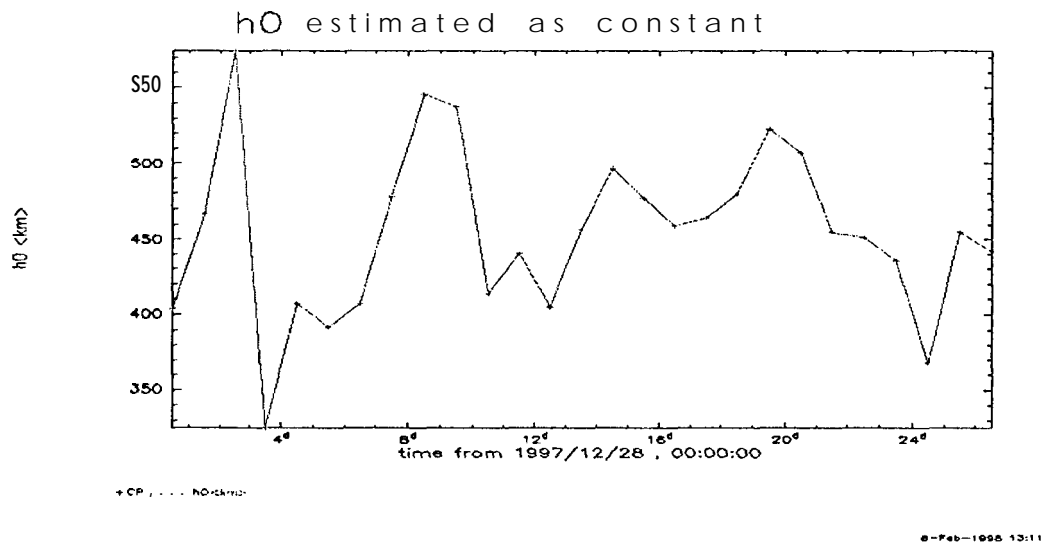


Figure 2: Daily estimated h_0 values from the CP1 fits [km].

Figure 2 shows a quite strong variation of the daily estimated h_0 values. But, as is pointed out in (Feltens, 1998), h_0 is only weakly estimable from pure TEC observable. The inclusion of satellite-to-satellite tracking (SST) data into the Chapman Profile model fits might improve this situation. Because for lack of such data, this could not be done yet, A combination of TEC data with other kinds of data, e.g. ionosonde data, might improve the situation too.

Figures 3 to 5 show a sequence different maps obtained for one day from the GE, CP and CP1 fits. All Figures have a vertical range from $+90^\circ$ to -90° in geographic latitude and a horizontal range from 0^h local time (-18°) to 24^h local time ($+18^\circ$) and are centered at 12^h local time (0°).

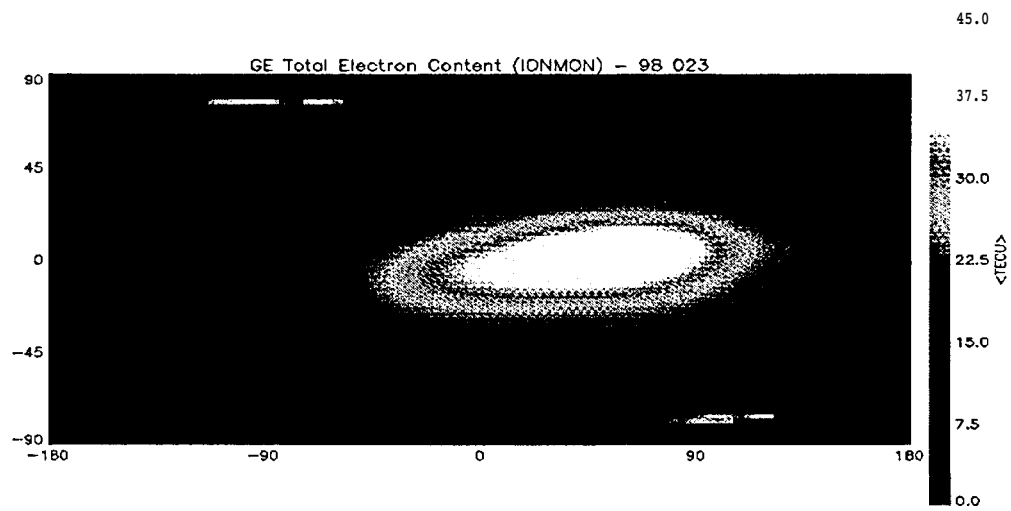


Figure 3: Global *TEC* map from GE fit for day 98023,

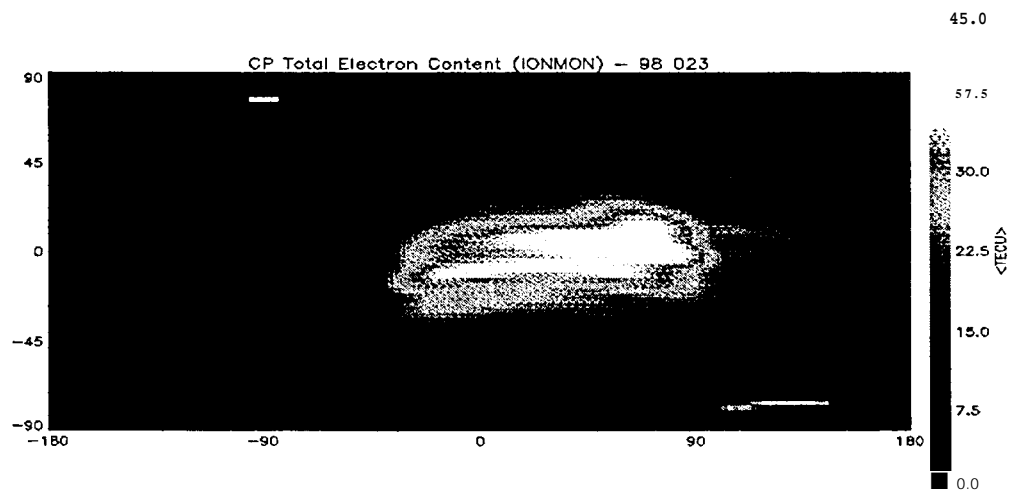


Figure 4a: Global *TEC* map from CP fit for day 98023,

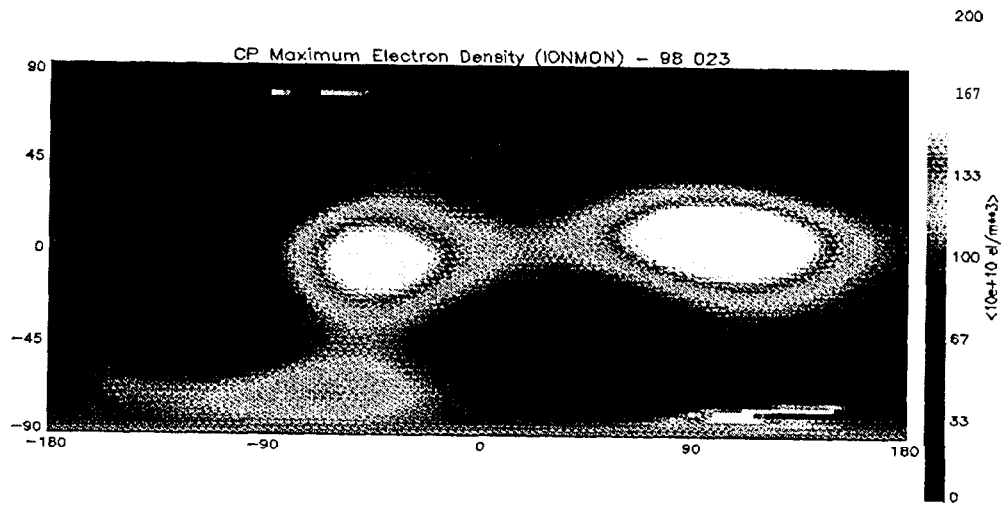


Figure 4b: Global N_0 map from CP fit for doy 98023.

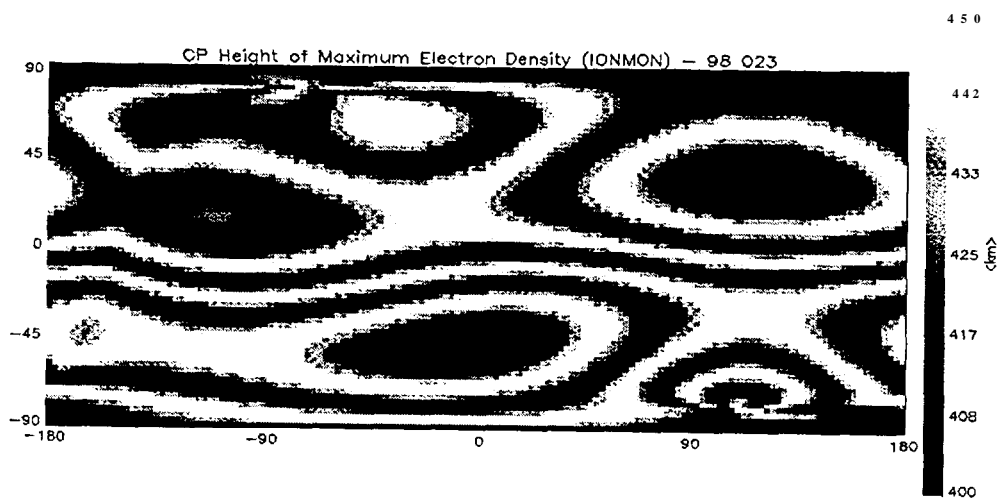


Figure 4c: Global h_0 map from CP fit for doy 98023.

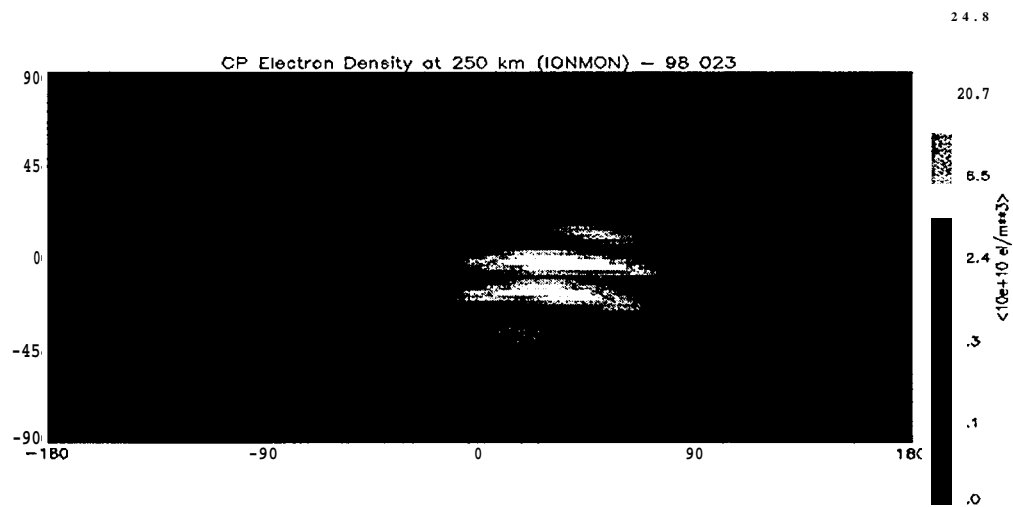


Figure 4d: Global electron density map at $h = 250 \text{ km}$ from CP fit for day 98023.

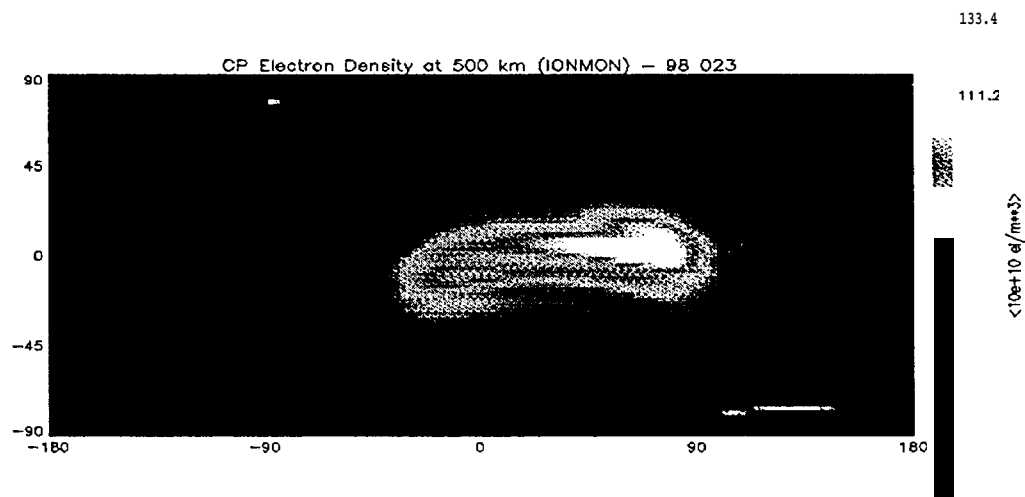


Figure 4e: Global electron density map at $h = 500 \text{ km}$ from CP fit for day 98023.

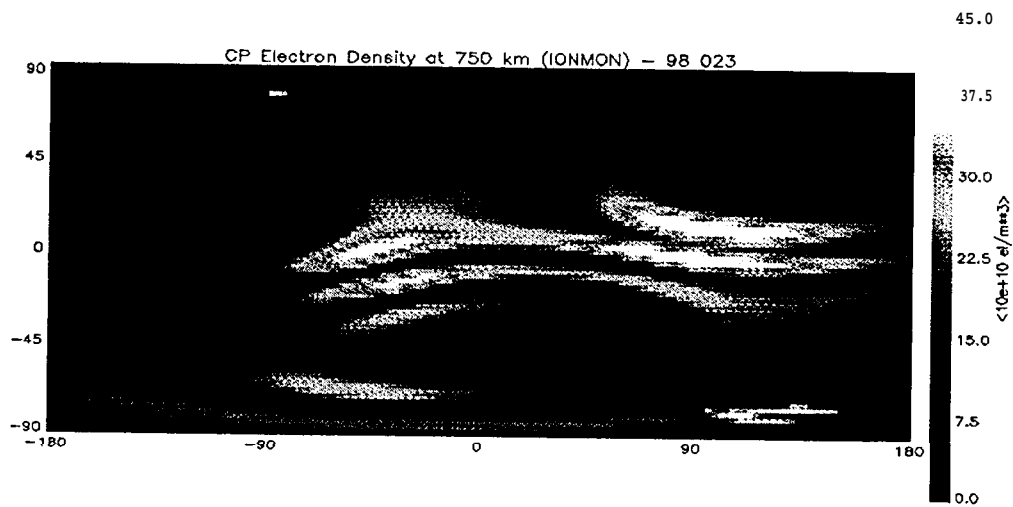


Figure 4f: Global electron density map at $h = 750 \text{ km}$ from CP fit for day 98023.

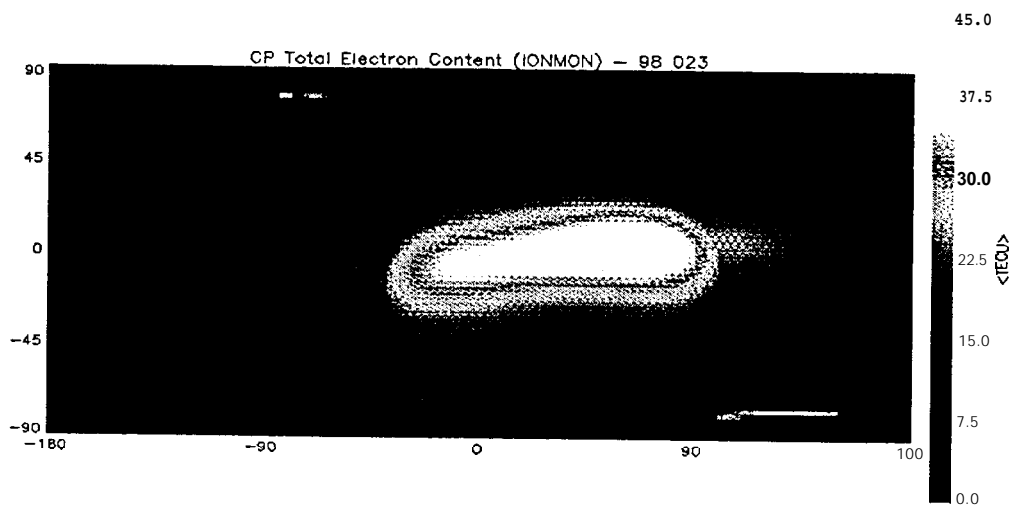


Figure 5: Global *TEC* map from CP1 fit for day 98023.

When comparing the TEC maps in Figures 3, 4a and 5, one recognizes an overall good agreement between the GE, CP and CP1 fit. Compared with the GE map, the two Chapman Profile maps present finer structures. This is especially valid for the map from the **CP** fit, since the height h_0 is not treated as constant but as extended sin-function single layer in this case. The estimation of both, N_0 and h_0 , makes the Chapman Profile models more flexible than the GE-function, thus allowing a better adaption to the TEC observation data. Additionally the 3-d geometry being intrinsic in the Chapman Profile models may enhance this flexibility. This 3-d geometry is ruled by the Sun's zenith angle χ (see Feltens, 1998).

The h_0 map shown in Figure 4c should not so strongly be interpreted as the real h_0 distribution, but more as the result of absorbing unmodeled effects in the CP fit.

Figures 4d to 4f present the electron density at different heights. Apart from the N_0 map of Figure 4b, the map for $h = 500$ km shows the highest electron density values, since it is closest to the height of maximum electron density. The lowest electron density can be seen in the map for $h = 250$ km, indicating a strong decrease of ionization by the solar radiation after having passed h_0 . The map for $h = 750$ km shows an overall lower niveau of electron density than the map for $h = 500$ km, which can be expected from theory - but at the borders the electron density can be higher at 750 km than at 500 km. This effect is also explained by Chapman Profile theory: Close to the terminator the height of maximum electron density is larger than at noontime (Feltens, 1998), and this effect propagates upwards and can be felt in 750 km altitude.

The above maps show abnormal peaks at high latitudes. Because of holes in the station net and the arrangement of orbital inclinations in GPS satellite constellation, there is a bad coverage around the poles. As consequence there are no observation data in these zones to which the **TEC** models could fix. This problem can only be overcome by densifying the station net in the polar regions (as far as new stations become available) - especially on the southern hemisphere.

Differential Code Biases

DLR Fernerkundungsstation **Neustrelitz** had provided differential code bias values with respect to which the **ESOC/IONMON** differential code biases could be compared. As example the values for four satellites are presented Figure 6 over the time span from 28 December 1997 to 23 January 1998:

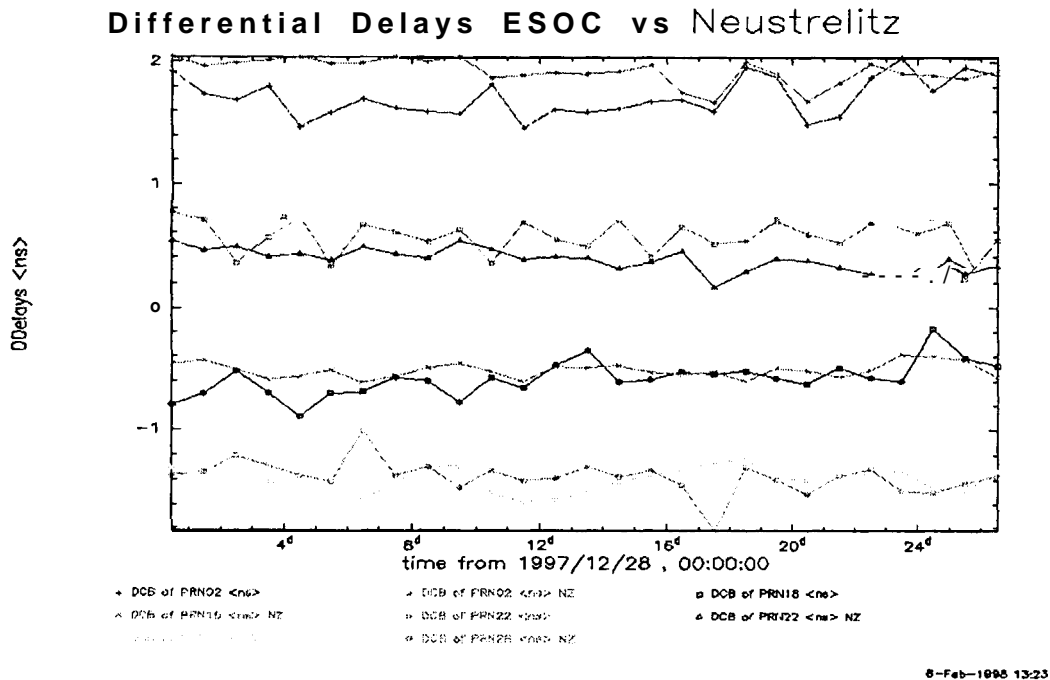


Figure 6: ESOC versus DLR Neustrelitz differential code bias values for PRNs 02, 18, 22,26.

Figure 6. shows an agreement between the Neustrelitz and the ESOC values within 0.3 ns over the whole period. An agreement of the same order was also found for the other GPS satellites. Additional comparisons with differential code bias values from the Astronomical Institute of the University of Beme confirmed this order of agreement,

CONCLUSIONS

ESOC has started with the routine evaluation of ionosphere products at the beginning of this year 1998. Three different kinds of global TEC maps and a set of receiver/satellite differential code bias values are produced daily. Of the three **TEC** maps two are based on a

Chapman Profile approach, thus providing also information on the ionosphere's electron distribution with respect to height.

Validation of achieved **TEC** map accuracy could so far only be done by analysis of **ESOC-internal** products. The common implementation of the IONEX software at all Analysis Centers will then allow for an easy and efficient **intercomparison** of ionosphere products.

Verification of internal accuracy was basically done with two methods:

- 1) By examination of the daily continuity of statistical parameters.
- 2) By comparison of TEC maps from different mathematical models for identical days.

Both methods confirmed stable and accurate IONMON model and software performance.

For the approval of estimated differential code biases, external values were available for comparison and showed an overall agreement in the order of 0.3 *ns*.

All in all ESOC'S operational ionosphere processing looks accurate and stable. The products are output in the **IONEX** format. ESOC is ready to contribute to an IGS ionosphere product.

REFERENCES

- Feltens, J., J.M. Dow, T.J. Martín-Mur, C. García Martínez and M.A. Bayona-Pérez, 1996, Verification of ESOC Ionosphere Modeling and Status of IGS Intercomparison Activity, IGS Presentation, in *Proceedings of the 1996 IGS Analysis Centers Workshop*, Silver Spring, MD, U. S.A., March 19-21, 1996, pp 205-219.
- Feltens, J., J.M. Dow, T.J. Martín-Mur, C. Garcia Martínez, F. Martínez-Fadrique and R. Piriz, 1997, Using GPS for Ionospheric Corrections of ESA Tracking Data, in *Proceedings of the 12th International Symposium on Space Flight Dynamics*, ESOC, Darmstadt, Germany, June 2-6, 1997, pp 121-125.
- Feltens, J., 1998, Chapman Profile Approach for 3-d Global TEC Representation, IGS Presentation, in *Proceedings of the 1998 IGS Analysis Centers Workshop*, ESOC, Darmstadt, Germany, February 9-11, 1998.
- Schaer, S., W. Gurtner and J. Feltens, 1997, IONEX: The Ionosphere Map EXchange Format Version 1, February 25, 1998, in *Proceedings of the 1998 IGS Analysis Centers Workshop*, ESOC, Darmstadt, Germany, February 9-11, 1998.

1

CHAPMAN PROFILE APPROACH FOR 3-D GLOBAL TEC REPRESENTATION

J. Feltens
EDS Industries (Deutschland) GmbH, based at
Flight Dynamics Division,
ESA, European Space Operations Centre,
Robert-Bosch-Str. 5, D-64293 Darmstadt, Germany

ABSTRACT

Until now, ESOC employed single layer algorithms to describe ionospheric TEC 2-dimensionally. Since the real ionosphere is a 3-dimensional phenomenon but not a 2-dimensional one, the idea arose to establish a physically more realistic 3-dimensional model, based on a Chapman Profile approach. The presentation of this new 3-dimensional TEC model will be the task of this paper.

The new 3-dimensional TEC model represents the ionosphere's electron density by a simple Chapman Profile, whereby the layer of maximum electron density N_0 acts as scaling factor and its height h_0 as profile parameter. N_0 and h_0 in turn are modeled as global single layers. The 3-dimensional TEC model uses so called "leveled TEC observables", derived from dual-frequency GPS tracking data, for the determination of its model parameters in a least squares fit. Beyond the evaluation of ground-based tracking data, the processing of SST data is possible too.

INTRODUCTION

This paper will concentrate on the presentation of the basic mathematical algorithms that were worked out to realize a 3-dimensional Chapman Profile TEC model. Numerical results and analyses obtained during an application of the new model to TEC observation data over a longer period of time, are presented in the paper "*Routine Production of Ionosphere TEC Maps at ESOC - First Results*" (Feltens et al., 1998), which is also part of these IGS workshop proceedings.

The presentation of mathematical algorithms in this paper had to be limited to an overview only. A complete mathematical description of the 3-dimensional Chapman Profile TEC model with all its background is given in (Feltens, 1998), and everything what can only be shown roughly here, is described in (Feltens, 1998) in detail.

This paper will start with the attempt to express GPS-derived leveled TEC observable mathematically in terms of a 3-dimensional TEC model based on a Chapman Profile. Since TEC observable do not stand for discrete ionospheric electron density values at certain

points, but represent the integral over all electron densities along the satellite signal path, solutions of the analytical integral over several forms of the Chapman Profile function will be presented, The basic Chapman Profile model parameters are the maximum electron density N_0 and its height h_0 . They will be modeled as global single layers. Key points of numerical applicability for practical use are geometrical aspects, the setting up of linearized observation equations and the establishment of initial values needed for least squares fits. Finally this paper will give some remarks on the estimability of N_0 and h_0 from pure TEC observable and then close with a conclusion.

CONCEPTION OF A CHAPMAN PROFILE MODEL

A TEC observable can mathematically be described as follows:

$$S \cdot (\tilde{\Phi}_1 - \tilde{\Phi}_2)_j^i = TEC_j^i + S \cdot c \cdot (d_j + d^i) + \varepsilon \quad (1)$$

$S \cdot (\tilde{\Phi}_1 - \tilde{\Phi}_2)_j^i$	carrier phase leveled to code observable or “TEC observable” measured between satellite i and ground station (or second satellite) j ,
S	$S = 9.52 [TECU/m]$, multiplication factor for GPS signals, for details see Equation (4.5) of TN-08 (Feltens, 1995a),
TEC_j^i	slant range TEC along signal path from satellite i to station (satellite) j ,
$S \cdot c$	$S \cdot c = 2.85 [TECU/s]$ multiplication factor to convert from [nanoseconds] into [TECU], for details see Equation (4.11) of TN-08,
d_j	differential hardware delay of station (or second satellite) j , normally given in [nanoseconds],
d^i	differential hardware delay of satellite i , normally given in [nanoseconds],
ε	TEC observation noise.

The Total Electron Content TEC is the integral of ionospheric electron density N_e along signal path:

$$TEC = \int_j^i N_e(s) ds \quad (2)$$

According to (Cappellari et al., 1976, page 7-46), the electron density N_e can at any point be represented as a function of height h_m and peak electron density N_m using a Chapman Profile:

$$N_e(z) = N_m \cdot e^{(1-z-e^{-z})} \text{ with } z = \frac{h-h_m}{H} \quad (3)$$

where

N_e	electron density at any arbitrary point along the Chapman Profile,
h	height above Earth surface at which N_e is wanted,
N_m	maximum electron density of the Chapman Profile,
h_m	height of maximum electron density N_m above Earth surface.
H	scale height.

N_m and h_m vary with the zenith angle χ of the Sun, i.e. with day time (see e.g. Ratcliffe, 1972). At noon N_m reaches its maximum and h_m its minimum. And during the time from sunset to sunrise h_m has its maximum and N_m its minimum. To achieve more generality it's convenient to refer Equation (3) to the values that N_m and h_m would reach at noon time. With $N_m(\chi = 0^\circ) = N_0$ and $h_m(\chi = 0^\circ) = h_0$ Equation (3) can be expressed as follows in terms of N_0 and h_0 (Ratcliffe, 1972):

$$N_e(z) = N_0 \cdot e^{(1-z - \sec\chi \cdot e^{-z})} \quad \text{with } z = \frac{h-h_0}{H} \quad (4)$$

where

χ	solar zenith distance,
N_0	maximum electron density of the Chapman Profile referred to $\chi = 0^\circ$,
h_0	height of maximum electron density N_0 above Earth surface at $\chi = (F')$.

The Chapman Profile theory assumes the scale height to be constant along the whole profile (Ratcliffe, 1972). According to (Cappellari et al., 1976) the scale height can be expressed as a function of h_0 as follows:

$$H = \frac{5}{3} \cdot \{30 + 0.2 \cdot (h_0 - 200)\} = \frac{h_0 - 50}{3} \quad [km] \quad (5)$$

Once N_0 and h_0 are known, Equation (4) can be used to calculate the electron density at any point and height along the Chapman Profile. Putting Equation (4) into Equation (2) and this into Equation (1) gives finally Equation (6) relating the Chapman Profile to the TEC observable:

$$S \cdot (\tilde{\Phi}_1 - \tilde{\Phi}_2)_j' = N_c \int_j^i e^{(1-z - \sec\chi \cdot e^{-z})} ds + S \cdot c \cdot (d_j + d_j') + \epsilon \quad (6)$$

Next a relation between the **integrand** ds and the profile variable z must be established: The differential triangle in Figure 1 indicates the following relation between differential increments dh in height and ds in slant range direction:

$$ds = \frac{dh}{\cos Z} \quad (7)$$

where

cosZ

cosine of slant range zenith distance.

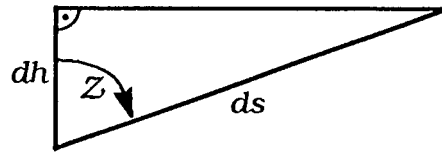


Figure 1: Differential triangle - relation between differential increment dh in height and differential increment ds in slant range direction.

And from Equation (4) the following relation between dz and dh can be derived:

$$dh = H \cdot dz \quad (8)$$

With the Relations (7) and (8) Equation (6) can thus be modified according to:

$$S \cdot (\tilde{\Phi}_1 - \tilde{\Phi}_2)_j^i = N_0 \cdot H \cdot \frac{1}{\cos Z} \cdot \int_{z_j}^{z_i} e^{(1-z-\sec\chi \cdot e^{-z})} dz + S \cdot c \cdot (d_j + d^i) + \epsilon \quad (9)$$

The $1/\cos Z$ -term can be understood as counterpart to the mapping functions used for single layer models (see e.g. Feltens, 1995a).

For several versions of the Chapman Profile function analytical integrals were found. The establishment of these integrals is presented in detail in (Feltens, 1998). Since such formulae developments are out of the scope of this paper, only the final integral functions can be presented here.

Analytical integral over the simplest form of the Chapman Profile function:

$$\int e^{(1-z-e^{-z})} dz = e^{(1-e^{-z})} \quad (10)$$

The Integral (10) was also confirmed by (Cappellari et al., 1976), where it is inherent in the Equations (7-146).

Analytical integral over the $\sec\chi$ -form of the Chapman Profile function:

$$\int e^{(1-z-\sec\chi \cdot e^{-z})} dz = \cos\chi \cdot e^{(1-\sec\chi \cdot e^{-z})} \quad (11)$$

Analytical integral over the $\sec\chi$ -form of the Chapman Profile function in terms of height h above ground:

$$\int e^{(1-\left(\frac{h-h_0}{H}\right)-\sec\chi \cdot e^{-\left(\frac{h-h_0}{H}\right)})} dh = H \cdot \cos\chi \cdot e^{(1-\sec\chi \cdot e^{-\left(\frac{h-h_0}{H}\right)})} \quad (12)$$

Only the $\sec\chi$ -form of the Chapman Profile function is of relevance for further considerations. Regarding the Integrals (11) and (12), Equation (9) can finally expressed as follows:

$$S \cdot (\tilde{\Phi}_1 - \tilde{\Phi}_2)_j^i = N_0 \cdot H \cdot \frac{\cos \chi}{\cos Z} \cdot e^{(1 - \sec \chi \cdot \cos Z) \cdot \frac{z_j}{H}} + S \cdot c \cdot (d_j + d^j) + \varepsilon \quad (13)$$

Equation (13) is that final equation which relates TEC observable to the integral over the Chapman Profile. Equation (13) is thus the base upon which the observation equations will be set up.

REPRESENTATION OF N_0 AND h_0 AS SINGLE LAYERS

N_0 and h_0 are clearly coupled with $\chi = 0^\circ$, i.e. with noon time (see Equation (4) above). So the coordinate origin for N_0/h_0 single layer development should be positioned at 12^h local time, i.e. at the Sun's maximum elevation above horizon. However, from ionosphere observations it is well known, that the diurnal maximum of electron density appears with a delay of about 2 hours. This effect has been accounted for in the software by calculating the Sun's position vector with a delay of 2 hours in such a way, that at 14^h the Sun's position of 12^h enters into the processing.

The software tests have shown that N_0 can be best modeled with a GE-function (Feltens, 1995 b). And these software tests also confirmed the method of computing the solar ephemerides with a 2 hours delay, since the maxima of the fitted No-GE-function and the Chapman Profile geometry ruled by χ did coincide under these conditions, thus causing the *rms* to minimize.

To model h_0 , special functions had to be worked out which force h_0 to get values in a predefined height range only. Two basic aspects had to be considered: 1) h_0 shall be modeled as smooth surface. 2) The surface functions should be designed so, that they can only reach values within predefined height limits. Since h_0 is referred $\chi = 0^\circ$, i.e. noontime, of the daily height variation, only the noontime values are of relevance for h_0 . Thus ignoring the daytime dependency, h_0 should only show variations depending mostly on solar activity. Expressed in numbers, these variations are in the range of $250 < h_0 \leq 400 \text{ km}$. However, the software tests have shown that the allowed height range should be set even narrower and slightly higher than 400 km :

$$ho_{min} = 400 \text{ km} \quad , \quad ho_{max} = 450 \text{ km} \quad \text{Ah.} = ho_{max} - ho_{min} = 50 \text{ km} \quad (14)$$

In operational use the allowed height range, as defined above in (14), should be adapted to the actual solar activity from time to time.

Of several candidates tried out, only the following approach, which appeared to be the most promising function to represent h_0 , is shown here. (Feltens, 1998) gives a complete overview over all candidates that were tried out for h_0 -modeling. The best candidate is a Sin-function enclosing another function $f(x,y)$ as its argument. The sin-function restricts the output values always to the range $-1 \leq \text{value} \leq 1$, and the internal function $f(x,y)$ causes -

if not linear - the unknown parameters not to be affected by a 2π -bias, the period of the sin-function, which could make convergence unstable. h_0 is then established by a proper scaling of the extended sin-function:

$$h_0 = \xi(x, y) = h_{0_{min}} + \frac{\Delta h_0}{2} \cdot \{1 + \sin[f(x, y)]\} \quad (15)$$

Instead of a sin-function, a cos-function could have been used too. But, since both should be equivalent, only the sin-function approach was implemented into the software.

Of several candidates the one **shown in Equation (16) was chosen for the inner function $f(x, y)$** . The first term $c \cdot \sin(x + y)$ has been included to enhance numerical stability:

$$f(x, y) = C \cdot \sin(x + y) + v_x \cdot \sin^2 x \cdot \cos x + \mu_x \cdot \sin x \cdot \cos^2 x + v_y \cdot \sin 2y \cdot \cos y + \mu_y \cdot \sin y \cdot \cos^2 y \quad (16)$$

with
 $C = 0.001$ numerically small constant

And the arguments x and y are defined as follows:

$$\begin{aligned} +90^\circ \geq x \geq -90^\circ & , & x = \Phi_m \\ 0^\circ \leq y \leq 180^\circ & , & y = \tau/2 \end{aligned} \quad (17)$$

where

Φ_m geomagnetic latitude,

τ local time.

The extended sin-function approach in the form presented above allows for the estimation of exactly 4 coefficients v_x, μ_x, v_y, μ_y . A generalization of Function (16) appears possible, but was not considered further. This might be a subject of future model extensions.

NUMERICAL REALIZATION

Integration of the Chapman Profile Formulae

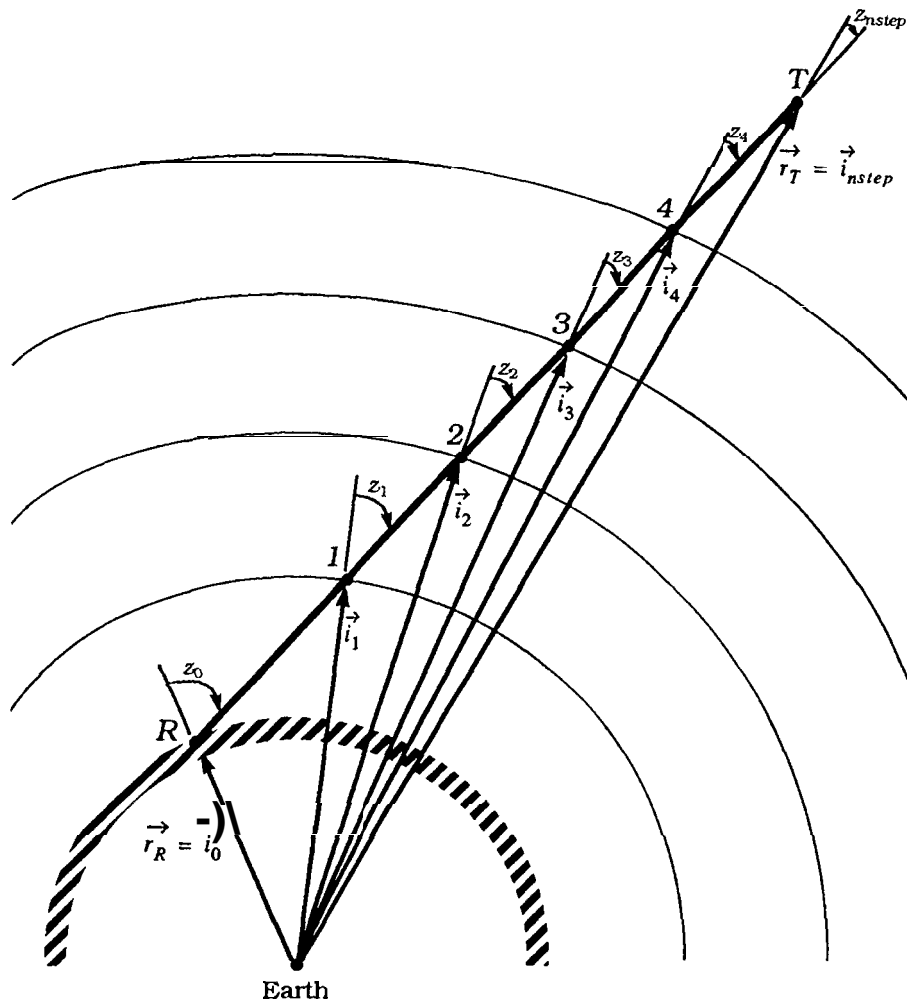


Figure 2: Change of zenith distance Z with height h .

In order to prepare the formulae of the preceding chapters for practical use, several aspects had to be considered:

- 1) The Integrals (11) and (12) were established under the assumption of **plane stratified** ionosphere layers, i.e. the satellite and solar zenith angles Z and χ were-assumed to be constant and independent of height - but the real ionosphere is, like the Earth, in first approximation a sphere.
- 2) The 3-dimensional **TEC** model shall also be usable for satellite-to-satellite tracking (SST) data. In the case of ground-based GPS tracking it is obvious that ionospheric signal delays can be expressed by one Chapman Profile. - However, at SST applications

geometrical conditions can arise, at which an ionospheric delay must be expressed by the sum of two Chapman Profiles.

- 3) (Feltens, 1995a, Section 5.3) presents a method to determine position vectors of satellite signal intersection points through the layer of maximum electron density. This algorithm assumes the shell height to be globally constant. However, the new model treats h_0 as single layer, i.e. there are variations in height, depending on geographic position. So the formulae of (Feltens, 1995a) must here be used in an iteration loop to find an intersection point through the No-layer.

Figure 2 shows how the **satellite zenith distance** Z changes with height h . The signal path is described by the range vector $\vec{p} = \vec{r}_T - \vec{r}_R$. In order to account for the changing satellite zenith distance Z , the following integration rule is exploited for Chapman Profile integration (see e.g. Bronstein and Semendjajew, 1979):

$$\int_a^d f(x) dx = \int_a^b f(x) dx + \int_b^c f(x) dx + \int_c^d f(x) dx, \quad a < b < c < d \quad (18)$$

The signal path s along which to be integrated is thus subdivided into equidistant intervals Δs . However, the signal path length is normally not an integer number of a predefined interval Δs . So the "actual integration step width" Δs is defined as follows:

$$nstep = \text{int}\left(\frac{s}{\Delta s}\right) + 1 \quad \text{and} \quad \Delta s = \frac{s}{nstep} \quad [km] \quad (19)$$

where

- s slant range, identical with the amount $|\vec{\rho}|$ of the range vector above,
- Δs "nominal integration step width",
- $nstep$ number of integration steps,
- int function corresponding to Fortran INT, i.e. cutting off the decimal digits.
- Δs "actual integration step width".

Integration is now done, starting at the lowest point of integration path and going upwards in steps of Δs to the highest point, in the way that at the beginning and ending of each interval Δs the position vectors \vec{i}_p on the slant range are determined:

$$\vec{i}_p = \vec{i}_0 + \frac{p \cdot \Delta s}{|\vec{\rho}|} \cdot \vec{\rho} \quad p = 1, 2, \dots, nstep \quad (20)$$

where (see Figure 2)

- \vec{i}_p position vector of an integration step **beginning/ending** point on slant range,
- \vec{i}_0 position vector of the lowest point of the integration path,
- \vec{i}_{nstep} position vector of the highest point of the integration path,
- $\vec{\rho}$ range vector defining slant range signal path $\vec{\rho} = \vec{r}_T - \vec{r}_R$.

As "actual integration step width",
p running integration step number,
nstep total number of integration steps.

Making the dot product of a position vector \vec{i}_p with the range vector \vec{p} gives the cosine of the satellite's zenith distance Z_p at that point *p* on the slant range:

$$\cos Z_p = \frac{\vec{i}_p \cdot \vec{p}}{|\vec{i}_p| \cdot |\vec{p}|} \quad (21)$$

And from the cosine values of two successive points *p* and *p-1* the means are built:

$$\cos Z_{p-1,p} = \frac{1}{2} \cdot (\cos Z_{p-1} + \cos Z_p) \quad (22)$$

What was shown in Figure 2 for the satellite zenith distance is in a similar way also valid for the Sun's zenith distance χ . So the solar zenith distance is handled in the same way as the satellite zenith distance was treated above: At each point \vec{i}_p where $\cos Z_p$ is computed, $\cos \chi_p$ is calculated too:

$$\cos \chi_p = \frac{\vec{i}_p \cdot (\vec{r}_\odot - \vec{i}_p)}{|\vec{i}_p| \cdot |\vec{r}_\odot - \vec{i}_p|} \quad (23)$$

where

\vec{r}_\odot the Sun's position vector,

The mean value being valid for the integration step between two successive points *p* and *p-1* is then:

$$\cos \chi_{p-1,p} = \frac{1}{2} \cdot (\cos \chi_{p-1} + \cos \chi_p) \quad \text{and} \quad \sec \chi_{p-1,p} = 1 / \cos \chi_{p-1,p} \quad (24)$$

On the other hand there is a significant difference between handling satellite zenith distances *Z* and solar zenith distances χ : Close to the terminator the Sun's zenith angle becomes $\chi = 90^\circ$, and beyond on the **nightside** $\chi > 90^\circ$. This causes the **sec χ -term** to become infinite at 90° and to change its sign beyond. The software tests have shown, that, when χ is approaching 90° , it should be frozen from a certain limit on for the whole nightside to a constant value. Of several values tried out $\chi = 70^\circ$ was found to be the best limit angle, i.e. for TEC modeling it is assumed that the electron content enclosed by the Chapman Profile does not go below that of $\chi = 70^\circ$ for the whole nighttime:

$$\text{i-f } \chi > 70^\circ \quad \rightarrow \quad \text{set } \chi = 70^\circ \quad (25)$$

The software tests have shown that the Chapman Profile integration **should** be restricted to a height range of **60-2000 km**. As appropriate step width $AS = 50 \text{ km}$ was identified. Before starting the integration, the software reduces integration path to that part of the whole slant range from ground station to satellite, which lies in that height range.

Establishment of Linearized Observation Equations

In order to obtain the **partials** with respect to the **unknowns** Equation (13) is written here again, now with the functional dependencies explicitly expressed:

$$S \cdot (\tilde{\Phi}_1 - 52) = N_0 \cdot H(h_0) \cdot \frac{\cos \chi}{\cos Z} \left. e^{(1 - \sec \chi \cdot e^{-z/h_0} H(h_0))} \right|_z^z + S \cdot c \cdot (d_j + d^i) + \varepsilon \quad (26)$$

and

$$z(h_0, H(h_0)) = \frac{h - h_0}{H(h_0)} \quad H(h_0) = \frac{h_0 - 50}{3} \text{ [km]}$$

The unknowns to be estimated in Equation (26) are the single layer coefficients N_{kl} and h_{nm} to represent $N_0(N_{kl})$ and $h_0(h_{nm})$, and the differential code bias values d_j and d^i . For the single layer coefficients N_{kl} and h_{nm} the **partials** $\partial\{S \cdot (\tilde{\Phi}_1 - \tilde{\Phi}_2)\} / \partial N_0$ and $\partial\{S \cdot (\tilde{\Phi}_1 - \tilde{\Phi}_2)\} / \partial h_0$ are needed anyway, and then the **partials** $\partial N_0 / \partial N_{kl}$ and $\partial h_0 / \partial h_{nm}$ are attached via chain rule to obtain the required **partials** $\partial\{S \cdot (\tilde{\Phi}_1 - \tilde{\Phi}_2)\} / \partial N_{kl}$ and $\partial\{S \cdot (\tilde{\Phi}_1 - \tilde{\Phi}_2)\} / \partial h_{nm}$ with respect to the unknowns needed for the observation equations. Knowledge of the **partials** $\partial\{S \cdot (\tilde{\Phi}_1 - \tilde{\Phi}_2)\} / \partial N_0$ and $\partial\{S \cdot (\tilde{\Phi}_1 - \tilde{\Phi}_2)\} / \partial h_0$ thus allows for the establishment of the **partials** for coefficients of any single layer model by applying the chain rule. Exploiting this fact, any single layer model can be extended for 3-dimensional Chapman Profile applications.

Regarding the geometrical aspects treated in the previous section and Equation (26), the **TEC** and its partial with respect to h_0 , which are both obtained via integration along the profile, can be expressed by the following summation formulae for practical use:

$$TEC(h) = N_0 \cdot H \cdot \sum_{p=1}^{nstep} \frac{1}{\cos Z_{p-1,p}} \cdot \left\{ \cos \chi_{p-1,p} \cdot e^{(1 - \sec \chi_{p-1,p} \cdot e^{-z})} - \cos \chi_{p-1,p} \cdot e^{(1 - \sec \chi_{p-1,p} \cdot e^{-z_{p-1}})} \right\} \quad (27)$$

and

$$\frac{\partial TEC(h)}{\partial h_0} = \frac{1}{3} \cdot \sum_{p=1}^{nstep} \frac{1}{\cos Z_{p-1,p}} \cdot \left\{ \cos \chi_{p-1,p} \cdot e^{(1 - \sec \chi_{p-1,p} \cdot e^{-z_p})} - \cos \chi_{p-1,p} \cdot e^{(1 - \sec \chi_{p-1,p} \cdot e^{-z_{p-1}})} \right\} + N_0 \cdot H \cdot \sum_{p=1}^{nstep} \frac{1}{\cos Z_{p-1,p}} \cdot e^{(1 - 2p - \sec \chi_{p-1,p} \cdot e^{-z_p})} \cdot \frac{\partial z_p}{\partial h_0} \cdot e^{(1 - z_{p-1} - \sec \chi_{p-1,p} \cdot e^{-z_{p-1}})} \cdot \frac{\partial z_{p-1}}{\partial h_0} \quad (28)$$

and the **partials** $\partial z_{p-1} / \partial h_0$ and $\partial z_p / \partial h_0$, being needed for Summation Formula (28):

$$\frac{\partial z_{p-1}}{\partial h_0} = \frac{-1}{H} \cdot \left\{ 1 + \frac{z_{p-1}}{3} \right\} \quad \text{and} \quad \frac{\partial z_p}{\partial h_0} = \frac{-1}{H} \cdot \left\{ 1 + \frac{z_p}{3} \right\}$$

The partial $\partial TEC(h) / \partial N_0$ is trivial:

$$\frac{\partial TEC(h)}{\partial N_0} = \frac{TEC(h)}{N_0} \quad (29)$$

If, for a SST measurement, the total integration path must be sub-divided into two sub-paths, two Chapman Profiles have to be integrated, and the final **partials** with respect to N_0 and h_0 are then obtained by summing up the **partials** of each Chapman Profile.

The **partials** for the receiver and satellite differential code bias d_j and d^i are simply:

$$\frac{\partial\{S \cdot (\tilde{\Phi}_1 - \tilde{\Phi}_2)\}}{\partial d_j} = S \cdot c = 2.85 \text{ (for GPS)} , \quad \frac{\partial\{S \cdot (\tilde{\Phi}_1 - \tilde{\Phi}_2)\}}{\partial d^i} = S \cdot c = 2.85 \text{ (for GPS)} \quad (30)$$

Getting Initial Values for the Unknowns

Since N_0 appears linear in the Chapman Profile function (see Equation (26)), its value needs not to be known a priori to establish the partial for it. Equation (29) shows that its partial is the **TEC** value normalized to N_0 . So using Equation (27) and summing up the **TEC** with $N_0 = 1$ gives the partial for N_0 without necessity of explicit knowledge of N_0 itself. However, a h_0 -value is needed to do this summation. During the first iteration h_0 is thus kept fixed to some initial values, and only values for the No-single layer coefficients are estimated. If N_0 is represented by a GE-function, this first iteration must be done in logarithmic mode (Feltens, 1995b and Feltens, 1998). From the second iteration on the h_0 -parameters are then estimated together with the No-parameters, using the No-coefficient values obtained from the first (or the previous) iteration as initial values. In the case h_0 is represented by an extended sin-function, the h_0 -coefficients are kept fixed with one $(v_x)_0, (\mu_x)_0, (v_y)_0, (\mu_y)_0 = 1$ (with respect to the predefined height range given in Equation (14)) during the first iteration.

h_0 's role is twofold: On one hand it is estimated as an unknown, on the other hand it is used to fix the intersection points through the No-layer in order to evaluate AJ_0 - and scale height EI -values there, and to compute the argument z of the Chapman Profile function. To evaluate the intersection points, N_0 , Eland z , the h_0 -single layer parameters of the previous iteration must thus be used. To make N_0 finally conform with h_0 , a last iteration is made with keeping h_0 again fixed, now to its recently estimated values, only estimating the N_0 -parameters and the differential code bias values.

ESTIMABILITY OF N_0 AND h_0 FROM TEC OBSERVABLE

The software tests have shown, that the Chapman Profile fits are rather insensitive against h_0 -variations, and estimated h_0 -parameters show only weak significance. This is obvious when keeping in mind that TEC observable are measurements of the integral over the electron density, and this integral is the area under the electron density profile. A **TEC** observable thus corresponds to such an area value. And an area value alone gives only the area's amount, saying nothing about the area's shape, i.e. the profile peak at h_0 can be extracted from the information provided by pure TEC observable only from effects caused by the varying elevations under which these observable were made. Because for lack of corre-

spending tracking data, the SST option could not be included into the software tests so far. It is hoped that the inclusion of SST data will improve the situation, since SST measurements are affected, depending on the geometrical conditions, by more varying parts of the ionosphere than ground-based tracking data. Inclusion of SST data might thus improve the resolution of profile parameters, such as h_0 .

The determination of No-parameters is stable, and No-single layer coefficients are estimated significantly. TEC models obtained when modeling N_0 with GE-functions appear to have the same order of accuracy as pure single layer GE-function fits - with the *rms* tending to be slightly better, i.e. Chapman Profile fits are of comparable accuracy as pure GE-function fits, but provide information on the ionosphere's third dimension - the height.

CONCLUSIONS

A mathematical model has been worked out allowing for the 3-dimensional representation of ionospheric TEC from TEC observation fits. These TEC measurements can be derived from GPS dual-frequency tracking data. The ionospheric TEC is modeled as the integral over simple Chapman Profiles with the layer of maximum electron density N_0 acting as scaling factor and its height h_0 as profile parameter. Both, N_0 and h_0 , are in turn represented as global single layers. For the modeling of h_0 special single layer functions were developed.

Since GPS-derived TEC observable represent the ionosphere's total electron content along signal path, no discrete electron density values are observed, but the integral over all electron densities along the signal path. Analytical solutions for the integral over several versions of the Chapman Profile function were found and implemented into the model. In order to account for certain geometrical aspects, the integral over the Chapman Profile function is finally evaluated by a mixture of analytical and numerical approach.

From its conception this Chapman Profile-founded model allows the evaluation of ground-based data as well as of SST data. However, for lack of SST data, software tests had so far to be restricted to the evaluation of ground-based data.

All in all the whole 3-dimensional TEC model is built up by simple mathematical formulae. From the model's and the software's conception and structure it is possible to combine it with every single layer and to include more complex ionosphere profiles in future steps of software extension.

The task of this paper was the presentation of the basic mathematical algorithms realizing the 3-dimensional TEC model. Analyses of numerical results, that came out when applying this model to TEC data fits, are presented in (Feltens et al., 1998), which is also published in these IGS workshop proceedings.

REFERENCES

- Bronstein, I.N. and K.A. Semendjajew, 1979, *Taschenbuch der Mathematik, Verlag Harri Deutsch, Thun und Frankfurt/Main, Vol 1+2.*
- Cappellari, J.O, C.E. Velez and A.J. Fuchs, 1976, Mathematical Theory of the Goddard Trajectory Determination System, Goddard Space Flight Center, X-582-76-77, Greenbelt, MD, U. S.A., April 1976, Section 7.6.2 'Ionosphere Models', pp 7-44-7-52.
- Feltens, J., 1995a, GPS TDAF Ionosphere Monitoring Facility, Mathematical Model Developments, in *GTDAF-TN-081s.s 1/- 11 Sep-95 (ESOC-internal document).*
- Feltens, J., 1995b, GPS TDAF Ionosphere Monitoring Facility, Examination of the Applicability of **Gauß-Type** Exponential Functions to Ionospheric Modeling, in *GTDAF-TN-09 Iss 1/- 11 Sep-95 (ESOC-internal document).*
- Feltens, J., 1998, GPS TDAF Ionosphere Monitoring Facility, Chapman Profile Model for the IONMON, in *GTDAF-TN-14 Iss 1/- 04 Mar-98 (ESOC-internal document).*
- Feltens, J., J.M. Dow, T.J. Martín-Mur, C. García Martínez and P. Bernedo, 1998, Routine Production of Ionosphere **TEC** Maps at **ESOC** - First Results, IGS Presentation, in *Proceedings of the 1998 IGS Analysis Centers Workshop, ESOC, Darmstadt, Germany, February 9-11, 1998.*
- Ratcliffe, J. A., 1972, An introduction to the ionosphere and magnetosphere, *Cambridge University Press, Great Britain, 1972.*

THE ROLE OF GPS DATA IN IONOSPHERIC MODELLING, MAPPING AND NOWCASTING

R. Leitinger,
Institut für Meteorologie und Geophysik,
Universität Graz, A-8010 GRAZ, Austria

ABSTRACT

The classical sources for ionospheric electron content (TEC) data are disappearing quickly. The ionospheric research community has to shift to Global Navigation Satellite Systems (GNSS, presently GPS and GLONASS) to gain TEC data from the plasma influence on the GNSS signals. This means a serious shift in policies and a necessity for enhanced research into the capabilities and the shortcomings of the „new” systems. One of the most serious consequences is the loss of temporal continuity. It has to be overcome by incorporation of **ionosonde** observations. The so-called „plasmasphere” problem also is a serious one if one is interested in long-term studies of ionospheric electron content or if TEC data are needed for correction of the ionospheric influence (e.g., ground to a height of 800 km).

Already now GNSS derived TEC data play a major role in ionospheric **modelling**, **mapping** and **nowcasting**. The importance of GNSS data for these purposes will increase quickly in the near future. Therefore close co-operation of institutions with ionospheric research and application capabilities with other users of GNSS signals is a necessity.

INTRODUCTION

The quantity of interest is the vertical ionospheric electron content (TEC). It is derived from the electron content along a slant ray path from the satellite transmitter (S) to the ground receiver (R):

$$I_{\nu} = \int_R^S N \, ds = \int_0^z N \frac{dh}{\cos \beta}$$

(N: electron density; ds : ray path element; dh : height element; β : zenith angle along ray; z is a „ceiling height” which depends on the observation method: for GPS observations it is the height of the satellite).

I_{ν} is not an observable: conversion of measured data (from a technical point of view phase differences) into I_{ν} values involves a „calibration” process.

Projection onto the vertical gives the (vertical) electron content (TEC):

$$I_{\parallel} = \frac{1}{\cos\beta} \int_0^z N \, dh = \frac{1}{\cos\beta} I_{\perp} = \frac{1}{\cos\chi} I_{\perp}$$

Since the electron density distribution along the ray RS is not known the projection is done in the following way: instead of the true mean for $(1/\cos\beta)$ an approximate value is taken $(1/\cos\chi; \chi = \beta(h_i))$: zenith angle in the „mean ionospheric height” or „shell height” h_i . If a fixed value is assumed for h_i , it is recommended to use 400 km. (At least in periods of high solar activity this value is too low in lower latitudes - in the vicinity of the crests of the equatorial anomaly and over the dip equator).

DATA SOURCES

In the past we had the following types of „satellite beacons” and could make use of three different „propagation effects”, namely the Faraday effect, the Group Delay effect (plasma influence on the modulation phase) and the Differential Doppler effect (plasma influence on carrier phase). Table 1 shows two „long-term” opportunities, namely the VHF beacons of the older types of geostationary communication satellites and the 150/400 MHz coherent beacons of the (US) Navy Navigation Satellite System (NNSS). The communication satellites needed the VHF beacons for navigation in the transfer phase and some were kept in continuous operation to allow observations of the Faraday effect (provided the polarisation of the beacon was elliptical and not nearly circular). A **geostationary** beacon provides a time constant ray path and therefore time continuous observations of ionospheric electron content with a „ceiling height” z of 2000 km (weighting because of the height dependence of the longitudinal component of the geomagnetic field, see, e.g., Titheridge, 1972). The NNSS satellites allow observations of the Differential Doppler effect (carrier phase difference; see, e.g., Leitinger et al., 1975). Since the satellites are in nearly circular and nearly polar orbits (in heights around 1100 km) evaluation of the observations essentially gives the latitude dependence of electron content. The transit time (around 20 minutes for an overhead pass) is short enough to neglect temporal variations of the ionization.

Table 1 also contains hints at the only two dedicated „experiments” which were available to the beacon satellite community: S-66 (Beacon Explorers B and C - A was a failure). BE-B provided global coverage for Faraday effect observations on two signals (40 and 41 MHz) and gave opportunity to construct the first regional models for electron content (see, e.g., Ebel et al., 1969). They suffered from the shortcomings one has with one satellite only, namely the coupling of local time variations and seasonal variations. The operation of the Beacon Explorers did not cover high solar activity. As far as it is known an other opportunity provided by S-66 was not used on a wider basis, namely the observation of carrier phase differences

(e.g., using the 40 and 360 MHz signals), The Beacon Explorers also had a 20 MHz beacon but because of interference problems (man mad noise) it could not be used from most locations.

The Radio Beacon Experiment on board of the **geostationary** communication research satellite ATS-6 was a very ambitious one (see Davies, 1980). One of the crucial achievements was the successful separation of (slant) **plasmaspheric** electron content from the total electron content. Thanks to ATS -6 RBE we have clear ideas about the **plasmaspheric** contribution for low solar activity.

Presently we **are** in a transition phase: The geostationary VHF beacons are faded out (they already have disappeared for Europe). NNSS has been decommissioned as a navigation system. Three to four satellites are kept in operation for ionospheric research purposes, hopefully for several more years. More and more the beacon satellite community has to shift to GPS (and GLONASS) data. This shift means a serious change in policy: most of the ionospheric research institutions will not be able to make their own GPS or GLONASS observations, they **rely** (and will have to continue to rely) on data collected for other purposes. It is very important to ensure that ionospheric expertise and research capabilities are preserved over the transition phase and that a multitude of comparisons of TEC data from **all** available sources are made.

Table 1: beacon opportunities of the past

Beacon satellites	frequencies (MHz)	propagation effects	properties & remarks
geostationary communication satellites	136...138	Faraday	fixed ray path, continuity in time, very good temporal resolution
polar orbiting NNSS	150/400	Diff. Doppler	scan in latitude, very good latitudinal resolution
Special Experiments:			
orbiting 1965-1969: S-66 (Beacon Explorers)	40/41	Faraday	
geostationary 1974-1977: ATS-6 RBE	40,41,140, 360 + modulation	Faraday, Diff. Doppler, Group Delay	separation of total content from ground to ATS-6 into ionospheric and plasmaspheric part

In the near future we will have GNSS plasma data only for long-term investigations which need observations conditions which remain as homogeneous as possible. Probably NNSS type beacons will be available from time to time on „experimental” basis.

It is important to note that continuous data collection and preservation is necessary not only for **long-term** investigations but for research into „**geophysical events**” as well. Presently the occurrence of such events (e.g., of ionospheric storms, large amplitude Traveling Ionospheric Disturbances, regional disturbances of other types) cannot be predicted and this author doubts very much that all „**events**“ of importance will be predictable in the future. „**Events**“ are studied after their occurrence (case studies with data from the data base).

TEC DATA COLLECTIONS AND THEIR USE

Ionospheric physics (and other branches of external geophysics) as well as many important applications need collections of ionospheric data. These data bases are used for typical „**long-term**“ investigations (mapping, **modelling**, system planning) and retrospectively for case studies and applications like corrections for propagation errors (first order errors in single frequency applications of satellite signals) and other uses of **nowcasting** procedures, Tables 2 and 3 give an overview.

Table 2: Use of TEC data bases for ionospheric physics

(1) „ Long-term “	Modelling, Mapping
	Solar cycle dependence
	Global Change
(2) „ Events “ (effects of)	Geomagnetic Storms
	Atmospheric Gravity Waves \Rightarrow TIDs
	Solar Flare Effects
	Others ? (Unexplained TEC excursions)

Table 3: Applications of TEC data

Geophysics: Ionization is important „ tracer “ for	Neutral atmosphere processes
	Magnetospheric processes
	Solar--terrestrial relations
Retrospective Applications:	TEC maps (testing, improving, refining)
	Correction of propagation errors (e.g., for single frequency altimetry)

	Retrospective nowcasting
	Retrospective updating of maps

The desired data density differs from application to application. Table 4 gives an overview for regional applications. Typical sizes of „regions“ are in the order of 30 to 50 degrees in latitude times 60 to 90 degrees in longitude. For lack of homogeneous coverage global studies are usually made by combining regional results (e.g., from Europe, the Americas, Australia, East Asia). Global TEC maps even with a much coarser resolution in latitude and longitude than regional ones would be of great value for global studies. From the point of view of geophysics and of applications for users the minimum would be one map per day for a given Universal Time („snapshot” maps) if temporal development can be assessed by means of data from a selection of observing points which are considered „typical“ for a region of **importance**. Ionosonde parameters (especially foF2 the maximum plasma frequency of the ionosphere and maximal electron density derived from it) are very well suited for monitoring of the temporal development of ionospheric disturbances. If more than one global map is produced per day it is recommended to construct the maps in Local Time (TEC over a grid in latitude and longitude for fixed LT). The minimum LT resolution would be 6 hours (4 maps per day, e.g., for 00 LT, 06 LT, 12 LT, 18 LT) but major improvements could be gained if the number of maps per day is larger. (8 maps per day already gives a very good impression on the temporal development of global storm disturbances.) However, it is important to note that global maps cannot replace regional ones.

Table 4: Desired data density (regional applications):

	At	As	$\Delta\phi$	$\Delta\lambda$
Regional Mapping	1 h	500 km	5"	15°
Most applications	15 min	500 km	5"	15°
Events:				
storms	15 min	200 km	2°	4°
LSTIDs	5 min	200 km	2°	4"

LSTIDs: Large Scale Travelling Ionospheric Disturbances

For ambitious applications like navigation of aircraft, land vehicles, ships in coastal waters and on rivers, etc., near real time regional maps are a necessity. The data behind such regional maps should be preserved for retrospective purposes.

Presently it is not realistic to assume that the whole globe will be covered with GNSS based regional maps with the resolution needed for ambitious applications. From the point of view of ionospheric physics important gaps will remain, e.g., over the oceans, and probably for many years over parts of Africa and Asia. One possibility to gain ionospheric data over remote areas is the use of GNSS occultation combined

with information on horizontal gradients of TEC. Global maps could help to bridge the gaps in the horizontal gradient information which is very scarce in the regions with poor coverage with ground stations.

From a geophysical point of view „higher latitudes” (Europe: N of 60°N) and „lower latitudes” (European/African sector: S of 35°N) are more important than the comparatively well known „mid latitudes”.

REMARKS AND CONCLUSIONS

(1) There is no doubt that GNSS data (ground based as well as occultation derived) will be the most important source of ionospheric „mass data” in the near future. This does not mean that these data can replace important research instruments like the Incoherent Scatter Radars. Furthermore optimal use of GNSS derived data makes it necessary to maintain the ionosonde network in operation. For many purposes electron content information is not sufficient. The ionosondes provide very valuable additional profile information and they provide temporal continuity for fixed locations which cannot be obtained from GNSS observations.

(2) For several reasons it is very important to continue NNSS observations as long as this is possible. They provide independent data and therefore possibilities to check the integrity of GNSS derived data, GNSS receiver calibration, etc. The spatial resolution of NNSS derived TEC is excellent and better than what can be gained from all other remote and in-situ measurements, Furthermore the „plasmasphere” problem is not yet solved for GNSS derived TEC: we know what to expect for times of low solar activity (mainly from ATS-6 RBE) but we have a lack of experience from high solar activity. Comparison of GPS data with NNSS data gives very valuable information about the **plasmaspheric** contribution in GNSS TEC.

(3) The transition from the classical TEC sources to GNSS means an important change in working conditions for the ionosphere research community: most of the research groups will not have their own receiving equipment but will have to rely on data collections (like IGS) and on close co-operation with other users of GNSS signals. It will be necessary to provide help and assistance to research groups in less developed countries. Regional data centers for GNSS derived TEC are a possible solution to data access problems in less developed countries.

(4) Close co-operation between international (global and regional) organisations for the use and application of ionospheric information is necessary to ensure optimal use of the novel data sources based on ground and space reception of GNSS signals. Since 1971 the International Beacon Satellite Group (presently Working Group G2 of the International Union for Radio Science - URSI) is an organisation which brings together scientists and engineers from different fields and from different regions

(chairman: R. Leitinger, Austria, co-chairmen: J.A. Klobuchar, USA, PVS Rama Rae, India). It is an important forum for the exchange of relevant information and experiences. It organizes Symposia in distances of two to three years (see Kersley, 1994 and Bencze and Leitinger, 1998 for the Proceedings of the two most recent Beacon Satellite Symposia). In recent years members of the Beacon Satellite Group have been involved extensively in assessing GPS as a data source for ionospheric research and for propagation errors in the application of transionospheric radio signals.

REFERENCES

- Bencze, P, and R. Leitinger (editors), 1998, Proceedings of the International Beacon Satellite Symposium 1997, Sopron, Hungary, 30 June-5 July, 1997. In print: *Acts Geodetica et Geophysics Hungarica*
- Davies, K., 1980, Recent progress in satellite Radio Beacon studies with particular emphasis on the ATS-6 Radio Beacon Experiment, *Space Sci. Rev.* 25, pp 357-430
- Ebel, A., G. Hartmann, R. Leitinger, G. Schmidt, J.P. Schödel, 1969, Vergleichende Auswertung von Faraday-Effekt-Beobachtungen zweier Empfangsstationen. *Zs. Geophysik* 35, pp. 373-411
- Kersley, L. (editor), 1994, Proceedings of the International Beacon Satellite Symposium, University of Wales, Aberystwyth, UK, 11-15 July 1994
- Leitinger, R., G. Schmidt, A. Tauriainen, 1975, An evaluation method combining the Differential Doppler measurements from two stations that enables the calculation of the electron content of the ionosphere. *J. Geophysics (Zs. Geophysik)* 41, pp. 201-213
- Titheridge, J. E., 1972, Determination of ionospheric electron content from the Faraday rotation of geostationary satellite signals. *Planet. Space Sci.* 20, pp. 353-369

MAPPING AND PREDICTING THE IONOSPHERE

Stefan Schaer, Gerhard Beutler, Markus Rothacher
Astronomical Institute, University of Berne
CH-3012 Berne, Switzerland

ABSTRACT

The Center for Orbit Determination in Europe (CODE) produces daily maps of the Earth's ionosphere on a regular basis since January 1, 1996. These global ionosphere maps (GIMs) are derived from exactly the same GPS tracking data — doubly difference carrier phase measurements — as those used for the determination of CODE core products delivered to the IGS like precise GPS orbits, earth orientation parameters (EOPs), station coordinates and velocities. For the ionospheric product we have to analyze the so-called *geometry-free* linear combination (LC), which primarily contains ionospheric information, as opposed to the ionosphere-free LC, which contains the “geometrical” information and completely eliminates the influence of the ionospheric refraction (ignoring higher-order terms). At present (March 1998), the GPS tracking network processed at CODE consists of more than 110 globally distributed stations of the International GPS Service for Geodynamics (IGS).

After reprocessing all 1995 IGS data using the “Bernese Processing Engine” [Rothacher et al., 1996a], a long-time series of daily GIM parameters covering a time span of about 3.2 years is at our disposal. On the one hand this ionosphere time series reveals the evolution of the total electron content (TEC) on a global scale, on the other hand it indicates that short-term as well as long-term predictions for CODE GIM parameters are possible. We discuss the time series for a few selected TEC parameters and develop a method to predict the TEC parameters. Furthermore, we describe how the temporal resolution can be increased when using spherical harmonic (SH) expansions to model the global TEC. First attempts estimating 2-hour maps are encouraging.

CODE'S IONOSPHERE PRODUCTS — AN OVERVIEW

The principles of the TEC mapping technique used at CODE were described in [Schaer et al., 1995] and [Schaer et al., 1996a].

At present the following ionosphere products are generated on a routine basis:

- 24-hour global ionosphere maps (GIMs) are produced using double-difference phase or phase-smoothed code observations. The phase-derived TEC maps proved their usefulness for ambiguity resolution (AR) on long baselines [Rothacher et al., 1996b].
- *Rapid* global maps are available with a delay of about 12 hours, the *final* ones after 3 days (in the IONEX format [Schaer et al., 1998]).
- Regional (European) maps are produced as well and are also used to support AR. On the average 90% of the initial carrier phase ambiguities can be resolved reliably — without making use of code measurements. Daily IONEX files containing hourly snapshots of the ionosphere are made available via anonymous ftp.
- Daily sets of differential code biases (DCBs) for all GPS satellites (and the contributing receivers) are estimated at CODE since October 1997.

Figure 1 shows the daily DCB estimates (dots) for 27 GPS satellites from day 022, 1998, to day 071, 1998, and the combined DCBs (circles) aligning all satellite-specific DCBs in the sense that the overall mean becomes *zero* (to obtain a virtual, but very stable reference). However, there are a couple of PRNs with *drifting* DCBs with respect to the remaining PRNs. PRN 08, which was launched few months ago, shows a significant drift of almost -0.5 ns over 50 days. We observe an increased root-mean-square error (RMS) for this satellite when assuming and modeling the DCBs as constant quantities (see Figure 1 and Table 1).

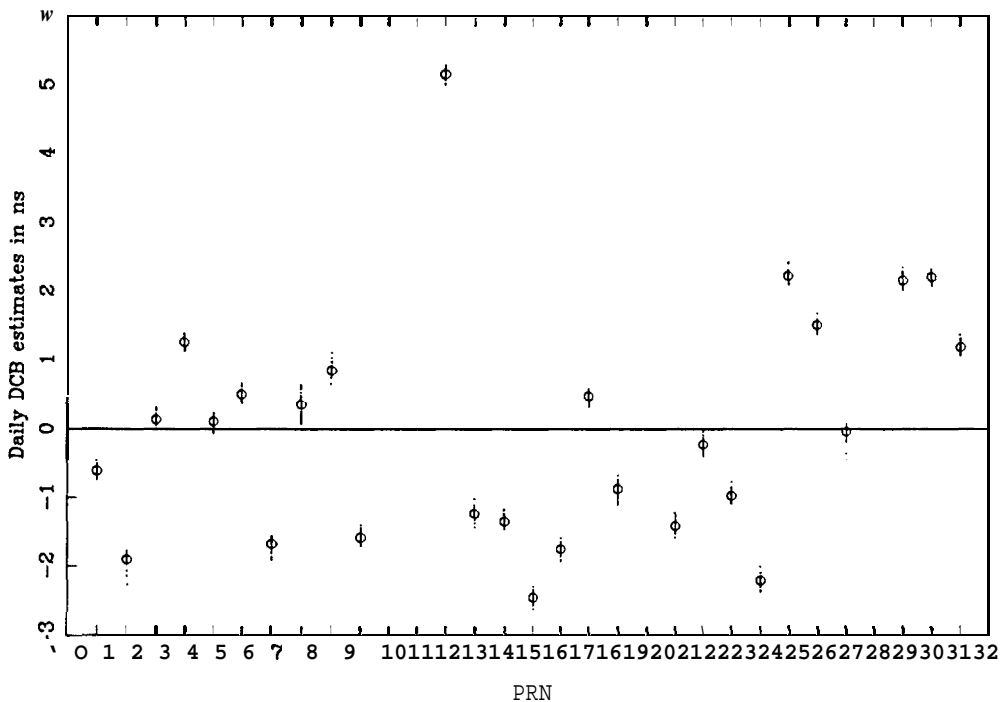


Figure 1. Daily PRN-specific DCB estimates (dots) for 27 GPS satellites from day 022, 1998, to day 071, 1998, and combined DCBs (circles)

The *combined* values of the satellite-specific DCBS taking into account the variance information of the individual solutions are listed in Table 1. In addition, the weighted RMS (WRMS) of the daily estimation is given for each PRN. The total WRMS of the 50-day DCB combination amounts to 0.08 ns. Let us mention that the estimated receiver-specific DCBs are of the order of ± 15 ns and show a day-to-day scattering highly depending on the station considered, Note that the DCB results presented here originate from a special solution where we simultaneously estimate n station-specific TEC models leading to $16n$ TEC plus $n + 27$ DCB parameters per day in total, where n is the number of stations processed.

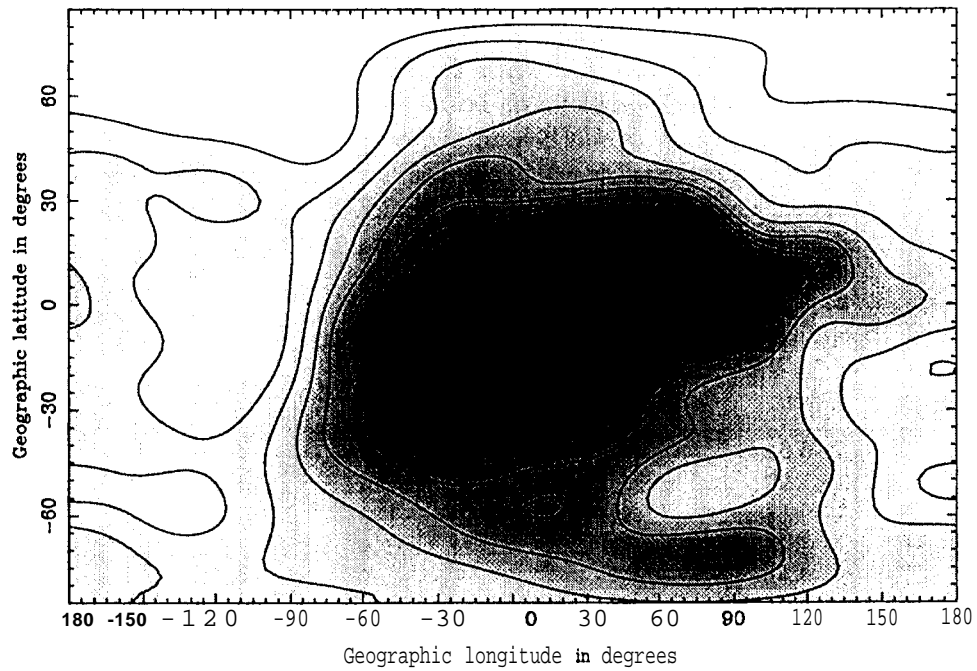
Table 1. Combined DCBS and weighted RMS errors of daily estimation

PRN	DCB (ns)	WRMS (ns)	PRN	DCB (ns)	WRMS (ns)
01	-0.63	0.06	17	-1.74	0.06
02	-1.90	0.07	18	+0.49	0.07
03	+0.14	0.06	19	-0.87	0.08
04	+1.26	0.06	21	-1.41	0.08
05	+0.11	0.07	22	-0.23	0.06
06	+0.51	0.07	23	-0.97	0.06
07	-1.68	0.11	24	-2.19	0.06
08	+0.35	0.16	25	+2.23	0.05
09	+0.86	0.07	26	+1.51	0.09
10	-1.57	0.07	27	-0.04	0.08
13	+5.16	0.06	29	+2.17	0.07
14	-1.22	0.07	30	+2.22	0.06
15	-1.34	0.07	31	+1.19	0.07
16	-2.43	0.08			

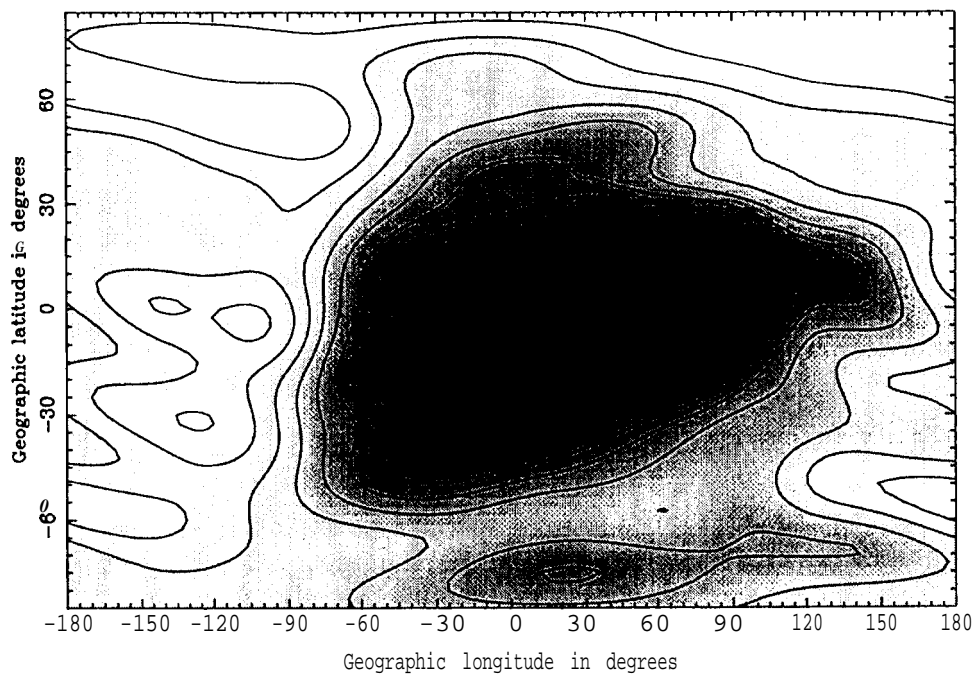
Figure 2 shows snapshots of (a) a phase-derived and (b) a code-derived 24hour TEC map for day 017, 1998 (taken at 12:00 UT). The number of contributing stations was 79 on that particular day. Light fields indicate small TEC, dark ones large TEC (up to 37.6 and 39.0 TECU here). The level lines are drawn at intervals of 2.5 TECU. There is no significant difference between the two maps.

LONG-TIME SERIES OF GLOBAL TEC PARAMETERS

The long-time series of global TEC parameters available at CODE covers over 1168 days and includes $(8 + 1)^2 = 81$ SH coefficients (the SH expansion was truncated at degree and order 8). The zero-degree SH coefficient representing the mean TEC on a global scale characterizes the ionospheric activity pretty well. The evolution of this particular TEC parameter during a period of low solar activity is shown in Figure 3. The daily estimates (dots) and a smoothed curve to better visualize the behavior are given. One recognizes a long-term trend caused by the 11-year solar cycle, annual and semi-annual variations, and relatively strong short-term fluctuations with periods of the order of 27 days due to the Sun's rotation. We clearly see maxima at equinox and minima at solstice, however, the minima in summer are more pronounced than those in winter. The recent ionospheric minimum was observed in summer 1996.



(a) *Phase-derived* TEC map



(b) *Code-derived* TEC map

Figure 2. 24-hour TEC maps for day 017, 1998

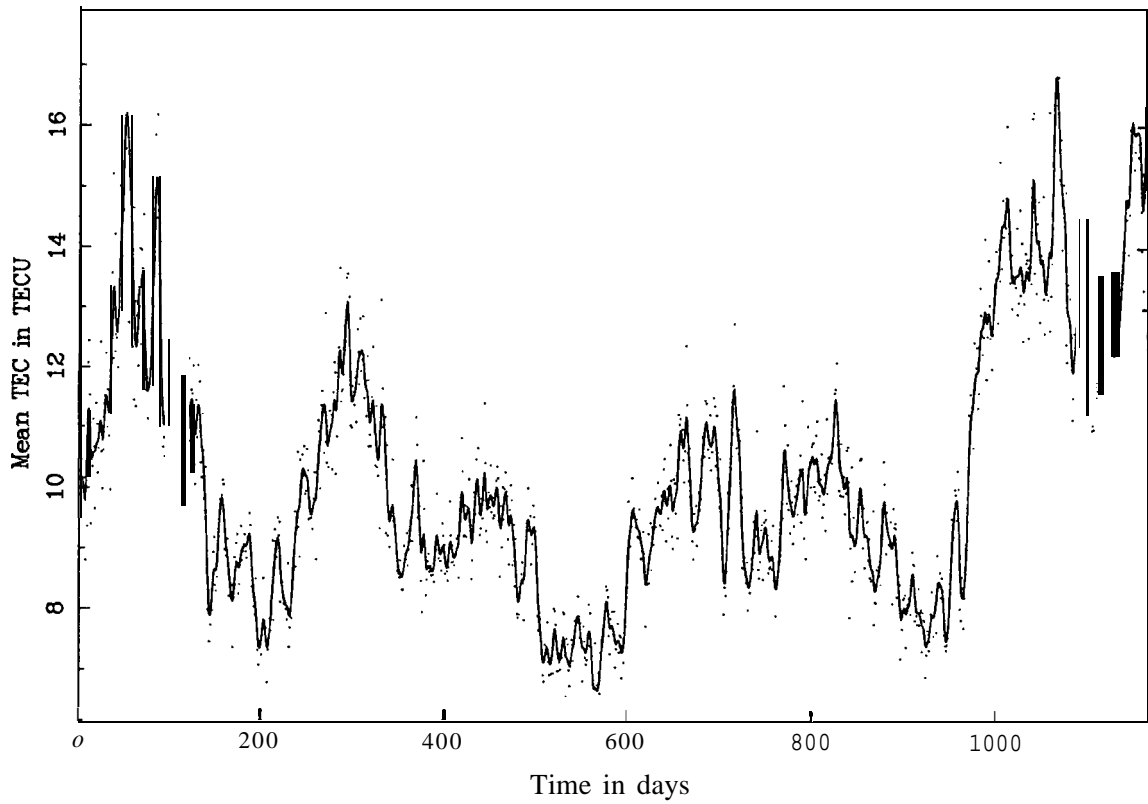
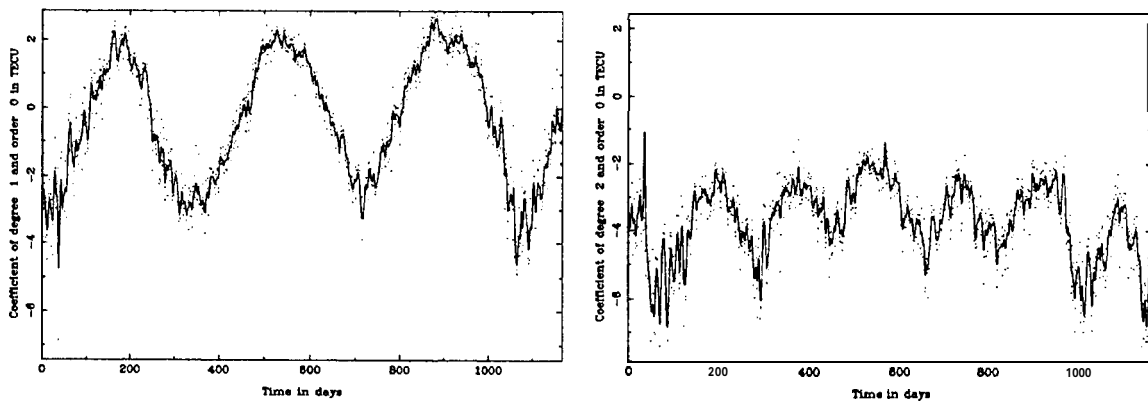


Figure 3. Zero-degree coefficient (mean TEC) from day 001, 1995 to day 072, 1998

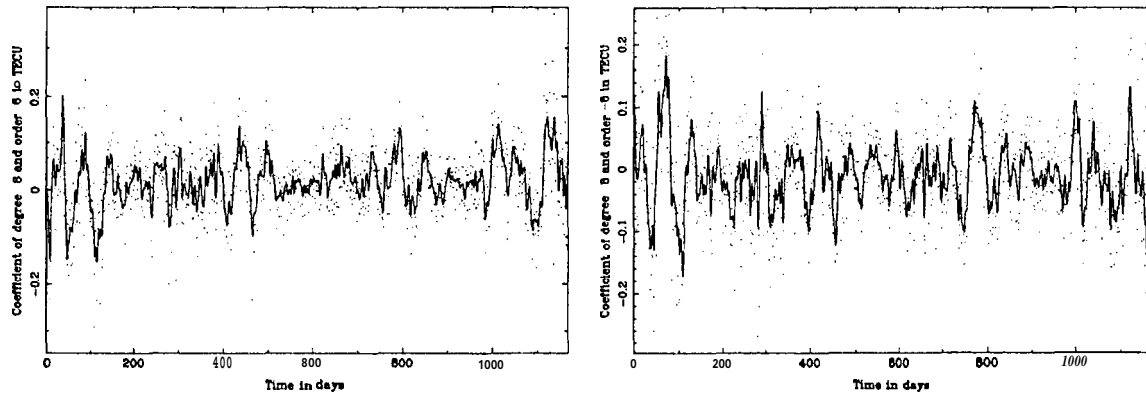
Figures 4 and 5 illustrate a few other SH coefficients showing similar periodicities and features as mentioned above.



(a) Term of degree 1 (and order 0)

(b) Term of degree 2 (and order 0)

Figure 4. Zonal SH terms



(a) Cosine term of degree 8 and order 6

(b) Sine term of degree 8 and order 6

Figure 5. Tesser SH terms

When correlating the mean TEC values and the 10.7-cm solar flux, the correlation factor is almost 0.8, reaching its maximum at a lag of 1 day.

PREDICTING THE IONOSPHERE

Let us split up the “ionospheric signal” l — a time series of SH TEC parameters $e_{ij}(t_k)$ — into a *deterministic* component d , which can be represented by a so-called trend function $\Phi(t)$, a *stochastic* component s , and a noise component n :

$$l = d + s + n \quad \text{or} \quad l - \Phi(x_0) = Ax + s + n. \quad (1)$$

As our trend function we use a harmonic expansion with a few prominent periods (11, 1, and 1/2 years)

$$\Phi(t) = a_0 + \sum_{i=1}^m (a_i \cos(\omega_i t) + b_i \sin(\omega_i t)) \quad \text{with} \quad \omega_i = \frac{2\pi}{\tau_i}. \quad (2)$$

The unknown parameters x of the trend function are estimated in a least-squares adjustment

$$x = (A^T C_{zz}^{-1} A)^{-1} A^T C_{zz}^{-1} (l - \Phi(x_0)), \quad (3)$$

where

$$x^T = [a_0, a_1, b_1, \dots, a_n, b_n] \quad \text{and} \quad C_{zz} = C_{ss} + C_{nn}. \quad (4)$$

C_{ss} and C_{nn} are the covariance matrices for the actual “signal” and the pure “noise”, respectively. Finally, if we perform short-term predictions (or interpolations), the *stochastic* component s is of interest, too:

$$\begin{bmatrix} s \\ n \end{bmatrix} = \begin{bmatrix} C_{ss} \\ C_{nn} \end{bmatrix} C_{zz}^{-1} (l - \Phi(x)). \quad (5)$$

The autocovariance function γ , which is used to set up the covariance matrices C_{ss} and C_{zz} , may be evaluated as

$$\gamma(h \Delta t) = \frac{1}{n} \sum_{k=1}^{n-|h|} (e_{ij}(t_k) - \Phi(t_k))(e_{ij}(t_{k+|h|}) - \Phi(t_{k+|h|})). \quad (6)$$

$h \Delta t$ denotes the lag; $\gamma(0)$ is the variance of the stochastic component.

The autocovariance function (ACF) of the mean TEC, i. e., the SH coefficient coo , is given in Figure 6. We notice that the ACF mainly reflects the Sun’s rotation period of approximately 27 days.

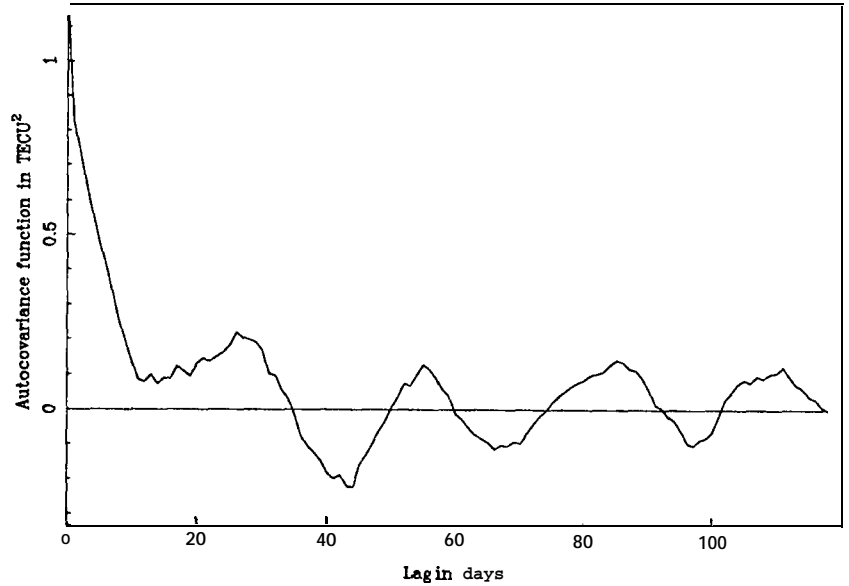
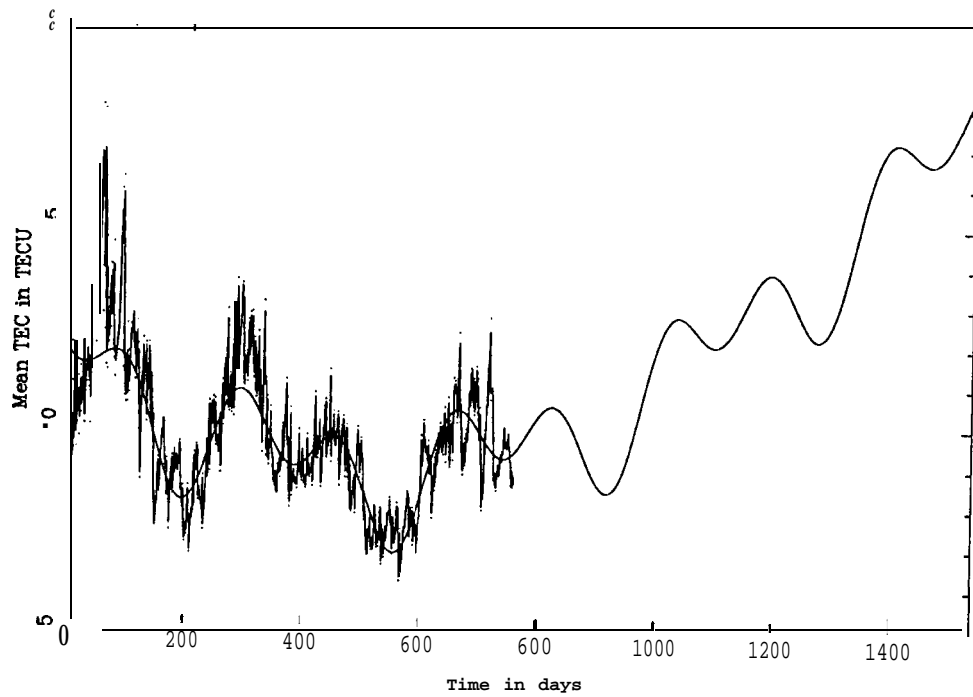
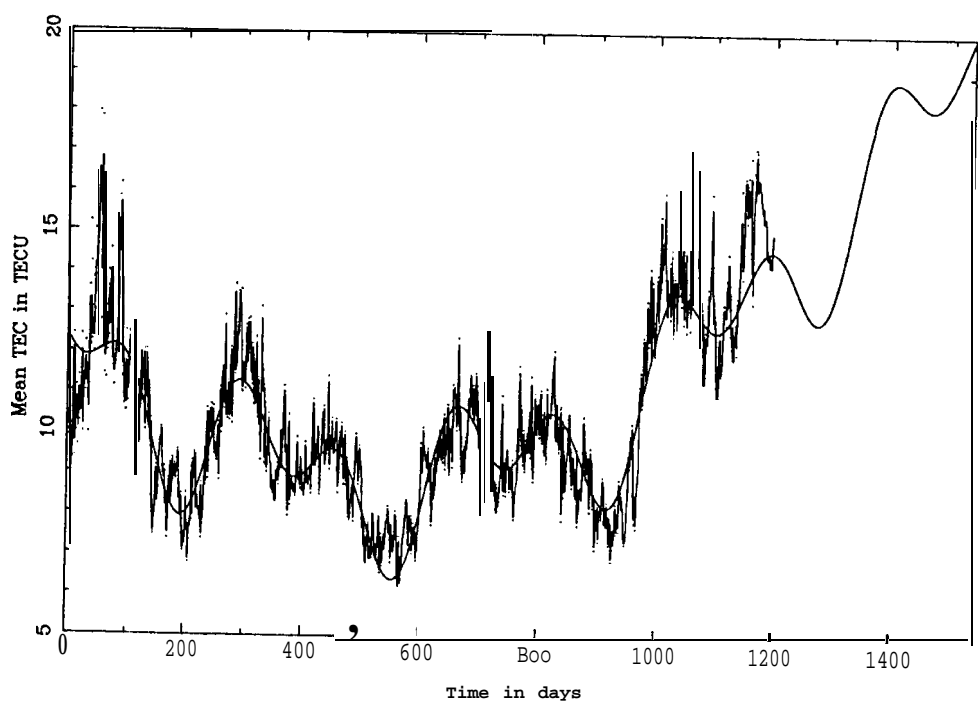


Figure 6. Autocovariance function of zero-degree coefficient for lags up to 120 days

Figure 7 shows the results when predicting (and interpolating) the mean TEC based on (a) a two-year time series *only* and (b) the complete time series. The daily GIM estimates are represented by dots. The trend function $\Phi(t)$ is given by the solid, smooths line and follows the general signal pretty well. It is amazing, considering that the time span of two years is quite short compared to a solar cycle, how well the extrapolated trend function shown in Figure 7a matches the real TEC observations shown in Figure 7b. The rapidly varying line also includes the *stochastic* component covering a prediction length of 30 days.



(a) 1995-1996 GIM data



(b) All GIM data

Figure 7. Prediction of mean TEC based on (a) a two-year time series and (b) the complete time series

When inspecting Figure 7 we see that the prediction consisting of $\mathbf{d} + \mathbf{s}$ does not exactly match the daily estimates because the matrix \mathbf{C}_{nn} is not a zero matrix but contains the variances provided by the primary ionosphere parameter estimation.

By performing the least-squares collocation step for each SH coefficient using the same prediction length, merging the predicted TEC coefficients to a full set of SH parameters, and writing a corresponding GIM file, we get a procedure that allows us to predict entire CODE GIMs! A software tool solving that task has been developed.

HIGH TEMPORAL RESOLUTION TEC USING SPHERICAL HARMONIC EXPANSIONS

In this section we discuss a method on how to increase the temporal resolution of the TEC representation when using spherical harmonic (SH) expansion.

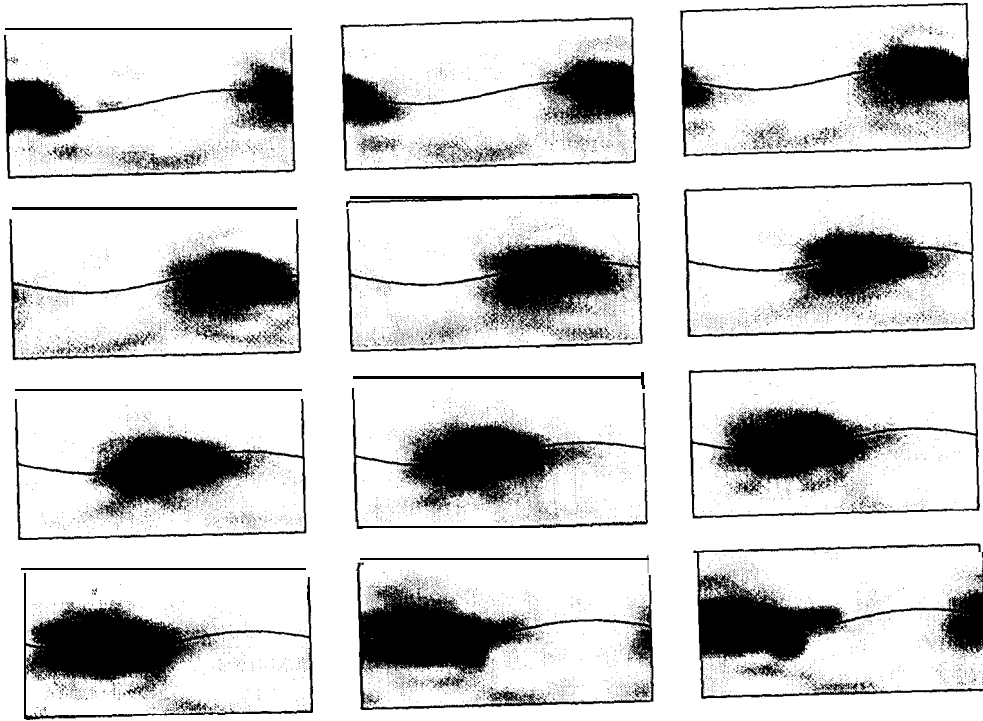
SH expansions are well suited to model time-independent quantities given on a spherical surface. When dealing with the ionosphere, the entire sphere is probed by GPS stations when deriving one-day TEC maps. The disadvantage is a poor temporal resolution because of the assumption of a “frozen” ionosphere co-rotating with the Sun. However, the general ionospheric behavior may well be described with daily TEC maps. When generating several TEC maps per day, one has to expect at times unreasonable — very high or negative — TEC estimates in regions where no stations are located. One may avoid such problems by limiting the variations between consecutive TEC maps with “relative” a priori constraints between consecutive maps by adding “relative” pseudo-observations of the type

$$\Delta e_{ij} = e_{ij}(t_k) - e_{ij}(t_{k-1}) = 0 \text{ for } k = 2, \dots, n \quad (7)$$

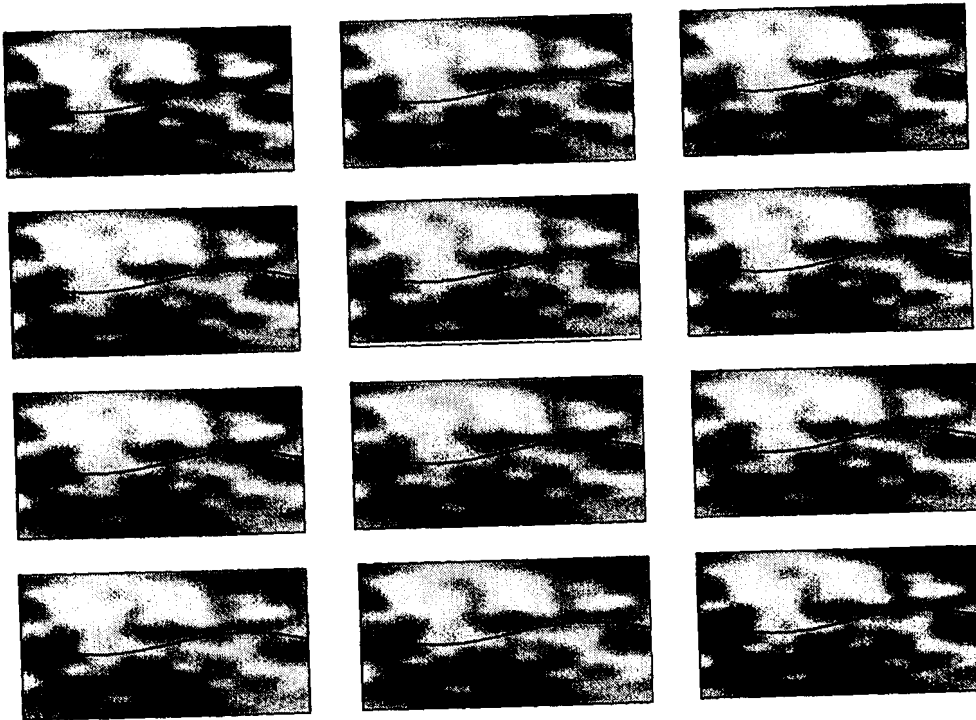
to the system of normal equations stemming from actual observations. Note that the a priori sigmas $\sigma_{\Delta e_{ij}}$ used for the pseudo-observations Δe_{ij} do not affect the “absolute” TEC determinations. Optimal values for these sigmas have to be found experimentally. Due to the fact that we deal with *normalized* SH coefficients, we may simplify this problem by setting $\sigma_{\Delta e_{ij}} \approx \sigma_{\Delta e}$.

A series of 12 2-hourly TEC maps (taken at 01:00, 03:00, . . . 23:00 UT) is shown in Figure 8a. The typical double-peak structure co-rotating with the Sun fairly well follows the geomagnetic equator, even when referring the TEC representation to a solar-geographic coordinate system. Nevertheless, Figure 8a indicates that a solar-geomagnetic reference frame is more appropriate.

The associated RMS maps shown in Figure 8b describe the formal accuracy of the TEC as a function of earth-fixed coordinates and basically reflect the station coverage. “Light” regions indicate small RMS (see, e. g., Europe or North America), “dark” regions mean large RMS (see, e. g., the region around the station O’Higgins, Antarctica). The ratio of the largest and smallest RMS is about 11. Such RMS maps may be included in IONEX files [Schaer et al., 1998].



(a) TEC maps



(b) RMS maps

Figure 8. 2-hourly TEC and RMS maps for day O17, 1998

SUMMARY

The CODE Analysis Center produces global and European ionosphere maps by analyzing double-difference phase observations (using an interferometric processing technique) and phase-smoothed code observations (processing one-way observations) on a regular basis. Some changes were recently made in our processing scheme: The elevation cut-off angle was decreased from 20 to 10 degrees and at the same time the elevation-dependent observation weighting defining $\text{Cos}^2 z$ as weight on the zero-difference level, where z is the zenith distance, was activated. The maximum degree of the SH expansion was increased from 8 to 12 in order to be able to resolve smaller TEC structures like, e. g., the equatorial anomaly.

A higher temporal resolution when using SH expansions is possible by limiting the variations in time with slight "relative" constraints between consecutive sets of SH coefficients. The 2-hour results obtained are very encouraging. The higher the temporal resolution, the less important it is whether a solar-geographic or a solar-geomagnetic reference frame is used.

Daily sets of differential code biases for the GPS satellites (and receivers) are estimated at CODE since October 1997. The day-to-day scatter of the satellite-specific DCBS is about 0.08 ns. Finally, an approach based on a least-squares collocation to predict global TEC was developed. Approaching the next solar maximum, the knowledge of the ionosphere becomes more and more important. The access to *fast* and *up-to-date* ionospheric information is required by many applications.

OUTLOOK

We will start to produce global ionosphere maps with a 2-hour resolution in the near future. Furthermore we intend to derive predicted ionosphere maps on a regular basis (e. g., 2-day predictions).

The generation of global maps statistically describing the fluctuations of the TEC as presented in [Schaer et al., 1996b] is planned. Reprocessing all global data since 1995 becomes more and more important in view of the progress made in the ionosphere modeling.

It is our declared goal to continuously map the ionosphere for (at least) the next period of high solar activity and to study in particular the impact of the ionosphere on the IGS core products. The establishment of a future IGS ionosphere product as discussed at the IGS AC Workshop in Darmstadt, Germany [Feltens and Schaer, 1998] is another reason to continue these efforts.

REFERENCES

- Feltens, J. and S. Schaer, 1998, IGS Products for the Ionosphere, *Proceedings of the IGS AC Workshop*, Darmstadt, Germany, February 9-11, 1998.
- Rothacher, M., G. Beutler, E. Brockmann, S. Fankhauser, W. Gurtner, J. Johnson, L. Merivart, S. Schaer, T. A. Springer, and R. Weber, 1996a, *The Bernese GPS Software Version 4.0*, September 1996, Astronomical Institute, University of Berne, Switzerland.

- Rothacher, M., G. Beutler, E. Brockmann, L. Mervart, S. Schaer, T. A. Springer, U. Wild, A. Wiget, C. Boucher, and H. Seeger, 1996b, Annual Report 1995 of the CODE Analysis Center of the IGS, *1995 Annual Report of the IGS*, September 1996, IGS Central Bureau, JPL, Pasadena, CA, USA, pp. 151-173.
- Schaer, S., G. Beutler, L. Mervart, M. Rothacher, and U. Wild, 1995, Global and Regional Ionosphere Models Using the GPS Double Difference Phase Observable, *Proceedings of the IGS Workshop on Special Topics and New Directions*, Potsdam, Germany, May 15-17, 1995, pp. 77-92.
- Schaer, S., G. Beutler, M. Rothacher, and T. A. Springer, 1996a, Daily Global Ionosphere Maps Based on GPS Carrier Phase Data Routinely Produced by the CODE Analysis Center, *Proceedings of the IGS AC Workshop*, Silver Spring, MD, USA, March 19-21, 1996, pp. 181-192.
- Schaer, S., M. Rothacher, T. A. Springer, and G. Beutler, 1996b, Mapping the Deterministic and Stochastic Component of the Ionosphere Using GPS, *EOS Transactions of the 1996 AGU Fall Meeting*, Vol. 77, No. 46, p. 142.
- Schaer, S., W. Gurtner, and J. Feltens, 1998, IONEX: The Ionosphere Map EXchange Format Version 1, February 25, 1998, *Proceedings of the IGS AC Workshop*, Darmstadt, Germany, February 9-11, 1998.

Contributed Papers on other Topics

Experiences of the BKG in Processing GLONASS and Combined GLONASS/GPS Observations

Heinz Habrich
Federal Agency for Cartography and Geodesy
D-60598 Frankfurt Main, Germany

Abstract

The Global Navigation Satellite System (GLONASS) is operated by the Russian Space Forces, Ministry of Defence of the Russian Federation. The satellite's constellation and the signal in space of both GLONASS and GPS are comparable. This enables a geodetic usage of GLONASS with the availability of a 48 satellites constellation in the case of a combination of GLONASS and GPS observations.

A joint effort of the Astronomical Institute of Beme (AIUB) and the Federal Agency for Cartography and Geodesy (BKG, former Institute of Applied Geodesy) has been established to modify the Bernese GPS Software for the processing of GLONASS and combined GLONASS/GPS observations. The reference system and the system time for GLONASS are different from the corresponding GPS quantities and have to be considered. New algorithms for ambiguity resolution and cycle slip detection are used to account for the satellite-specific GLONASS frequencies. The BKG has processed GLONASS and combined GLONASS/GPS phase observations. The performed processing steps include the generation of combined GLONASS/GPS orbit files, cycle slip corrections and the resolution of the carrier phase ambiguities.

Introduction

GLONASS observations can be processed similarly to GPS, provided two basic characteristics are taken into consideration: (1) The broadcast satellite's positions refer to the PZ-90 reference frame and the system time is synchronized to UTC(Moscow). (2) GLONASS satellites transmit it's signal on satellite-specific frequencies. The first item is of importance for the combined processing of GLONASS and GPS observations. Orbit files must refer to a unique reference frame and the GLONASS system time has to be transformed to GPS time. At BKG combined orbit files in the SP3-format are generated. The second item has to be modelled carefully in the carrier phase observation equations.

The double difference observations show a new bias term, which effects the integer ambiguity parameters and the cycle slip detection.

The new ambiguity resolution algorithm solves successively for the integer ambiguities. Therefore the effect of the new bias term on the ambiguities is reduced to a minimum. In order to assign cycle slips to the correct satellites, a new iterative approach is used. Cycle slips detected by triple differences are applied to the correct single difference. New ambiguities are introduced, if cycle slips can not be assigned to a single satellite. The *new* approaches for ambiguity resolution and cycle slip correction can be used for GLONASS and GPS or combined GLONASS/GPS observations.

The BKG is operating a permanent GLONASS/GPS receiver at it's Fundamental Station **Wetzell**. Recorded observations are available in the **RINEX** format.

Generation of Combined GLONASS/GPS Orbits

In order to process combined GLONASS/GPS observations an orbit file containing navigation messages of both GLONASS and GPS satellites has to be generated. Table 1 shows differences of the two systems which are most relevant for a combination.

	GLONASS	GPS
Reference System	PZ-90	WGS-84
System Time	GLONASS time, UTC - GLONASS <1 μ sec (since July 1, 1997)	GPS time, GPS - UTC = 12 sec (January 1998)
Broadcast Ephemerides	satellite's position, velocity and acceleration, every 15 and 45 min	modified Kepler elements, every full hour
Carrier Frequency	L1 :1602 + k* 0.5625 MHz L2: 1246+ k* 0.4375 MHz ,k=1,2,...,24	L1: 1575.42 MHz L2: 1227.60 MHz

Table 1: GLONASS/GPS System Differences

A combined orbit file in the **WGS-84** reference system, referred to the GPS time scale, can be generated in the **SP3-format**. The required transformations are shown in Figure 1, supporting the existence of both GLONASS and GPS **RINEX** navigation files. Concerning GLONASS, the **RINEX** format has currently been extended [Gurtner, 1997]. GPS position coordinates for the **SP3-file** epochs are calculated from Kepler elements. Epochs of the GLONASS navigation data are transferred to GPS time through adding an integer number of seconds (e.g. 12 sec for January 1998). The position, velocity and

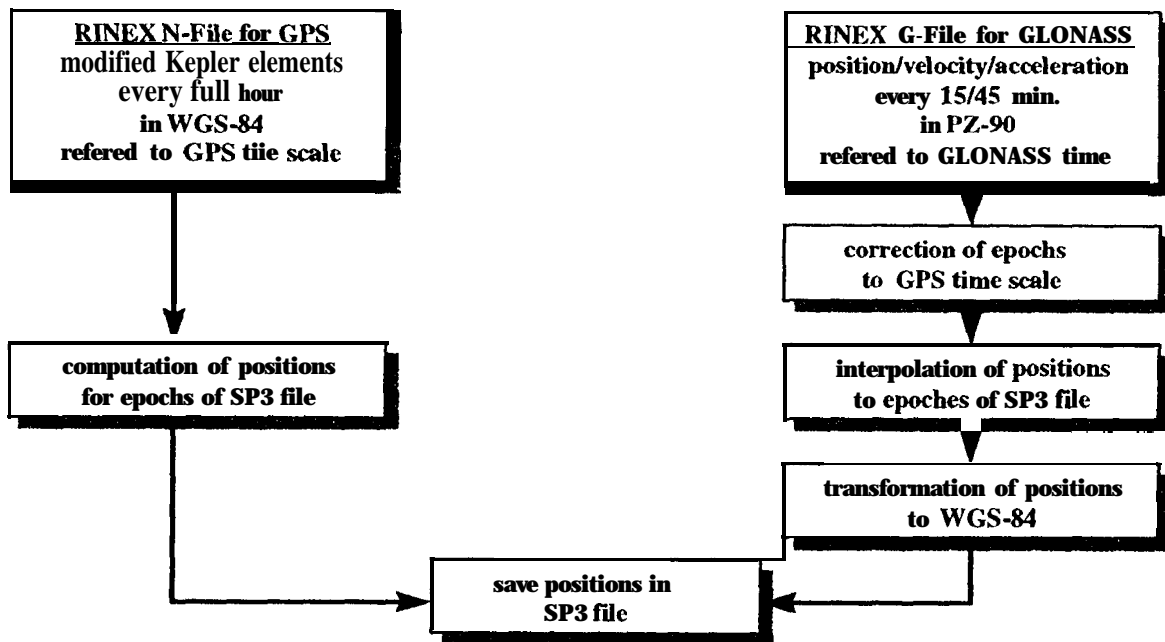


Figure 1: Generation of Combined SP3-Orbit Files

acceleration of the GLONASS satellites are given for the epochs of the broadcast ephemerides and used to compute the position for the SP3-file epochs. For the interpolation of positions we use formulas according to [ICD, 1995] within a time interval of 15 min. These formulas are given in Table 2 and account for the

- central part of Earth's gravitational potential,
- zonalgeopotential effects characterized by C_{20} ,
- . approximate transformation between celestial and terrestrial coordinate system,
- . accelerations caused by sun and moon,

The Runge-Kutta method can be used for the necessary numerical integrations. Figure 2

$$\begin{aligned}
 \ddot{x} &= -\frac{\mu}{r^3} \cdot x + \frac{3}{2} \cdot C_{20} \cdot \frac{\mu \cdot a^2}{r^5} \cdot x \cdot \left(1 - \frac{5 \cdot z^2}{r^2}\right) + \omega^2 \cdot x + 2 \cdot \omega \cdot \dot{y} + \ddot{X} \\
 \ddot{y} &= -\frac{\mu}{r^3} \cdot y + \frac{3}{2} \cdot C_{20} \cdot \frac{\mu \cdot a^2}{r^5} \cdot y \cdot \left(1 - \frac{5 \cdot z^2}{r^2}\right) + \omega^2 \cdot y - 2 \cdot \omega \cdot \dot{x} + \ddot{Y} \\
 \ddot{z} &= -\frac{\mu}{r^3} \cdot z + \frac{3}{2} \cdot C_{20} \cdot \frac{\mu \cdot a^2}{r^5} \cdot z \cdot \left(3 - \frac{5 \cdot z^2}{r^2}\right) + \ddot{Z}
 \end{aligned}$$

Table 2: Approximate Equation of Motion for GLONASS Satellites

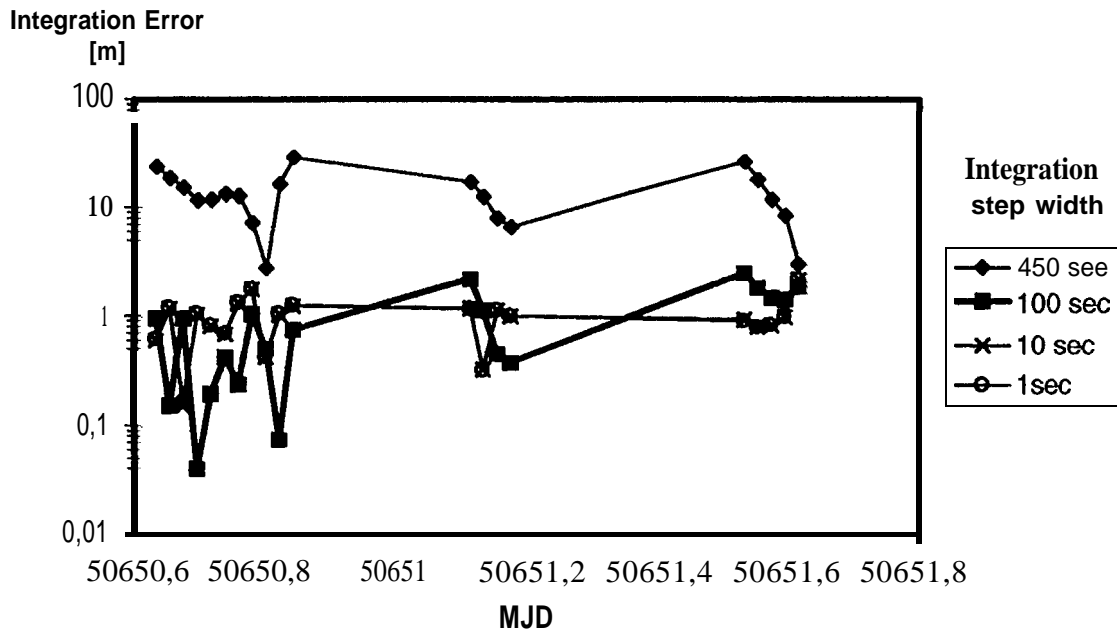


Figure 2: Numerical Integration error for X-Component, 15 min intervals

shows the discrepancies between a forward integration for the X-component (initial value is the broadcast position for epoch i) and a backward integration (initial value is the broadcast position for epoch $i + 30 \text{ rein}$) for the epoch $i + 15 \text{ min}$, using four different integration step widths (450, 100, 10 and 1 sec). The 10 sec and 1 sec integration step width lead to nearly identical results.

The GLONASS satellite positions are transformed from PZ-90 to WGS-84 and then stored in the SP3-format. Two sets of approximate transformation parameters have been estimated in 1996 as given in Table 3.

$\begin{bmatrix} x \\ y \\ z \end{bmatrix}_{\text{WGS-84}} = \begin{bmatrix} 1 & -0.33'' & 0 \\ 0.33'' & 1 & 0 \\ 0 & 0 & 1 \end{bmatrix} \cdot \begin{bmatrix} u \\ v \\ w \end{bmatrix}_{\text{PZ-90}}$	<p>Roßbach et al. 1996</p> <p>Post-fit residuals: 30 - 40 cm</p>
$\begin{bmatrix} x \\ y \\ z \end{bmatrix}_{\text{WGS-84}} = \begin{bmatrix} 0 \\ 2.5\text{m} \\ 0 \end{bmatrix} + \begin{bmatrix} 1 & -0.39'' & 0 \\ 0.39'' & 1 & 0 \\ 0 & 0 & 1 \end{bmatrix} \cdot \begin{bmatrix} u \\ v \\ w \end{bmatrix}_{\text{PZ-90}}$	<p>Misra et al. 1996</p> <p>Post-fit residuals: 1 - 30 m</p>

Table 3: Transformation Parameters, PZ-90 to WGS-84

The combined **SP3-file** includes also clock corrections for **GLONASS** and GPS satellites. Clock and frequency corrections are transmitted by the GLONASS satellites and are used to compute the satellite clock correction for the **SP3-file** epochs.

Phase Observable

The satellite specific frequencies (**resp.** wavelengths) have to be **modelled** correctly for the phase observable. This leads to the following observation equations:

Zero Difference Observable

$$\Psi_k^i = c \cdot \tau_k^i + N_k^i \cdot \lambda^i + c \cdot \Delta t_k - c \cdot \Delta t^i$$

where

c	=	Velocity of light
τ_k^i	=	Signal travel time between satellite i and receiver k , including the tropospheric and ionospheric bias
N_k^i	=	Unknown integer number of cycles (ambiguity)
λ^i	=	Nominal wavelength of signal from satellite i
Δt^i	=	Satellite clock error at time of emission
Δt_k	=	Receiver clock error at time of reception

Single Difference Phase Observable

$$\Delta\Psi_{kl}^i = c \cdot \Delta\tau_{kl}^i + N_{kl}^i \cdot \lambda^i + c \cdot \Delta t_{kl}$$

where

$$\begin{aligned}\Delta\tau_{kl}^i &= \tau_k^i - \tau_l^i \\ N_{kl}^i &= N_k^i - N_l^i \\ \Delta t_{kl} &= t_k - t_l\end{aligned}$$

Double Difference Phase Observable

$$\Delta\Delta\Psi_{kl}^{ij} = c \cdot \Delta\Delta\tau_{kl}^{ij} + N_{kl}^{ij} \cdot \lambda^i + N_{kl}^j \cdot \Delta\lambda^{ij}$$

where

$$\begin{aligned}\Delta\Delta\tau_{kl}^{ij} &= \Delta\tau_{kl}^i - \Delta\tau_{kl}^j \\ \Delta\lambda^{ij} &= \lambda^i - \lambda^j \\ N_{kl}^{ij} &= N_{kl}^i - N_{kl}^j\end{aligned}$$

The double differences show the new bias term $b^{ij} = N_{kl}^j \cdot \Delta\lambda^{ij}$ which

- destroys the integer nature of the ambiguities,
- . depends on the wavelength differences of the two satellites
- . needs single difference ambiguities N_{kl}^j to be known.

The integer ambiguities may be found, if the bias term is smaller than 0.1 cycles. This is true for small wavelength differences of the two satellites or if the single difference ambiguities are known with an accuracy of a few cycles. Table 4 shows examples in units of the reference wavelength λ_0 .

	$\Delta\lambda$ [cycles of λ_0]	maximum allowed N_{kl}^j for $b_{ij} \leq 0.1$ [cycles of λ_0]
GLONASS-GLONASS (rein)	0.0035	285
GLONASS-GLONASS (max)	0.0081	12
GPS-GLONASS (max)	0.0253	4

Table 4: Numerical Values for Single Difference Bias Term

For the minimum wavelength difference for two GLONASS satellites the single difference ambiguities N_{kl}^j have to be known within an accuracy of 285 cycles which is possible, e.g. after computing a Code single point positioning.

Ambiguity Resolution

The single difference bias term causes problems for the ambiguity resolution. With the assumption, that the single difference ambiguities N_{kl}^j are known with an accuracy of e.g. 200 cycles, we can resolve the ambiguities of satellite pairs with small wavelength differences, but not for those with larger wavelength differences (see Table 4). To overcome this problem, an iterative approach is used.

The ambiguities of satellite pairs with small wavelength differences are solved first. The following iterations show significant smaller RMS errors for the single difference ambiguities and allow the ambiguity resolution for satellite pairs with larger wavelength difference. The ambiguity resolution algorithm can be summarised to six steps as given in Table 5.

The RMS errors for double difference ambiguities as computed in step 3) of Table 5 are given in Figure 3; the RMS errors depend on the wavelength difference of the two satellites. Due to the single difference bias term, for small wavelength differences the double difference ambiguities can be fixed to an integer number with the first iteration. The rectangular symbols show the RMS errors of the corresponding iteration step, when the ambiguities were fixed to an integer. Due to the iterative procedure, even for large wavelength differences the RMS values are smaller than 0.1 cycles.

-
- 1) Set up n single difference ambiguities N_{kl}^j for n satellites as unknown parameters (singular).
 - 2) Introduce a priori constraint for N_{kl}^j (e.g. 300 cycles) and compute first solution vector with covariance matrix.
 - 3) Compute all possible double difference ambiguities N_{kl}^{jj} and the corresponding formal errors (integer destroyed by bias term).
 - 4) Fix the best determined double difference ambiguity to an integer number.
 - 5) Eliminate one single difference ambiguity from the normal equation system. If $\Delta\lambda \neq 0$:
 - a) Normal equation system is now regular.
 - b) RMS error of N_{kl}^j decreases significantly in next iteration.
- Next iteration, (n-1) single difference ambiguities N_{kl}^j may be eliminated.
- 6) Estimate the unresolved N_{kl}^j as real value in the final solution.
-

Table 5: Ambiguity Resolution Approach

Figure 4 shows the RMS errors of the single difference ambiguities as computed in each iteration step. In each of the first eleven iterations one ambiguity between two GPS satellites (identical wavelength) has been resolved. This does not improve the RMS error. In the twelfth iteration step the wavelength difference of the corresponding satellite pair was not equal zero, leading to a decreased RMS error for the single difference ambiguities.

Figure 5 shows the fractional parts of the ambiguities, solved for pairs of two GPS satellites, two GLONASS satellites and a GPS/GLONASS satellite pair.

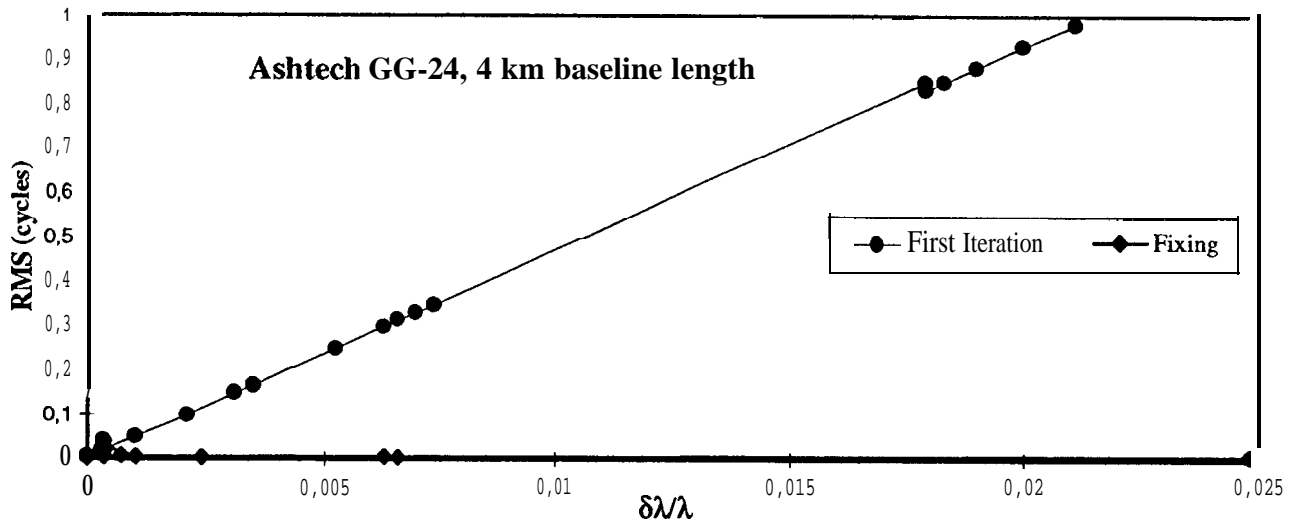


Figure 3: RMS Error of Double Difference Ambiguities

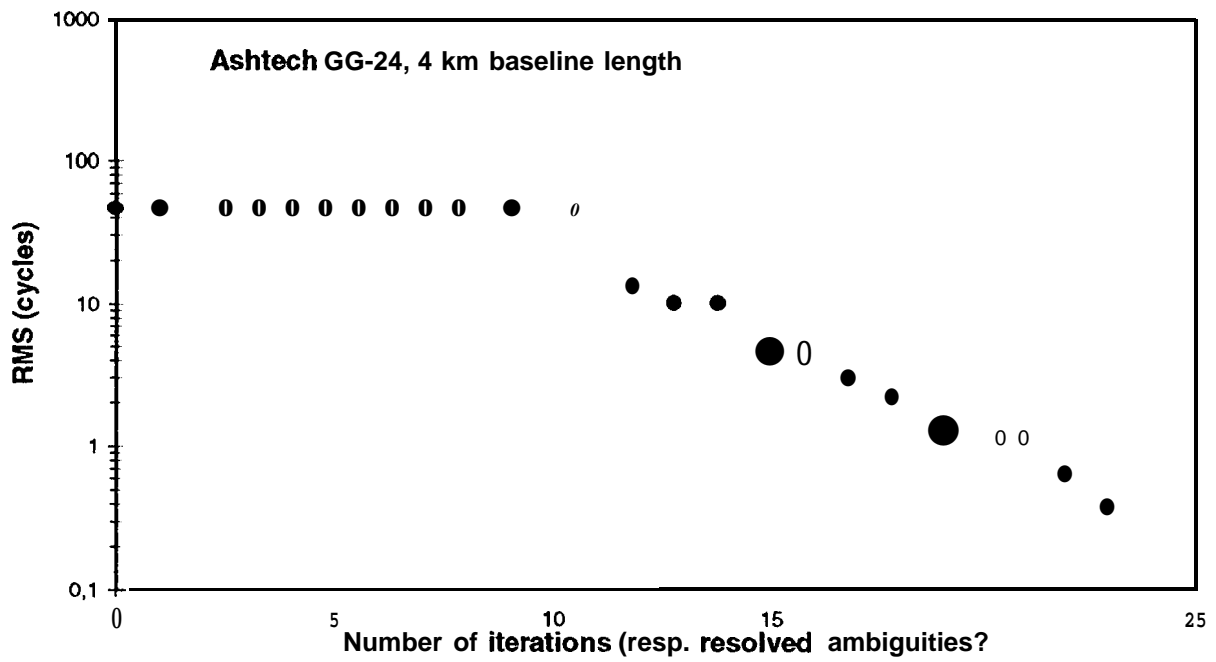


Figure 4: RMS Error of Single Difference Ambiguities

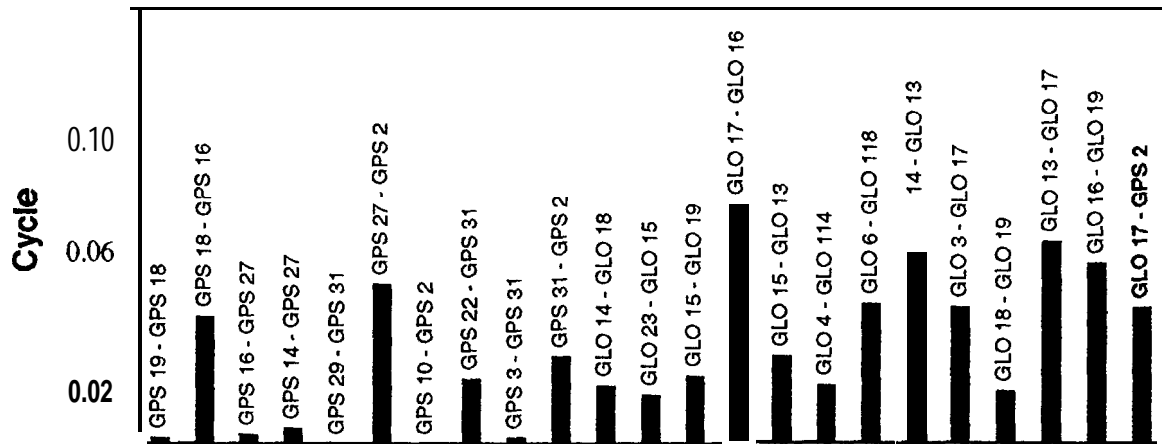


Figure 5: Fractional Parts of Resolved Ambiguities

Cycle Slip Detection

Two general qualities characterise the cycle slip detection for satellite specific frequencies:

- . A Cycle slip has to be assigned to the responsible involved satellite, i.e. applied to the correct single difference.
- New ambiguities have to be introduced for cycle slips, which can not be assigned to a specific satellite.

In order to detect cycle slips, the triple difference residuals can be interpreted as

$$\Delta\Delta\Delta r_{kl}^{ij}(t_2 - t_1) = b_i \cdot \lambda^i - b_j \cdot \lambda^j$$

with

$$b_i = N_{kl}^i(t_2) - N_{kl}^i(t_1)$$

$$b_j = N_{kl}^j(t_2) - N_{kl}^j(t_1).$$

The formulas above lead to following facts:

- Residuals are close to zero, if no cycle slip occurs.
- Residuals are singular for the determination of **b_i and b_j** .
- The difference (**$b_i - b_j$**) **can not be determined**, because $\lambda^i - \lambda^j \neq 0$.
- The cycle slip can be assigned to a single satellite, as soon as **b_i or b_j** is known (i.e. equal zero).

Three examples for cycle slips and the corresponding triple difference residuals are given in Table 6. A cycle slip of size „one cycle” was assumed for satellite i (resp. j) in example 1 (resp. 2). This slips will be detected, but can not be assigned to a specific satellite, because the triple difference residuals are not significantly different ($\Delta\lambda^{ij}$ is small compared to λ^i or λ^j). The cycle slips assumed for example 3 may not be detected.

Example	b_i	b_j	$\Delta\Delta\Delta r_{kl}^{ij}(t_2-t_1)$
1	1	0	λ^i
2	0	-1	$\lambda^i - \Delta\lambda^{ij}$
3	1	1	$\Delta\lambda^{ij}$

Table 6: Cycle slips in triple difference residuals

In order to calculate the integer numbers of cycles for the single difference observation corrections, the triple difference residuals have to be converted into units of cycles. Figure 6 shows two alternative methods for this conversion.

The integer numbers are destroyed by a bias term in both cases. Besides the wavelength difference, the bias term depends on the size of the slip (first formula) or the relative receiver clock error (second formula). Using the second formula, one can reduce the influence of the bias term through an estimation of the receiver clock error.

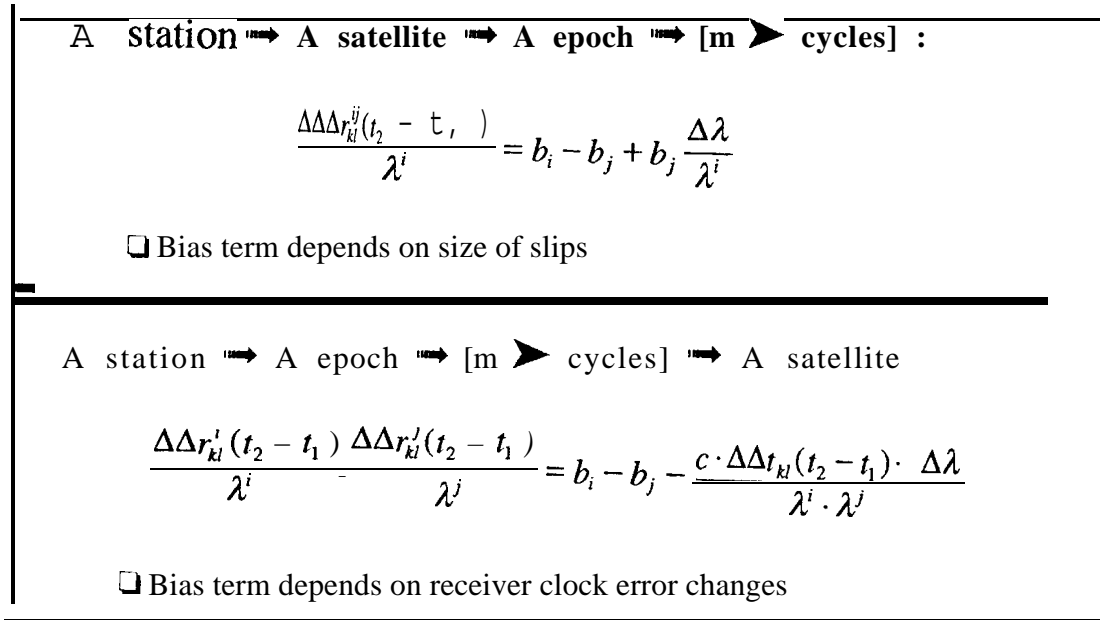


Figure 6: Triple Difference Residuals in Units of Cycles, two approaches

-
- 1) Compute triple difference residuals for all satellite pairs and select pairs with „no slip”.
 - 2) Find satellite pair with smallest $\Delta\lambda$ in all satellites with „no slip” and set $b_i=b_j=0$.
 - 3) Find satellite pair „with slip” which includes one of the „clean” satellites and assign the cycle slip to the other satellite.
 - 4) Correct cycle slip to the single difference observation and start next iteration.
 - 5) Introduce new ambiguities for cycle slips which could not be assigned to a single satellite.
-

Table 7: Iterative Approach for Cycle Slip Correction

Obviously the bias term is smallest, for smallest wavelengths differences of the two satellites. This leads to an iterative approach for cycle slip correction. A scheme for this algorithm is given in Table 7.

GLONASS Permanent Station Wettzell

The BKG operates a combined **GLONASS/GPS** dual frequency receiver at the Fundamental Station in **Wettzell** on a permanent basis. The receiver of type 3S-Navigation R10W40 has been installed in January 1996. Due to receiver failures an observation gap occurred in 1997. The receiver has been re-installed in January 1998 for a permanent tracking.

The receiver operates in the following mode:

- . Up to 5 GLONASS satellites on L 1, C/A-code,
- . up to 5 GPS satellites on L1, C/A-code,
- up to 8 GLONASS satellites on L2, P-code,
- 30 sec. measurement interval
- . receiver clock synchronisation to UTC,
- time transfer mode enabled.

The observation and navigation data are available in the **RINEX** format from BKG's anonymous ftp-server <[igs.ifag.de](ftp://igs.ifag.de)>.

Conclusion

It has been demonstrated, that GLONASS and combined GLONASS /GPS carrier phase observations can be processed. As a joint effort of AIUB and BKG, the Bernese GPS Software has been modified for the new requirements. Combined orbit files for GLONASS and GPS satellites were generated in the SP3-format. New approaches for ambiguity resolution and cycle slip detection were used, in order to take satellite specific frequencies into consideration. A satellite constellation of up to 48 satellites (combination of GLONASS and GPS) can be used for geodetic applications.

References

- Gurtner W. (1997): *RINEX, The Receiver Independent Exchange Format Version 2*, updated revision, Astronomical Institute University of Berne
- ICD (1995): *GLONASS Interface Control Document*, Coordinational Scientific Information Center of Russian Space Forces, Moscow, Russia
- Misra P. N., Abbot R. I., Gaposchkin E.M. (1996): *Transformation Between WGS-84 and PZ-90*, Proceedings of the 9th International Technical Meeting of the Satellite Division of the Institute of Navigation, ION GPS-96, Kansas City, Missouri
- Roßbach U., Habrich H., Zarraoa N. (1996): *Transformation Parameters Between PZ-90 and WGS-84*, Proceedings of the 9th International Technical Meeting of the Satellite Division of the Institute of Navigation, ION GPS-96, Kansas City, Missouri

PRECISE AUTONOMOUS EPHEMERIS DETERMINATION FOR FUTURE NAVIGATION SATELLITES

Miguel.M. Romay-Merino, Patrick van Niftrik

GMV, Isaac Newton 11, P.T.M. Tres Cantos, E-28760 Madrid, Spain

ABSTRACT

Ephemeris errors are one of the major contributors to the total UERE (User Equivalent Range Error) budget. The user positioning accuracy can be determined as the product between the UERE and the DOP (Dilution of Precision). To minimise the total positioning errors accurate ephemeris shall be computed in real time. In this paper the different algorithms that can be used to compute accurate orbits in real time are presented. They can be classified in:

- . On ground orbit determination algorithms
- . On-board orbit determination algorithms

This paper will be focused on on-board or autonomous orbit determination algorithms. Results obtained using simulated data indicate that those techniques would be able to provide accurate ephemeris if accurate tracking data is available.

REAL TIME ORBIT DETERMINATION ALGORITHMS

Three types of algorithms can be considered for orbit determination:

1. Dynamic algorithms
2. Reduce dynamic algorithms
3. Geometric algorithms

Geometric algorithms are not able to provide the required accuracy for high orbiting satellites, therefore those algorithms will not be considered here.

Dynamic algorithms are based on the integration of the satellite motion equations. Very accurate dynamic models are currently available, therefore it would be possible to

compute high accurate orbits using this type of algorithms. Their major drawback is that they require a significant amount of computational time, so they are in principle not valid for real time applications. In the other hand these algorithms are able to compute accurate orbit predictions, so orbit predictions could be used to compute in real time the ephemeris message to be sent to the user. This technique is schematically represented in the following figure:

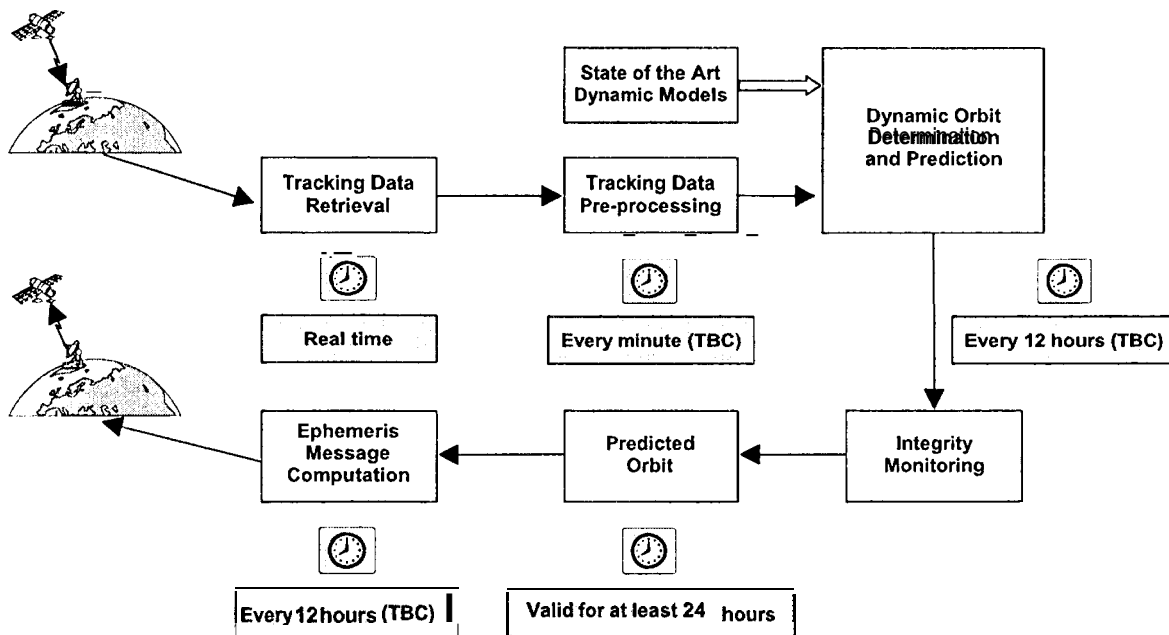


Figure 1 Schematic representation of a real time dynamic orbit determination algorithm

The tracking data is collected at the different ground stations and it is sent in real time to the MMCC (Mission Management Control Centre). At the MMCC the tracking data is retrieved and pre-processed shortly after the arrival. At regular time intervals (i.e. every 12 hours) the orbit determination program runs, and after an integrity check a new orbit prediction will be available. This orbit prediction will be valid for the next hours (for high orbiting satellites at least 24 hours), a very simple orbit model will be fitted to the predicted orbit, and the parameters of this model will be sent to the users (ephemeris message). With the ephemeris message the users will be able to determine the position of any satellite in the constellation at any epoch with the desired accuracy.

This technique requires to send the data to the MMCC, there a heavy processing is required, and then the ephemeris message has to be sent to the satellite, and finally the satellite will send back the ephemeris message to the users.

This scheme can be severely simplified if two way measurements (satellite-ground station-satellite) are considered, then the processing can be done on-board, where also the

ephemeris message will be computed and finally this message will be send to the users. If the integrity monitoring could also be done on-board the MMCC will not be responsible for any orbit determination activity.

This technique is schematically represented in the following figure:

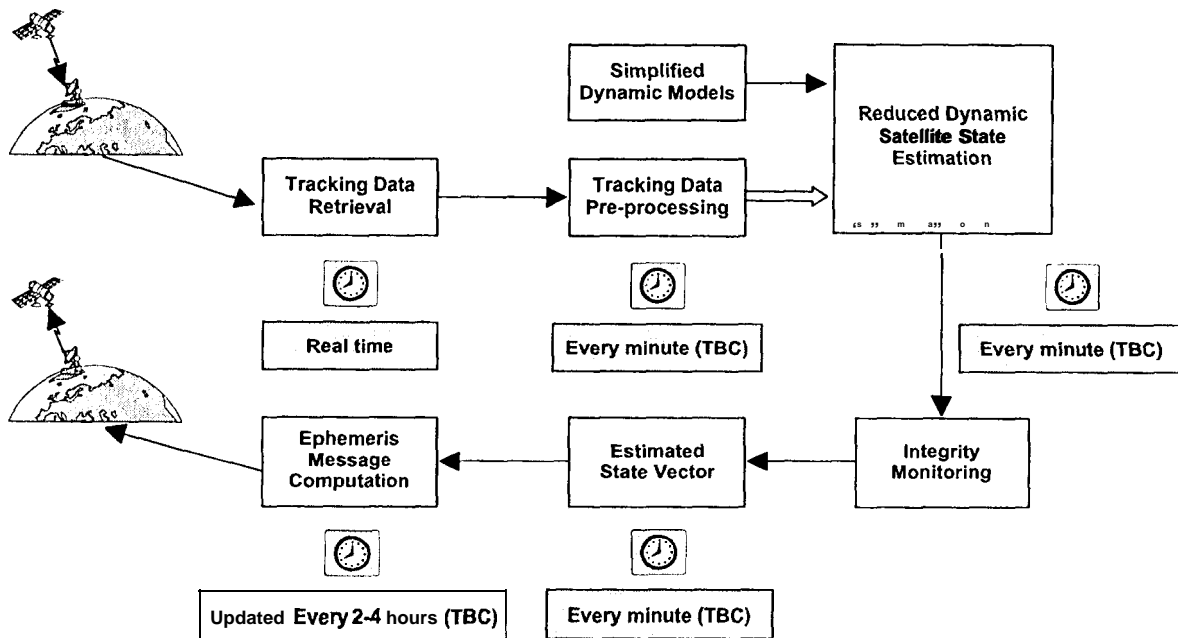


Figure 2 Schematic representation of a real time reduced dynamic orbit determination algorithm

This type of algorithms are only able to work in real time if the reduce dynamic algorithm is able to accomplish some very stringent requirements, like:

- . Low computational loads
- . Real time
- . Accuracy
- Integrity

The core of the proposed strategy is the estimation module. The estimation module which is proposed is a least squares algorithm including measurement's weight and a priori information. It can be demonstrated that this algorithm can be equivalent to a classical batch least squares algorithm, but also to a Kalman filter. The different parameters of the filter can be adjusted in order to have a classical batch, or a Kalman filter, or an intermediate algorithm. Most of the already existing on-board orbit determination packages are based in the use of Kalman filters, while most of the on-

ground orbit determination algorithms are based in the use of least squares batch algorithms. Both algorithms have some advantages and drawbacks:

- The major advantage of the least squares batch algorithms is their robustness, this is very important for an on board GNSS orbit determination where stringent integrity requirements are imposed. The major drawback of the batch algorithms is that they usually require heavy computations, and that they are not able to work in real time. They will only be able to work in real time if accurate predictions are computed, but accurate predictions can only be computed in combination with accurate dynamic models, which in principle is not compatible with an on-board orbit determination concept.
- The major advantage of the Kalman filters is their capability to work in real time, every time a measurement is received a new estimation of the state can be computed, The major drawback of these algorithms is their low robustness, as they are very sensitive to anomalous measurements or events. They require very often a fine tuning of the noise and information matrices. It would be difficult to fulfil the integrity requirements using a Kalman filter algorithm.

As it has been mentioned before, the proposed algorithm is a combination of the two described algorithms. Therefore it would be possible to combine the high robustness (integrity) and accuracy of the least squares batch algorithms, with the real time capabilities of the Kalman filters. The least square algorithm with a priori information is briefly described here.

If an estimate and the associated covariance matrix are known at a time t_j , and an additional observation or observation sequence is obtained at a time t_k , the estimate and the observation can be combined in a straight forward manner to obtain the new estimate \hat{x}_k .

The estimate \hat{x}_j and P_j (covariance matrix) are propagated forward to t_k , using the following expressions:

$$\begin{aligned}\bar{x}_k &= \Phi(t_k, t_j) \hat{x}_j \\ \bar{P}_k &= \Phi(t_k, t_j) P_j \Phi^T(t_k, t_j)\end{aligned}$$

Where $\Phi(t_k, t_j)$ represents the transition or propagation matrix. The problem to be considered can be stated as follows:

Given \bar{x}_k, \bar{P}_k and some measurements ($y_k = H_k x_k + \varepsilon_k$), where the observation error is random with zero mean and specified covariance ($E[\varepsilon_k \varepsilon_k^T] = R_k \delta_{kj}$ and $E[(x_j - \hat{x}_j) \varepsilon_k^T] = 0$) find the best linear minimum variance unbiased estimate of x_k .

The solution to the problem can be obtained just by considering the a priori information as measurements. The problem can be solved using a normal least squares filter. Note that if \hat{x}_j is unbiased, \bar{x}_k will be unbiased since $E[\bar{x}_k] = \Phi(t_k, t_j)E[\hat{x}_j]$. Hence, \bar{x}_k can be interpreted as an observation and the following relations will hold

$$\begin{aligned} y_k &= H_k x_k + \varepsilon_k \\ \bar{x}_k &= x_k + \eta_k \end{aligned}$$

where

$$\begin{aligned} E[\varepsilon_k] &= 0, \quad E[\varepsilon_k \varepsilon_j^T] = R_k, \quad E[\eta_k] = 0 \\ E[\eta_k \varepsilon_k^T] &= 0 \text{ and } E[\eta_k \eta_k^T] = \bar{P}_k \end{aligned}$$

Now if the following definitions are used

$$y = \begin{bmatrix} y_k \\ \dots \\ \bar{x}_k \end{bmatrix} \quad H = \begin{bmatrix} H_k \\ \dots \\ I \end{bmatrix} \quad \varepsilon = \begin{bmatrix} \varepsilon_k \\ \dots \\ \eta_k \end{bmatrix} \quad R = \begin{bmatrix} R_k & 0 \\ \dots & \dots \\ 0 & \bar{P}_k \end{bmatrix}$$

The observation equations can be expressed as $y_k = H_k x_k + \varepsilon_k$, and the weighted least squares solution can be applied to obtain the following estimate for \hat{x}_j .

$$\hat{x}_k = (H^T R^{-1} H)^{-1} H^T R^{-1} y$$

In view of the previous definitions:

$$\hat{x}_j = \left\{ \begin{bmatrix} H_k^T & : & I \end{bmatrix} \begin{bmatrix} R_k^{-1} & 0 \\ \dots & \dots \\ 0 & \bar{P}_k^{-1} \end{bmatrix} \begin{bmatrix} H_k \\ \dots \\ I \end{bmatrix} \right\}^{-1} \left\{ \begin{bmatrix} H_k^T & : & I \end{bmatrix} \begin{bmatrix} R_k^{-1} & 0 \\ \dots & \dots \\ 0 & \bar{P}_k^{-1} \end{bmatrix} \begin{bmatrix} y_k \\ \dots \\ \bar{x}_k \end{bmatrix} \right\}$$

or in expanded form,

$$\hat{x}_k = (H_k^T R_k^{-1} H_k + \bar{P}_k^{-1})^{-1} (H_k^T R_k^{-1} y_k + \bar{P}_k^{-1} \bar{x}_k)$$

The covariance associated with the new estimate is

$$P_k = E[(\hat{x}_k - x_k)(\hat{x}_k - x_k)^T] = (H_k^T R_k^{-1} H_k + \bar{P}_k^{-1})^{-1}$$

The following remarks are pertinent to the previous equations:

1. The vector y_k may be only a single observation or it may include an entire batch of observations.
2. The a priori estimate, \bar{x}_k , may represent the estimate based on a priori initial conditions or the estimate based on the reduction of a previous batch of data.

The approach proposed is then based on the processing of small batches of data (around a few minutes) but using the covariance matrix obtained in the previous batch estimation as additional observations for the current batch. The arc length of the process shall be adjusted (envisaged value 5 minutes) and the weight to be given to the measurements and the a priori information (covariance matrix) shall also be adjusted. Those parameters will be adjusted by considering the stringent integrity requirements. The real time capabilities are obtained thanks to the way the ephemeris to be sent to the user is computed. This message is computed by performing a fit, in a least squares sense, of the parameters of a simple orbit model to the latest estate estimates. The parameters of the model are sent to the user at regular time intervals. For a satellite flying at a geosynchronous altitude, those parameters will remain valid over a period not shorter than two hours.

To test the feasibility of this type of algorithms the precise orbit determination software BAHN (developed at ESA/ESOC) has been taken. The BAHN software is a batch least squares algorithm, and it has been converted into a reduce dynamic algorithm by performing some minor modifications. Those modifications are schematically represented in Figure 4 and Figure 4.

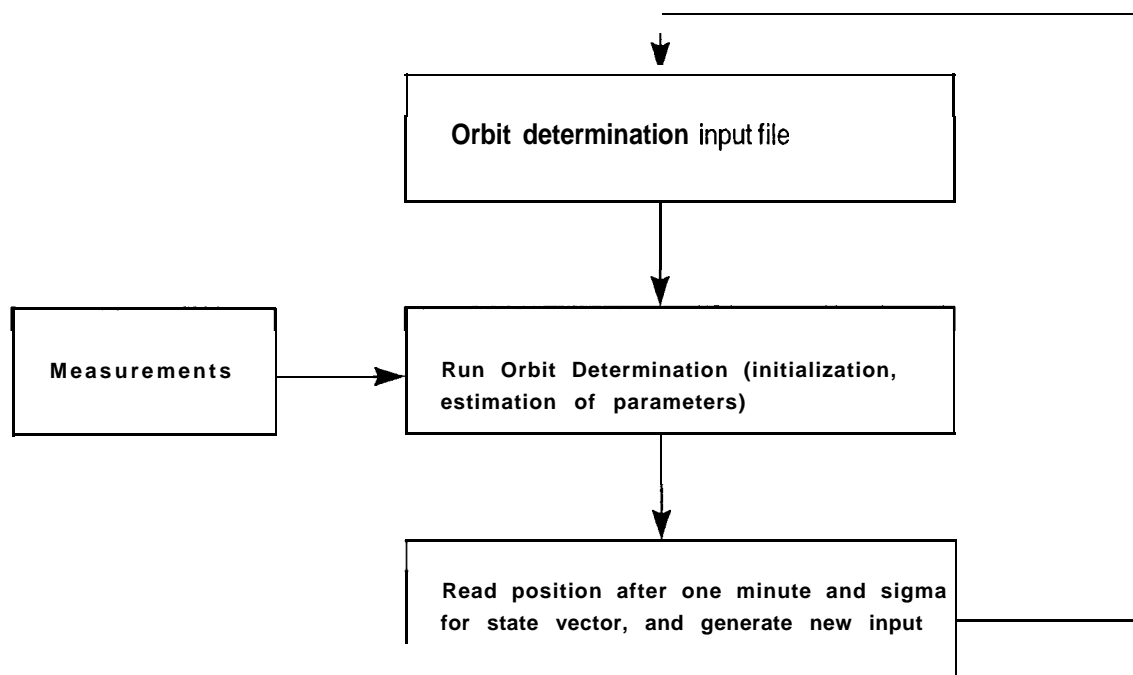


Figure 3 Schematic representation of the implemented algorithm

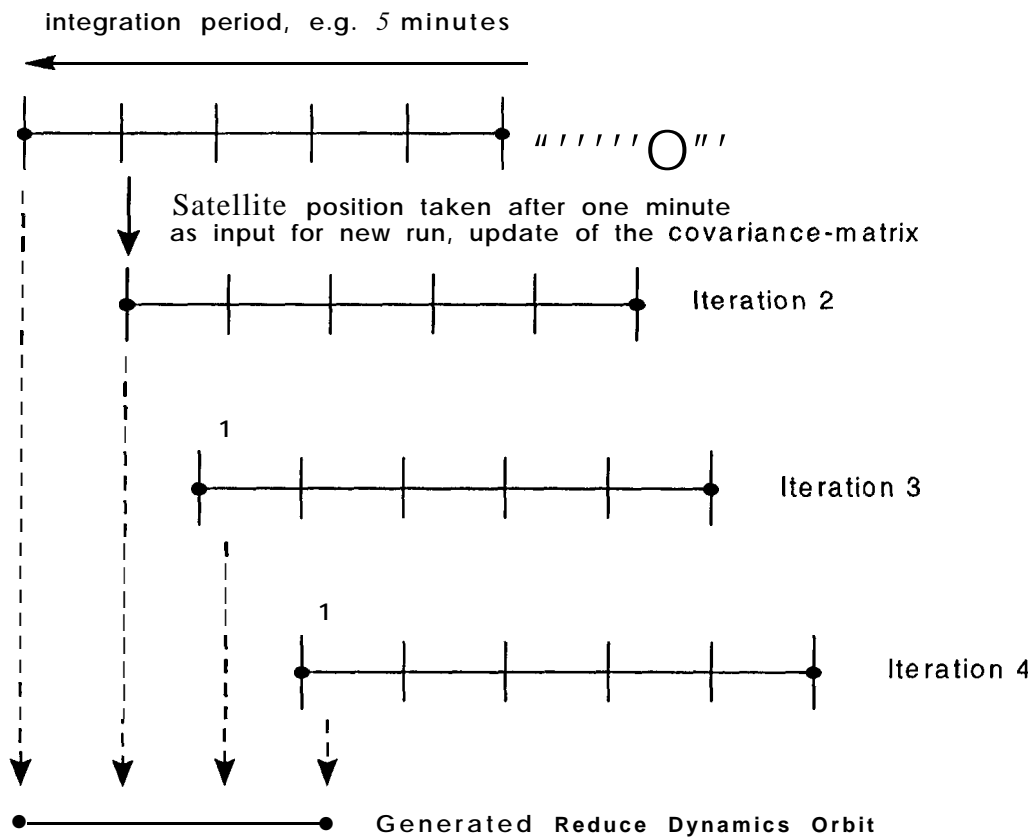


Figure 4 Schematic representation of the implemented algorithm

SIMULATION RESULTS

To test the performances of the implemented algorithms some simulations have been performed. The orbit selected has been an inclined geosynchronous orbit (IGSO) as future satellite navigation systems may be based on those orbits. The ground tracks described by an European GNSS constellation composed by satellites flying in GEO and IGSO orbits is represented in Figure 5.

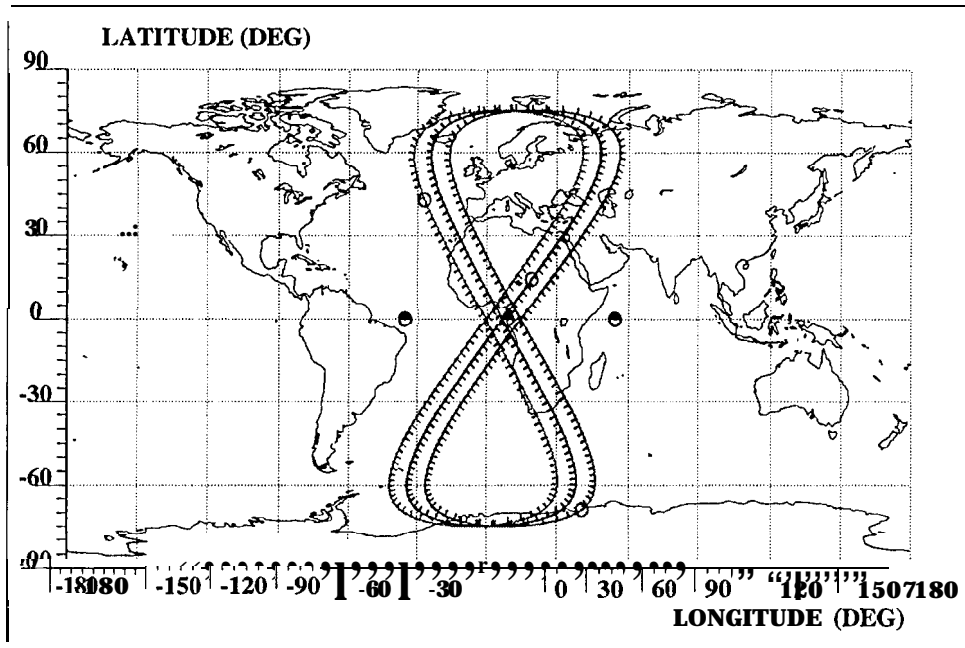


Figure 5 Ground track for the ENSS constellation

To simulate the tracking data realistic errors have been introduced in the models affecting the satellite motion, and the measurements. Simulations have been validated by using real data from GPS and GEO satellites, unfortunately it has not been possible to validate the measurement simulation process using real data from an IGSO satellite, as there are no satellites flying in those orbits.

Measurements (two way range) have been simulated with a measurement rate of 5 seconds. The dynamic models used for the measurements generation are represented in the table below, there also the models that have for been used for the orbit computation are represented.

Item	Generation of measurements	Short arc determination
Gravity field	JGM (9x9)	GEMT3 (2x0)
Solar perturbations	Used	Not Used
Lunar perturbations	Used	Not Used
Solid tide perturbations	Used	Not Used
Ocean tide perturbations	Schwiderski (6x6)	Not used
c.p.r. accelerations	Not used	Used

Table 1 Dynamic models considered

A total arc length of 4 hours was studied. Figure 6 shows this ground track of the satellite for that period.

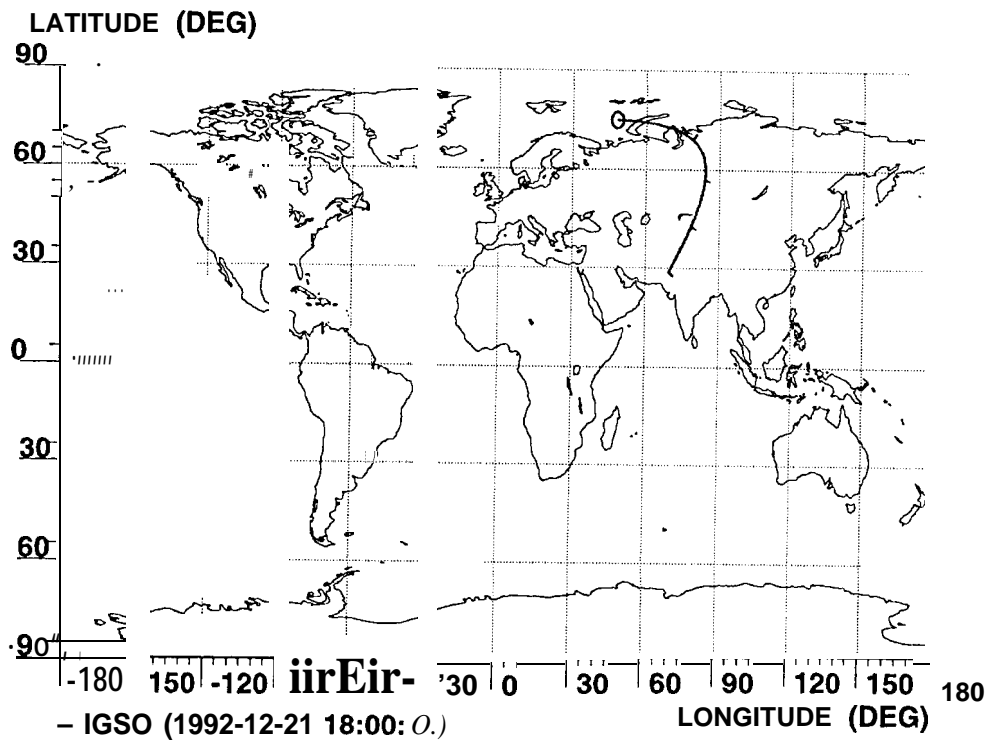


Figure 6: Part of the satellite arc from the IGSO used for the reduce dynamic orbit determination simulations

Three different tracking stations network were studied. First the case with only European tracking stations. Those consist of the following stations:

- Reykjavik
- Hammerfest
- Rome
- . Aberdeen
- Stilly
- . Ankara
- Munich
- . Cádiz.

This network will be referred to as “European”. A second case is the case with tracking stations divided more regular] y over the Earth’s surface with respect to the satellite orbit. These stations are:

- . Hammerfest
- . Cádiz

- Ankara
- . Usuda
- . Djakarta
- Ceylon
- . Alaska
- . Malindi
- . Irkutsk

This network will be referred to as “Well Distributed”, As a last case a network is used with good geometry but with only a very few tracking stations. This network consists of the following stations:

- Hammerfest
- Malindi
- Irkutsk
- Cádiz

This network will be referred to “Reduced Network”. All the stations used for the analysis here are depicted on the map in Figure 7.

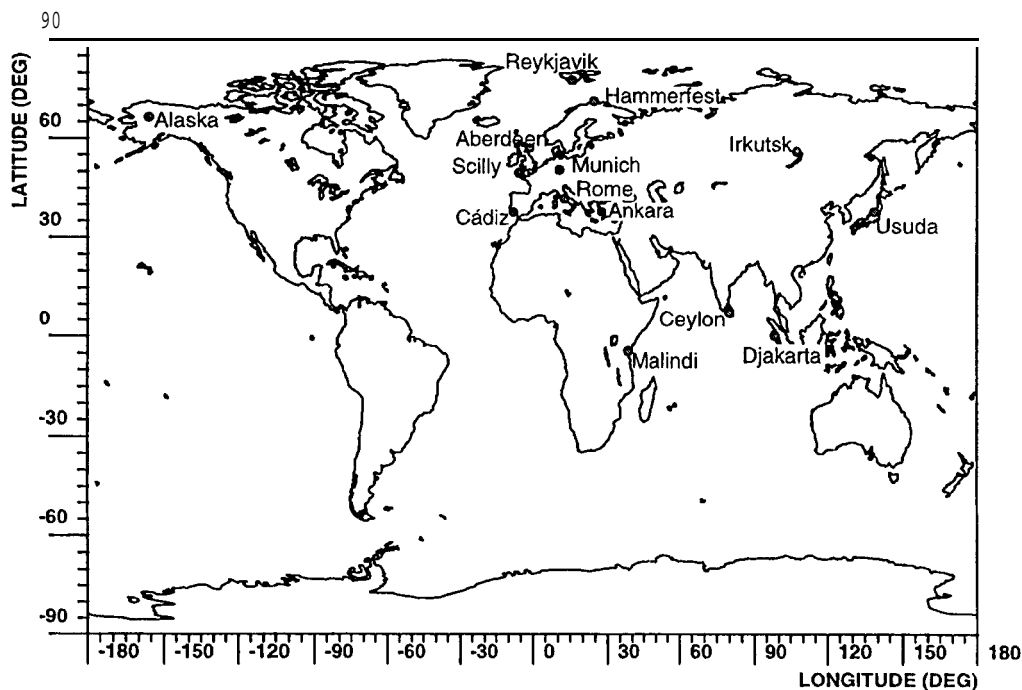


Figure 7: Tracking stations used for different case of reduce dynamic orbit determination

First from the generation of the simulated measurements a reference orbit was created. This orbit was used as the true orbit. Then with different set-ups for the tracking network, orbits were calculated using the reduce dynamic algorithm. The resulting orbits were compared with the reference orbit by means of the RMS of the differences in radial, along track and cross track direction. This was done for the three tracking station network for two different case.

- . The first case is the nominal case optimal for the reduce dynamic algorithm, i.e., very good measurements are present for all stations. This means measurements have been generated with a noise of 10 cm and no station dependent biases are present.
- . The second case is to see the effect of measurements with more noise and with biases. A noise of 1 meter was used and for **all** stations biases were generated with a sigma of 5 meters, This was only done for the European network and the emphasis here is more on the effects of the biases. One case will be studied in which the biases are estimated and in the other case the biases will not be estimated in the process

The following table depicts the results for the first case, with the three different tracking station network and good measurements (no biases and measurements with a sigma of 10 cm)

Tracking network	Radial (cm)	Along track (cm)	Cross track (cm)	Total RMS (cm)
European network	10.17	36.53	92.98	57.97
Well Distributed Network	2.50	17.39	11.59	12.15
Reduced Network	3.62	47.24	8.29	57.85

Table 2 Estimated accuracy of the computed orbits

These results show the power of the reduce dynamic algorithm in the presence of good measurements. All three cases give results well below a meter and in the case of the Well Distributed Network the differences are even on the decimetre level. The results for the Reduced Network are a little misleading because in the first part of the orbit determination the **Malindi** station is not tracking the satellite. When Malindi was within the visibility of the satellite it was observed that the results were comparable with that of the Well Distributed Network. Therefore the following conclusions can be made:

- . Reduce dynamic orbit determination is **very powerful** if **accurate measurements are present** with a geometrically well distributed network of ground stations. Also only a few ground stations, but with **good geographical distribution** lead to good results.

For the second case, with measurements with 1 metre noise and station dependent biases the results are depicted in following table.

Tracking network	Radial (cm)	Along track (cm)	Cross track (cm)	Total RMS (cm)
European, biases estimated	1106.92	1731.63	8915.14	5282.16
European, biases fixed	60.58	1601.27	1182.96	1149.95

Table 3 Estimated accuracy of the computed orbits

These results indicate that the reduce dynamic algorithm loses its strength when no precise measurements are present. The case in which the station dependent biases were estimated showed no convergence and was only deteriorating in means of orbit differences.

The case in which the biases were not estimated shows better performance, but still in the order of meters. However, the difference here is that the orbit seemed to be converging. This can be seen in Figure 8.

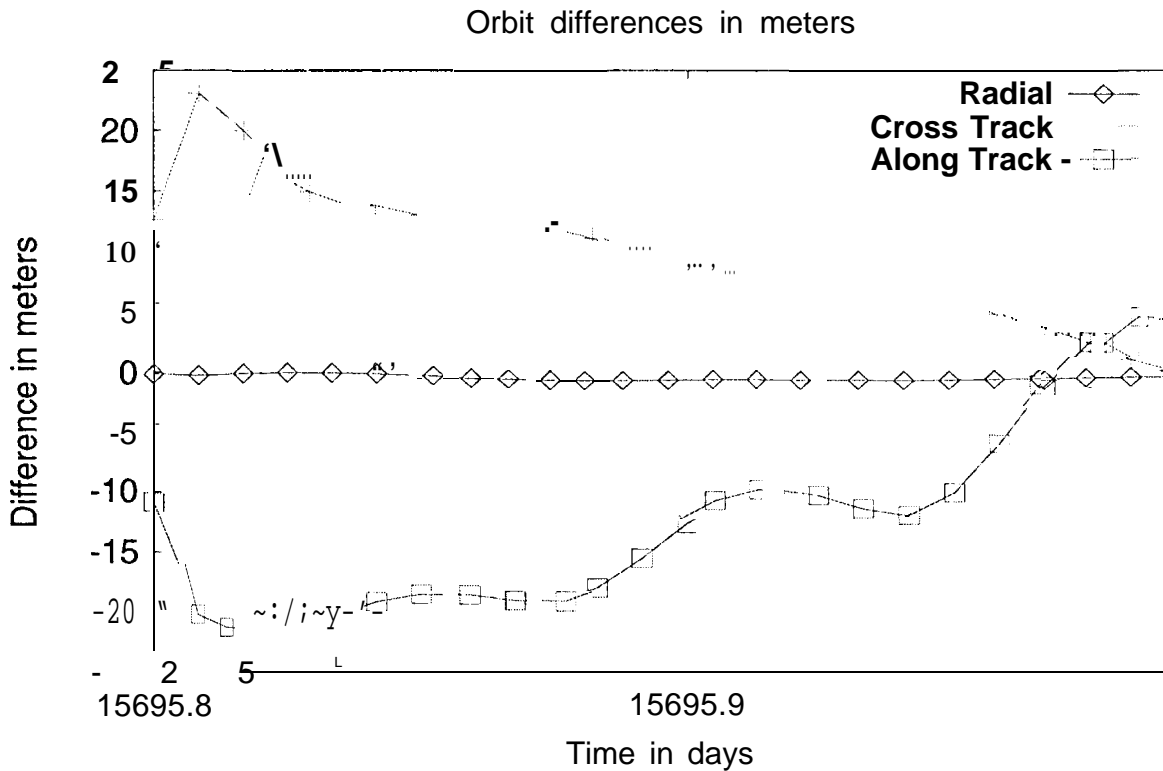


Figure 8: Plot of orbit differences in radial, along track and cross track direction for the reduce dynamics algorithm with a European network and the biases fixed

The time it takes to complete one iteration (in this case this correspond to five minutes of data) on a Sun Spare Ultra, is about 10 seconds. It has to be reminded here that this can even be faster if the orbit determination package is modified in a proper way so that it is not initializing all of its parameters each time it is run. It can be concluded therefore that the reduce dynamic algorithm can be successfully used for real time purposes. Moreover

it is believed that, with dedicated software development, it is even suited for on-board orbit determination, since the dynamic models used for the reduce dynamics are quite simple.

The capability of the reduce dynamic algorithms to compute accurate orbits during manoeuvre periods has been evaluated. Some orbital manoeuvres have been simulated and orbits have been computed using reduce dynamic algorithms. The major conclusion of this analysis is:

- . The orbit determination accuracy to be achieved during manoeuvre periods is about the same as the obtained in periods without manoeuvres. Therefore the results presented in previous tables are also representative for manoeuvre periods. The orbit determination accuracy to be achieved is therefore not driven by the manoeuvre execution but for the tracking data quality.

CONCLUSIONS

The following conclusions have been derived from the analysis:

- A reduced dynamic algorithm has been derived from a state of the art dynamic algorithm. The reason for that has only been to tests the performances of the algorithm, but if an on-board implementation is required it would be better to start from a fairly simple orbit propagator, almost keplerian.
- It has been demonstrated that this type of algorithms will allow to accomplish the very stringent accuracy, integrity and continuity requirements for a future global navigation system.
- Results from preliminary simulations indicate that the describe algorithm is able to provide very accurate ephemeris if accurate measurements, from a well distributed network of ground stations, are available.
- This algorithm can be used for autonomous orbit determination, or to estimate orbits during critical periods, like manoeuvres.

ARP PROJECT: ABSOLUTE AND RELATIVE ORBITS USING GPS

Tomás J. Martin Mur
European Space Operations Centre, European Space Agency
D-64293 Darmstadt, Germany

Carlos García Martínez
GMV at ESOC

ABSTRACT

ESA's Automated Transfer Vehicle (ATV), a logistic and supply spacecraft for the International Space Station (ISS), will use GPS as the main positioning system for absolute and long range relative navigation. The ATV Rendez-vous **Predevelopment (ARP)** program is being carried out to increase European expertise on automated rendez-vous technologies. This program includes three Flight Demonstrations in which data from GPS receivers **on-board** two nearby spacecraft are collected, so they can be used to validate relative navigation algorithms using GPS, ESOC is participating in the project by computing absolute reference trajectories using precise GPS orbits and clocks. These trajectories are then compared with the results from the relative trajectory algorithm.

INTRODUCTION

GPS has been proposed as tracking or scientific instrument for several future ESA spacecraft. One of them will be the ATV, that will serve as a logistic and supply vehicle for the International Space Station. GPS is going to be used to determine the long and medium range relative position of the ATV with respect to the ISS. For this GPS receivers and the associated antennas will be installed in both spacecraft. Before the concept can be used operationally, it is **necessary** to fine-tune it and validate it by using flight experiments with other spacecraft and ground simulations. The ATV Rendez-vous **Predevelopment (ARP)** program has the goal of validating methods for relative navigation, including relative GPS navigation. Within this program three Flight Demonstrations have taken place to collect GPS and other data from spacecraft performing **rendez-vous**. These data are then processed on-ground to test and validate on-board algorithms for relative navigation. Independent reference trajectories are

needed in order to use them as yardstick against which the results of the relative navigation algorithm can be compared.

ESOC was asked to calculate absolute trajectories using GPS as a relatively independent yardstick with respect to the relative trajectories that are computed using common-view differential observations.

THE ARP FLIGHT DEMONSTRATIONS

The three ARP Flight Demonstrations (**FD**) have already taken place. In all of them GPS receivers have been simultaneously operated in two spacecraft performing rendez-vous. The receivers used were SPS receivers modified to output raw measurement data. They produced C/A pseudorange, and **L1** carrier and **doppler** and they had between 6 and 12 channels, The baseline for **ATV** is to use one-frequency receivers with a number of channels and antennas that should ensure a common visibility of at least four GPS satellites.

ARP **FD-1** took place between November 19 and December 4, 1996. It was performed during the **STS-80** Shuttle flight and it involved the Shuttle acting as chaser spacecraft and the Orfeus-SPAS retrievable satellite acting as target. The **Orfeus-SPAS** was equipped with the 9-channel Laben **ARP** GPS receiver and the Shuttle had the 6-channel Trimble TANS Quadrex receiver. Data (GPS and **GNC**) were simultaneously collected during a free-flight period and during retrieval.

ARP **FD-2** took place in May 1997 during Shuttle flight **STS-84** to the **MIR** space station. For this flight the Laben **ARP** GPS receiver was installed on the Shuttle and the GPS data from **MIR** was obtained from the MOMSNAV receiver. This receiver has two blocks of 6-channels and each of them is connected to one antenna, one to a out-looking antenna in the **Priroda** module and the other to a side-looking antenna in the same module. Simultaneous data was collected only during separation.

ARP **FD-3** took place in September/October 1997 during Shuttle flight **STS-86** to the **MIR** space station. The configuration was the same as for **FD2** and it seems that simultaneous data from both the docking and the **un-docking** will be available. The data from **MIR** had to be brought back to the ground on physical support by a later **flight** of the Shuttle (**Soyuz** for **FD2**).

POST-FLIGHT PROCESSING AT ESOC

ESOC processed the GPS data together with **GNC** data and IGS products [**Martín** Mur et al, 1997]. The **GNC** data is used to model the spacecraft attitude and the possible thruster firings, The IGS products that are used are ESOC'S final orbits and 30 second clocks. The approach that is used to determine the trajectories in the **ARP** context has to be different to that used for standard GPS **POD** because the data is collected over periods of only a few hours, the spacecraft involved may be performing attitude or orbit **manoeuvres**, the receivers are one

frequency SPS models and because the spacecraft altitude is so low, non-propulsive dynamics (specially drag) can not be modeled to a very high degree of accuracy.

The approach that we follow is to use pseudorange and phase observable corrected with the ESOC precise orbit and clock products for the GPS satellites. Spacecraft state parameters, including clock parameters, are obtained using a precise orbit propagator together with a Square Root Information Filter (**SRIF**). The propagator includes empirical accelerations, and the SRIF produces filtered and smoothed estimates of the parameters, including empirical accelerations, and the **covariance**.

So far the data for FD1 and FD2 have been processed and we expect to receive and process the data for FD3 in the next months.

CRITICAL ASPECTS FOR ARP TRAJECTORY ESTIMATION

The critical aspects for this work, as already identified in our preparatory activities [Martín Mur et al, 1995], are the following:

- Receiver characterization and performance
- Dynamical modeling
- Ionospheric correction

Receiver characterization is important because three different receivers from three different manufactures are being used. These receivers do not output **RINEX** standard GPS observable because they do not produce simultaneous carrier and pseudorange measurements for all channels, the pseudorange is output in the form of ambiguous code phase and time tags do not follow the **RINEX** standard. Each receiver uses a different data format and the data has to be preprocessed to correct biases that sometimes are not well defined. The receivers were designed to provide SPS solutions, in this way their precision and accuracy are not as good as for geodetic receivers. As an example, the pseudorange specification for the Laben receiver was of 10 m error. This may be enough for stand alone SPS (considering that selective availability has 30 m rms error), but it is not good when the receivers are used in differential mode.

Dynamical modeling is a problem because the spacecraft are flying very low (400 km), they have large and changing drag and solar radiation pressure areas. Furthermore they may be performing orbit and attitude control thrusting that are only known to a level of about 3 mm/S^2 and have moving parts that change the centre of mass location in body fixed axes. This has made it necessary to implement the estimation of empirical acceleration in our filter.

The ionospheric perturbation on carrier and code can not be calculated from the measurements because only one frequency is available and the high pseudorange noise precludes the use of techniques as those discussed in [Martín Mur et al, 1995] like the **code-carrier** ionospheric free combination. Ionospheric corrections from ground based receivers are of no avail because the spacecraft are flying not below but through the ionosphere, even

close to the maximum. It was decided to use the integration of the **IRI-95** electron density model [Bilitza 1990], despite the fact that it does not include the effect of the **plasma**sphere on the carrier phase advance or the code delay.

RESULTS FOR THE FIRST TWO FLIGHT DEMONSTRATIONS

For FD1 [Martin Mur, 1997] data were collected during two phases, a dynamically quiet phase in between deployment and retrieval and a dynamically noisy phase during retrieval including grappling of the **Astropas** by the Shuttle Remote Manipulation System (**RMS**). Carrier phase could be fitted to the centimeter level and pseudorange to the five meter level. The accuracy of the trajectories that were obtained is estimated to be about 30 cm rms for the in-between phase and about 1 meter for the retrieval, with degraded performance during grappling.

For FD2 [Martín Mur, 1998] data were recorded only during the separation and in that phase the Shuttle made a number of attitude correction **manoeuvres**. Data from the **side**-looking antenna in MIR were of questionable quality and it seems that the behavior of the MOMSNAV receiver is not yet fully understood. Solutions have been obtained with residuals in the centimeter range for phase and in the 5 meter range for pseudorange and it is expected that the solution accuracy is in the 1 meter rms **level**.

CONCLUSION

We have demonstrated the capability of producing improved trajectories for spacecraft using one frequency GPS receivers and IGS products. It is important to realize that the limiting factor for this kind of trajectory estimation is not the accuracy of precise GPS products, but by the accuracy of the measurements. For precise relative navigation the best results would be obtained using receivers that have been designed for the purpose, i.e. that can produce simultaneous, low noise carrier phase and pseudorange measurements.

REFERENCES

- Bilitza, D. (cd.) (1990), International Reference Ionosphere 1990, **NSSDC 90-22**, Greenbelt, Maryland, 1990.
- Martin Mur, Tomás J., J. Dow, N. Bondarenco, S. Casotto, J. Feltens and C. García Martínez (1995), Use of GPS for Precise and Operational Orbit Determination at ESOC, Proceedings of the ION GPS-95, September, 1995.
- Martín Mur, Tomás J., J. Dow, C. García Martínez (1997), Absolute and Relative Navigation of Spacecraft Using GPS: The ATV Rendez-vous Predevelopment Flight Demonstrations, Proceedings of the 12th International Symposium on Space Flight Dynamics, June, 1997.
- Martin Mur, Tomás J. (1997), ESOC **ARP-FD1** Trajectory Reconstitution Analysis, ESA/ESOC, September, 1997.
- Martin Mur, Tomás J., C. Garcia Martínez (1998), ESOC **ARP-FD2** Trajectory Reconstitution Analysis, **ESA/ESOC**, February, 1998.

Poster Summary Papers

IGS Related Activities at the Geodetic Survey Division of Natural Resources Canada

C. Huot, P. Tétreault, Y. Mireault., P. Heroux,
R. Ferland, D. Hutchison and J. Kouba

Summary

In 1997 NRCan started submission to IGS of predicted orbits and estimated tropospheric delays. In 1998 NRCan will also start contributing ionosphere products in the recently adopted IGS IONEX format. No major modifications were made to the NRCan estimation strategy since the 1997 IGS Workshop except for the addition of new stations and the correction of erroneous ocean loading coefficients.

Rapid and Predicted Orbits and Clock Products

NRCan continues to use JPL's GIPSY-OASIS II software for its GPS processing along with the strategy described in the IGS Annual Reports. A new station selection strategy based on using at least one out of n stations in various geographic sub-region of the IGS tracking network was implemented. The strategy ensures that a network with a strong geometry is available early enough in the day to allow sufficient time to process and submit to IGS the daily rapid solutions. The new strategy has resulted in a more consistent quality of the NRCan rapid products which currently have rms of about 10 cm for satellite positions and 0.5 ns for satellite clocks with respect to IGR products. Rapid Earth Orientation Parameters (EOP) solutions are also submitted. The better selection of stations also resulted in fewer failures to submit rapid solutions to IGS on time. However, for some regions within the IGS tracking network, it is still difficult to consistently retrieve data on time for the processing.

In addition to the rapid orbits and clocks NRCan also provides predicted orbits on a daily basis to IGS. A 2-day prediction is obtained from 4 IGR rapid orbit solutions by estimating 6 Keplerian elements and 9 radiation pressure parameters using the Bernese software version 3.5. The IGR x and y Pole position series are used along with the Bulletin A UT 1 series to provide the necessary Earth Orientation Parameters. The use of the Bulletin A UT1 series, initiated on GPS Week 934, has improved the z-rotation orientation of the NRCan predicted orbits as can be seen on Figure 1. An annual trend of about 10 cm in amplitude has been observed in the z-translation orientation of the NRCan predicted orbits (not shown here). NRCan predicted orbits are currently about 50 cm median RMS with respect to IGR orbits for non-eclipsing satellites and about 100 cm for eclipsing satellites.

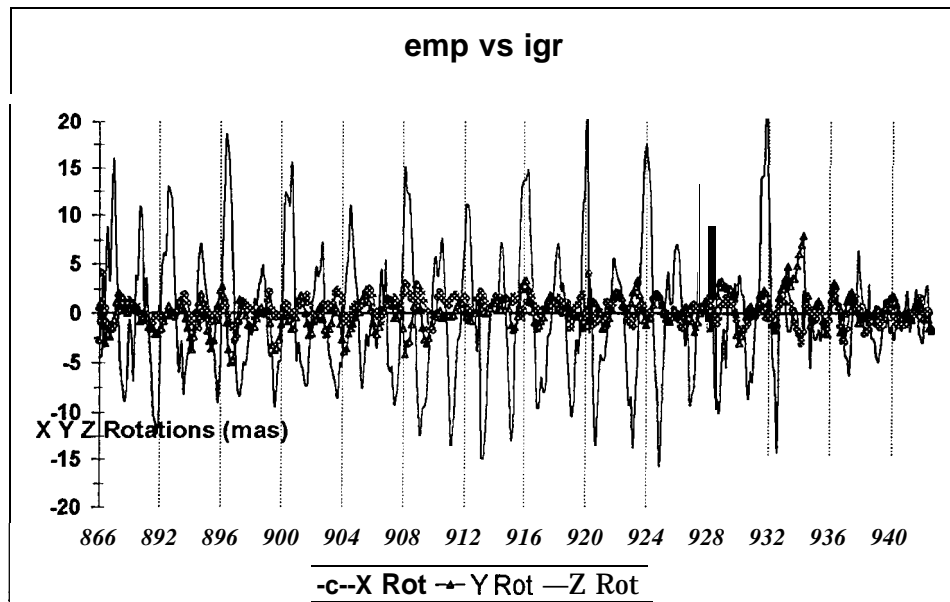


Figure 1. NRCan Predicted vs IGR orbits

Ionospheric Modeling

NRCan, in support of the Canadian Active Control System (CACS), has developed a regional grid model of ionospheric delays and is currently implementing a global solution in the IONEX format for future submission to IGS. The NRCan ionospheric model is currently based on 10 to 15 regional stations covering the Canadian territory. It is computed using carrier phase smoothed pseudo-range observations with an elevation cut-off angle of 15 degrees and elevation dependent weighting. A spherical single layer shell at 350 km elevation and a $\cos z$ mapping function are used. The model has a 24 hour temporal resolution and uses a sun-fixed/geographic reference frame. Table 1 presents the precise point positioning monthly averaged daily rms which can be currently achieved with the single layer model and satellite differential code biases.

Table 1. Point positioning using NRCan ionospheric modeling

**Monthly Average of Daily RMS
Position Estimates at 15 min. intervals
Station NRC1, January 1998**

Latitude	<u>RMS (m)</u>		<u>Processing Mode</u>
	Longitude	Height	
1.3	0.7	3.6	L1
1.0	0.7	1.7	L1 + SLM
0.8	0.4	1.1	L1 + SLM + CAL
0.5	0.4	1.1	L3

L1 = L₁ Frequency
SLM = Single Layer Model
CAL = Satellite Differential Code Bias
L3 = Ionospheric Free Combination

Final Orbits, Clocks and Station Coordinate Products

A problem with NRCan ocean loading coefficients which resulted in a strong signal with a 13.7 day period in the NRCan 2.5 year station position residual series was corrected on February 23, 1997. A recent spectral analysis of the NRCan station position residual series for GPS Weeks 894 to 938 confirmed that the erroneous ocean loading coefficients were indeed responsible for the artificial 13.7 day signal.

Table 2 presents the weekly averaged differences between the NRCan and ITRF/IGS products computed for stations, orbits and EOP'S estimates. UTI-UTC was not included due to its long-term drift, which prevailed in the weekly averaged means and sigmas.

Table 2. Weekly Averaged Differences Between NRCan and ITRF/IGS Products
For weeks 0836 to 0932.

<u>Solution</u>		<u>Translation (cm)</u>			<u>Rotation (mas)</u>			<u>Scale(ppb)</u>
		T1	T2	T3	R1	R2	R3	Sc
Stations	(a)	0.0	-0.4	-0.2	-0.092	-0.017	-0.002	0.47
sigmas		0.1	0.2	0.1	0.044	0.025	0.016	0.33
Orbits	(b)	0.0	1.5	0.4	-0.352	0.072	-0.335	0.08
sigmas		0.8	0.9	0.6	0.145	0.129	0.285	0.09
EOP (c)					-0.316	0.116		
sigmas					0.142	0.154		

- (a) Combined NRCan weekly SINEX coord. solutions vs ITRF coord. for the 13 IGS fiducial stations.
 (b) Weekly averaged transformations between NRCan and IGS daily orbits.
 (c) Weekly averaged differences between NRCan and IGS daily polar motion.
-

ESA/ESOC IGS ANALYSIS CENTRE POSTER SUMMARY

Carlos García Martínez (GMV at ESOC), John Dow (ESA/ESOC),
Tomás Martín Mur (ESA/ESOC), Joachim Feltens (EDS at ESOC),
Pelayo Bernedo (GMV at ESOC).

INTRODUCTION

The following are the main sheets of the poster that was presented in the workshop. It summarizes the current status and results of the ESOC IGS Analysis Centre.

ESOC ANALYSIS CENTRE: MAJOR CHANGES SINCE FEBRUARY 96

Date	Change
02/96	Estimation of small delta-v impulses every 12 hours for the whole constellation to allow velocity discontinuity
11/02/96	ESA SINEX file available
30/06/96	New reference frame ITRF94. Subdaily polar motion according to Ray model. Antenna phase centre correction with the model IGS 01 .PCV. Estimation of EOP rates,
31/03/97	Estimation of sine and cosine radial one cycle per revolution empirical acceleration (instead of impulses every 12 hours)
09/03/97	Saastamoinen tropospheric model replaced the Willman one
02/04/97	ESA predicted orbits available
21/04/97	Deadline of rapid orbits reduced from 23:00 to 21:00 UTC
22/07/97	Hatanaka compression implemented for the analysis and for the data distribution of the ESA receivers
30/11/97	Ocean loading implementation based on the Schemeck model

RAPID AND FINAL ORBITS

DIFFERENCES BETWEEN RAPID AND FINAL ORBITS

	FINAL	RAPID
PROCESSING STARTED	3 or 4 days after last collected data depending on data availability	at 14:00 UTC independent on data availability
PROCESSING TIME	12 hours	4 hours for 30 stations
ARC (hours)	12+24+12	12+ 24
NORMAL EQUATIONS FOR SINEX GENERATION o u T P u T	YES	NO

The orbit **modelling** is common. Per satellite we estimate the following parameters:

- Position and velocity at epoch.
- Scale for Rock 4T, y-bias, sine and cosine radial component one cycle per revolution empirical accelerations. These parameters replaced the delta-v impulses every 12 hours for all the satellites in March 1997.
- For **eclipsing satellites** the observations are excluded half an hour before and after the eclipse. Delta-v are estimated in the three orbital components at eclipse exit time.
- Any delta-v due to spacecraft **manoeuvres**.

PREDICTED ORBITS

Earth fixed positions taken from the rapid IGS solution are used as basic observable. The number of days for the fit is variable, currently set to four. If the IGR rapid orbit is not accessible our corresponding rapid solution plus cop's are used instead. Measurements of the last day have a weight three times the one of the initial days.

Per satellite are estimated **Rock 4T scale factor, ybias and sine and cosine one cycle per revolution empirical accelerations in the three orbital directions**. The initial state vector is taken from the corresponding rapid solution. It is also estimated.

Earth orientation parameters are taken from the rapid solution for the fit interval and from the IERS rapid service for the prediction. xp, yp and ut1 in the prediction interval are corrected **for the offset with respect to the IGS rapid eop's**.

Satellites are deweighted if

- they have been deweighted in the rapid solution
- are missing any of the days of the rapid combination
- are in eclipse period
- the orbit determination fit of the 4 igr orbits is poor.

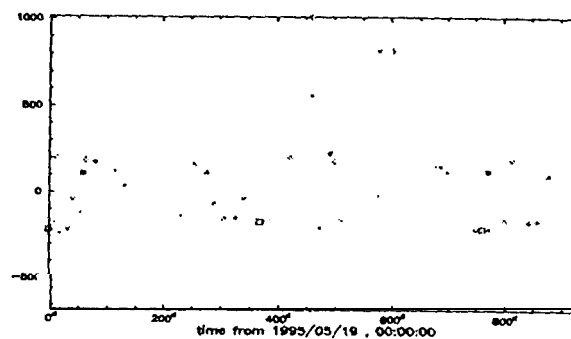
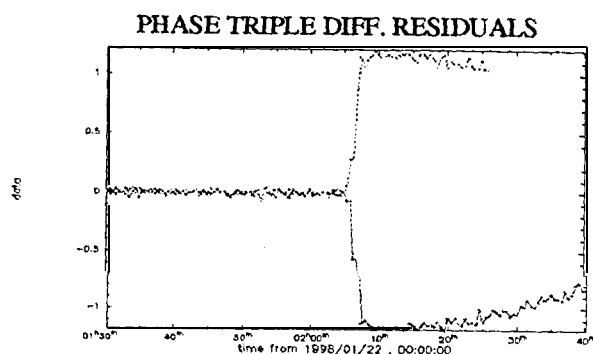
Satellites with a extremely bad fit in the 4 day igr interval are replaced by the propagation of our last rapid solution. It has been proven that a propagation of a smaller arc gives better results.

ESTIMATION OF MANOEUVRES

Manoeuvres must be previously announced in the NANU'S and at least two receivers must track the manoeuvring satellite to detect the firing time. **Two** methods have been developed:

- Study of residuals of the phase triple differences. The time is determined by looking for a step in the triple differences. The preliminary delta-v value is estimated by energy change.
- Use of carrier phase time differences, An algorithm has been developed to detect delta-v changes based on the comparison of the observations to a propagated orbit.

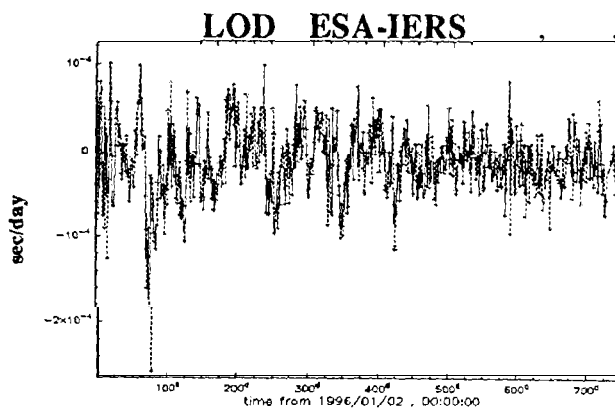
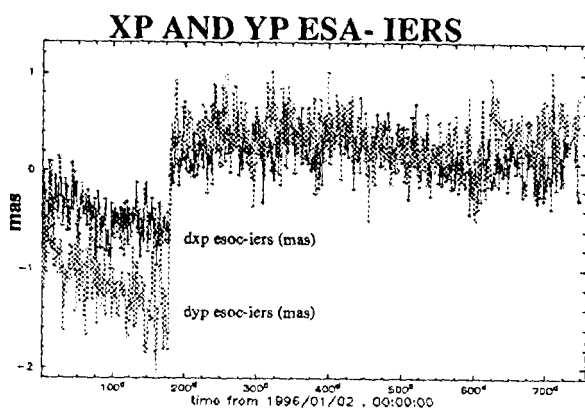
Our orbit determination program **BAHN** estimates the impulse in three directions.



EARTH ORIENTATION PARAMETERS

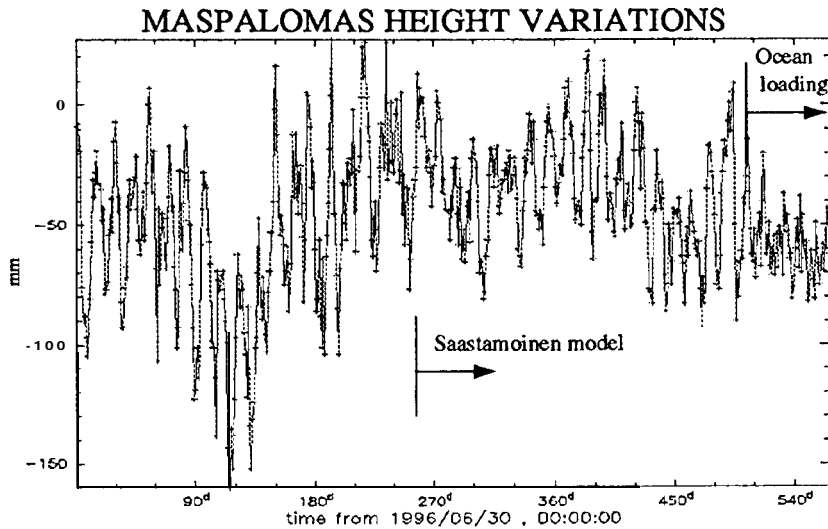
Below are shown the differences of our estimations respect to the Bulletin B. Several improvements have been registered in the last two **years**, mainly due to the adoption of the Ray **subdiurnal** model in June 1996 and the estimation of one cycle per revolution empirical accelerations since March 1997.

The change to ITRF94 produced the **discontinuities** that can be seen in the pole comparison plot. The offset for our solution was about 0.82 mas in xp and 1.73 in yp.



STATION COORDINATES

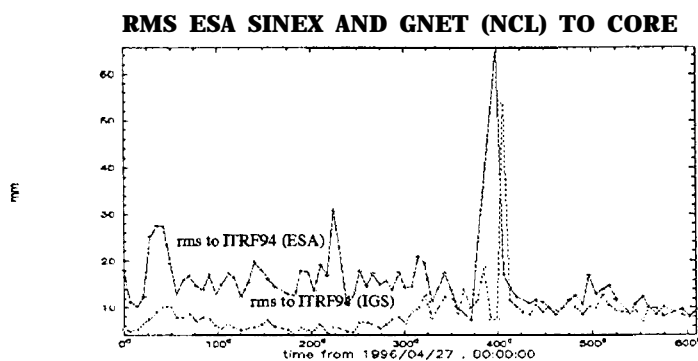
The stability of the station coordinates has been improved, especially in the vertical component, with the implementation of the **Saastamoinen** tropospheric model in March 1997 and also with the consideration of ocean loading based on the **Scherneck** model. That can be clearly seen below on the height estimation of **Maspalomas**, a station very much affected by the ocean loading effect. Several tidal effects, specially the fortnightly one, have been substantially reduced.



TRANSFORMATIONS FROM ESA SINEX TO ITRF

In this plots therms is presented for a time span of about two years. The ESA rms, scale factor and dy have converged to the igs solution since the introduction of the Saastamoinen model in March 1997.

The first 60 days of the plot the reference is **ITRF93** and it was changed to **ITRF94** on June 1996.

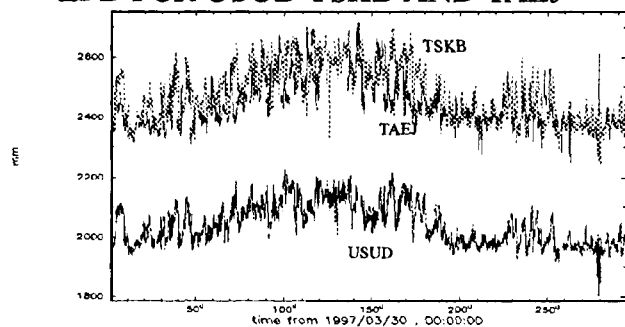


TROPOSPHERIC ESTIMATES

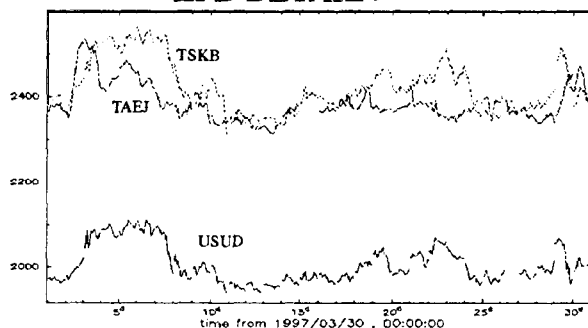
Tropospheric zenith path delays are produced in our routine analysis. They are estimated along with orbits, cop's and station coordinates. We use the **Saastamoinen** model since March 1997. The model consists of two hourly step functions with apriori values taken from the previous day.

In the following examples the results for three stations, USUD, TSKB and TAEJ from the same region are presented. The three curves show the same seasonal variation. Taejon and Tsukuba are located close to the sea level while **Usuda** is at about 1500 meters height. That explains the difference of about 400 mm between the curves. The geographical proximity between **Usuda** and **Tsukuba** makes both profiles to look very similar in spite of the height difference.

ZPD FOR USUD TSKB AND TAEJ



ZPD DETAIL



CONCLUSIONS AND OUTLOOK

- Since the beginning of 1997 we have incremented our IGS contribution with the production of predicted orbits.
- Rapid and final orbit solutions have improved through the estimation of empirical cyclic accelerations.
- Our products, especially station coordinates and atmospheric products, have been very positively affected by the implementation of the Saastamoinen tropospheric **model** and the **ocean loading**,
- The routine computation of ionospheric products has been recently started.
- Tests will be carried out to try to improve the dynamical model of the satellites, especially the eclipsing ones. This can have a positive impact in the predictions and rapid orbits when the visibility is poor. The arc lengths will be reviewed.
- **Glonass** data processing capabilities will be implemented in time for **IGEX'98**.
- We are currently using our orbits and clocks for the Automated Transfer Vehicle /Automatic Rendezvous Pre-development (A TV/A TV) **project, to demonstrate the capability to perform automated rendezvous operations using GPS.**

RECENT IGS ANALYSIS CENTER ACTIVITIES AT JPL

David C. Jefferson, Yoaz E. Bar-Sever, Michael B. Heflin,
Michael M. Watkins, Frank H. Webb, James F. Zumberge
Jet Propulsion Laboratory, California Institute of Technology
Pasadena, CA 91109 USA

SUMMARY

JPL activities as an IGS Analysis Center continued; regular deliveries of rapid (1 -day), and precise GPS orbits and clocks, Earth orientation parameters, and free-network ground station coordinates (now in SINEX 1.0) were maintained. Daily troposphere estimates in the IGS exchange format are now available. The estimation of site-specific tropospheric gradients have further improved the accuracy of our solutions. In 1998, a larger subset of the newly-augmented group of 47 IGS fiducial stations was put in use, and all freed-network solutions are made to align with ITRF96. Enhancements have been made to our site selection and automation processes. A timeline of our analysis strategy is shown in Table 1.

Table 1. Analysis evolution since 1997.

<u>Action</u>	<u>Date</u>
Produce troposphere files in IGS Exchange format	Jan 26, 1997
Produce station coordinate files in with SINEX 1.0 format	Jan 26
Produce free-network transformation files routinely	Apr 15
Do not process satellites not found on rapid-service orbit	Apr 23
Estimate tropospheric gradients	Aug 24
Use TurboRogue MAD2 (in place of MADR) as a fiducial site	Nov 9
Correct mismodeling of SRP for PRN03	Nov 9
Use NRC1 (instead of ALGO) as default reference clock	Dec 14
Use 32 hour nominal orbit interval, map final orbits for 30 hours	Feb 1, 1998
Use ITRF96 coordinates and velocities for 22+ subset of 47 IGS fiducials	Mar 1
Use free-network estimates in troposphere products	Mar 15

MAJOR NEW STRATEGIES AND PRODUCTS

Troposphere Solutions

Beginning with GPS week 890. JPL contributes solutions to the IGS troposphere estimate combination. These **files** contain our daily estimates of the total (wet + dry) **zenith** tropospheric delay at each site used in the **global** solution. Troposphere **parameters** are estimated using a satellite elevation cutoff of 15 degrees. The format of the troposphere products was designed by Yoaz Bar-

Sever (**JPL**) and Gerd Gendt (**GFZ**). Starting with GPS week 920, tropospheric gradients were added to the list of **parameters** estimated for each ground station. In implementing this strategy, the following **modifications** were made to the initial estimation process:

- The two gradient parameters are modeled as random walk with a sigma of 0.03 **cm/sqrt(hour)** and are estimated every five minutes.
- The **Niell** troposphere mapping function has replaced the **Lanyi** mapping function.
- The random walk sigma on the estimated zenith wet delay has been reduced from 1.02 **cm/sqrt(hour)** to 0.30 **cm/sqrt(hour)**.
- The carrier phase **post-fit** residual rejection criterion has been reduced **from** 5.0 cm to 2.5 cm.
- Beginning week 949, troposphere products are representative of the **free-network** estimates (freed-network prior to this).

The JPL solutions are archived as

<ftp://sideshow.jpl.nasa.gov/pub/jpligsac/<www>/jpl<www><d>.tro.Z>

Reference Frame

Beginning week 947, orbits, Earth orientation, **SINEX** station coordinates, and daily transformation **files align** with the **ITRF96** reference frame. Nominal monument coordinates and velocities are taken from ftp://igsb.jpl.nasa.gov/igsb/station/coord/ITRF96_IGS_RS47.SNX.Z, and antenna heights from <ftp://igsb.jpl.nasa.gov/igsb/station/general/igs.snx>. As we use only 37 stations in our daily processing, we select a subset of the 47 sites designated by the **IGS** as **fiducials** in the following **manner**:

- Automatically include and constrain the following 22 sites when available ALGO DAV1 FAIR FORT GOL2 HARK IRKT KERG IUT3 KOKB KWJ1 MAC1 MAD2 MALI **OHIG** ONSA **SANT TID2** TSKB **WTZR YAR1** YELL.
- **Allow** the **remaining** 15 sites to be selected normally, based on geographic distribution. Constrain any of these that are **IGS fiducials** to their **ITRF96** values.

The north-east-vertical transformation agreement between our 7-year **ITRF94** solution and **ITRF96** is 2, 2, and 11 mm for positions, and 1, 2, and 7 **mm/yr** for velocities.

RESULTS

One metric of performance is day-to-day orbit consistency. Figure 1 is a plot of **JPL** orbit repeatability (**3drms**) since 1995. Each data point indicates the median over **all** satellites and days for a particular **GPS week**. The daily number for a given **satellite** indicates the degree to which the precise orbit agrees with those of adjacent days near the midnight boundary. Weeks during which AS was off are marked with an 'X'. Contributing factors to the improving trend are the continuing expansion of the global network, the use of global phase ambiguity resolution, and the estimation of tropospheric gradients.

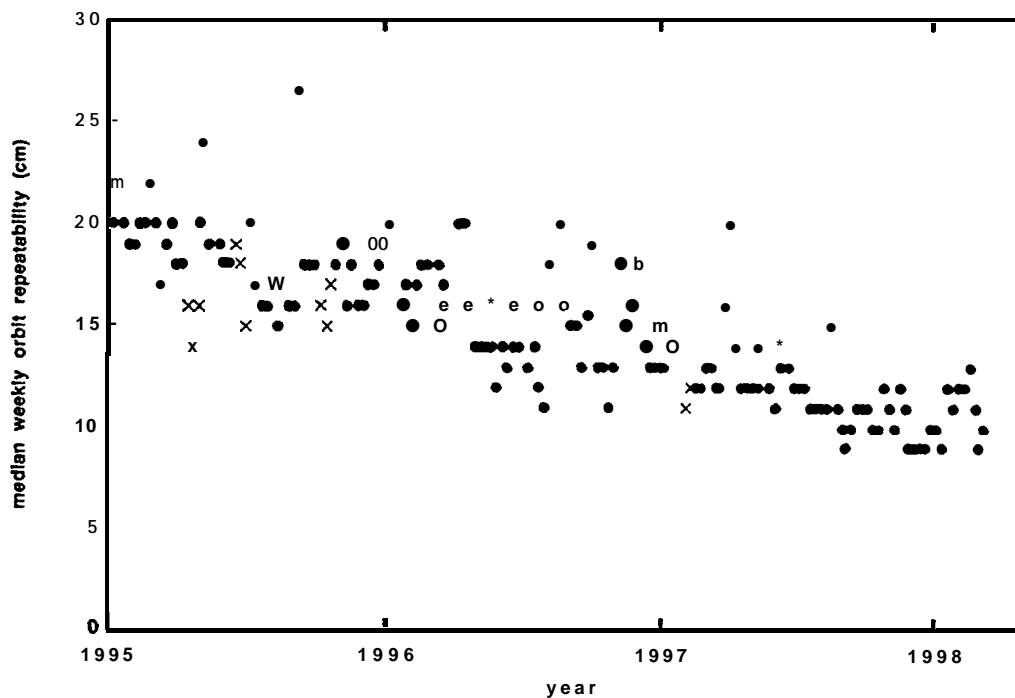


Fig. 1. JPL orbit repeatability (3drms) since 1995.

Acknowledgement The work described in this paper was carried out by the Jet Propulsion Laboratory, California Institute of Technology, under contract with the National Aeronautics and Space Administration.

REFERENCES

Bar-Sever, Y. E., P. M. Kroger and J. A. Borjesson, *Estimating Horizontal Gradients of Tropospheric Path Delay with a Single GPS Receiver*. (Submitted for publication. Copies available upon request.)

Jefferson, D. C., M. B. Heflin, M. M. Watkins, F. H. Webb, J. F. Zumberge, Jet Propulsion Laboratory *IGS Analysis Center Report, 1996*, in *IGS 1996 Annual Report*, J. F. Zumberge, D. E. Fulton, R. E. Neilan, editors, IGS Central Bureau, Jet Propulsion Laboratory, Pasadena, CA, 1997

A REVIEW OF GPS RELATED ACTIVITIES AT THE NATIONAL GEODETIC SURVEY

Mark Schenewerk, Steve Mussman, Gerry Mader and Everett Dutton
National Geodetic Survey, NOAA
Silver Spring, MD 20910 USA

INTRODUCTION

The following, originally presented in poster format, is a brief summary of activities at the National Geodetic Survey (NGS) related to or of interest to the International GPS Survey for Geodynamics (IGS). First, a brief summary of orbit production and the quality of those products is given. This is followed by a description of a new effort to estimate total electron content (TEC) over the United States using the IGS and Continuously Operating Reference Station (CORS) network. These estimates are summarized in the form of TEC maps which are made available via the World Wide Web (WWW).

A SUMMARY OF ORBIT PRODUCTION AT NGS FOR 1997

- GPS ephemerides are made using the daily, 24 hour Receiver Independent EXchange (RINEX) data files processed with the page4 program.
- The observable is **double-differenced**, ionosphere-free phase with a data interval of 30 seconds and 15 degree observation elevation cutoff.
- The data are automatically edited with manual verification of the auto-editing.
- For the rapid products, initial conditions (position, velocity, two radiation pressure scale factors) are taken from the last epoch of the previous day's ephemeris. For the final products, the rapid is the source for the a priori orbital values.
- The National Earth Orientation Service, NEOS, Bulletin A (SERIES 7) e-mailings are used for a priori pole information. This series is updated for the Sunday production and kept for an entire week.
- The coordinates of the sanctioned sites are held constrained at the level of the sigmas distributed with the coordinates (Kouba, 1996). Two additional sites: MATE and MDO1 are also constrained. For the rapid products, additional sites may be constrained if significant data outages occur.
- The Cartwright and Taylor (1971 and Cartwright and Edden, 1973) solid Earth tidal potential, complete through degree three but including the newest Shida and Love numbers was used to removed the solid earth tide but no model for atmospheric or ocean-loading was applied.
- No ocean or atmospheric loading corrections are made.
- The standard antenna phase patterns were used (Rothacher and Mader, 1996).
- The hydrostatic (dry) component of the atmosphere was modelled and removed using Saastamoinen (1972) zenith delay and NMF mapping functions (Neill,

1996), A seasonal model for the surface temperature, pressure and relative humidity was used at all sites. Two hour wet tropospheric delays are estimated for all sites.

- Phase biases are estimated. No phase biases were fixed to their integer values.
- No operational changes have been made since January 12, 1997. The only software change occurred on June 30, 1997 when the automatic editor was upgraded.

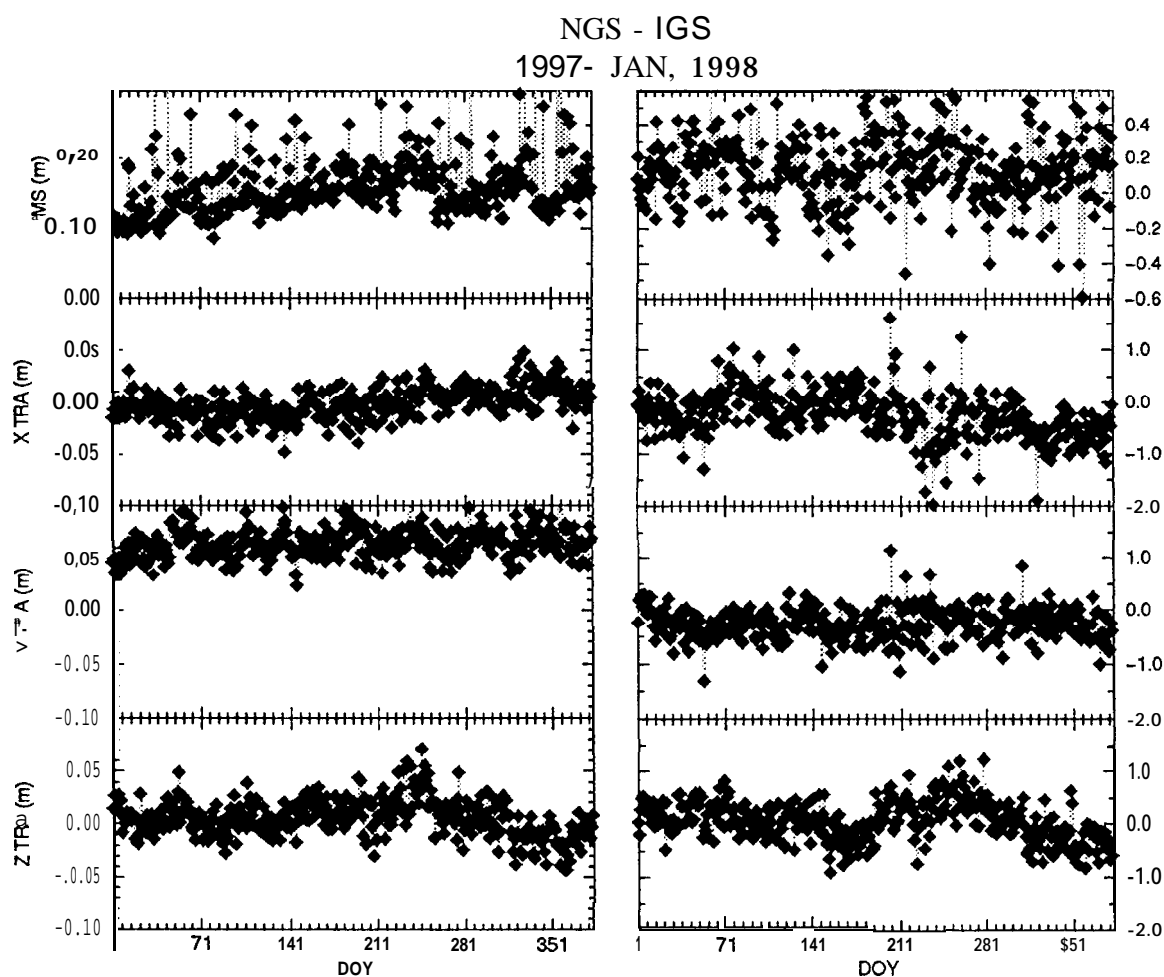


Figure 1 Comparison of the NGS product to the IGS Final. The panels show the RMS of fit, and the seven parameters of the transformation which yields the best fit. TRA = translation; ROT = rotation

NOAA-NEOS A @ Fri Feb 607:10:54 EST 1998
 $x = 0.737(0.383)$ $y = 0.548(0.481)$ $utl - utc = -0.060(0.374)$

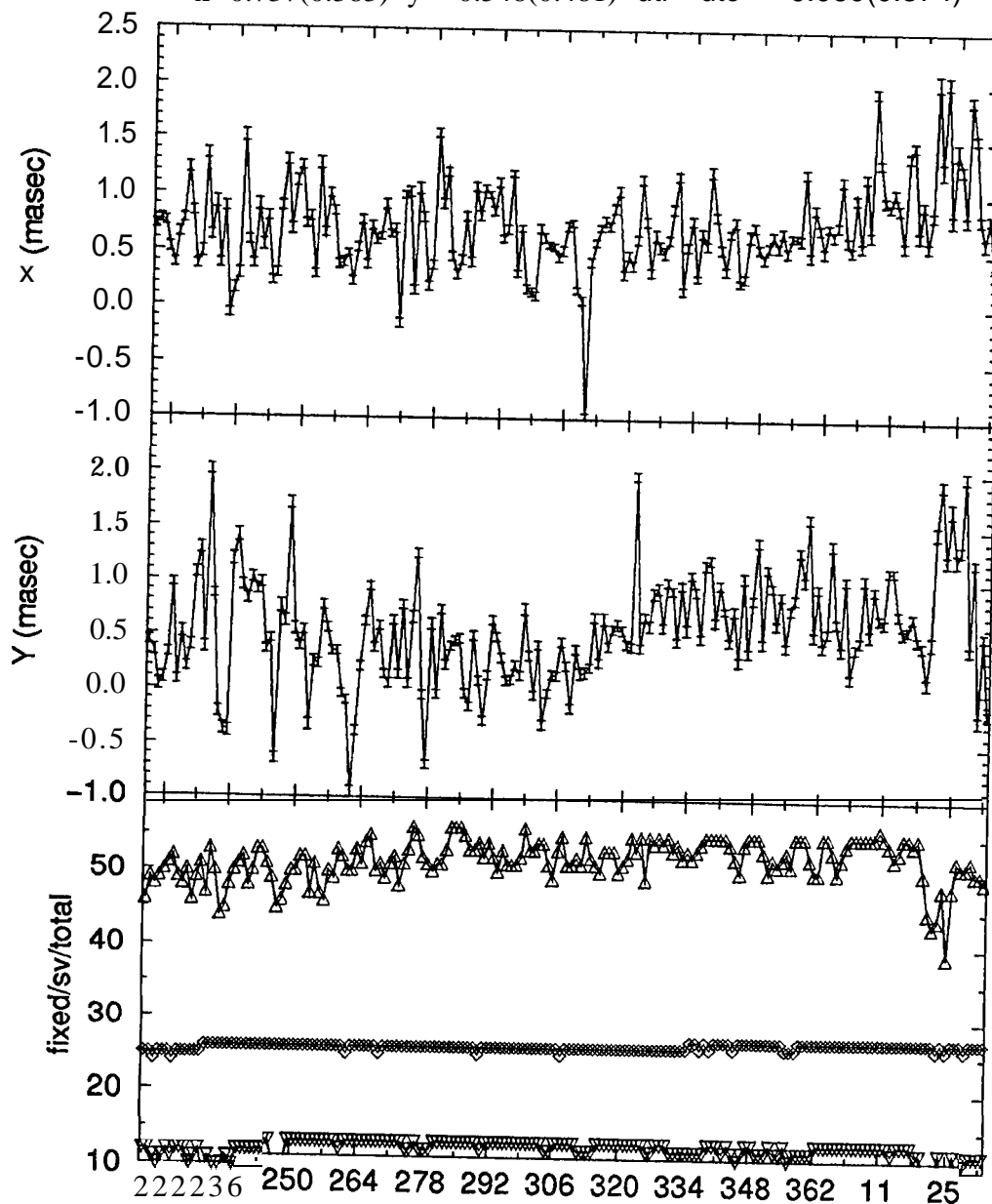


Figure 2 Comparison of the NGS X and Y Earth orientation parameters to the NEOS Bulletin A. The bottom panel shows the number of constrained, i.e. fixed sites (inverted triangles), satellites (diamonds), and total number of sites in each solution (triangles),

TOTAL ELECTRON CHANGES IN THE IONOSPHERE DURING IONOSPHERIC STORMS AS MEASURED BY THE CORS NETWORK OF GPS RECEIVERS

At each station of the CORS network, local models of TEC were constructed from carrier phase. These are displayed in the form of maps. Geomagnetic storms on 10 January, 15 May and 10 October, 1997 were studied in detail and are presented here. The TEC changes associated with the three event shown here depend strongly on latitude. Maps are plotted of the daily maximum TEC minus the maximum of the average for several nearby days. This is a measure of the strength of the event which is independent of local time.

Developmental movies of the ionospheric maps for selected days are available at <http://www.grdl.noaa.gov/GRD/GPS/Projects/TEC>

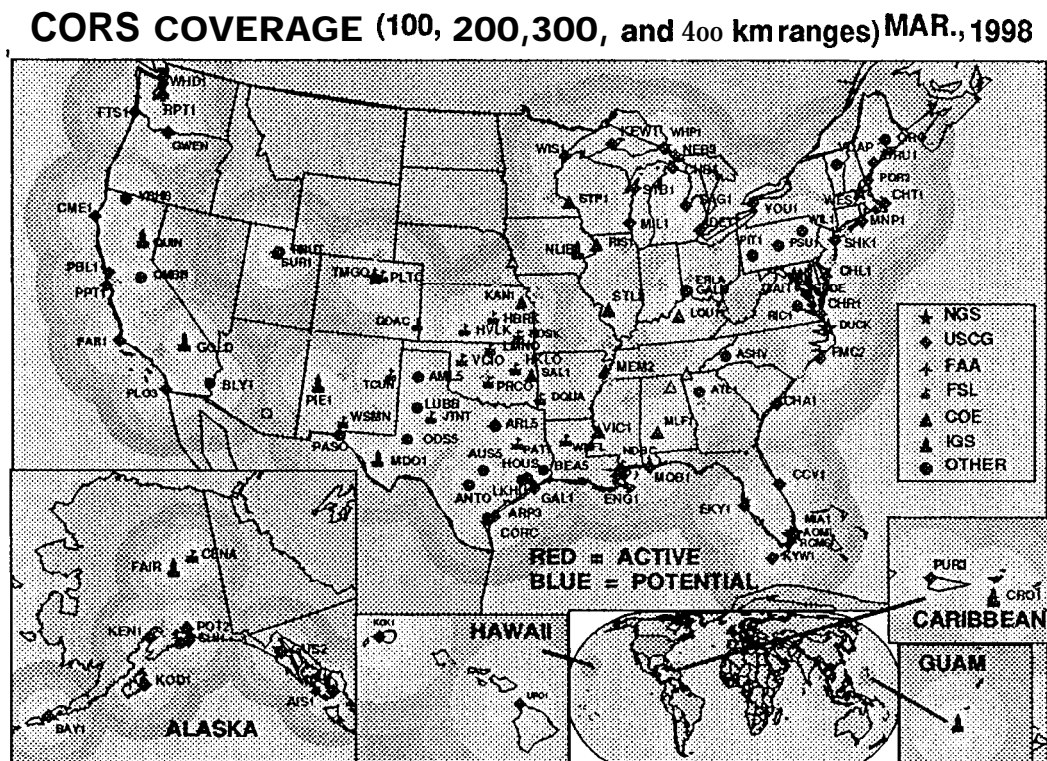


Figure 3 The CORS network as of March, 1998. Note that several IGS tracking sites are redistributed through the CORS data center.

TEC from the CORS Network

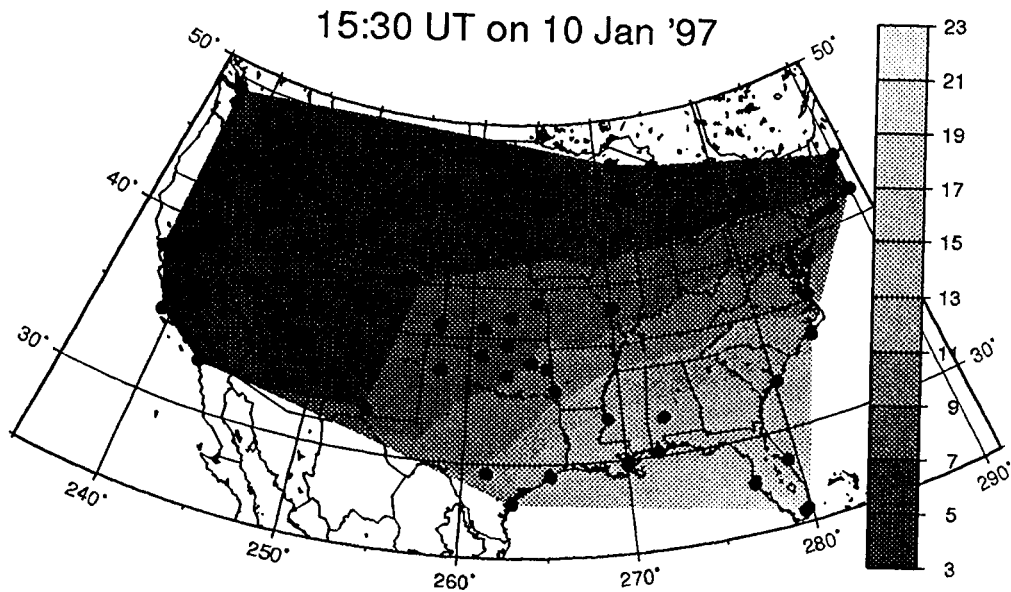


Figure 4 TEC map for 15:30 UTC on January 10, 1997

Storm Anomaly on 10 Jan '97

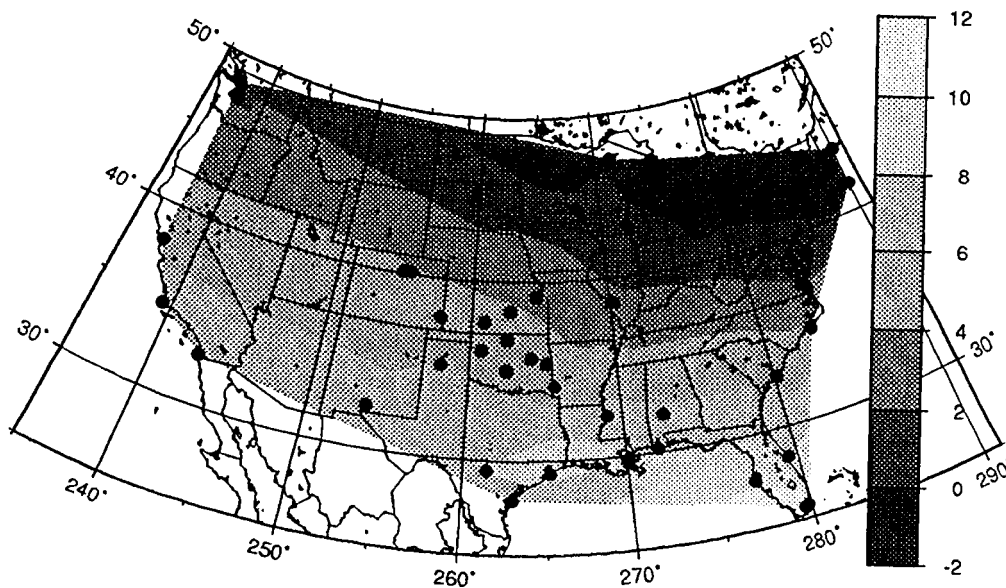


Figure 5 TEC maximum for January 10, 1997 minus the typical, average maximum for this period.

Storm Anomaly on 15 May '97

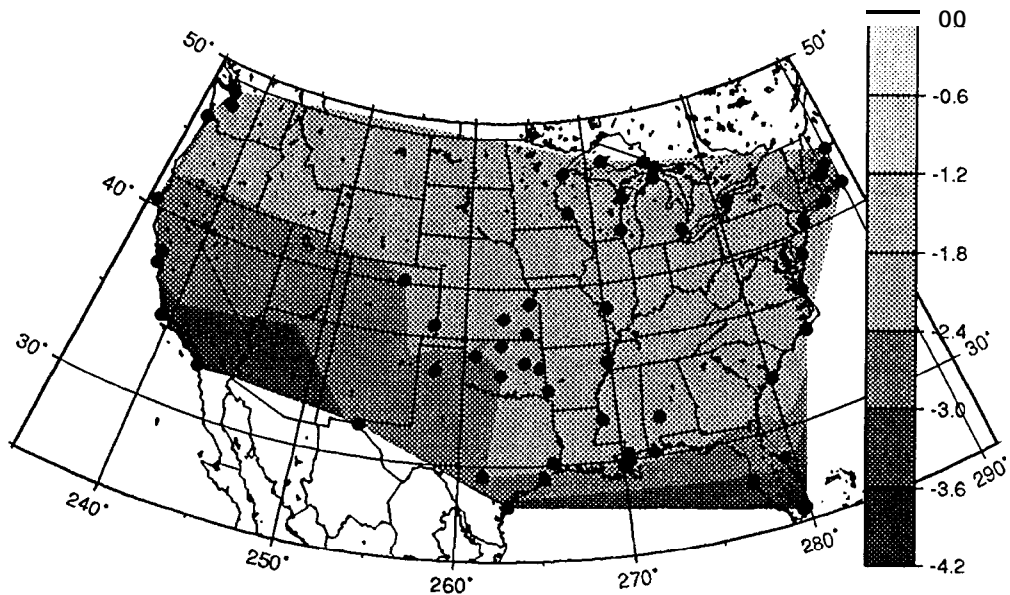


Figure 6 TEC maximum for May 15, 1997 minus the typical, average maximum for this period.

Storm Anomaly on 10 Oct '97

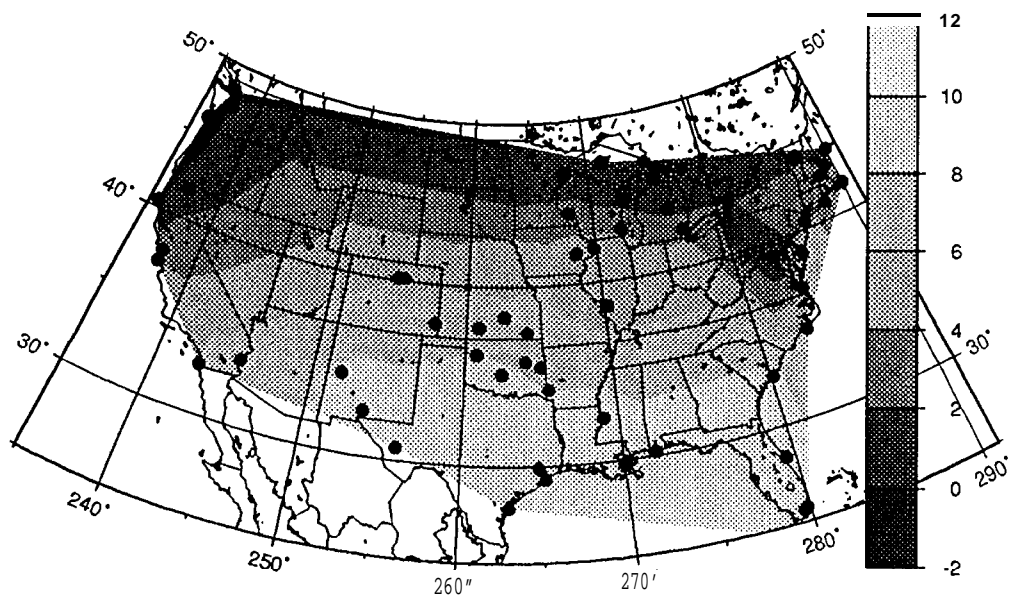


Figure 7 TEC maximum for October 10, 1997 minus the typical average maximum for this period.

REFERENCES

- Cartwright, D.E., and R.J. Taylor, New computations of the tide-generating potential, *Geophys. J.R. astr. Soc.*, **23**, 45-74, 1971.
- Cartwright, D. E., and A.C. Edden, Corrected tables of tidal harmonics, *ibid*, 33, 253-264, 1973,
- Kouba, J., Personal communication via **email** with subject "Comments on ITRF94 (fwd)", June 11, 1996.
- Rothacher, M. and Mader, G.L., Personal communication via **email** with subject "Antenna Phase Center Corrections IGS_01", June 30, 1996.
- Niell, A.E., Global mapping functions for the atmosphere delay at radio wavelengths, *J. Geophys. Res.*, **101(B2)**, 3227-3246, 1996.
- Saastamoinen, J., Atmospheric correction for the troposphere and stratosphere in radio ranging of satellites, in **The Use of Artificial Satellites for Geodesy**, *Geophys. Monogr. Ser. 15* (S.W. Henriksen et al., eds.), AGU, Washington, D. C., 247-251, 1972.

U.S. NAVAL OBSERVATORY: CENTER FOR RAPID SERVICE AND PREDICTIONS

J.R. Ray, J.R. Rohde, P. Kammeyer, and B.J. Luzum
Earth Orientation Dept., U.S. Naval Observatory
Washington, DC 20392 USA

INTRODUCTION

The mission of the U.S. Naval Observatory (USNO) includes determining the positions and motions of the Earth, Sun, Moon, planets, stars and other celestial objects, providing precise time, measuring the Earth's rotation, and maintaining the master clock for the U.S. The Earth Orientation (EO) Department contributes to this mission by collecting suitable observations and performing data analyses to determine and predict the orientation of the terrestrial reference frame within the celestial reference frame. The key parameters determined and disseminated are polar motion coordinates, universal time (UT1), precession, and **nutation**. The user community includes the U.S. Department of Defense, other U.S. government agencies, scientific researchers, and the general public. The primary applications are for high-accuracy navigation and positioning with an emphasis on real-time uses.

In order to accomplish these objectives, USNO collaborates closely with a large number of other groups and organizations. In particular, the U.S. National Earth Orientation Service (NEOS) is a partnership with the National Aeronautics and Space Administration (NASA) and the National Oceanic and Atmospheric Administration (NOAA) primarily to organize joint VLBI (very long baseline interferometry) operations to monitor Earth orientation. NEOS serves as the VLBI coordinating center for the International Earth Rotation Service (IERS). USNO and NEOS have an enduring commitment to VLBI in order to maintain accurate knowledge of UT1, the celestial pole, and the celestial reference frame, which is realized by the positions of about 600 extragalactic radio sources. This responsibility is shared with several non-U.S. agencies which contribute essential observing time on their VLBI telescopes.

As with VLBI, the capabilities of GPS also serve important USNO mission objectives. For that reason we have participated actively with the IGS since its inception. Recently, the US NO role in the IGS has grown and further expansion is expected. This report summarizes the current status and future prospects for US NO involvement with GPS and the IGS, together with some recent results.

IERS SUB-BUREAU FOR RAPID SERVICE AND PREDICTION

NEOS serves as the IERS Sub-bureau for Rapid Service and Prediction of Earth orientation parameters (EOPs). This function is carried out by the EO Dept. at USNO. EOP results contributed by many analysis centers derived from observations by VLBI, satellite laser ranging (SLR) to LAGEOS, lunar laser ranging (LLR), or GPS are combined into a homogeneous daily time series which is updated and distributed twice each week as *IERS Bulletin A*. Combined EOP values for the recent past are published together with predictions extending a year into the future.

In recent years, the *Bulletin A* polar motion results have been dominated by the precise determinations of the IGS combined Final products, with the Rapid series being used for the most recent measurements. The Rapid determinations are quite important for *Bulletin A* by providing timely, high-quality results which are most significant for polar motion predictions needed by real-time users. The recent accuracy of these series is estimated to be about 0.1 mas (per component) for the Finals and 0.2-0.3 mas for the Rapids. It is expected that implementation of the much more robust and improved terrestrial reference frame realization proposed by Kouba *et al.* (1998), where the coordinates and velocities of 47 sites are constrained to their ITRF96 values, will produce significantly more stable polar motion results. This, in turn, should improve the quality and reliability of current and near-term predictions of polar motion.

In addition to polar motion, *IERS Bulletin A* has become increasingly reliant on IGS estimates of length of day (LOD). The IGS started producing an official LOD product on 02 March 1997 using a weighted combination of LOD results submitted by each IGS Analysis Center (AC). To calibrate for LOD biases, each series is compared with the most recent 21 days of non-predicted UT1 values from *Bulletin A* (Kouba and Mireault, 1997; Ray, 1996). Shortly after its advent, the IGS combined LOD results were introduced into the *Bulletin A* combination to extend the UT 1 value of the most recent VLBI determination forward by integration. A few months later an independent set of GPS-based estimates of universal time, derived at USNO and described below, were also included in *Bulletin A*. About two weeks of the most recent estimates are used, after calibration in offset and rate compared to overlapping UT 1 results from VLBI. These two series together have proven very successful in extending UT 1 results forward from the latest VLBI determinations, which may have a latency of up to about a week. As a consequence, the last non-predicted UT1 value in *Bulletin A* is now generally more accurate than 100 μ s, usually considerably more so.

Errors in predicted EOP values are a significant source of systematic error in the IGS Predicted orbits, although they rarely dominate the overall error budget. Martin Mur *et al.* (1998) have stressed the need for improved EOP predictions for use in computing the IGS Predicted orbits. Partly to address this concern, refinements already under development were implemented in *Bulletin A* on 03 March 1998 (Ray and Luzum, 1998). The current and previous performance of the predicted polar motion variation is shown in Table 1. It can be seen that the improvement is most significant for the shortest prediction intervals (53% for 1 day) but diminishes over longer spans. Research is continuing into further improvements, which are likely to be implemented later in 1998.

For real-time users, given two updates of *Bulletin A* each week, the longest prediction interval is 7 days (for Tuesday updates compared with the previous Thursday issue which normally contains most recent data from 2 days earlier). This means that real-time users should experience polar motion errors no greater than about 2.4 mas (in an RMS sense per component). When the IGS delivery schedule for its Rapid products advances from 21:00 UTC to 16:00 UTC each day (by the end of 1998) this will allow each *Bulletin A* update to be performed during Washington afternoons with a reduced data latency of 1 day rather than the current 2 days. Thus the maximum prediction interval for real-time users will shorten to 6 days with an associated RMS polar motion error of about 2.0 mas. The *Bulletin A* update schedule could be changed to Monday/Thursday from the current Tuesday/Thursday to further reduce the maximum prediction interval to 5 days with an RMS polar motion error of about 1.7 mas. This has not been done in the past because most U.S. holidays occur on Mondays.

Table 1. Errors in *IERS Bulletin A* predictions for polar motion. The values tabulated are RMS scatters per component based on a retrospective analysis of actual polar motion variations during 1994- 1998.

predictions interval (days)	polar motion error (milliarcseconds)	
	previous	current
1	0.442	0.206
2	0.882	0.515
3	1.322	0.893
4	1.749	1.296
5	2.143	1.682
6	2.497	2.044
7	2.820	2.374
10	3.712	3.282
15	5.186	4.705

Predictions of UT1 variation are more problematic because the geophysical excitation is an order of magnitude larger than for polar motion. To reduce UT1 prediction errors will require very close coordination between the IGS and the IERS Sub-bureau, with heavy reliance on IGS Rapid LOD estimates and perhaps necessitating daily updates of *Bulletin A*.

As part of its contribution to the IGS, USNO prepares regular reports and plots of the performance of each IGS Analysis Center (AC) compared with *Bulletin A*, which are available at <http://maia.usno.navy.mil/bulletin-a.html>. Additional analysis reports are prepared occasionally to assess changes in IGS performance or to evaluate the geophysical implications (see for example Eubanks *et al.*, 1998).

IGS RAPID SERVICE ASSOCIATE ANALYSIS CENTER

Given the significance of the IGS results and our increasing reliance upon them, it is natural for USNO also to contribute actively as a data analysis center. Beginning 23 April 1997 USNO officially became a contributor to the IGS Rapid products. Originally we intended to eventually begin submitting Final and other products to become a full IGS AC. Since that time, however, other GPS-related activities have developed, such as the IGS/BIPM timing project (Ray, 1998), which are more closely tied to the USNO mission and therefore take higher priority. Given limited resources, USNO would, for the time being, prefer not to assume the additional responsibilities of a full AC. We suggest that the IGS recognize Rapid Service Associate Analysis Centers (RSAACs) as contributors of rapid service and prediction products. We plan to begin producing and contributing predicted GPS orbits during 1998.

An emerging interest at USNO is improved GPS orbits for a variety of real-time applications, including precise time transfer. This requires the highest quality Rapid and Predicted orbits and EOPs. These interests mesh naturally with full participation in the IGS/BIPM timing project. In support of this, USNO has already deployed a TurboRogue SNR12 receiver in Washington, DC connected to the USNO Master Clock (MC) as its

frequency reference. A second receiver is being deployed at Falcon Air Force Base in Colorado Springs, site of the USNO Alternate Master Clock (AMC) and the operations center for GPS. The MC and AMC are kept closely synchronized by regular two-way satellite time transfer (TWSTT) observations. These IGS sites can therefore serve as important comparison sites in the IGS/BIPM project.

Basic features of the USNO analysis strategy are summarized in Table 2. The software used is GIPSY/OASIS II, developed and maintained by JPL.

Table 2. USNO Analysis Strategy.

Software	GIPSY/OASIS II (vers. 4.8)
Observable	carrier phase & pseudo-range at 7.5 min.
Arc length	3+24 hr.
Network	30 global sites (usually)
Elevation cutoff	15 deg.
Sat. parameters	initial position & velocity, rad. pressure scale & Y-bias as constants, X,Z rad. pressure scales as stochastic
Attitude	yaw rates for eclipsing sats.

GPS DETERMINATIONS OF UNIVERSAL TIME

Elsewhere Kamrneyer (1998) has described his method to determine UT1 -like variations from an analysis of GPS orbit planes as estimated for IGS Rapid submissions. Briefly, the Earth-fixed GPS ephemerides determined operationally at USNO are compared to orbit planes propagated using a modeled radiation pressure acceleration normal to each orbit plane. For each satellite, the modeled acceleration is expressed relative to the projection of the Sun direction on the orbit plane and depends only on the angle from the orbital angular momentum to the Sun. The models being used were obtained empirically from observed experience when this angle was greater than 90° during 1994-1995. For each satellite, there is a unique axial rotation angle which brings the observed Earth-fixed positions into alignment with the propagated orbit plane. Since the propagated orbit plane of each satellite is different from its osculating orbit plane in an inertial frame, offsets are added to the rotation angles to form single-satellite estimates of GPS-based universal time. The median of these values for the 13 satellites modeled gives the UT estimate reported to *Bulletin A*.

Kammeyer's results show quite encouraging short-term performance. The relatively slow drifts allow sliding segments of these data to be including in the *Bulletin A* combination after calibration only for an offset and a rate. The residual scatter is about 75 μ s over 3-week intervals. The procedure is described above and has proven very successful in extending more accurate but less timely VLBI measurements of UT1 to nearer real-time. Over longer spans these GPS-based determinations drift systematically, up to about 600 μ s in six months.

Several improvements can be made. The long-term drifts reflect deficiencies in empirical models for the orbit plane motions. With the longer series of orbits now available, better models should be feasible. In particular, the present models are based

on data collected before the current yaw bias was implemented. Models can be constructed for all satellites, not just the 13 currently being used. The procedure could be applied to the more precise and reliable IGS combined orbits rather using the USNO orbits.

REFERENCES

Eubanks, T. M., J.R. Ray, and B. J. Luzum, The atmospheric excitation of rapid polar motions, *Eos Trans. American Geophysical Union*, in press 1998.

Kammeyer, P., Determination of a UT1-like quantity by comparing GPS positions to propagated orbit planes, in preparation 1998.

Kouba, J., and Y. Mireault, Analysis Coordinator report, in *International GPS Service for Geodynamics, 1996 Annual Report*, edited by J.F. Zumberge, D.E. Fulton, and R.E. Neilan, Jet Propulsion Laboratory, Pasadena, California, pp. 55-100, 1997.

Kouba, J., J. Ray, and M.M. Watkins, IGS reference frame realization, in 1998 *IGS Analysis Center Workshop Proceedings*, European Space Operations Centre, Darmstadt, Germany, (this volume), in press 1998.

Martín Mur, T. J., T. Springer, and Y. Bar-Sever, Orbit predictions and rapid products, in 1998 *IGS Analysis Center Workshop Proceedings*, European Space Operations Centre, Darmstadt, Germany, (this volume), in press 1998.

Ray, J., GPS measurement of length-of-day: Comparisons with VLBI and consequences for UT1, in *1996 IGS Analysis Center Workshop Proceedings*, edited by R.E. Neilan, P.A. Van Scoy, and J.F. Zumberge, Jet Propulsion Laboratory, Pasadena, California, pp. 43-60, 1996.

Ray, J., The IGS/BIPM time transfer project, in 1998 *IGS Analysis Center Workshop Proceedings*, European Space Operations Centre, Darmstadt, Germany, (this volume), in press 1998.

Ray, J., and B. Luzum, Improved polar motion predictions, IGS Electronic Mail #1816, <http://igscb.jpl.nasa.gov/igscb/mail/igsmail/igsmess>. 1816, 27 Feb. 1998.

THE IGS REGIONAL NETWORK ASSOCIATE ANALYSIS CENTER FOR SOUTH AMERICA AT DGFI

Wolfgang H. Seemueller, Hermann Drewes
Deutsche Geodaetisches Forschungsinstitut (DGFI)
D-80539 Muenchen, Germany

INTRODUCTION

Early in 1996 the International GPS Service for Geodynamics (IGS) called for participation in a pilot project to densify the IERS Terrestrial Reference Frame (ITRF) by regional networks and a distributed data processing by Regional Network Associate Analysis Centers (RNAAC). DGFI is acting on behalf of the SIRGAS project (Sistema de Referencia Geocentric para America del Sur) as a RNAAC for South America. Beginning in mid of 1996 all available data of permanently observing GPS stations in the mainland of South America and surrounding regions are processed routinely and forewarned as SINEX files to the IGS Global Data Centers.



Fig. 1: Regional Network processed by RNAAC SIRGAS

SUMMARY

The RNAAC SIRGAS coordinate solutions are generated weekly using the Bernese Processing Engine (BPE version 4.0, Rothacher and Mervart, 1996), starting with the beginning of the pilot project to densify the IERS Terrestrial Reference Frame (ITRF) in June 1996. The regional network consists of 22 GPS stations (fig. 1), seven of nine Brazilian GPS stations are processed by RNAAC exclusively.

Conclusions from the analysis are

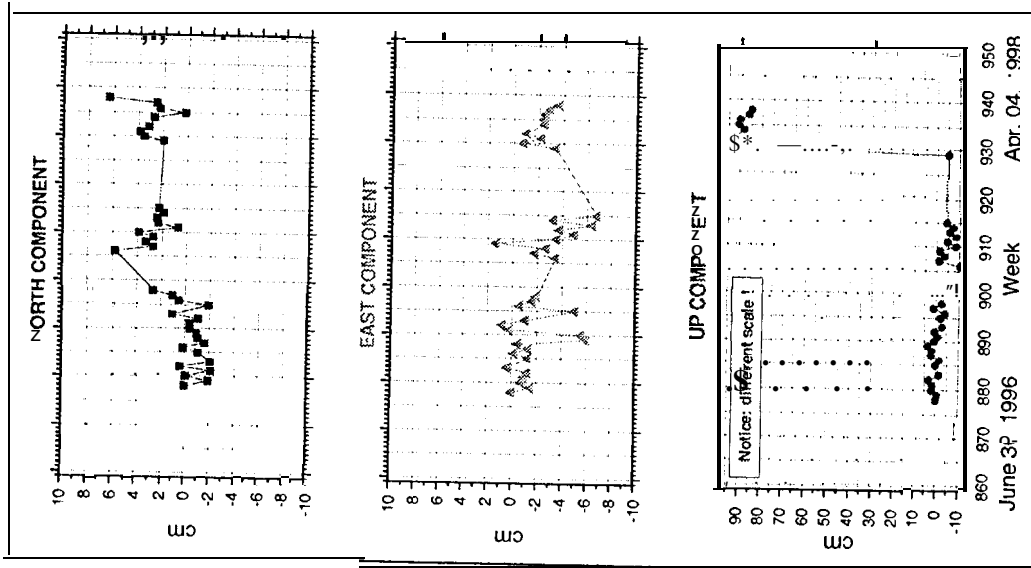
- Note: the vertical scale of the figures is 20 cm normally, except when the variations are bigger; then you see a mark that the scale differs.
- Posters 1 to 3 are the original posters shown in Darmstadt, they are reduced from DIN AO to DIN A4, and therefore they are not very nicely readable.
- To have a clearer insight to the discrepancies all comparisons for all stations are shown on one page each (figures 2 to 10)
- A rough analysis of processing results is demonstrated in the figures 2 to 10. We show the deviations in North, East and Up components of selected stations for the internal consistency (variations of weekly SIR R solutions with respect to the first solution), the diurnal variations of RNAAC solutions with respect to the first solution (only for problematic periods), and the external consistency by comparison of SIR R SINEX with the GNAAC'S P-Sinex solutions (after Helmert transformation because the SIR R-SINEX solutions are free network solutions).
- The deviations are typically in the sub-centimeter level for horizontal components and in the 1 to 2 cm level for the vertical (see Fig. 8 and 9). The small deviations of the seven Brazilian exclusive RNAAC SIRGAS stations (see e.g. Fig. 10, station President Prudente) are due to the fact that no other Analysis Center is processing these data, i.e. only the RNAAC SIRGAS solution is included in the "combination".
- Figures 2 to 7 show the deviations for IGS stations with problematic periods only. For GPS week 910 to 920 the deviations between the SIR R solutions and the GNAAC polyhedron solutions from Newcastle University increase, but this is not valid for the comparison with the MIT solutions. This is the case especially for station Limon (Fig.2), Arequipa, Ascension and Santiago de Chile (Fig. 5 to 7). The diurnal variations of SIR R solutions don't figure out this abnormal behaviour. The GNAAC Newcastle will solve this problem
- Station Limon/Costa Rica shows a jump in the Up component of about +90 cm from day 97305 to 97306 (Fig.2). Nothing is reported in the IGSMail about a change. The reason for this discontinuity is unknown.
- The Up component of station Kourou (Fig.3) is strongly varying in the daily solutions, this valid for the weekly solutions also.

REFERENCE

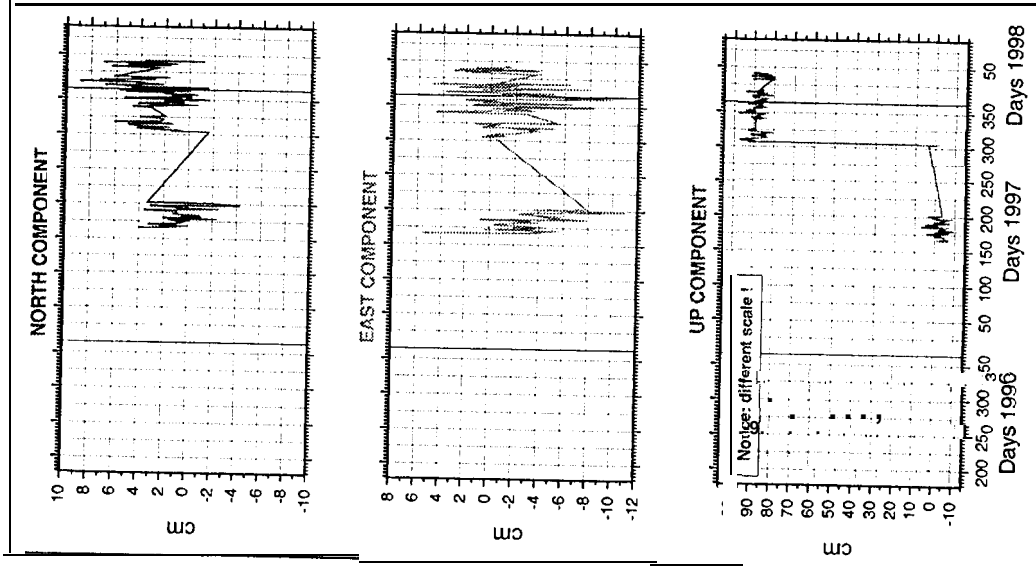
Rothacher, M. and Mervart, L. (eds.): Bernese GPS software 4.0. Astronomical Institute, University of Berne, 1996.

IGS STATION LIMON

Variations of weekly SIR R solutions with respect to first solution



variations of daily SIR R solutions with respect to first solution



Comparison of diff. SIR R and GNAAC P after Helmert transf.

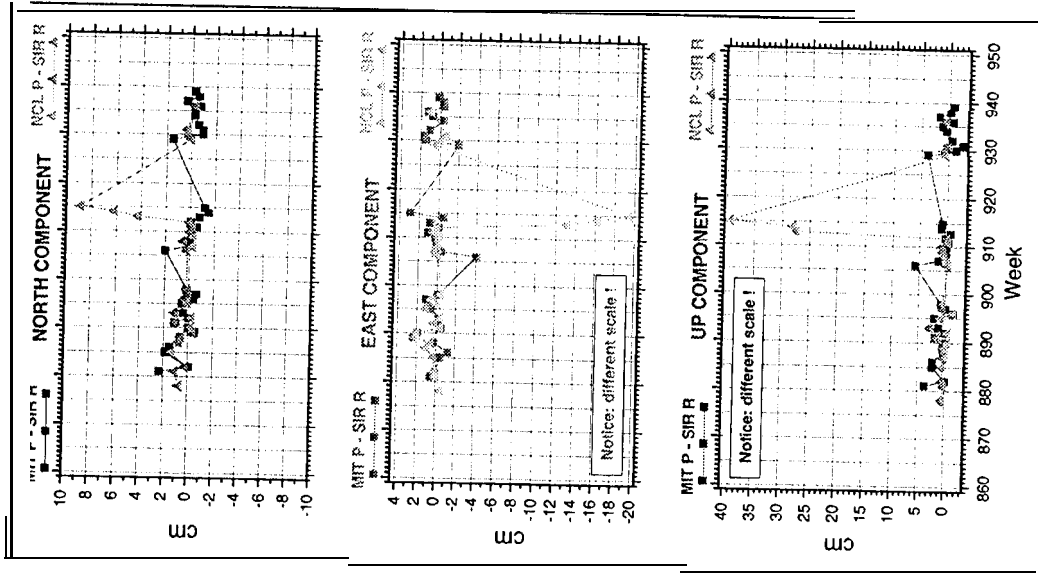


Fig. 2: Internal and External comparison of RNAAC SIR solutions (Station Limon)

IGS STATION KOUROU

Variations of weekly SIR R solutions with respect to first solution

Variations of daily SIR R solutions with respect to first solution

Comparison of cliff. SIR R and GNAAC P after Helmert transf.

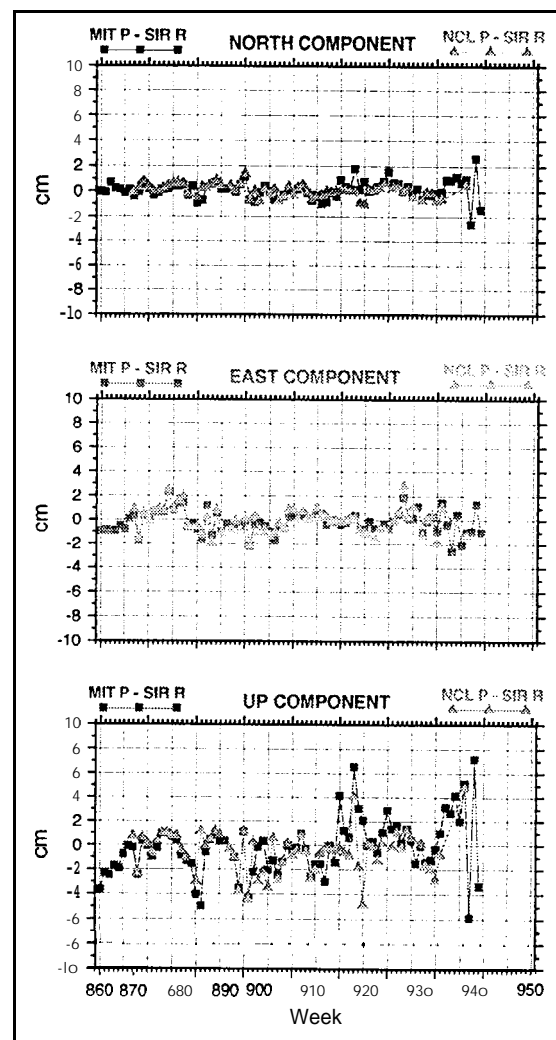
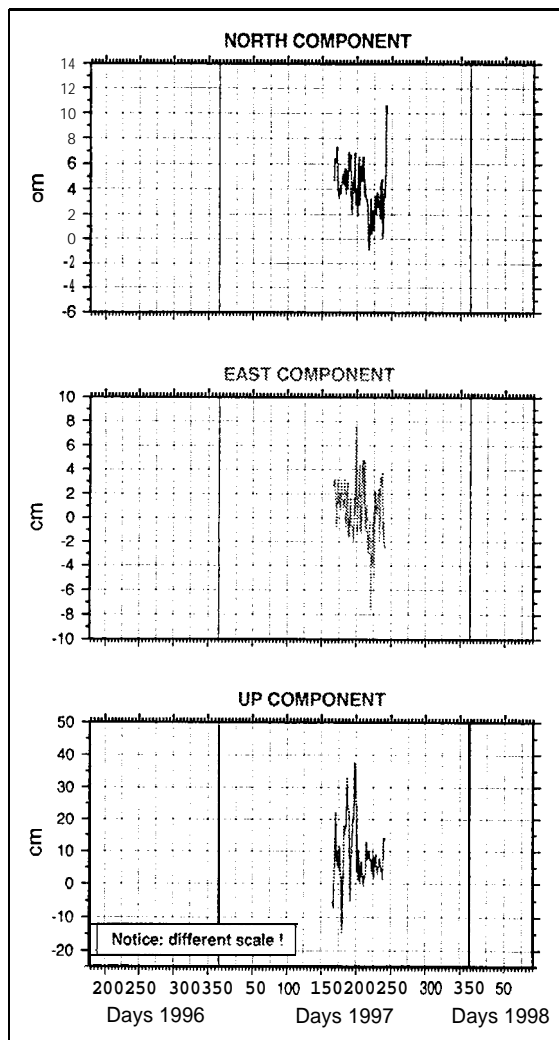
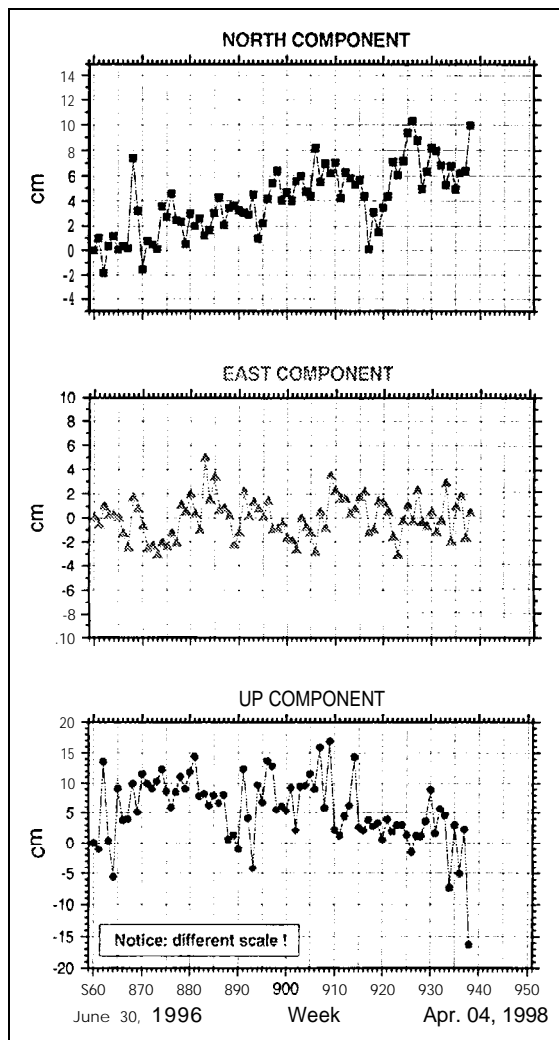
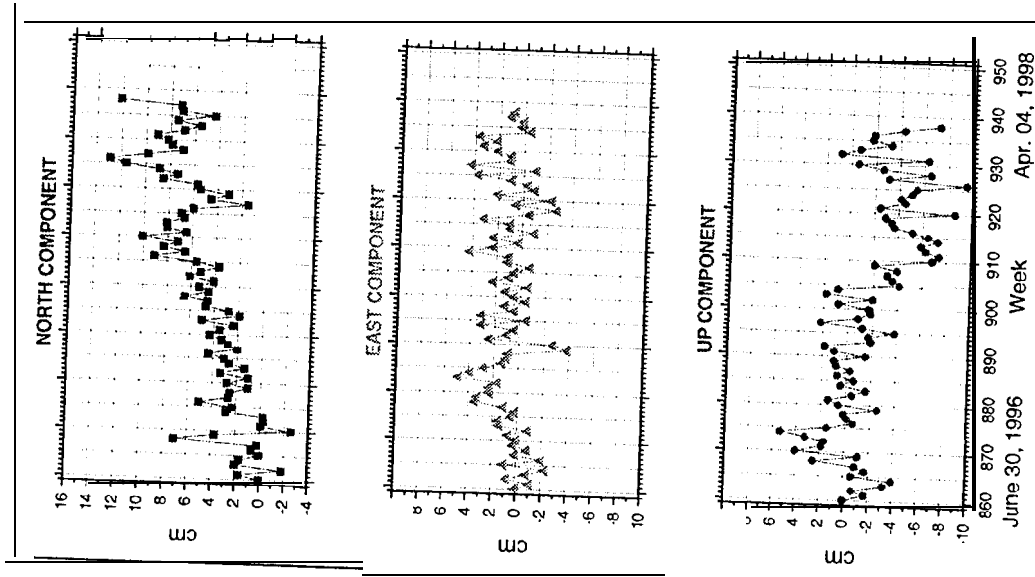


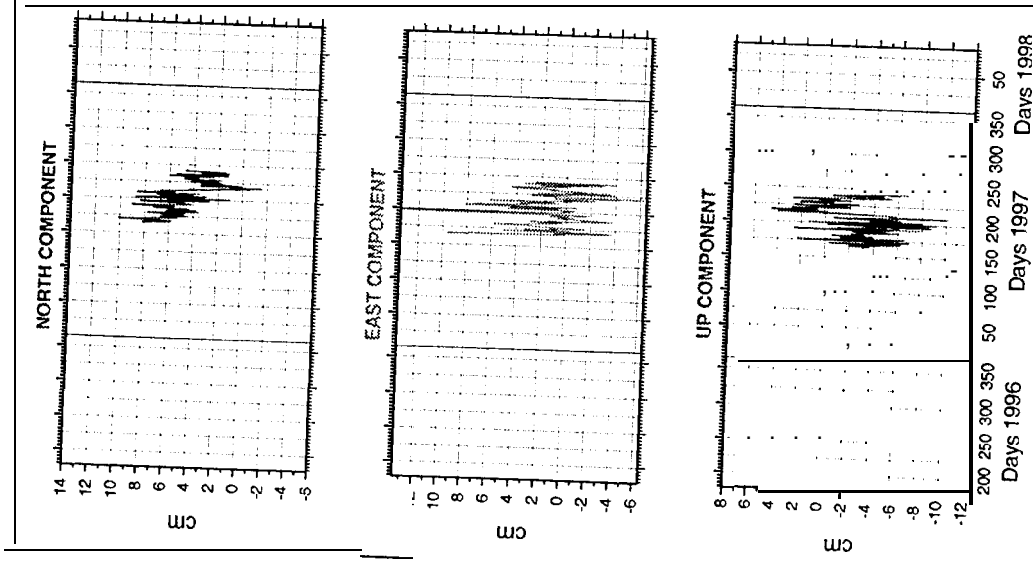
Fig. 3: Internal and External comparison of RNAAC SIR solutions (Station Kourou)

IGS STATION ST. CROIX

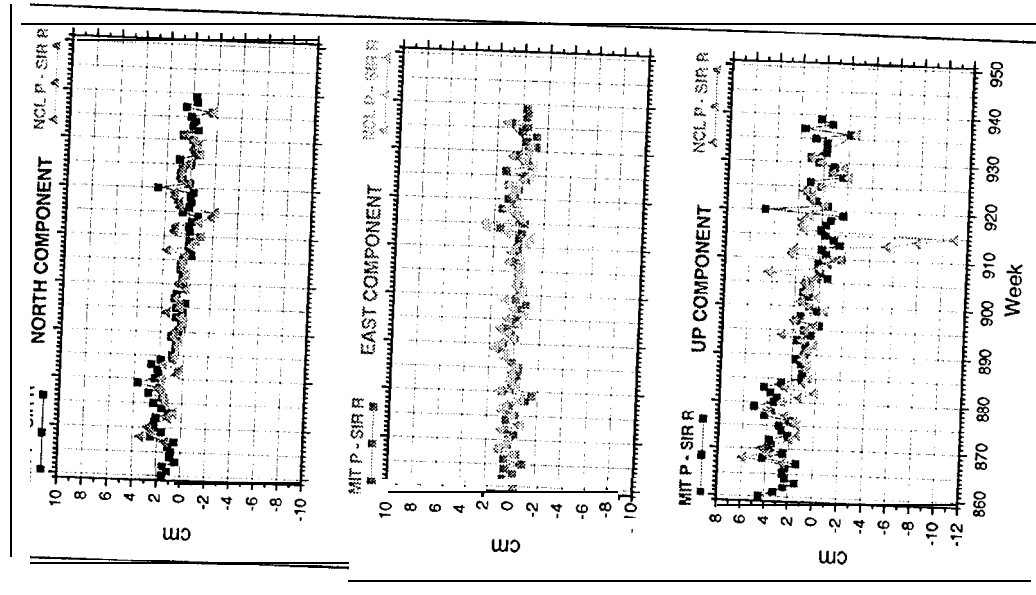
Variations of weekly SIR R solutions with respect to first solution



Variations of daily SIR R solutions with respect to first solution



Comparison of diff. SIR R and GNAC P after Helmert transf.

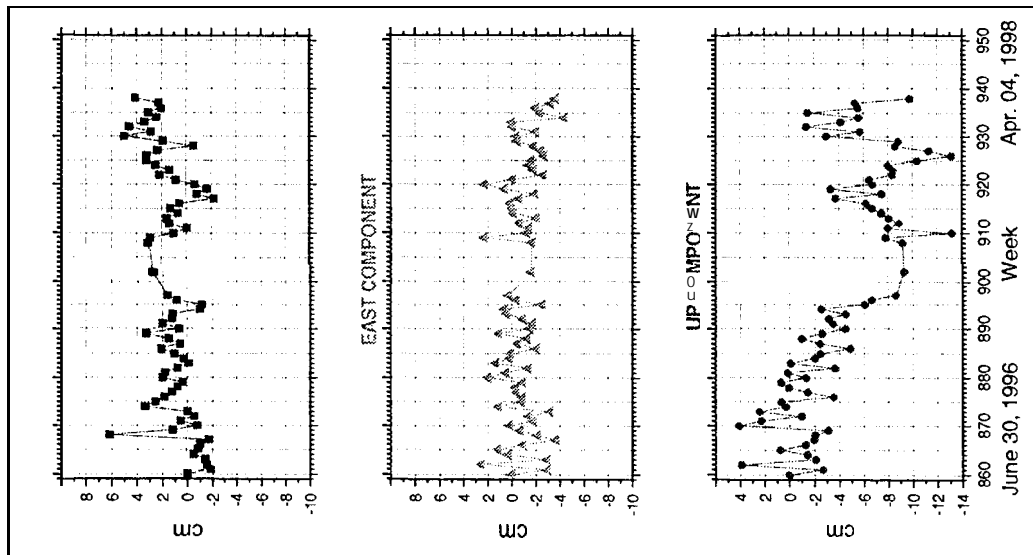


F g

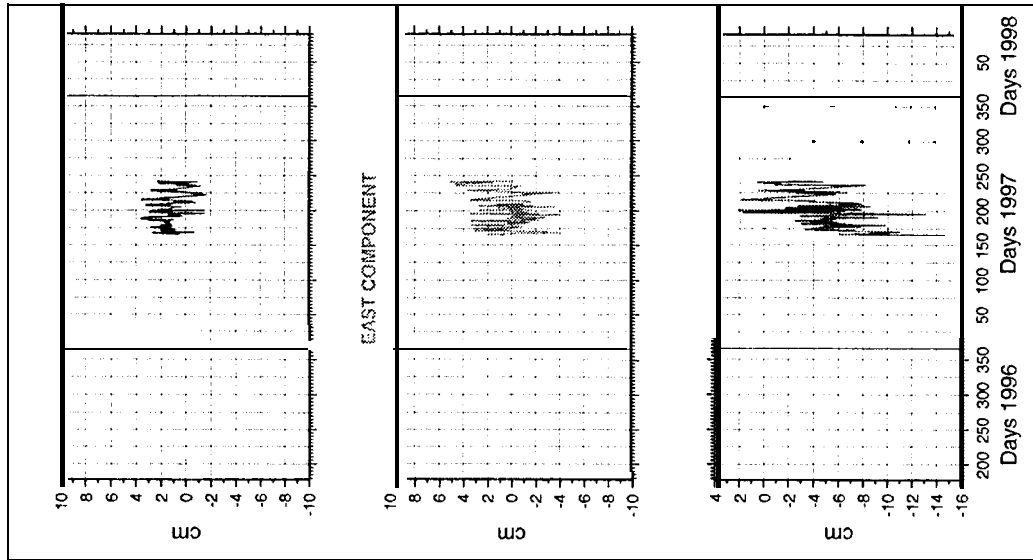
STATION ST. CROIX IGS

IGS STATION AREQUIPA

Variations of weekly SIR R solutions with respect to first solution



Variations of daily SIR R solutions with respect to first solution



Comparison of diff. SIR R and GNAAC P after Helmert trans.

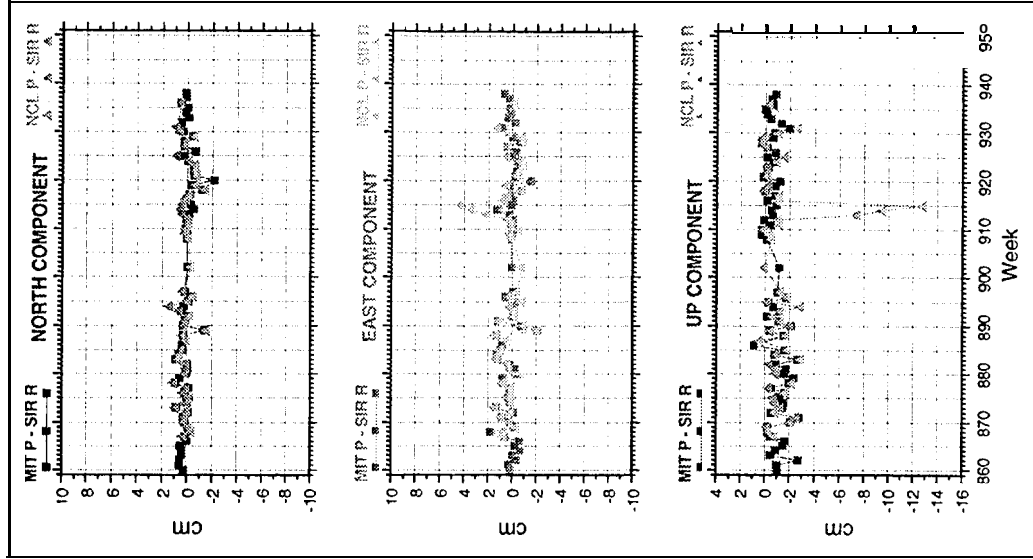


Fig. 5: Internal and External comparison of RNAAC SIR solutions (Station Arequipa)

IGS STATION SANTIAGO

Variations of weekly SIR R solutions with respect to first solution

Variations of daily SIR R solutions with respect to first solution

Comparison of cliff. SIR R and GNAAC P after Helmert transf.

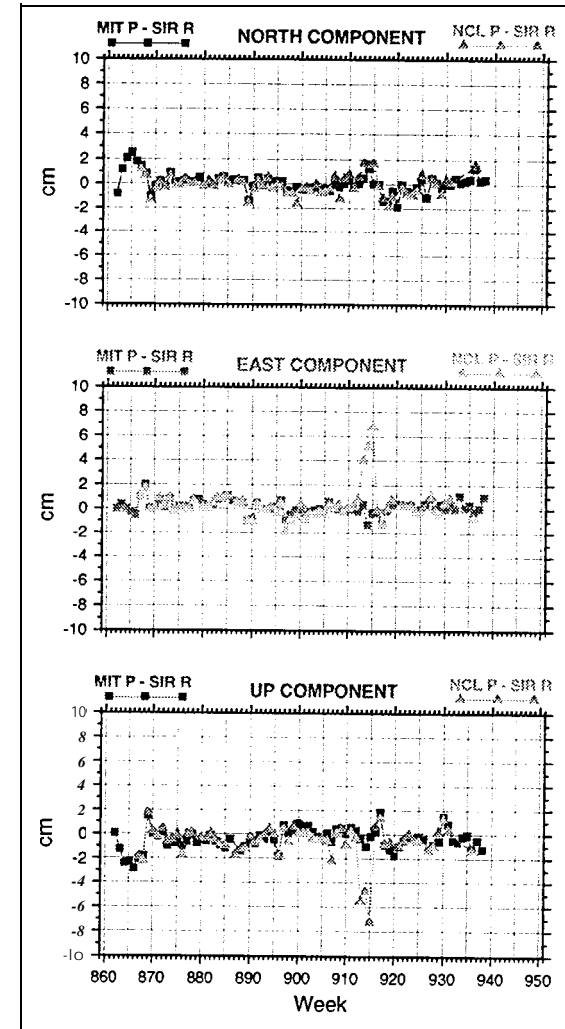
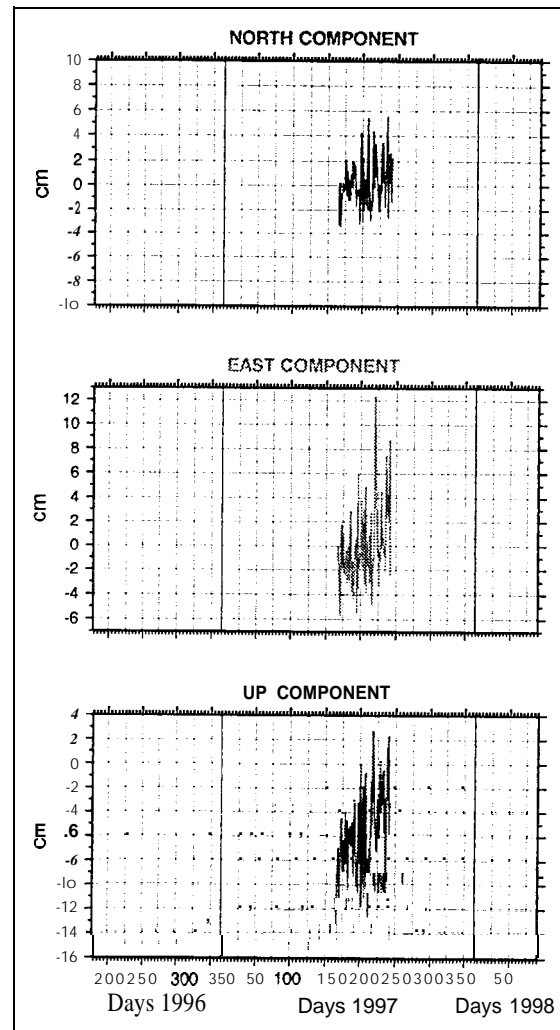
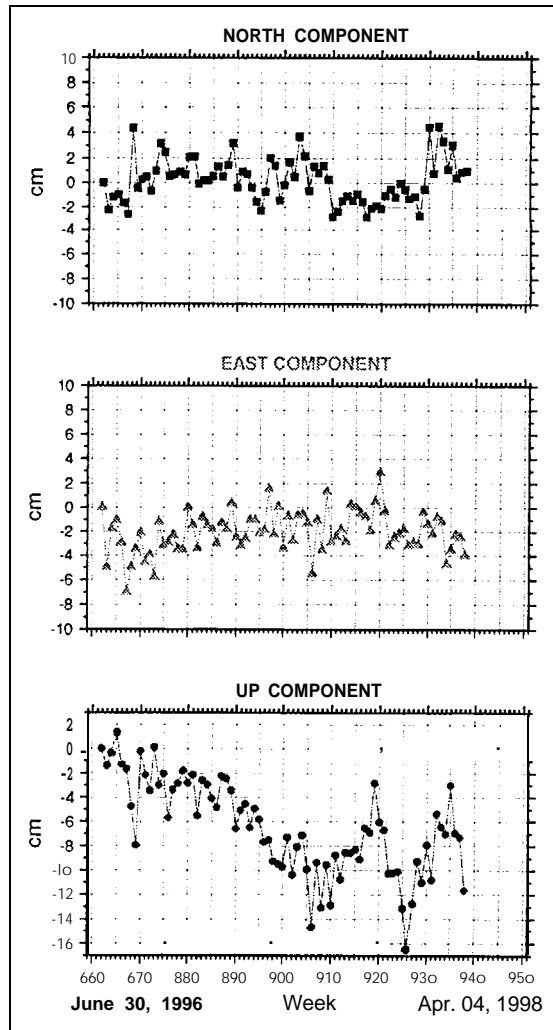
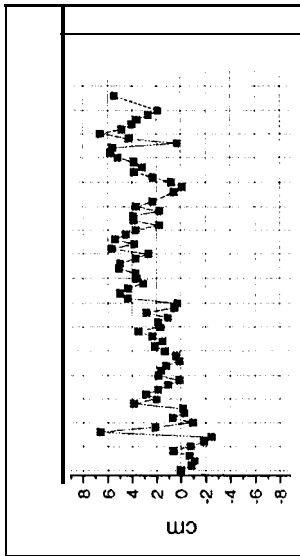


Fig. 6: Internal and External comparison of RNAAC SIR solutions (Station Santiago de Chile)

IGS STATION ASCENSION

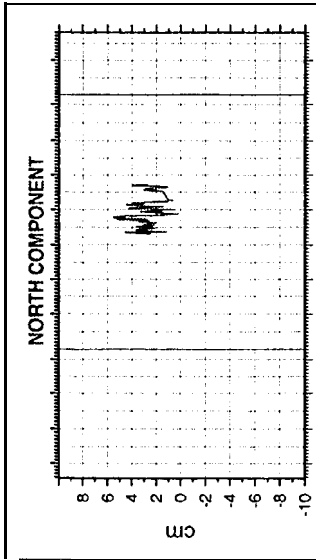
Variations of daily SIR R solutions with respect to first solution



Variations of

with

to first solution



Comparison of diff. SIR R and GNAAC P

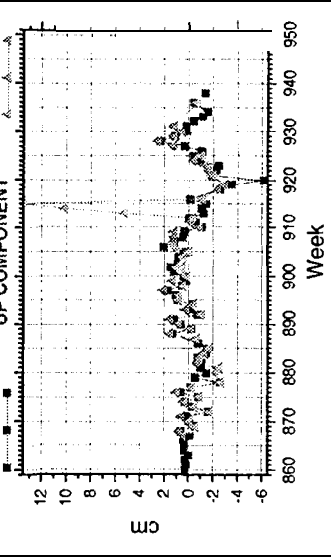
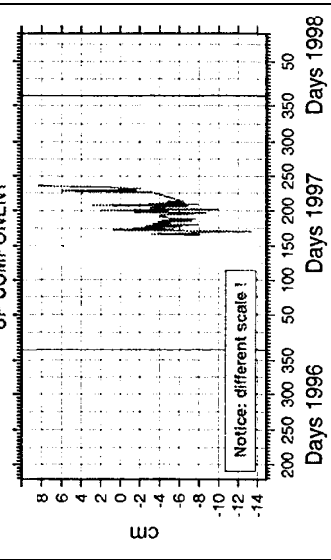
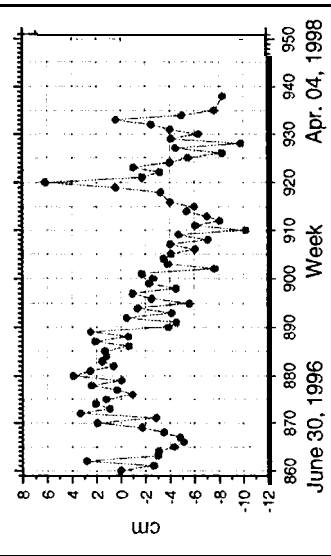
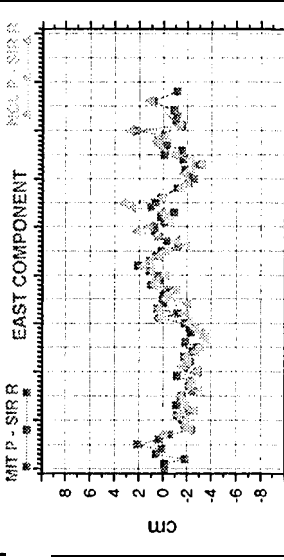
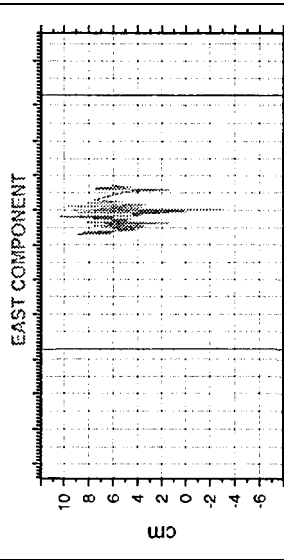
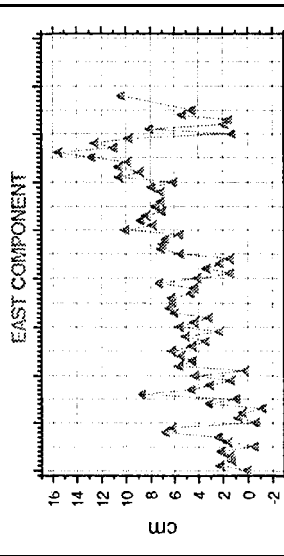
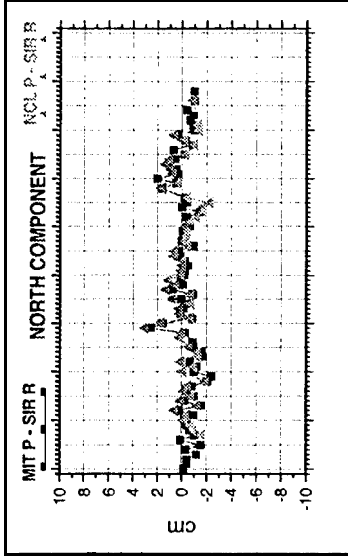


Fig. 7: Internal and External comparison of RNAAC SIR solutions (Station ASCENSION)

IGS STATION BRASILIA

Variations of weekly SIR R solutions with respect to first solution

Variations of daily SIR R solutions with respect to first solution

Comparison of cliff. SIR R and GNAAC P after Helmert transf.

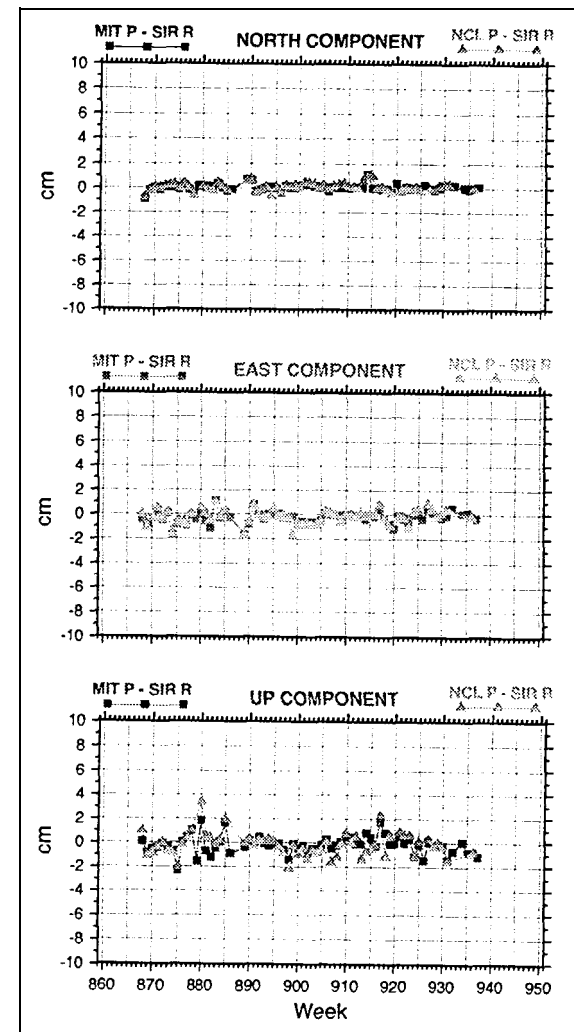
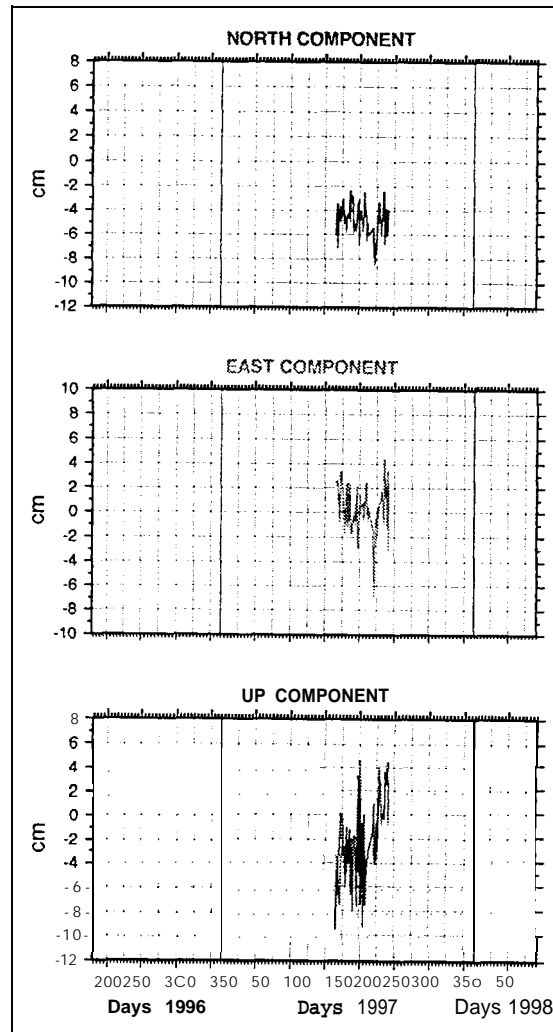
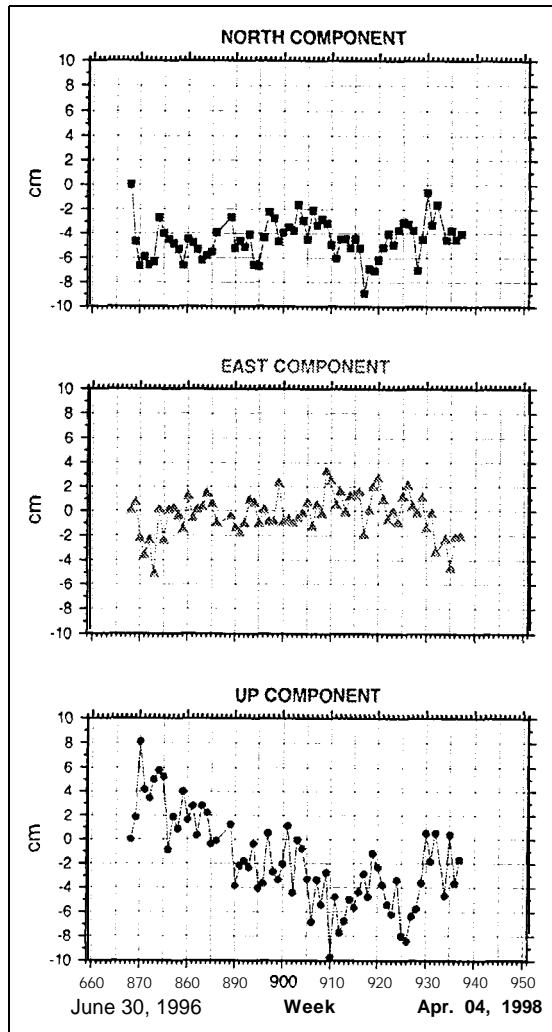
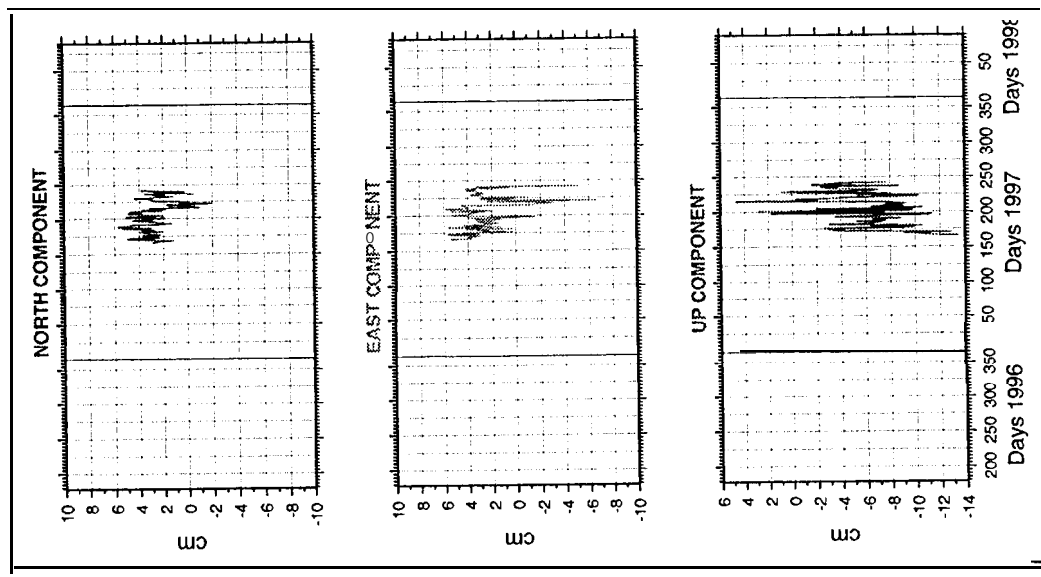


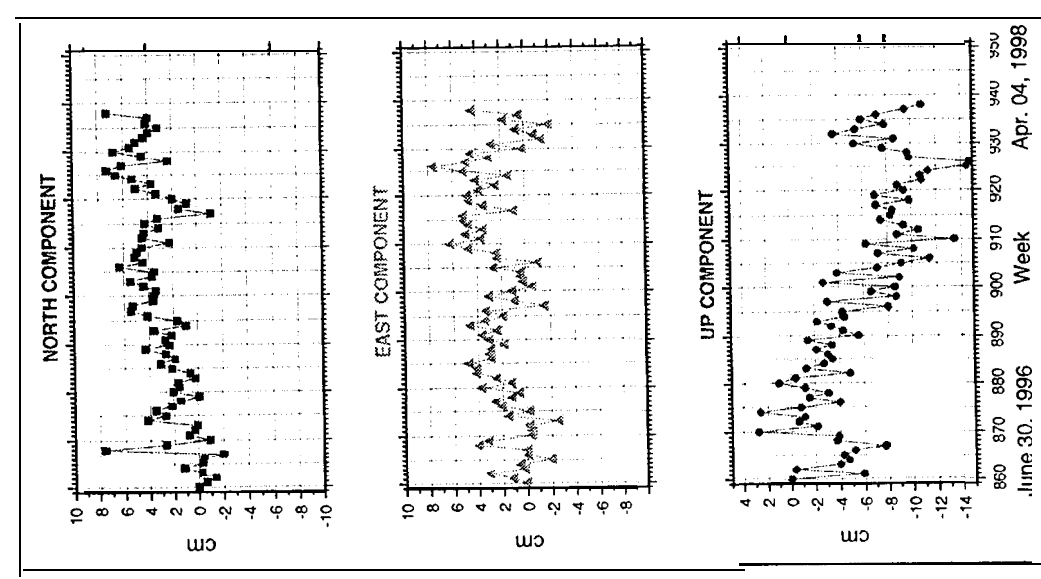
Fig. 8: Internal and External comparison of RNAAC SIR solutions (Station Brasilia)

IGS STATION FORTALEZA

Variations of daily SIR R solutions with respect to first solution



Variations of weekly SIR R solutions with respect to first solution



Comparison of diff. SIR R and GNAAC P after Helmert transf.

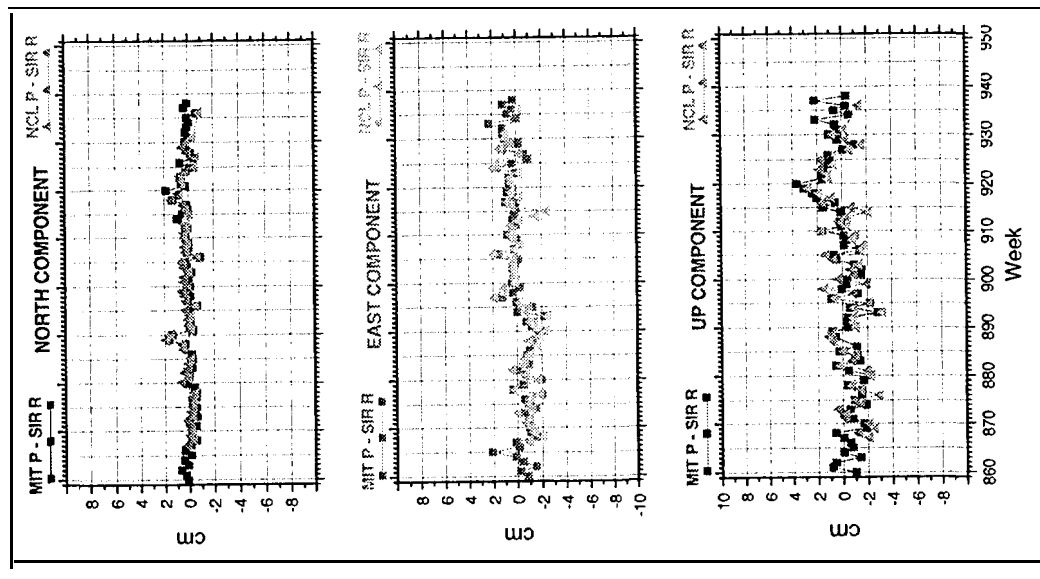


Fig. 9: Internal and External comparison of RNAAC SIR solutions (station Fortaleza)

STATION PRESIDENTE PRUDENTE

Variations of weekly SIR R solutions with respect to first solution

Variations of daily SIR R solutions with respect to first solution

Comparison of cliff. SIR R and GNAAC P after Helmert transf.

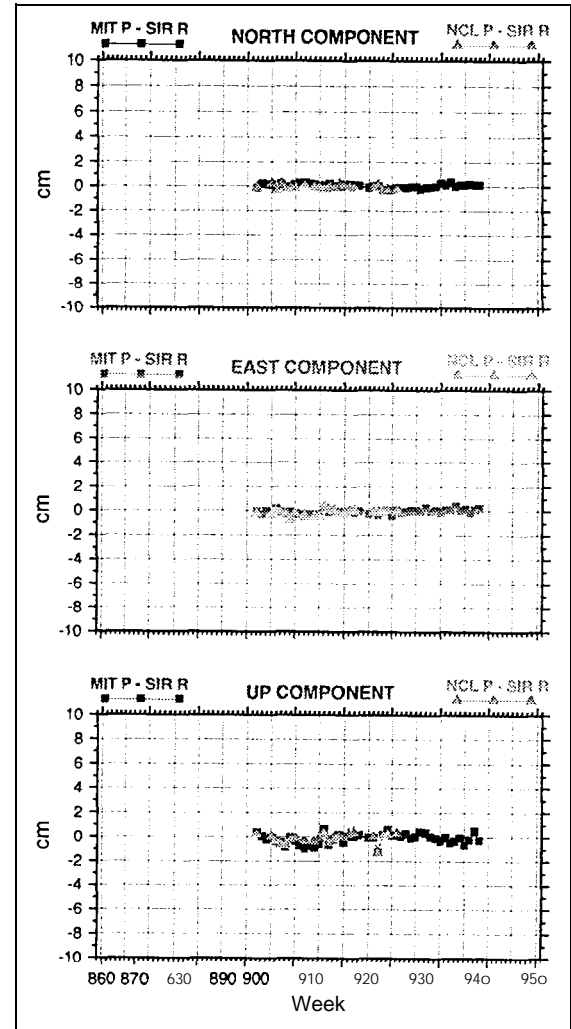
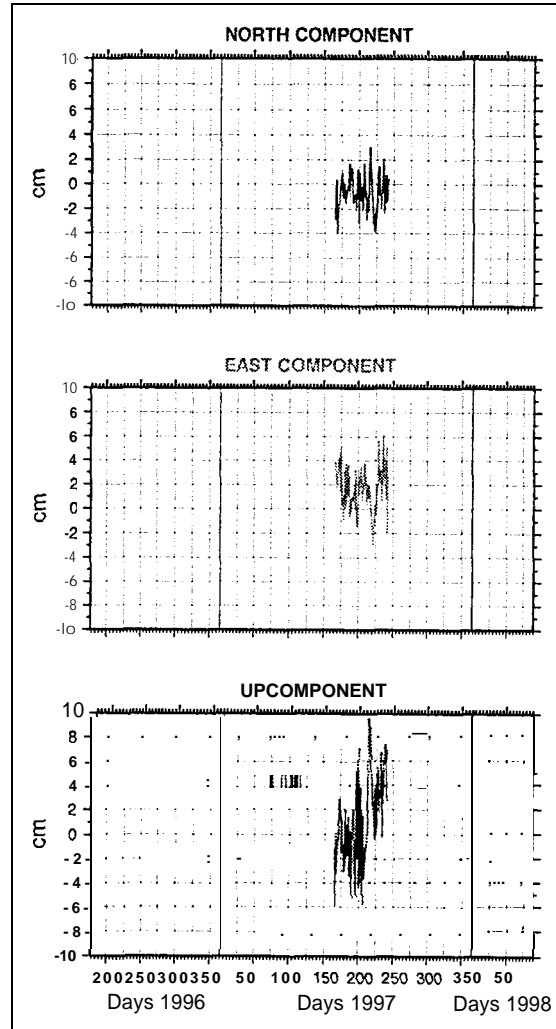
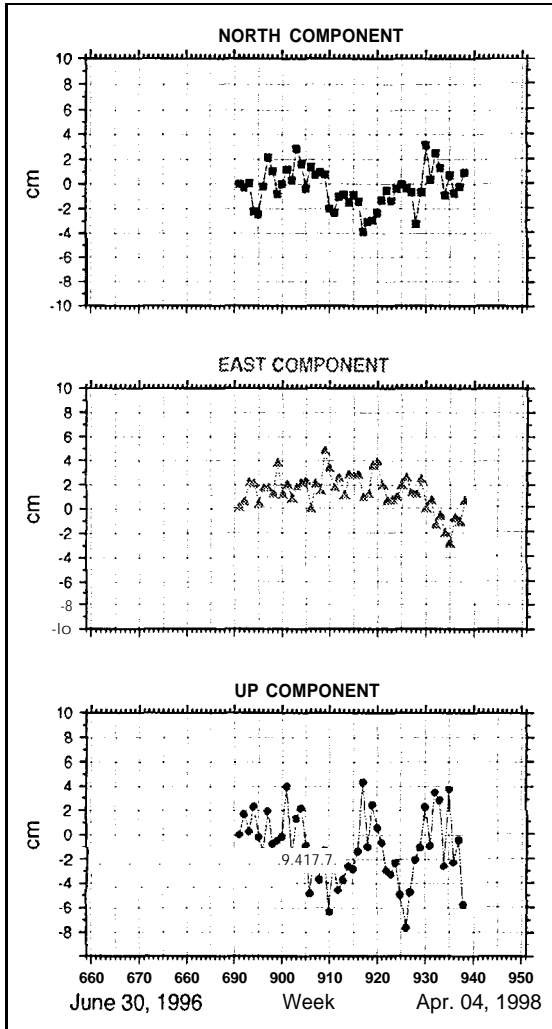
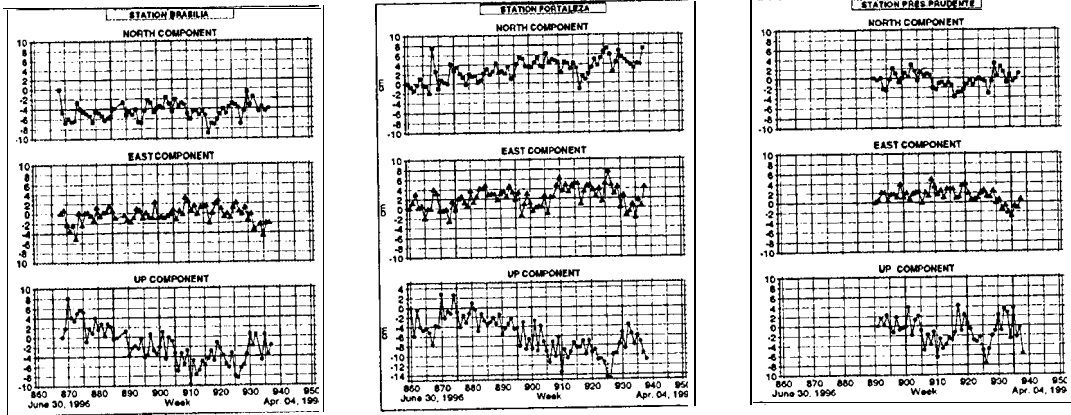


Fig. 10: Internal and External comparison of RNAAC SIR solutions (Station Presidente Prudence)

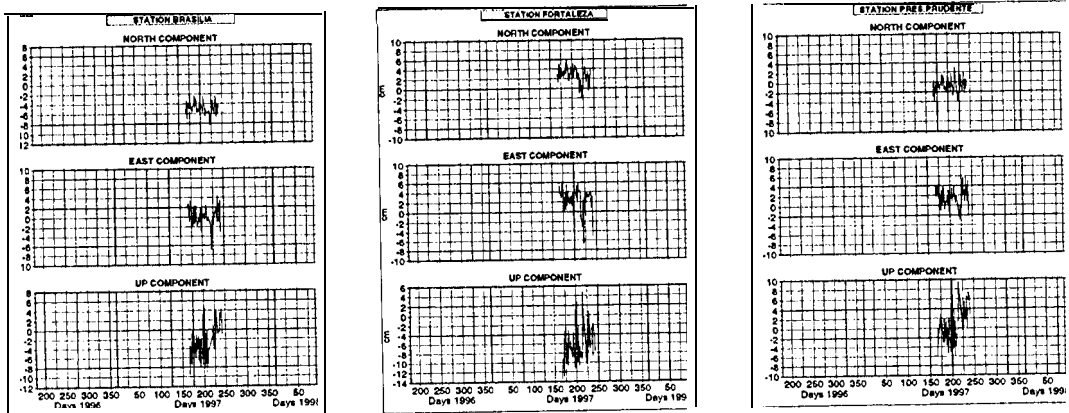
IGS Regional Network Associate Analysis Center SIRGAS
(IGS RNAAC SIR)

Brazilian GPS Stations

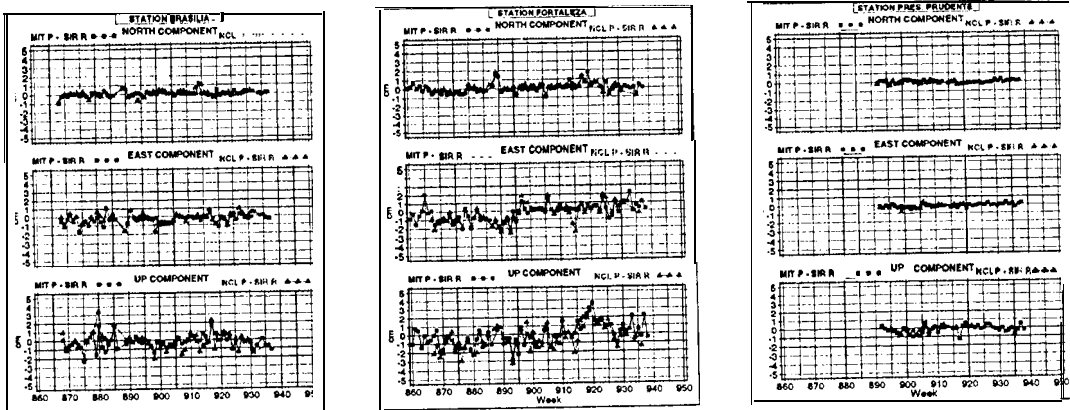
Internal Consistency of RNAAC SIR Weekly Solutions
Variations of Weekly SIR R Solutions with respect to the first Solution



Diurnal Variations of RNAAC SIR Solutions
Variations of Daily SIR R Solutions with respect to the first Solution



Comparison of SIR R-SINEX with GNAAC's P-SINEX Solutions
Differences in North, East and Up Components after Helmert Transformation



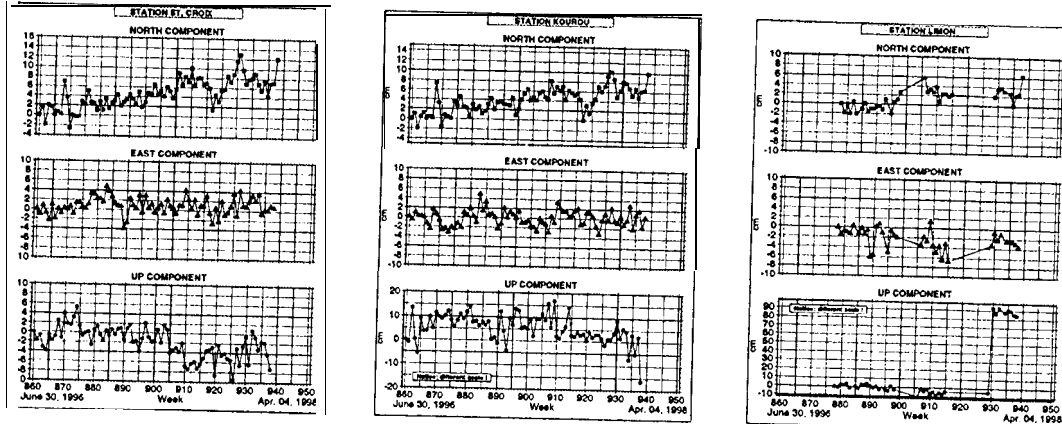
IGS

Poster 1: Selected Brazilian GPS Stations

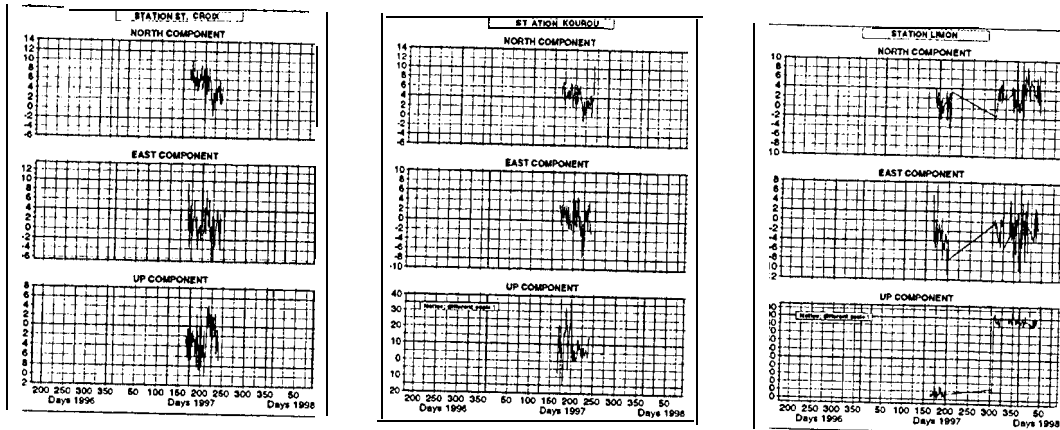
IGS Regional Network Associate Analysis Center SIR(2AS)
(IGSRNAAC SIR)

IGS Stations with Problematic Periods

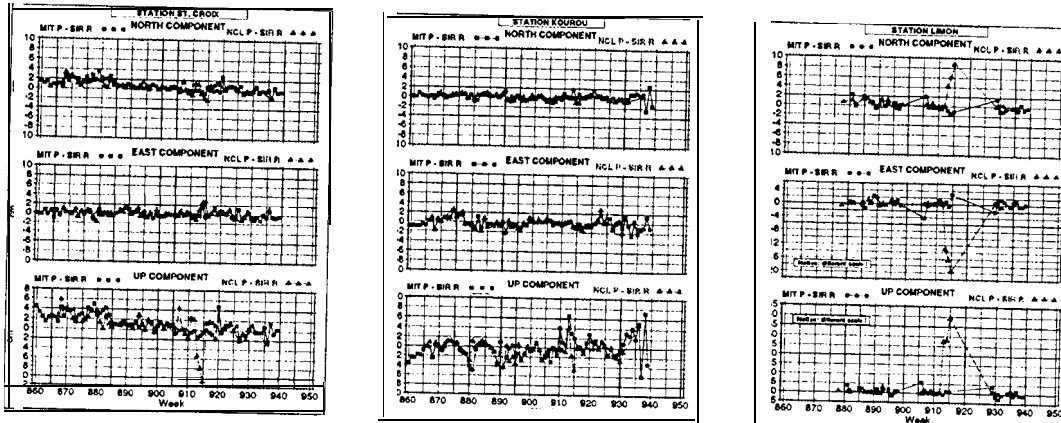
Internal Consistency of RNAAC SIR Weekly Solutions
Variations of Weekly SIR R Solutions with respect to the first Solution



Diurnal Variations of RNAAC SIR Solutions
Variations of Daily SIR R Solutions with Respect to the first Solution



Comparison of SIR R-SINEX with GNAAC's P-SINEX Solutions
Differences in North, East and Up Components @ m. Helmert Transformation

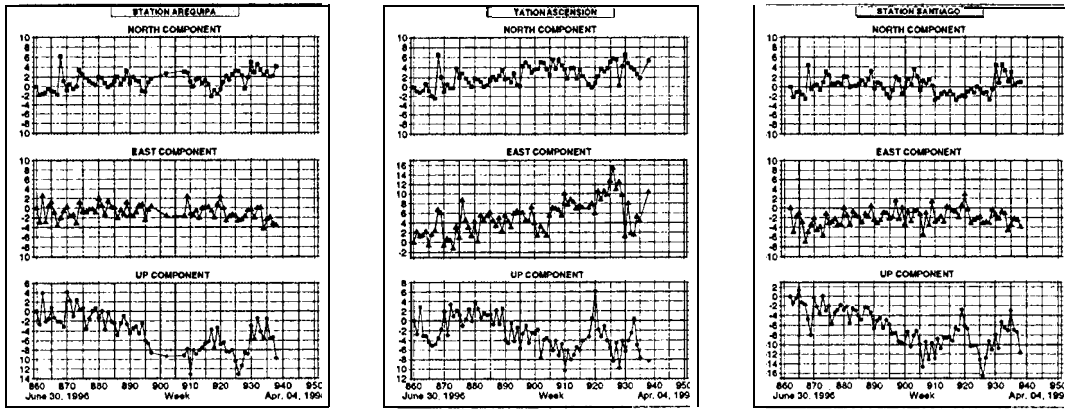


Poster 2: IGS Stations with Problematic Periods

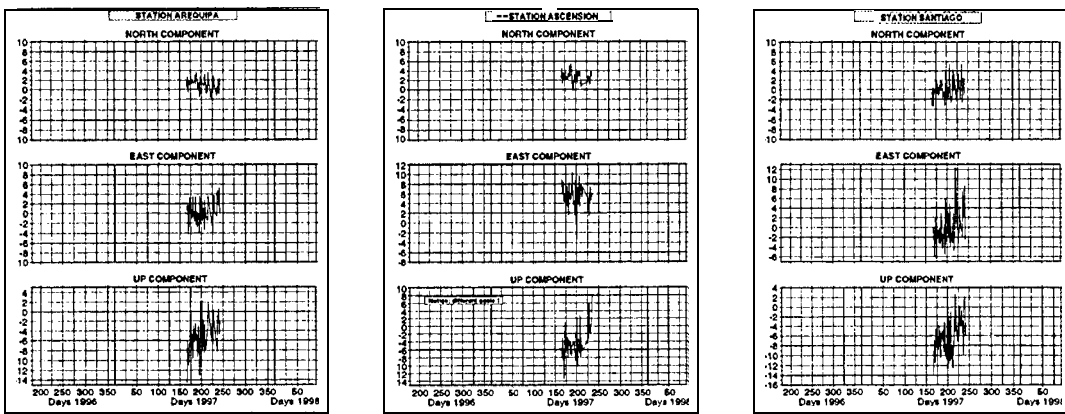
IGS Regional Network Associate Analysis Center SIRGAS
(IGS RNAAC SIR)

IGS Stations with Problematic Periods

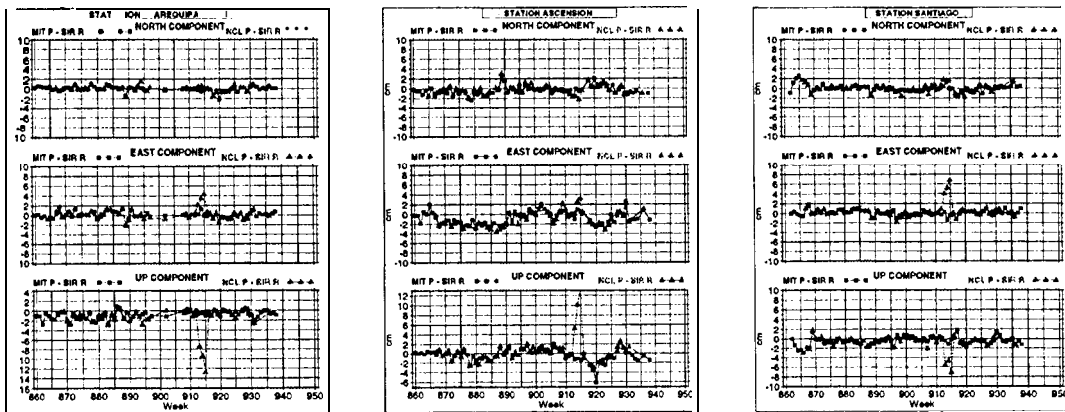
Internal Consistency of RNAAC SIR Weekly Solutions
Variations of Weekly SIR R Solutions with respect to the first Solution



Diurnal Variations of RNAAC SIR Solutions



Comparison of SIR R-SINEX with GNAAC's P-SINEX Solutions
Differences in North, East and Up C m - a n . , Helmert Transformation



Poster 3: IGS Stations with Problematic Periods

*Ra'ed Ka war, Geoffrey Blewitt, and Phil Davies**

Department of **Geomatics**, University of Newcastle upon Tyne, UK

ABSTRACT

The Newcastle (NCL) **GNAAC** has been operational for two years. It produces weekly combined solutions for the GNET, and the PNET (i.e., **densified GNET**); based on the ACS and **RNAACs** data respectively. In our poster at this workshop, we present the current status of the NCL **GNAAC**, summary of data submission and analysis, strategies, and some of the weighted RMS postfit residuals of the AC solutions with respect to the NCL **GNAAC** solutions.

INTRODUCTION

The Newcastle Global Network Associate Analysis Center (NCL **GNAAC**) was established in 1995 as a response to the call for participation in the pilot project of the IGS distributed processing scheme for the **densification** of the **ITRF**. This scheme has two components: the combined analysis (**G-SINEX**) of the Analysis Centers' coordinate solutions (**A-SINEX**); and the integration (**P-SINEX**) of regional network submissions (**R-SINEX**). The NCL **GNAAC** commenced producing coordinate weekly combined solution files, **G-SINEX**, from GPS week 817. Since GPS week 0834 the NCL **GNAAC** started to include station discrepancy information for each Analysis Center. With regard to the **P-SINEX** component, this started in year 1996.

NCL GNAAC STATUS

In November 1997 and due to the change over of the NCL **GNAAC** operator; there were some reports not retrieved from both the GNET and the PNET. The GNET

* Currently at Ordnance Survey, Southampton, UK

reports were all recovered and routine operation started again. With respect to the PNBT report we are still working on that.

SUMMARY OF DATA SUBMISSION AND ANALYSIS

As previously mentioned we analyze data from ACS and RNAACs. Figure 1 shows a bar diagram for the sources of the A-SINEXS that we analyze. It seem fairly obvious that most of the ACS have been submitting data to the CDDIS on time. Figure 2 shows that the NCL GNAAC should be routinely analyzing solutions from 6 RNAACs: AUS, GIA, PGC, GSI, SIR and EUR. However, this is not the case, solutions from only three or four RNAACS are being analyzed routinely. There are two reasons behind this: the first, and most important is that the RNAACS are not submitting data to the CDDIS on time; and the second is caused by our recent strategy to analyze only the stations that have a formal log file at the IGS CB (see next section).

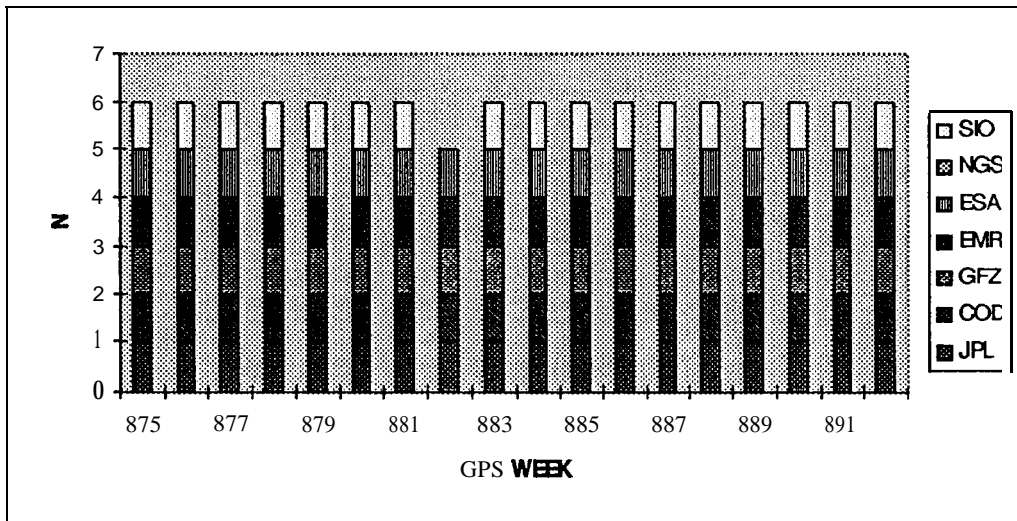


Figure 1: The number and sources of A-SINEX data analysed.

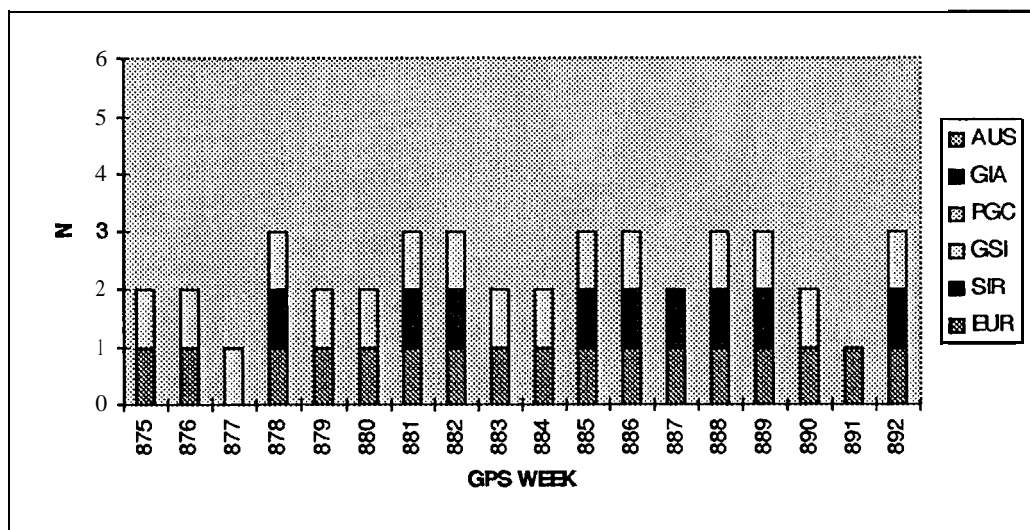


Figure 2: The number and sources of A-SINEX data analysed.

STRATEGY

Since October 1997 an automatic **catalogue** update system has been put in place at NCL. This system downloads theloghist.txt file, maintained by the IGS CB, and create history **SINEX** file that is used for station information. The adoption of this policy means that there will be no discrepancy of the history block at A- & P-SINEX, and only stations that have official log files will be analyzed. Consequently, many stations have been thrown away out of our analysis, and sometime all of an RNAAC'S data are rejected as a result of this.

RESULTS

Figure 3 shows the Weighted Root Mean Square (**WRMS**) in mm for the postfit residuals, from the **A-SINEX** to the NCL **G-SINEX**. It is noticed that the maximum value is about 25 mm of the postfit residuals which emphasizes the importance of combining the **A-SINEXs** to one solution.

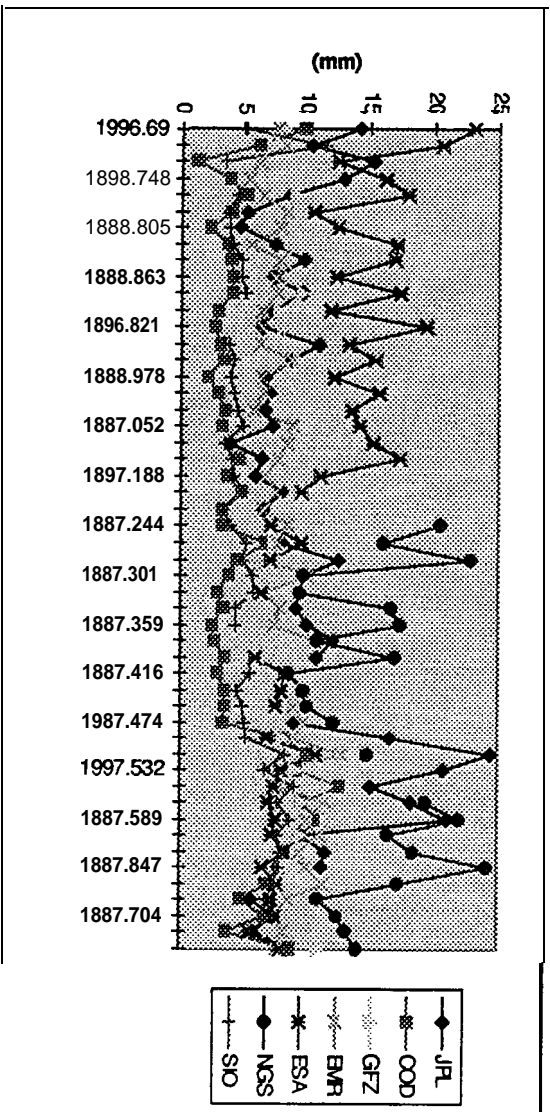
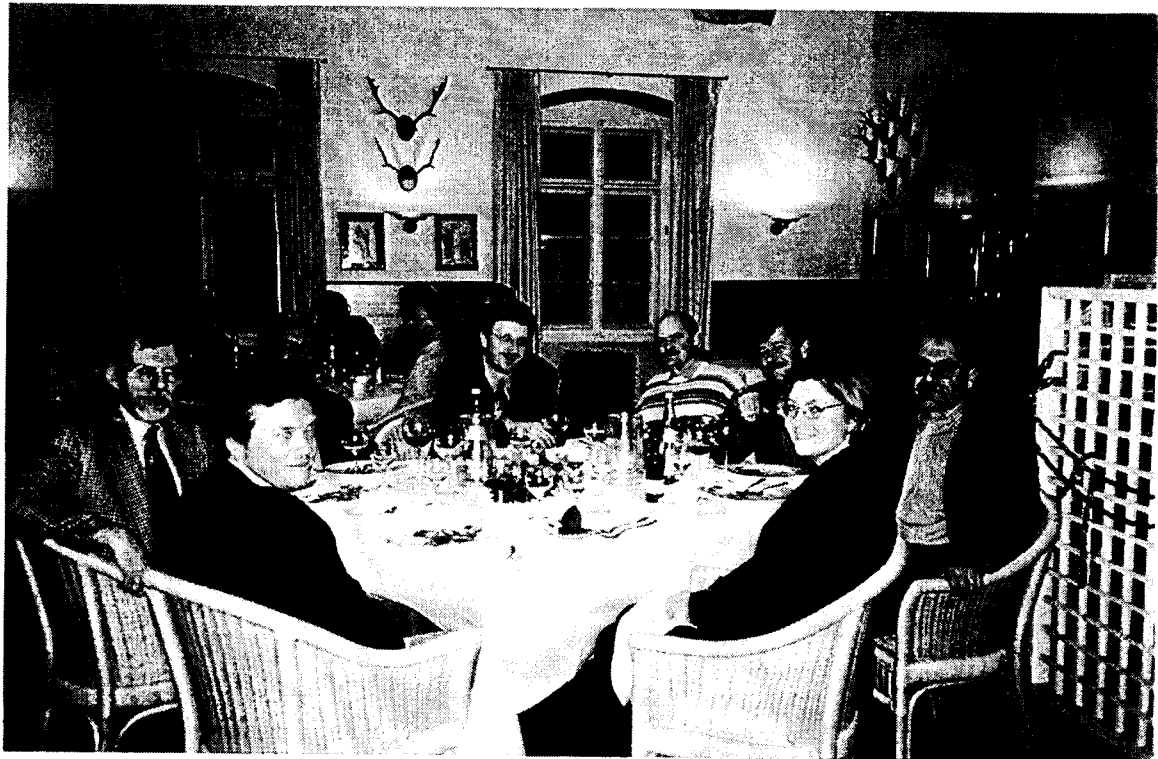


figure 3: P tti residuals' 1g RMS (mm) (A-SINEXs to NCL G-SINEX).



IGS Workshop Dinner, Jagschloss Kranichstein, Darrnstadt, 10 February 1998.
(Photos courtesy of Ruth Neilan, JPL.)